ARO 26588.1-EG-CF

AD-A217 189

(2)

Compendium of Abstracts and Viewgraphs

2nd International Workshop on Composite Materials and Structures for Rotorcraft

Army Research Office
American Helicopter Society
Rensselaer Polytechnic Institute

September 14 & 15, 1989

SECURITY CLASSIFICATION OF THIS PAGE

REPORT DOCUMENTATION PAGE

Form Approved
OMB No. 0704-0188

1a. REPORT SECURITY CLASSIFICATION Unclassified	1b. RESTRICTIVE MARKINGS N.A.
2a. SECURITY CLASSIFICATION AUTHORITY N.A.	3. DISTRIBUTION/AVAILABILITY OF REPORT Unlimited
2b. DECLASSIFICATION/DOWNGRADING SCHEDULE N.A.	
4. PERFORMING ORGANIZATION REPORT NUMBER(S) N.A.	5. MONITORING ORGANIZATION REPORT NUMBER(S) ARO 26588.1-EG-CF
6a. NAME OF PERFORMING ORGANIZATION Rensselaer Polytechnic Institute 6b. OFFICE SYMBOL (If applicable) RPI	7a. NAME OF MONITORING ORGANIZATION Army Research Office
6c. ADDRESS (City, State, and ZIP Code) 110 8th St., Troy, N.Y. 12180	7b. ADDRESS (City, State, and ZIP Code) P. O. Box 12211, Research Triangle Park, N.C. 27709-2211
8a. NAME OF FUNDING/SPONSORING ORGANIZATION Army Research Office 8b. OFFICE SYMBOL (If applicable) ARO	9. PROCUREMENT INSTRUMENT IDENTIFICATION NUMBER DAAL03-89-G-0003
8c. ADDRESS (City, State, and ZIP Code) P.O. Box 12211 Research Triangle Park, N.C. 27709-2211	10. SOURCE OF FUNDING NUMBERS PROGRAM ELEMENT NO. / PROJECT NO. / TASK NO. / WORK UNIT ACCESSION NO.

11. TITLE (Include Security Classification)
2nd International Workshop on Composite Materials and Structures for Rotorcraft

12. PERSONAL AUTHOR(S)
R. J. Diefendorf

13a. TYPE OF REPORT	13b. TIME COVERED	14. DATE OF REPORT (Year, Month, Day)	15. PAGE COUNT
(see #16)	FROM 12/1/88 TO 11/30/89	Sept. 14 & 15, '89	N.A.

16. SUPPLEMENTARY NOTATION
Compendium of Abstracts and Viewgraphs (of presentations)

17. COSATI CODES			18. SUBJECT TERMS (Continue on reverse if necessary and identify by block number)
FIELD	GROUP	SUB-GROUP	Rotorcraft Composite Materials & Structures

19. ABSTRACT (Continue on reverse if necessary and identify by block number)

A workshop was conducted, dealing with the fundamentals of composite constituent materials and laminates as they influence applications to advanced rotorcraft developments. Included in the purview of the workshop were the theory, numerical analysis, fabrication, testing, and inspection of thermoset & thermoplastic resin matrix and metal matrix composites as they may have advantage for rotors, fixed airframe, drive system, controls, and engine "cold section" components.

A total of 23 technical presentations were made in six sessions. There were, in addition Keynote, Luncheon and Banquet Addresses. Although general announcements were made to 157 leaders in these fields, attendance was by invitation only. A total of 61 workshop participants attended, representing 5 U.S. and 2 European helicopter manufacturers; 8 U.S. and 1 European universities; 6 U.S. government agencies; and 5 U.S. materials industry companies.

20. DISTRIBUTION/AVAILABILITY OF ABSTRACT ☐ UNCLASSIFIED/UNLIMITED ☒ SAME AS RPT. ☐ DTIC USERS	21. ABSTRACT SECURITY CLASSIFICATION Unclassified
22a. NAME OF RESPONSIBLE INDIVIDUAL R. G. Loewy	22b. TELEPHONE (Include Area Code) 518-276-6594 22c. OFFICE SYMBOL Institute Professor

DD Form 1473, JUN 86 Previous editions are obsolete. SECURITY CLASSIFICATION OF THIS PAGE

RENSSELAER POLYTECHNIC INSTITUTE

workshop on

Composite Materials and Structures

September 14th and 15th, 1989

GENERAL CHAIRMAN - Professor R. J. Diefendorf
Rensselaer Polytechnic Institute

STEERING COMMITTEE -

Dr. Gary Anderson, Chairman	- U.S. Army Research Office
Carl Albrecht	- Boeing Helicopter
G. Reis Alsmiller	- Bell Helicopter
John Dugundji	- M.I.T.
Wolf Elber	- U.S. Army AATD
Samuel Garbo	- Sikorsky Aircraft
William Krueger	- DuPont
Andrew Logan	- McDonnell Douglas Helicopter
John Zugschwert	- AHS

AGENDA

2nd ARO-AHS-RPI WORKSHOP ON COMPOSITE MATERIALS AND STRUCTURES FOR ROTORCRAFT

Room 4050 CII

September 14th

8:15-8:20 AM	WELCOME - R. *Judd Diefendorf* (Rensselaer Polytechnic Institute)
8:20-8:40 AM	KEYNOTE ADDRESS: *Thomas L. House*, Technical Director, U.S. Army Aviation Systems Command and Technical Director, American Helicopter Society, "Composite Structures for Rotorcraft— Meeting the Military Application Challenge"
SESSION I:	CHAIRMAN - *Christian K. Gunther (Boeing Helicopters)* Rotor Technology
8:45-9:15 AM	*"Rotor Blade Root End Design: To Wind or Drill?", A. *Stevenson*, Westland Helicopters Ltd., Yeovil, Somerset, United Kingdom.
9:15-9:45 AM	*"Structural Strength and Stiffness Analysis of Composite Rotor Components for Best Material Efficiency", A. *Barth*, Messerschmitt-Bolkow Blohm, GmbH, Munich, West Germany.
9:45-10:15 AM	"Stress Analysis of Composite Rotor Blades", *M. Borri and G. Ghiringhelli*, Politecnico di Milano, Milano, Italy.
10:15-10:30 AM	B R E A K (CII Lounge)
SESSION II:	CHAIRMAN - *Paul A. Lagace (Massachusetts Institute of Technology)* Composite Structural Design
10:30-11:00 AM	*"Composite Challenges on the V-22", *M. K. Stevenson*, Bell Helicopter, Fort Worth, Texas.
11:00-11:30 AM	"Analysis and Design of Curved Composite Beams", *O. A. Bauchau and A. W. Peck*, Rensselaer Polytechnic Institute, Troy, New York.
11:30-12:00 PM	"Dynamic Characteristics of Thin-Walled Composite Beams", *L. W. Rehfield*, University of California-Davis, Davis, California, *A. R. Atilgan and D. H. Hodges*, Georgia Institute of Technology, Atlanta, Georgia.
12:00-12:30 PM	"Evaluation of Composite Components on the Bell 206L and Sikorsky S-76 Helicopters", *D. J. Baker*, NASA-Langley, Hampton, Virginia.
12:30-1:50 PM	L U N C H (Rensselaer Union, Rm 241-243)
1:15-1:45 PM	LUNCHEON ADDRESS: *Joseph Goldberg*, Program Manager, Sikorsky Aircraft-UTC, "Composite Developments in Rotor Systems"

[CONTINUED on PAGE 2]

September 14th

SESSION III: *CHAIRMAN - Robert W. Arden (U.S. Army AVSCOM)*
Tailored Laminates

2:00-2:30 PM "The Reduction of Hygrothermal Effects on Tension-Torsion Coupling in Composite Rotor Blades", S. C. *Hill*, Rensselaer Polytechnic Institute, Troy, New York.

2:30-3:00 PM "Importance of Elastic Tailoring in Design Analysis of Thin-Walled Composite Beams", A. R. *Atilgan*(*), L. W. *Rehfield*(**), and D. H. *Hodges*(*), (*)Georgia Institute of Technology, Atlanta, GA, (**)University of California-Davis, Davis, California.

3:00-3:30 PM "Toward Understanding the Tailoring Mechanisms for Thin-Walled Composite Tubular Beams", L. W. *Rehfield*, University of California-Davis, Davis, California and A. R. *Atilgan*, Georgia Institute of Technology, Atlanta, Georgia.

3:30-3:45 PM **B R E A K (CII Lounge)**

SESSION IV: *CHAIRMAN - Sanford S. Sternstein (Rensselaer Polytechnic Institute)*
Structural Integrity and Damage Mechanisms

3:45-4:15 PM "Damage Resistance in Rotorcraft Structures", E. A. *Armanios* and B. H. *Fortson*, Georgia Institute of Technology, Atlanta, Georgia.

4:15-4:45 PM "Biaxial Fatigue of Epoxy Matrix Composites", E. *Krempl*, Rensselaer Polytechnic Institute, Troy, New York.

4:45-5:15 PM "Structural Tailoring Techniques for Increased Delamination Resistance of Laminated Composites", A. J. *Vizzini* and W. R. *Pogue III*, University of Maryland, College Park, Maryland.

5:15-5:45 PM "Generalized Structural Integrity Assurance: Application to Rotorcraft", W. T. *Matthews*, U.S. Army Materials Technology Laboratory, Watertown, Massachusetts.

6:00-9:00 PM **C O C K T A I L S A N D B A N Q U E T (Sage Dining Hall)**

7:45-8:15 PM BANQUET SPEAKER: ***Jack D. Floyd***, Deputy Director, Super Team LHX Joint Program Office, Bell Helicopter/McDonnell-Douglas Helicopter Co., "LHX— A New Composite Helicopter"

[CONTINUED on PAGE 3]

September 15th

SESSION V: CHAIRMAN - *Jeffrey A. Hinkley* (NASA-*Langley*)
Thermoplastics versus Thermosets

8:15-8:45 AM "The Adhesion of Carbon Fibers to Thermoset and Thermoplastic Polymers", *W. D. Bascom*, University of Utah, Salt Lake, Utah.

8:45-9:15 AM "Compression Failure and Delamination in Thermoplastic Composites", *S. S. Sternstein*, Rensselaer Polytechnic Institute, Troy, New York.

9:15-9:45 AM "Advanced Thermoplastic Composite Structures for Rotorcraft Applications", *J. F. Pratte*, E. I. DuPont De Nemours & Co., Wilmington, Delaware.

9:45-10:15 AM "Thermoplastic Prepreg Product Forms", *T. L. Greene*, BASF, Charlotte, North Carolina.

10:15-10:45 AM "Advanced Thermoset Resin Systems", *W. T. McCarvill*, Hercules, Inc., Magna, Utah.

10:45-11:00 AM B R E A K (CII Lounge)

SESSION VI: CHAIRMAN - *George J. Schneider* (*Sikorsky Aircraft Division*, UTC)
Intelligent Structures and Active Control

11:00-11:30 AM *"Embedded Actuation and Processing in Intelligent Materials", *E. F. Crawley, K. B. Lazarus, and D. J. Warkentin*, Massachusetts Institute of Technology, Cambridge, Massachusetts.

11:30-12:00 PM "Dynamically-Tunable Smart Composites Featuring Electro-Rheological Fluids", *M. V. Gandhi and B. S. Thompson*, Michigan State University, East Lansing, Michigan.

12:00-12:30 PM *"Active Dynamic Tuning Utilizing SMA Composites", C. A. *Rogers*, Virginia Polytechnic Institute and State University, Blacksburg, Virginia.

12:30-1:00 PM "A Review of Active Noise Control Strategies for Reduction of Rotorcraft Interior Noise", *J. D. Jones*, Purdue University, West Lafayette, Indiana.

1:00-2:15 PM L U N C H (Fac/Staff Center Meeting Room - Sage Dining Hall)

A D J O U R N

*INVITED PAPERS

KEYNOTE ADDRESS

Thomas L. House
Technical Director
U.S. Army Aviation Systems Command
and
Technical Director
American Helicopter Society

"Composite Structures for Rotorcraft--
Meeting the Military Application Challenge"

UNAVAILABLE PRIOR TO PRESENTATION

SESSION I

ROTOR TECHNOLOGY

Christian K. Gunther
Boeing Helicopter Co.
Chairman

"Rotor Blade Root End Design: To Wind or Drill?"

Andrew Stevenson

Westland Helicopters Ltd., Yeovil, Somerset, U.K.

ARO-AHS-RPI 2nd International Workshop on
COMPOSITE MATERIALS AND STRUCTURES
FOR ROTORCRAFT

September 14 and 15, 1989

Rensselaer Polytechnic Institute
Troy, New York

UNAVAILABLE PRIOR TO PRESENTATION

Structural Strength And Stiffness Analysis Of Composite Rotor Components For Best Material Efficiency

Armin Barth

Messerschmitt-Bölkow-Blohm GmbH

Helicopter Division

Munich, Germany

Contents

- Rotor Concepts
  - Bearingless Main and Tail Rotors
  - Elastomeric Bearing Main and Tail Rotors (FEL)
- Design of FEL Main Rotor Hub
  - Structural Analysis
  - Experimental Verification

BO 105 / BK 117 Main Rotor (Hingeless)

MBB Helicopter Division

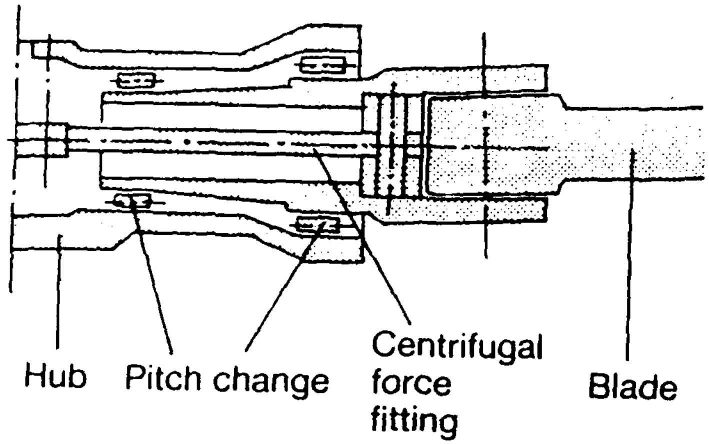

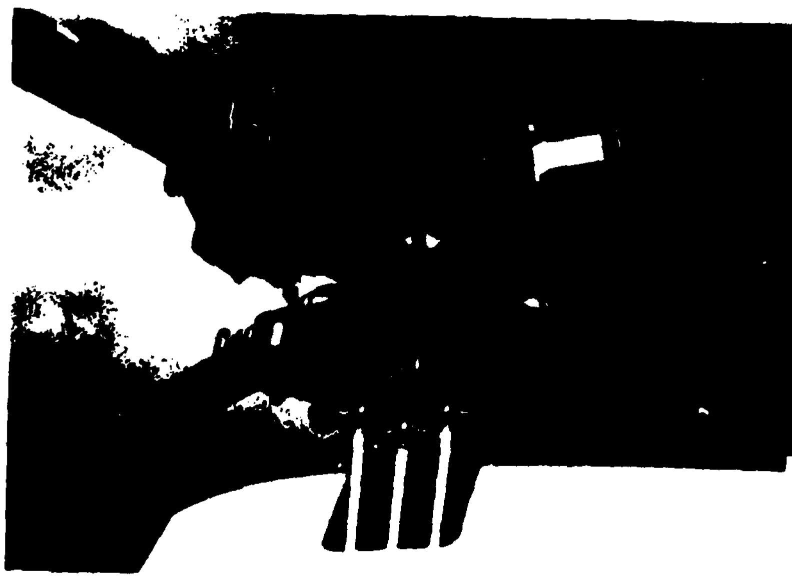

Bearingless Rotor Concepts
Stages of Developement

MBB Helicopter Division

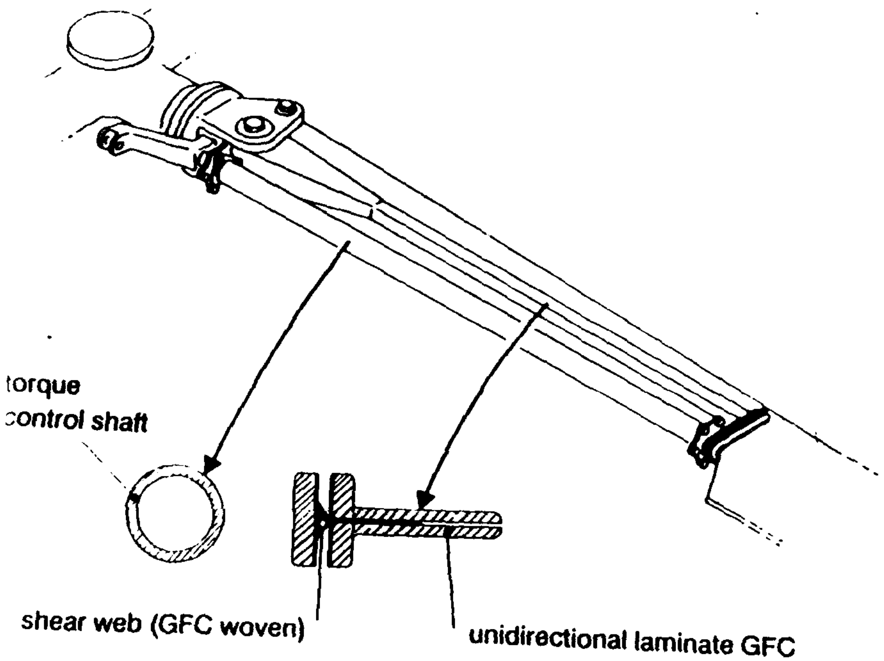

Experimental System

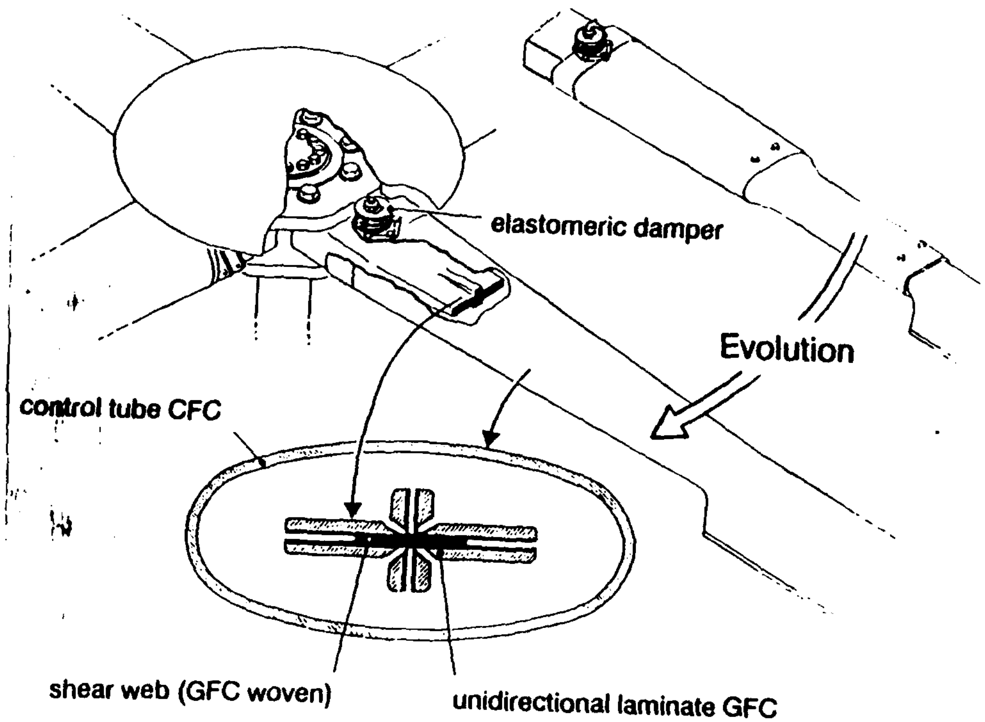

Prototype I (Telescopic Control Tube)

Prototype II (Blade With Integrated Control Tube)

Bearingless Rotor Concepts
Experimental Rotor

MBB Helicopter Division

Experimental Bearingless Rotor on Whirl Tower

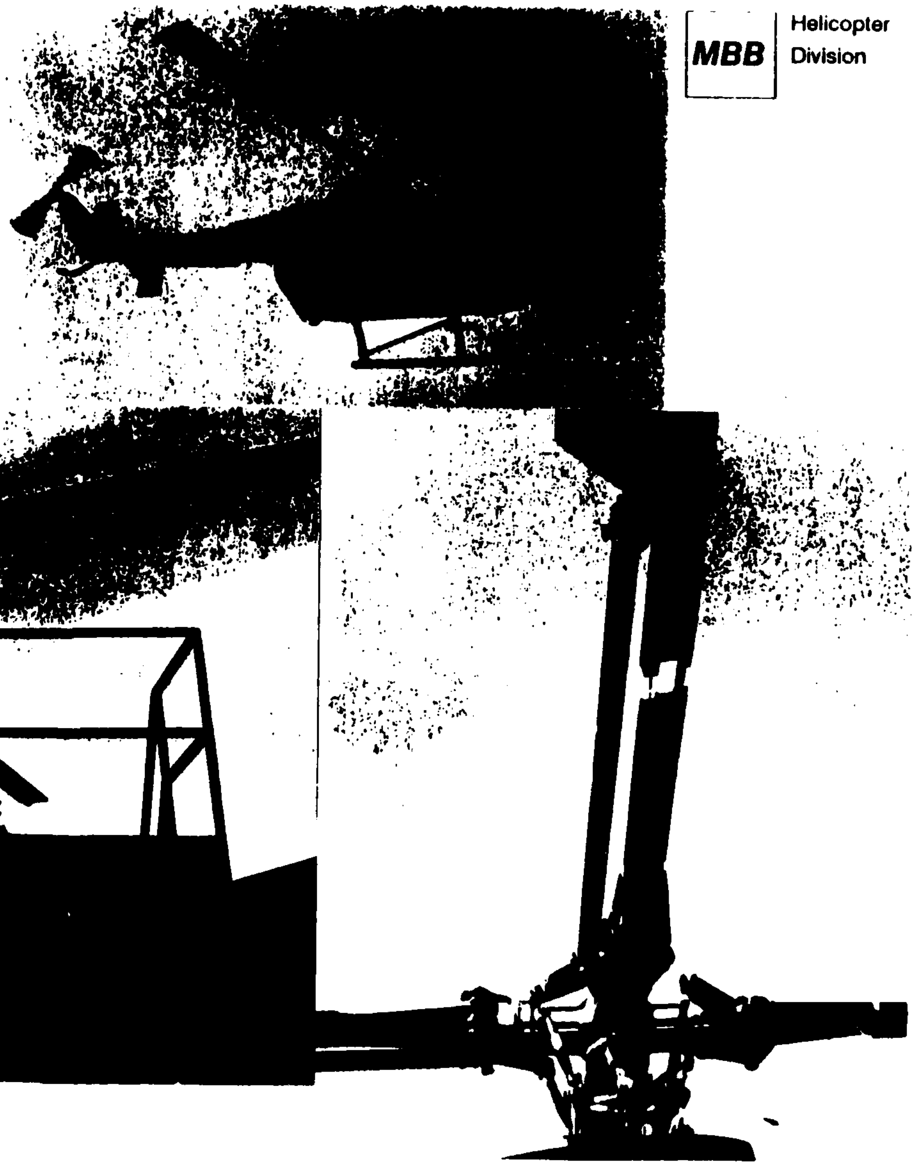

Flight Testing on the BO 105

Bearingless Rotor Concepts
Prototype I, Telescopic Control Tube

MBB Helicopter Division

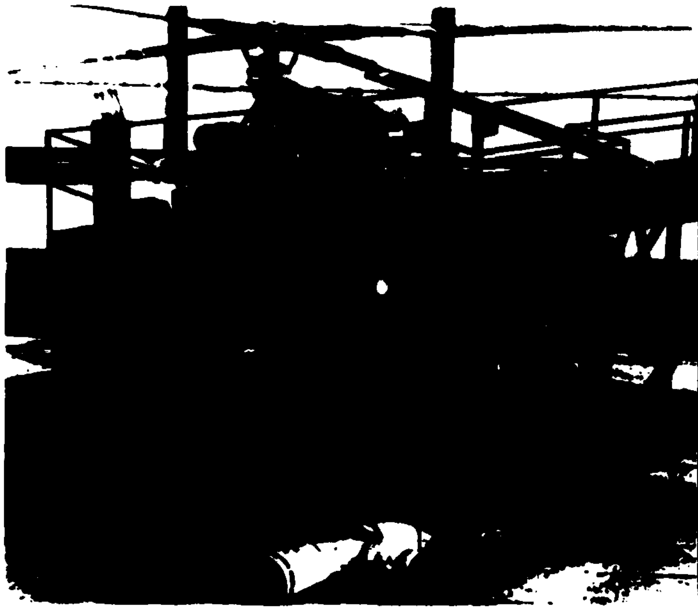

Prototype I on Whirl Tower

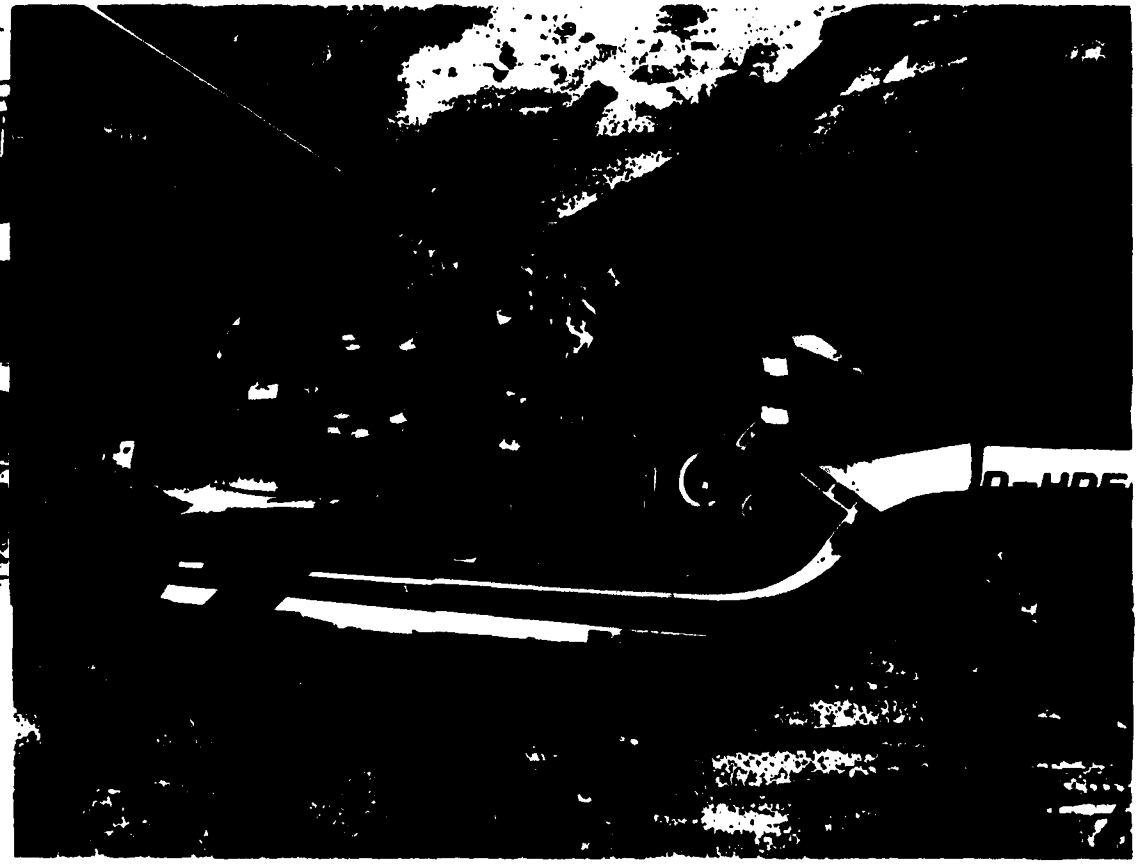

Flight Testing of the Prototype I on the BO 105

Bearingless Rotor Concepts

Prototype II, Blade with Integrated Control Tube

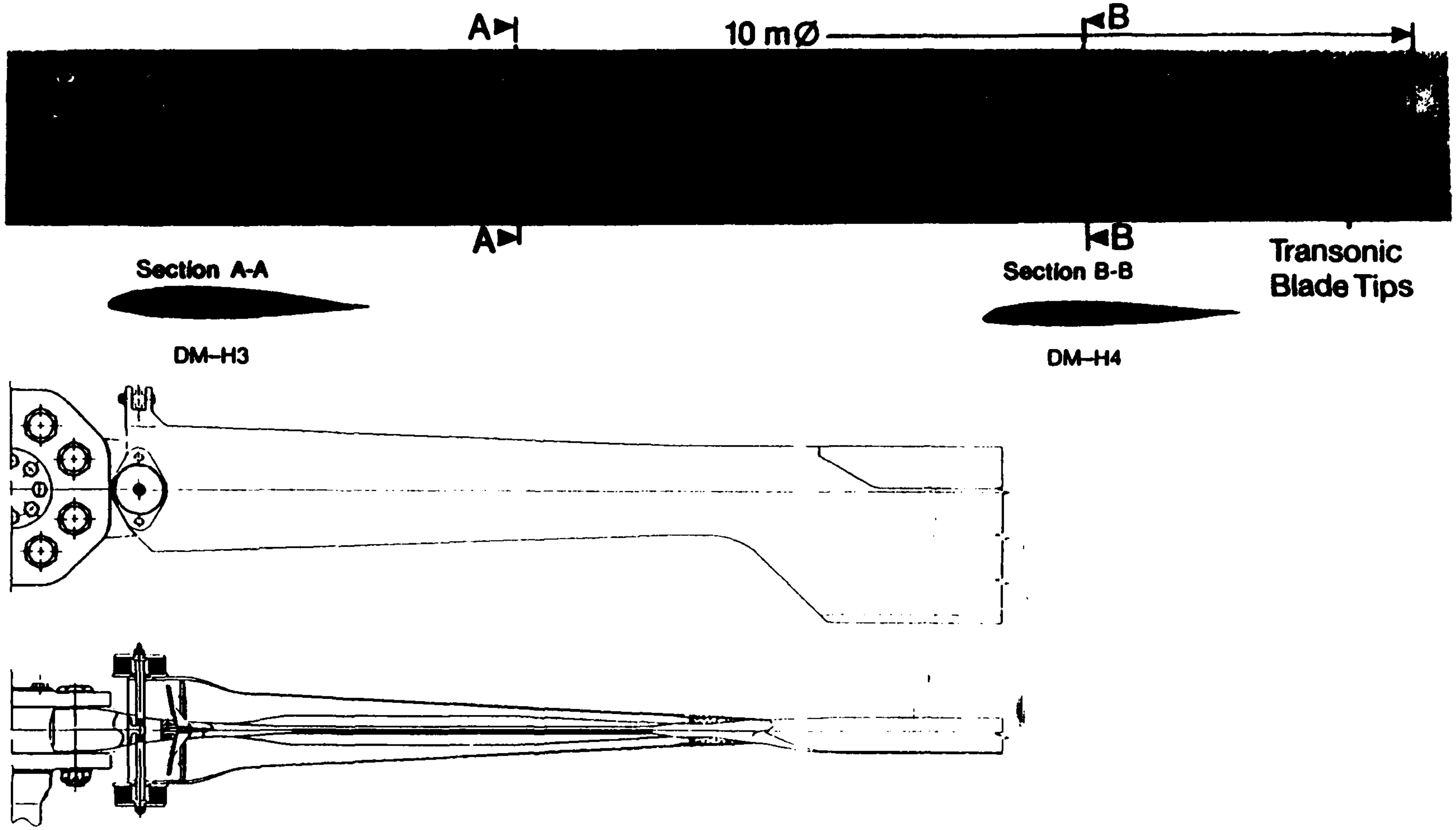

Complexity of Rotor Blade with Blade Attachment

The Bearingless Rotor on the BO 108

MBB Helicopter Division

Bearingless Rotor Concepts
Experimental Tail Rotor (Soft Inplane)

MBB Helicopter Division

Flight Testing of the Composite Tail Rotor on the BK 117

Bearingless Tail Rotor

Bearingless Composite Tail Rotor with Control Tube

MBB Helicopter Division

Fiber Elastomeric Bearing (FEL) Tail Rotor

MBB Helicopter Division

- Flight tested on BO 105
- In use on the new BO 108

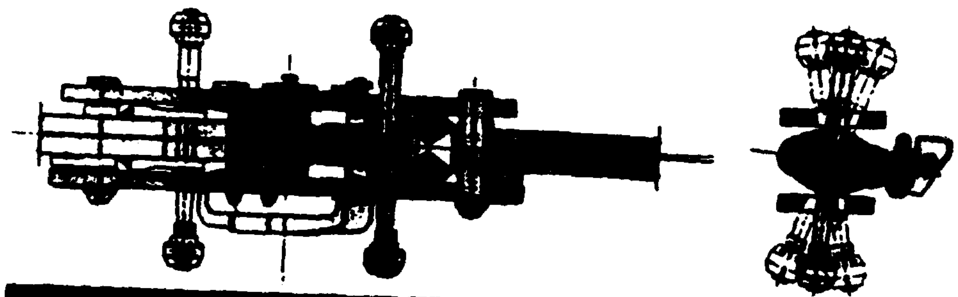

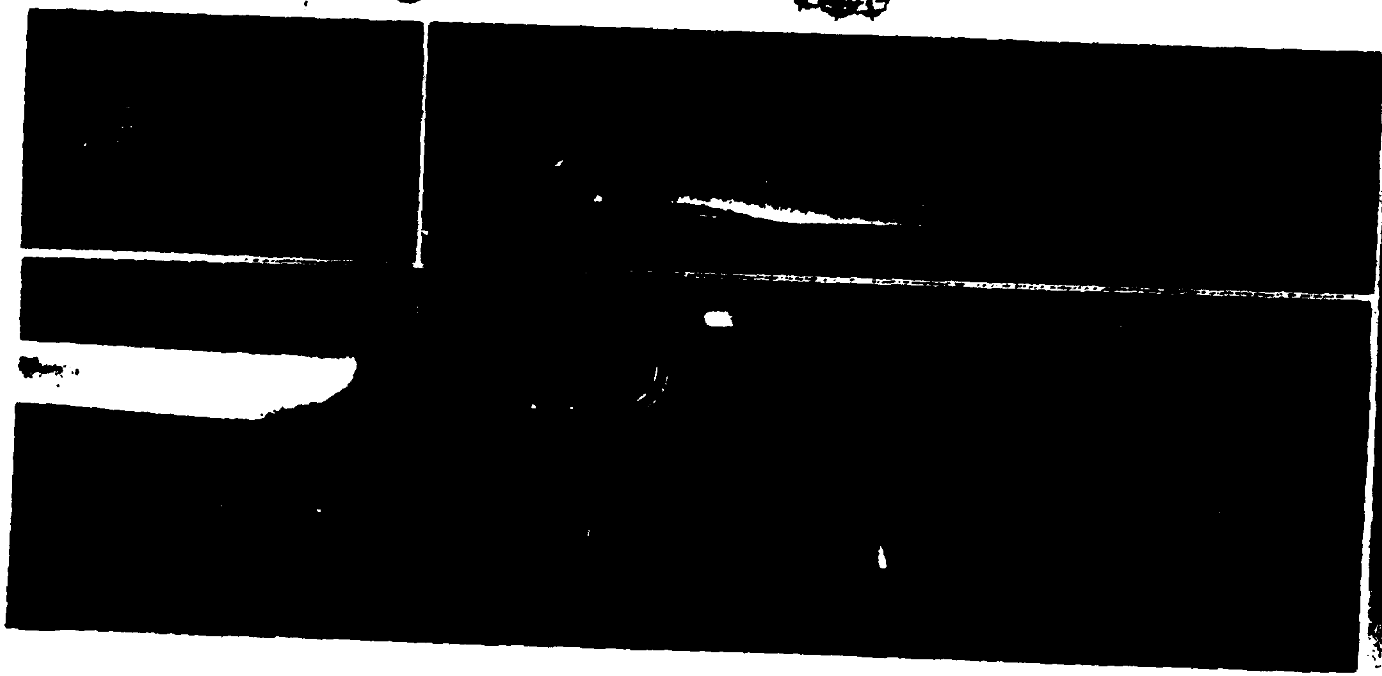

Main Rotor System with Elastomeric Bearings (FEL)

MBB Helicopter Division

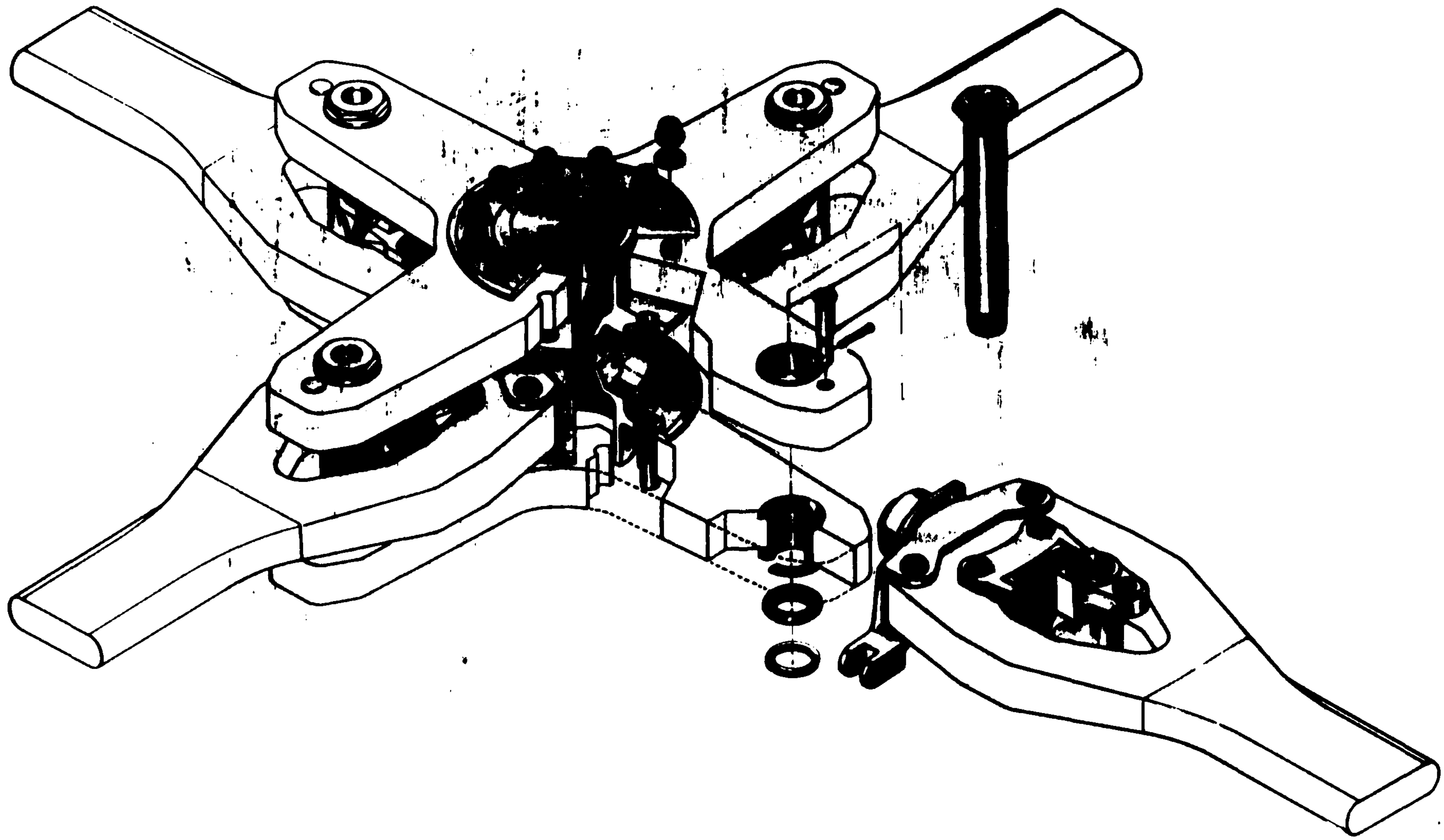

FEL Rotor on the Anti-Tank Helicopter PAH-2

MBB Helicopter Division

Main Rotor Hub
FEM Idealization of the Basic Version

MBB Helicopter Division

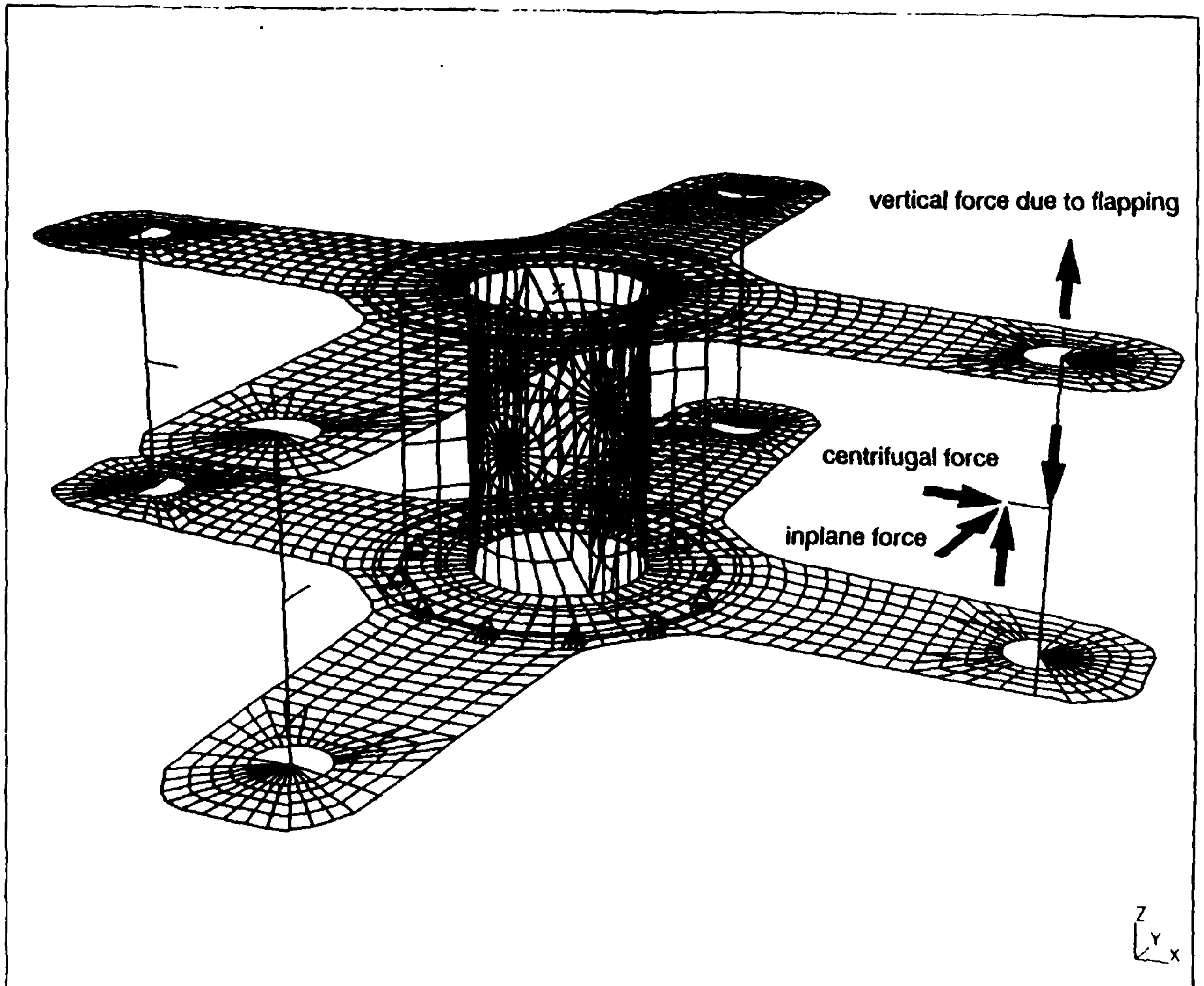

Deformed Geometry Due to Centrifugal Force, Flapping and Lead-Lag Bending

MBB Helicopter Division

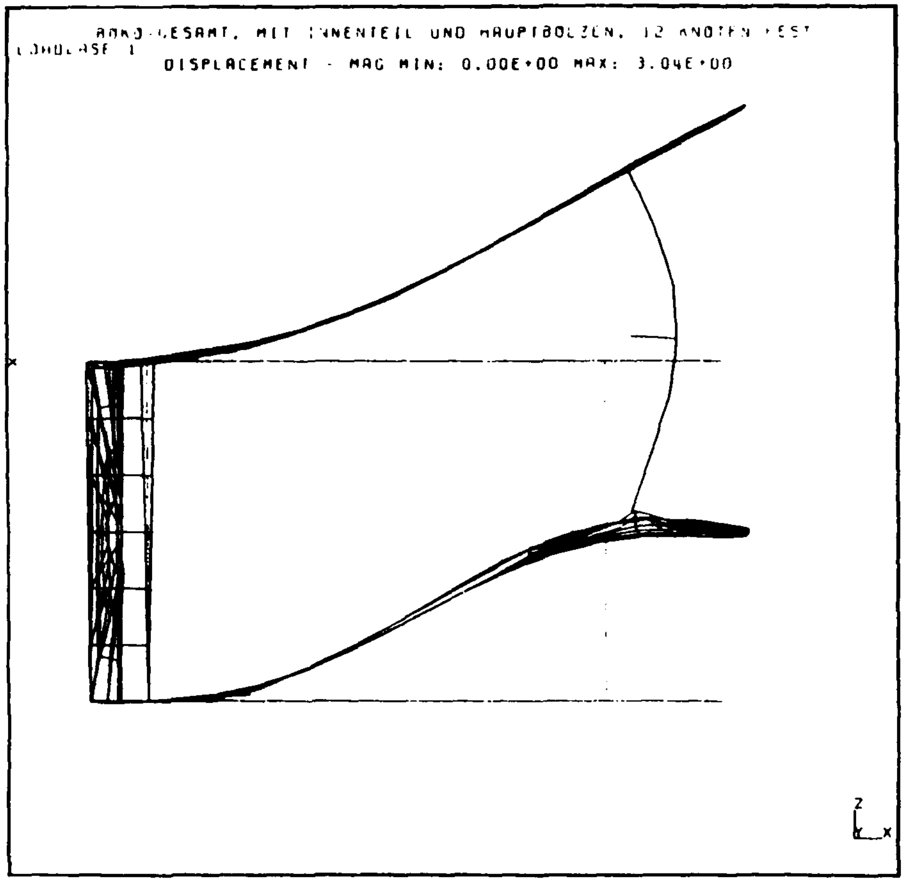

Static Load

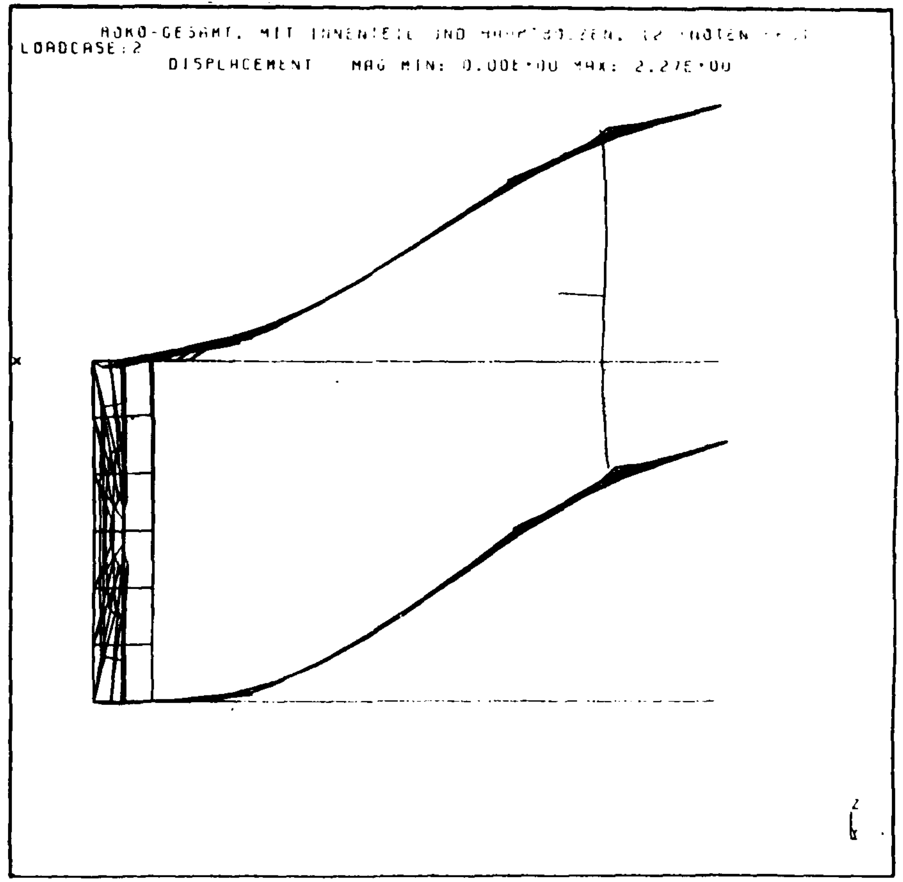

Alternating Load

Shape Influence on Stress Concentration

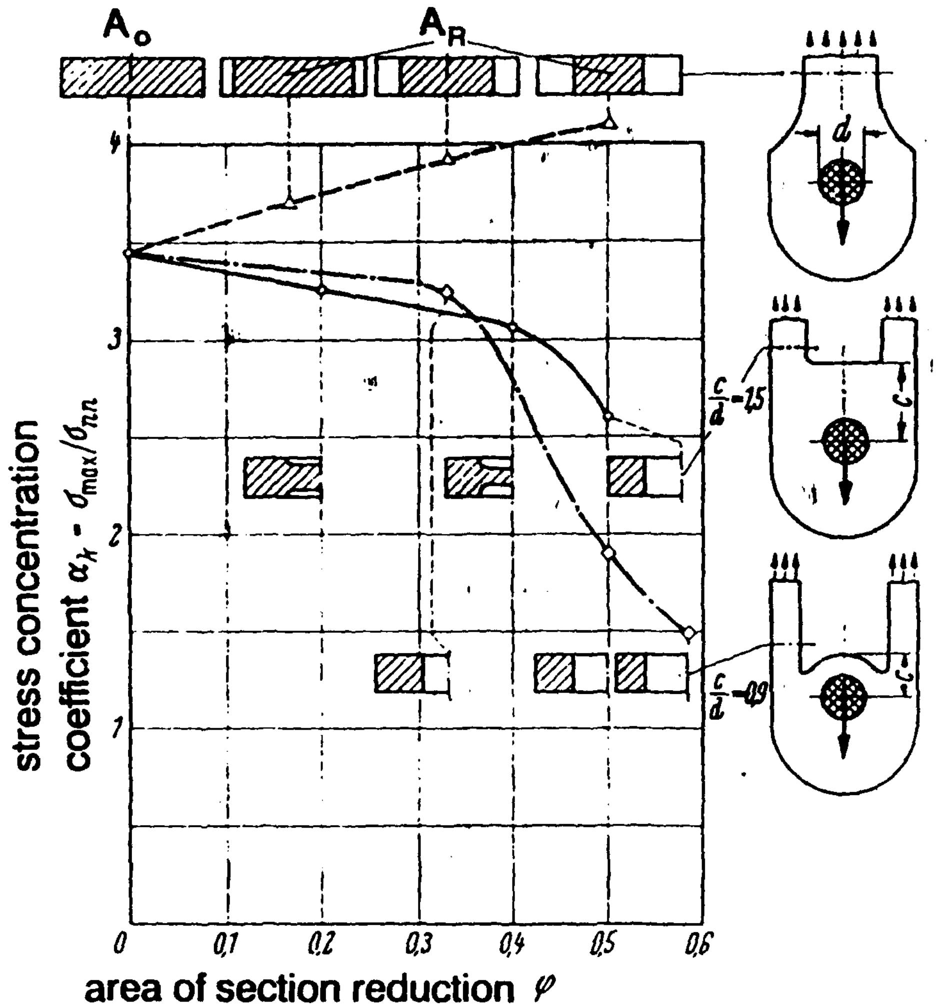

$\varphi = 1 - A_R / A_o$

A_R = residual area of section

A_o = basic area of section

Quarter Model of Main Rotor Hub (Solid Elements)
CFC Hub Plates with Cutout

MBB Helicopter Division

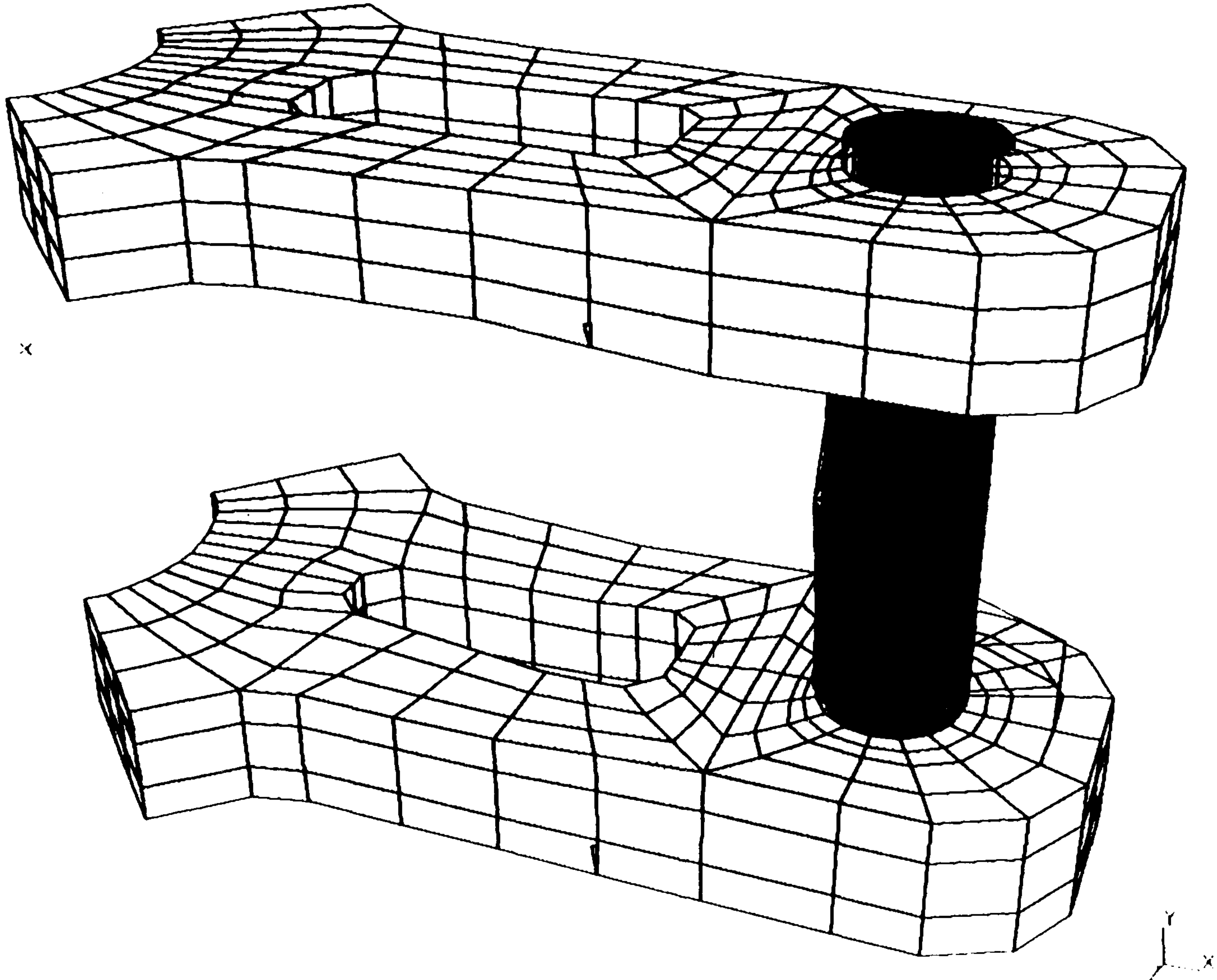

Deformed Geometry Due to Centrifugal Force, Flapping and Lead-Lag Bending

MBB Helicopter Division

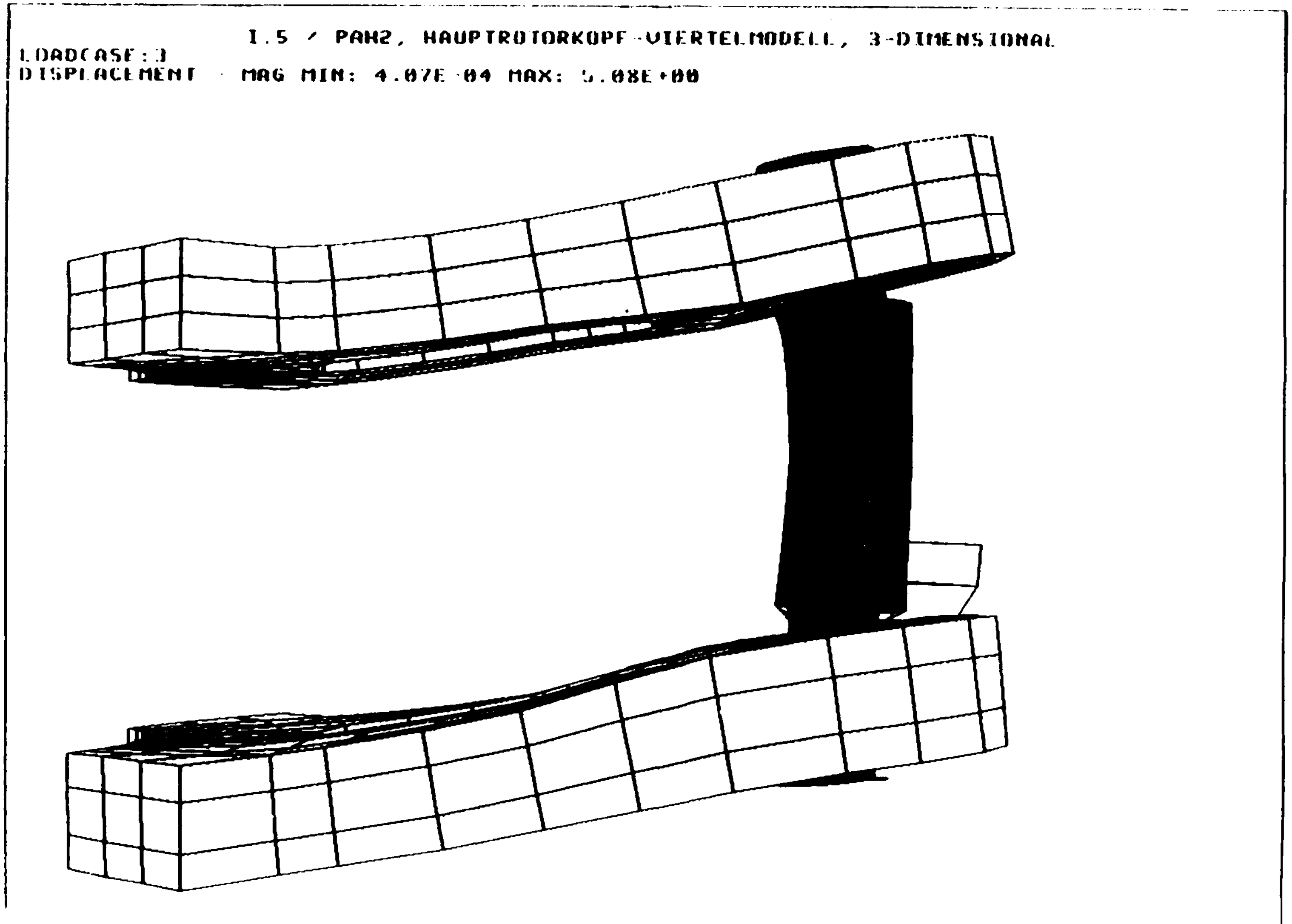

Stress Distribution / Bottom Hubplate

MBB Helicopter Division

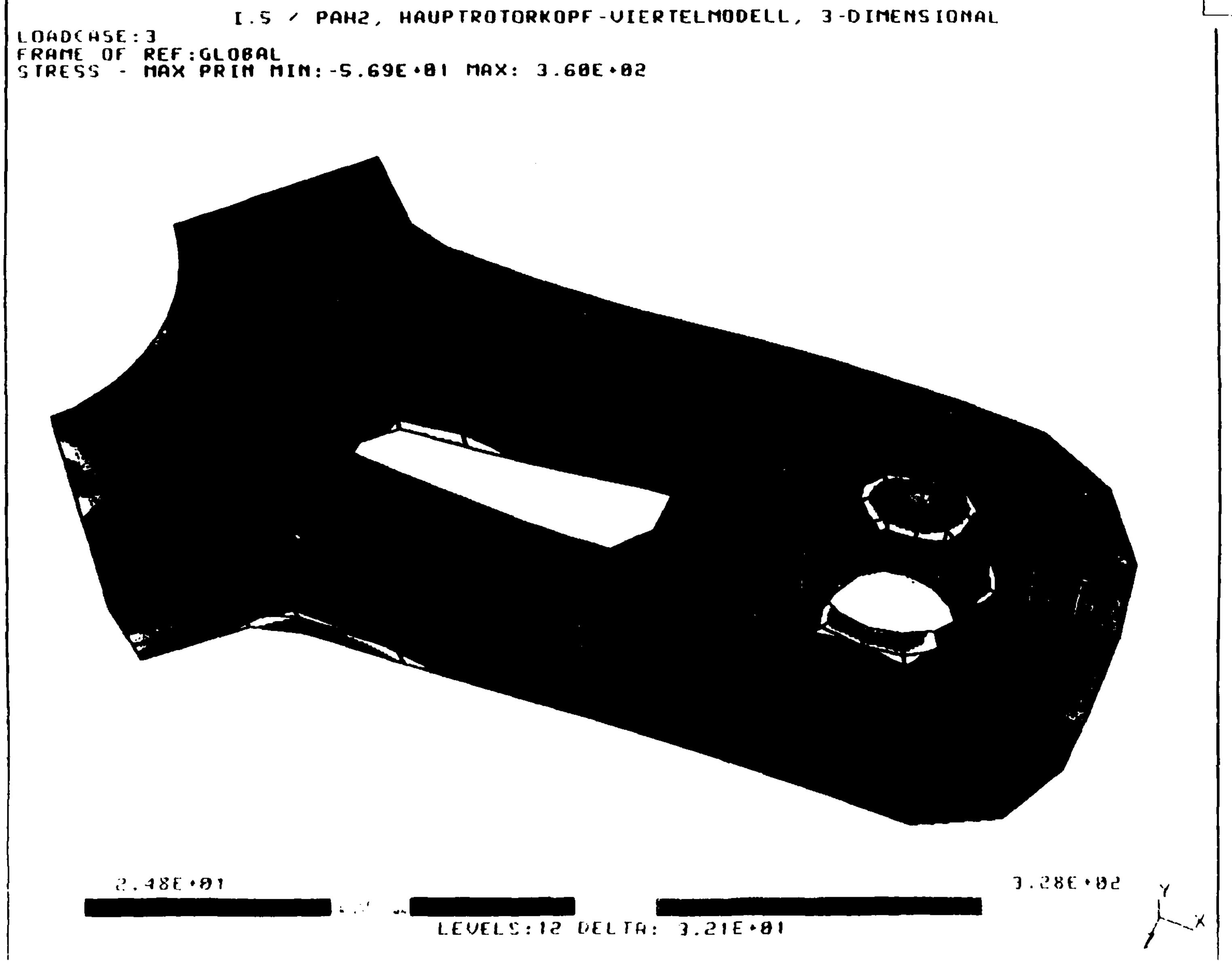

Comparison of Stress Distribution in Top and Bottom Hubplate

MBB Helicopter Division

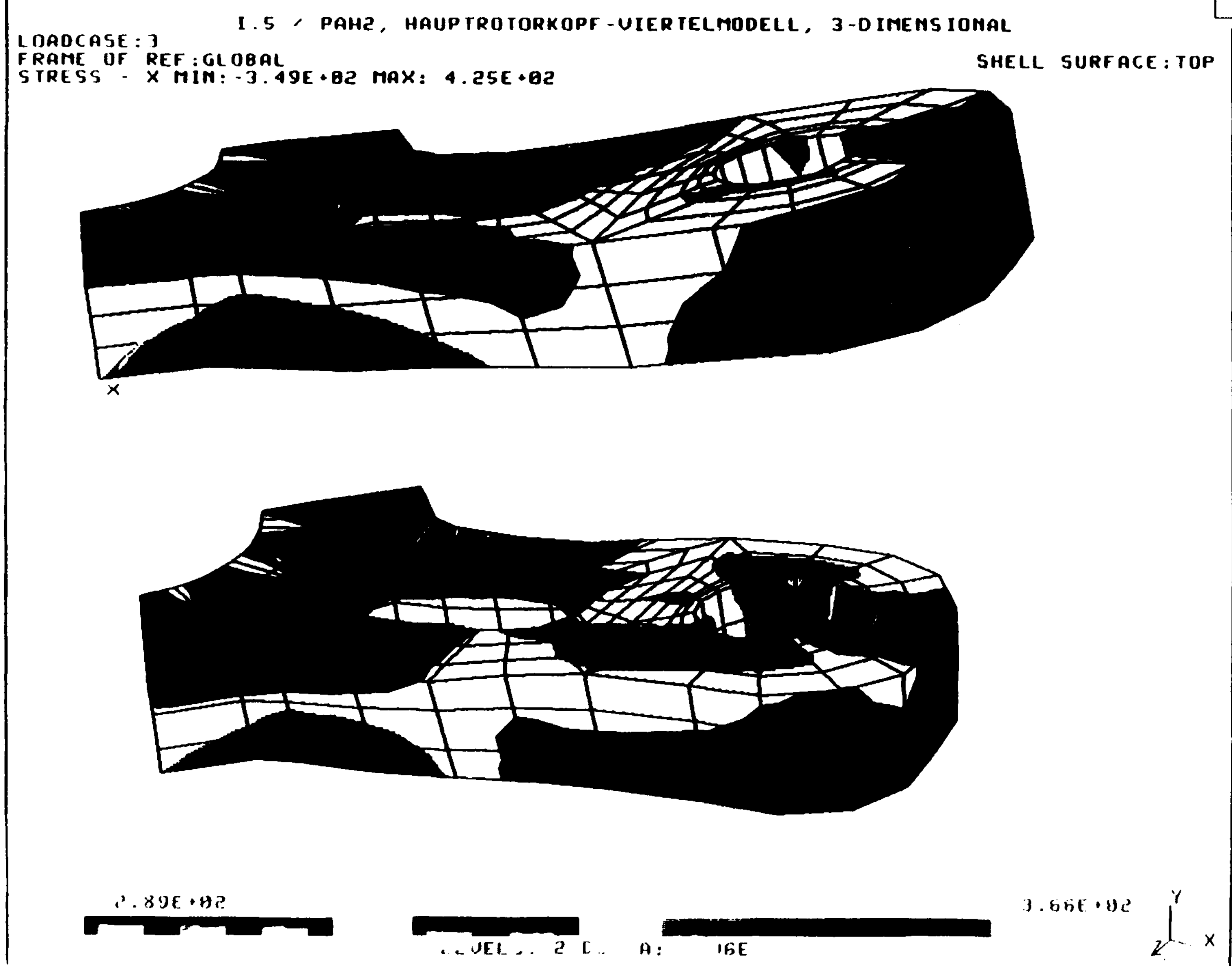

Weight Reduction of Different Configurations

MBB Helicopter Division

Rotor Hub Plate Configuration	Deformation in Centrifugal Force Fitting [mm]	Weight Reduction of Hub Plates [%]
Basic Version Top + Bottom Plate Same Thickness	3.2	0
20% Thickness Reduction of Top Plate 10% Thickness Reduction of Bottom Plate	4.2	-14.
Large Cutout Without Thickness Reduction	4.3	-24.
Small Cutout 20% Thickness Reduction of Top Plate 10% Thickness Reduction of Bottom Plate	4.9	-24.

CFC Test Specimens

MBB Helicopter Division

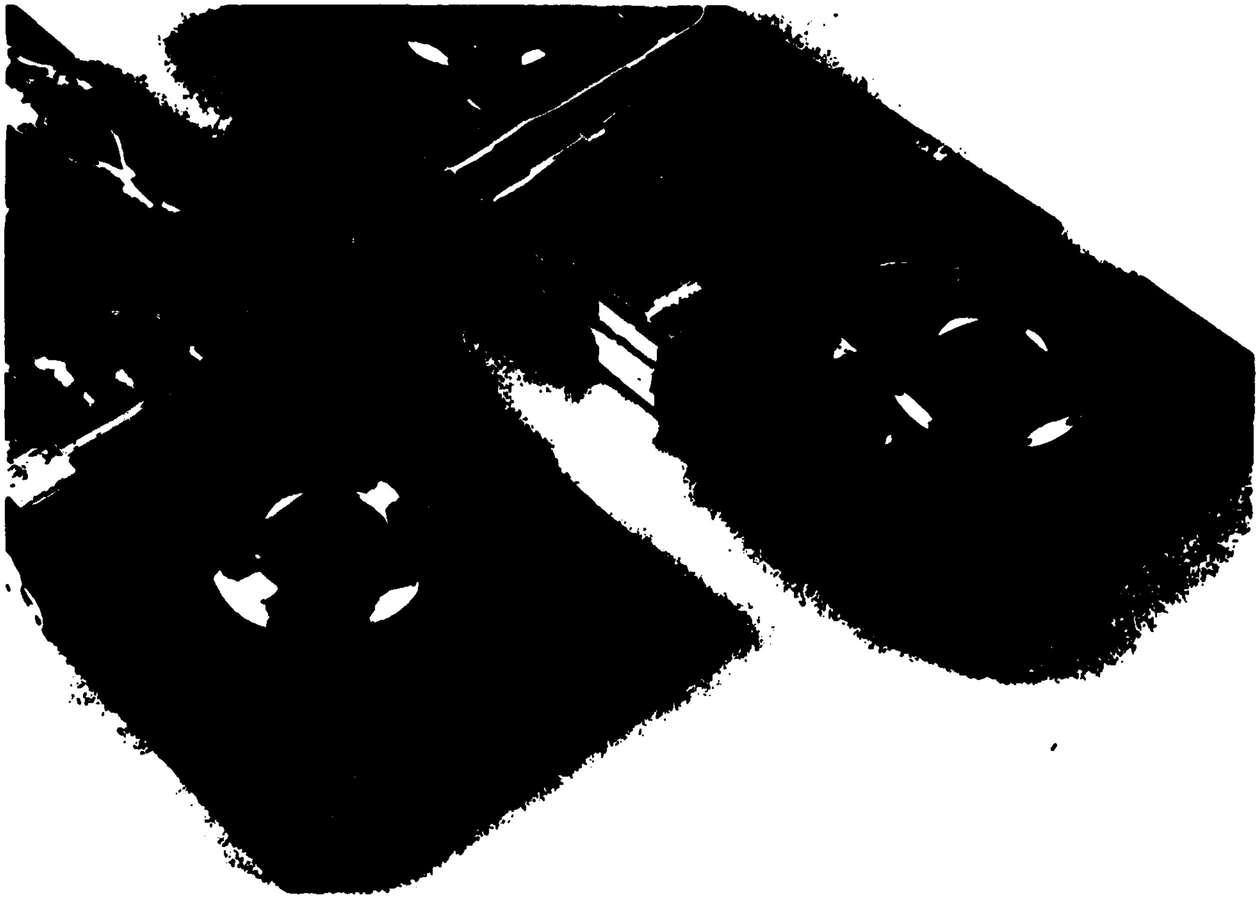

Rupture Due to Dynamic Loading R=0.11

Dynamic Strength of the Test Specimens

MBB Helicopter Division

- Low Decrease of the Strength Versus Load Cycles

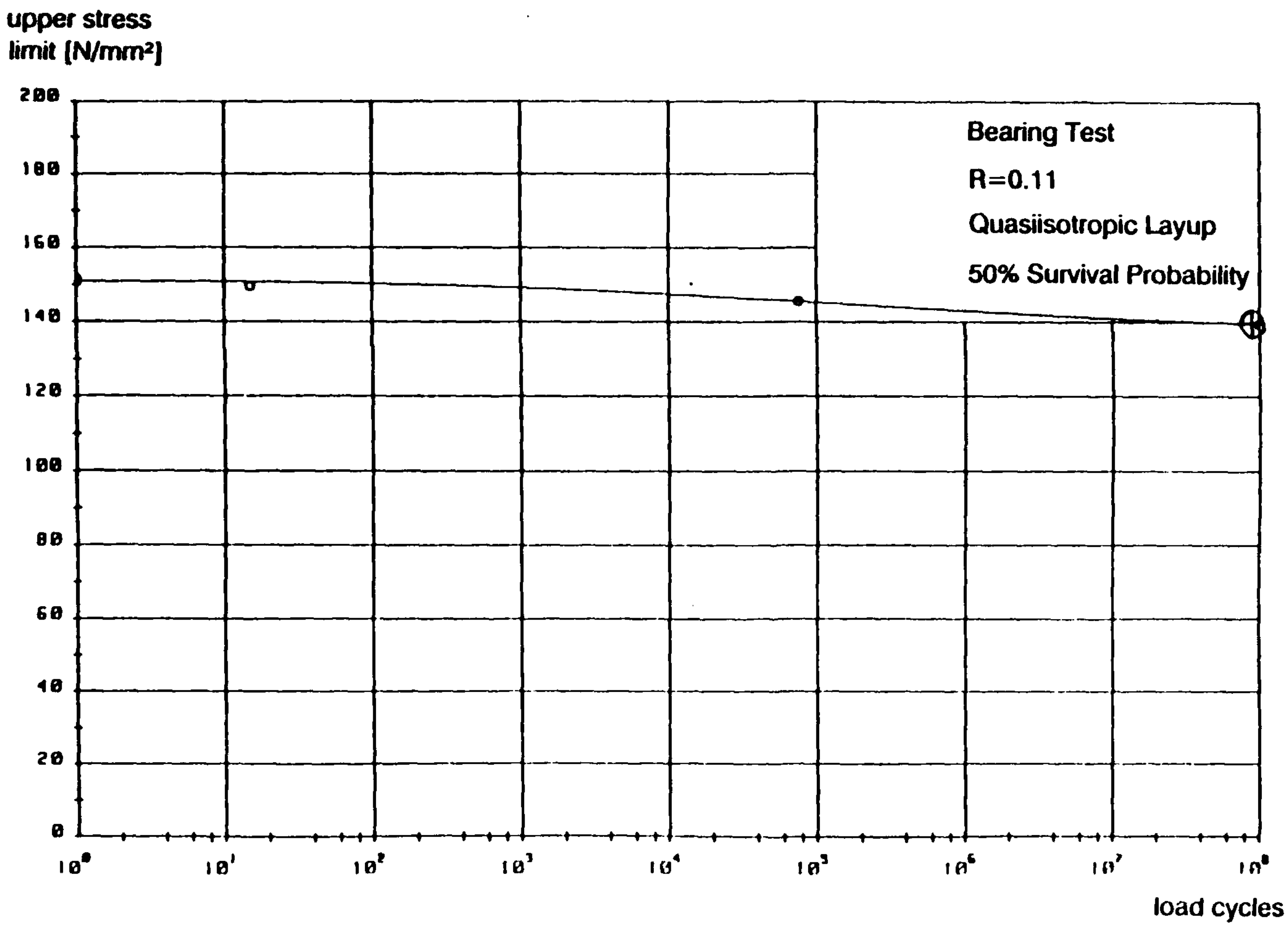

Shear Stress Distribution in Isotropic Beam Cross Sections Due to Transverse Forces

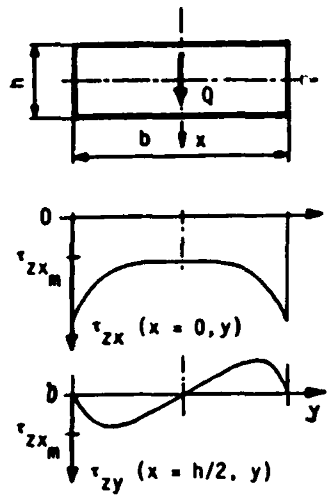

$\tau_{zx_{max}}$ $(x=0,\ y=\pm\ b/2)$

$\tau_{zy_{max}}$ $(x=\pm\ h/2,\ y)$

$\tau_{zx_m} = \frac{Q}{b \cdot h}$

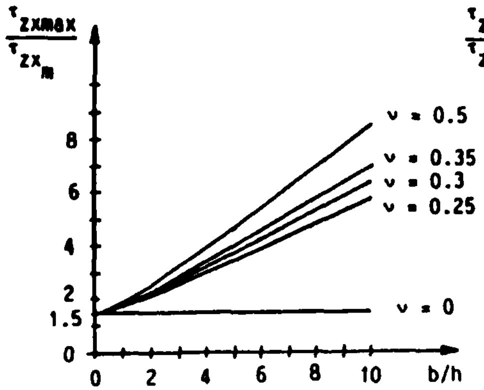

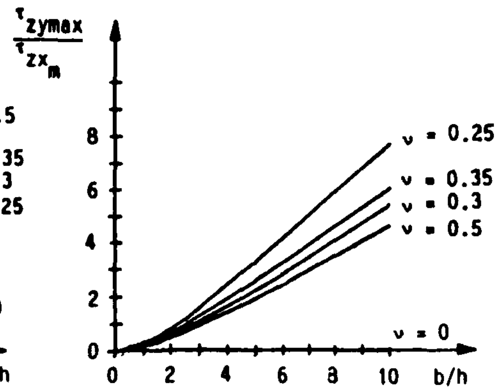

Shear Stress Reduction with Chamfer Rotor Hub Plates

MBB Helicopter Division

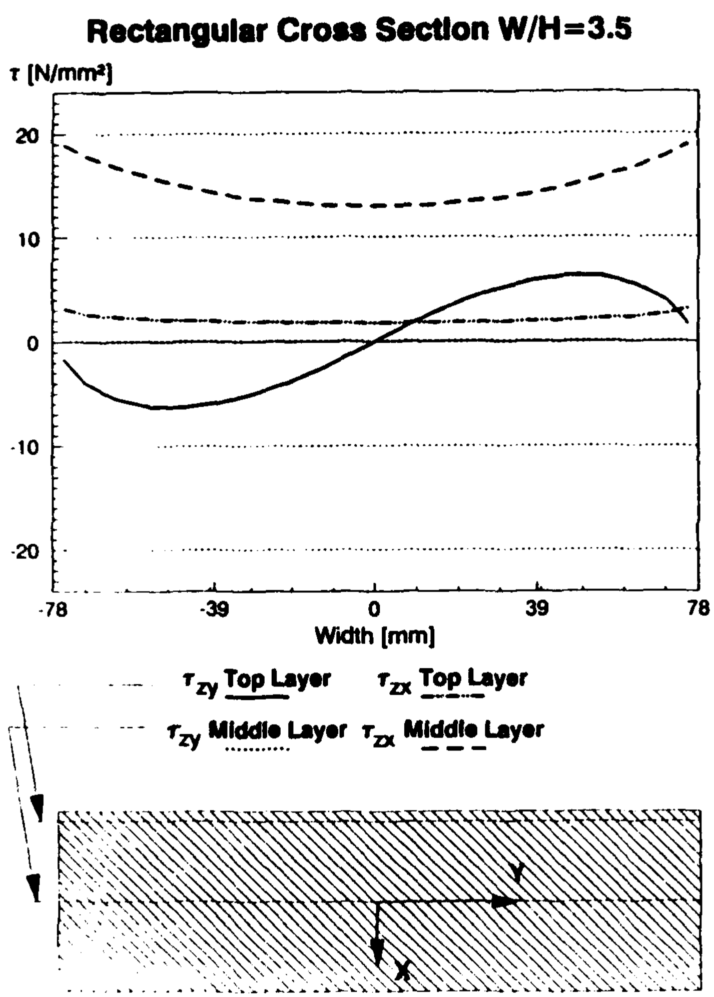

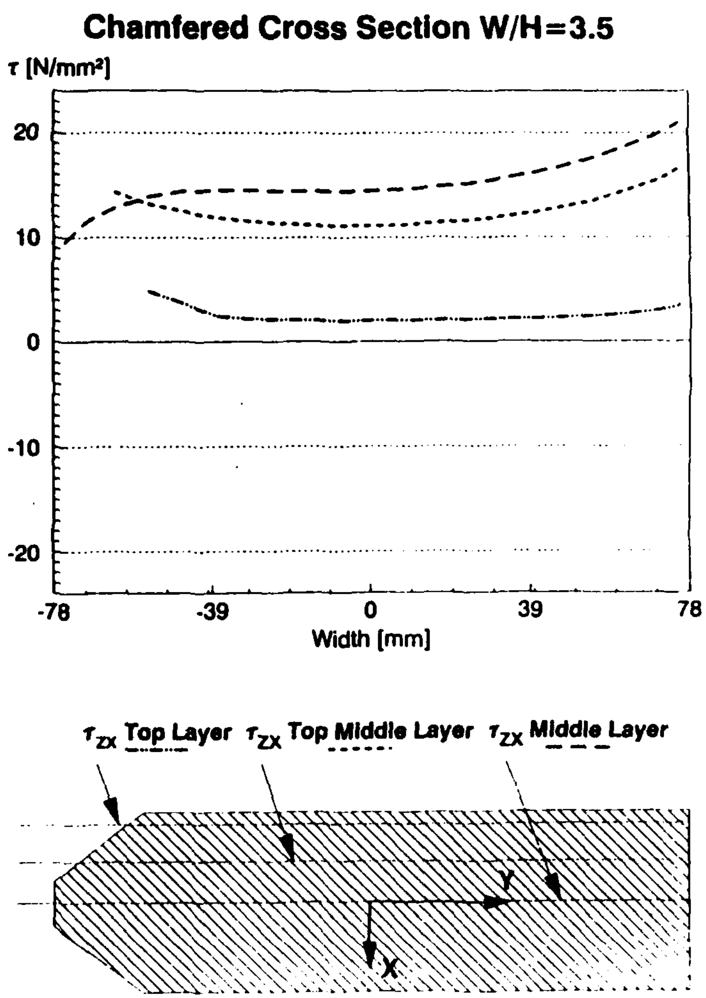

FEL Rotor Hub in Test Rig

MBB Helicopter Division

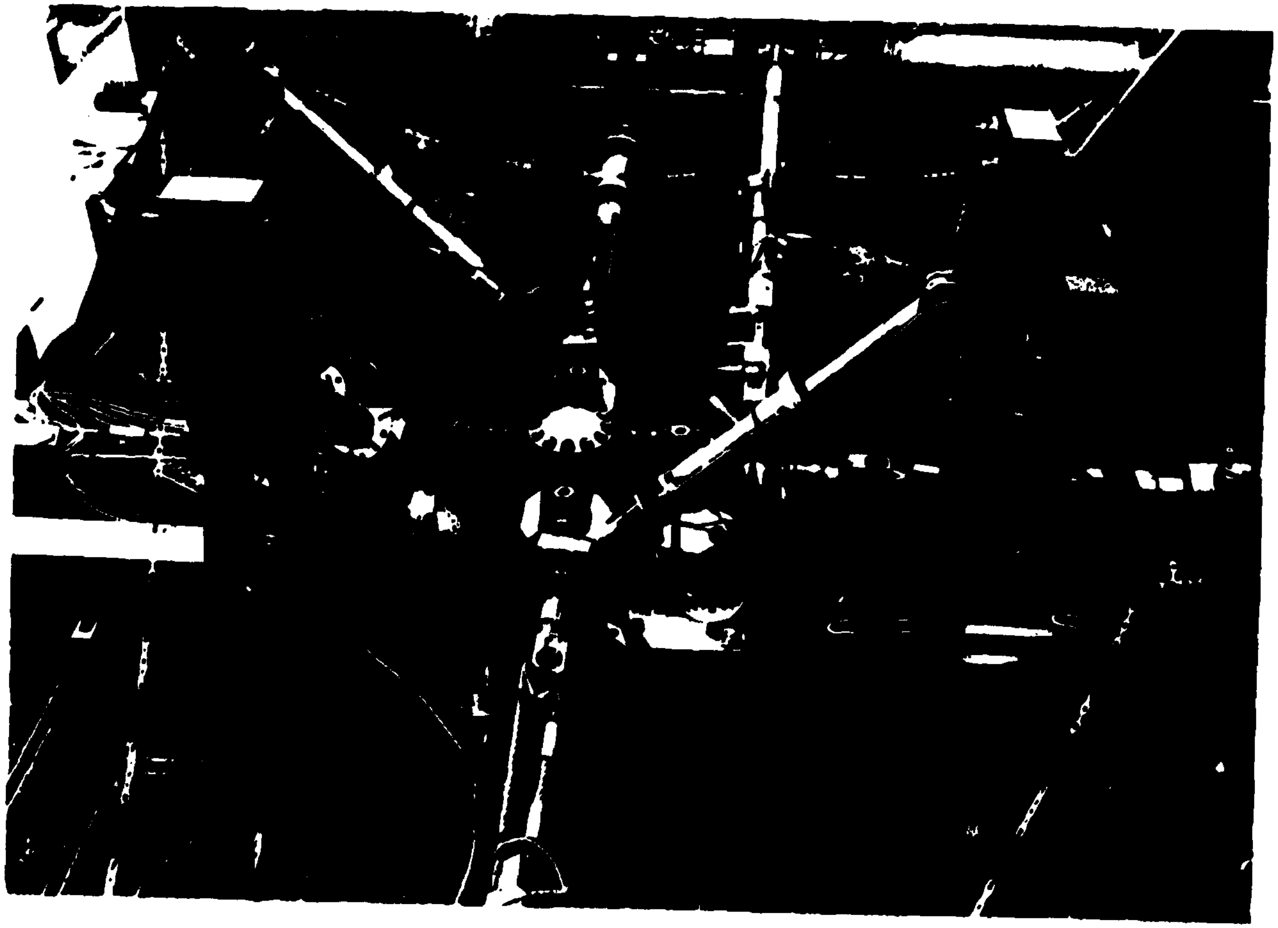

CFC Rotor Hub Under Combined Loads

Stress Analysis of Composite Rotor Blades

Marco Borri   Gianluca Ghiringhelli

Dipartimento di Ingegneria Aerospaziale
Politecnico di Milano - Milano - ITALY

Abstract

The design of Composite Rotor Blades requires the analysis of tridimensional stress states including interlaminar stresses.

Despite the powerfulness of modern computers, standard tridimensional finite elements approximations of the entire rotor blade are not yet considered feasible, because of the high degree of accuracy required in the material properties of the blade cross section. As a consequence, the problem is generally formulated in two different consecutive steps. The first step considers the stress analysis of the blade cross section. This is modeled as a two dimensional continuum, and the following analyses are performed:

- Eigensolution analysis of self equilibrated modes and of the diffusion lenghts
- Particular solutions under prescribed stress resultants

The second step is mainly devoted to the dynamical behavior of the entire blade. Here the blade is usually considered as a one dimensional continuum. Under this approximation, in general, the following computations are performed;

- Trim solution under steady flight conditions
- Linear stability analysis of Floquet's type

The subdivision of the problem into two steps is equivalent to the metod of separation of variables first proposed by De S.Venant which, as it is well known, is exact only for slender, straight and untwisted beams under applied loads to the edges, but it is also applicable to curved, twisted and swept

beams undergoing small strains. The present discussion focuses on the cross section analysis. This is usefull even if the overall behavior of the beam is geometrically non linear, as it happens in helicopter baldes.

In our formalism we take into account the effects of built in twist, curvature and swept so that geometrical coupling of tension and torsion can be also accounted for. Since in composite helicopter rotor blades the inplane and out of plane warping can strongly influence the stress distribution, we start from the two dimensional Finite Element idealization of the cross section of the blade while an exact integration along the beam axis is performed.

The program developed can supply the following outputs:

- Mass and stiffness matrices with due consideration of all possible couplings e.g. bending-torsion, torsion-tension, shear-tension, that can be achieved with any kind of anisotropic materials.
- All the components of the stress and strain tensors under prescribed forces and moments resultant in the usual beam sense, i.e. discarding the boundary perturbations.
- Eingensolutions in terms of displacement and diffusion length.

As far as materials are concerned, the program can take into account every kind of nonhmogeneity and anisotropy, and it may also be considered as an advanced and easy-to-use tool for isotropic beam analysis. The effectiveness of this approach mainly resides on the fact that discretization occours on the cross section only. For instance, an idealization by 500-1000 degrees of freedom of the section leads to a problem of small size; however it enables the performance of a detailed analysis that three dimensional schemes would make extremely expensive and practically unfeasible in the preliminary design phases. As a matter of fact, the program has already been employed also as an analysis modulus in optimization processes for composite blade sections.

Some experimental test performed on straight composite blade specimens had shown a good correlation wiht the numerical results.

Comparison with three dimensional analysis in the case of twisted and curved beams showed the formidable effectiveness of the present approach.

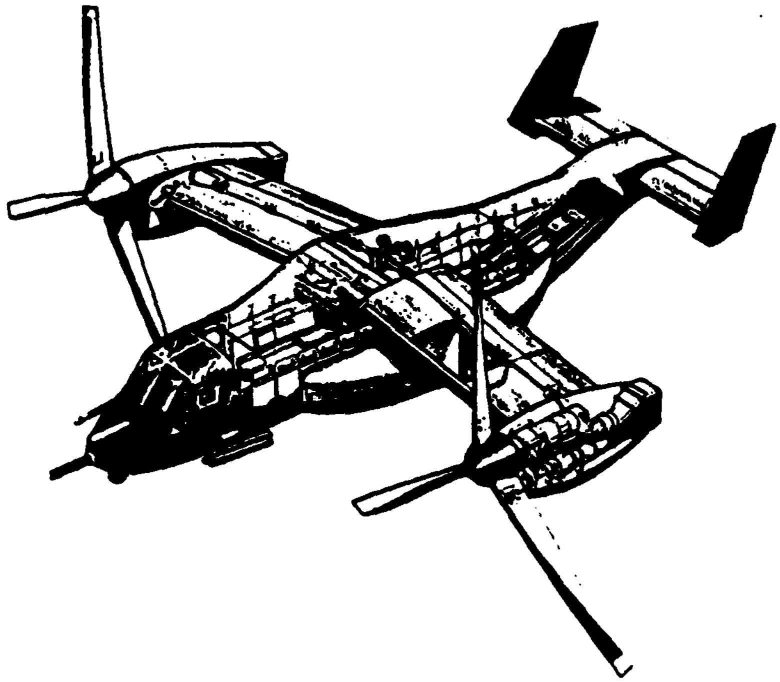

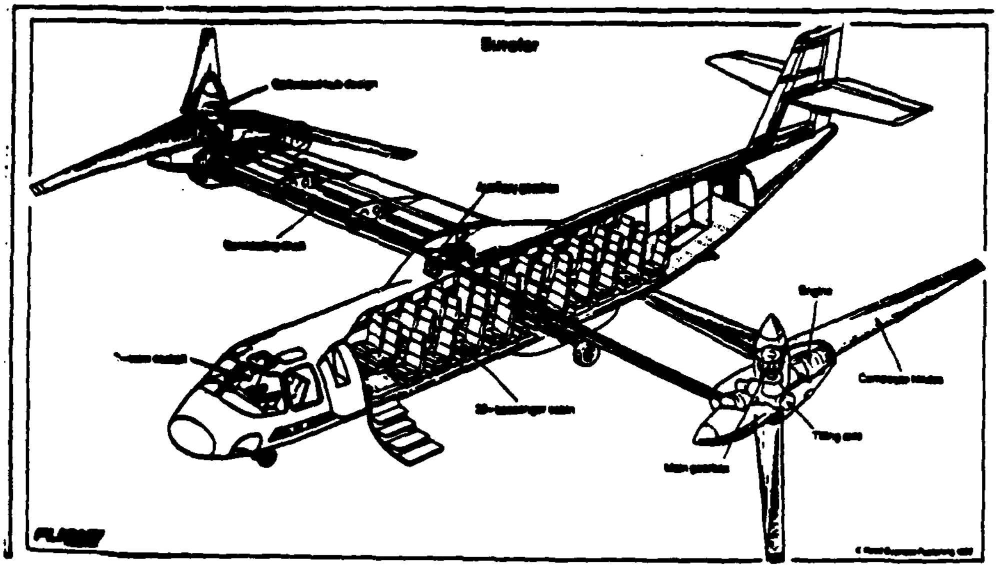

Twisted and Curved Beams Geometry

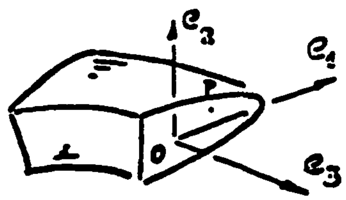

$O = O(y)$

$P - O = y^1 e_1 + y^2 e_2$

- y^1, y^2 cartesian coordinates on the cross section
- $y = y^3$ curvilinear abscissa of the reference line
- $e = e_3 = e_1 \times e_2$ unit normal to the cross section
- $\dfrac{\partial O}{\partial y} = \tau$ unit tangent to the reference line
- $\dfrac{\partial e_p}{\partial y} = k \times e_p$ $\quad k$ curvature and twist vector

In general $e \neq \tau$ (swept beam)

- Cross section components of a Tensor

$$v = v_p e_p \qquad v_p = v \cdot e_p$$

$$T = e_p T_{pq} e_q \qquad T_{pq} = e_p \cdot T \cdot e_q$$

- Corotational derivative of a Tensor

$$\frac{\partial^* v}{\partial y} = e_p \frac{\partial v_p}{\partial y} = \frac{\partial v}{\partial y} - k \times v$$

$$\frac{\partial^* T}{\partial y} = e_p \frac{\partial T_{pq}}{\partial y} e_q = \frac{\partial T}{\partial y} - k \times I \cdot T + T \cdot k \times I$$

Metric Tensor

$$dP = g_1\,dy^1 + g_2\,dy^2 + g_3\,dy^3$$

- g_k Covariant basis vectors

$$g_1 = e_1 \qquad g_2 = e_2 \qquad g_3 = \tau + k \times (P - O)$$

$$\sqrt{g} = g_1 \times g_2 \cdot g_3 = e_1 \times e_2 \cdot g_3 = e_3 \cdot g_3$$

Volume element $dv = \sqrt{g}\,dy^1 dy^2 dy^3$

- g^k Contravariant basis vectors

$$g^1 = g_2 \times g_3/\sqrt{g} \qquad g^2 = g_3 \times g_1/\sqrt{g} \qquad g^3 = g_1 \times g_2/\sqrt{g}$$

$$\underset{p}{g_k} = g_k \cdot e_p = \begin{bmatrix} 1 & 0 & \underset{1}{g_3} \\ 0 & 1 & \underset{2}{g_3} \\ 0 & 0 & \underset{3}{g_3} \end{bmatrix}$$

$$\underset{1}{g_3} = \tau_1 - k_3 y^2$$

$$\underset{2}{g_3} = \tau_2 + k_3 y^1$$

$$\underset{3}{g_3} = \tau_3 + k_1 y^2 - k_2 y^3 = \sqrt{g}$$

$$\underset{p}{g^k} = g^k \cdot e_p = \frac{1}{\sqrt{g}} \begin{bmatrix} \sqrt{g} & 0 & 0 \\ 0 & \sqrt{g} & 0 \\ -\underset{1}{g_3} & -\underset{2}{g_3} & 1 \end{bmatrix}$$

Cross section Components vs Tensorial Components

$$v = v^k g_k = v_k g^k = \underset{p}{v} e_p$$

$$\underset{p}{v} = \underset{p}{g}^k v_k = \underset{p}{g}_k v^k$$

$$\mathbf{T} = e_p \underset{pq}{T} e_q = T_{ik} g^i g^k \quad \text{etc...}$$

$$\underset{pq}{T} = T_{ik} \underset{p}{g}^i \underset{q}{g}^k \quad \text{etc...}$$

$$\underset{pq}{v} = v_{ik} \underset{p}{g}^i \underset{q}{g}^k = \underset{p}{e} \cdot \frac{\partial v}{\partial y^k} \underset{q}{g}^k = e_p \cdot \frac{\partial v}{\partial e_q} = \nabla_{e_q} v \cdot e_p$$

- $\underset{pq}{v}$ are the components with respect to the c.s. basis vectors of the covariant derivative along the basis vectors itself

$$\underset{p\kappa}{v} = \frac{\partial \underset{p}{v}}{\partial y^\kappa} \qquad \kappa = 1,2$$

$$\underset{p3}{v} = \nabla_e v \cdot \underset{p}{e} = \underset{p}{e} \cdot \frac{\partial v}{\partial e} = \underset{3}{g}^k \frac{\partial \underset{p}{v}}{\partial y^k} + \underset{3}{g}^3 K \times v \cdot \underset{p}{e}$$

- Covariant derivative along the normal to the cross section

$$\nabla_e v = e \cdot \nabla v = \underset{3}{g}^k \frac{\partial v}{\partial y^k} + \underset{3}{g}^3 K \times v$$

Virtual Work Principle for a Beam Slice

$dA = dy^1 dy^2$

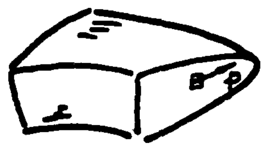

$$\frac{\partial}{\partial y}\int_A p \cdot \delta s \, dA = \int_A \sigma : \delta\varepsilon \sqrt{g}\, dA$$

p cross section traction

σ stress tensor 6 components

ε strain tensor 6 components

δs virtual displacement

$$T = \int_A p \, dA$$ stress resultant

$$M = \int_A (P-O) \times p \, dA$$ stress moment resultant

Referring to the cross section basis vectors

$$\frac{\partial}{\partial y}\int_A p^q \, \delta s_q \, dA = \int_A \sigma^{pq} \, \delta\varepsilon_{pq} \sqrt{g}\, dA$$

$$\delta\varepsilon_{pq} = \delta s_{p|q} + \delta s_{q|p}$$

Finite Elements Approximation

- $\dfrac{\partial}{\partial y}\displaystyle\int_A \delta s \cdot p \, dA = \int \delta \varepsilon : \sigma \sqrt{g}\, dA$

  $\sigma = D\varepsilon$

- $s = N(y^1, y^2)\, U \qquad s' = N(y^1, y^2)\, U' \qquad (\ )' = \dfrac{\partial}{\partial y}$

  $\varepsilon = \beta(y^1, y^2)\, U' + \beta(y^1, y^2)\, U$

$$\begin{Bmatrix} \delta U' \\ \delta U \end{Bmatrix}^T \begin{Bmatrix} P \\ P' \end{Bmatrix} = \begin{bmatrix} \delta U' \\ \delta U \end{bmatrix}^T \begin{bmatrix} M & C^T \\ C & E \end{bmatrix} \begin{Bmatrix} U' \\ U \end{Bmatrix}$$

$$P = \int_A N^T p \, dA \qquad P' = \frac{\partial}{\partial y} \int_A N^T p \, dA$$

$$M = \int_A \beta^T D \beta \sqrt{g}\, dA, \quad C = \int_A \beta^T D \beta \sqrt{g}\, dA, \quad E = \int_A \beta^T D \beta \sqrt{g}\, dA$$

$$\begin{Bmatrix} P \\ P' \end{Bmatrix} = \begin{bmatrix} M & C^T \\ C & E \end{bmatrix} \begin{Bmatrix} U' \\ U \end{Bmatrix}$$ FIRST ORDER EQUILIBRIUM EQUATION

or:

$$MU'' + (C^T - C)U' + EU = 0$$ SECOND ORDER EQUILIBRIUM EQUATION

Symmetric skewsymmetric Symmetric

- Eigenanalysis
  - Eigenvalue — diffusion length
  - Eigenvectors — Self equilibrated modes

Particular solution under prescribed stress resultant

- Equilibrated stress resultants

$$\frac{\partial^*}{\partial y} T + K \times T = 0 \qquad T = \int p \, dA$$

$$\frac{\partial^*}{\partial y} M + K \times M + \tau \times T = 0 \qquad M = \int (P-O) \times p \, dA$$

- Displacement resolution

$s = u + \varphi \times (P-O) + w$ — 6 times Redundant

$u = u(y)$ — Rigid translation of the cross section

$\varphi = \varphi(y)$ — Rigid rotation of the cross section

$w = w(y^1, y^2, y^3)$ — 3D warping of the cross section

- Appropriate definition of the warping

$$\int w \cdot p \, dA = 0 \qquad w \text{ true warping}$$

- Internal virtual work in terms of stress resultants only

$$\int \delta \varepsilon : \sigma \sqrt{g} \, dA = \delta\left(\frac{\partial u}{\partial y} + \tau \times \varphi\right) \cdot T + \delta \frac{\partial \varphi}{\partial y} \cdot M$$

$\frac{\partial u}{\partial y} + \tau \times \varphi$ — Linear cross section strain

$\frac{\partial \varphi}{\partial y}$ — Angular cross section strain

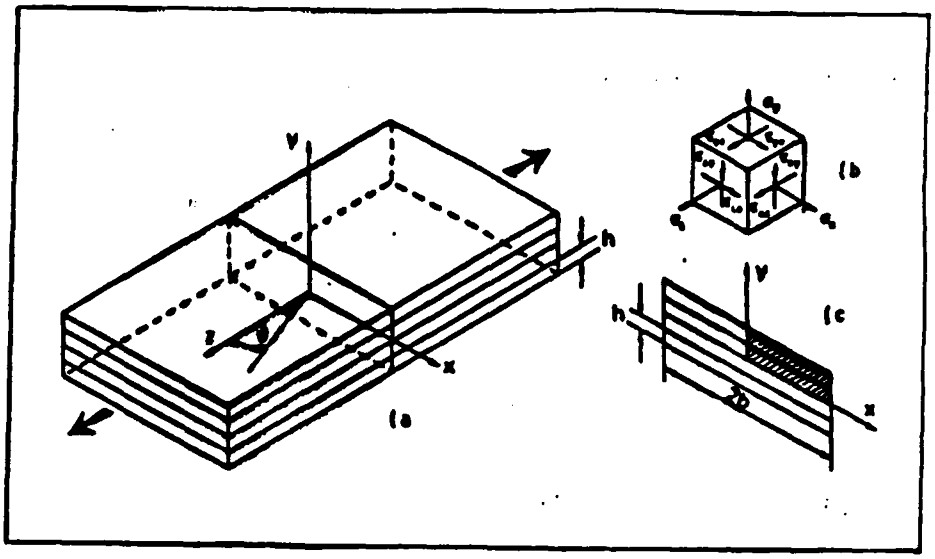

Fig. 2. a) Four plies laminate configuration; b) 3-D Stress components; c) a z = constant plane.

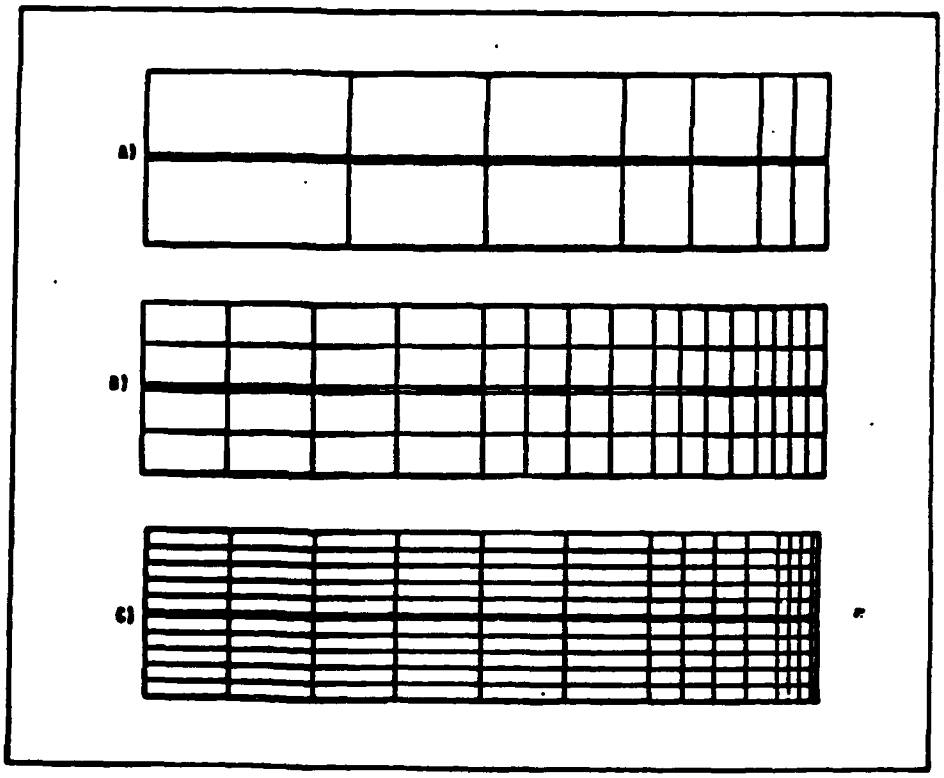

Fig. 3. A) Coarse mesh; B) Medium mesh; C) Fine mesh.

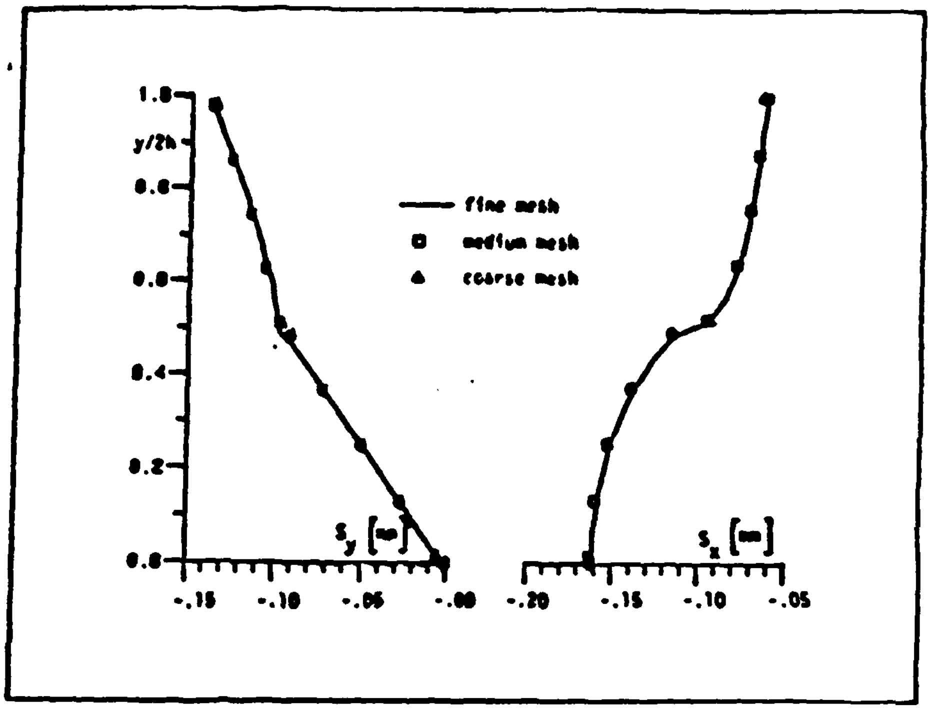

Fig. 5. Significant warping components s_x and s_y.

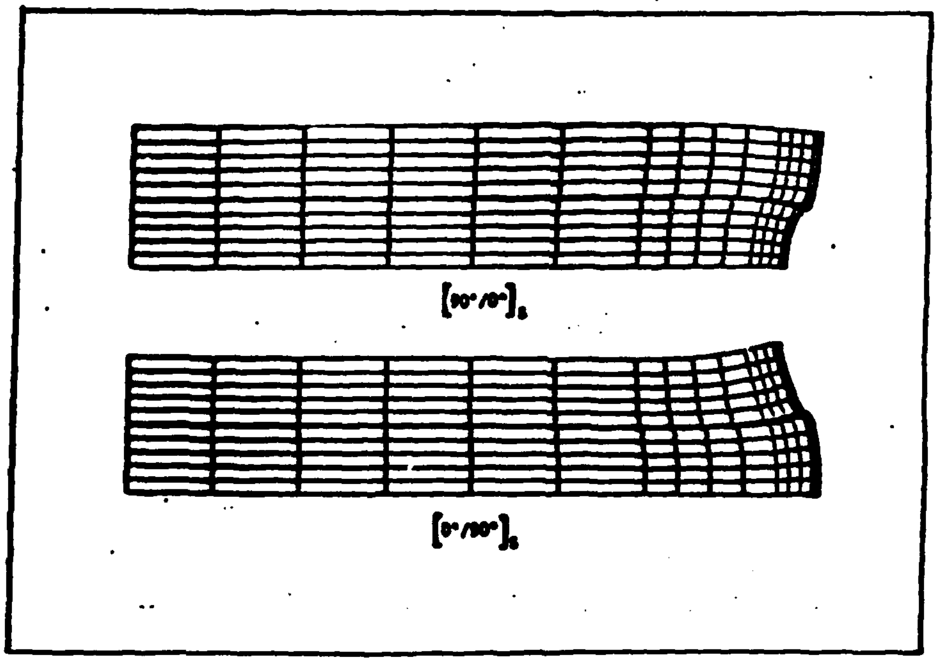

Fig. 6. Fine mesh deformed shapes.

11

ESEMPI DI APPLICAZIONE

TRAVE A SEZIONE QUADRATA
DIMENSIONI DELLA SEZIONE 120x120 mm

TRAVE CURVA

RAGGIO DI CURVATURA 200 mm
LUNGHEZZA 200x3.14 mm

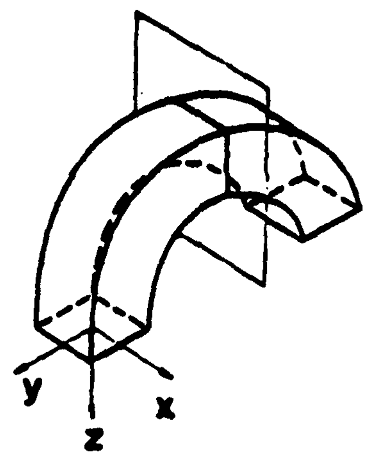

TRAVE SVERGOLA

ROTAZIONE ESTREMITA' 180°
LUNGHEZZA 628.3 mm

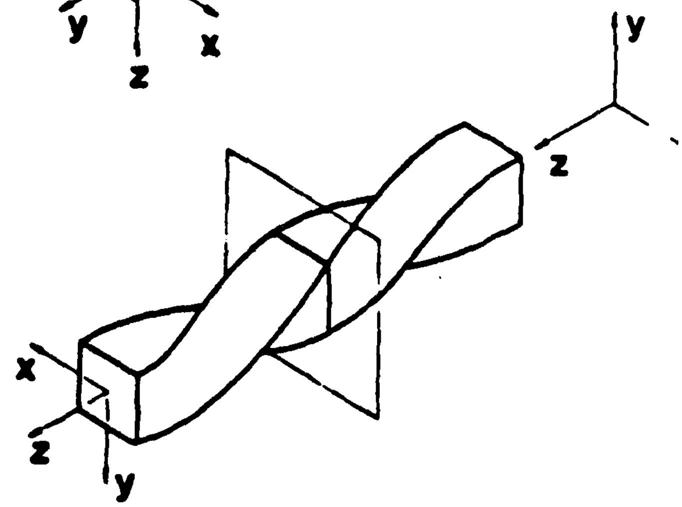

CONDIZIONI DI CARICO

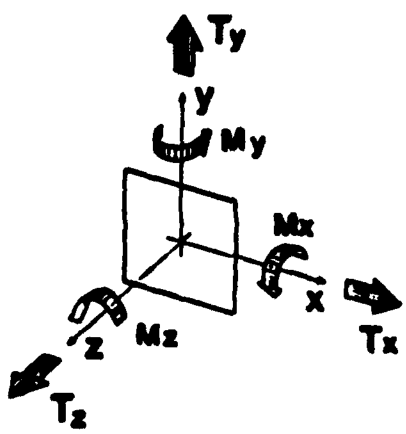

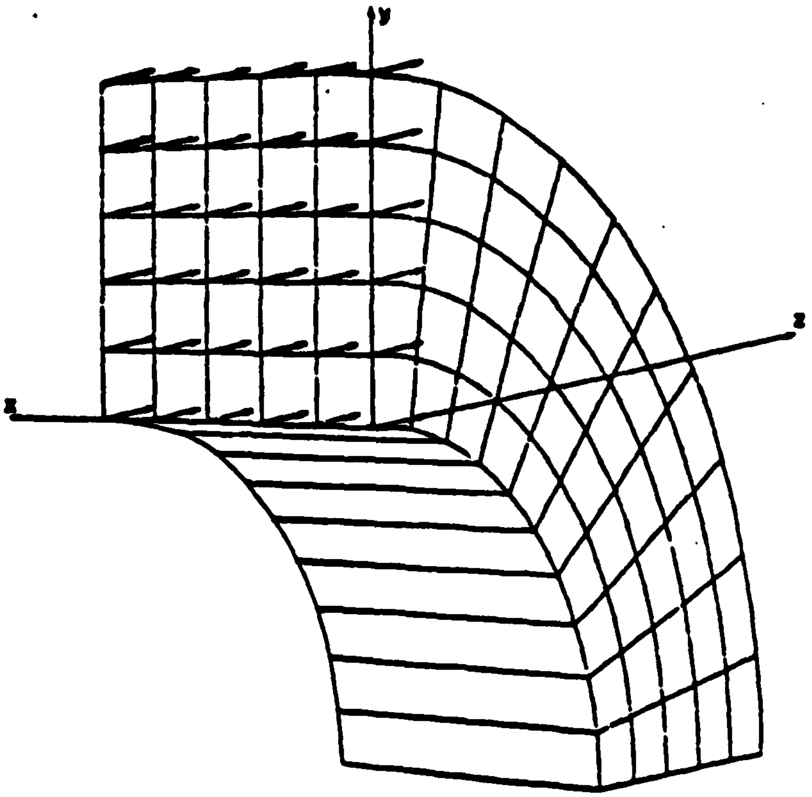

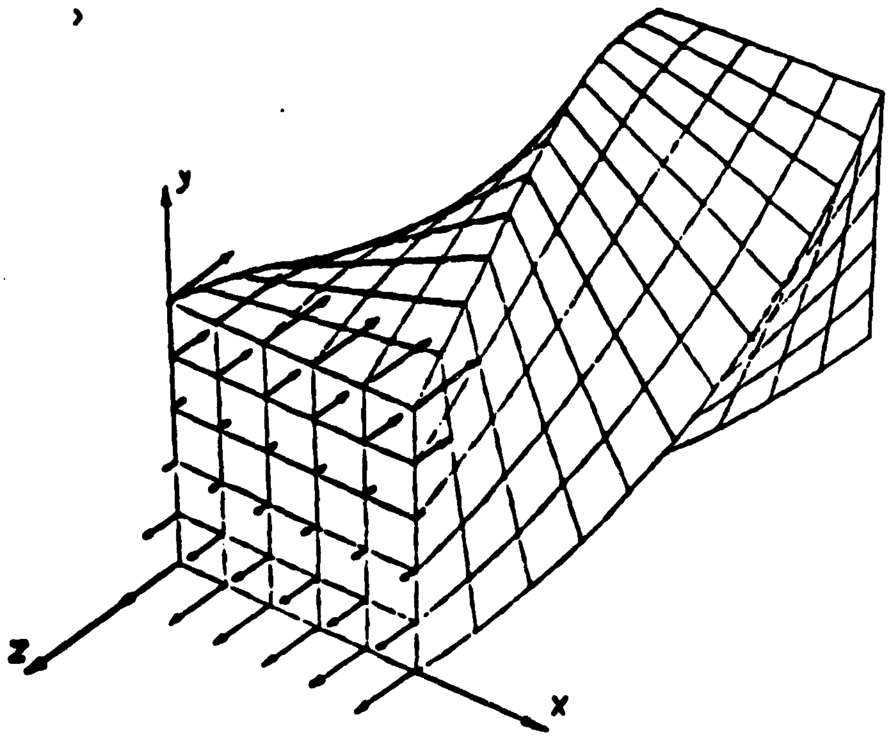

SCHEMA AD ELEMENTI FINITI TRI-DIMENSIONALE
PER ANALISI DI CONFRONTO

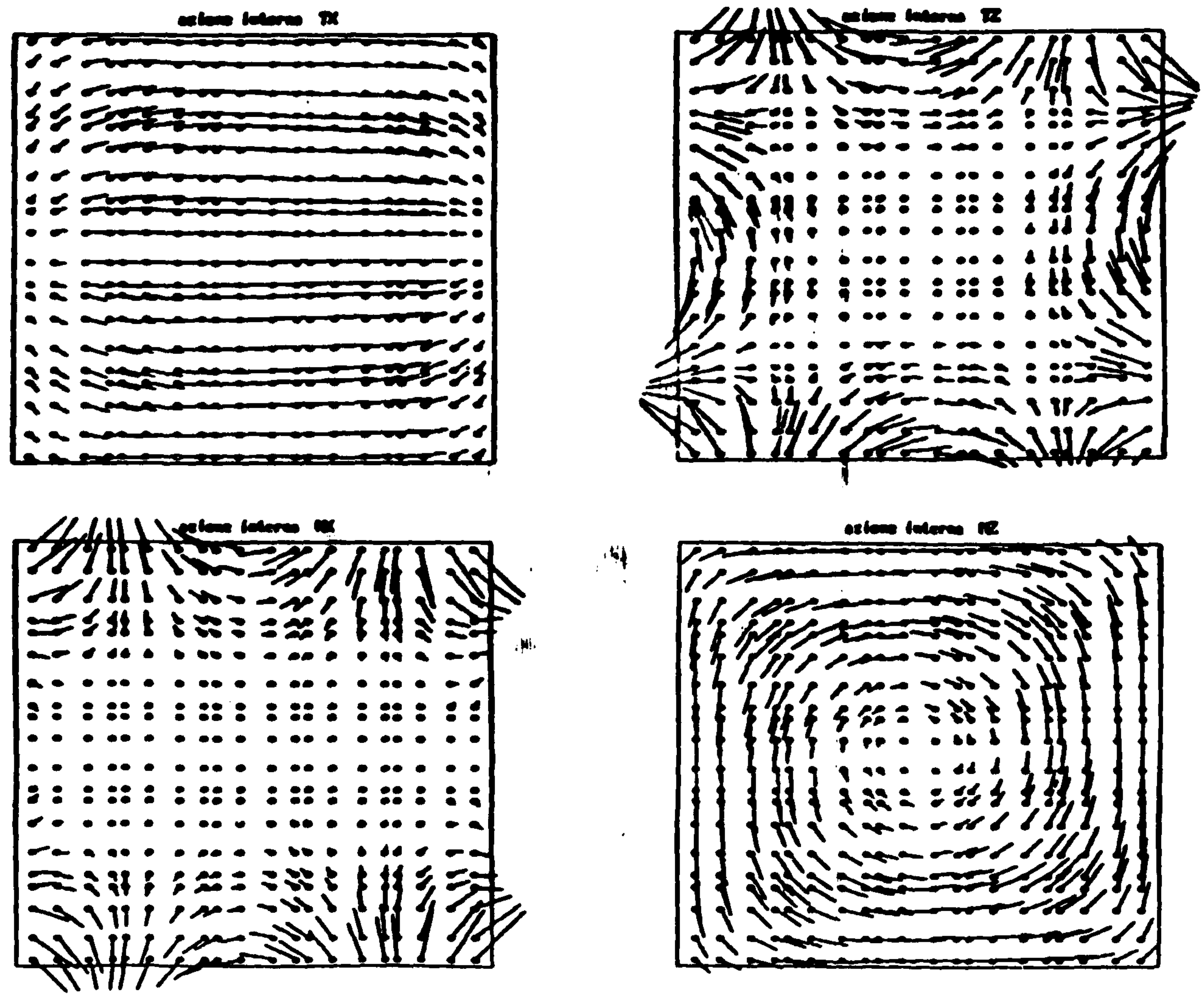

DISTRIBUZIONE DELLA τ NEL PIANO SEZIONE DELLA TRAVE SVERGOLA

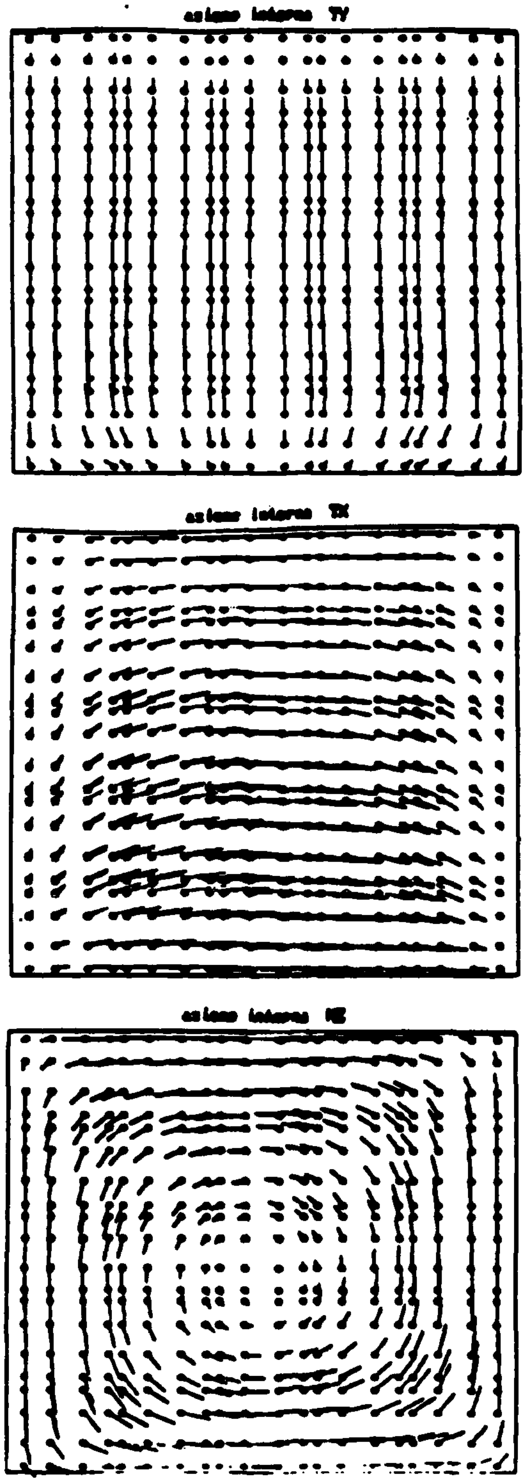

DISTRIBUZIONE DELLA τ NEL PIANO

SEZIONE DELLA TRAVE CURVA

SESSION II

COMPOSITE STRUCTURAL DESIGN

Paul A. Lagace
Massachusetts Institute of Technology
Chairman

"Composite Challenges on the V-22"

M. Keith Stevenson

Bell Helicopter, Fort Worth, Texas

ARO-AHS-RPI 2nd International Workshop on
COMPOSITE MATERIALS AND STRUCTURES
FOR ROTORCRAFT

September 14 and 15, 1989

Rensselaer Polytechnic Institute
Troy, New York

UNAVAILABLE PRIOR TO PRESENTATION

ANALYSIS AND DESIGN OF CURVED COMPOSITE BEAMS

ARO-AHS-RPI WORKSHOP ON
COMPOSITE MATERIALS AND
STRUCTURES FOR ROTORCRAFT
TROY,NY

September 14–15, 1989

O.A. BAUCHAU

A.W. PECK

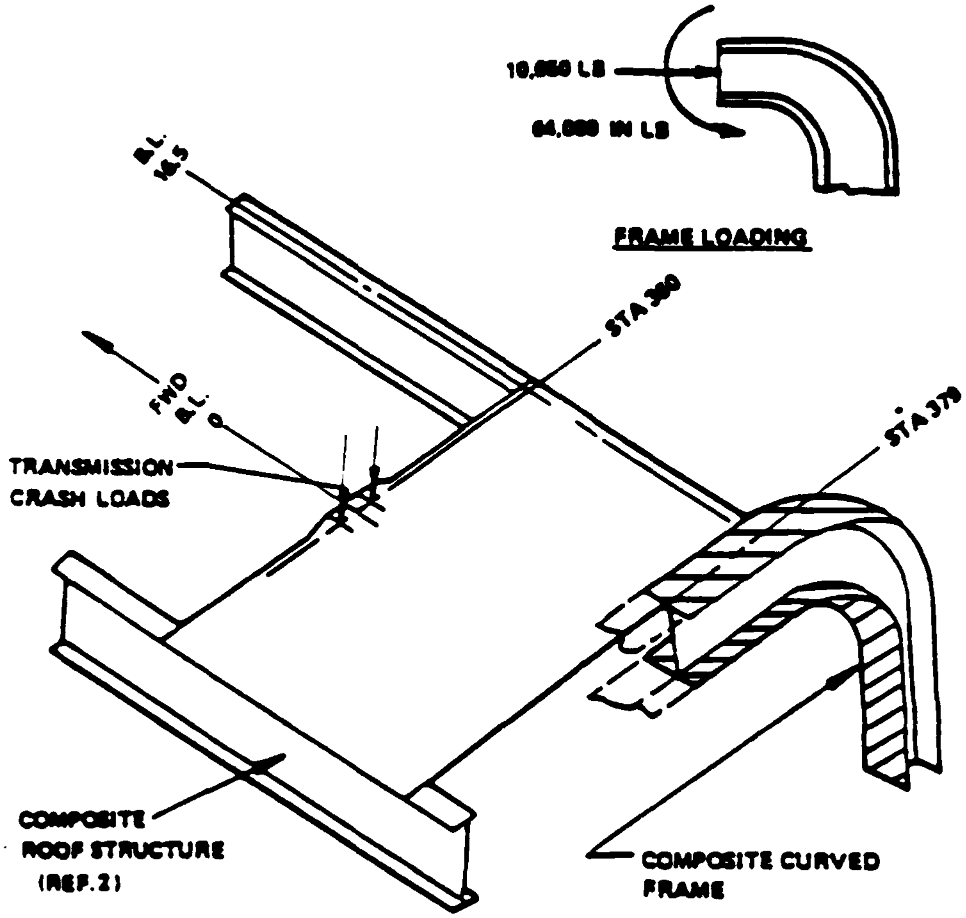

Figure 1. Composite Curved Frame Selected from BLACK HAWK Cabin Fuselage

Design of Straight and Curved I-Beams

STRAIGHT I-BEAM

- The web carries the shear force (shear stresses)

- The flanges carry the bending moment (axial stresses)

CURVED I-BEAM

- The web must carry the shear force (shear stresses) AND resist the crushing stresses

- The flanges must carry the bending moment (axial stresses) AND the curling stresses

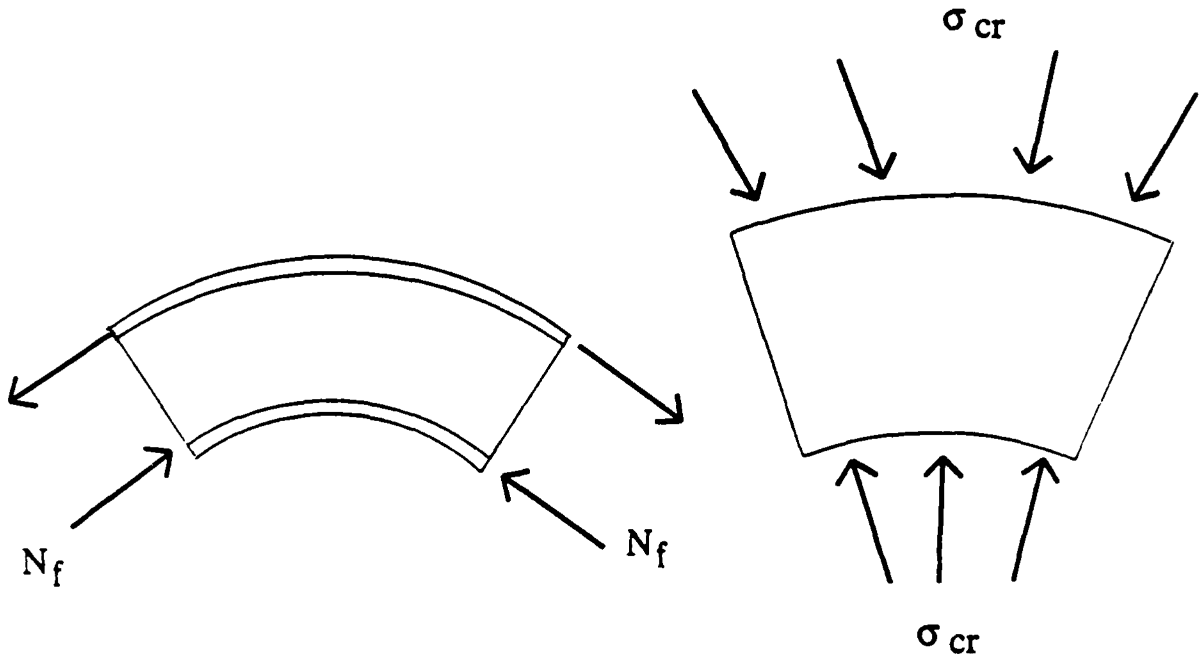

CRUSHING OF THE WEB

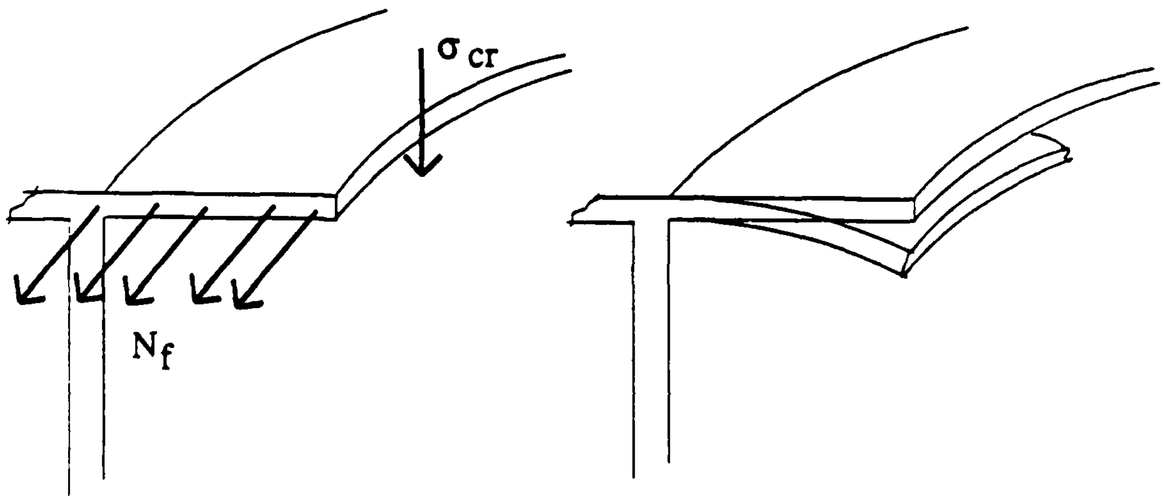

CURLING OF THE FLANGES

Specimen Configuration

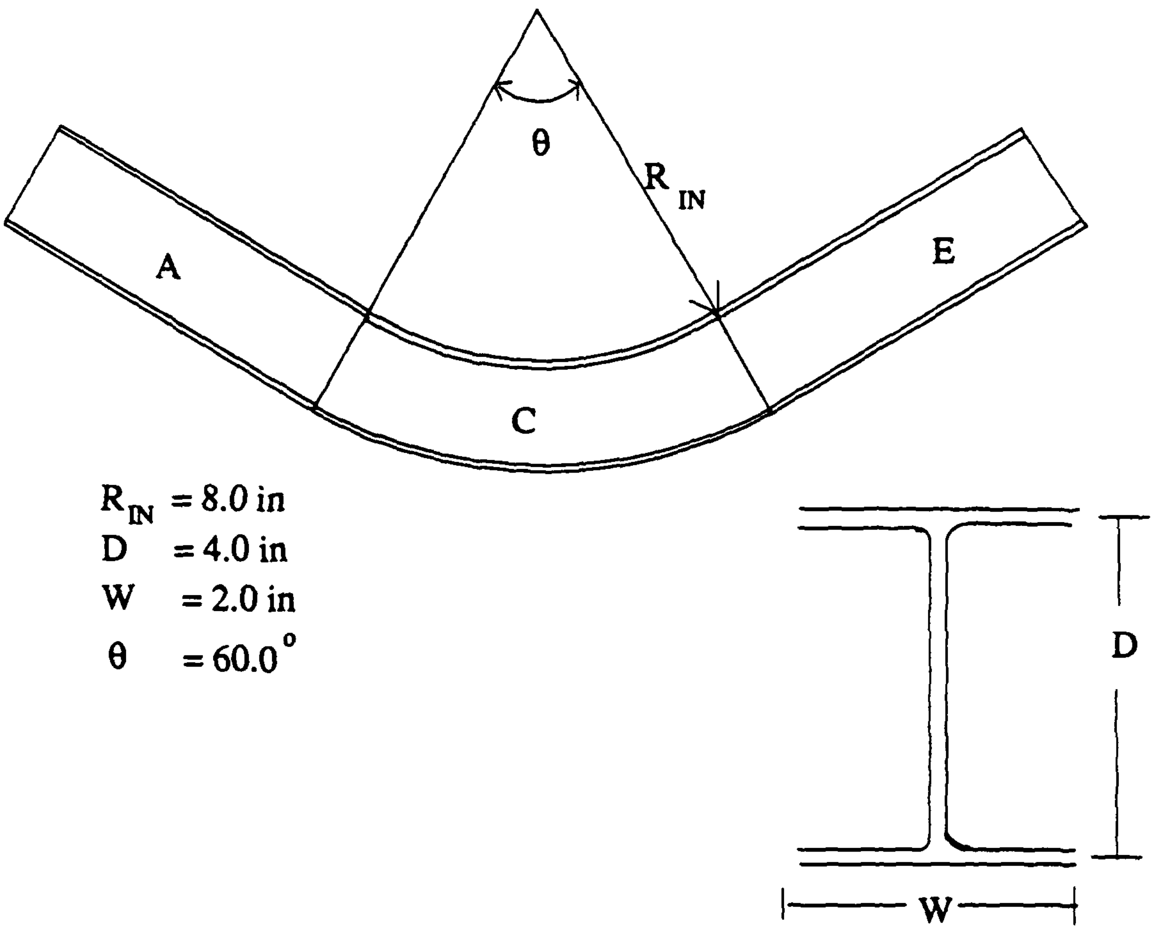

R_{IN} = 8.0 in
D = 4.0 in
W = 2.0 in
θ = 60.0°

MATERIAL
Graphite prepreg tape (250° F cure)
Fiberite HY -E12481F

Numerical Investigation

Finite element model of the test specimen was performed using the ABAQUS code

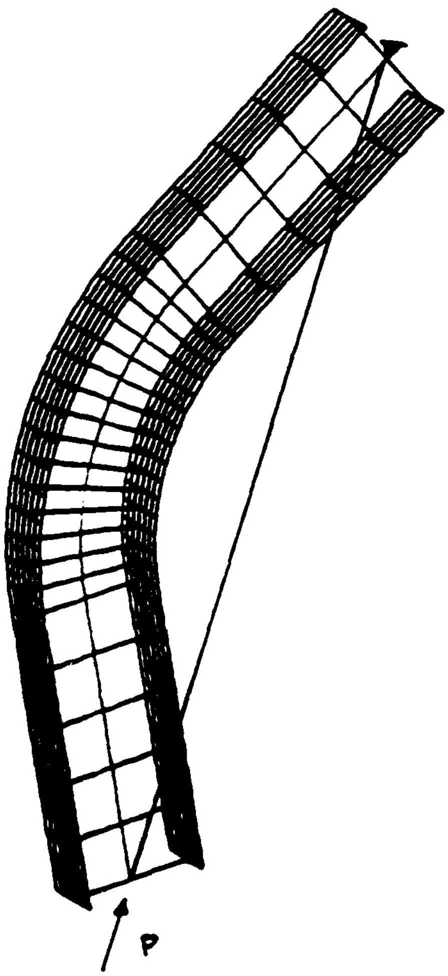

- **1500 grid points (~7000 DOF's)**
- **350 8– noded shell elements**

ANALYTICAL SOLUTION

General Differential Equation

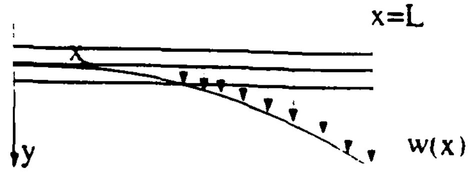

$$D_{22}w^{iv} + \frac{E_{11}t_f}{R_f^2}w = \frac{\sigma_o t_f}{R_f}$$

$$\overline{x} = \frac{x}{L} \qquad \overline{w} = \frac{w}{t_f}$$

Non – Dimensional Form

$$\overline{w^{iv}} + 4\alpha^4\,\overline{w} = \overline{\sigma_o}$$

$$\alpha^4 = \left[3\frac{E_{11}}{D_{22}}\frac{1}{\left(\frac{R_f}{L}\right)^2\left(\frac{t_f}{L}\right)^2}\right]$$

$$\overline{\sigma_o} = 12\left(\frac{\sigma_o}{D_{22}}\right)\frac{1}{\left(\frac{t_f}{L}\right)^3\left(\frac{R_f}{L}\right)}$$

Strain Relation

$$\epsilon = \epsilon_o - \frac{w}{R_f} = \epsilon_o C(\alpha, \overline{x})$$

where $C(\alpha, \overline{x}) = c(\alpha)\,ch(\alpha) -$

$$\frac{1}{ch^2(\alpha) + c^2(\alpha)}\quad [ch(\alpha)\,sh(\alpha) + c(\alpha)\,s(\alpha)] \times [c(\alpha\overline{x})\,sh(\alpha\overline{x}) - s(\alpha\overline{x})\,ch(\alpha\overline{x})]$$

$$+ \left[ch^2(\alpha) - c^2(\alpha)\right] \times [s(\alpha\overline{x})\,sh(\alpha\overline{x})]$$

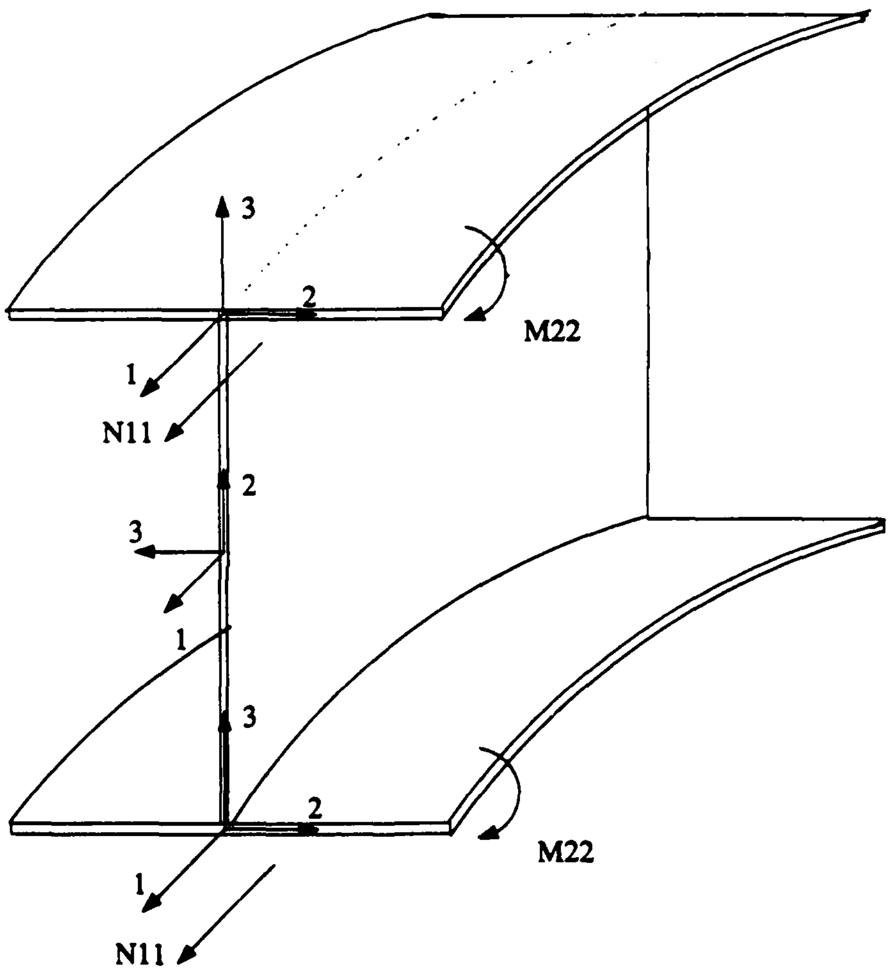

CURVED BEAM LOCAL COORDINATE AXES

N11 VS FLANGE POSITION

LOWER FLANGE, GR/EP T300-5208

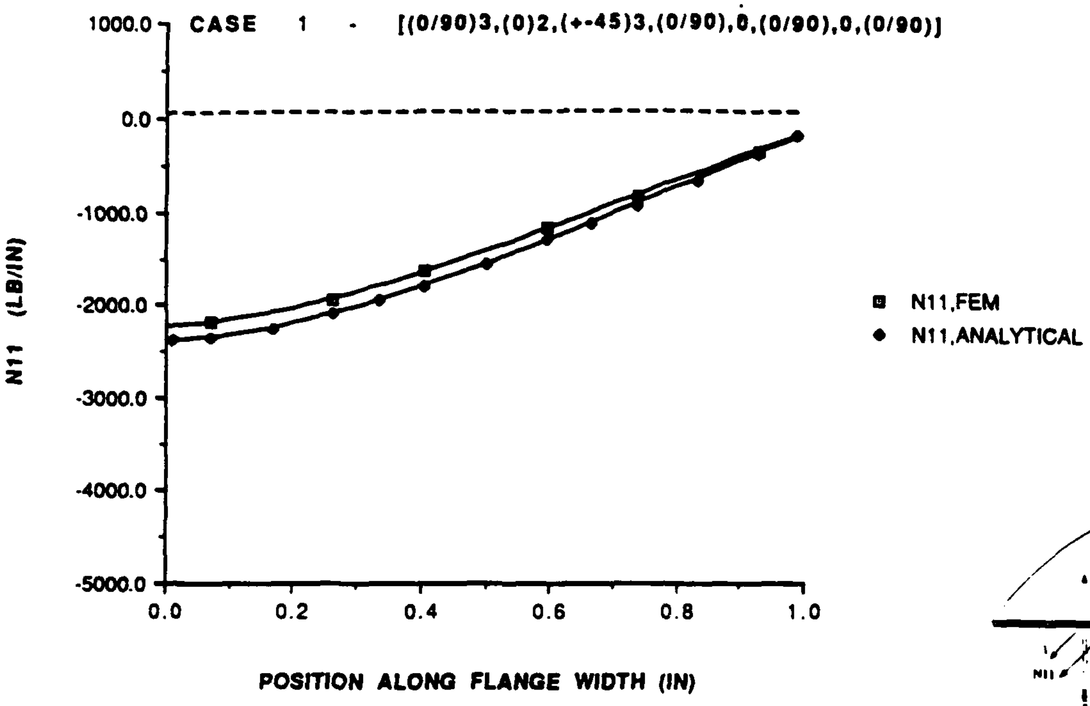

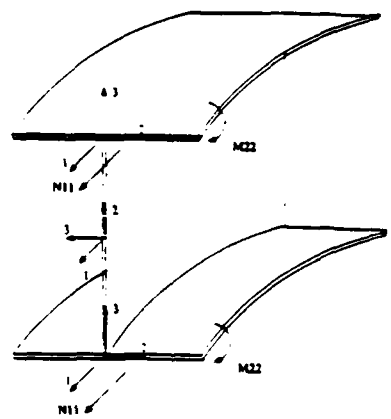

CURVED BEAM LOCAL COORDINATE AXES

M22 VS FLANGE POSITION

LOWER FLANGE, GR/EP T300-5208

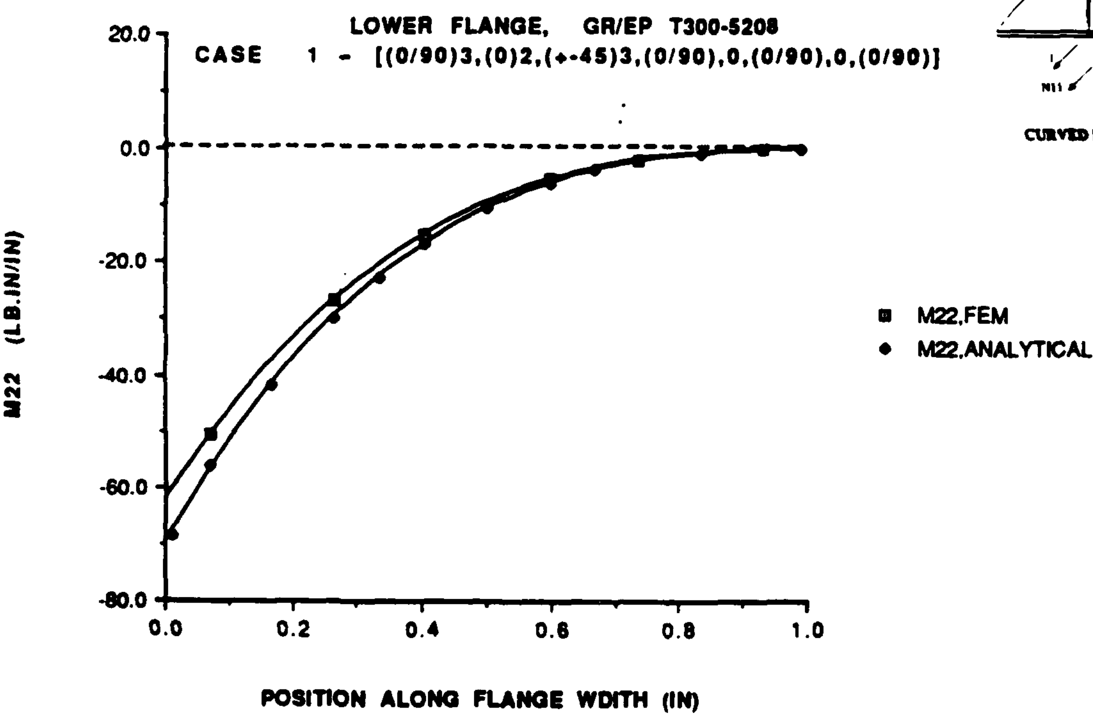

N11 VS FLANGE POSITION

UPPER FLANGE, GR/EP T300-5208

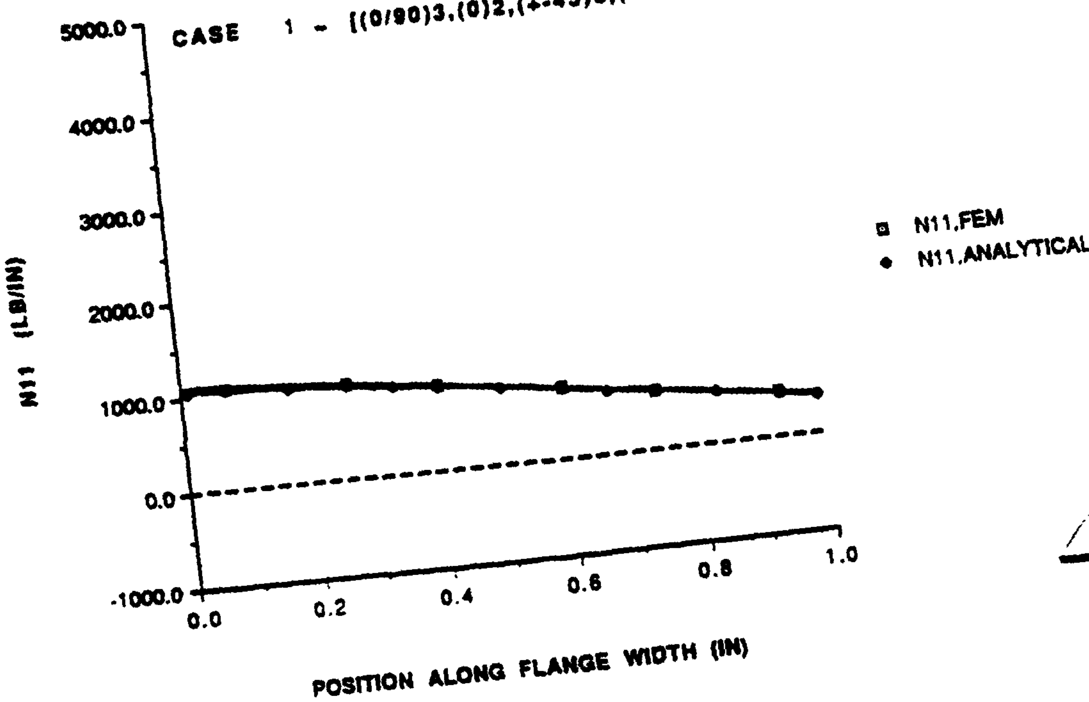

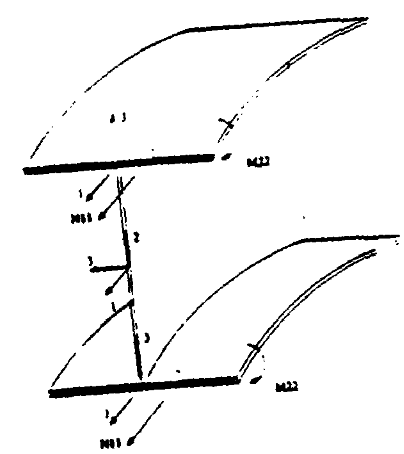

CURVED BEAM LOCAL COORDINATE AXE

M22 VS FLANGE POSITION

UPPER FLANGE, GR/EP T300-5208

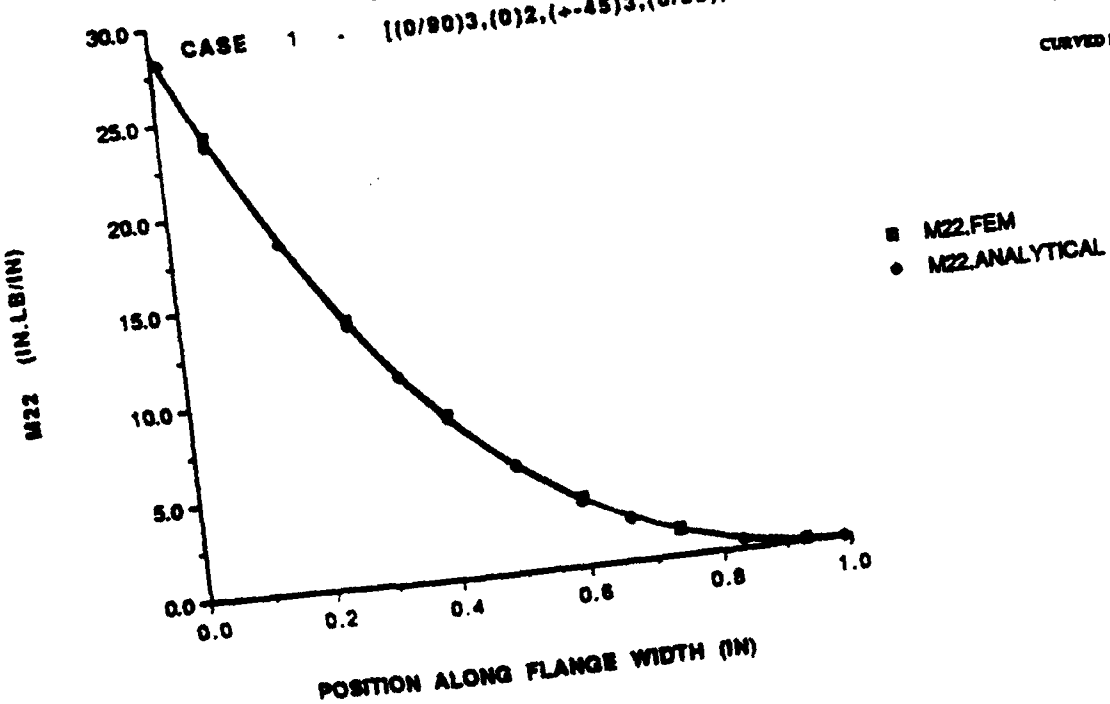

N11 VS FLANGE POSITION

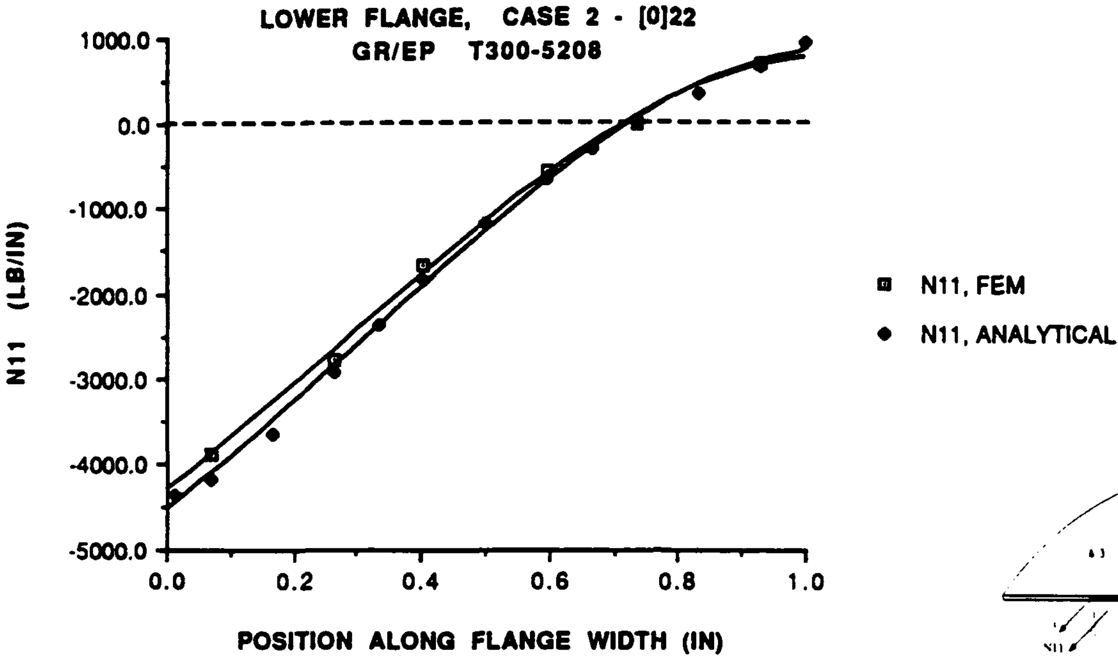

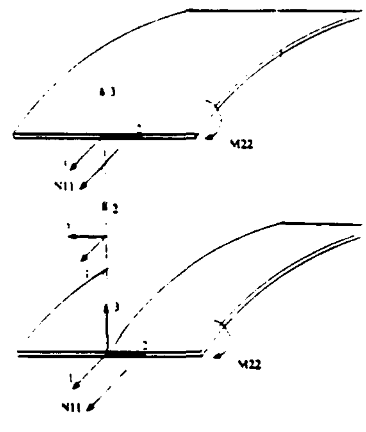

CURVED BEAM LOCAL COORDINATE AXES

M22 VS FLANGE POSITION

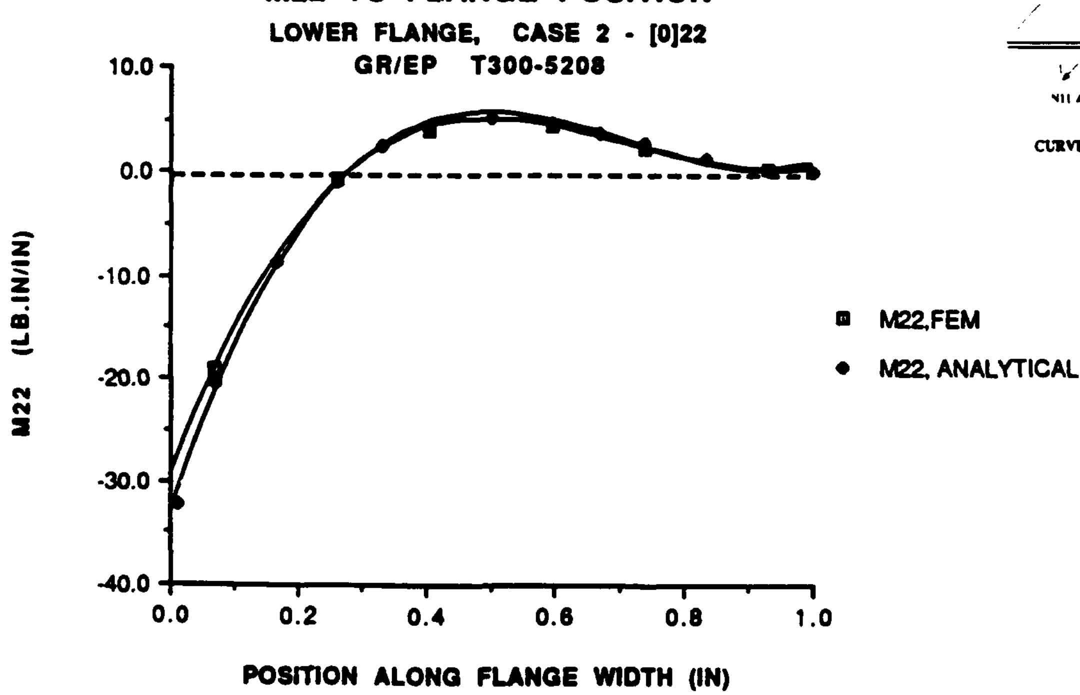

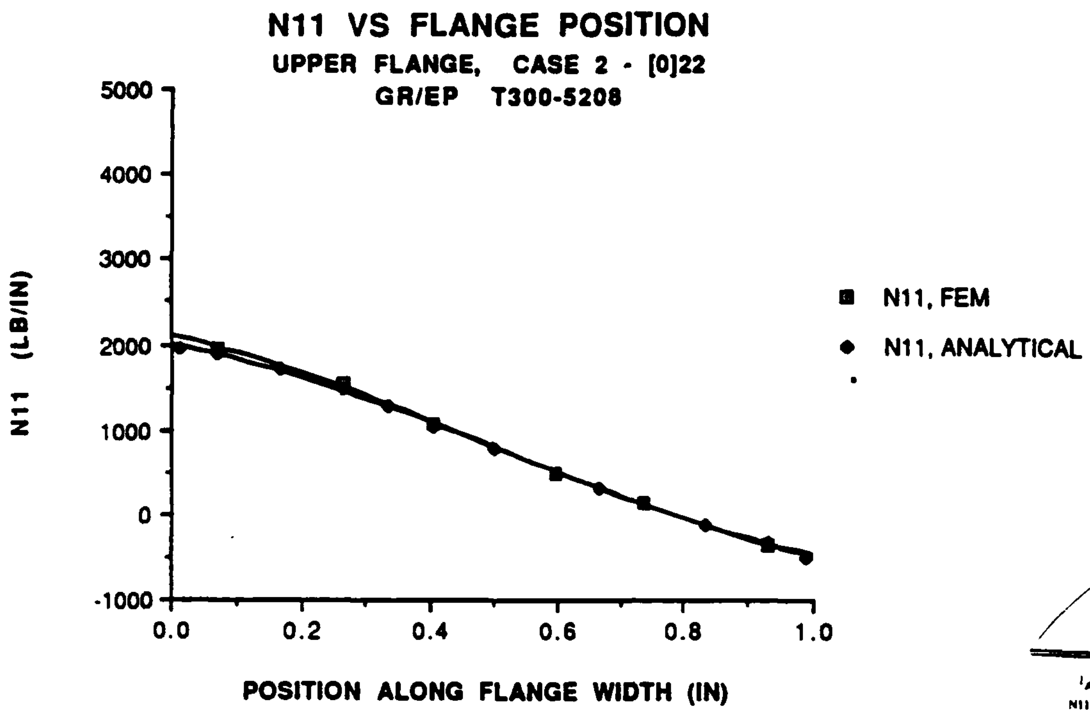

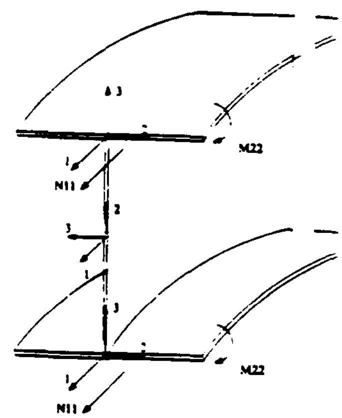

CURVED BEAM LOCAL COORDINATE AX

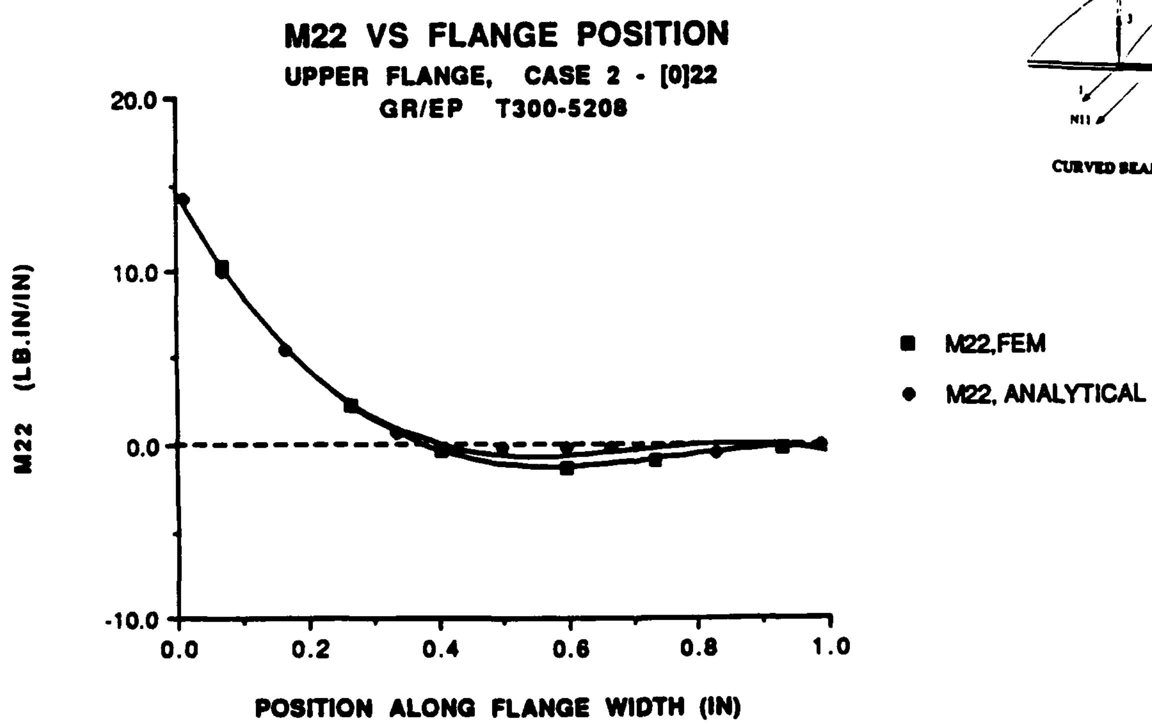

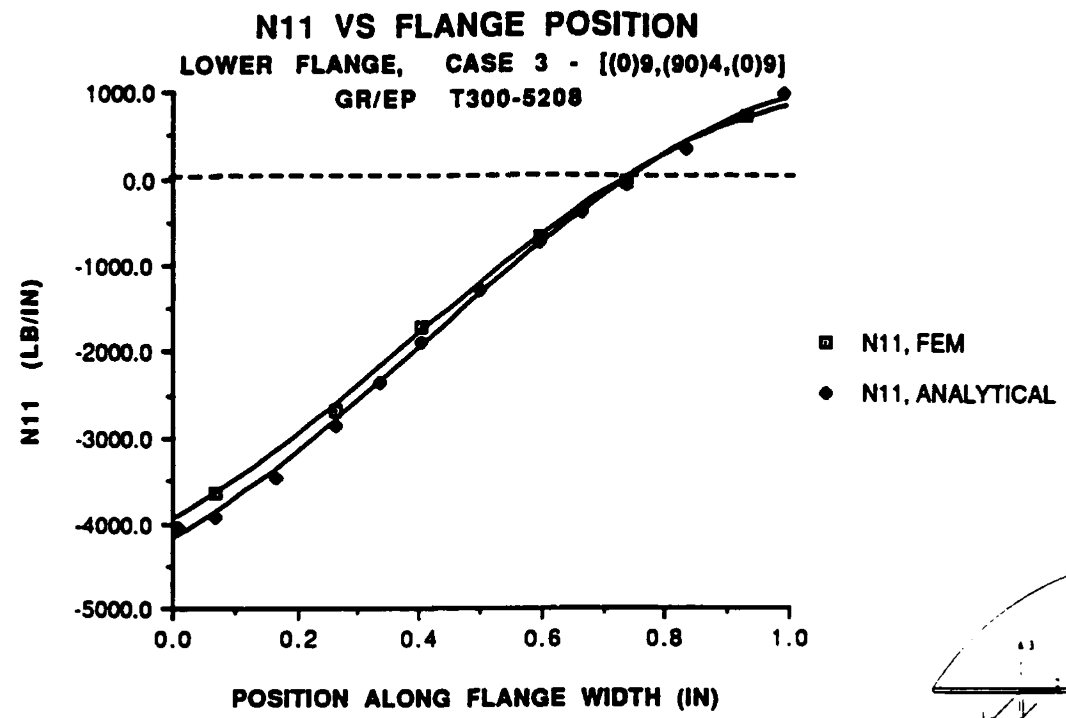

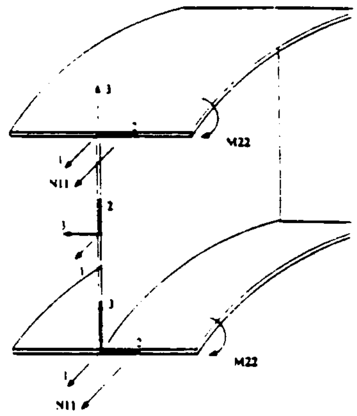

CURVED BEAM LOCAL COORDINATE AXE:

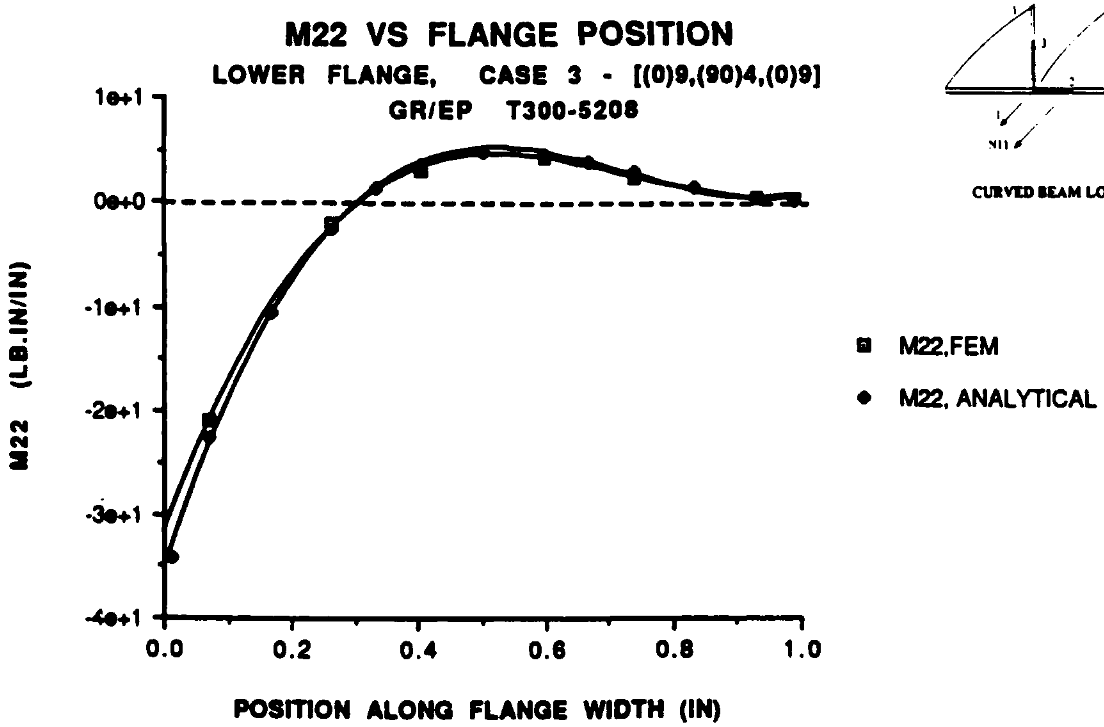

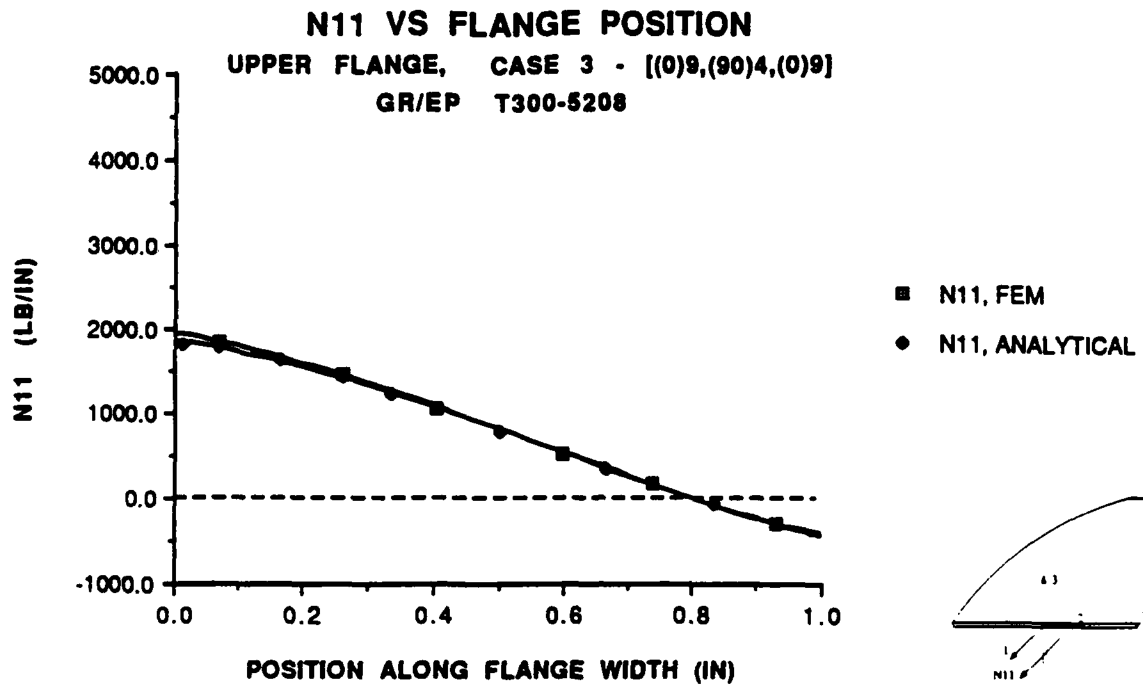

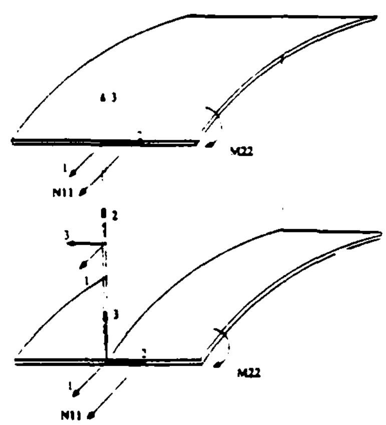

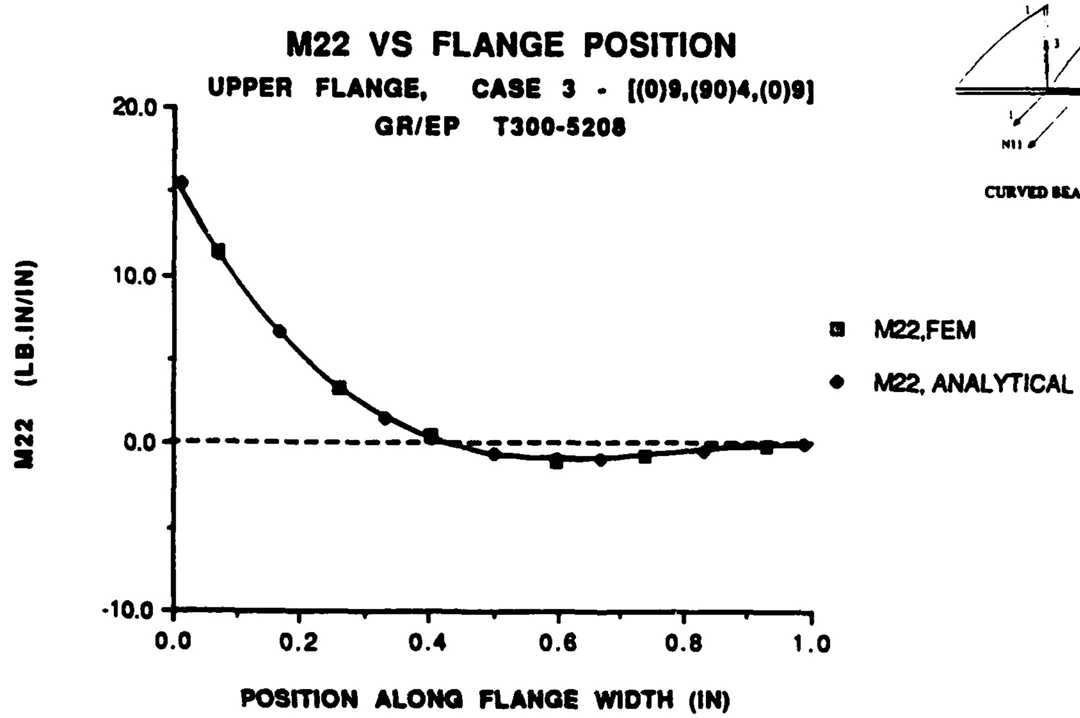

CURVED BEAM LOCAL COORDINATE A

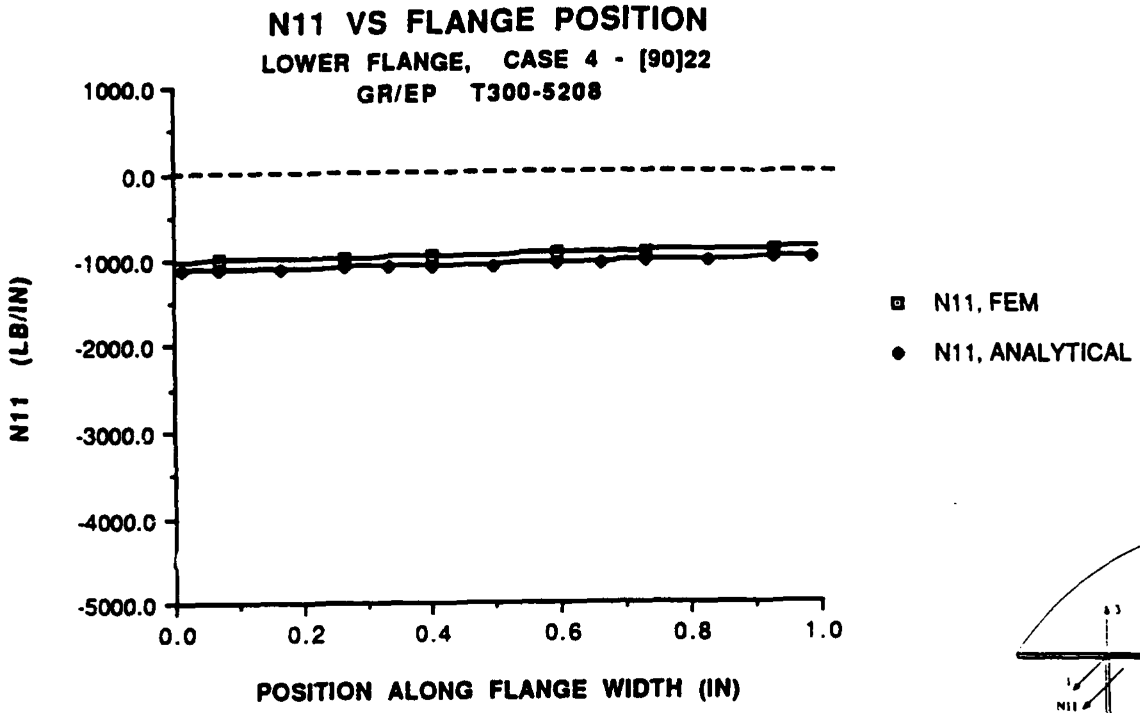

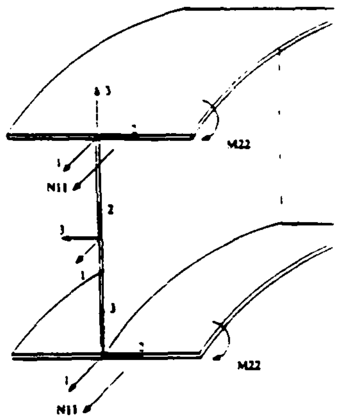

CURVED BEAM LOCAL COORDINATE A

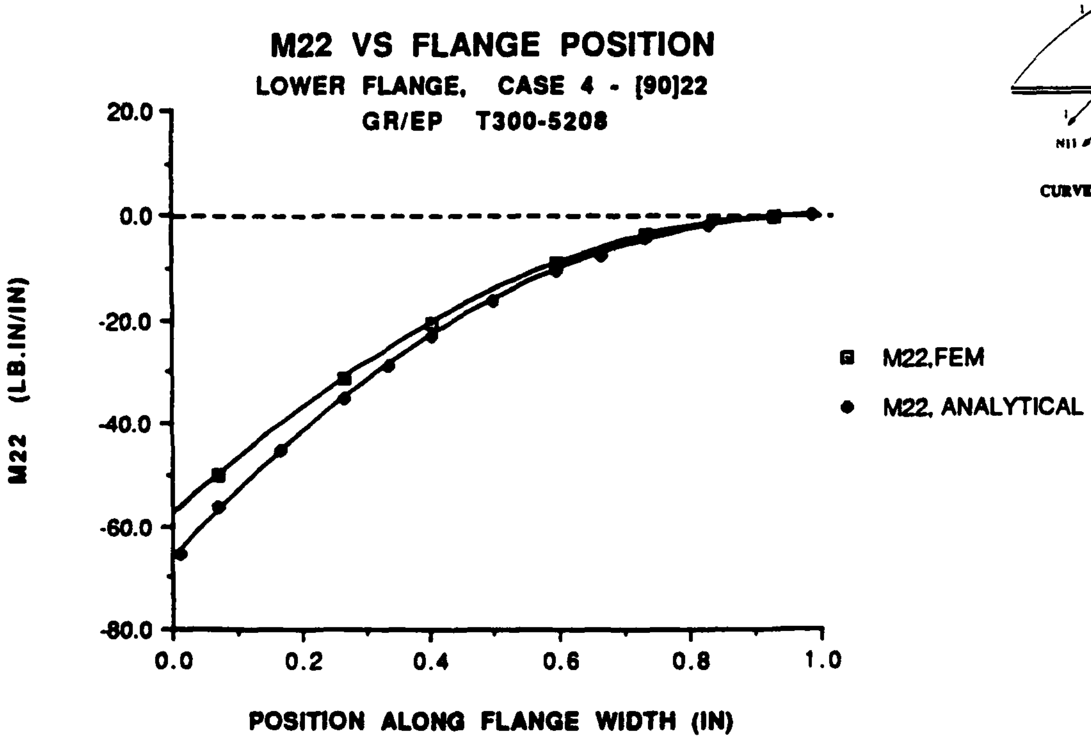

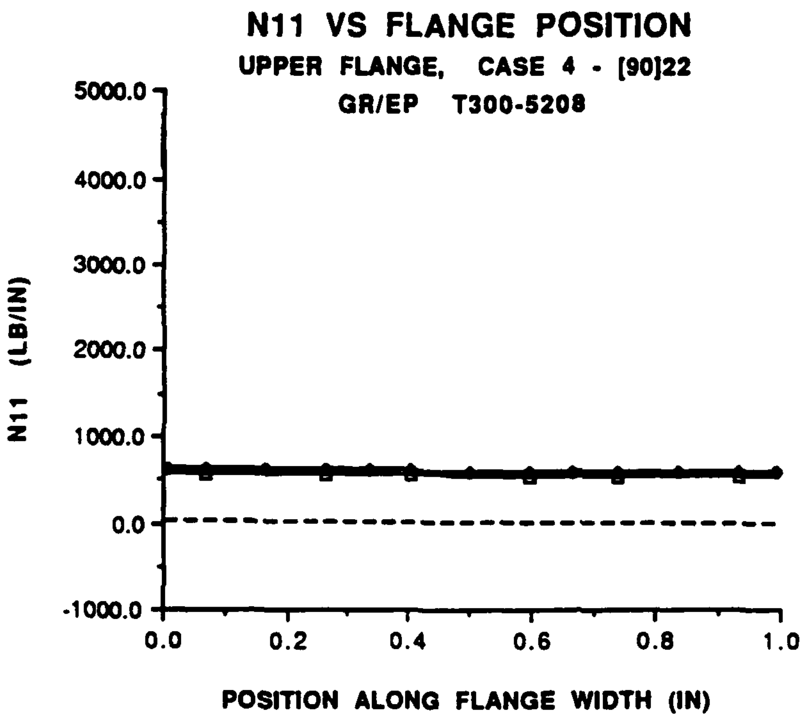

N11, FEM

N11, ANALYTICAL

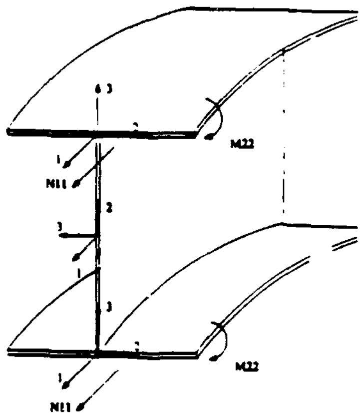

CURVED BEAM LOCAL COORDINATI XES

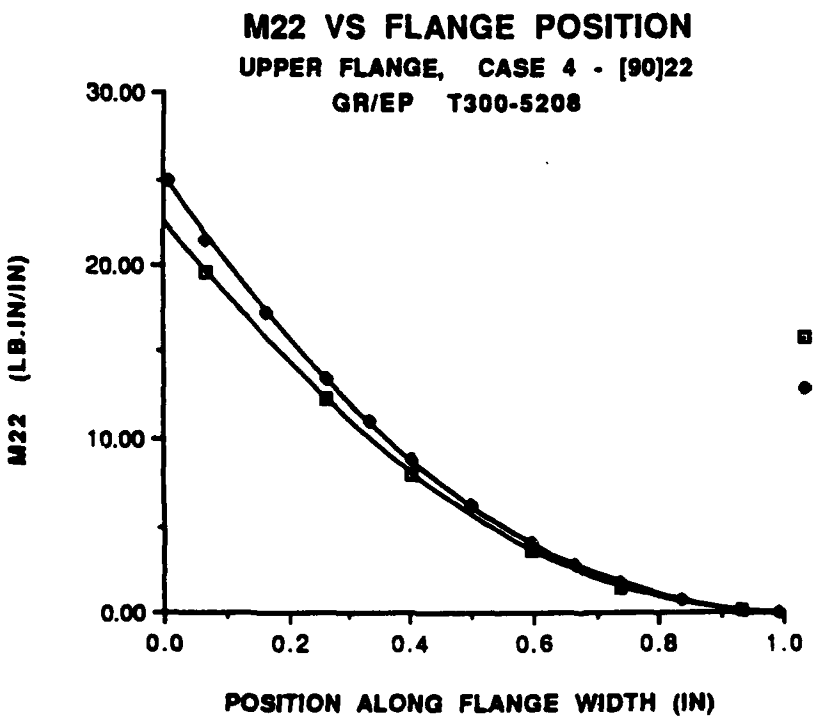

M22,FEM

M22, ANALYTICAL

P/Po VS ALPHA

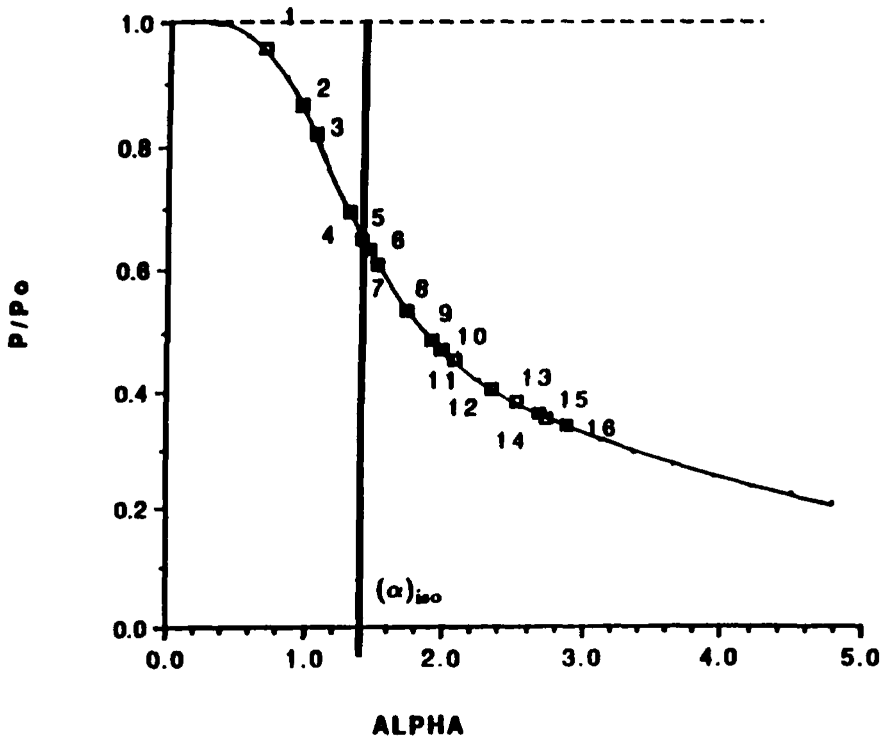

P = Total Load in Flange, With Curling

P_O = Total Load in Flange, Without Curling

$$\frac{P}{P_O} = \frac{1}{\alpha}\,\frac{\sin(\alpha)\cos(\alpha) + \sinh(\alpha)\cosh(\alpha)}{\cos(\alpha) + \cosh(\alpha)}$$

LAMINATE LAYUPS

1 – $[90]_{22}$

2 – $[\pm 60]_{11}$

3 – $[(90)_8, (0)_6, (90)_8]$

4 – $[(0)_3, (90)_{16}, (0)_3]$

5 – $[(\pm 45)]_{11}$

6 – $\left[(0/90)_2, (\pm 45)_2, (0)_2, (90)\right]_{SYM}$

7 – $[(0)_4, (90)_{14}, (0)_4]$

8 – $[(0/90)_2, (0)_{14}, (0/90)_2]$

9 – $\left[(\pm 45)_2, (0)_6, (\pm 45), (0)_6, (\pm 45)_2\right]$

10 – $\left[(0)_4, (\pm 45)_7, (0)_4\right]$

11 – $[(\pm 30)]_{11}$

12 – $[(0)_6, (\pm 45)_5, (0)_6]$

13 – $[(\pm 20)]_{11}$

14 – $\left[(0)_9, (90)_4, (0)_9\right]$

15 – $[(0)_9, (\pm 45)_2, (0)_9]$

16 – $[0]_{22}$

$$\alpha^4 = \left[3\left(\frac{E_{11}}{D_{22}}\right)\frac{1}{\left(\frac{R_f}{L}\right)^2\left(\frac{t_f}{L}\right)^2}\right]$$

$$\left[\frac{\alpha}{(\alpha)_{iso}}\right]^4 = \left[\left(\frac{E_T}{E_L}\right), \left(\frac{E_L}{E_T}\right)\right]$$

GEOMETRY

$t_f = 0.110$ in $\quad R_f = 7.975$ in

$L = 1.000$ in

MATERIAL

T300 – 5208 GR/EP

$\alpha = [0.688, 2.880]$

Minimum and Maximum Values of Alpha and Corresponding (P/Po) for Various Materials

MATERIAL NUMBER	MATERIAL TYPE	Ex (GPa)	Ey (GPa)	MIN ALPHA	(P/Po)	MAX ALPHA	(P/Po)
1	T300-5208 Gr/Ep	181.0	10.3	0.6863	0.9586	2.8770	0.3403
2	Hi Modulus Gr 500 GPa	245.0	10.0	0.6316	0.9697	3.1260	0.3162
3	Hi Modulus Gr 700 GPa	490.0	10.0	0.5311	0.9845	3.7170	0.2685
4	B(4)/5505 Boron/Ep	204.0	18.5	0.7711	0.9365	2.5600	0.3755
5	AS/3501 Gr/Ep	138.0	8.96	0.709	0.9532	2.7830	0.3501
6	Scotchply 1002	38.6	8.27	0.956	0.8682	2.0650	0.4500
7	Kevlar 49/Ep	76.0	5.5	0.729	0.9483	2.7090	0.3582
	Isotropic			1.4051	0.6519	1.4051	0.6519

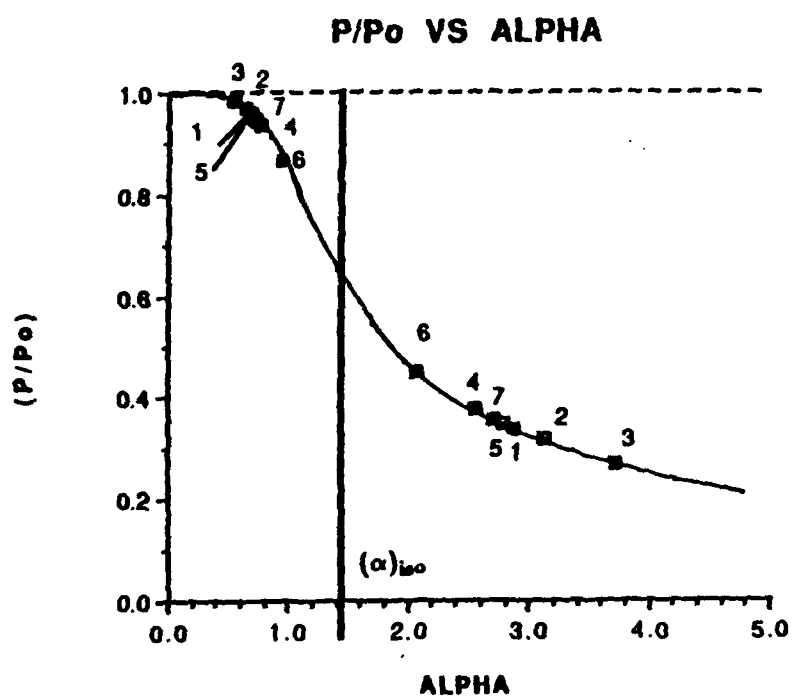

MATERIALS

1 – T300 – 5208, GR/EP

2 – High Modulus Graphite, 500 GPa

3 – High Modulus Graphite, 700 GPa

4 – B (4) /5505, B/EP

5 – AS/3501, GR/EP

6 – SCOTCHPLY 1002

7 – KEVLAR 49/EP

GEOMETRY

$t_f = 0.110$ in $R_f = 7.975$ in

$L = 1.00$ in

Γ = Total Load in Flange, With Curling

Γ_O = Total Load in Flange, Without Curling

$$\frac{\Gamma}{\Gamma_O} = \frac{1}{\alpha}\,\frac{\sin(\alpha)\cos(\alpha) + \sinh(\alpha)\cosh(\alpha)}{\cos(\alpha) + \cosh(\alpha)}$$

(N/No), (M/Mo) VS ALPHA

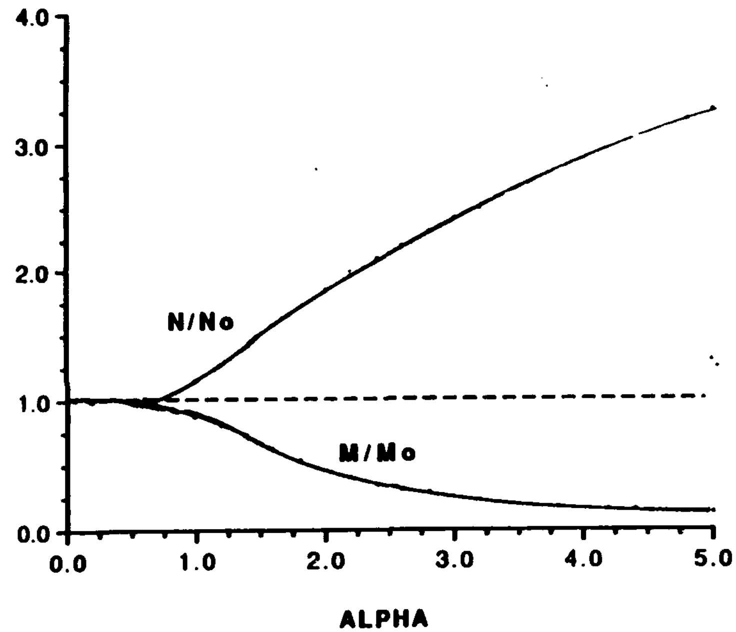

$$\alpha^4 = \left[3\left(\frac{E_{11}}{D_{22}}\right) \frac{1}{\left(\frac{R_f}{L}\right)^2 \left(\frac{t_f}{L}\right)^2} \right]$$

$$\left[\frac{\alpha}{(\alpha)_{iso}}\right]^4 = \left[\left(\frac{E_T}{E_L}\right), \left(\frac{E_L}{E_T}\right)\right]$$

GEOMETRY

$t_f = 0.110$ in $R_f = 7.975$ in

$L = 1.000$ in

MATERIAL

T300 – 5208 GR/EP

N_r Axial Load at the root, With Curling

$N_{r,w/o}$ = Axial Load at the root, Without Curling

$$\frac{N_r}{N_{r,w/o}} = \frac{E_{11}\epsilon(\alpha, \bar{x} = 0.)}{E_{11}\epsilon(\alpha = 0., \bar{x} = 0.)}$$

M_r = Moment at the root, With Curling

$M_{r,w/o}$ = Moment at the root, Without Curling

$$\frac{M_r}{M_{r,w/o}} = \left(\frac{N_r}{N_{r,w/o}}\right) \frac{1}{\alpha^2} \frac{\sin^2(\alpha) + \sinh^2(\alpha)}{\cos^2(\alpha) + \cosh^2(\alpha)}$$

ABS(N11) VS ALPHA

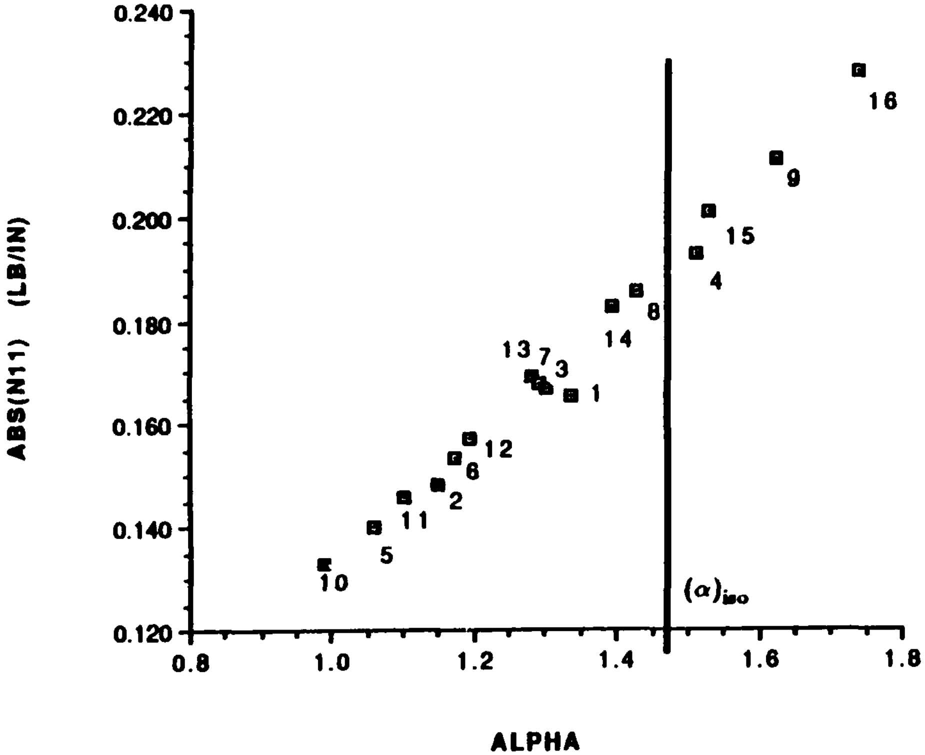

MII . . . E . . .

1 – $[90_1, (\pm 45)_4, 0_1]_{sym}$

2 – $[90_3, (\pm 45)_3, 0_1]_{sym}$

3 – $[90_2, (\pm 45)_3, 0_2]_{sym}$

4 – $[90_1, (\pm 45)_3, 0_3]_{sym}$

5 – $[90_5, (\pm 45)_2, 0_1]_{sym}$

6 – $[90_4, (\pm 45)_2, 0_2]_{sym}$

7 – $[90_3, (\pm 45)_2, 0_3]_{sym}$

8 – $[90_2, (\pm 45)_2, 0_4]_{sym}$

9 – $[90_2, (\pm 45)_2, 0_5]_{sym}$

10 – $[90_7, (\pm 45)_1, 0_1]_{sym}$

11 – $[90_6, (\pm 45)_1, 0_1]_{sym}$

12 – $[90_5, (\pm 45)_1, 0_3]_{sym}$

13 – $[90_4, (\pm 45)_1, 0_4]_{sym}$

14 – $[90_3, (\pm 45)_1, 0_5]_{sym}$

15 – $[90_2, (\pm 45)_1, 0_6]_{sym}$

16 – $[90_1, (\pm 45)_1, 0_7]_{sym}$

$$\alpha^4 = \left[3\left(\frac{E_{11}}{D_{22}}\right)\frac{1}{\left(\frac{R_f}{L}\right)^2\left(\frac{t_f}{L}\right)^2}\right]$$

$$\left[\frac{\alpha}{(\alpha)_{iso}}\right]^4 = \left[\left(\frac{E_T}{E_L}\right)\cdot\left(\frac{E_L}{E_T}\right)\right]$$

GEOMETRY

$t_f = 0.100$ in $\quad R_f = 7.975$ in

$L = 1.00$ in

MATERIAL

T300 – 5208 GR/EP

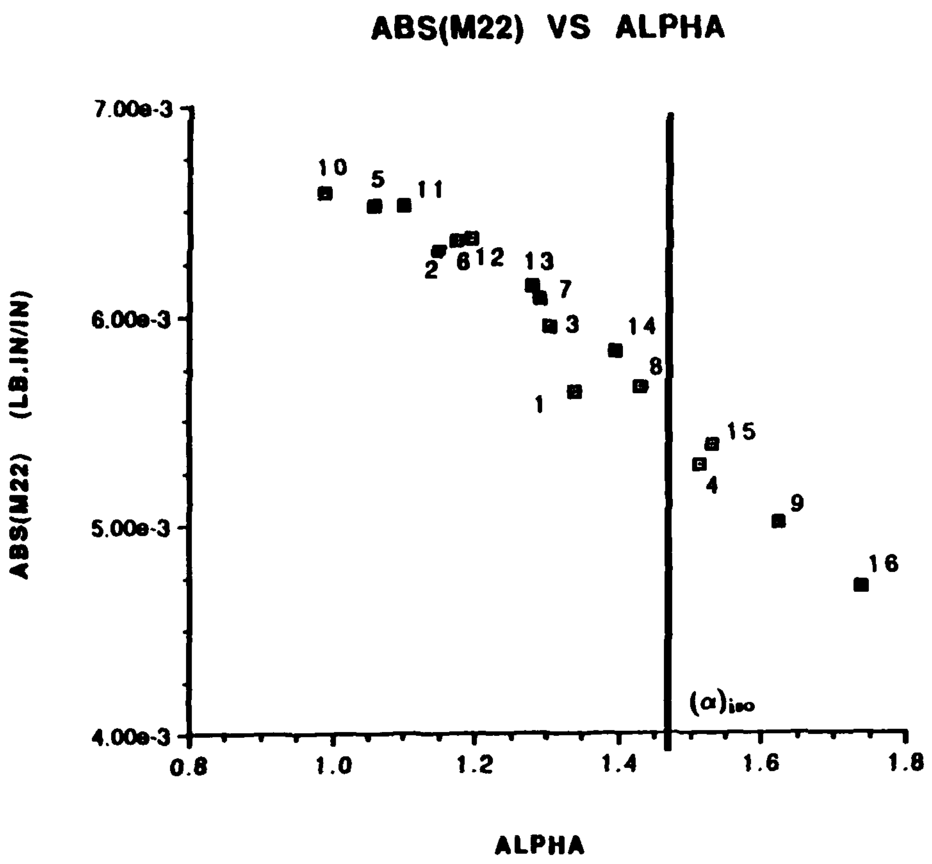

LAMINATE LAY – UPS

1 – $[90_1, (\pm 45)_4, 0_1]_{sym}$

2 – $[90_3, (\pm 45)_3, 0_1]_{sym}$

3 – $[90_2, (\pm 45)_3, 0_2]_{sym}$

4 – $[90_1, (\pm 45)_3, 0_3]_{sym}$

5 – $[90_5, (\pm 45)_2, 0_1]_{sym}$

6 – $[90_4, (\pm 45)_2, 0_2]_{sym}$

7 – $[90_3, (\pm 45)_2, 0_3]_{sym}$

8 – $[90_2, (\pm 45)_2, 0_4]_{sym}$

9 – $[90_2, (\pm 45)_2, 0_5]_{sym}$

10 – $[90_7, (\pm 45)_1, 0_1]_{sym}$

11 – $[90_6, (\pm 45)_1, 0_1]_{sym}$

12 – $[90_5, (\pm 45)_1, 0_3]_{sym}$

13 – $[90_4, (\pm 45)_1, 0_4]_{sym}$

14 – $[90_3, (\pm 45)_1, 0_5]_{sym}$

15 – $[90_2, (\pm 45)_1, 0_6]_{sym}$

16 – $[90_1, (\pm 45)_1, 0_7]_{sym}$

$$\alpha^4 = \left[3\left(\frac{E_{11}}{D_{22}}\right)\frac{1}{\left(\frac{R_f}{t}\right)^2\left(\frac{t_f}{L}\right)^2}\right]$$

$$\left[\frac{\alpha}{(\alpha)_{iso}}\right]^4 = \left[\left(\frac{E_T}{E_L}\right), \left(\frac{E_L}{E_T}\right)\right]$$

GEOMETRY

$t_f = 0.100$ in $\quad R_f = 7.975$ in

$L = 1.00$ in

MATERIAL

T300 – 5208 Gr/EP

MAXIMUM BENDING MOMENT VS ALPHA

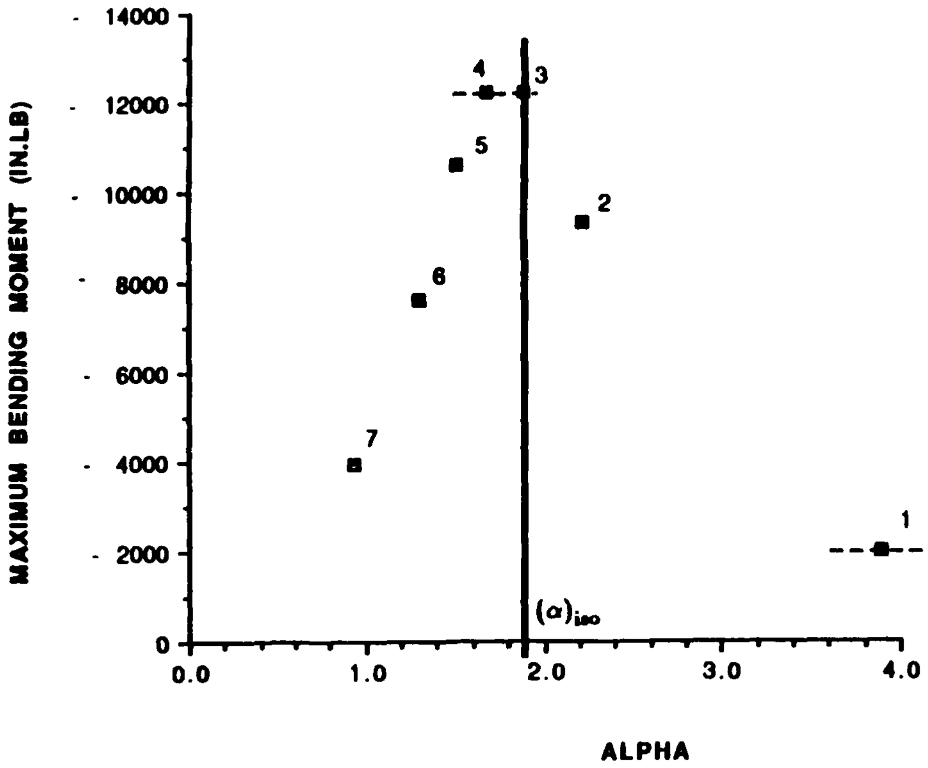

LAMINATE LAY – UPS

1 – $[0_6]_{sym}$

2 – $[90, 0_5]_{sym}$

3 – $[90_2, 0_4]_{sym}$

4 – $[90_3, 0_3]_{sym}$

5 – $[90_4, 0_2]_{sym}$,

6 – $[90_5, 0]_{sym}$

7 – $[90_6]_{sym}$

$$\alpha^4 = \left[3\left(\frac{E_{11}}{D_{22}}\right) \frac{1}{\left(\frac{R_f}{L}\right)^2 \left(\frac{t_f}{L}\right)^2} \right]$$

$$\left[\frac{\alpha}{(\alpha)_{iso}}\right]^4 = \left[\left(\frac{E_T}{E_L}\right) \cdot \left(\frac{E_L}{E_T}\right)\right]$$

GEOMETRY

$t_f = 0.060$ in $\quad R_f = 7.975$ in

$L = 1.00$ in

MATERIAL

T300 – 5208 GR/EP

MAXIMUM BENDING MOMENT VS ALPHA

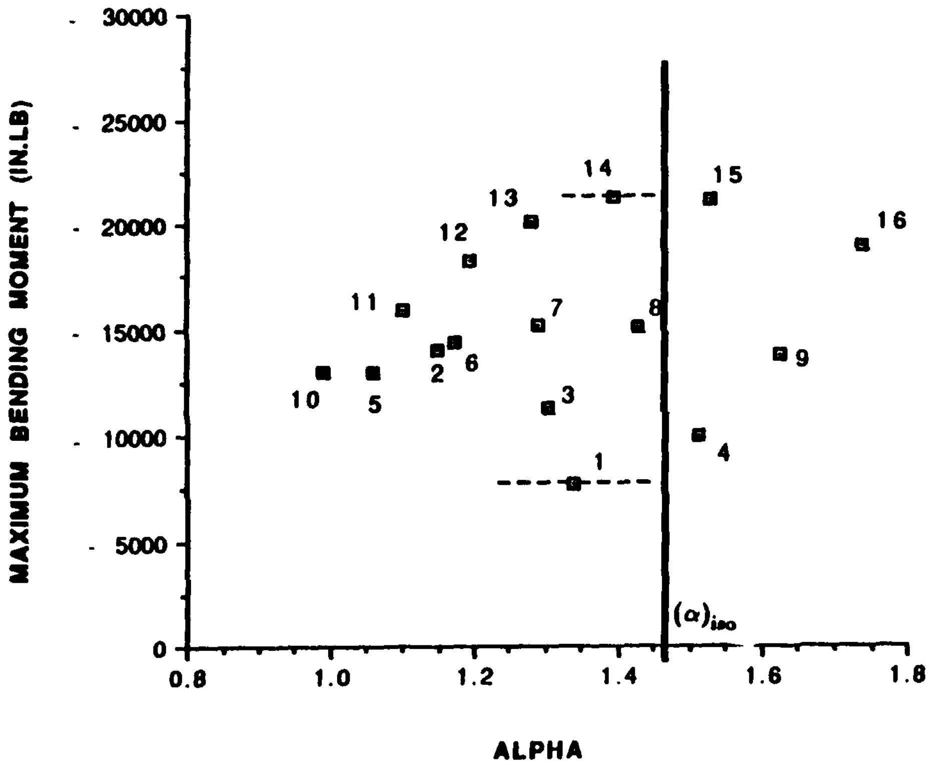

LAMINATE LAY – UPS

1 – $[90_1, (\pm 45)_4, 0_1]_{sym}$

2 – $[90_3, (\pm 45)_3, 0_1]_{sym}$

3 – $[90_2, (\pm 45)_3, 0_2]_{sym}$

4 – $[90_1, (\pm 45)_3, 0_3]_{sym}$

5 – $[90_5, (\pm 45)_2, 0_1]_{sym}$

6 – $[90_4, (\pm 45)_2, 0_2]_{sym}$

7 – $[90_3, (\pm 45)_2, 0_3]_{sym}$

8 – $[90_2, (\pm 45)_2, 0_4]_{sym}$

9 – $[90_1, (\pm 45)_2, 0_5]_{sym}$

10 – $[90_7, (\pm 45)_1, 0_1]_{sym}$

11 – $[90_6, (\pm 45)_1, 0_1]_{sym}$

12 – $[90_5, (\pm 45)_1, 0_3]_{sym}$

13 – $[90_4, (\pm 45)_1, 0_4]_{sym}$

14 – $[90_3, (\pm 45)_1, 0_5]_{sym}$

15 – $[90_2, (\pm 45)_1, 0_6]_{sym}$

16 – $[90_1, (\pm 45)_1, 0_7]_{sym}$

$$\alpha^4 = \left[3\left(\frac{E_{11}}{D_{22}}\right)\frac{1}{\left(\frac{R_f}{L}\right)^2\left(\frac{t_f}{L}\right)^2}\right]$$

$$\left[\frac{\alpha}{(\alpha)_{iso}}\right]^4 = \left[\left(\frac{E_T}{E_L}\right), \left(\frac{E_L}{E_T}\right)\right]$$

GEOMETRY

$t_f = 0.100$ in $\quad R_f = 7.975$ in

$L = 1.00$ in

MATERIAL

[illegible]00 – [illegible]08 Gr/EP

Conclusions

• 1 – Good correlation was found between the predictions of a 3–D FEM model of laminated composite I-beams with a strong curvature and a "Strength of Material" analytical model.

• 2 – The stress distribution in the flanges is characterized by a single parameter

$$\alpha^4 = \left[3\frac{E_{11}}{D_{22}}\frac{1}{\left(\frac{R_f}{L}\right)^2\left(\frac{t_f}{L}\right)^2}\right]$$

Material stiffness effects are

$$\left(\frac{\alpha}{\alpha_{iso}}\right)^4 \in \left[\frac{E_L}{E_T}, \frac{E_T}{E_L}\right]$$

• 3 – The lay-up and stacking sequence of the flanges drastically affects overall load carrying capability. Up to a factor of 5 was observed.

• 4 – A nearly "quasi-isotropic" lay-up seems to yield the highest strength.

• 5 – The question remains open as to whether the I configuration is desirable in beams with strong curvature.

"Dynamic Characteristics of Thin-Walled Composite Beams"

Lawrence W. Rehfield
University of California, Davis, California

Ali R. Atılgan and Dewey H. Hodges
Georgia Institute of Technology, Atlanta, Georgia

DERIVATION BY PRINCIPLE OF VIRTUAL WORK

- CONSISTENCY
- SIMPLICITY OF DERIVATION
- GOVERNING KINETIC EQUATIONS
- NATURAL/GEOMETRIC BOUNDARY CONDITIONS

KINEMATICS

$$\gamma^{o}_{xy} = \beta_z + V_{,x} \tag{1}$$

$$\gamma^{o}_{xz} = \beta_{,y} + W_{,x} \tag{2}$$

$$\gamma^{o}_{xs} = \gamma^{o}_{xy}\frac{dy}{ds} + \gamma^{o}_{xz}\frac{dz}{ds} + \frac{2Ae}{c}\,\phi_{,x} \tag{3}$$

$$u = U(x) + y\beta_z + z\,\beta_y + \underline{\psi(s)\,\phi_{,x}} \tag{4}$$

$$v = V(x) - z\phi(x) \tag{5}$$

$$w = W(x) + y\,\phi(x) \tag{6}$$

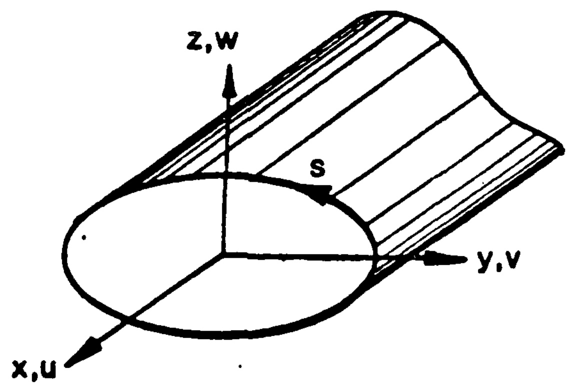

GENERALIZED FORCE RESULTANTS

$$(N, M_y, M_z) = \oint N_{xx}(1, z, y)ds$$

$$(Q_y, Q_z) = \oint N_{xs}\left(\frac{dy}{ds}, \frac{dz}{ds}\right) ds$$

$$M_x = \frac{2A_e}{c}\oint N_{xs}\, ds$$

$$Q_w = \oint N_{xx}\psi\, ds$$

CONSTITUTIVE RELATIONS

$$\begin{bmatrix} N_{xx} \\ N_{ss} \\ N_{xs} \end{bmatrix} = \underline{A} \begin{bmatrix} \varepsilon^{o}_{xx} \\ \varepsilon^{o}_{ss} \\ \gamma^{o}_{xs} \end{bmatrix}$$

$$N_{ss} \approx 0$$

$$\begin{bmatrix} N_{xx} \\ N_{xs} \end{bmatrix} = \underline{K} \begin{bmatrix} \varepsilon^{o}_{xx} \\ \gamma^{o}_{xs} \end{bmatrix}$$

ELASTIC LAW

$$\begin{bmatrix} N \\ Q_y \\ Q_z \\ M_x \\ M_y \\ M_z \\ Q_w \end{bmatrix} = \underset{7 \times 7}{C} \begin{bmatrix} U_{,x} \\ \gamma^o_{xy} \\ \gamma^o_{xz} \\ \phi_{,x} \\ \beta_{y,x} \\ \beta_{z,x} \\ \phi_{,xx} \end{bmatrix}$$

25 INDEPENDENT STIFFNESSES

VIBRATION BEHAVIOR

- EXTENSION - TWIST
- BENDING

CONSIDER LOWER MODES ONLY

EXTENSION-TWIST VIBRATION

$$C_{11}U'' + \underline{C_{14}\phi''} + M\omega^2 U = 0$$

$$\underline{C_{14}U''} + C_{44}\phi'' + I\omega^2\phi = 0$$

MODELING APPROXIMATIONS

- Coupled modes
- Statically uncoupled modes (M or I neglected)
- Uncoupled modes (C_{14} neglected)

STATICALLY UNCOUPLED FREQUENCIES

ARE RELATED TO CLASSICALLY

UNCOUPLED FREQUENCIES

$$\omega_{IT} = (\omega_{IT})_{CL} \ (1-\beta)^{1/2}$$

$$\omega_{IE} = (\omega_{IE})_{CL} \ (1-\beta)^{1/2}$$

COUPLED FREQUENCIES

$$\omega^2_{1,2} = \frac{(\omega^2_{IT} + \omega^2_{IE}) \pm \left[(\omega^2_{IT} - \omega^2_{IE})^2 + 4\beta\, \omega^2_{IT}\omega^2_{IE}\right]^{1/2}}{2(1-\beta)}$$

FIG. 1

MODEL ROTOR CROSS SECTION

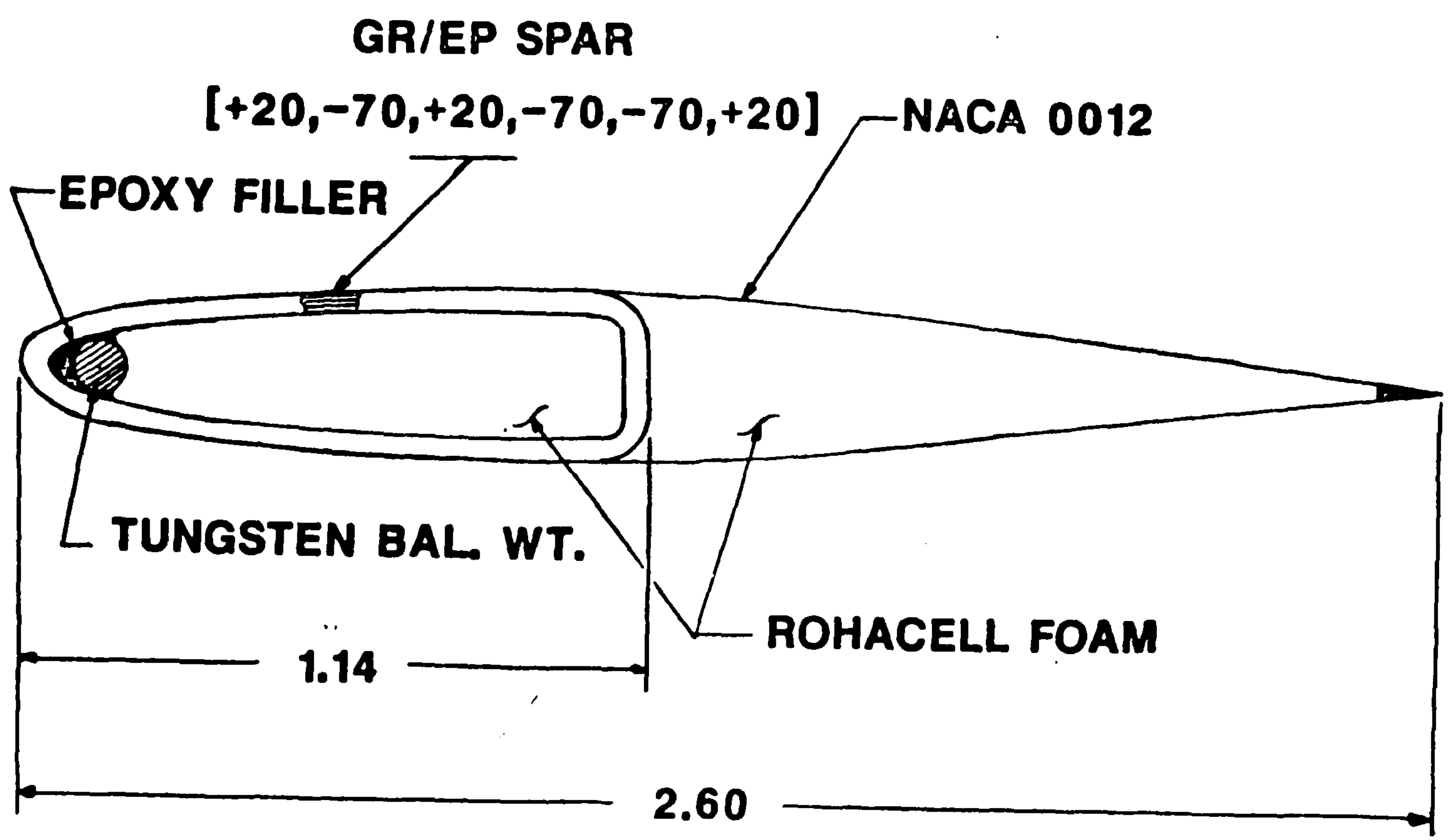

<u>LANGLEY MODEL ROTOR BLADE</u>

<u>EXTENSION-TWIST VIBRATION FREQUENCIES</u>

COUPLED MODES

$\omega_1 = 10.33$ $\omega_2 = 33.81$

STATICALLY UNCOUPLED MODES

$\omega_{IT} = 10.96$ $\omega_{IE} = 22.80$

CLASSICALLY UNCOUPLED MODES

$(\omega_{IT})_{CL} = 15.34$ $(\omega_{IE})_{CL} = 31.92$

BENDING VIBRATIONS

- IGNORE SHEAR DEFORMATION
  EFFECTS IF $L/d >> 1$.
  (SLENDER BEAMS)

- MODES ARE (ALMOST) UNCOUPLED

BENDING VIBRATIONS

- $C^{*}_{55} = C_{55}\,(1-\beta_1)$

- $\omega = \omega_{BE}\,(1-\beta_1)^{1/2}$

$(\omega_{BE})_1 = 5.89$

$\omega_1 = 4.05$

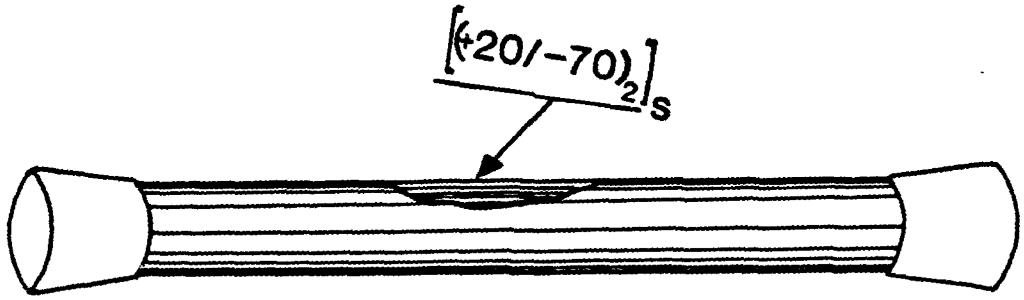

Schematic of the Langley model composite tube

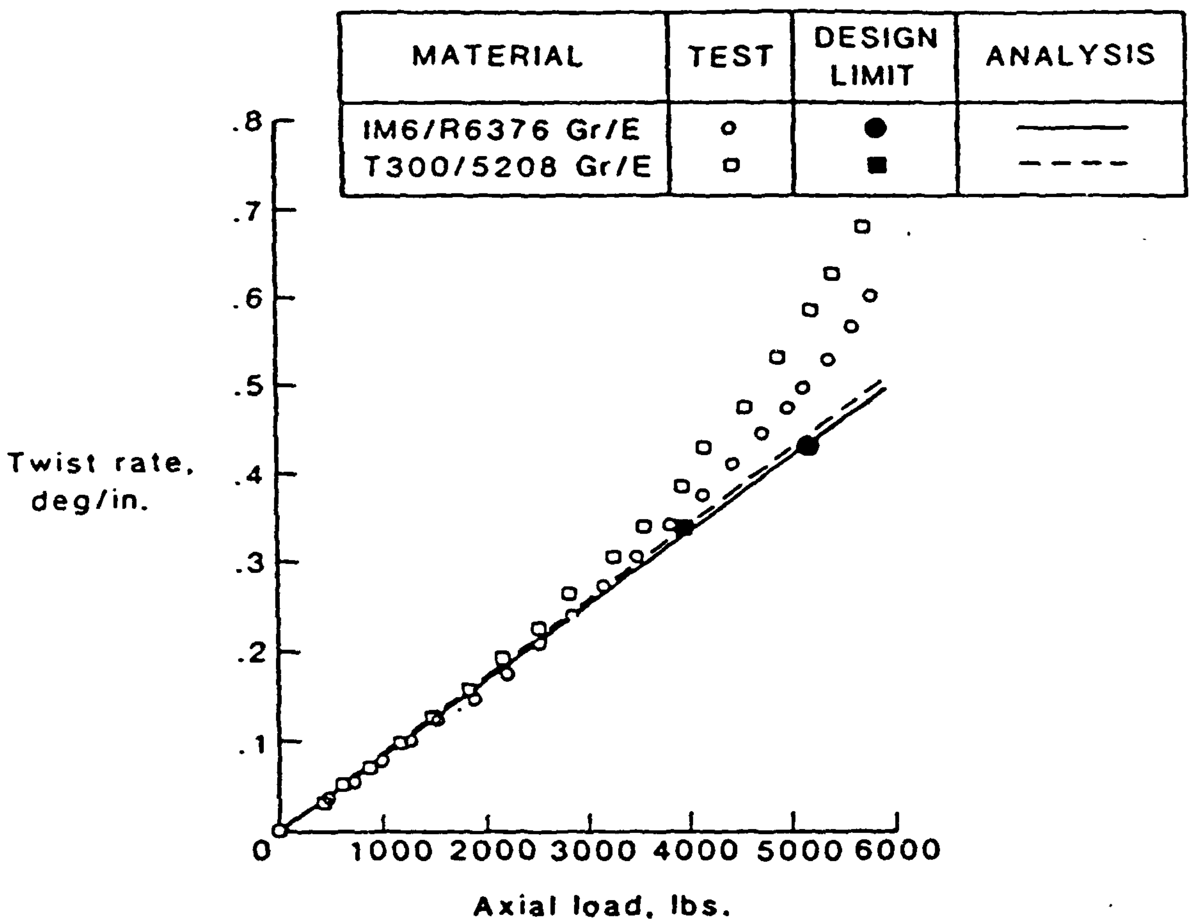

Static test correlations for Langley model tube

Stiffnesses of the Langley model tube

Stiffnesses	Calculated Values
C_{11}, lb	0.8456×10^6
C_{22}, lb	0.1056×10^6
C_{33}, lb	0.1056×10^6
$C_{44}, lb - in^2$	0.2771×10^5
$C_{55}, lb - in^2$	0.5681×10^5
$C_{66}, lb - in^2$	0.5681×10^5
$C_{14}, lb - in$	0.9735×10^5
$C_{25}, lb - in$	-0.4867×10^5
$C_{36}, lb - in$	0.4867×10^5

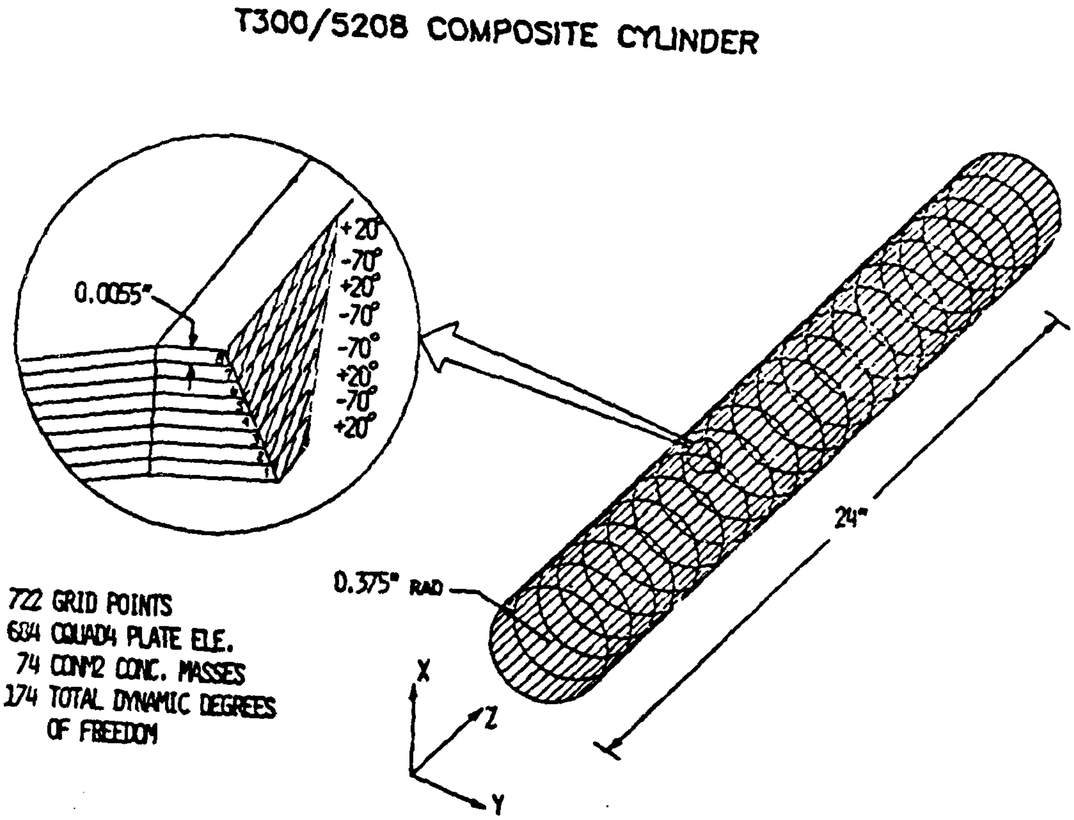

The finite element model of the Langley tube

MODE SHAPES:
Coupled Modes

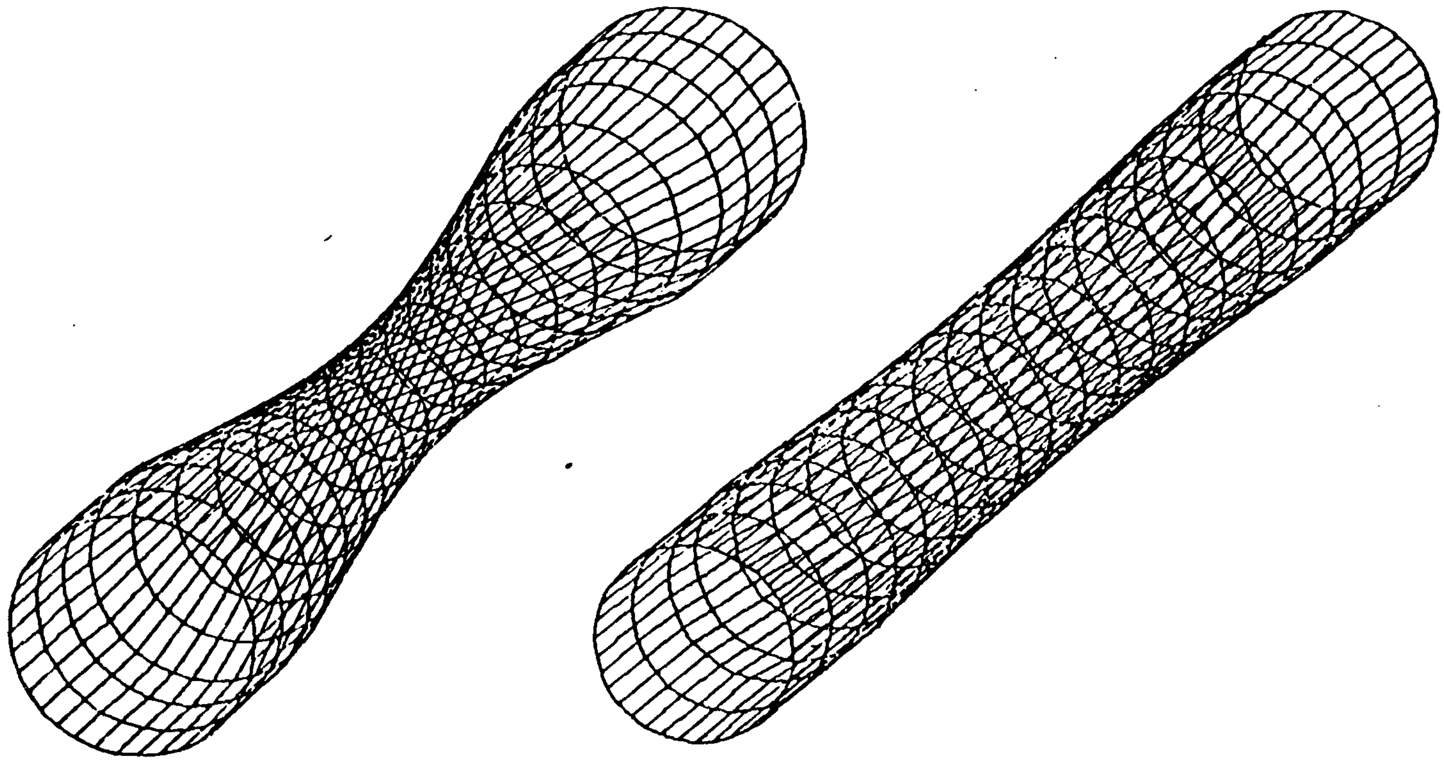

1st torsion   1st extension

MODE SHAPES:
Finite Element Analysis

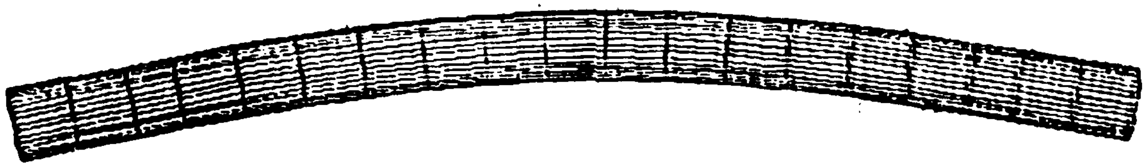

1st bending

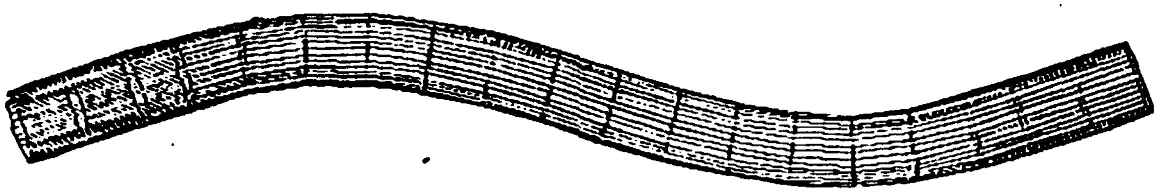

2nd bending

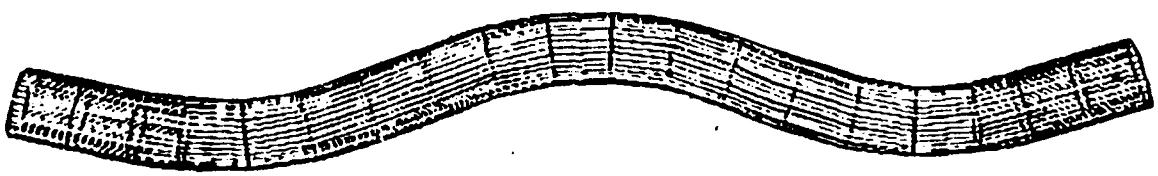

3rd bending

Free-free vibration results for the Langley model tube

MODE	EXPERIMENTAL	FEM 1 (SHELL)	FEM 2 (BEAM)	ANALYTICAL MODEL
BENDING	319	337	337	341
TORSION	583	592	653	606

Clamped-free vibration results for the Langley model tube

Modes	Transfer Matrix	Analytical Method
Coupled bending	58.73	58.88
Coupled extension-torsion	312.07	312.11

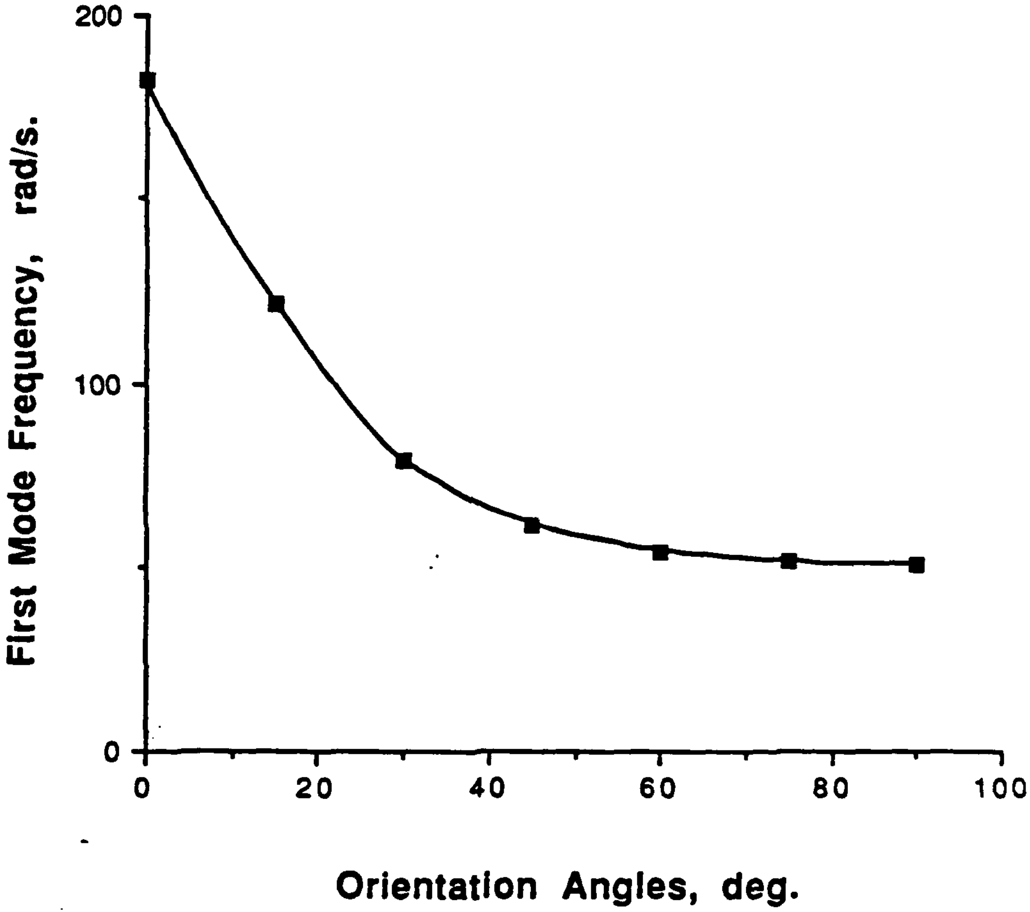

Alteration of the first mode bending frequency with the orientation angle

VIBRATION SUMMARY

- EXTENSION-TWIST MODES MUST BE TREATED AS COUPLED.

- BENDING MODES ARE UNCOUPLED

  - SCALE BE RESULTS

  - REDUCE STIFFNESSES FOR MASS COUPLING

EVALUATION OF COMPOSITE COMPONENTS ON THE BELL 206L AND SIKORSKY S-76 HELICOPTERS

Donald J. Baker

Aerostructures Directorate
USAARTA (AVSCOM)

NASA Langley Research Center
Hampton, Virginia

COMPOSITE COMPONENT DURABILITY PROGRAM OBJECTIVES

- Determine durability and maintainability of flight components
- Determine strength and stiffness retention of components after flight service
- Determine effect of environment on statically exposed specimens
- Compare strength retention of flight components and exposed specimens

OUTLINE

206L Program

S-76 Program

- Component description
- Flight service evaluation
- Residual strength tests
- Ground based environmental exposure tests
- Summary

OBJECTIVE OF BELL 206L PROGRAM

- Determine the durability of composite airframe structures in the commercial helicopter environment

- Establish confidence and accelerate acceptance of composite structures in commercial helicopters

SCOPE OF FLIGHT SERVICE EVALUATION

- Forty shipsets of components installed by operators
- Four general locations in the U. S. and Canada
- Periodic inspections
- Six shipsets removed at 1, 3, 5, 7 and 10 year intervals and returned for static test

LOCATION OF COMPOSITE COMPONENTS ON BELL MODEL 206L HELICOPTER

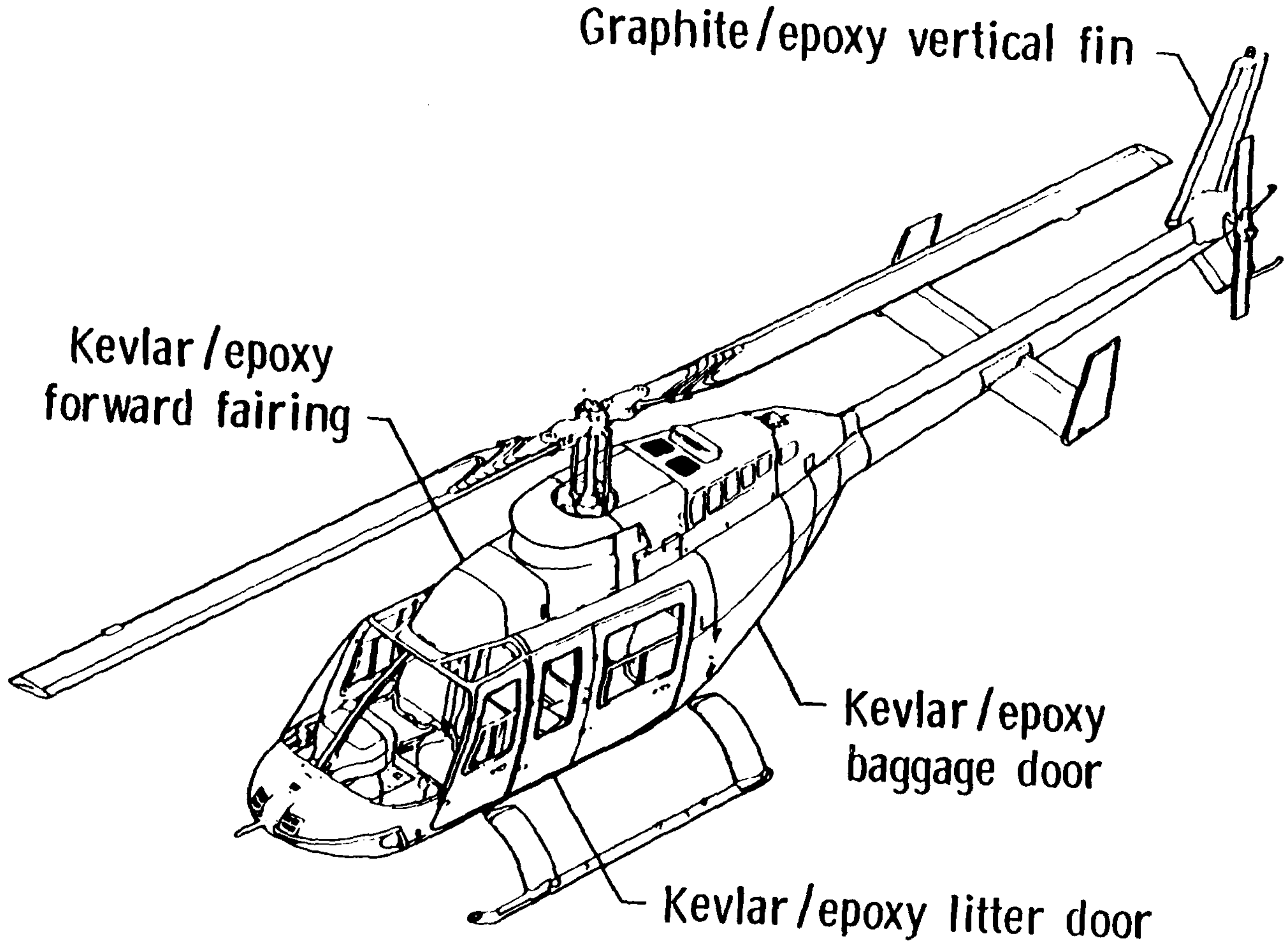

BELL 206L HELICOPTER COMPOSITE COMPONENTS

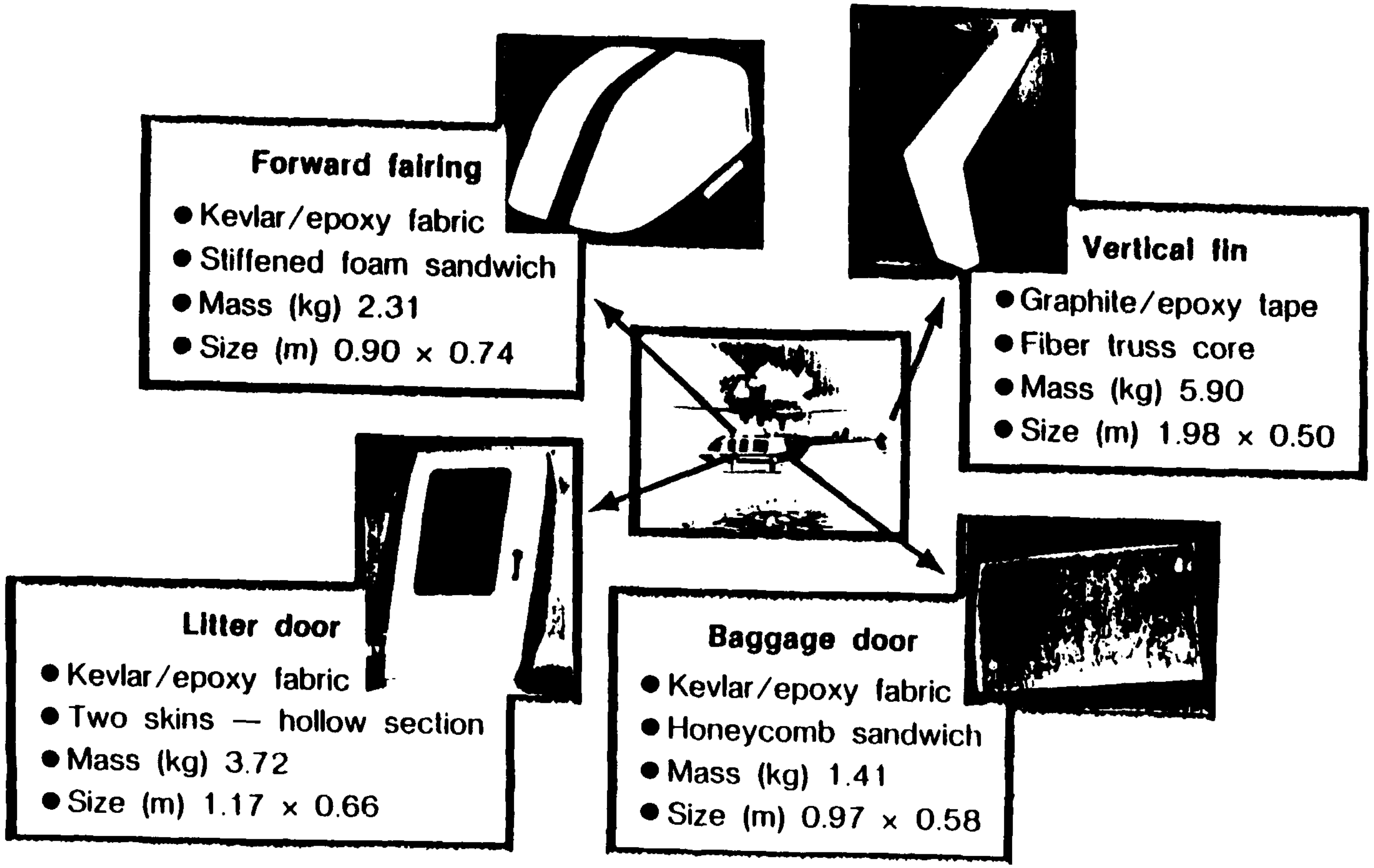

DISTRIBUTION OF BELL 206L HELICOPTERS WITH COMPOSITE COMPONENTS

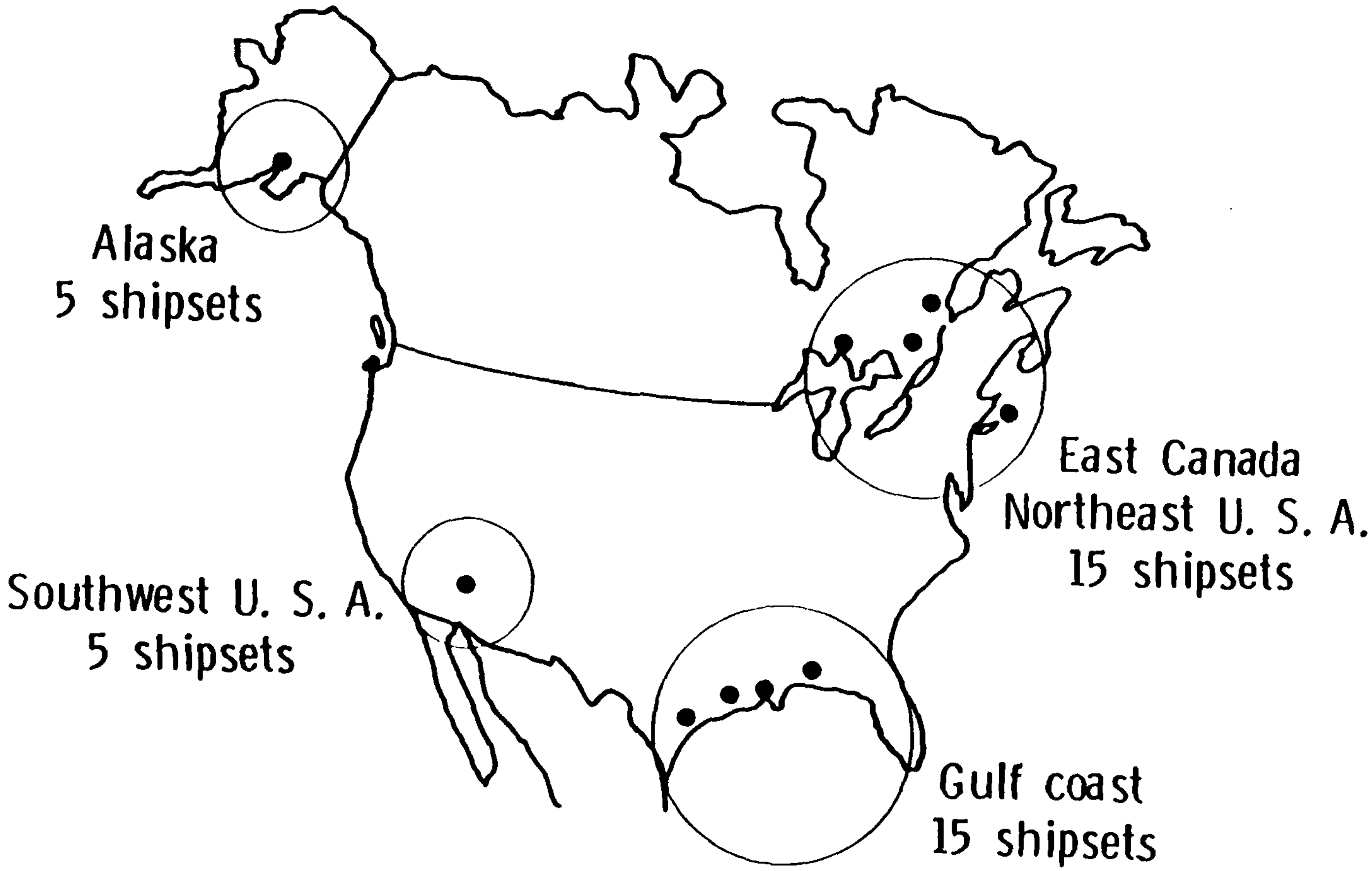

SUMMARY OF FLIGHT HOURS BY REGION

Region	Flight hours through 1988
Gulf of Mexico	67919
Northeast USA and East Canada	38195
Southwest USA	7920
Alaska	8321
Total	122355

SERVICE EXPERIENCE

- Forward fairing
  - Cracks on inner skin near latch on two doors revealed by 1985 inspection
  - Operators bonded a metal plate to underside of fairing for antenna grounding
- Vertical fin
  - Cracked paint on Kevlar leading edge caused by ground handling personnel
  - Lightning strikes on two fins

SERVICE EXPERIENCE

- Litter door
  - Metal hinge failures
  - Skin buckling on four doors located in Southwest U. S. A.
- Baggage door
  - Cracking of unsupported corners
  - Large disbonds between outer skin and NOMEX core

FAILURE LOADS FOR VERTICAL FIN

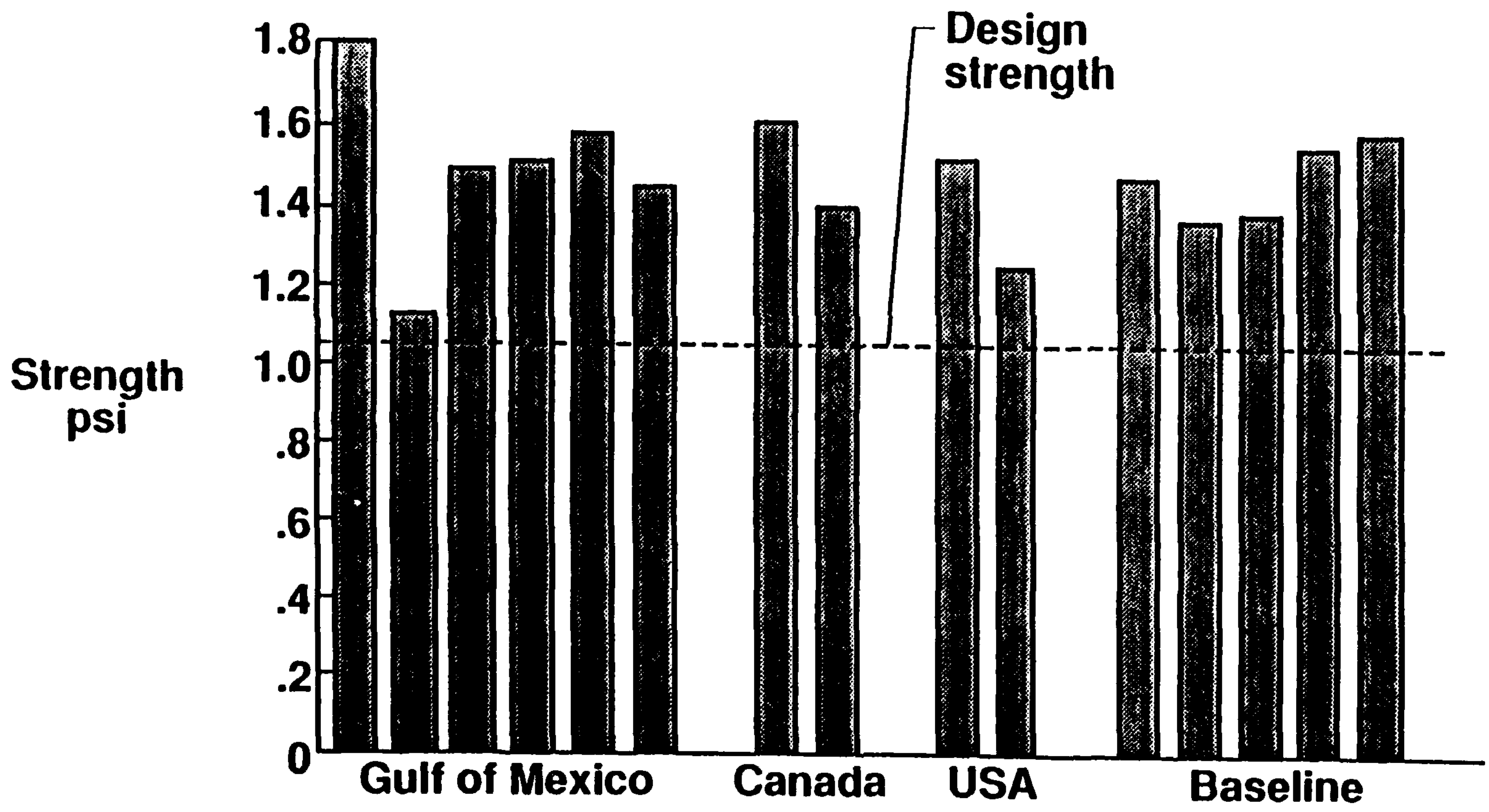

SLOPE OF LOAD DEFLECTION CURVES FOR VERTICALFIN

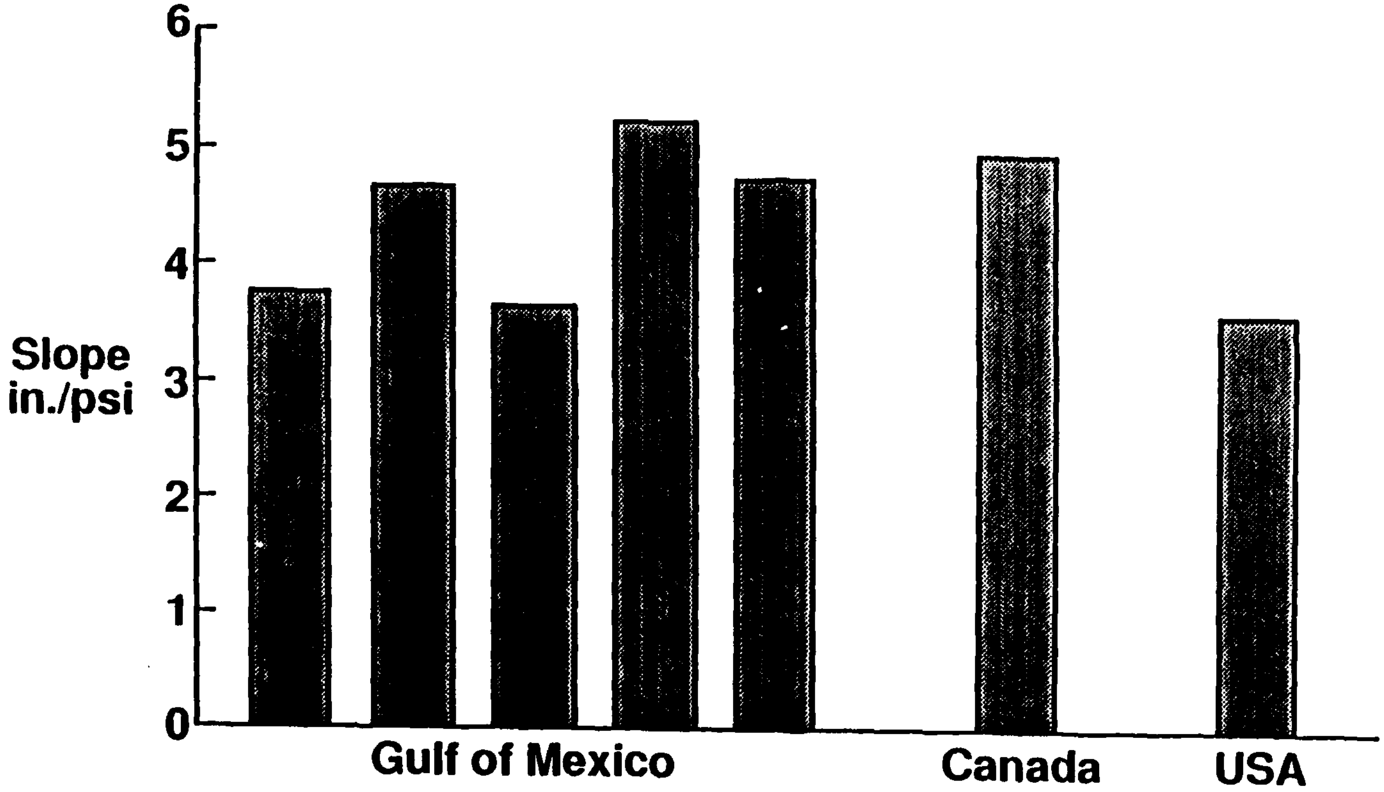

SLOPE OF LOAD DEFLECTION CURVES FOR BAGGAGE DOORS

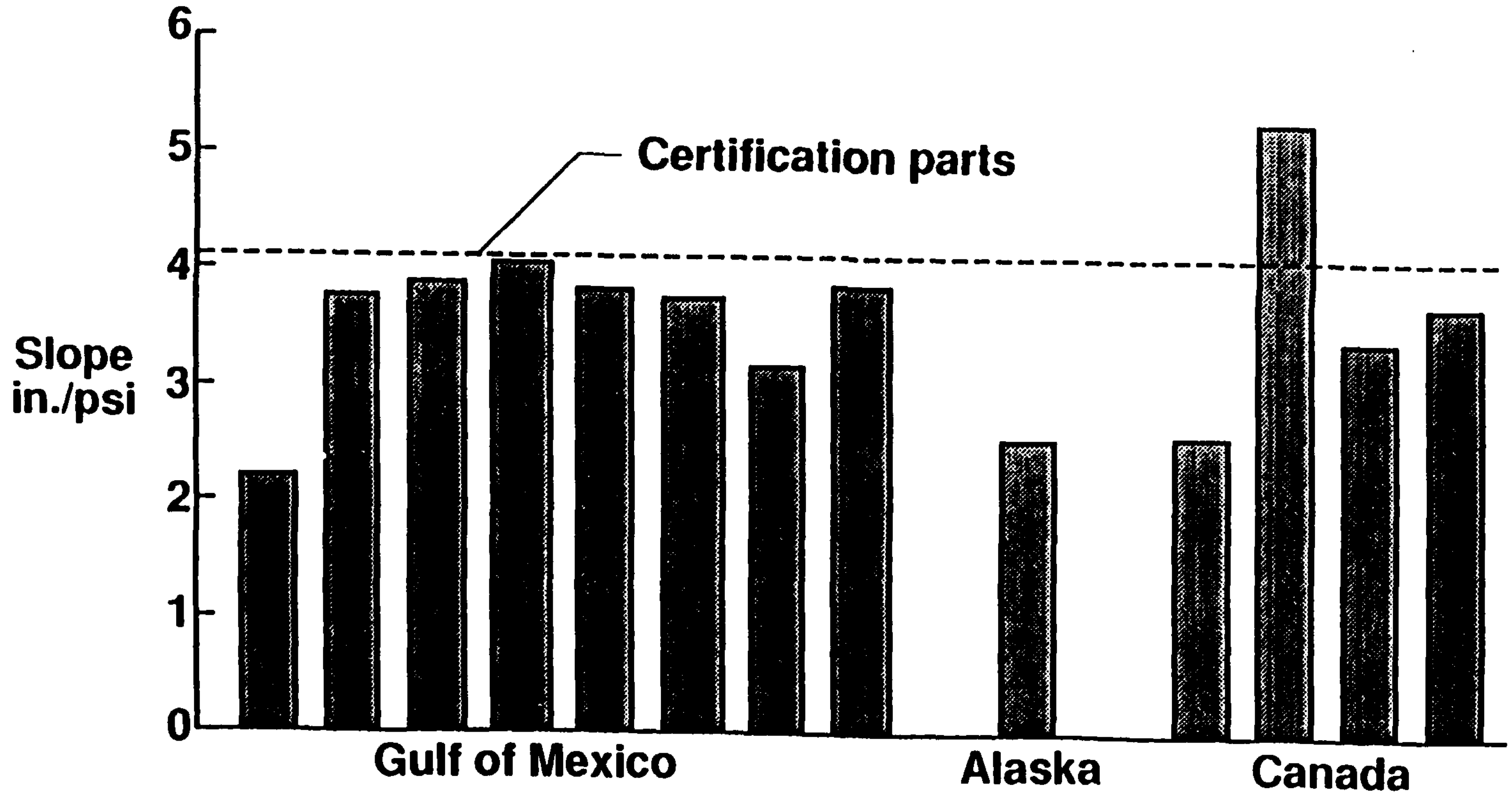

FAILURE LOADS FOR BAGGAGE DOORS

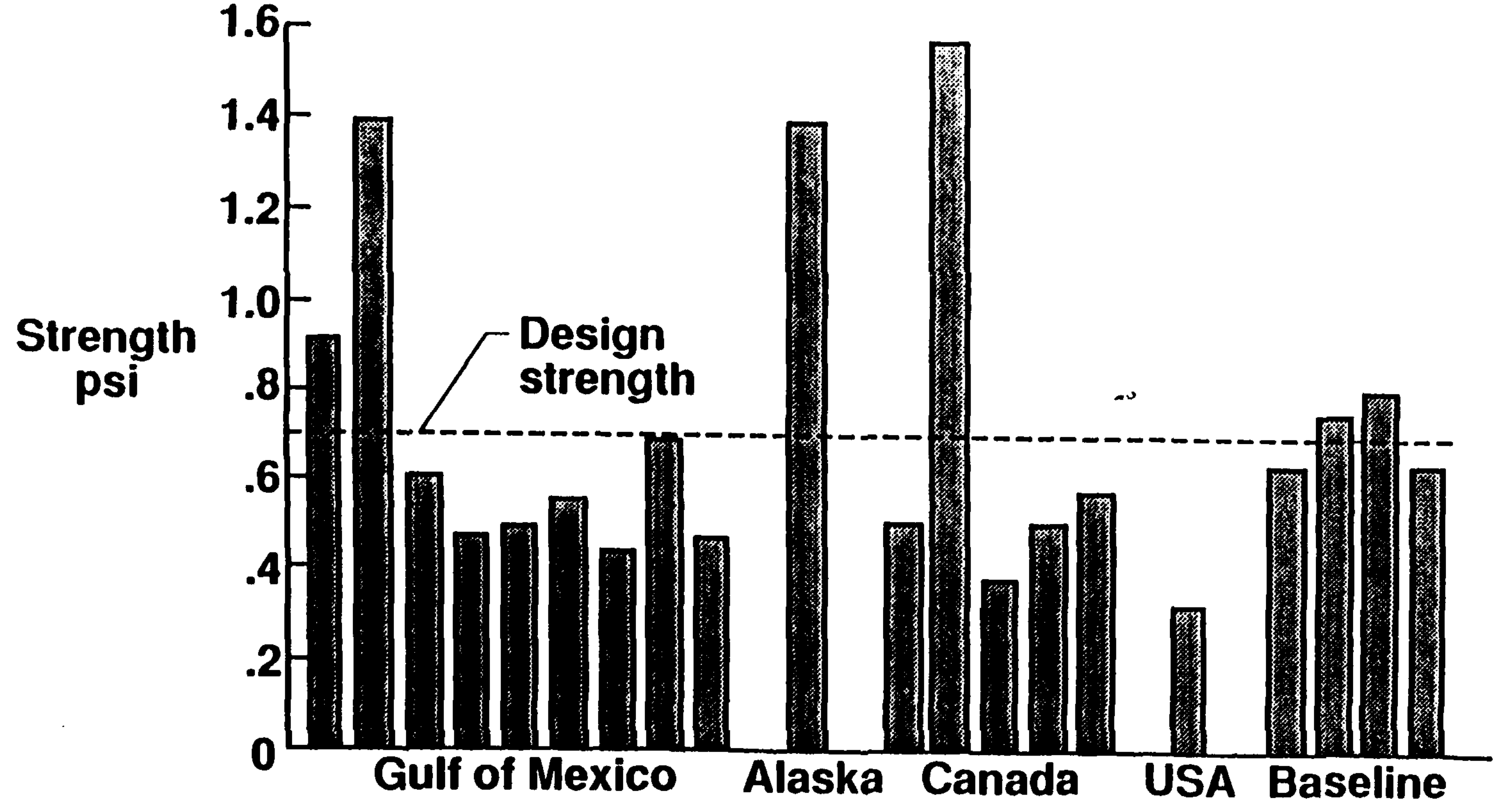

LOCATIONS OF GROUND BASED ENVIRONMENTAL EXPOSURE OF COMPOSITE MATERIALS USED IN BELL 206L COMPONENTS

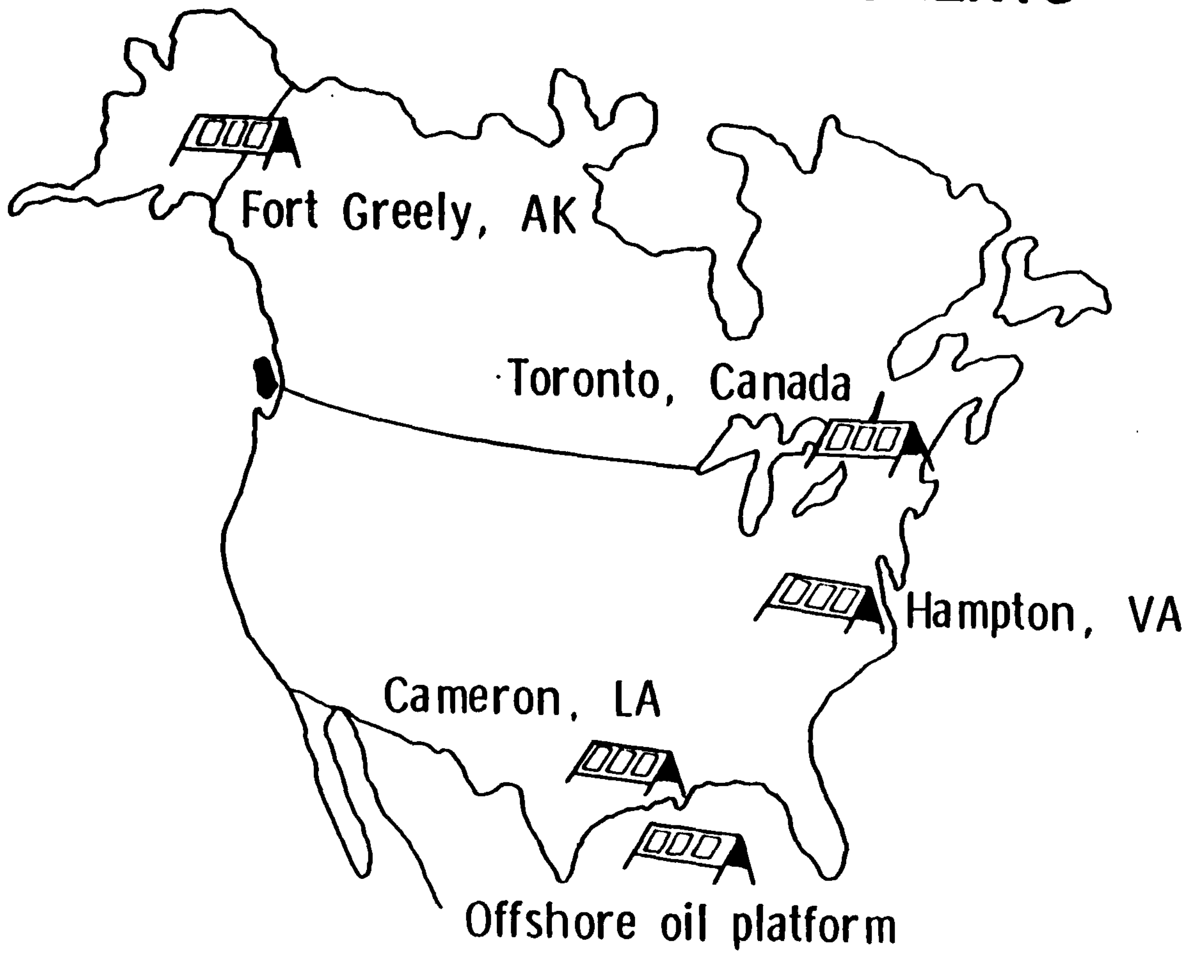

RESIDUAL STRENGTH OF COMPOSITE MATERIALS AFTER EXPOSURE

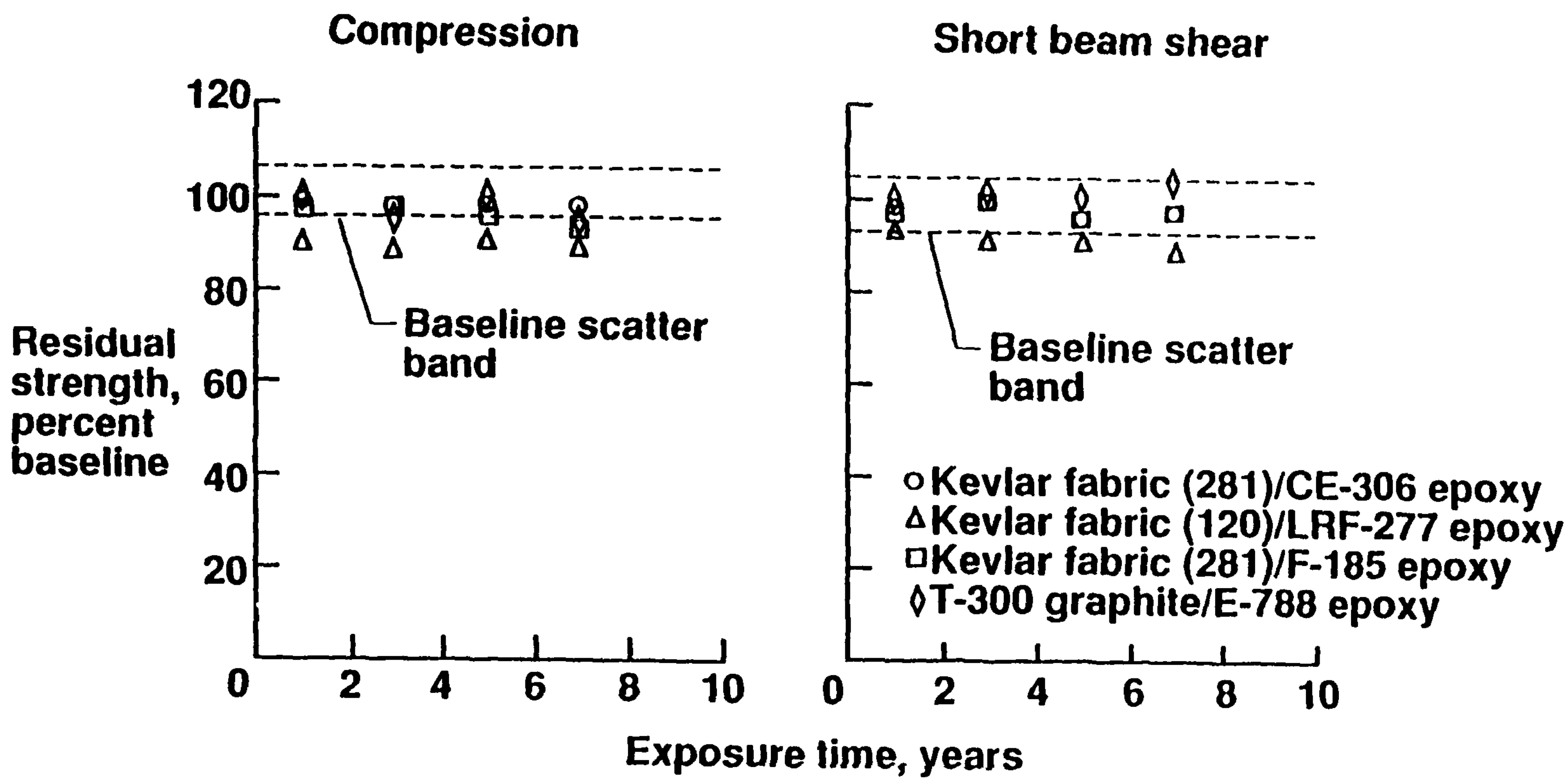

SUMMARY OF BELL 206L PROGRAM

- Composites have performed well in service
  - 122,000 hours of flight service accumulated
  - Very few problems in service
  - Strength of vertical fin exceeded the required design strength after service
  - 35 percent of baggage doors exceeded the design strength after service
- Residual short beam shear and compression strengths of ground exposure specimens exceed 88 percent of baseline after 5 years of exposure

OBJECTIVE OF SIKORSKY S-76 PROGRAM

- Determine the effects of flight service on statically and dynamically loaded composite components in production helicopters
- Correlate real-time in-service environmental effects with accelerated laboratory tests

COMPOSITE COMPONENTS IN FLIGHT SERVICE ON SIKORSKY S-76 HELICOPTER

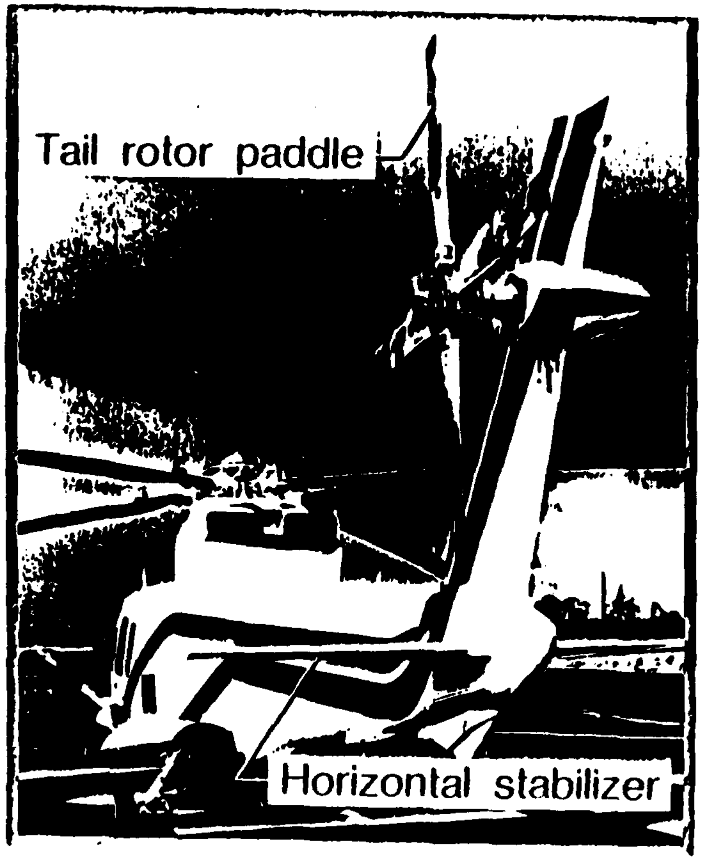

EVALUATION OF PRIMARY COMPOSITE COMPONENTS FROM SIKORSKY S-76 HELICOPTER

Tail rotor

- Graphite/epoxy spar
- Glass/epoxy skin
- Weight (kg) 6.6
- Size (m) 2.4 × .2

Horizontal stabilizer

- Graphite-Kevlar/epoxy spar
- Kevlar/epoxy skin
- Nomex honeycomb sandwich
- Weight (kg) 18.1
- Size (m) 2.9 × .8

SCHEDULE FOR REMOVAL OF S-76 COMPONENTS FROM SERVICE

Component	Years of service							
	2	3	4	5	6	7	8	9
Horizontal stabilizer	X		X		X		X	
Tail rotor spar	X	X	X	X		X		X
		X		X		X		
		X						

EFFECT OF FLIGHT SERVICE ON STRENGTH OF SIKORSKY S-76 COMPOSITE HORIZONTAL STABILIZER

Stabilizer test condition	Flight time, hr	Service region	Failure		Remarks
			Maximum static load, % DLL	Fatigue cycles	
After 17 months of commercial service	1600	Louisiana Gulf Coast	220	—	Torque box h/c core and splice plate failure
After 56 months of commercial service	3999	Louisiana Gulf Coast	—	Completed 500 000 at baseline certification load + 302 000 cycles at 105 % of baseline	No failure Failure
After 59 months of commercial service	4051	Louisiana Gulf Coast	—	Completed 500 000 cycles at baseline certification load + 59 980 cycles at 123 % of baseline	No failure Failure

EFFECT OF SERVICE ENVIRONMENT ON S-76 COMPOSITE TAIL ROTOR SPARS

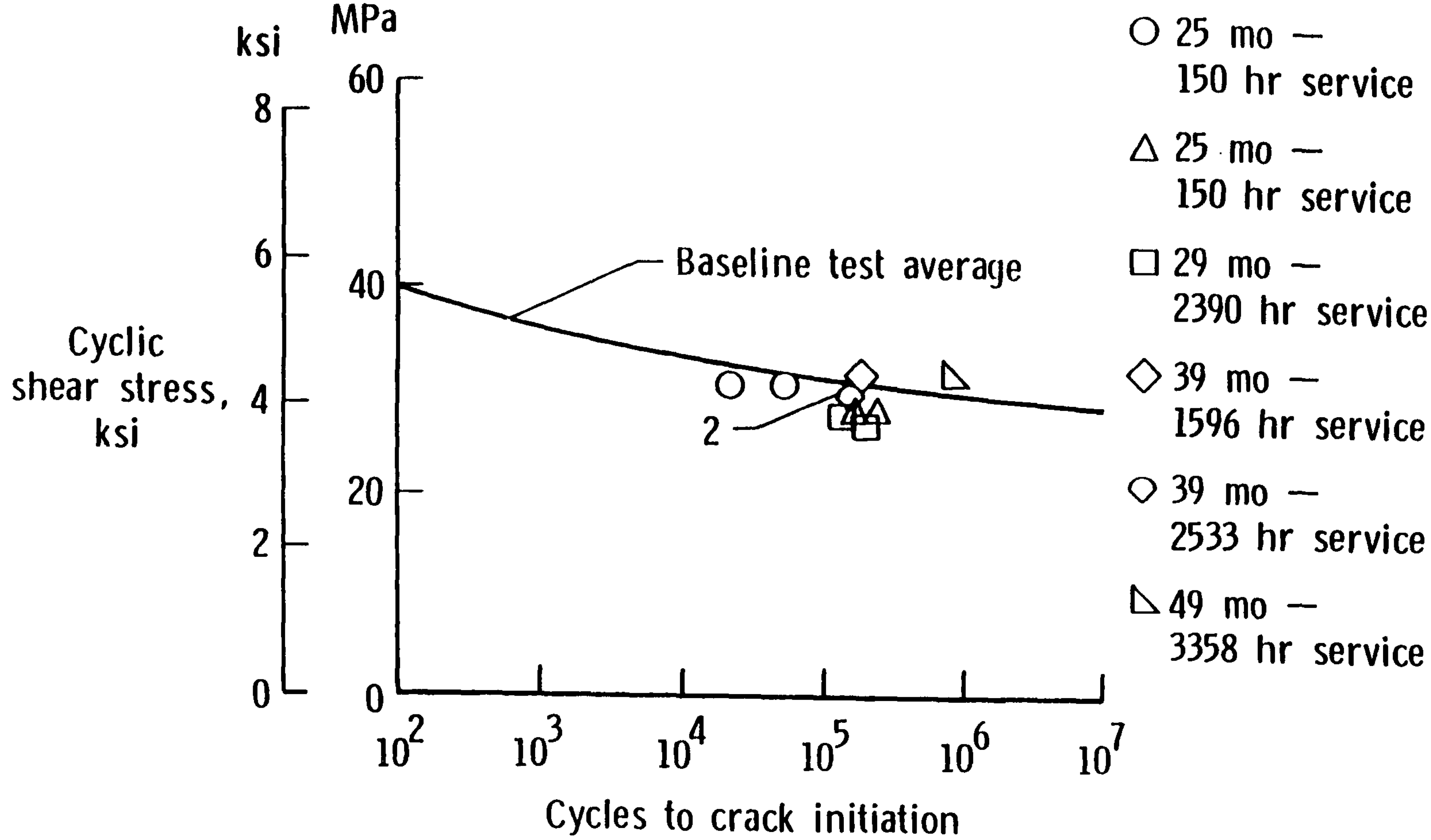

MOISTURE CONTENT OF S-76 TAIL ROTOR SPARS

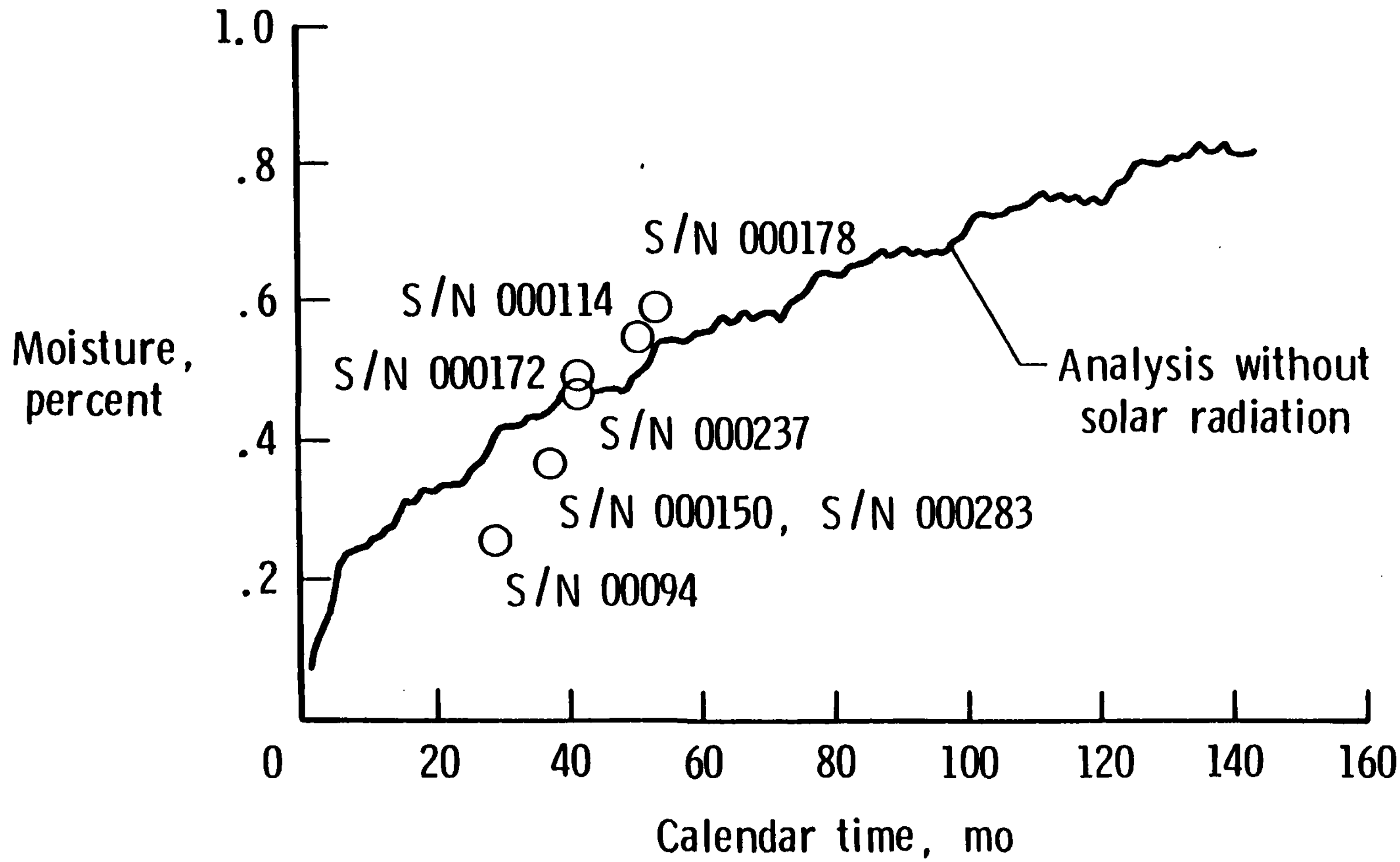

EFFECT OF MOISTURE ON THE RESIDUAL STRENGTH OF ASI/6350 GRAPHITE EPOXY

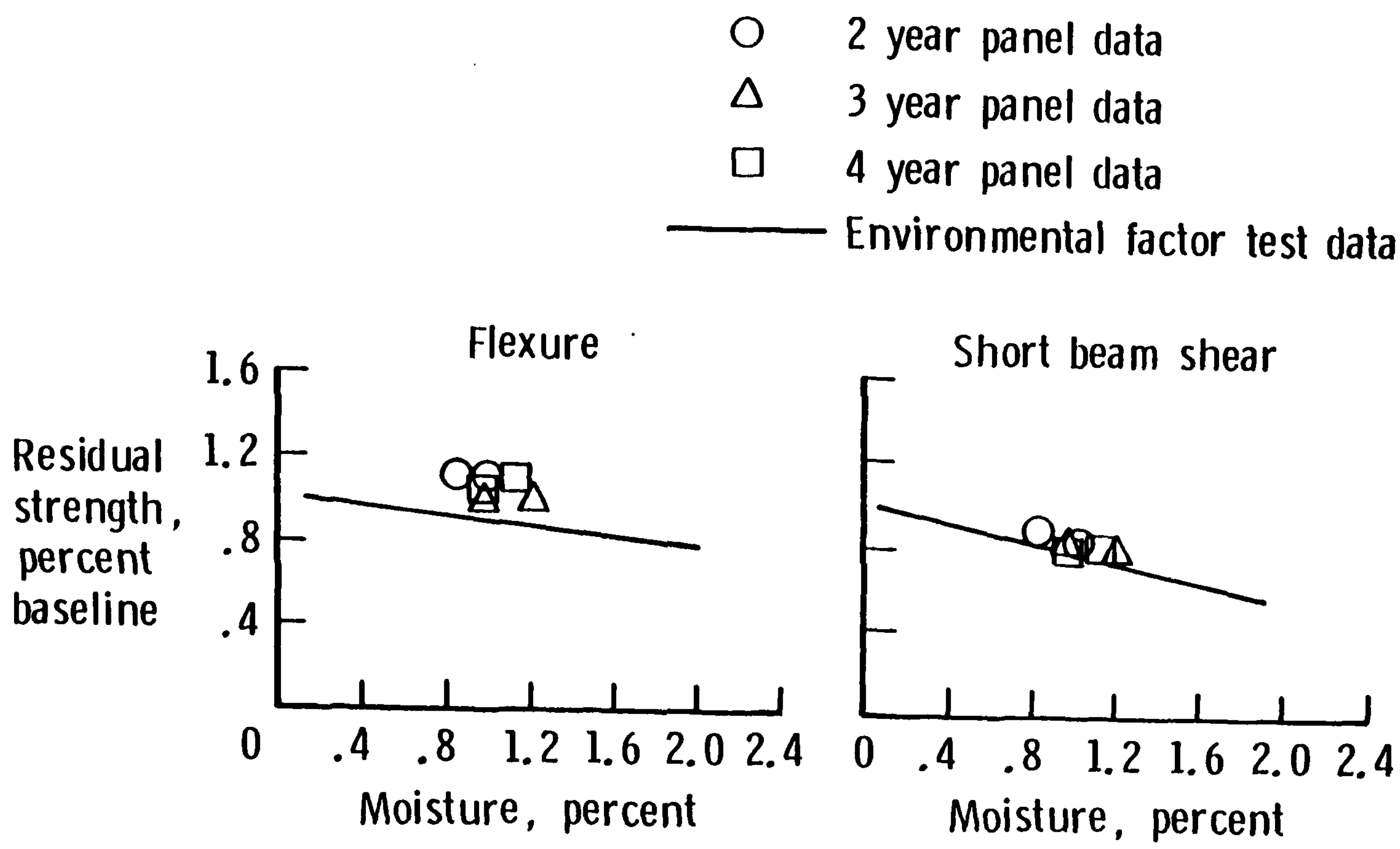

SUMMARY OF SIKORSKY S-76 PROGRAM

- 53146 hours accumulated on 14 components
- Residual strength of stabilizer with 17 months service was 220 percent of design ultimate load
- Fatique lives of stabilizers with 56 and 66 months of service exceeded certification
- Tail rotor spars retained 94 percent of baseline strength after 5 years
- Residual flexure and short beam shear strengths exceed the accelerated tests after outdoor exposure

LUNCHEON ADDRESS

Joseph Goldberg
Program Manager
Sikorsky Aircraft-UTC

"Composite Developments in Rotor Systems"

UNAVAILABLE PRIOR TO PRESENTATION

SESSION III

TAILORED LAMINATES

Robert W. Arden
U. S. Army AVSCOM
Chairman

THE REDUCTION OF HYGROTHERMAL EFFECTS ON TENSION-TORSION COUPLING IN COMPOSITE ROTOR BLADES

Stephen C. Hill

Rensselaer Polytechnic Institute

September 14, 1989

THE REDUCTION OF HYGROTHERMAL EFFECTS ON TENSION-TORSION COUPLING IN COMPOSITE ROTOR BLADES

- Introduction and Background
- Theoretical Work
    - Tension-Torsion Coupling
    - Hygrothermal Model
- Experimental Work
- Conclusions

TENSION-TORSION COUPLING: Twisting response of rotor blade to axial tension.

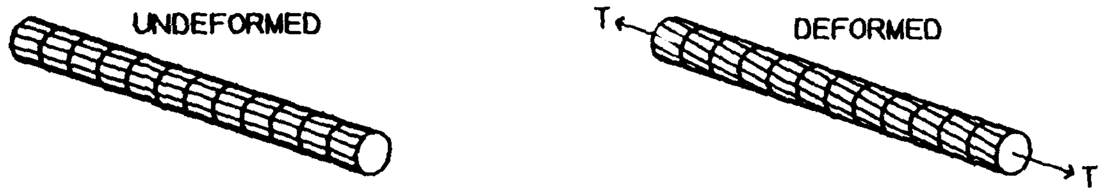

HYGROTHERMAL EFFECTS (TEMPERATURE AND MOISTURE): Change the properties of the matrix which can alter the coupling response.

RESEARCH THRUST:

- Measure changes in coupling caused by HT effects.
- Develop predictive mathematical models of coupling.
- Minimize changes in coupling from HT effects while preserving the coupling.

BACKGROUND

HYGROTHERMAL EFFECTS

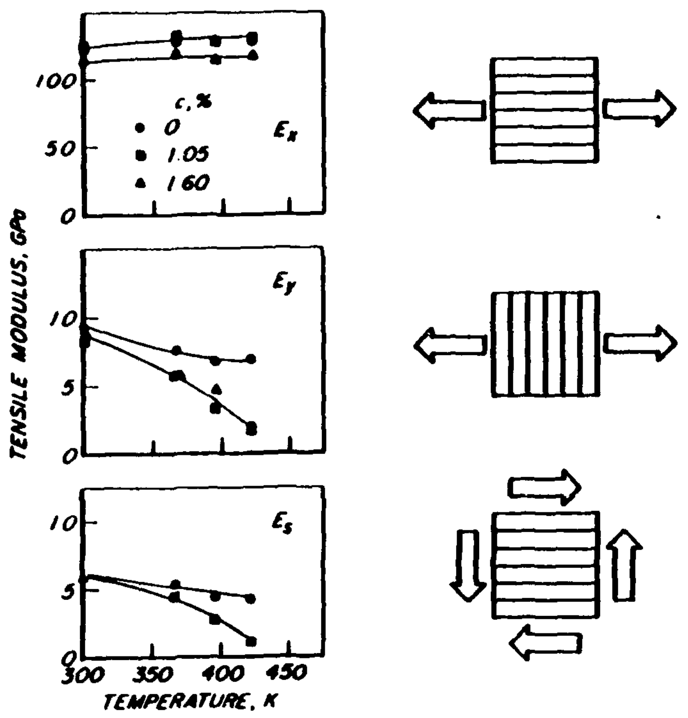

Tsai, S. W. and Hahn, H. T.
Introduction to Composite Materials
Technomic, 1980, p. 384.

COUPLING

- Performance
  - Nixon, M. - NASA Langley
  - Bauchau, O., and Bryan, P.
    - Rensselaer Polytechnic
- Aeroelastic Tailoring
  - Hong and Chopra
    - University of Maryland

Why is coupling desirable?

- Variation of performance with changing rotor speeds.
- Aeroelastic tailoring.

Current rotor blades do *not* use tension-torsion coupling.

Why aren't HT effects as great a concern for current rotor blades?

- HT changes affect matrix properties.
- Current designs use 0° fibers for bending and ±45° fibers for torsion. <u>These modes are fiber-dominated.</u> (Coupling depends on matrix-dominated modes.)

WHERE DOES COUPLING COME FROM?

- Single unidirectional ply:

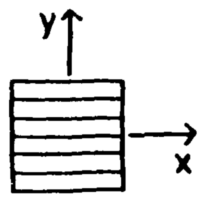

$$\begin{Bmatrix} \sigma_x \\ \sigma_y \\ \sigma_s \end{Bmatrix} = \begin{bmatrix} Q_{xx} & Q_{xy} & 0 \\ Q_{xy} & Q_{yy} & 0 \\ 0 & 0 & Q_{ss} \end{bmatrix} \begin{Bmatrix} \epsilon_x \\ \epsilon_y \\ \epsilon_s \end{Bmatrix}$$

- Transform to laminate axes.

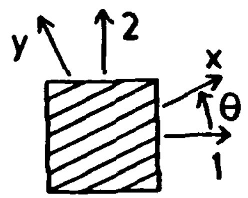

$$\begin{Bmatrix} \sigma_1 \\ \sigma_2 \\ \sigma_6 \end{Bmatrix} = \begin{bmatrix} Q_{11} & Q_{12} & Q_{16} \\ Q_{12} & Q_{22} & Q_{26} \\ Q_{16} & Q_{26} & Q_{66} \end{bmatrix} \begin{Bmatrix} \epsilon_1 \\ \epsilon_2 \\ \epsilon_6 \end{Bmatrix}$$

Note: Non-zero Axial-Shear Coupling Term.

- Integrate through laminate thickness.

$$\begin{Bmatrix} N_1 \\ N_2 \\ N_6 \end{Bmatrix} = \begin{bmatrix} A_{11} & A_{12} & A_{16} \\ A_{12} & A_{22} & A_{26} \\ A_{16} & A_{26} & A_{66} \end{bmatrix} \begin{Bmatrix} \epsilon_1 \\ \epsilon_2 \\ \epsilon_6 \end{Bmatrix} \Rightarrow \begin{Bmatrix} \epsilon_1 \\ \epsilon_2 \\ \epsilon_6 \end{Bmatrix} = \begin{bmatrix} a_{11} & a_{12} & \boxed{a_{16}} \\ a_{12} & a_{22} & a_{26} \\ \boxed{a_{16}} & a_{26} & a_{66} \end{bmatrix} \begin{Bmatrix} N_1 \\ N_2 \\ N_6 \end{Bmatrix}$$

Coupling between axial force and shear deformation.

FOR THIN-WALLED TUBES:

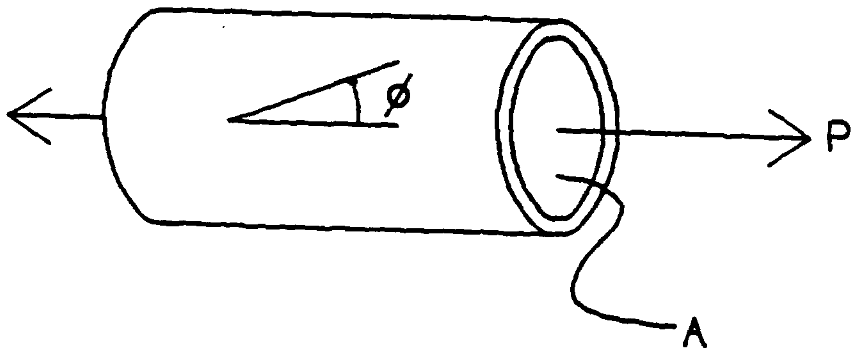

TWIST RATE

$$\phi' = -\frac{a_{16}}{2A} P$$

NOTE DEPENDENCE ON TENSION-TORSION COUPLING TERM (a_{16})

THERMAL STRAIN AND ISOTROPY

- SHEAR STRAIN MAY ALSO BE CREATED BY THERMAL EFFECTS.

- PLY AXES

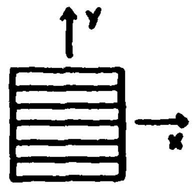

$$\begin{Bmatrix} \epsilon_x \\ \epsilon_y \\ \epsilon_s \end{Bmatrix}^{THERMAL} = \begin{Bmatrix} \alpha_x \\ \alpha_y \\ 0 \end{Bmatrix} \Delta T$$

NOTE: NO THERMAL SHEAR STRAIN IN PLY AXIS SYSTEM

- TRANSFORM TO LAMINATE AXES

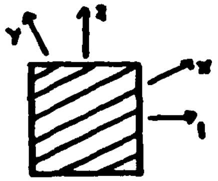

$$\begin{Bmatrix} \epsilon_1 \\ \epsilon_2 \\ \boxed{\epsilon_6} \end{Bmatrix}^{THERMAL} = \begin{Bmatrix} \alpha_1 \\ \alpha_2 \\ \alpha_6 \end{Bmatrix} \Delta T$$

THERMAL SHEAR STRAIN WILL PRODUCE TUBE TWIST DUE TO TEMPERATURE CHANGE.

- $[\theta/\theta+90]_T$ LAMINATES USED FOR TUBE WALLS
  - THERMALLY ISOTROPIC : $\alpha_{6\,LAMINATE} = 0$, NO THERMAL SHEAR
  - TENSION - TORSION COUPLING EXISTS : $a_{16} \neq 0$

MODEL OF HYGROTHERMAL EFFECTS

- Lump HT effects into single parameter, η: $\eta = \eta(T, c)$
- Use this as a modifier of shear modulus

  $$\boxed{Q_{ss} = \bar{Q}_{ss}\,\eta(T, c)}$$

  $\bar{Q}_{ss}$ is some reference value of shear modulus.
- Why only modifiy shear modulus?
  - Shear modulus dominates tension-torsion coupling.
  - Other matrix-dominated parameters show smaller effects.
- Example of η from experimental data:

  $$\eta(T;c) = (0.9449) + (5.578\times10^{-3})T - (68.83\times10^{-6})T^2$$

LAMINATES STUDIED

- Built from hygrothermally-isotropic laminates.
- Single Material
  - $[(\theta/\theta+90)]_T$
- Hybrid laminates (more than one material)
  - Since shear effects play most important role, use reinforcing fibers to counteract shear.
  - $[(\theta/\theta+90)^{G}_{\zeta_G}/(\theta\pm45)^{F}_{\zeta_F}]_T$

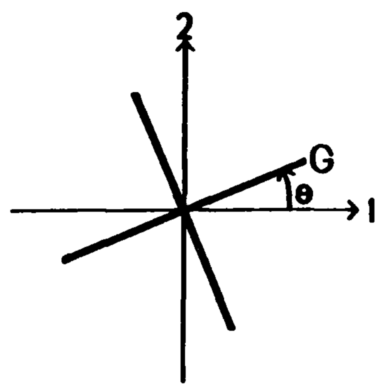

$[(\theta/\theta+90)]_T$

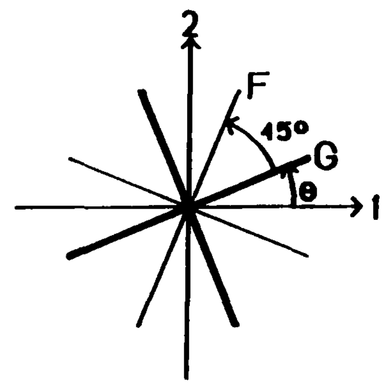

$[(\theta/\theta+90)^{G}_{\zeta_G}/(\theta\pm45)^{F}_{\zeta_F}]_T$

OPTIMAL LAYUP FOR HYBRID LAMINATE

- Tension-torsion coupling term has same form for both laminates:

$$\boxed{\bar{a}_{16} = \frac{1}{4}(\sin 4\theta)\,\bar{a}_c^o(\eta)}$$

  Optimization of coupling due to geometric (θ) and HT (η) effects may be performed separately.

- Geometry used to maximize coupling: $\theta = 22.5°$

- Want to minimize effect of η on coupling
  - Need ζ^f which minimizes change in coupling due to HT effects.
  - This results in cubic equation for ζ^f.
  - Difficult to get feel for what happens physically from solution to this equation.
  - Rely on numerical results.

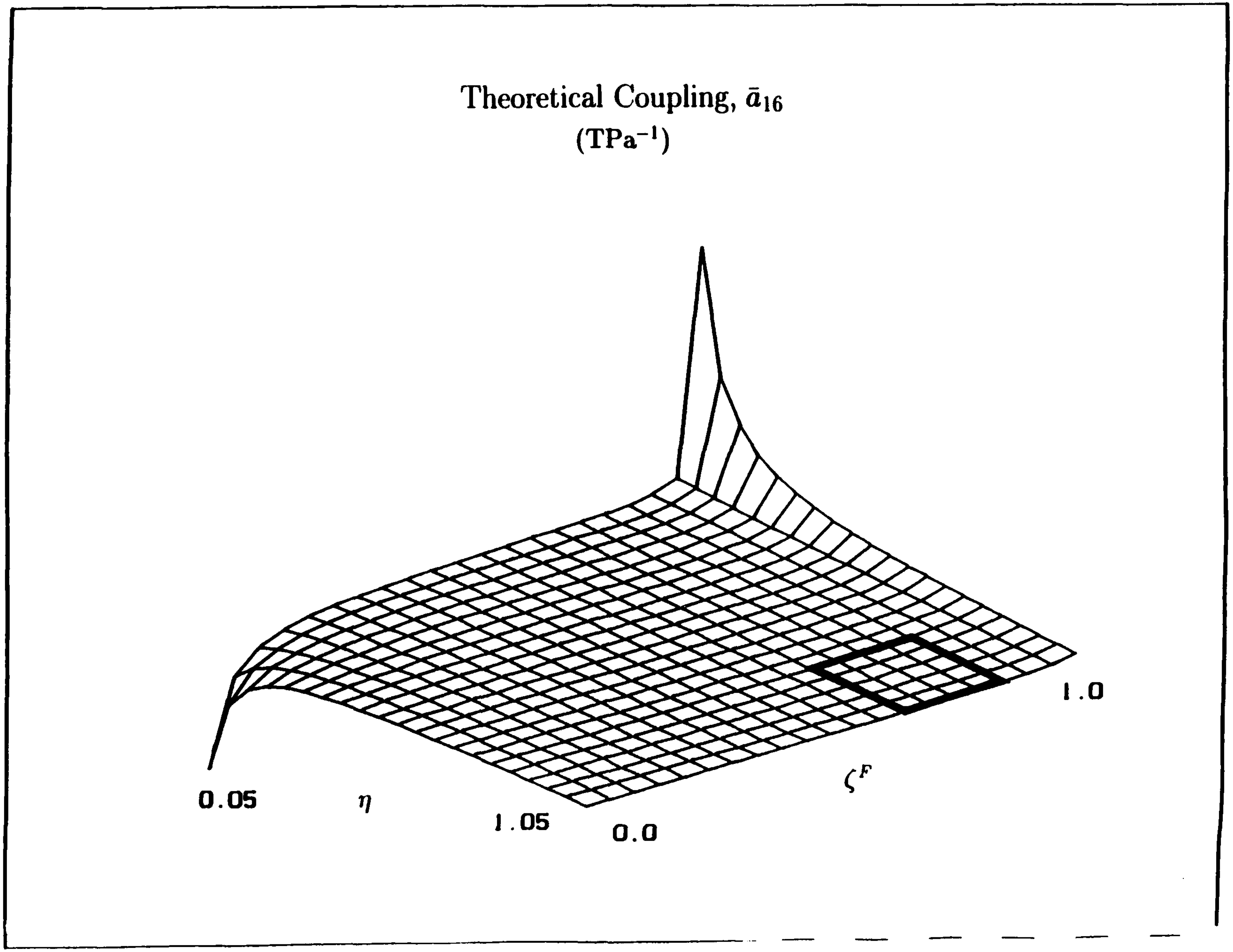

Theoretical Coupling, $\bar{a}_{16}$
(TPa^{-1})
0.05
η
1.05
0.0
ζ^F
1.0

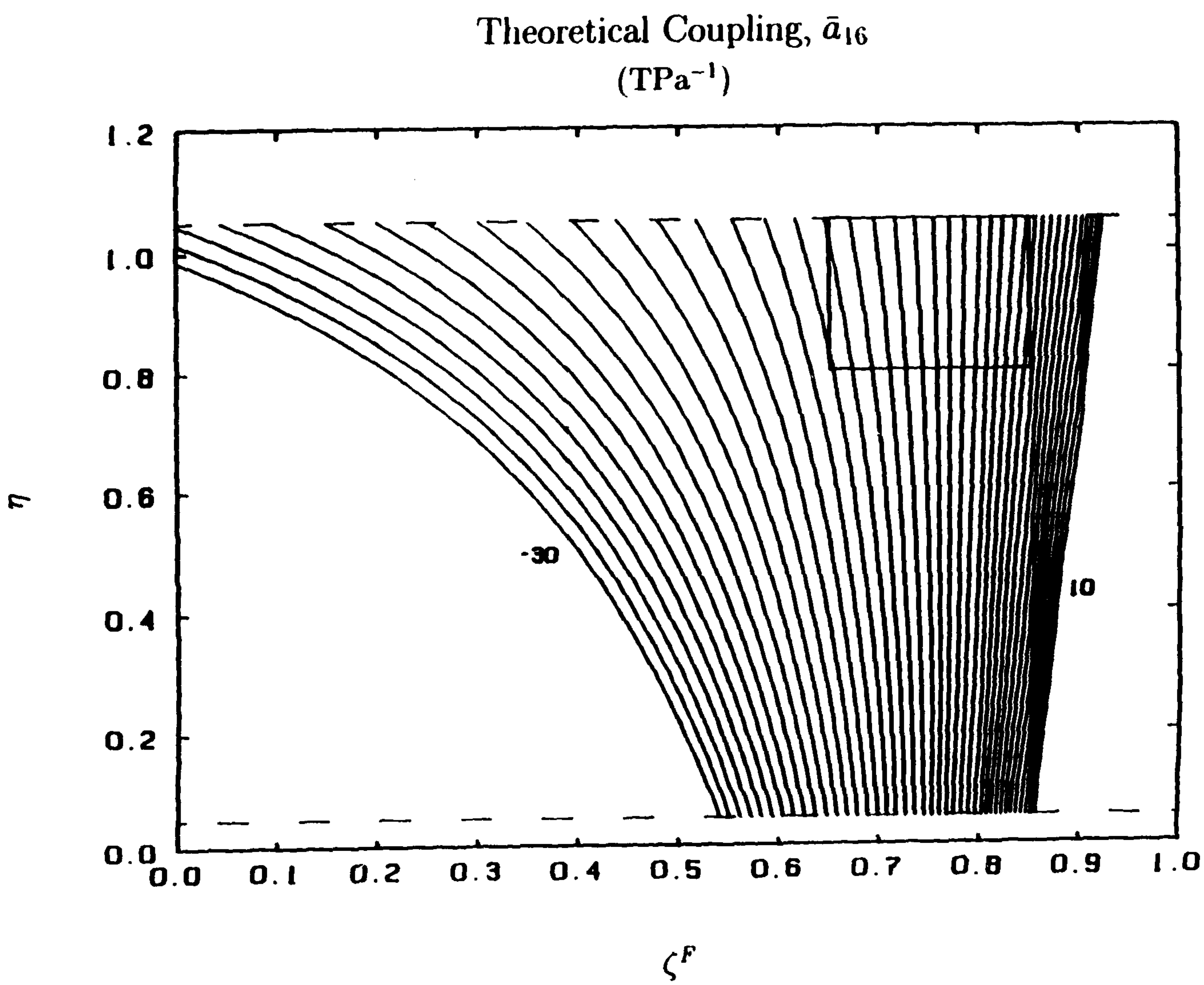
Theoretical Coupling, $\bar{a}_{16}$
(TPa^{-1})
η
ζ^F
-30
10
0.0
0.1
0.2
0.3
0.4
0.5
0.6
0.7
0.8
0.9
1.0
1.2

Thickness Ratio ζ^F as Function of η for $\left[(\Theta/\Theta+90)^G_{\zeta^G} / (\Theta \pm 45)^F_{\zeta^F}\right]_T$ Laminates

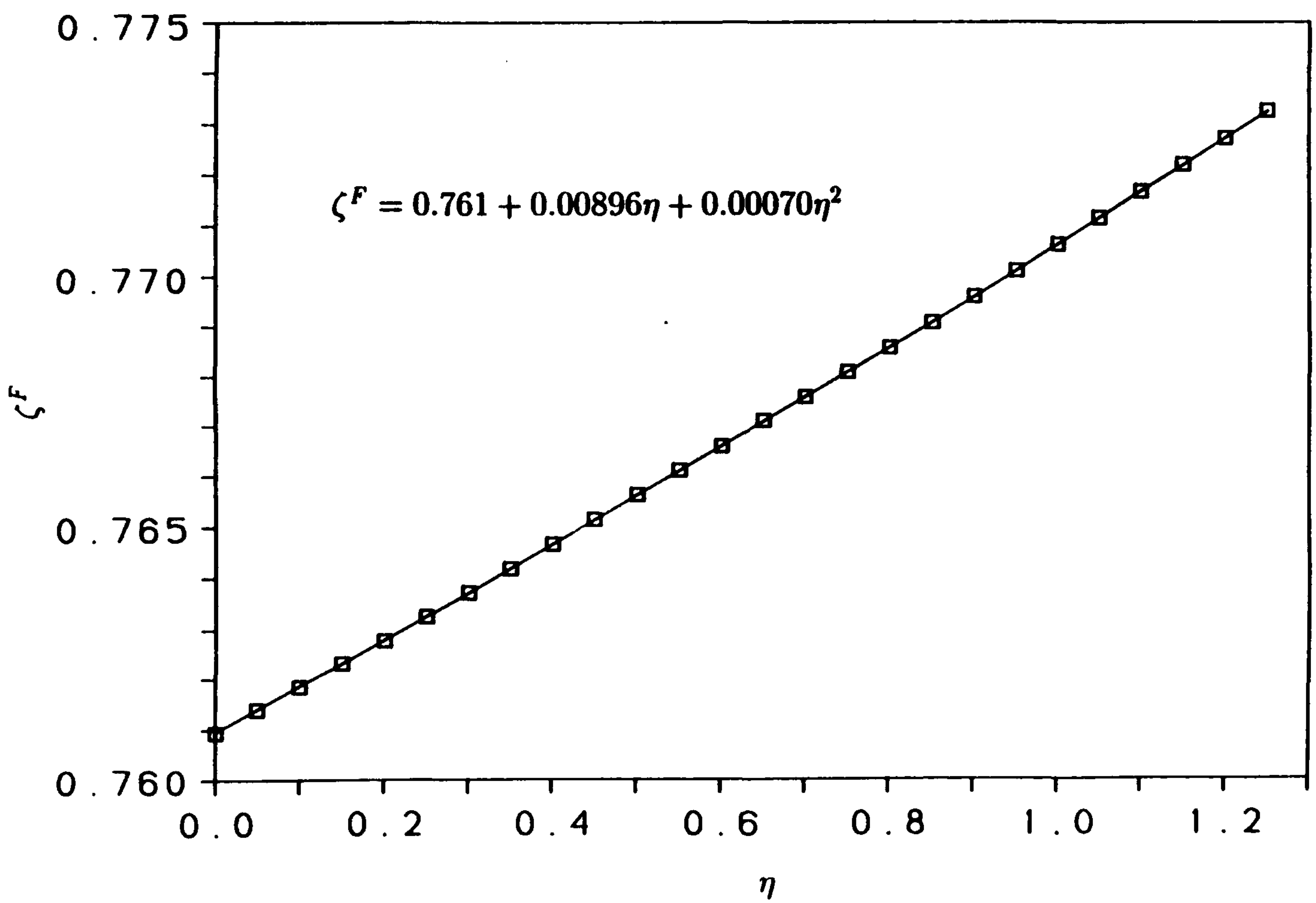

Theoretical Hygrothermal Variation of Coupling $\bar{a}_{16}$ for Various ζ^F's for $\left[(\Theta/\Theta+90)^G_{\zeta^G}\,/\,(\Theta\pm 45)^F_{\zeta^F}\right]_T$ Laminates

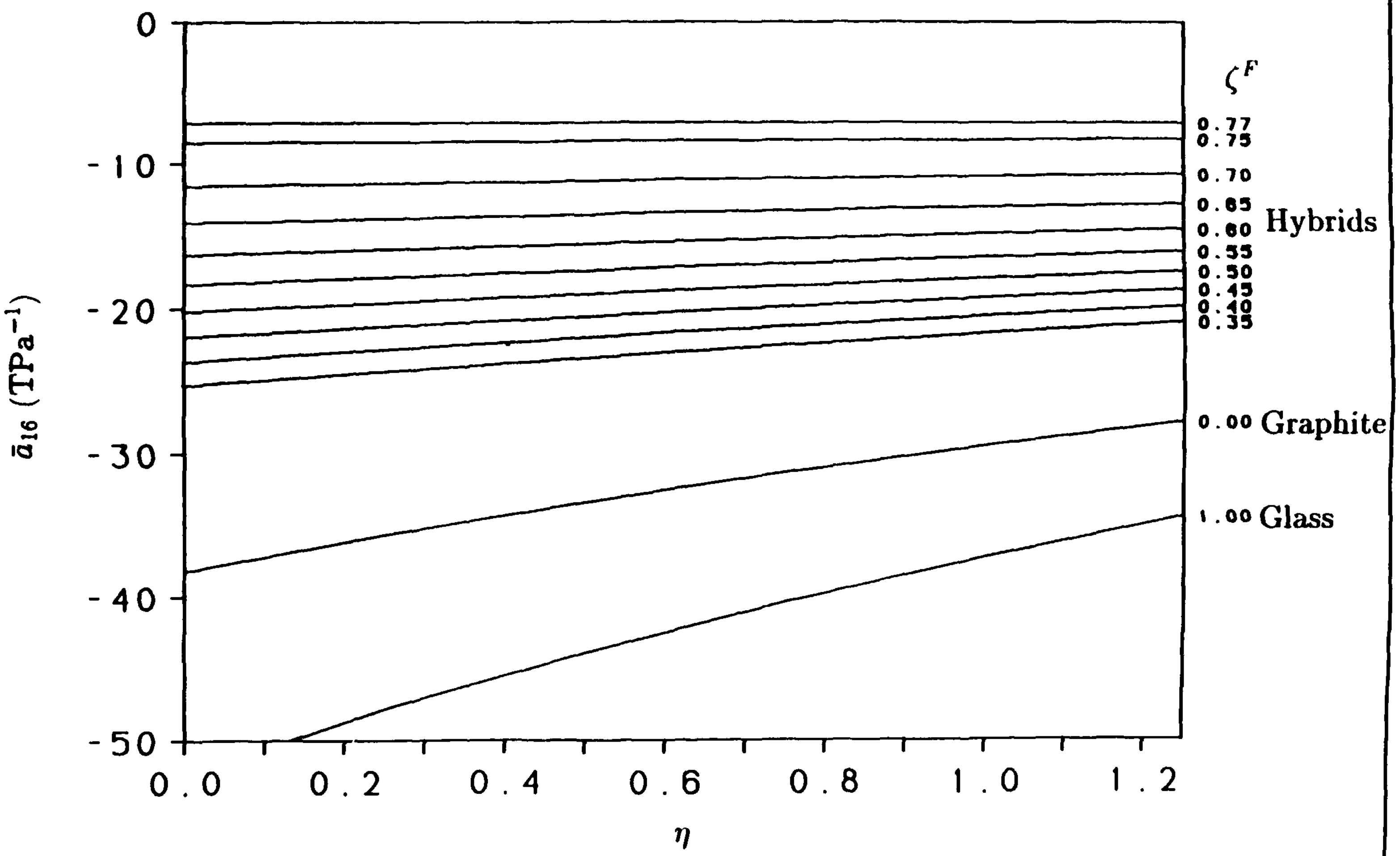

EXPERIMENTAL WORK

TEST SPECIMENS

- Circular Cylinders
  - 12" long, 1" diameter
  - Thin-walled
- Why circular cross-section?
  - Ease of construction
  - Similarity to rotor blade torque box
  - Does not warp out-of-plane
    - Simplifies mounting

TESTS

- Vary temperature and moisture content
- Applied Torsion
  - Unidirectional laminates $[0_2]_T$
  - Measure shear modulus
- Applied Tension
  - Various laminates $[\theta/\theta+90]_T$ etc.
  - Measure coupling

TEST RIG

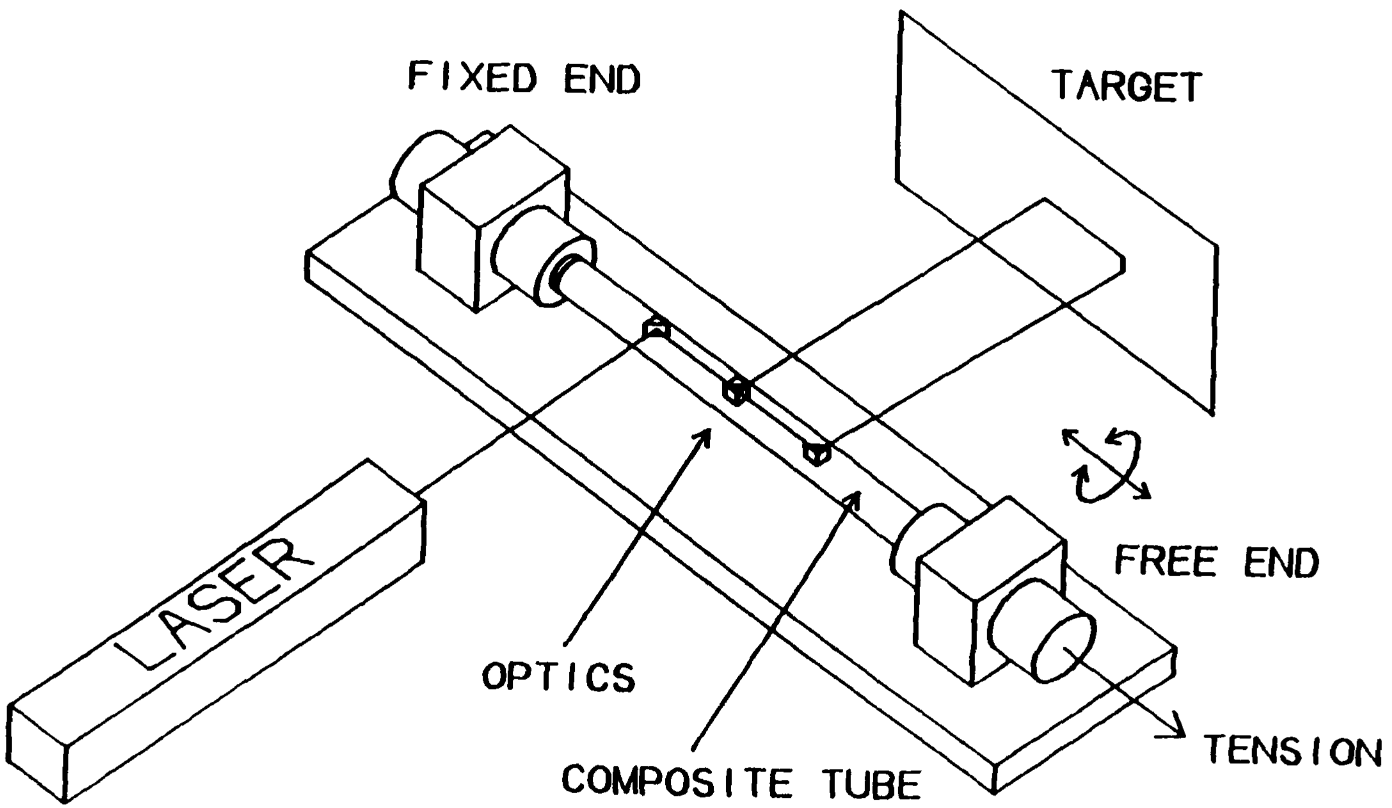
FIXED END
TARGET
LASER
OPTICS
FREE END
COMPOSITE TUBE
TENSION

Experimental Shear Modulus for Dry Conditions

$c = 0.0218\%$

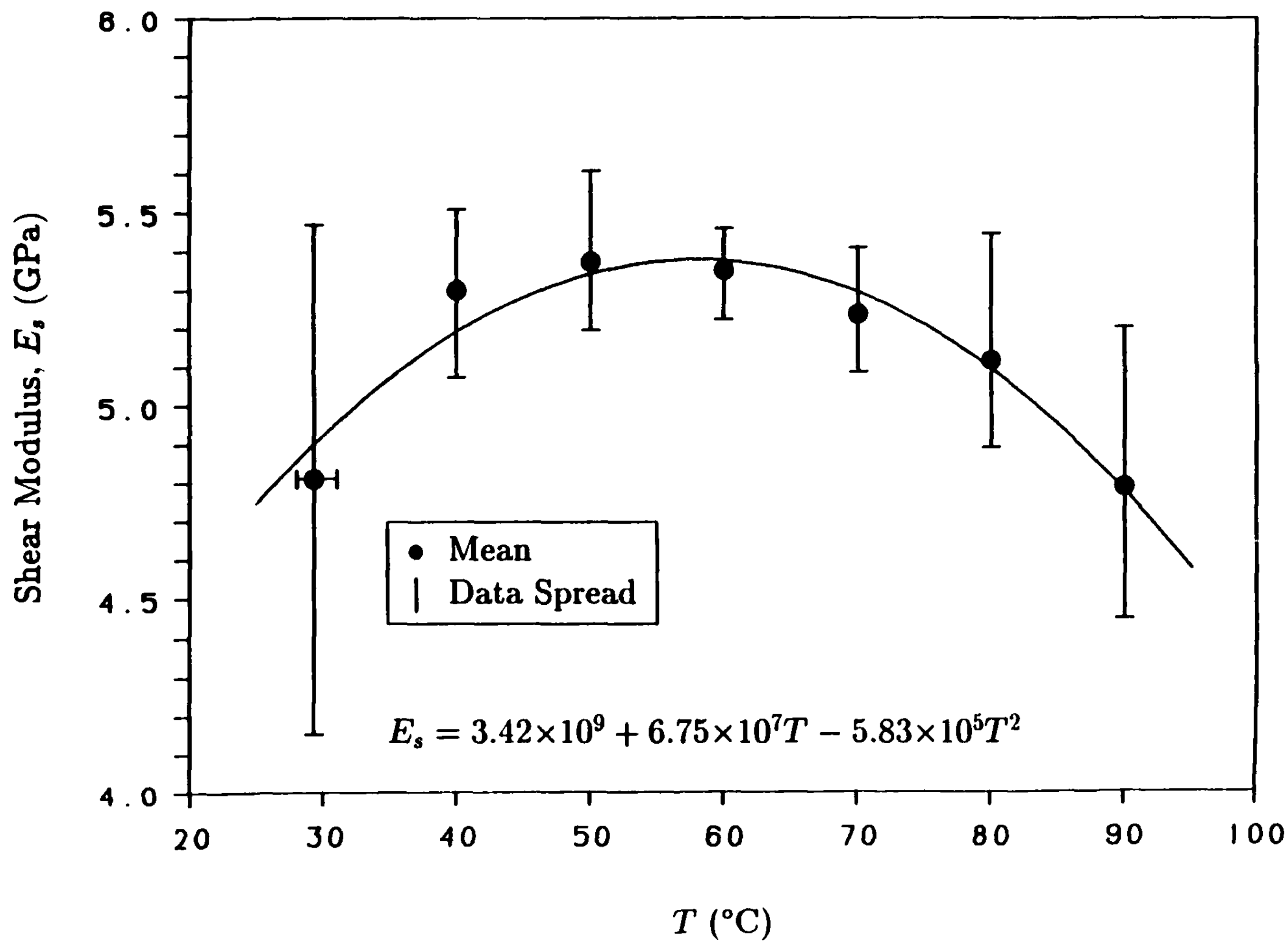

Experimental Shear Modulus for Room-Air Conditions

$c = 0.243\%$

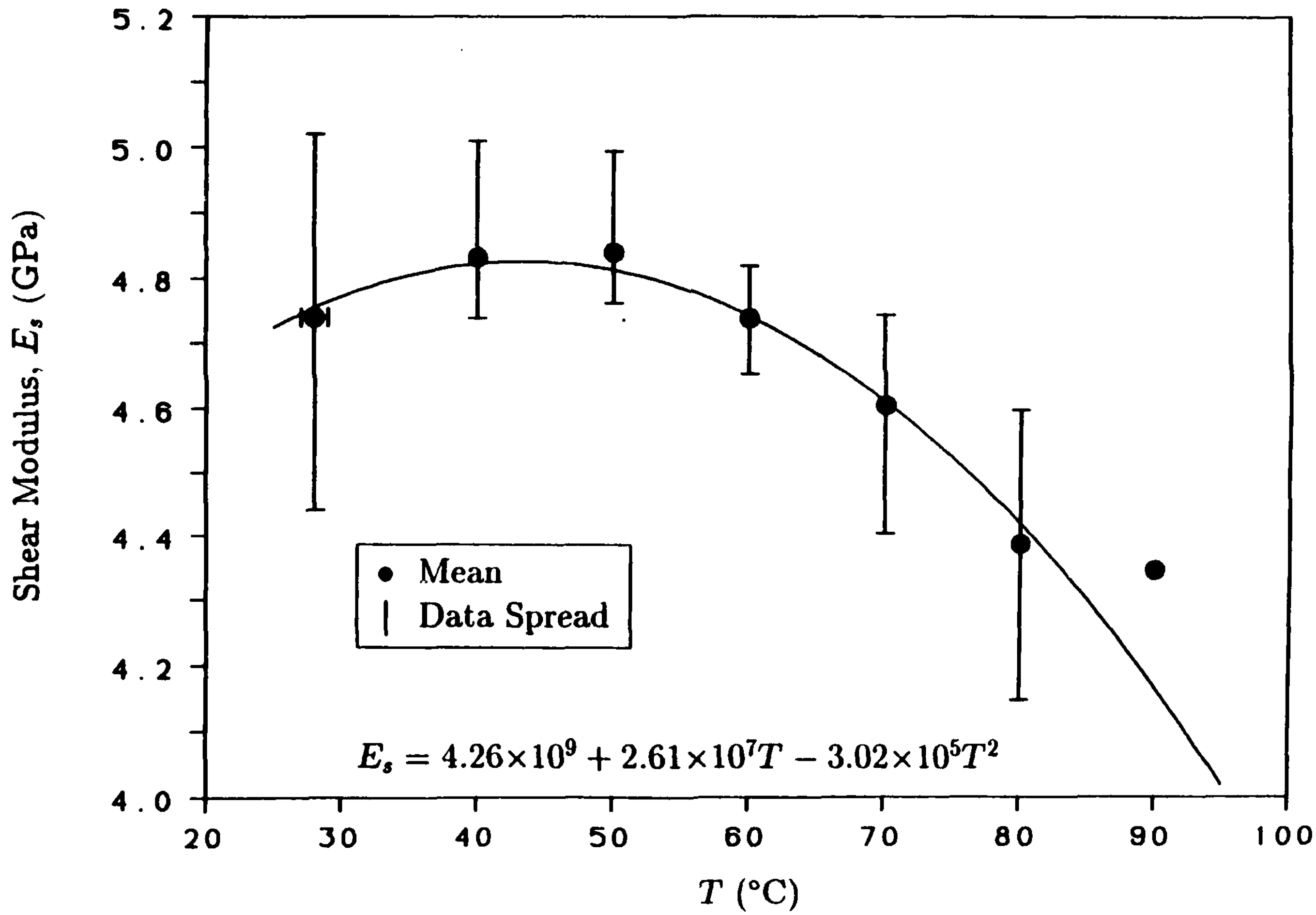

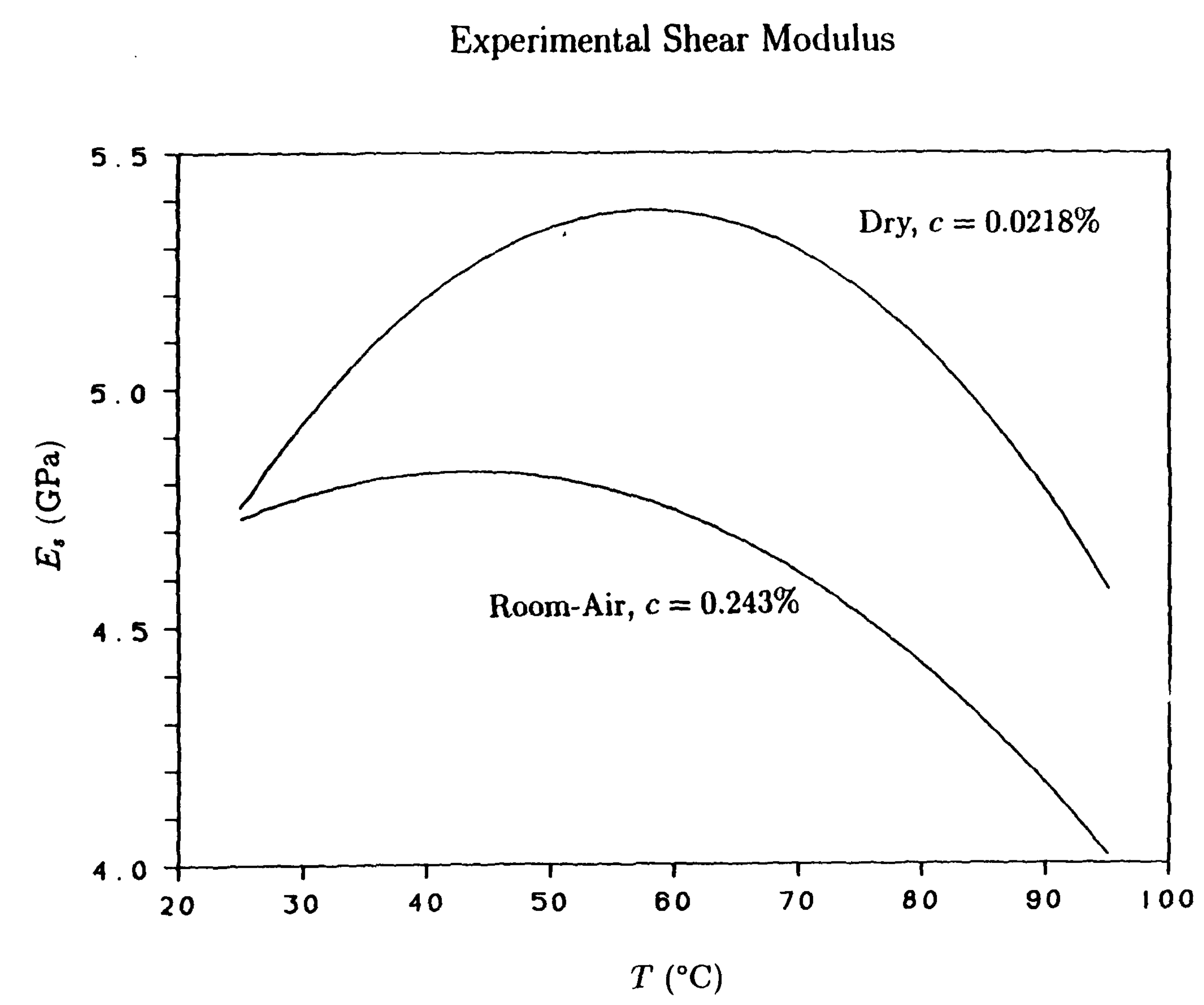
Experimental Shear Modulus
Dry, c = 0.0218%
Room-Air, c = 0.243%
E_s (GPa)
5.5
5.0
4.5
4.0
20
30
40
50
60
70
80
90
100
T (°C)

Experimental Coupling for $[\Theta/\Theta + 90]_{mT}$ Laminates

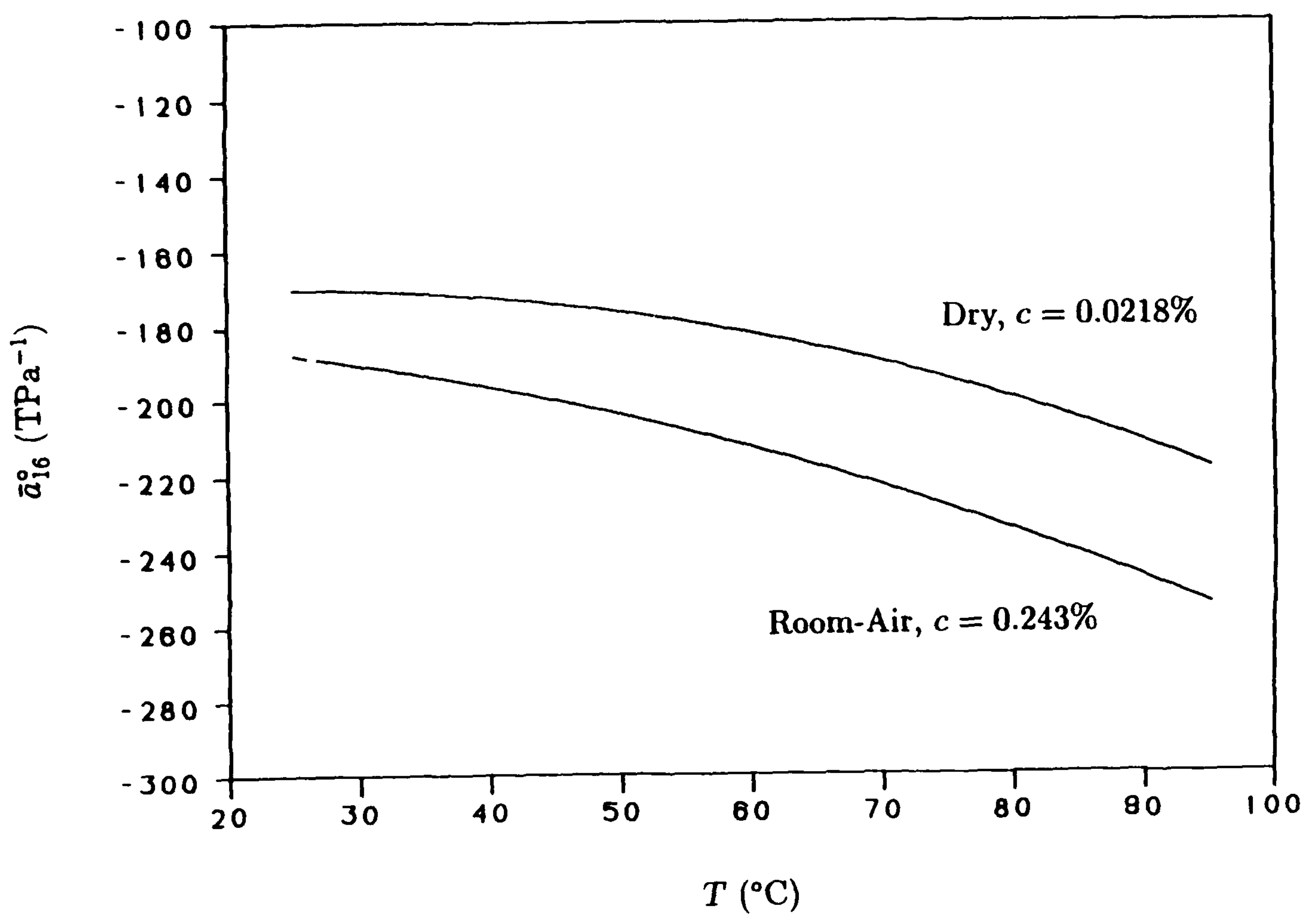

Experimental Variation of Coupling, $\bar{a}_C$, for Various ζ^F's

Room Air, $\left[(\Theta/\Theta+90)^G_{\zeta^G} / (\Theta\pm 45)^F_{\zeta^F}\right]_T$ Laminates

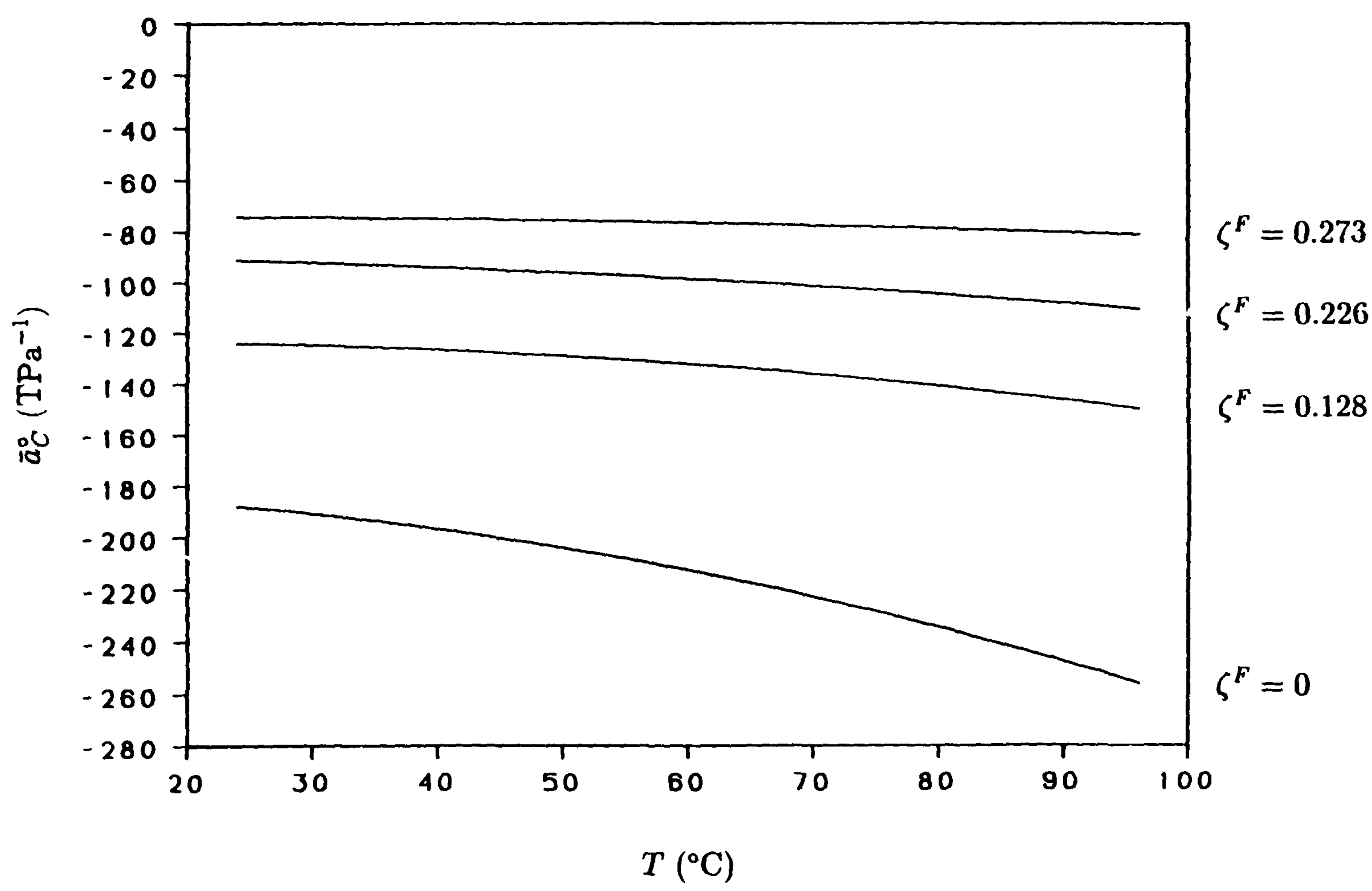

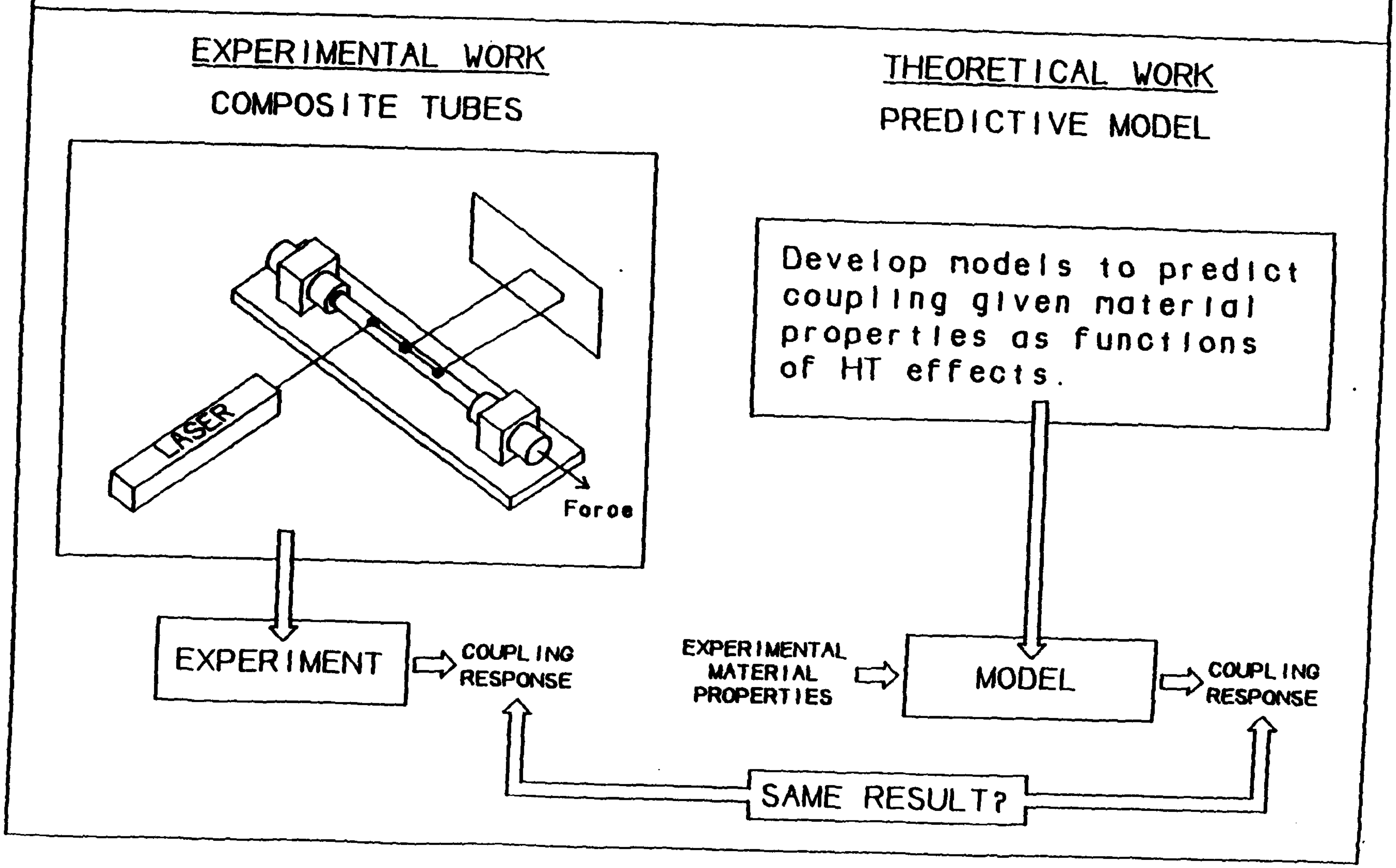
EXPERIMENTAL WORK
COMPOSITE TUBES
LASER
Force
EXPERIMENT
COUPLING RESPONSE
THEORETICAL WORK
PREDICTIVE MODEL
Develop models to predict coupling given material properties as functions of HT effects.
EXPERIMENTAL MATERIAL PROPERTIES
MODEL
COUPLING RESPONSE
SAME RESULT?

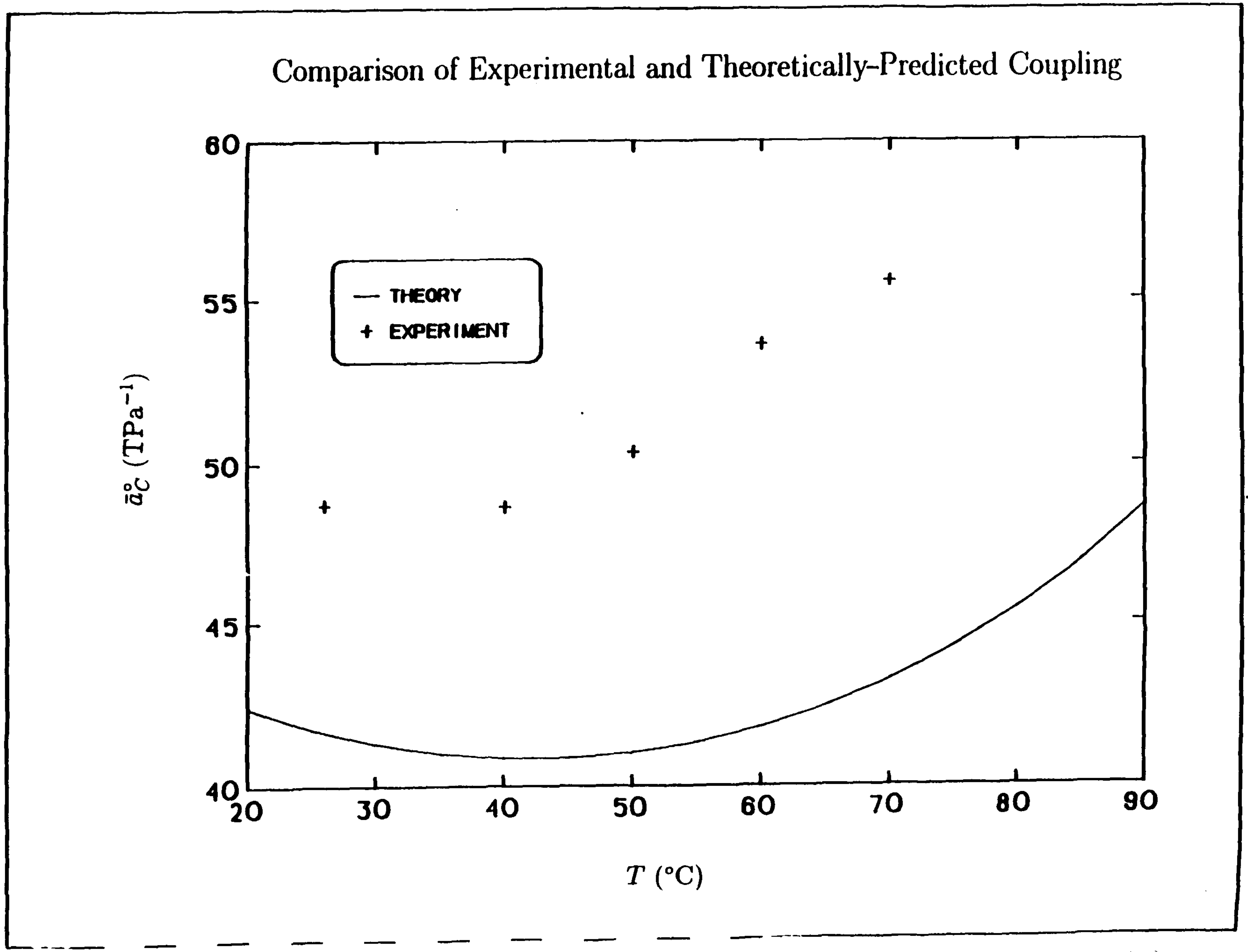

Comparison of Experimental and Theoretically-Predicted Coupling
THEORY
EXPERIMENT
60
55
50
45
40
20
30
40
50
60
70
80
90
$\bar{a}_C^\circ$ (TPa^{-1})
T (°C)

CONCLUSIONS

- Hygrothermal effects can have a significant influence on material properties.
- It is possible to design laminates with the desired tension-torsion coupling which exhibit minimal or no variation due to hygrothermal effects.

"Importance of Elastic Tailoring in Design Analysis of Thin-Walled Composite Beams"

Ali R. Atılgan
Georgia Institute of Technology, Atlanta, Georgia

Lawrence W. Rehfield
University of California, Davis, California

and

Dewey H. Hodges
Georgia Institute of Technology, Atlanta, Georgia

ACCOMPLISHMENTS IN MODELING FOR THIN-WALLED COMPOSITE BEAMS

- Rehfield and Atilgan (1986) (New Coupling Mechanisms, Warping and Shear Deformation Models)
- Rehfield and Atilgan (1987) (Single Cell)
- Rehfield, Atilgan and Hodges (1988) (Multicell)
- Rehfield, Hodges and Atilgan (1988) (Nonclassical Effects)
- Rehfield and Atilgan (1989) (Tailoring Mechanisms)
- Rehfield and Atilgan (1989) (Buckling Behavior)
- Rehfield, Atilgan and Hodges (1989) (Dynamic Characteristics)
- Rehfield, Atilgan and Hodges (1989) (Shear Center and Elastic Axis Revisited)

SIMPLE ANALYTICAL METHODS PROVIDE

- INSIGHT, INTUITION, "FEEL" - THE ESSENCE OF GOOD DESIGN
- UNDERSTANDING OF BEHAVIOR IN TERMS OF BASIC PRINCIPLES
  - CAUSE/EFFECT RELATIONSHIPS
  - INTRINSIC POTENTIAL/LIMITATIONS
- RELIABLE TREND INFORMATION
  - EVALUATE COMPETITIVE CONCEPTS
  - SELECT CONFIGURATION
- RAPID, EFFICIENT, ECONOMICAL ANALYSIS TURNAROUND FOR THE DESIGN ENVIRONMENT

Equilibrium and Force-Deformation Relationships

Assuming membrane behavior of the plies

$$\begin{Bmatrix} N_{xx} \\ N_{ss} \\ N_{xs} \end{Bmatrix} = [A] \begin{Bmatrix} \varepsilon_{xx} \\ \varepsilon_{ss} \\ \gamma_{xs} \end{Bmatrix}$$

With the hoop stress equal to zero or

$$N_{ss} = 0$$

we have

$$\begin{Bmatrix} N_{xx} \\ N_{xs} \end{Bmatrix} = [K] \begin{Bmatrix} \varepsilon_{xx} \\ \gamma_{xs} \end{Bmatrix}$$

Equilibrium and Force-Deformation Relationships (continued)

The K's are stiffnesses given by

$$K_{11} = A_{11} - \frac{A_{12}^2}{A_{22}}$$

$$K_{12} = A_{16} - \frac{A_{12}A_{26}}{A_{22}}$$

$$K_{22} = A_{66} - \frac{A_{26}^2}{A_{22}}$$

The principle of virtual work leads to generalized internal forces of the form

$$\oint_{\Gamma} N_{xx}(1, z, -y, \psi)ds = (N, M_y, M_z, Q_\omega)$$

$$\oint_{\Gamma} N_{xs}\left(\frac{dy}{ds}, \frac{dz}{ds}, \frac{2A}{c}\right)ds = (Q_y, Q_z, M_x)$$

Equilibrium and Force-Deformation Relationships (continued)

The constitutive relations can be put into a matrix form relating the generalized strains u to the generalized forces F

$$F = Cu$$
$$u = SF$$

where

$$u = \langle U_{,x} \ \gamma_{xy} \ \gamma_{xz} \ \phi_{,x} \ \beta_{y,x} \ \beta_{z,x} \ \phi_{,xx} \rangle^T$$
$$F = \langle N \ Q_y \ Q_z \ M_x \ M_y \ M_z \ Q_\omega \rangle^T$$

A choice of the reference axis so that

$$\oint_\Gamma K_{11}\, y ds = \oint_\Gamma K_{11}\, z ds = \oint_\Gamma K_{11}\, yz ds = 0$$

leaves the stiffness matrix C consisting of 25 independent constants

The compliance matrix S is simply the inverse of C

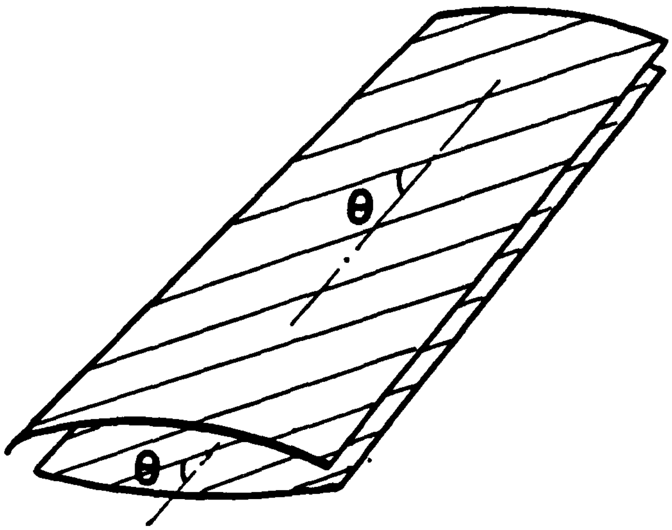

Ply orientation for circumferentially asymmetrical stiffness

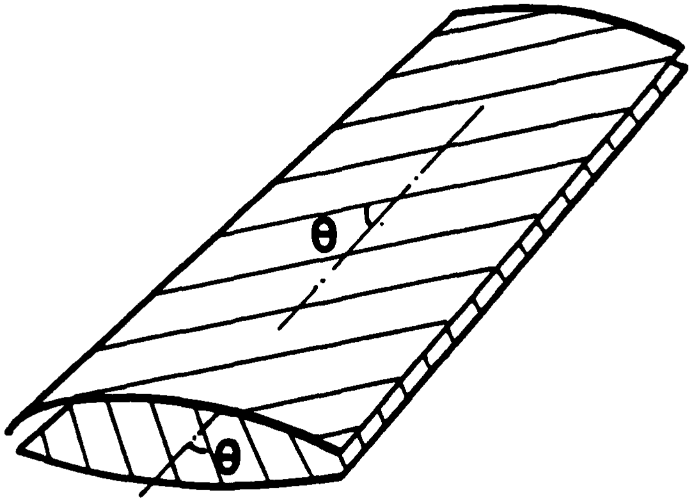

Ply orientation for circumferentially uniform stiffness

EXTENSION-TWIST COUPLING

CREATES BLADE PITCH

CHANGES WITH RPM

TILT ROTOR PERFORMANCE TRENDS

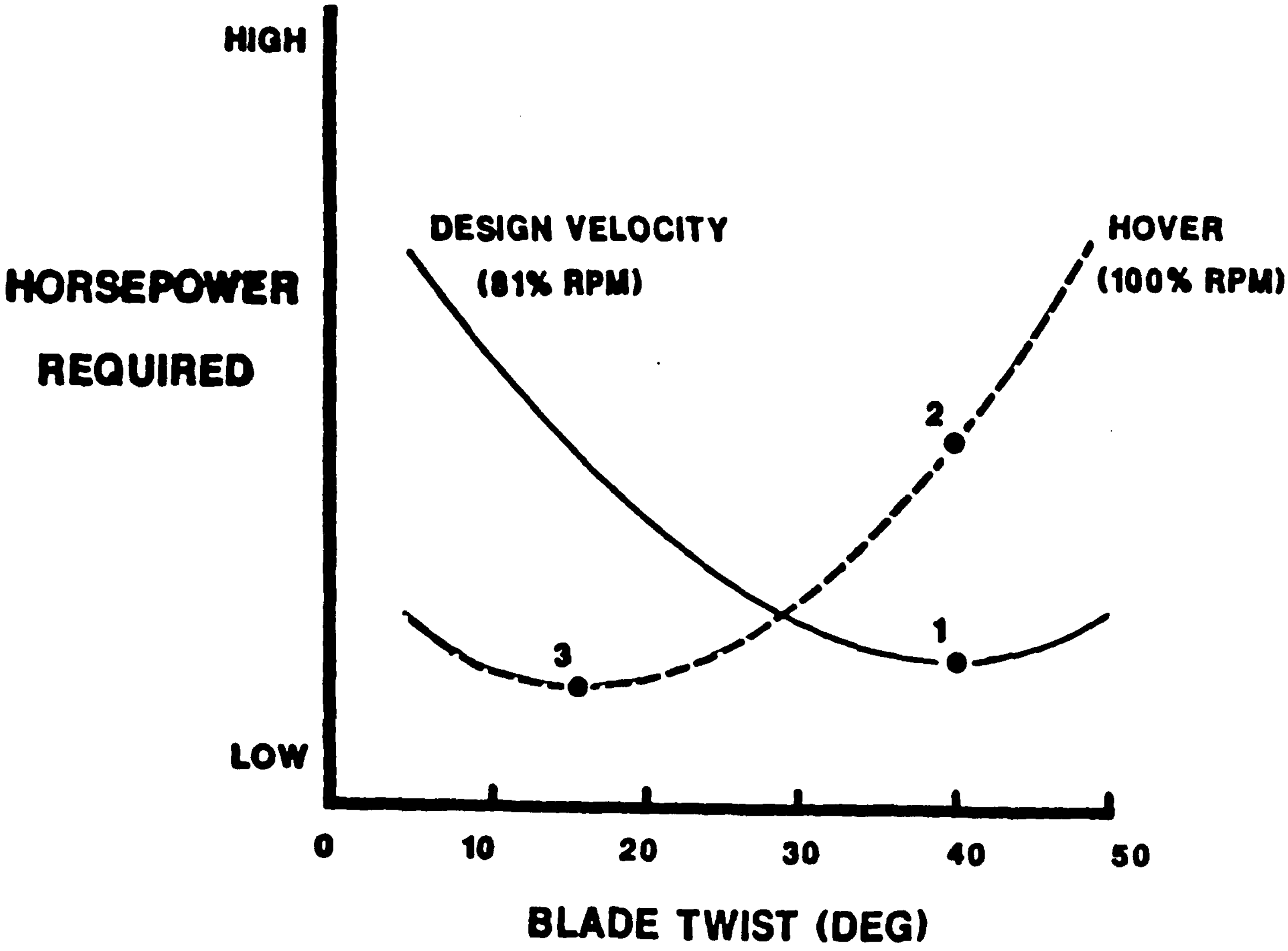

TAILORING PARAMETER

$$\beta = C_{14}^2 \Big/ C_{11}\, C_{44} = K_{12}^2 \Big/ K_{11}\, K_{22}$$

$$\beta_1 = C_{25}^2 \Big/ C_{22}\, C_{55} = g_1\, \beta$$

$$\beta_2 = C_{36}^2 \Big/ C_{33}\, C_{66} = g_2\, \beta$$

β = TAILORING PARAMETER

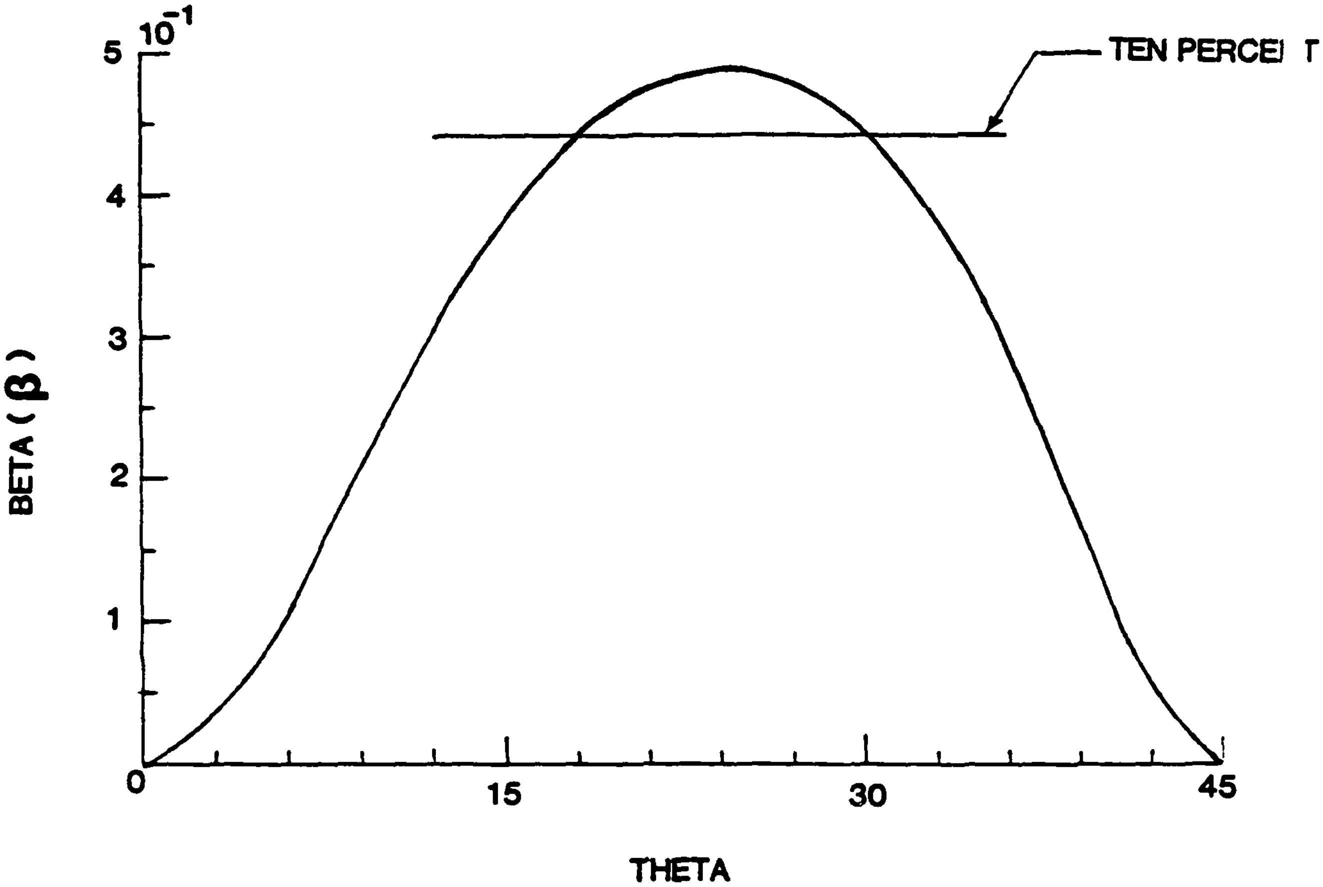

Alteration of the elastic tailoring parameter with the orientation angle

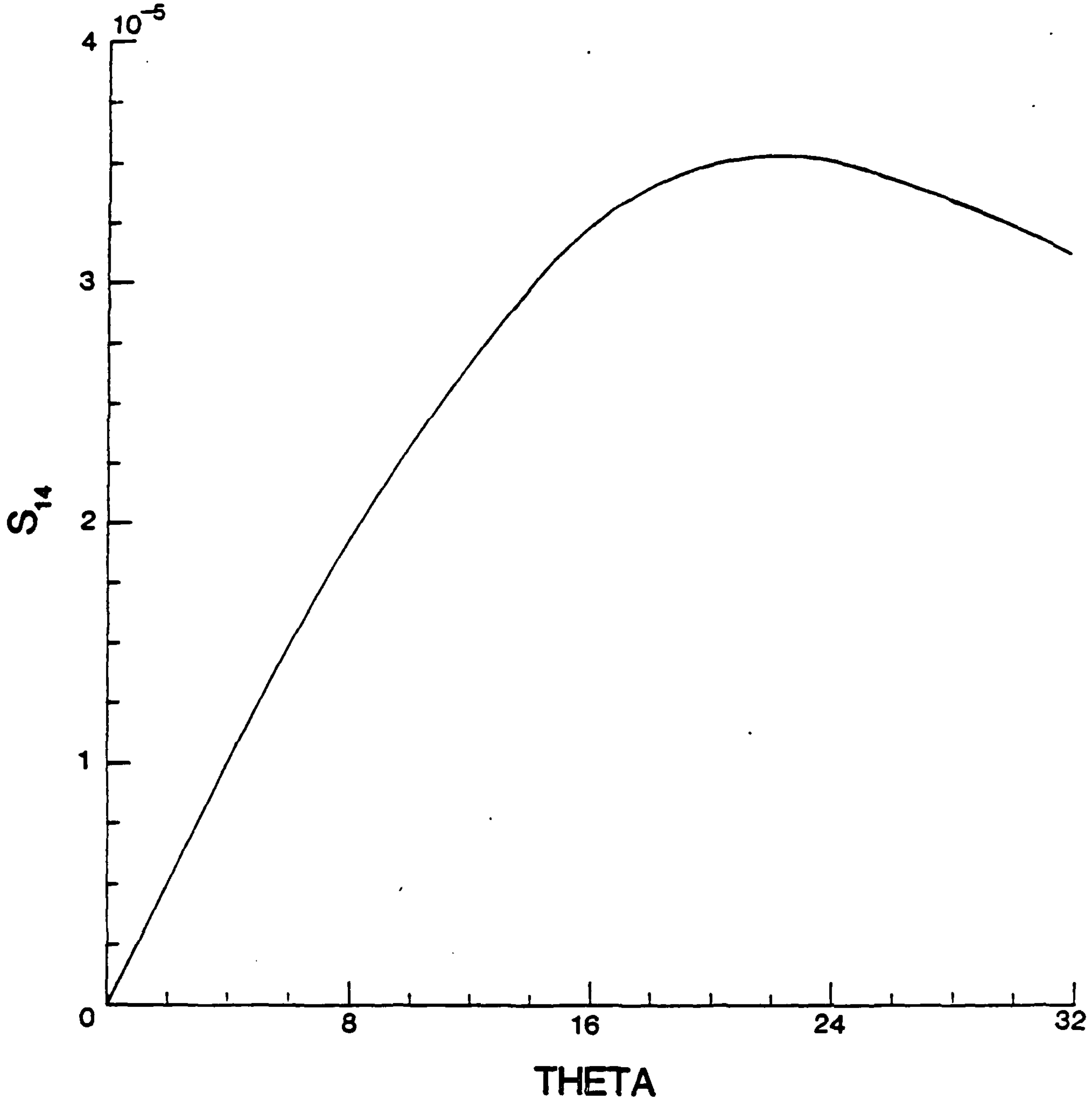

Alteration of the extension-twist flexibility with the orientation angle

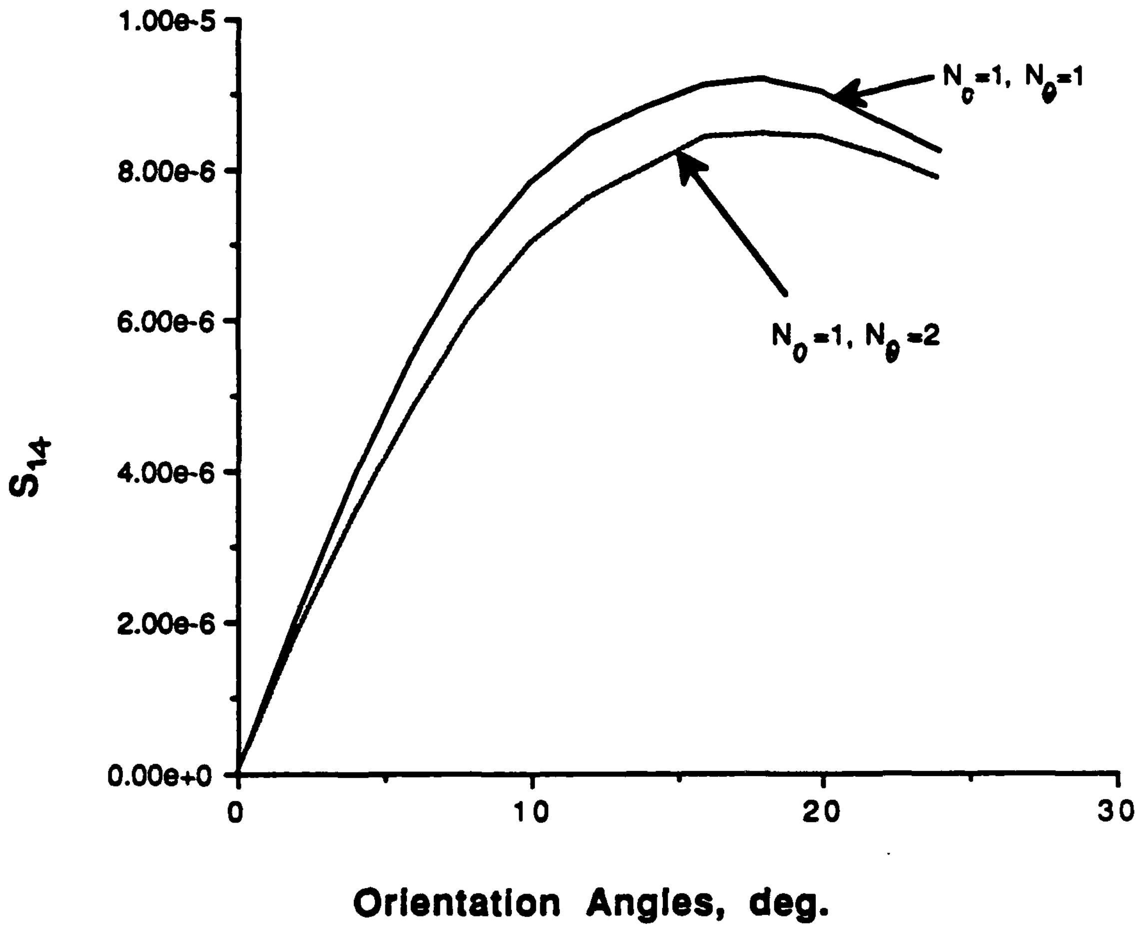

Effect of 0° and angle plies on the extension-twist flexibility

TWIST ANGLE PREDICTIONS

- ADDITION OF TORSION-RELATED WARPING EFFECTS

$$\bar{M}_x = C_T \, \phi,_x - \underline{C_{77} \, \phi,_{xxx}}$$

- REDUCED STIFFNESS (ELASTIC COUPLING)

$$C_T/C_{44} = 0.51$$

- $$\lambda^2 = \frac{C_T L^2}{C_{77}}$$

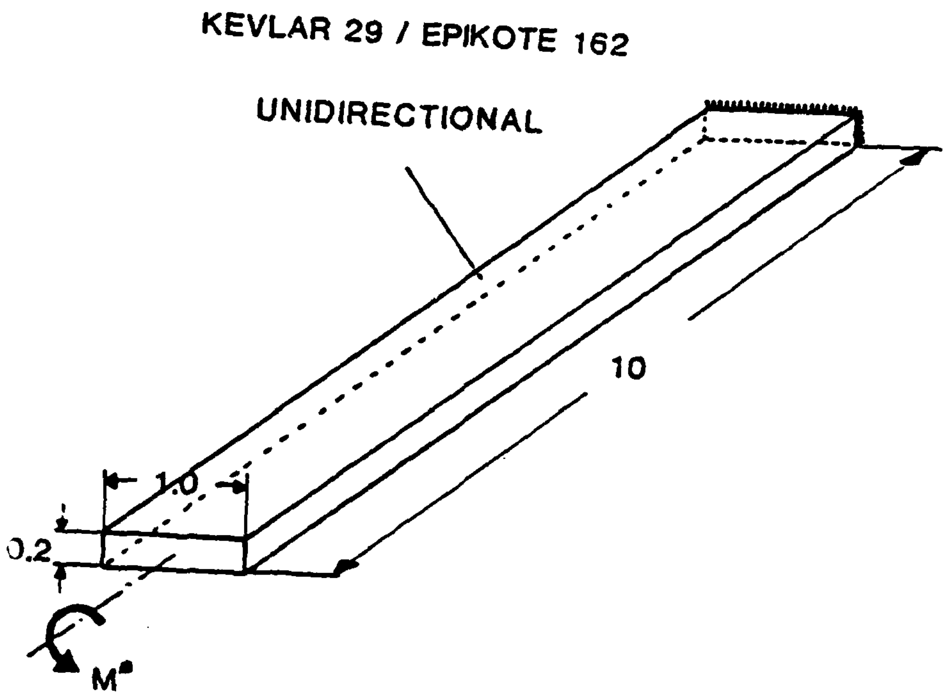

Slender cantilever beam with rectangular cross section subjected to end moment

Prediction of Twist Angle (continued)

The underlined term is the influence of warping, the effect of which on the tip twist angle is obvious

$$\phi\Big|_{\xi=1} = \frac{M_x^* L}{C_T}\left(1 - \underline{\frac{1}{\lambda}}\right)$$

For isotropic beams the decay length parameter is

$$\lambda^2 = \frac{G}{E}\frac{12L^2}{a^2(1-\alpha)^2}$$

which, because of material properties, is always large

However, for composite beams with a uniform layup (*K*'s constant)

$$\lambda^2 = \frac{K_{22}(1-\beta)}{K_{11}}\frac{12L^2}{a^2(1-\alpha)^2}$$

where

$$\beta = \frac{C_{14}^2}{C_{11}C_{44}}$$

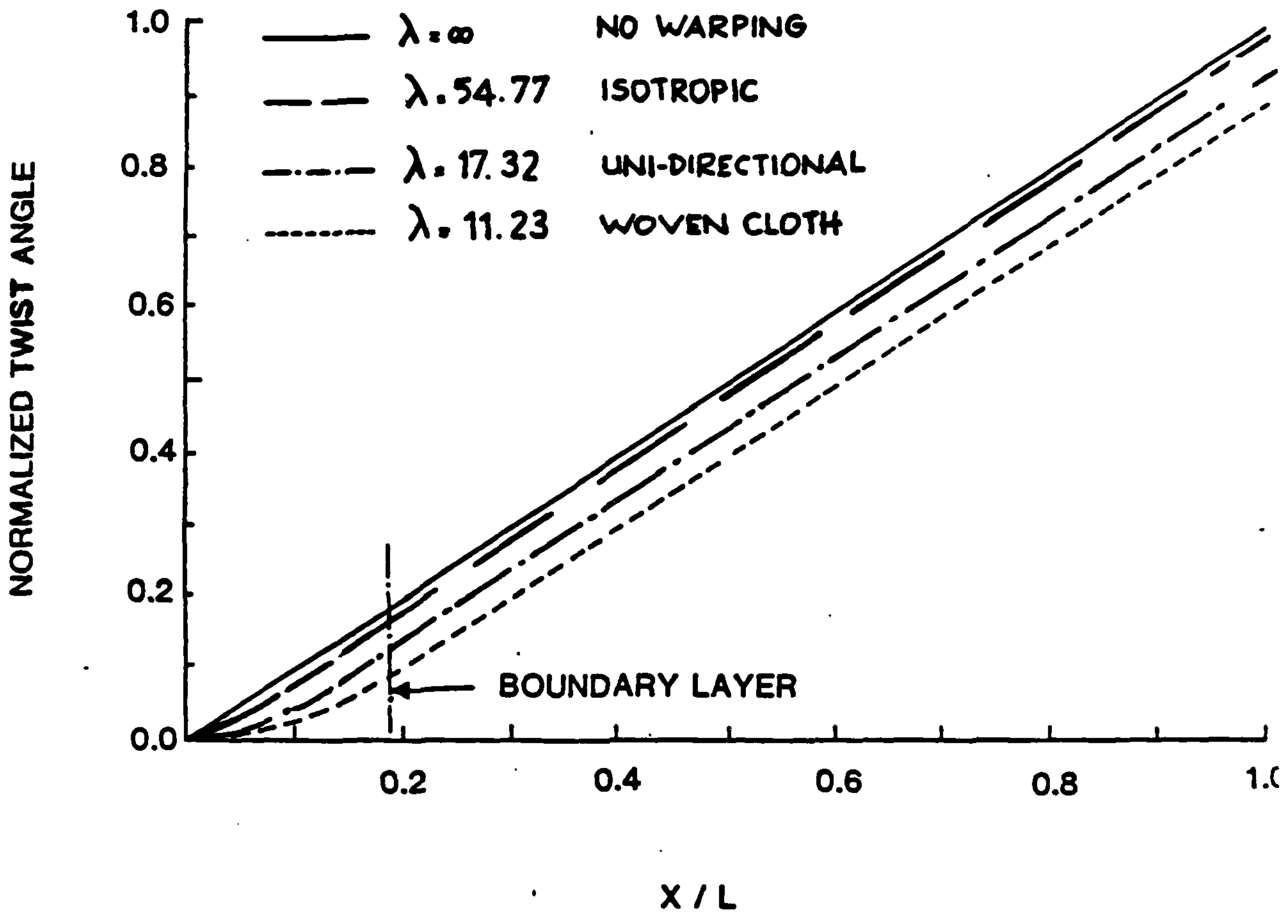

Twist angle predictions due to end torque with different material systems.

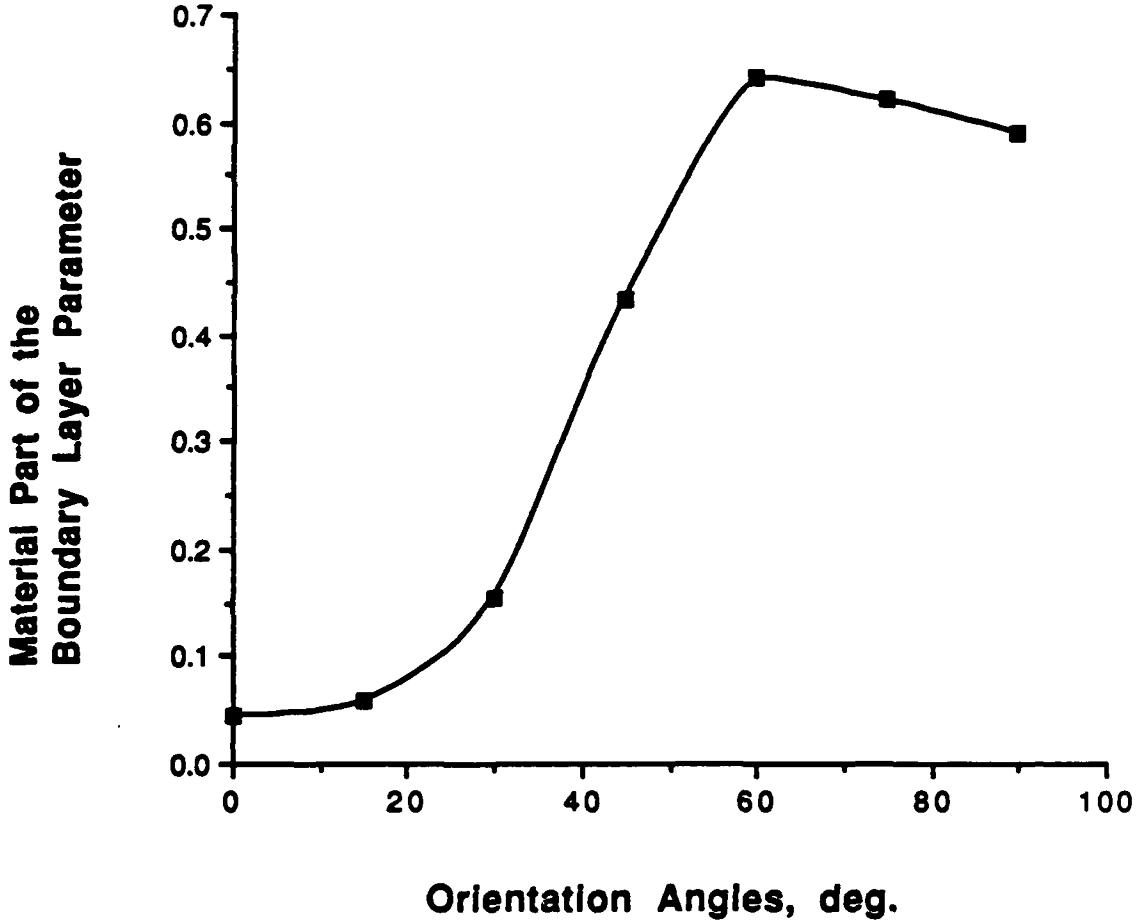

Alteration of the boundary layer parameter with the orientation angle

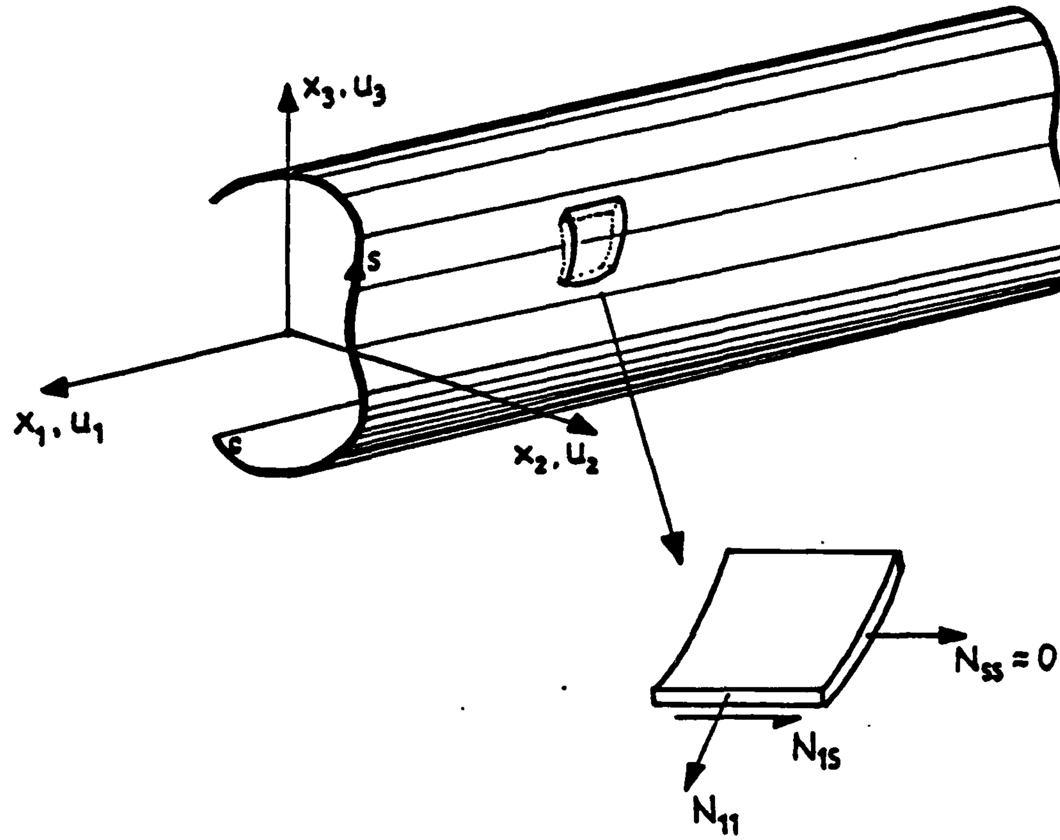

Thin-walled open cross section beam model

KINEMATICS

$$
\begin{aligned}
u_1 &= U_1(x) + x_2\beta_3 + x_3\beta_2 + \psi(s)\phi' \\
u_2 &= U_2(x) - (x_3 - x_3^s)\phi(x_1) \\
u_3 &= U_3(x) - (x_2 - x_2^s)\phi(x_1) \\
\gamma_{12} &= \beta_3 + U_2' \\
\gamma_{13} &= \beta_2 + U_3' \\
\gamma_{1s} &= \gamma_{12}\frac{dx_2}{ds} + \gamma_{13}\frac{dx_3}{ds} \\
\gamma_{11} &= U_1' + x_2\beta_3' + x_3\beta_2' + \psi\phi'' + \frac{1}{2}{u_2'}^2 + \frac{1}{2}{u_3'}^2
\end{aligned}
$$

COMPRESSIVE BUCKLING EQUATIONS

$$-M_3'' + P\left(U_2'' + x_3^s \phi''\right) = 0$$

$$-M_2'' + P\left(U_3'' - x_2^s \phi''\right) = 0$$

$$-M_1' + P\left(\frac{C_\rho}{C_{11}}\phi'' + x_3^s U_2'' - x_2^s U_3''\right) = 0$$

CONSTITUTIVE EQUATIONS

$$M_3 = C_{26}\gamma_{12} + C_{36}\gamma_{13} + C_{66}\beta_3'$$

$$M_2 = C_{25}\gamma_{12} + C_{35}\gamma_{13} + C_{55}\beta_2'$$

$$M_1 = C_{44}\phi' - C_{77}\phi''$$

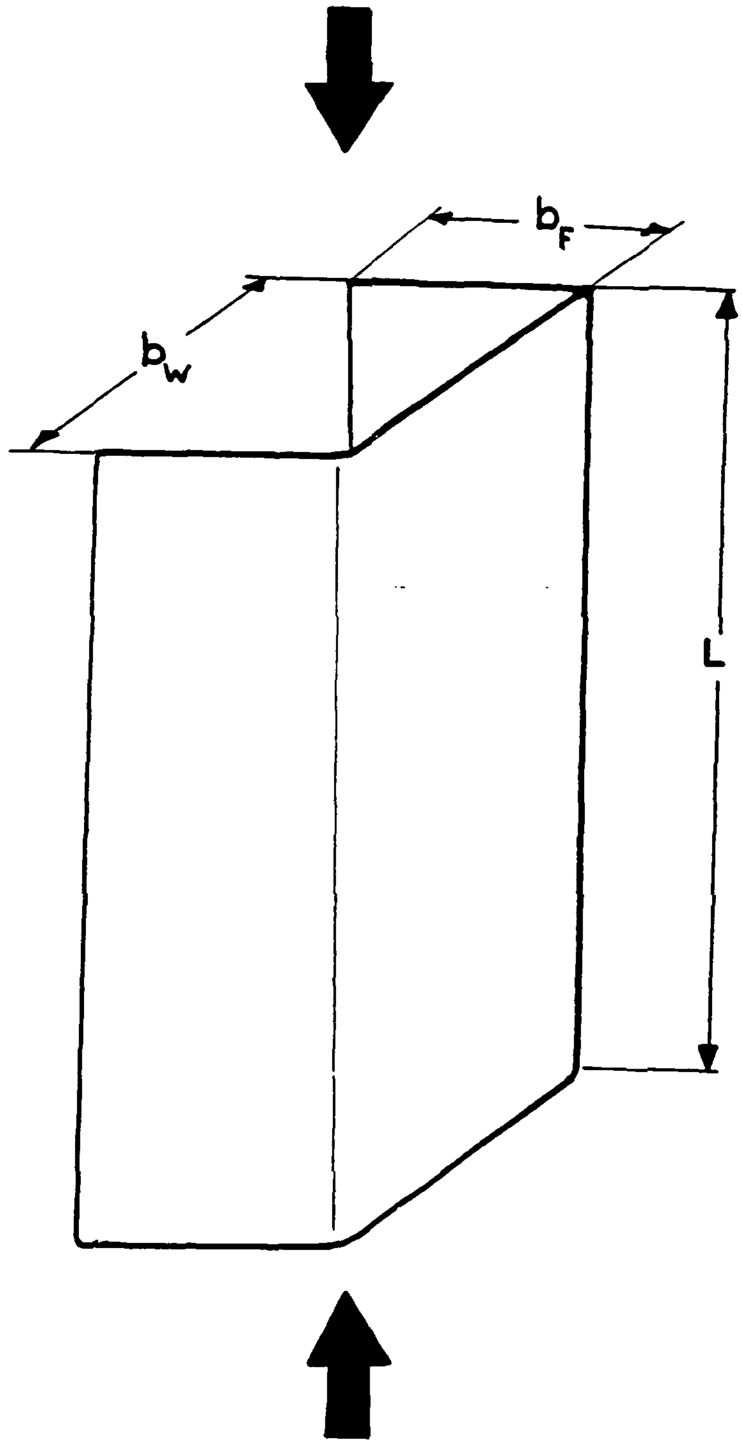

Schematic of a channel section subjected to compressive loading

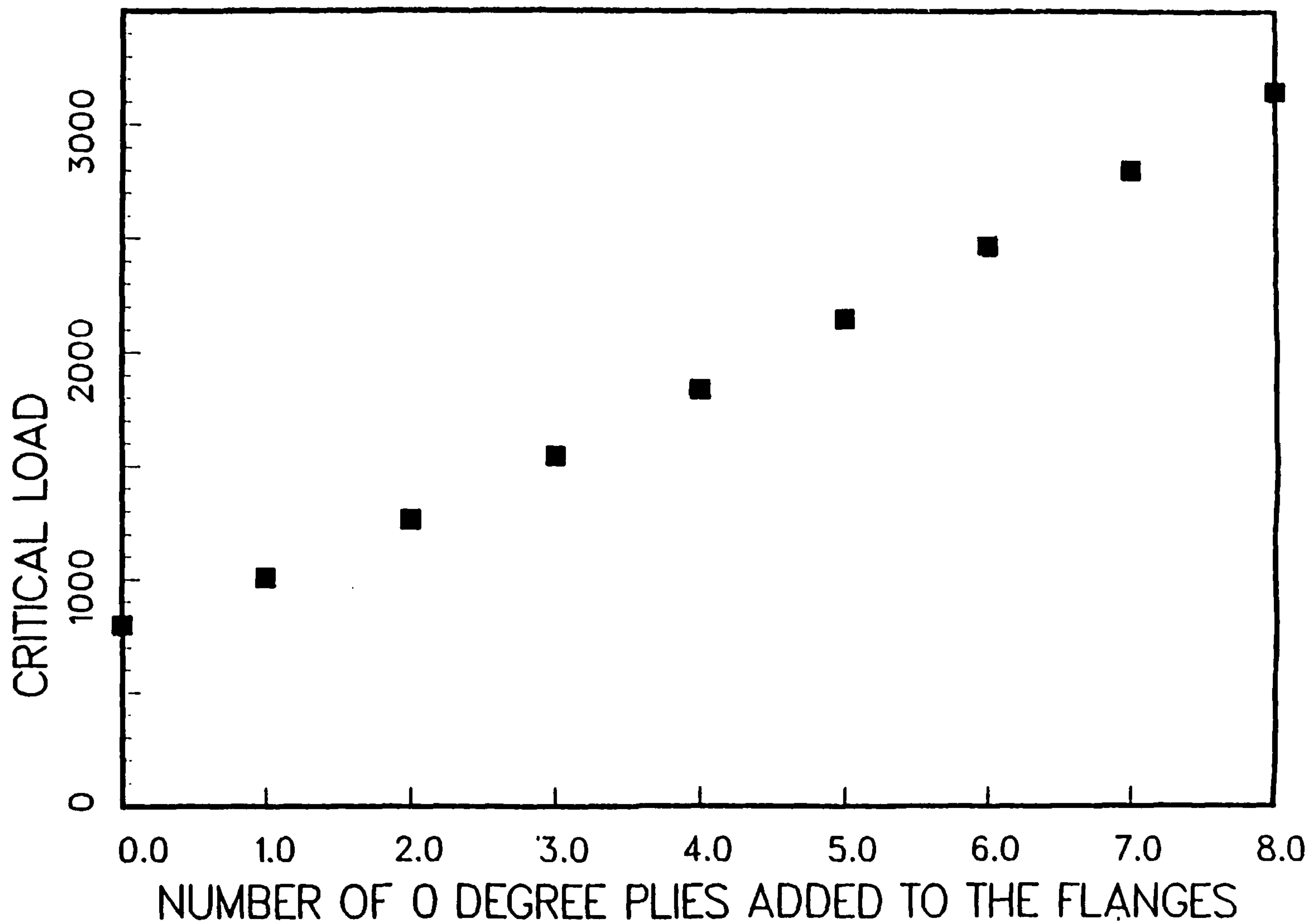

Critical buckling loads for a channel section with different ply orientations.

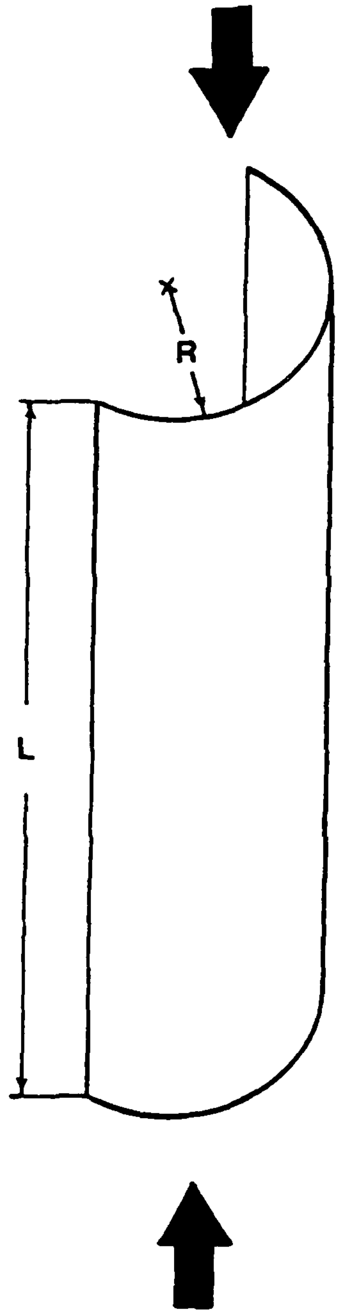

Schematic of a semi-circular cross section subjected to compressive loading

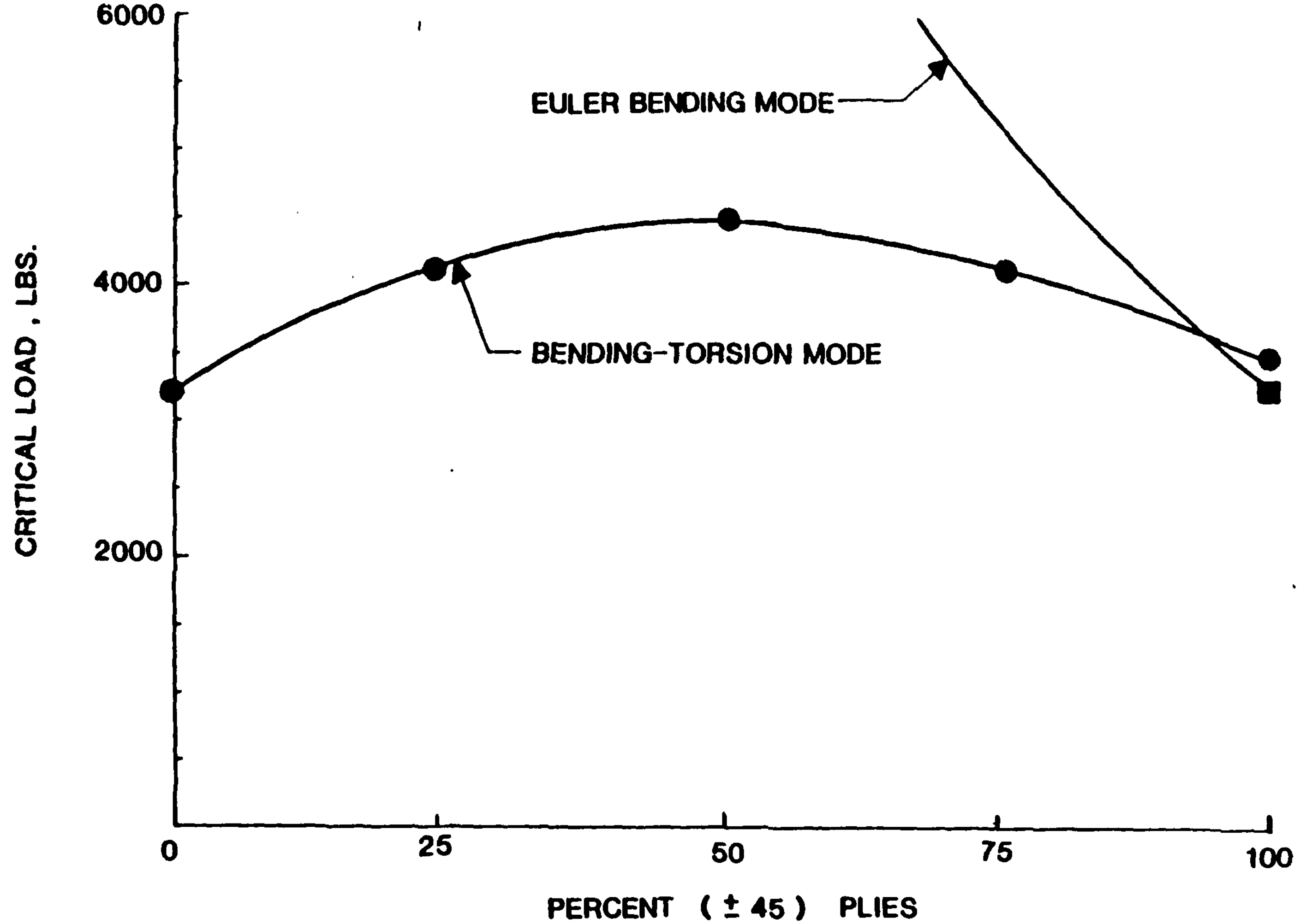

Critical buckling loads for a semi-circular cross section with different ply orientations (AS-4/3501-6 Gr/E, $\frac{L}{R} = 15$)

Beam Cross-Section and Specimen No.	Dimensions	Material Properties	Ply Layup
Channel 1	L (Beam Length): 19 in. b_F (Flange Width): 1.25 in. bw (Web Width): 1.25 in. t_w (Wall Thickness): 0.080 in. R (Corner Radius): 0.125 in.	Material: AS4-3502 GR/EP E_1: 17.8 x 10^6 psi E_2: 1.51 x 10^6 psi ν_{12}: 0.331 G_{12}: 0.844 x 10^6 psi	$[\pm45/0/90]_{2s}$
Channel 2	L (Beam Length): 19 in. b_F (Flange Width): 1.25 in. bw (Web Width): 1.25 in. t_w (Wall Thickness): 0.080 in. R (Corner Radius): 0.125 in.	Material: AS4-3502 GR/EP E_1: 18.3 x 10^6 psi E_2: 1.51 x 10^6 psi ν_{12}: 0.331 G_{12}: 0.844 x 10^6 psi	$[\pm45/\mp45/90/$[illegible]$_3]$
Channel 3	L (Beam Length): 12 in. b_F (Flange Width): 0.75 in. bw (Web Width): 1.25 in. t_w (Wall Thickness): 0.080 in. R (Corner Radius): 0.125 in.	Material: AS4-3502 GR/EP E_1: 18.1 x 10^6 psi E_2: 1.51 x 10^6 psi ν_{12}: 0.331 G_{12}: 0.844 x 10^6 psi	$[\pm45/0/90]_{2s}$

Beam cross section dimensions, material properties and ply layup for buckling load comparison

Beam Cross Section and Specimen No.	Buckling Load, lbs.		
	Experiment	Present	Vlasov Analysis
Channel 1	7000	7943	9872
Channel 2	6830	8917	12540
Channel 3	9670	11565	15830

Comparison of buckling loads for clamped-free boundary condition

Channel-4 Properties

Material: AS4/3501-6

L (Beam Length)	: 12in.	$E_1 = 20.2\ 10^6$
b_f (Flange Width)	: 1.75in.	$E_2 = 1.61\ 10^6$
b_w (Web Width)	: 1.75in.	$\nu_{12} = 0.3$
t_w (Wall Thickness	: 0.06in.	$G_{12} = 0.87\ 10^6$

Buckling Load, lbs.

Layup	Analysis	Experiment	Present
$[\pm 15/0]_{2s}$	2061	2144	2313

Comparison of buckling loads for simply supported bouindary condition

Cross sections	Buckling Load, lbs.		
	SD	Hybrid SD	Error %
Channel - 1	7943	8365	5.3
Channel - 2	8917	9630	8.0
Channel - 3	11565	12048	4.2

Comparison of buckling loads

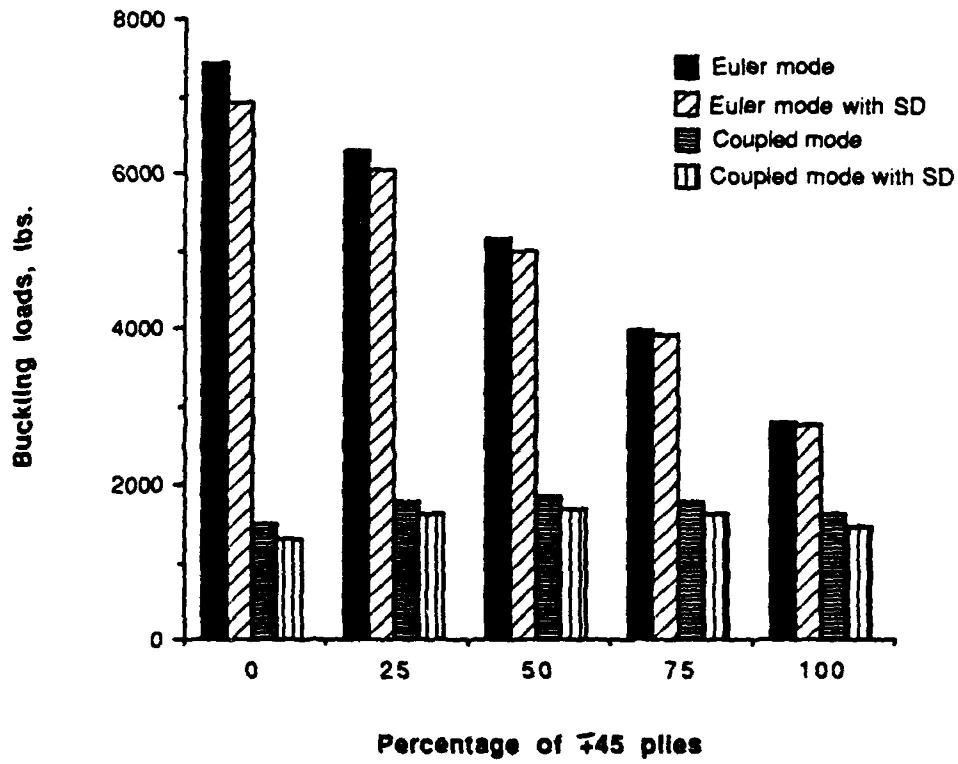

8000
6000
4000
2000
0
Buckling loads, lbs.
Euler mode
Euler mode with SD
Coupled mode
Coupled mode with SD
0
25
50
75
100
Percentage of ∓45 plies

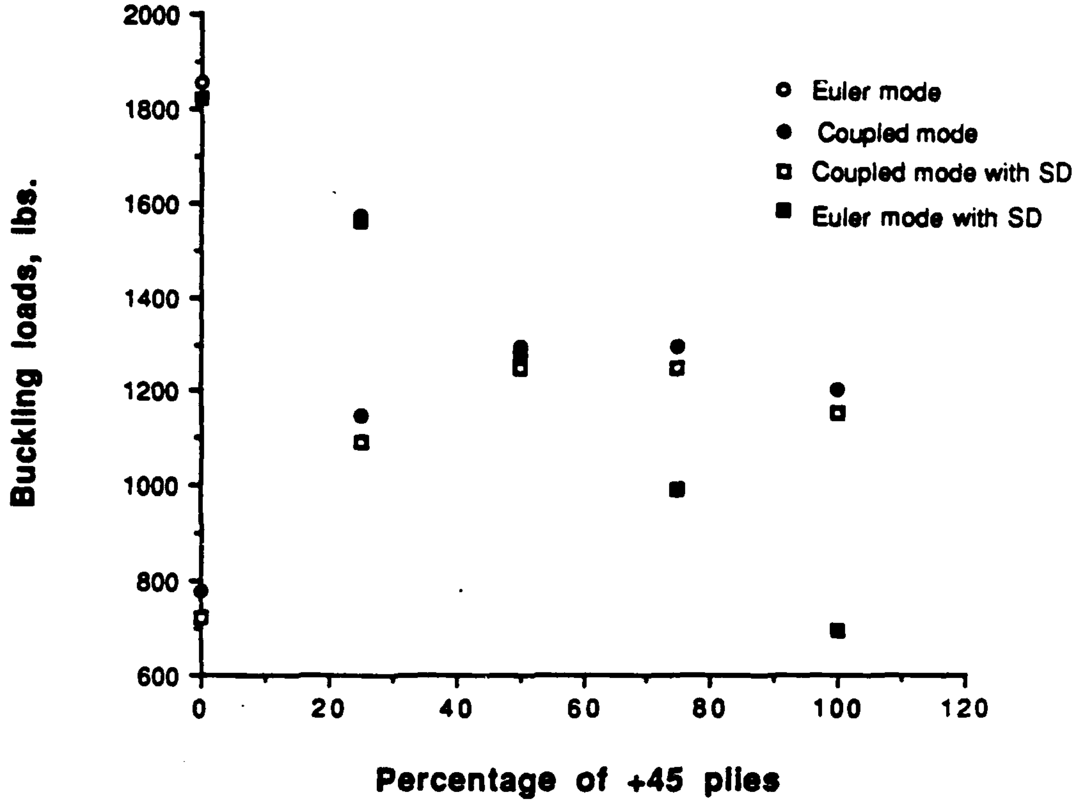

Critical buckling loads for a semi-circular cross section with different ply orientations (S2/5245C G/E. $\frac{L}{R} = 30$)

<u>GENERAL OBSERVATIONS</u>

- TAILORING PARAMETER IDENTIFIED
- STIFFNESSES ARE <u>REDUCED</u> BY ELASTIC COUPLING
  - SIMPLE RULES

"Toward Understanding the Tailoring Mechanisms for Thin-Walled Composite Tubular Beams"

Lawrence W. Rehfield
University of California, Davis, California

and

Ali R. Atılgan
Georgia Institute of Technology, Atlanta, Georgia

COMPOSITE ROTOR BLADE MODELING

OBJECTIVE

DEVELOP A THEORETICAL MODEL SUITABLE FOR REPRESENTING COMPOSITE ROTOR BLADE DESIGNS

- DYNAMIC AND OVERALL STRESS ANALYSES
- AEROELASTIC TAILORING

SIMPLE COMPOSITE BEAM MODELS

- MANSFIELD AND SOBEY (1979)
- MANSFIELD (1981)
- VALISETTY AND REHFIELD (1984)
- BAUCHAU (1985)
- REHFIELD (1985)
- REHFIELD AND ATILGAN (1987)
- REHFIELD AND ATILGAN (1987)

THEORY FOR COMPOSITE SINGLE CELL BEAMS

- KINEMATICALLY BASED
- CONSISTENT
- SIMPLE TO DERIVE
- ARBITRARY WALL LAYUP AND ELASTIC COUPLING

KINEMATICS

$$\gamma^{o}_{xy} = \beta_z + V_{,x} \tag{1}$$

$$\gamma^{o}_{xz} = \beta_y + W_{,x} \tag{2}$$

$$\gamma^{o}_{xs} = \gamma^{o}_{xy}\frac{dy}{ds} + \gamma^{o}_{xz}\frac{dz}{ds} + \frac{2Ae}{c}\,\phi_{,x} \tag{3}$$

$$u = U(x) + y\beta_z + z\,\beta_y + \underline{\psi(s)\,\phi_{,x}} \tag{4}$$

$$v = V(x) - z\,\phi(x) \tag{5}$$

$$w = W(x) + y\,\phi(x) \tag{6}$$

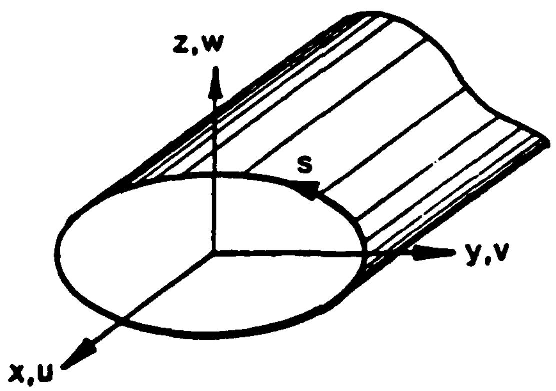

GENERALIZED FORCE RESULTANTS

$$(N, M_y, M_z) = \oint N_{xx}(1, z, y)\,ds$$

$$(Q_y, Q_z) = \oint N_{xs}\left(\frac{dy}{ds}, \frac{dz}{ds}\right) ds$$

$$M_x = \frac{2A_e}{c} \oint N_{xs}\, ds$$

$$Q_w = \oint N_{xx} \psi \, ds$$

FUNDAMENTAL ASSUMPTIONS

- N_{ss} NEGLECTED
- CROSS SECTIONS PRESERVED

$$(N_{xx}\ N_{xs})^T = \begin{bmatrix} K_{11} & K_{12} \\ K_{12} & K_{22} \end{bmatrix} (\epsilon_{xx}\ \gamma_{xs})^T$$

ELASTIC LAW

$$\begin{bmatrix} N \\ Q_y \\ Q_z \\ M_x \\ M_y \\ M_z \\ Q_w \end{bmatrix} = \underset{7 \times 7}{C} \begin{bmatrix} U_{,x} \\ \gamma^o_{xy} \\ \gamma^o_{xz} \\ \phi_{,x} \\ \beta_{y,x} \\ \beta_{z,x} \\ \phi_{,xx} \end{bmatrix}$$

25 INDEPENDENT STIFFNESSES

IMPROVED TWISTING KINEMATICS

- SHEAR CENTER OFFSET
- VARIABLE SHEAR STRAIN

$$\gamma_T = \frac{2A}{c} \Phi_{,x} \alpha(s)$$

$$\alpha(s) = C \Big/ \left(K_{22}(1-\beta) \oint \frac{ds}{K_{22}(1-\beta)} \right)$$

$$\beta = (K_{12})^2 \Big/ K_{11}K_{22}$$

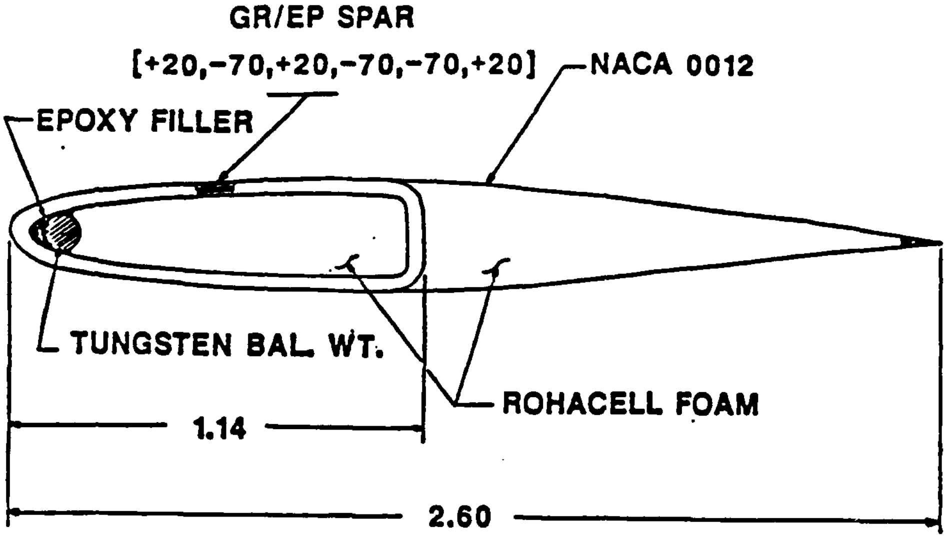
GR/EP SPAR
[+20,-70,+20,-70,-70,+20]
NACA 0012
EPOXY FILLER
TUNGSTEN BAL. WT.
ROHACELL FOAM
1.14
2.60

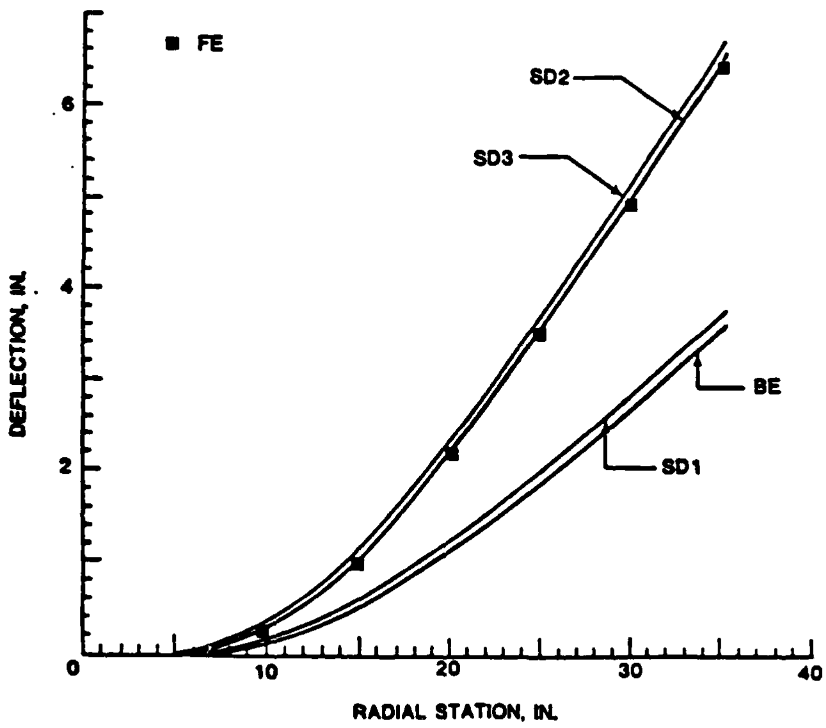
FE
SD2
SD3
BE
SD1
DEFLECTION, IN.
RADIAL STATION, IN.
0
2
4
6
10
20
30
40

ARCHETYPE MECHANISMS FOR ELASTIC TAILORING

- EXTENSION-SHEAR COUPLING IN CRYSTALS:

  W. VOIGT, 1928

- BENDING-TWIST COUPLING (CRYSTALS):

  W.F. BROWN, JR., 1940

- EXTENSION-SHEAR COUPLING IN WOOD AND PLYWOOD; R.F.S. HEARMON, 1943

- EXTENSION-TWIST COUPLING (PROPELLERS):

  M.M. MUNK, 1949

- TWO NEW COUPLING MECHANISMS (TUBES):

  L.W. REHFIELD, 1985

  L.W. REHFIELD, A.R. ATILGAN

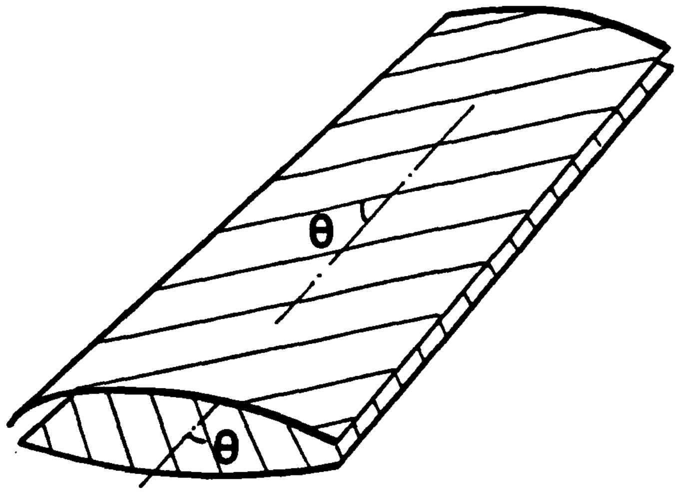

Ply Orientation for Circumferentially Uniform Stiffness

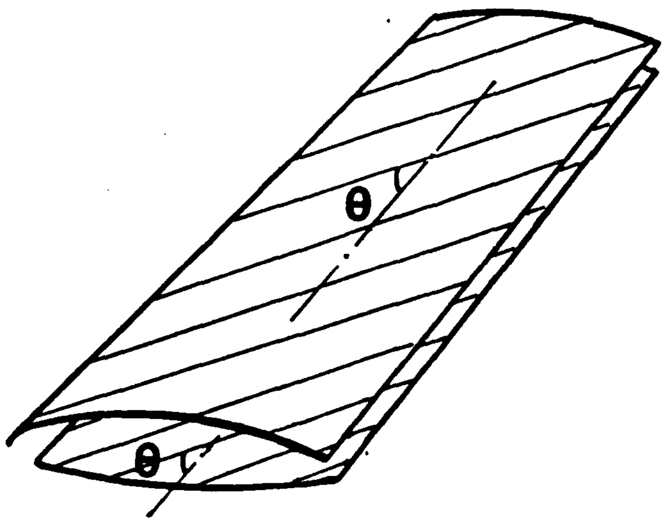

Ply Orientation for Circumferentially Asymmetrical Stiffness

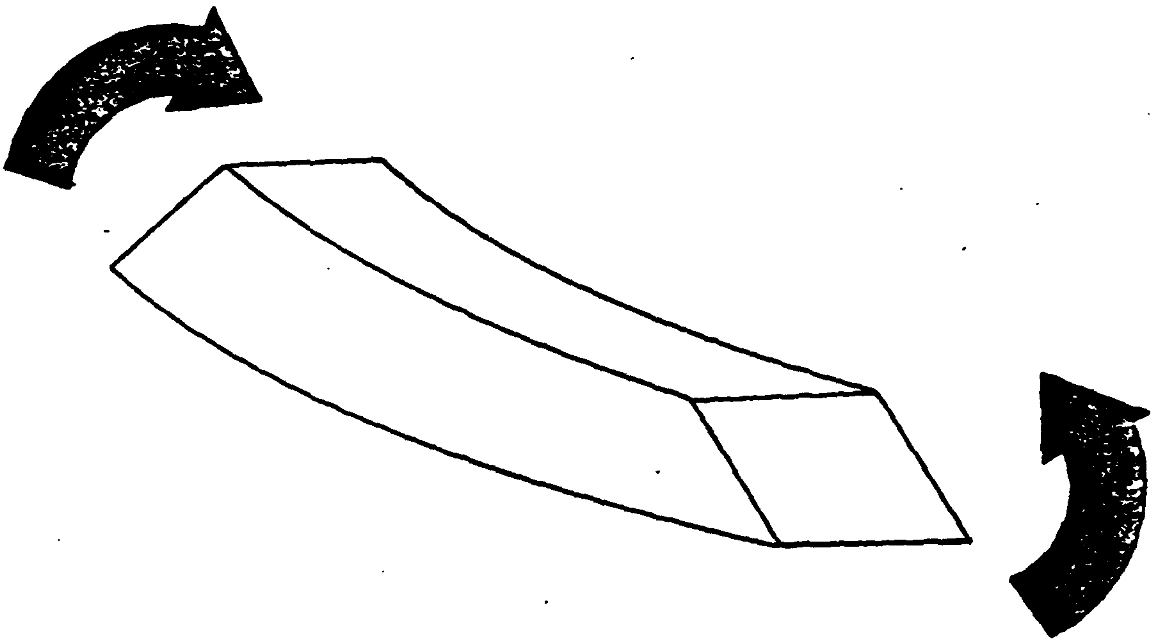

BENDING - TRANSVERSE SHEAR COUPLING

SHEAR-BENDING COUPLING

$$\beta_{y,x} = S_{25}\, Q_y + S_{55}\, \underline{M_y}$$

$$\beta_{z,x} = S_{36}\, \underline{Q_z} + S_{66}\, M_z$$

$$\beta_y = \gamma^{\circ}_{xz} - W_{,x}$$

$$\beta_z = \gamma^{\circ}_{xy} - V_{,y}$$

PRIMARY NONCLASSICAL EFFECTS

SD2 MODEL: $W,_{xx} = - S_{55} M_y$

$$S_{55} = (C_{55} - \underline{C_{25}^2/C_{22}})^{-1}$$

$$(S_{55}\ C_{55})^{-1} = 0.51$$

$$V,_{xx} = (S_{25} - S_{36})Q_z$$

- INCREASED DIRECT FLEXIBILITY

- OFF AXIS BENDING

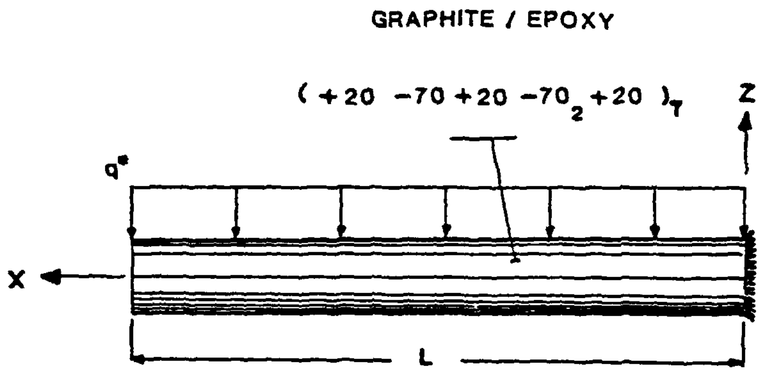

GRAPHITE / EPOXY
(+20 -70 +20 -70$_2$ +20)$_T$
Z
q*
X
L

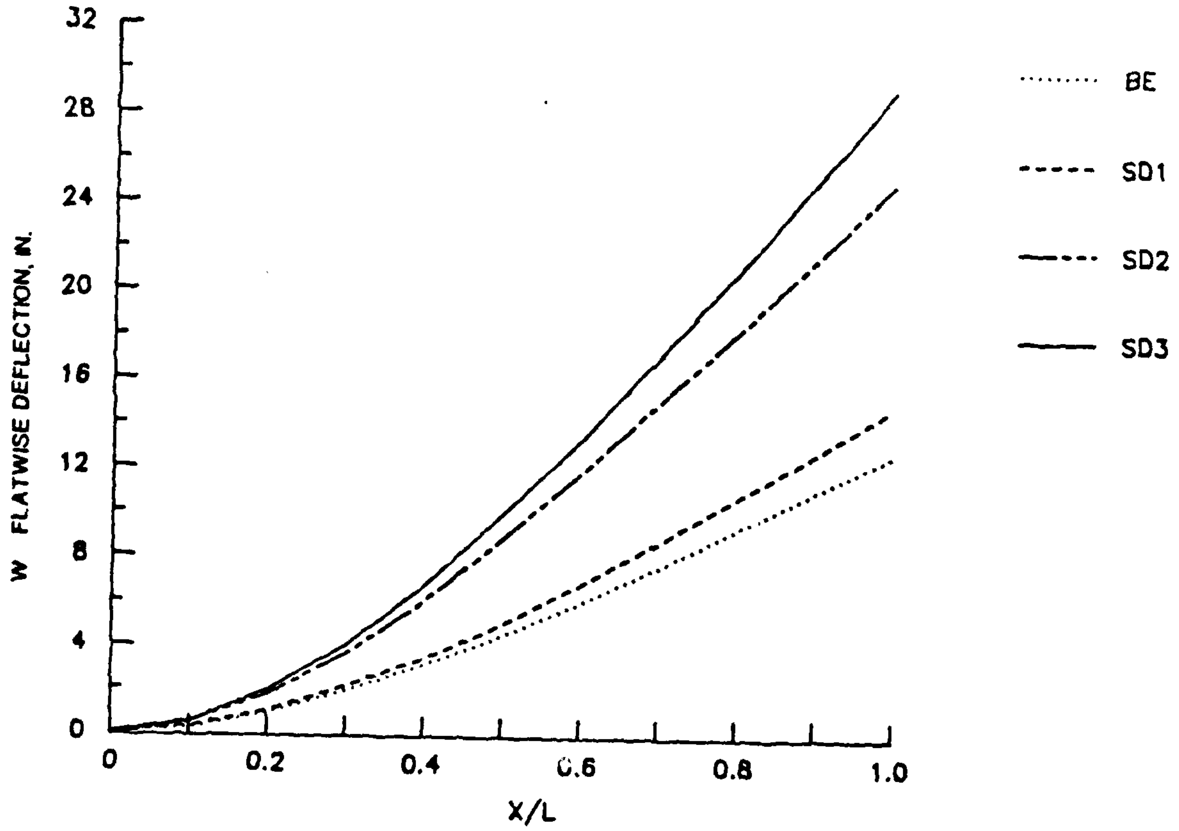

W FLATWISE DEFLECTION, IN.
32
28
24
20
16
12
8
4
0
0
0.2
0.4
0.6
0.8
1.0
X/L
BE
SD1
SD2
SD3

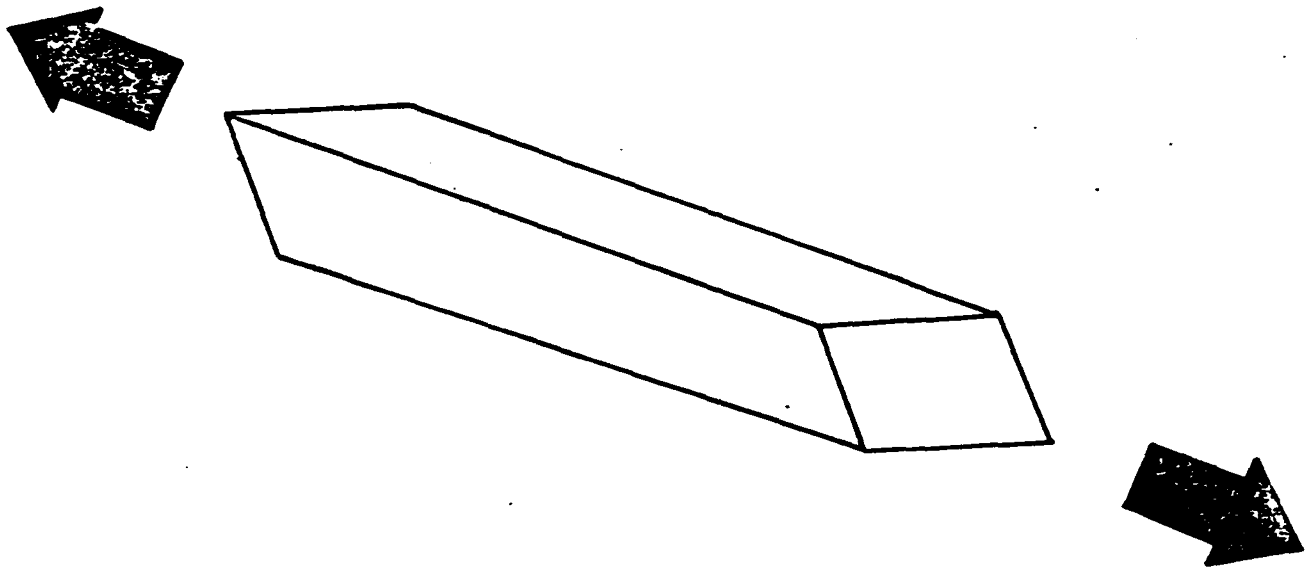

EXTENSION - TRANSVERSE SHEAR COUPLING

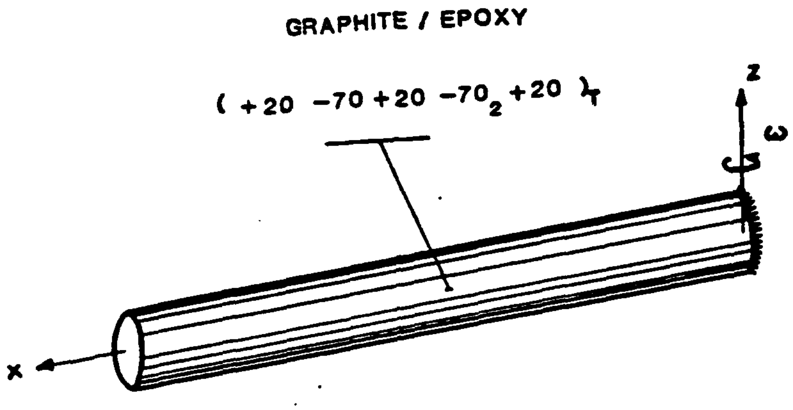

GRAPHITE / EPOXY
(+20 -70 +20 -70$_2$ +20)$_T$
z
ω
x

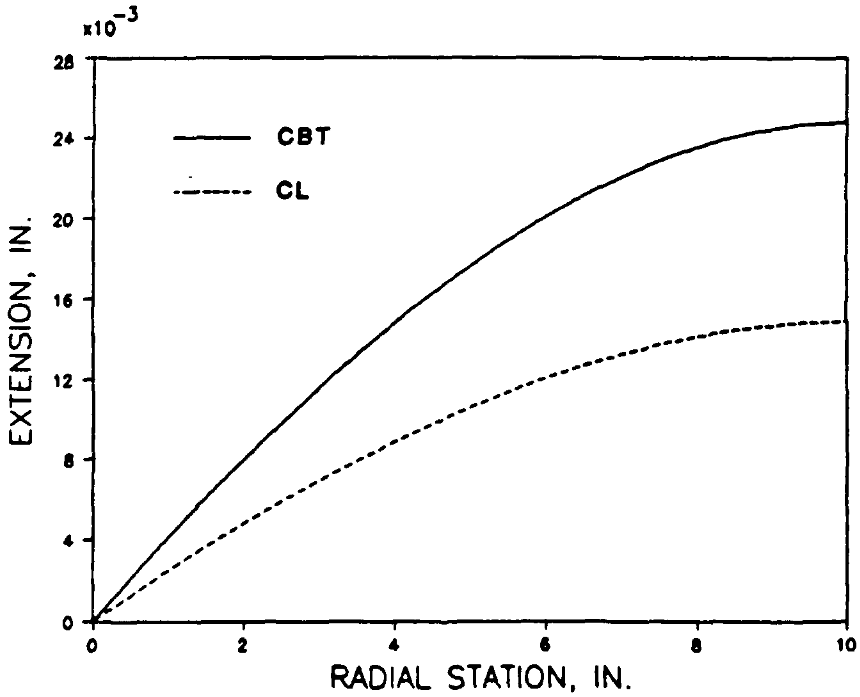

x10^{-3}
CBT
CL
EXTENSION, IN.
RADIAL STATION, IN.
0
4
8
12
16
20
24
28
2
6
10

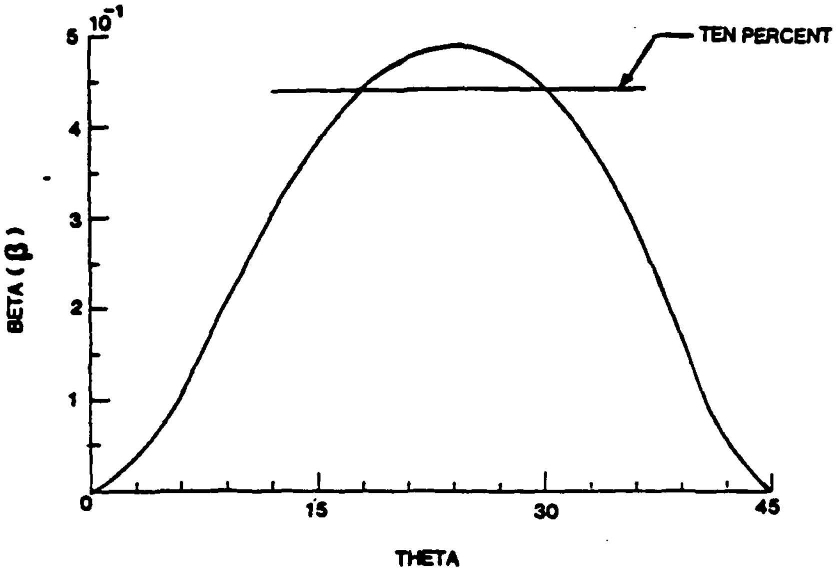

10^-1
5
4
3
2
1
0
15
30
45
BETA (β)
THETA
TEN PERCENT

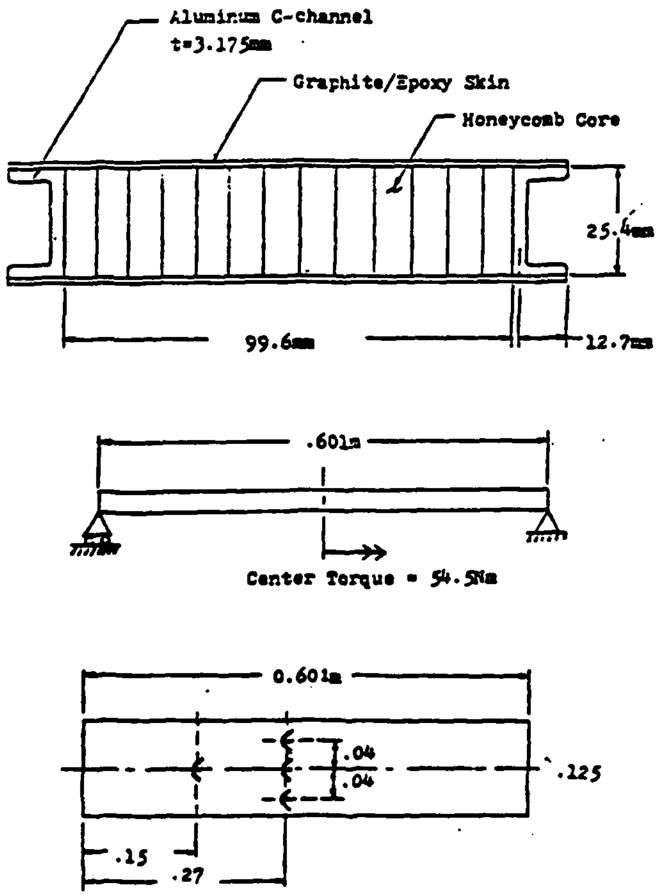

Aluminum C-channel
t=3.175mm
Graphite/Epoxy Skin
Honeycomb Core
25.4mm
99.6mm
12.7mm
.601m
Center Torque = 54.5Nm
0.601m
.04
.04
.125
.15
.27

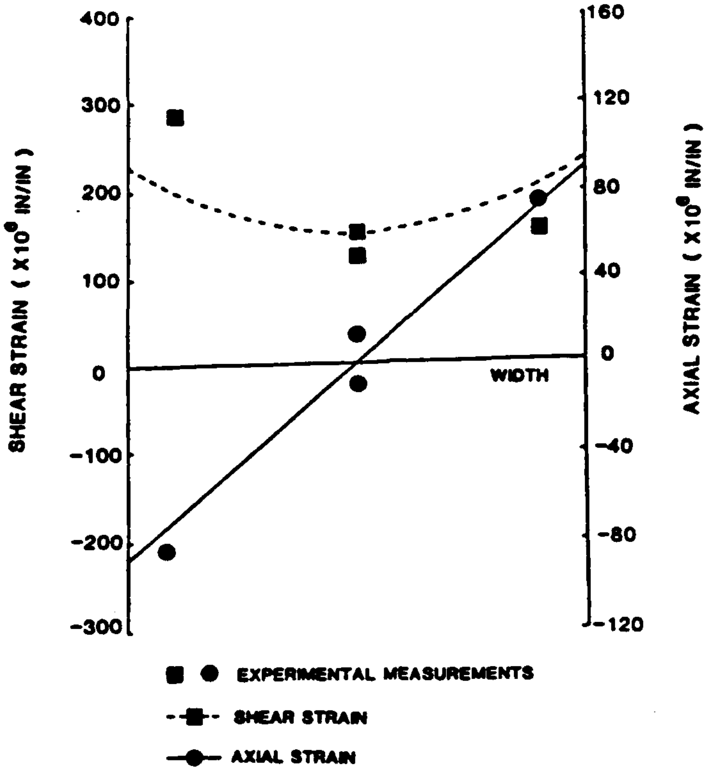

BALANCED DESIGN

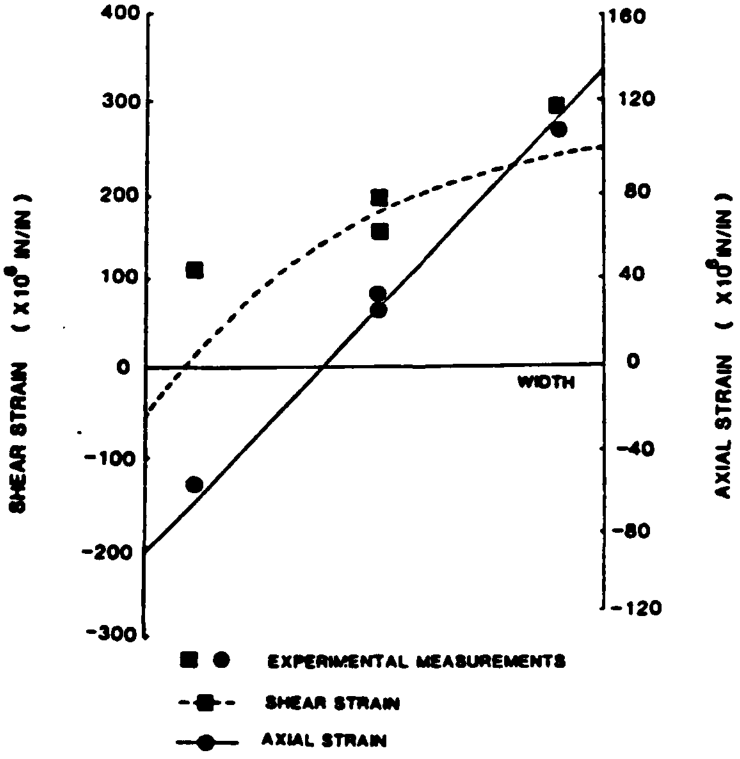

UNBALANCED DESIGN

<u>CONCLUSIONS</u>

- STRUCTURAL TECHNOLOGY BASE ADEQUATE
- EFFECTIVE STIFFNESSES ARE <u>REDUCED</u> BY ELASTIC COUPLING
- CONSEQUENCES ON SYSTEM PERFORMANCE MUST BE ASSESSED

SESSION IV

STRUCTURAL INTEGRITY AND DAMAGE MECHANISMS

Sanford S. Sternstein
Rensselaer Polytechnic Institute
Chairman

DAMAGE RESISTANCE IN ROTORCRAFT STRUCTURES

Erian A. Armanios and Bryan H. Fortson
Center of Excellence for Rotary Wing Aircraft Technology
Georgia Institute of Technology
Atlanta, Georgia 30332-0150

2nd ARO-AHS-RPI Workshop
on Composite Materials and Structures for Rotorcraft
September 14th, 1989

FUNDAMENTAL ISSUE

- Resistance to Damage Growth is Essential to :
  - Detection
  - Damage Tolerance
  - Retirement for Cause

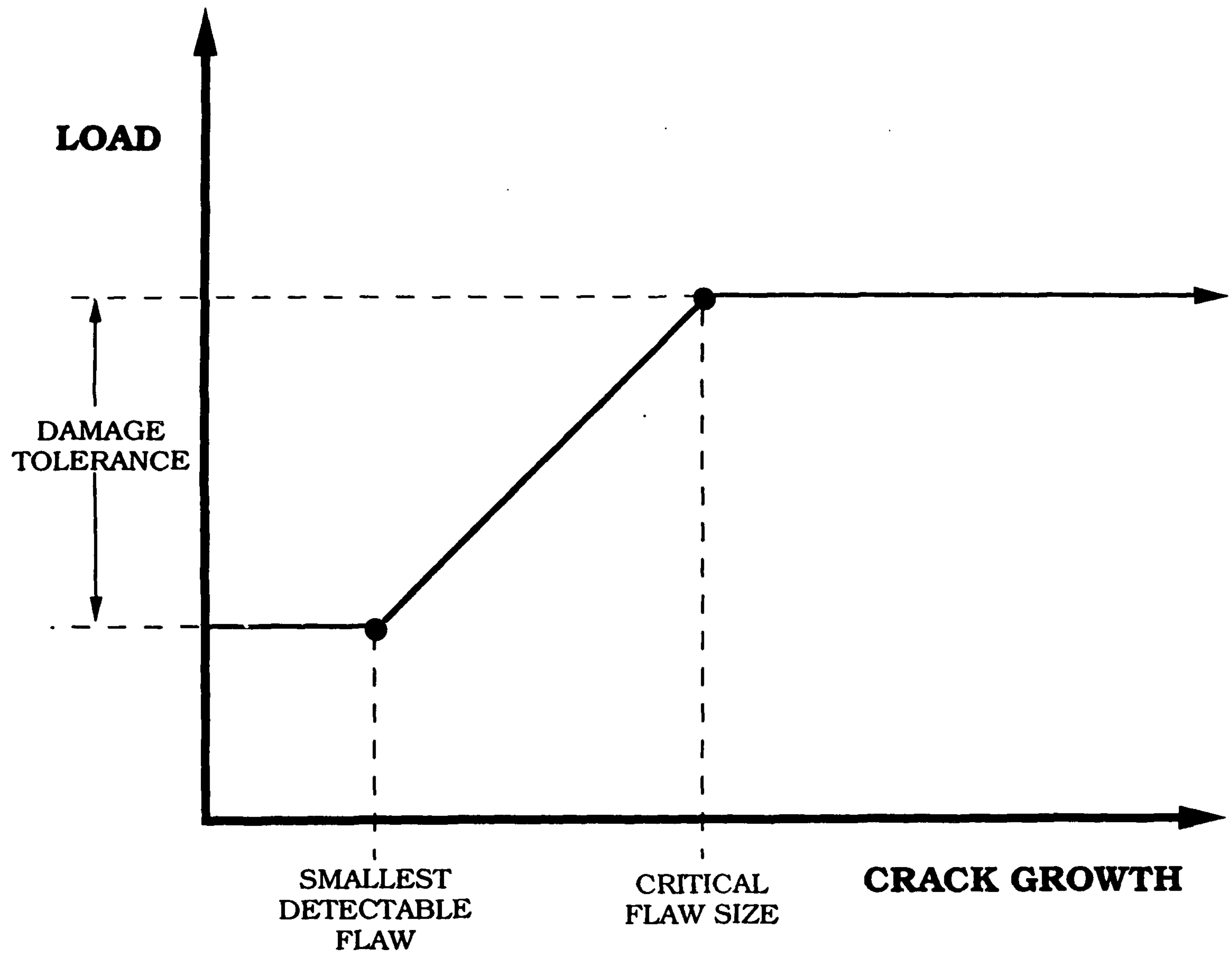
LOAD
DAMAGE
TOLERANCE
SMALLEST
DETECTABLE
FLAW
CRITICAL
FLAW SIZE
CRACK GROWTH

OBJECTIVES

- Identify damage modes in laminated composites
- Obtain a fundamental understanding of behavior
    - Primary modes
    - Accompanying secondary modes
- Investigate interaction of damage modes
    - Resistance and containment of primary modes

DAMAGE MODES IN LAMINATED COMPOSITE ROTORCRAFT STRUCTURES

- Delamination
  - Free Edge
  - Local
- Fiber Pullout and Breakage
- Matrix Microcracking

→ Interaction of Damage Modes

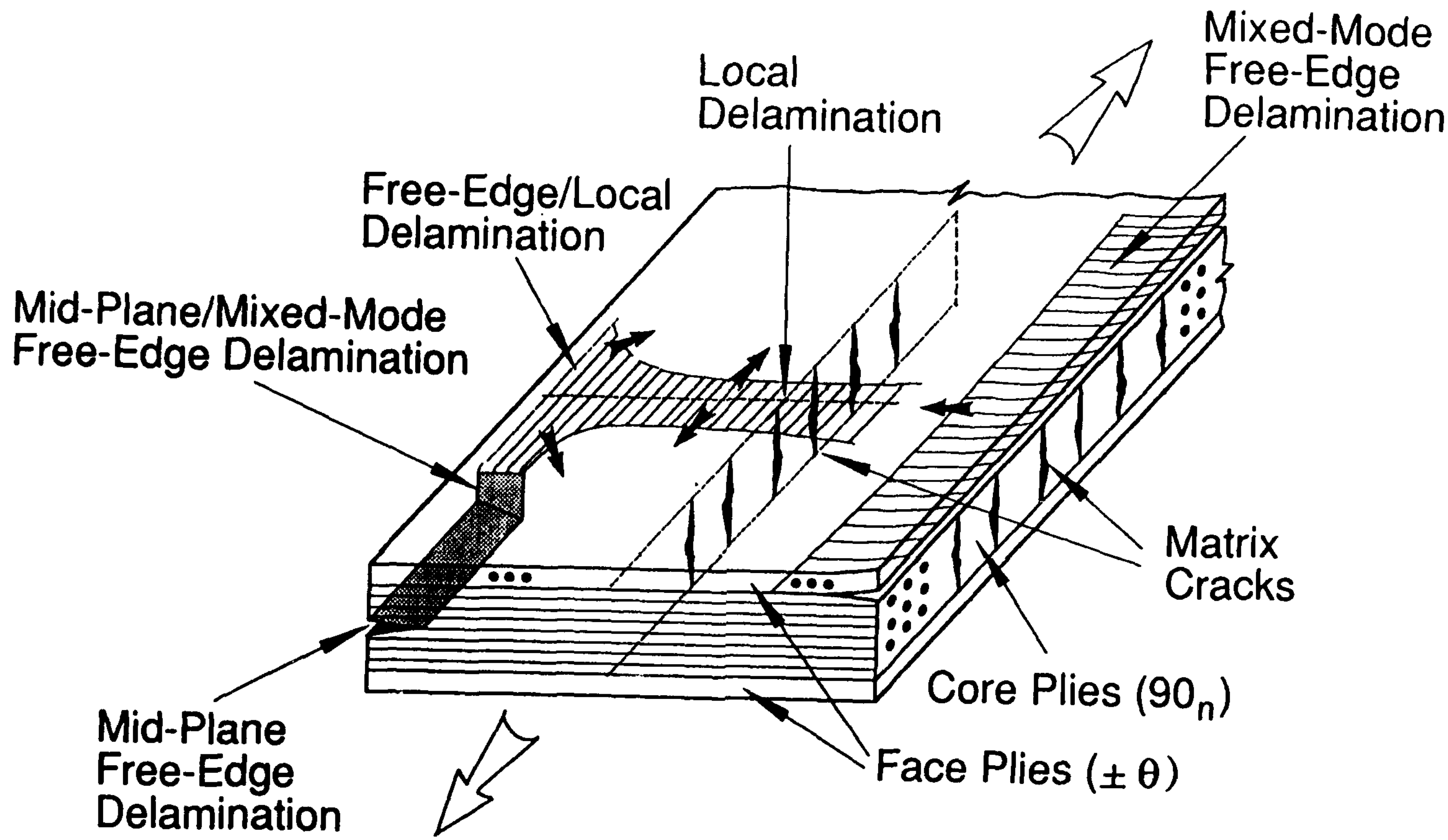

DAMAGE MODES

APPROACH

- Design and test generic laminate configurations to isolate a primary damage mode
  - geometry
  - material
- Characterize damage growth
  - load vs. growth data
- Correlate with fracture surface morphology

CONFIGURATION DESIGN

- Ply drop / Taper
  - Unidirectional layup
  - Two material systems:
    * AS4/3501-6
    * AS4/BP907

PLY-DROP CONFIGURATION

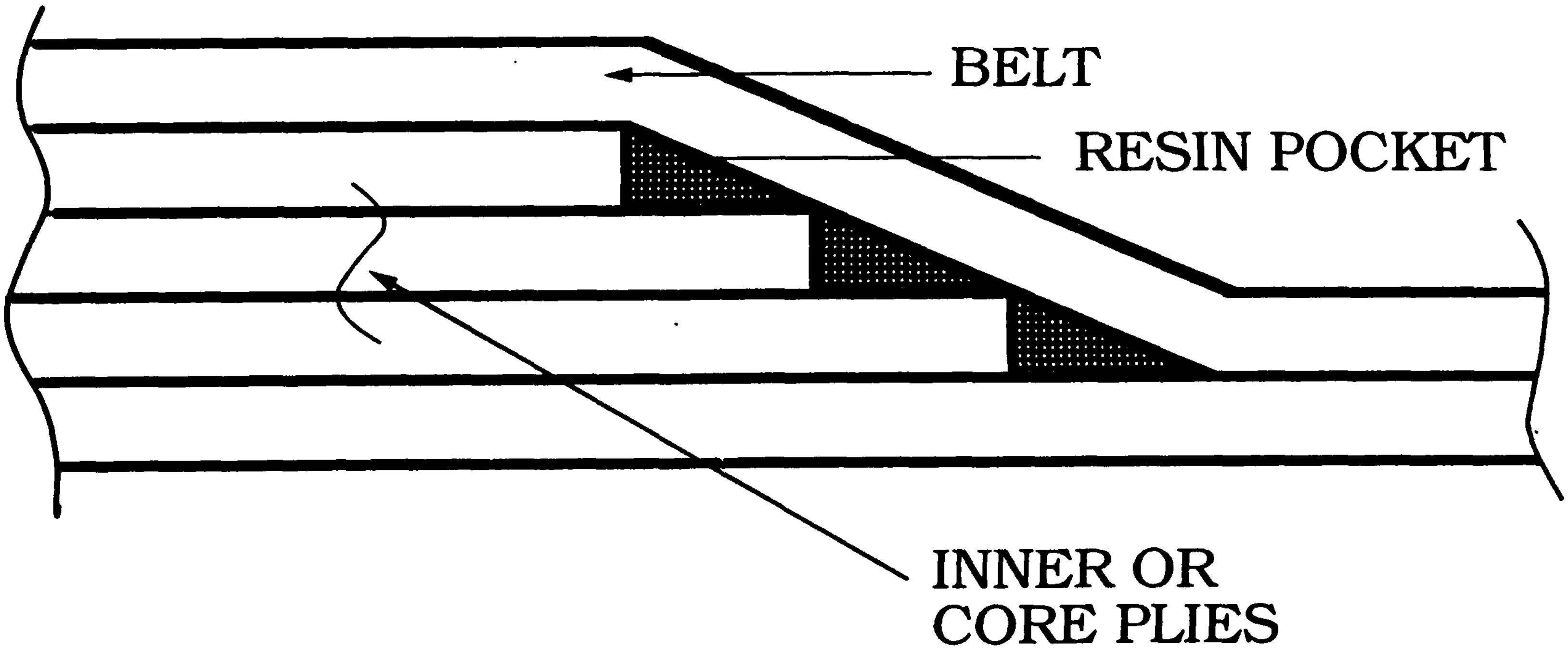

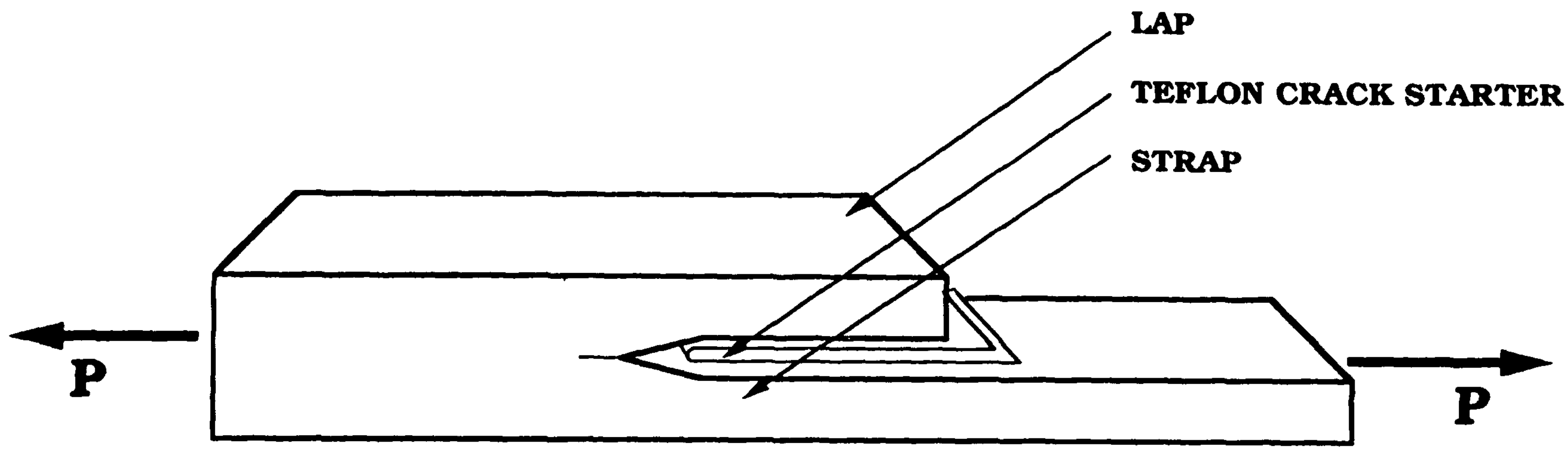
LAP
TEFLON CRACK STARTER
STRAP
P
P

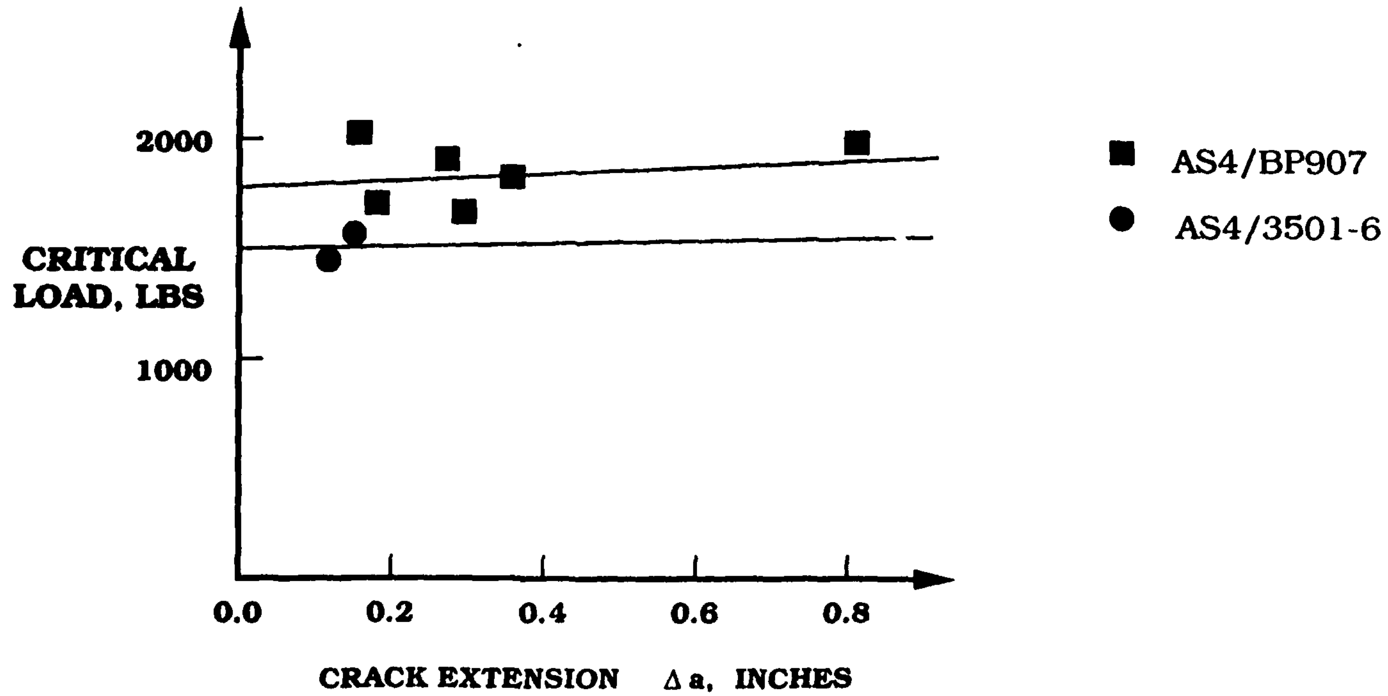
CRITICAL LOAD, LBS
2000
1000
0.0
0.2
0.4
0.6
0.8
CRACK EXTENSION Δa, INCHES
AS4/BP907
AS4/3501-6

FRACTURE SURFACE MORPHOLOGY

- Use of statistical approach to quantify damage modes
  - Interface failure
  - Matrix shear
  - Matrix cracking
  - Defects
- Correlate with load vs. crack growth

STATISTICAL APPROACH

- Mann-Whitney U-test
    - Nonparametric
    - Requires no knowledge of distribution
    - 95% efficient
- Compare area fractions of morphologies in adjacent data sets

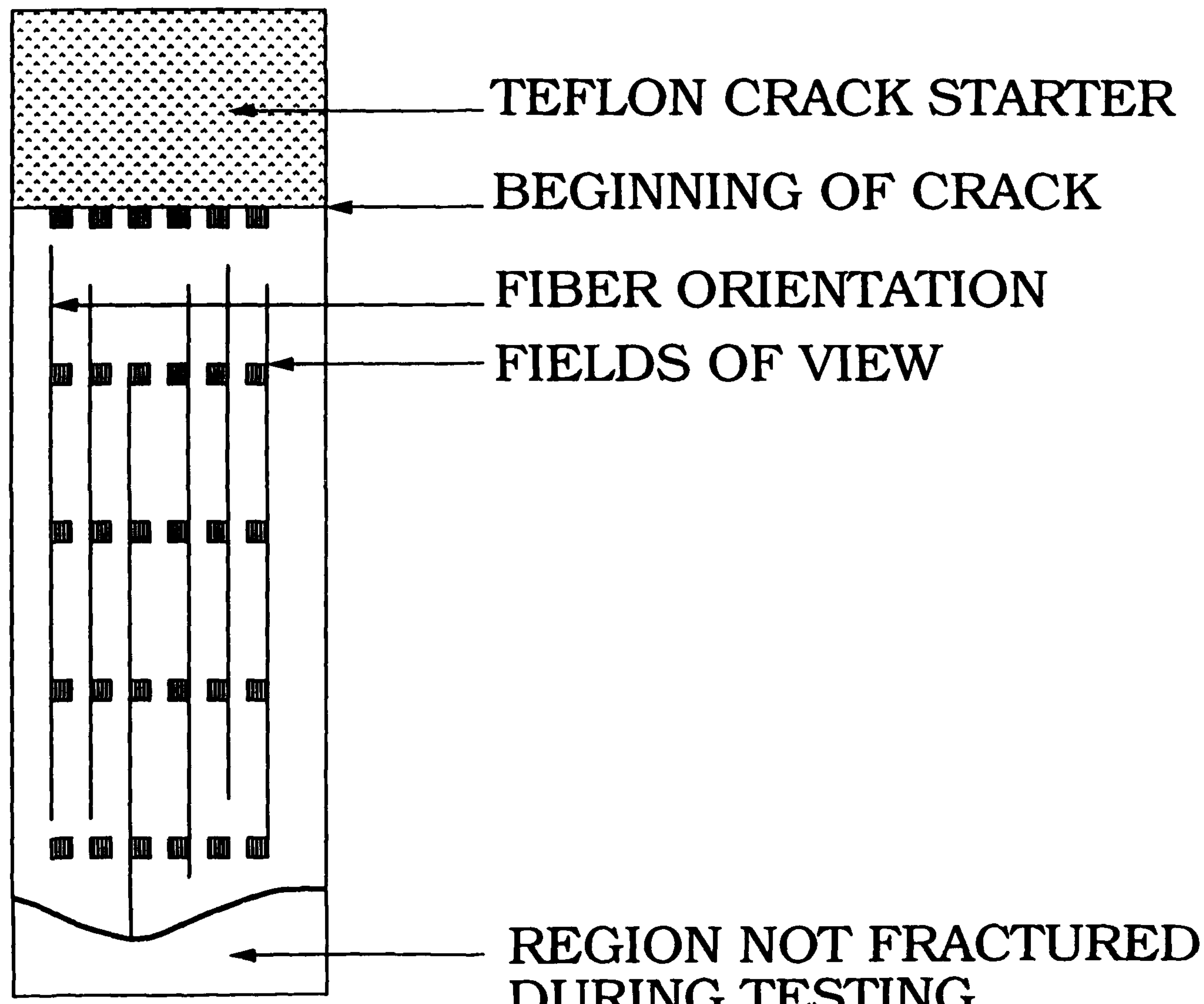
TEFLON CRACK STARTER
BEGINNING OF CRACK
FIBER ORIENTATION
FIELDS OF VIEW
REGION NOT FRACTURED
DURING TESTING

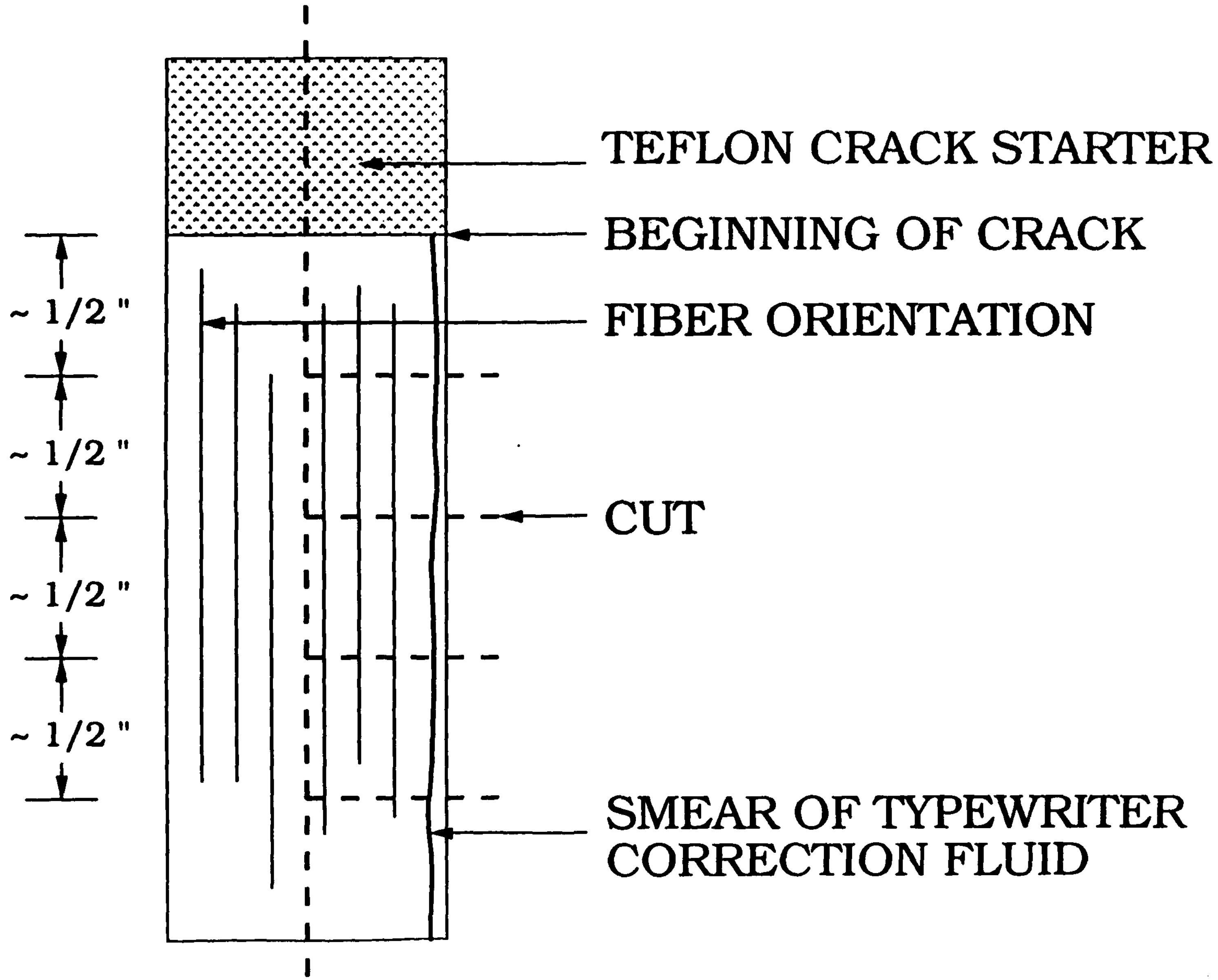
TEFLON CRACK STARTER
BEGINNING OF CRACK
FIBER ORIENTATION
CUT
SMEAR OF TYPEWRITER CORRECTION FLUID
~ 1/2 "
~ 1/2 "
~ 1/2 "
~ 1/2 "

POINT-COUNTING APPROACH

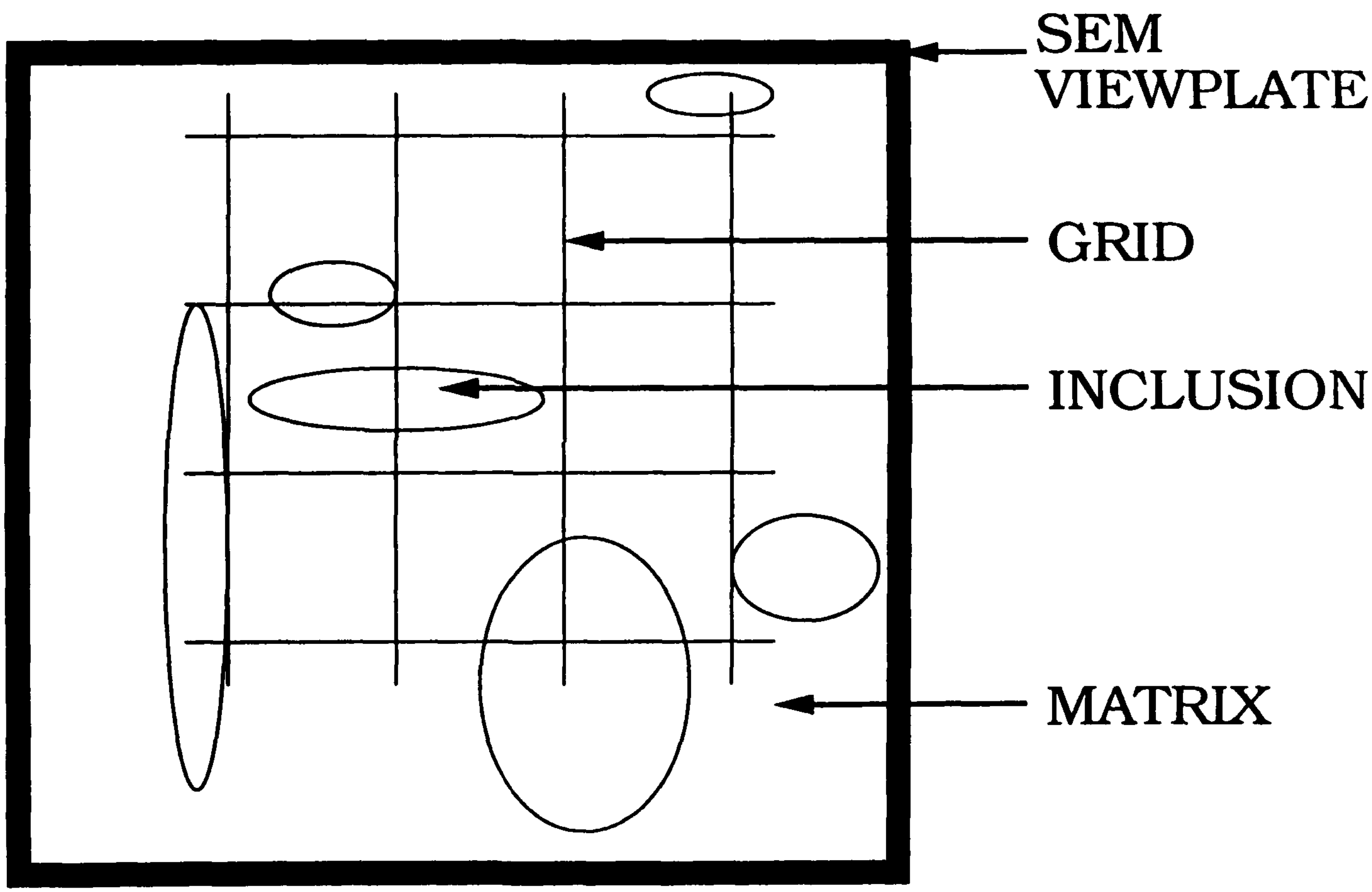

AN EXAMPLE
FROM A BRITTLE SYSTEM

STATISTICAL RANGE	ARREST LOCATION
15.6 mm - 17.6 mm	18.3 mm
26.2 mm - 28.2 mm	24.4 mm

BRITTLE SYSTEM EXAMPLE (continued)

- FIRST ARREST:
  - Interface failure increases
  - Shearing failure decreases
  - Matrix cracking increases
- SECOND ARREST:
  - Above events reversed
- SUGGESTS ARREST IS TRANSITION BETWEEN DAMAGE MODES

DAMAGE RESISTANCE DESIGN

- Develop a secondary vehicle to retard delamination
  - Matrix microcracking at delamination front
- Alter layup
  - Increase matrix loading
  - Quasi-isotropic layup

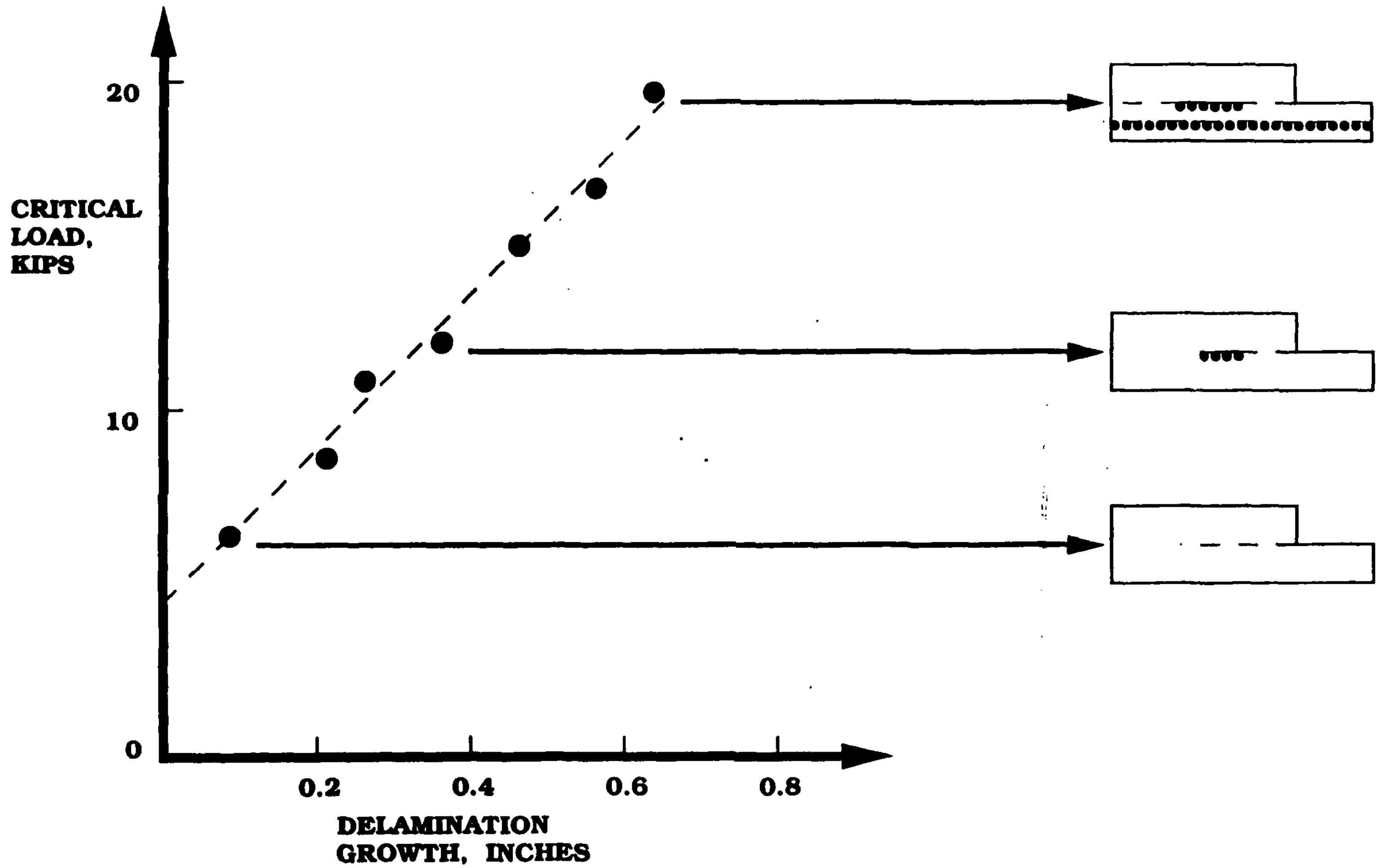
CRITICAL
LOAD,
KIPS
20
10
0
0.2
0.4
0.6
0.8
DELAMINATION
GROWTH, INCHES

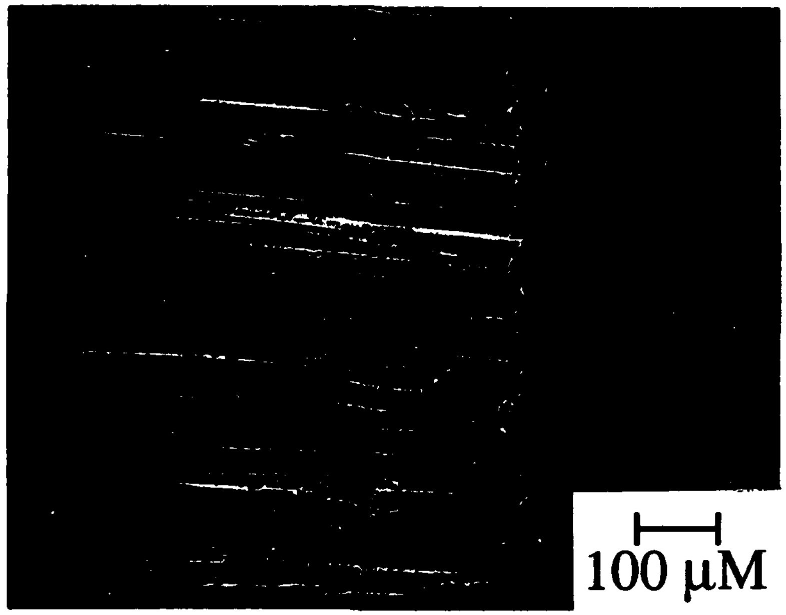
100 μM

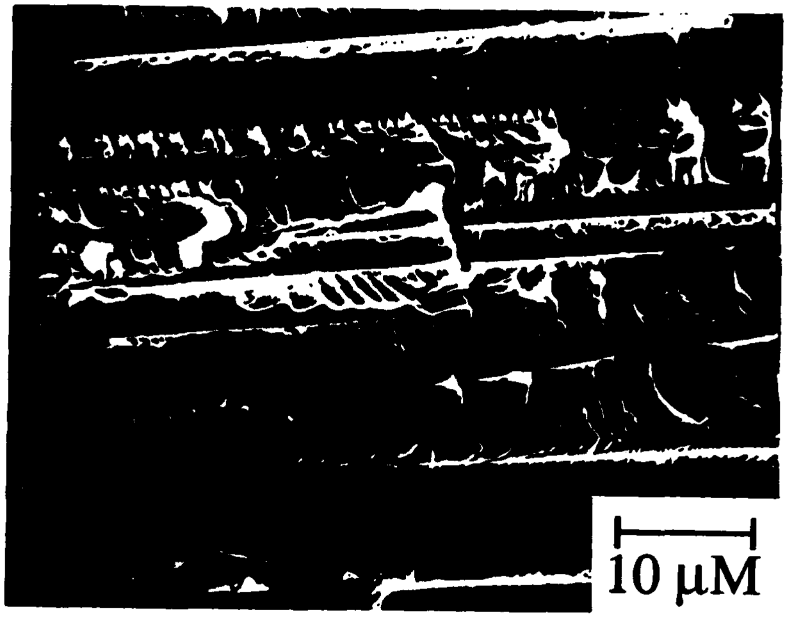
10 µM


1 µM

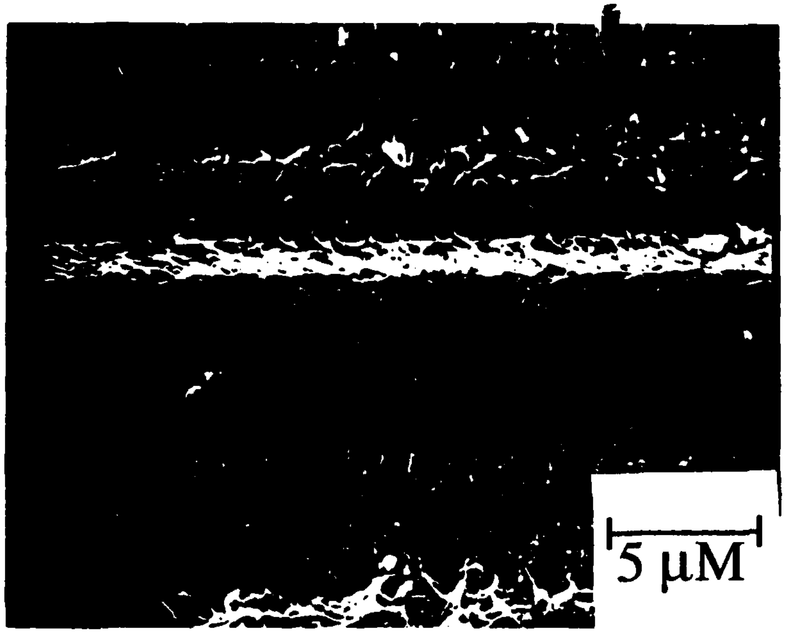
5 μM

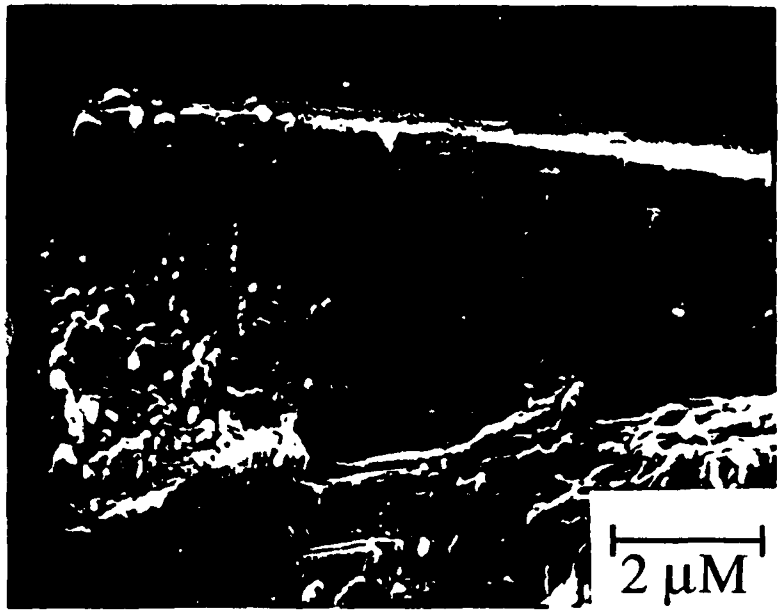
2 μM

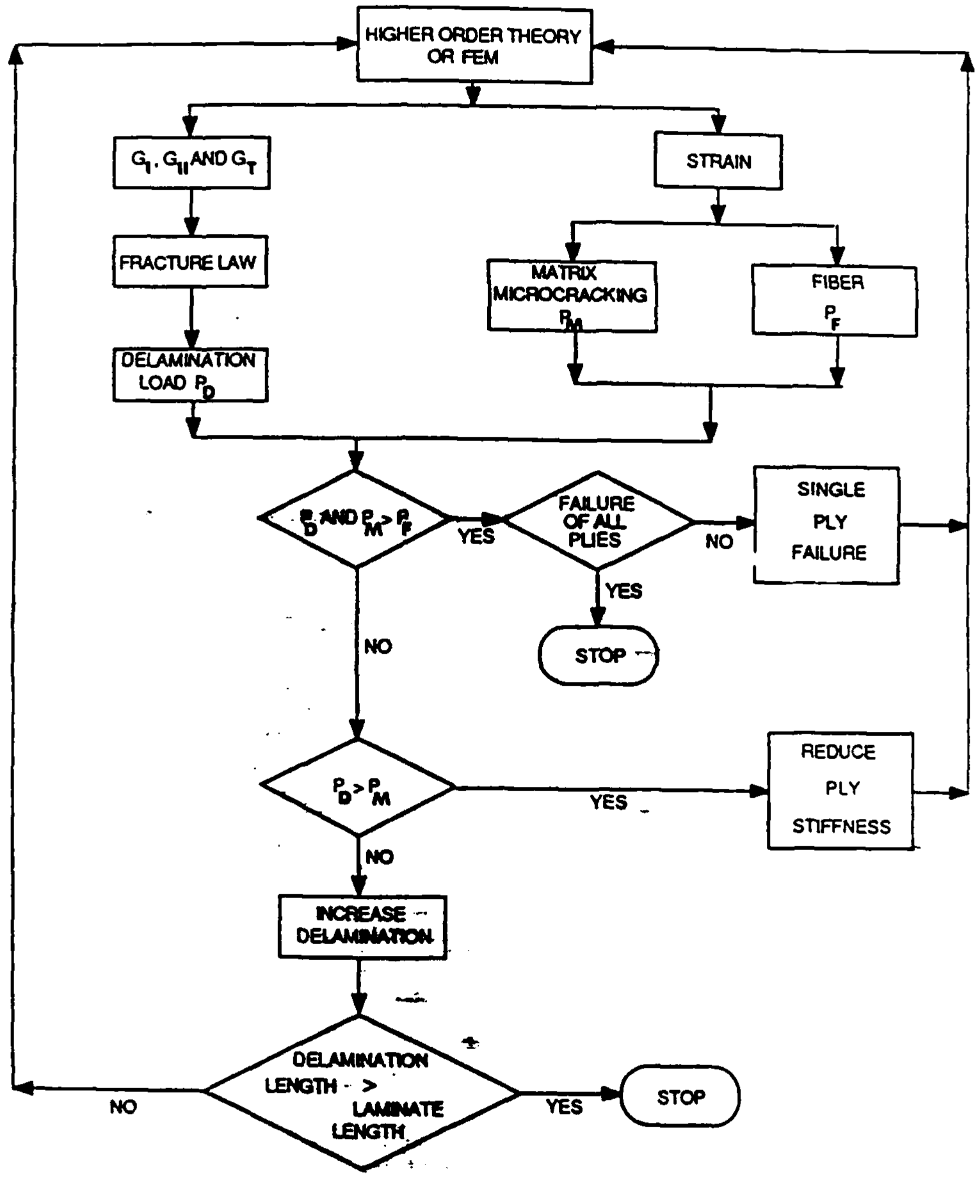
HIGHER ORDER THEORY OR FEM
G_I, G_{II} AND G_T
STRAIN
FRACTURE LAW
MATRIX MICROCRACKING P_M
FIBER P_F
DELAMINATION LOAD P_D
P_D AND P_M > P_F
YES
FAILURE OF ALL PLIES
NO
SINGLE PLY FAILURE
YES
STOP
NO
P_D > P_M
YES
REDUCE PLY STIFFNESS
NO
INCREASE DELAMINATION
DELAMINATION LENGTH > LAMINATE LENGTH
NO
YES
STOP

CONCLUSION

- Interaction of damage modes can lead to improvement in damage resistance by tailoring
  - Ply thickness
  - Ply orientation
  - Matrix and fiber material

Biaxial Fatigue and Deformation Behavior of Gr/E Composites

Erhard Krempl

Department of Mechanical Engineering,
Aeronautical Engineering & Mechanics
Rensselaer Polytechnic Institute
Troy, N. Y. 12180-3590

The Effect of Interlaminar Normal Stresses on the Uniaxial Zero–to–Tension Fatigue Behavior of Graphite/Epoxy Tubes

Erhard Krempl and Deukman An*
Mechanics of Materials Laboratory
Rensselaer Polytechnic Institute, Troy, NY 12180–3590

During the past several years, the Mechanics of Materials Laboratory of RPI has developed a method to obtain biaxial fatigue data under axial/torsion loading. A thin–walled tubular specimen can be made from prepregs by a lay–up procedure and tested in an MTS servohydraulic axial/torsion testing machine with computer control. We have provided completely reversed load–controlled fatigue data on Gr/Epoxy materials under uniaxial and combined loadings using $[\pm 45]_s$ and $[0/\pm 45]_s$ lay–ups [1–3]. The edgeless specimen eliminates suspected end effects and can be used for tests involving significant compressive loading. Near unidirectional Gr/Epoxy and Kevlar/Epoxy specimens were fatigue tested in uniaxial loading for negative R–ratios [3].

It was suspected that the thin–walled tubular specimen would not provide "true material fatigue data" because of the presence of interlaminar tensile stresses introduced by the curvature. They would promote early delamination of the plies. To check on this hypothesis zero–to–tension fatigue tests were run on Gr/Epoxy $[\pm 45]_s$ tubes with and without pressurization. The pressure levels were chosen so as to compensate the suspected interlaminar tensile stresses. Fatigue test results in the range from 10^4 to 10^6 cycles with and without pressurization are within the same reasonable scatterband. It is concluded that the interlaminar tensile stresses do not affect the fatigue performance.

Restraint of lateral motion by inserting a tightly fitting metal mandrel into the bore of the tube had a significant beneficial effect on the static and the fatigue strength of the tubes. This improvement could be used in practical applications.

REFERENCES

[1] Krempl, E. and Niu, T. M., *Journal of Composite Materials, 16*, 1982, pp. 172–187.

[2] Niu, T. M., "Biaxial Fatigue of Graphite/Epoxy $[\pm 45]_s$ Tubes,"D. Eng. thesis, Rensselaer Polytechnic Institute, May 1983.

[3] Krempl, E., Elzey, D. M., Hong, B. Z., Ayar, T. and Loewy, R. G., *Journal of the American Helicopter Society, 33*, 1988, pp. 3–10.

*Now at Pusan National University, Pusan, Korea.

I. SPECIMEN, EQUIPMENT

II. BIAXIAL FRACTURE SURFACE

III. BIAXIAL FATIGUE RESULTS

IV. DISCUSSION

Fatigue Test Specimens in Use

Strip (ASTM)

Thinwalled tubes

Cruciform (plane) Specimen

Test Specimens

Strip	*Tubular*
tensile loading	tension/compress.
edge effects	no edge effects
axial loading	axial,torsion, press.
off-axis shear only	on/off-axis shear

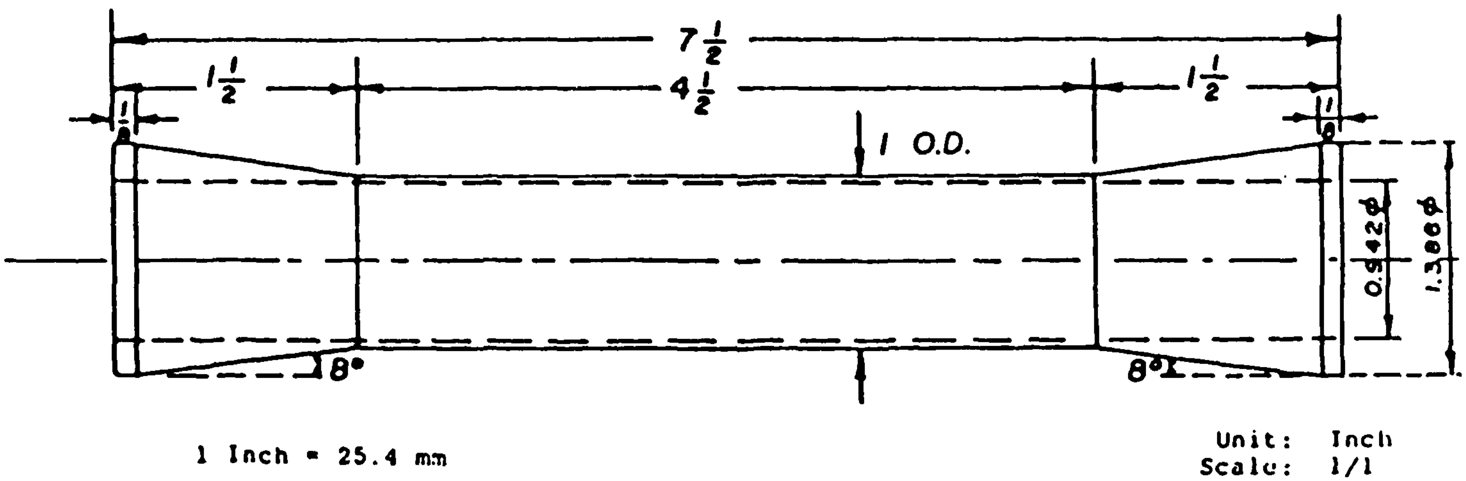

Figure 1 Thin-walled tube specimen.

SPECIMEN

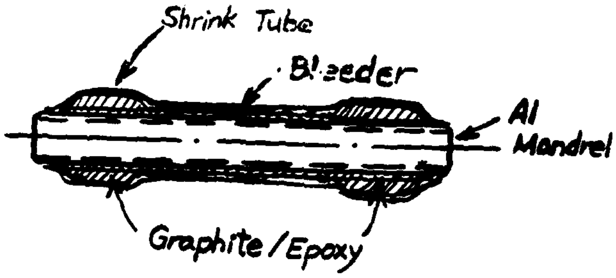

MATERIAL:

FIBERITE HY-E 1048 A1E PREPREG
T-300 UNION CARBIDE GR FIBER

Cure
79°C: 20 MIN PREHEAT, HOLD 30 min.
121°C 150 MIN 0.69 MPA CURING
SLOW COOLING TO ROOM TEMPERATURE

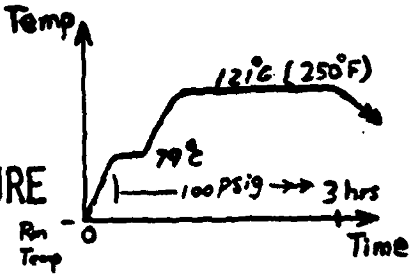

60% FIBER VOLUME

THIN-WALLED TUBES. OD 25.4 MM;
WALL THICKNESS 1.5 MM; LENGTH 190 MM
$[\pm 45]_s$

AXIAL: MATRIX BEHAVIOR DOMINATES DEFORMATION

TORSION: FIBER BEHAVIOR DOMINANT

J. COMPOSITE MATERIALS 16, 172-187 (1982)

SPECIMEN I FIXTURE

EXTENSOMETER

- DIAMETRAL, AXIAL
- BIAXIAL. AXIAL AND ANGULAR DISPLACEMENT

TESTING MACHINE

- MTS TENSION-TORSION SERVOHYDRAULIC TEST SYSTEM
- MTS 463 CONTROL AND DATA INTERFACE, TEKTRONIX 4025 TERMINAL

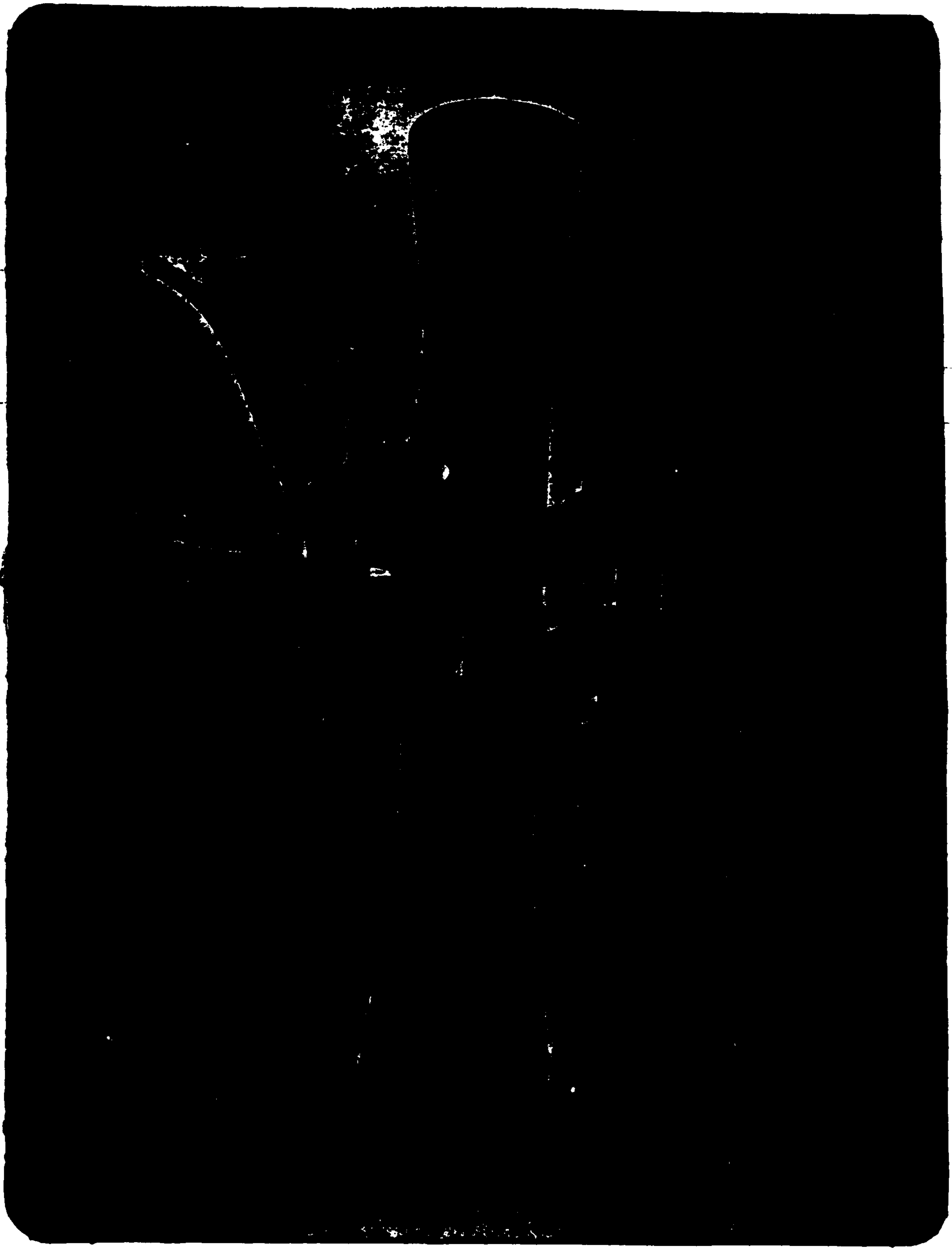

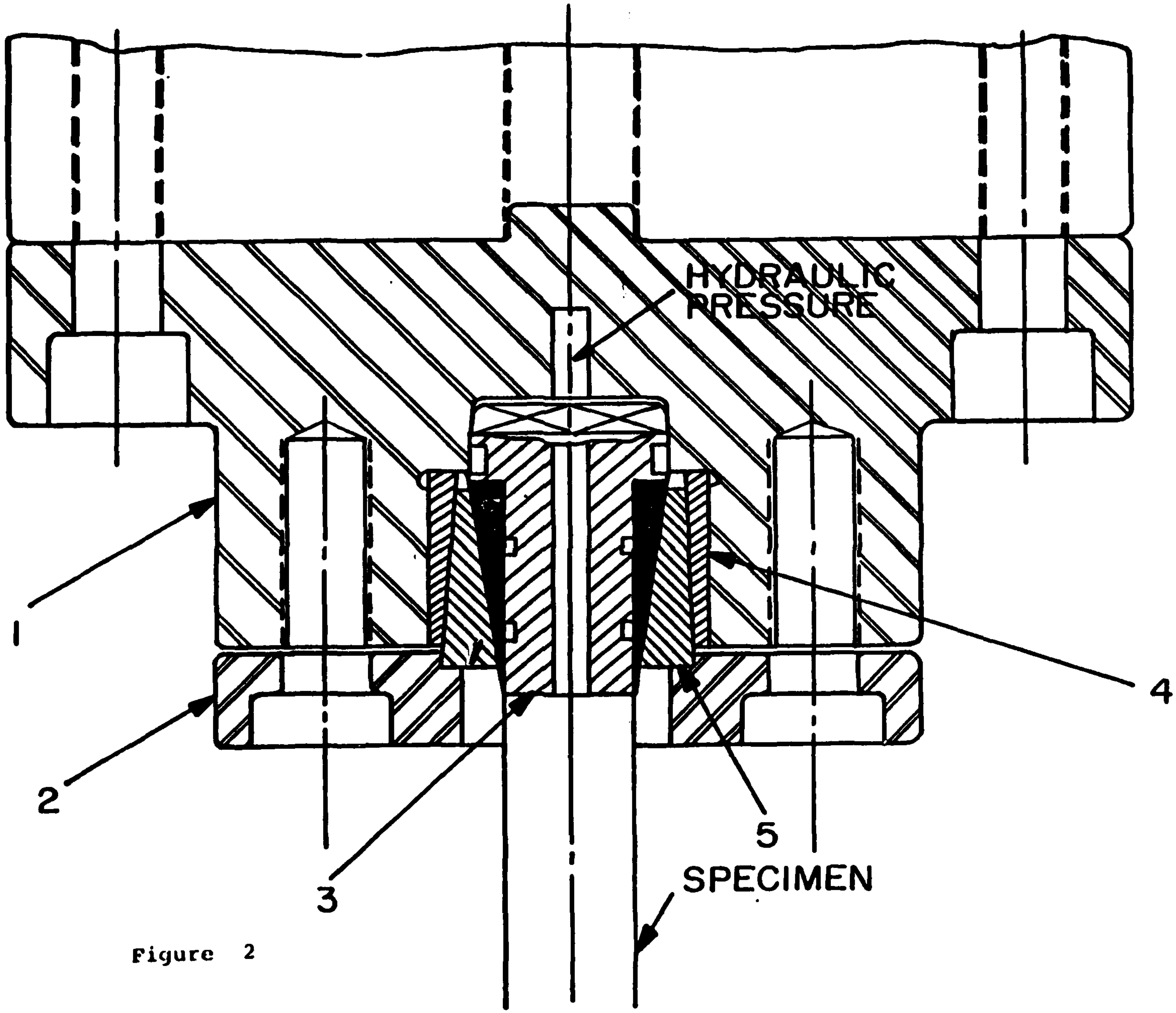

Figure 2

I. SPECIMEN, EQUIPMENT

II. BIAXIAL FRACTURE SURFACE

III. BIAXIAL FATIGUE RESULTS

IV. DISCUSSION

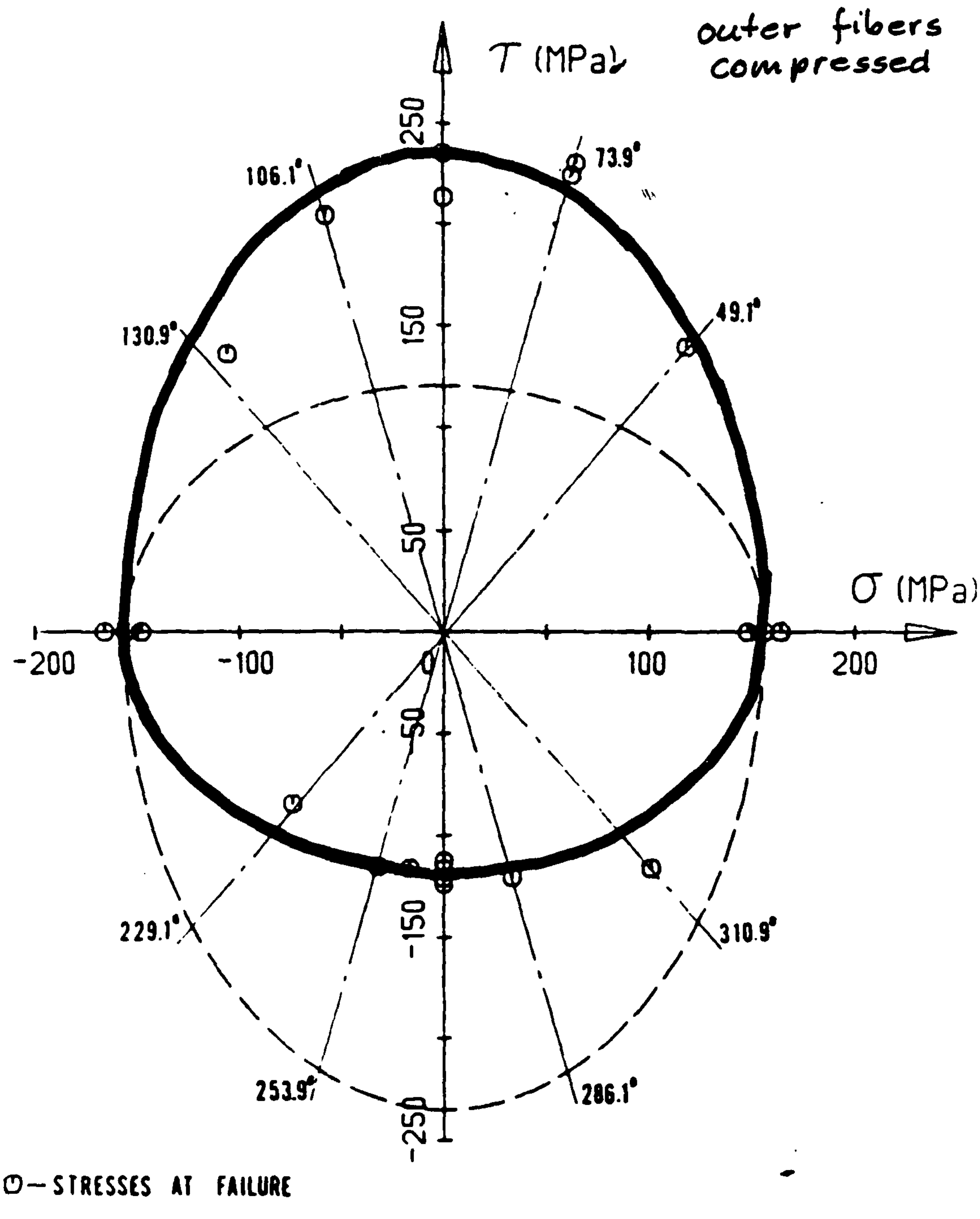

Figure 22 Fracture locus of graphite/epoxy $[\pm 45]_s$ tubes. It can be composed of two distinct surfaces.

STATIC TEST RESULTS $[\pm 45]_s$

- ELASTIC MODULI IN TENSION, COMPRESSION (± TORSION) ARE EQUAL
- INELASTIC, TIME-DEPENDENT DEFORMATION BEYOND 25% OF AXIAL ULTIMATE AND BEYOND 50% OF TORSIONAL ULTIMATE
- TENSILE AND COMPRESSIVE STRENGTH EQUAL ± 150 MPA
- ULTIMATE TORSION STRENGTH DEPENDS STRONGLY ON DIRECTION OF TWIST
  - \+ 190 MPA (OUTER FIBERS COMPR.)
  - \- 130 MPA (OUTER FIBERS TENS.)

WHY IS STATIC TORSION STRENGTH HIGHER WHEN OUTSIDE FIBERS ARE COMPRESSED?

EFFECTIVE RIGIDITY IS HIGHER IN THIS CASE THAN WHEN OUTER FIBERS ARE TENSED.

FAILURE MODE IS LOCAL (NOT EULER) BUCKLING. DELAMINATION ENHANCED DURING NEGATIVE TWIST.

WORST CASE NEGATIVE TWIST AND COMPRESSION ($\theta = 49°$).

PECULIAR SHAPE OF $\tau - \gamma$ DIAGRAM DUE TO LOCAL BUCKLING.

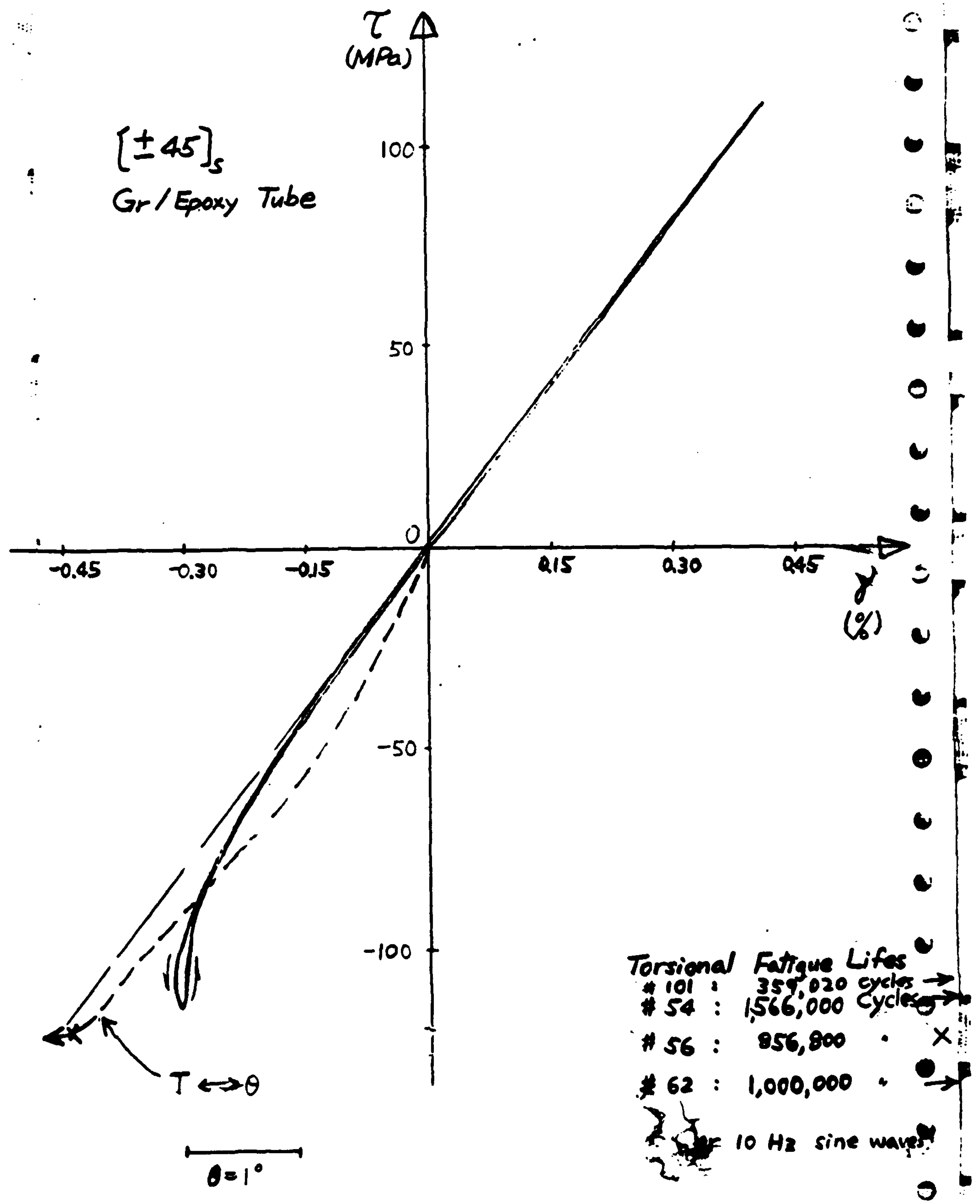

τ (MPa)
[±45]s
Gr / Epoxy Tube
100
50
0
-50
-100
-0.45
-0.30
-0.15
0.15
0.30
0.45
γ (%)
T ↔ θ
θ = 1°
Torsional Fatigue Lifes
101 : 359,020 cycles
54 : 1,566,000 Cycles
56 : 856,800
62 : 1,000,000
10 Hz sine waves

I. SPECIMEN, EQUIPMENT

II. BIAXIAL FRACTURE SURFACE

III. BIAXIAL FATIGUE RESULTS

IV. DISCUSSION

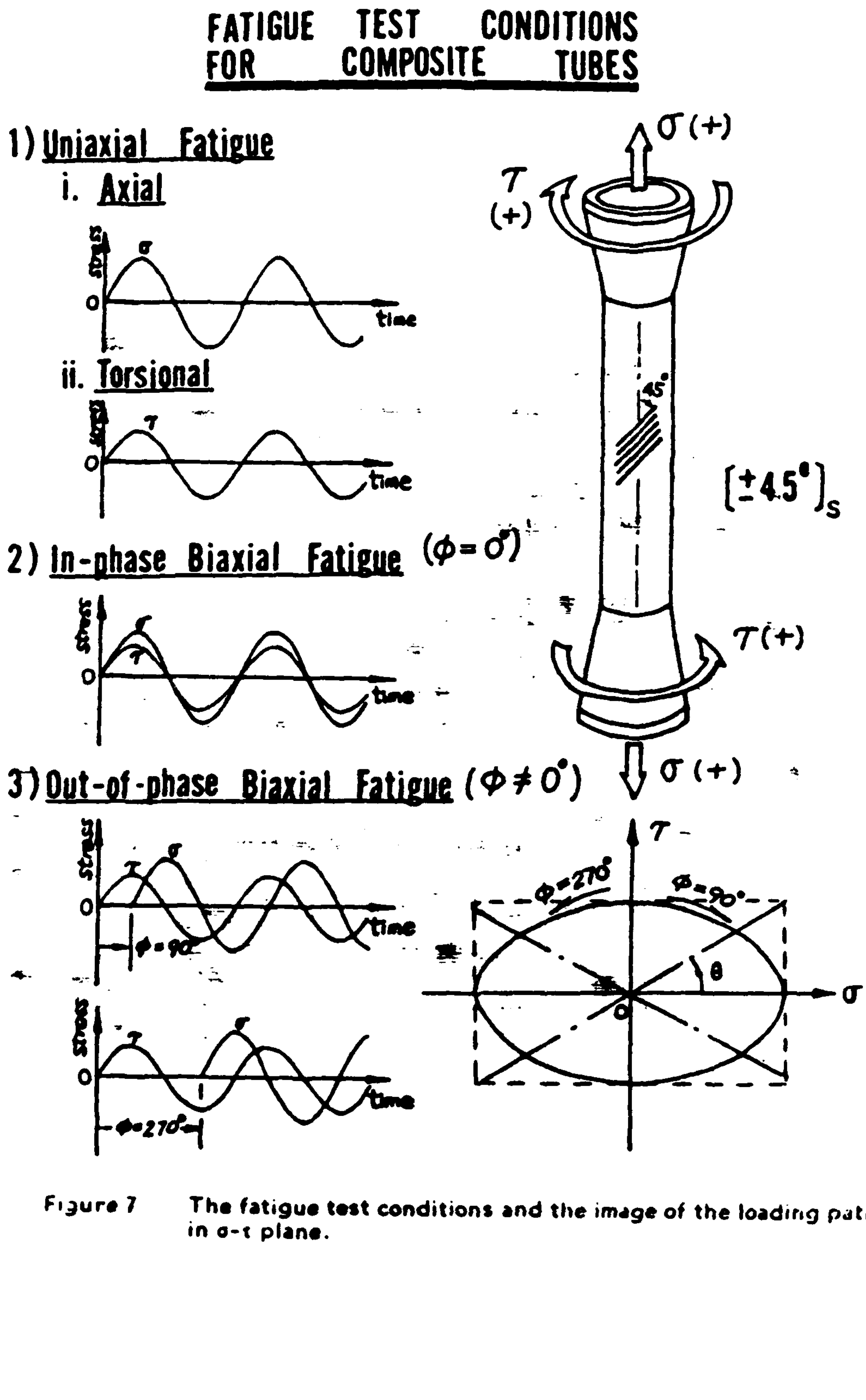

Figure 7 The fatigue test conditions and the image of the loading paths in σ-τ plane.

PARAMETERS

ROOM TEMPERATURE, AIR LOAD CONTROL, R = -1

IN PHASE

θ = 49°, 74°, 106°, 131°

TAN θ = SHEAR ST.A. /AXIAL ST.A.

OUT OF PHASE

θ = 49° ONLY

ϕ = 90° AND 270°

FREQUENCY

1 Hz

0.1 Hz AND 0.01 Hz FOR AXIAL AND θ = 49°
IN-PHASE TESTS

CYCLES-TO-FAILURE

$10^2 - 10^6$

MAJORITY < 10^5

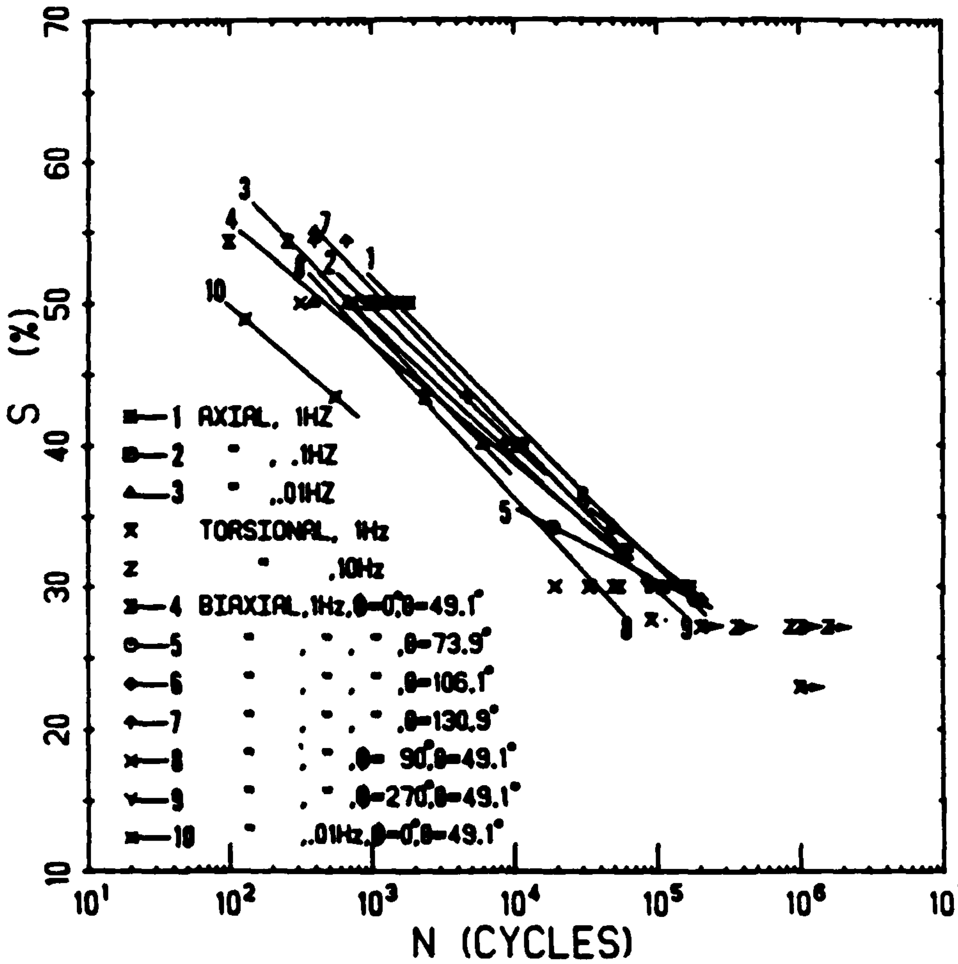

Figure 76 Fatigue life based on biaxial equivalent stress, sinusoidal loading, R=-1.

$$S^2 = \left(\frac{\sigma_a}{\sigma_u^+}\right)^2 + 0.078\left(\frac{\tau_a}{\tau_u^-}\right)^2$$

EFFECTIVE STRESS

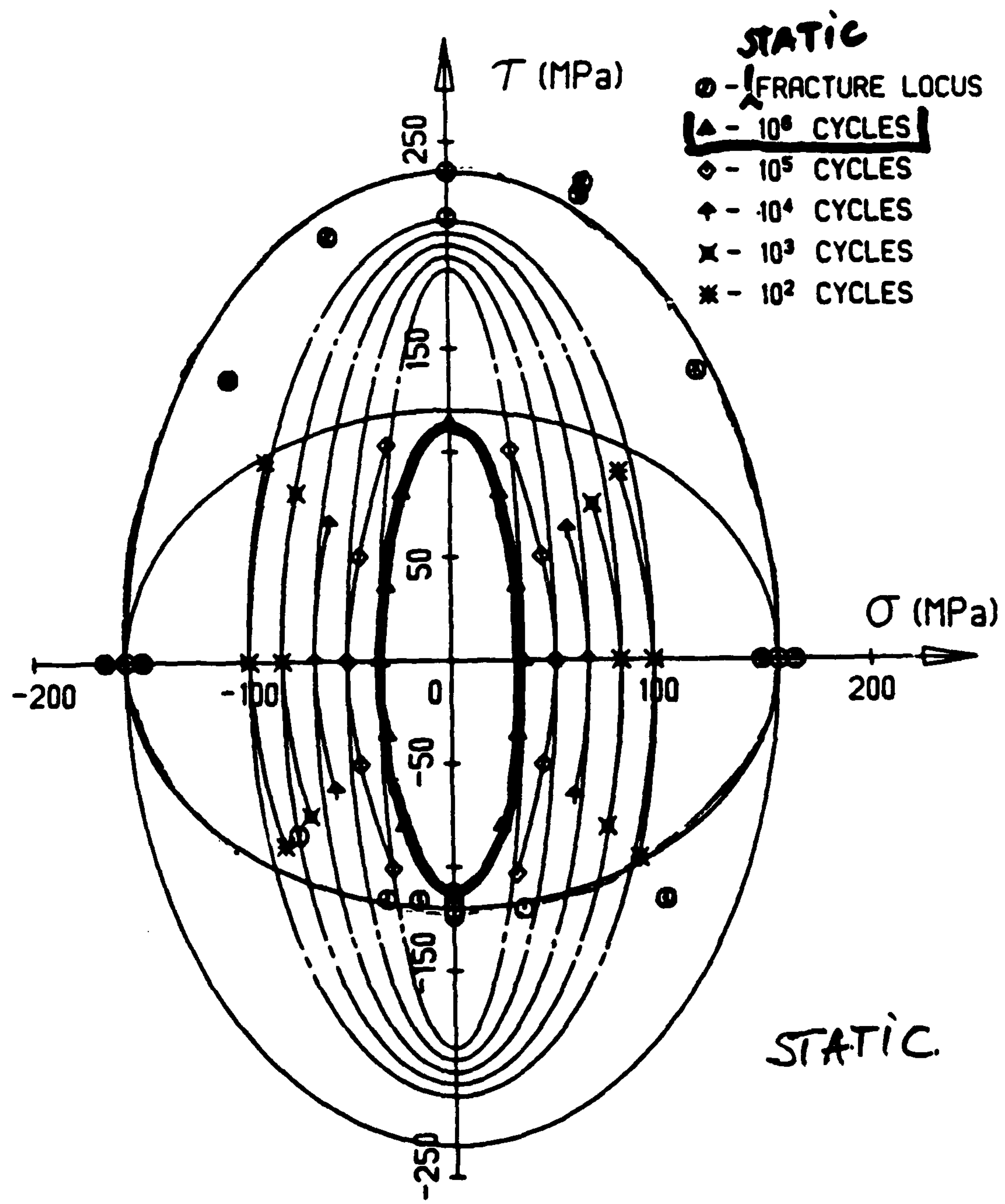

Figure 77 Iso-fatigue life curves of [±45]s graphite/epoxy tubes based in the σ-τ plane at R=-1 and 1 Hz. The solid contours with symbols represent the fatigue lives in the presence of buckling; the concentric ellipses would represent the fatigue lives without buckling. Static results are also shown.

FATIGUE PERFORMANCE LIMITED BY LOCAL BUCKLING

TIME DEPENDENCE CAUSES A REDUCTION OF FATIGUE LIFE

I. SPECIMEN, EQUIPMENT

II. BIAXIAL FRACTURE SURFACE

III. BIAXIAL FATIGUE RESULTS

IV. DISCUSSION

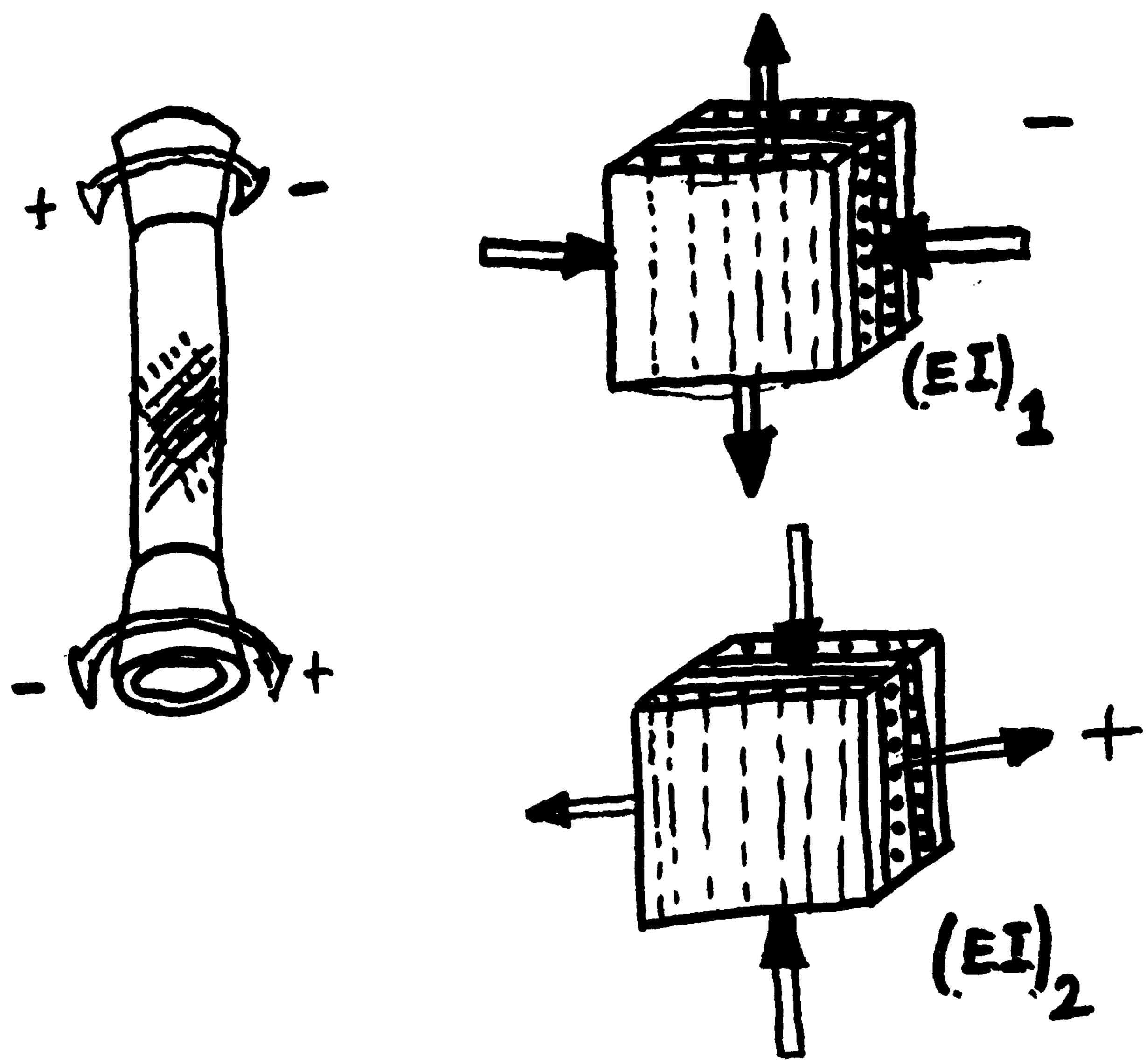

$(EI)_1 < (EI)_2$

EFFECTIVE RIGIDITY IS HIGHER IN THIS CASE THAN WHEN OUTER FIBERS ARE TENSED.

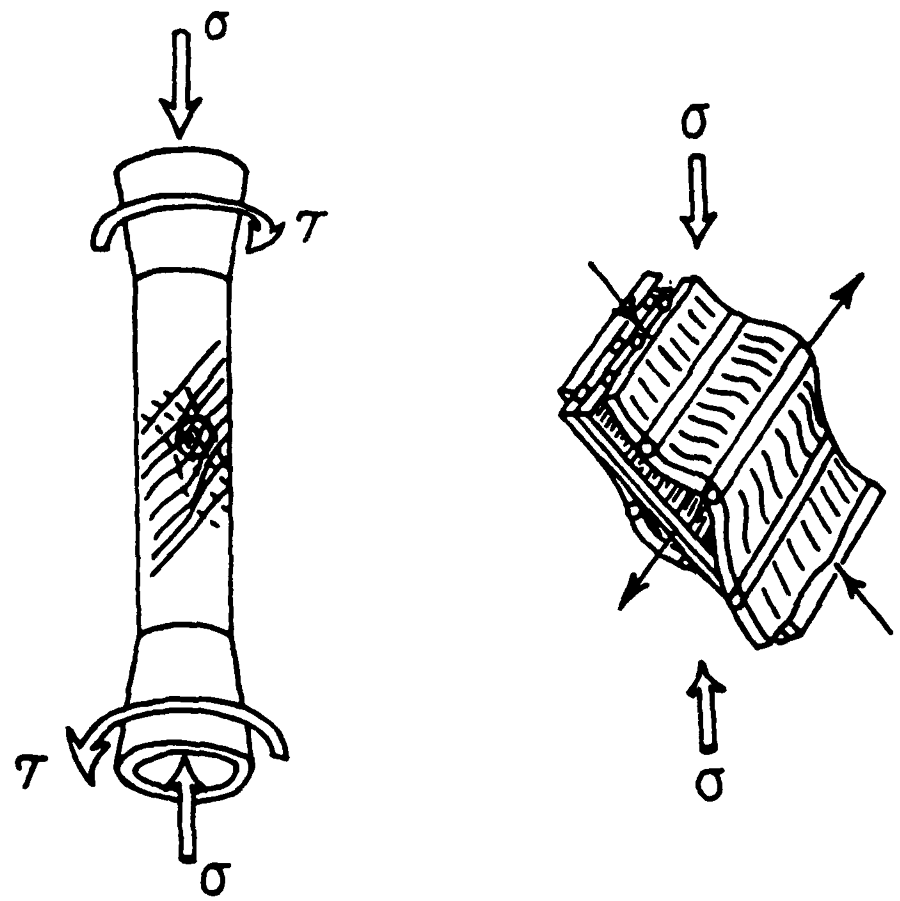

Figure 74 Sketch of deformation of a $[\pm 45]_s$ tube under combined compression and negative twist.

WORST CASE NEGATIVE TWIST AND COMPRESSION
(θ = 49°).

FATIGUE TEST RESULTS

R = -1. LOAD CONTROL AXIAL LOADING

- FATIGUE STRENGTH IS LOW
- THERE IS AN INFLUENCE OF FREQUENCY
- CHANGES IN HYSTERESIS LOOP SIGNIFICANT TOWARDS END OF LIFE
- APPEARANCE OF FATIGUE FRACTURE NOT DIFFERENT FROM STATIC FRACTURE

FATIGUE BEHAVIOR OF
UNIDIRECTIONAL COMPOSITES (KEVLAR 49/EPOXY)

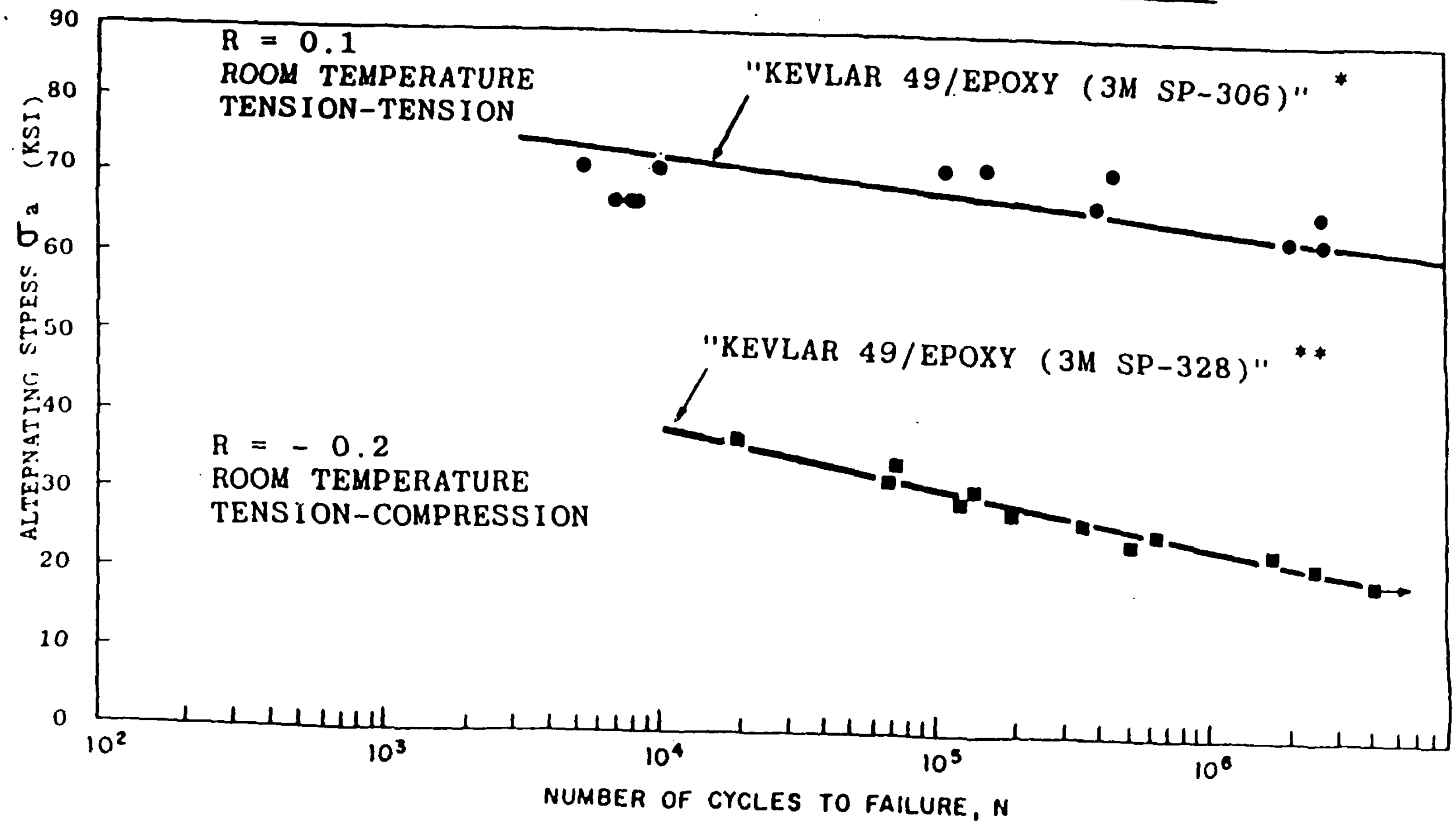

* Courtesy DU PONT Co. DATA MANUAL FOR KEVLAR 49 ARAMID III.
** ARO-RPI Composite Fatigue Research

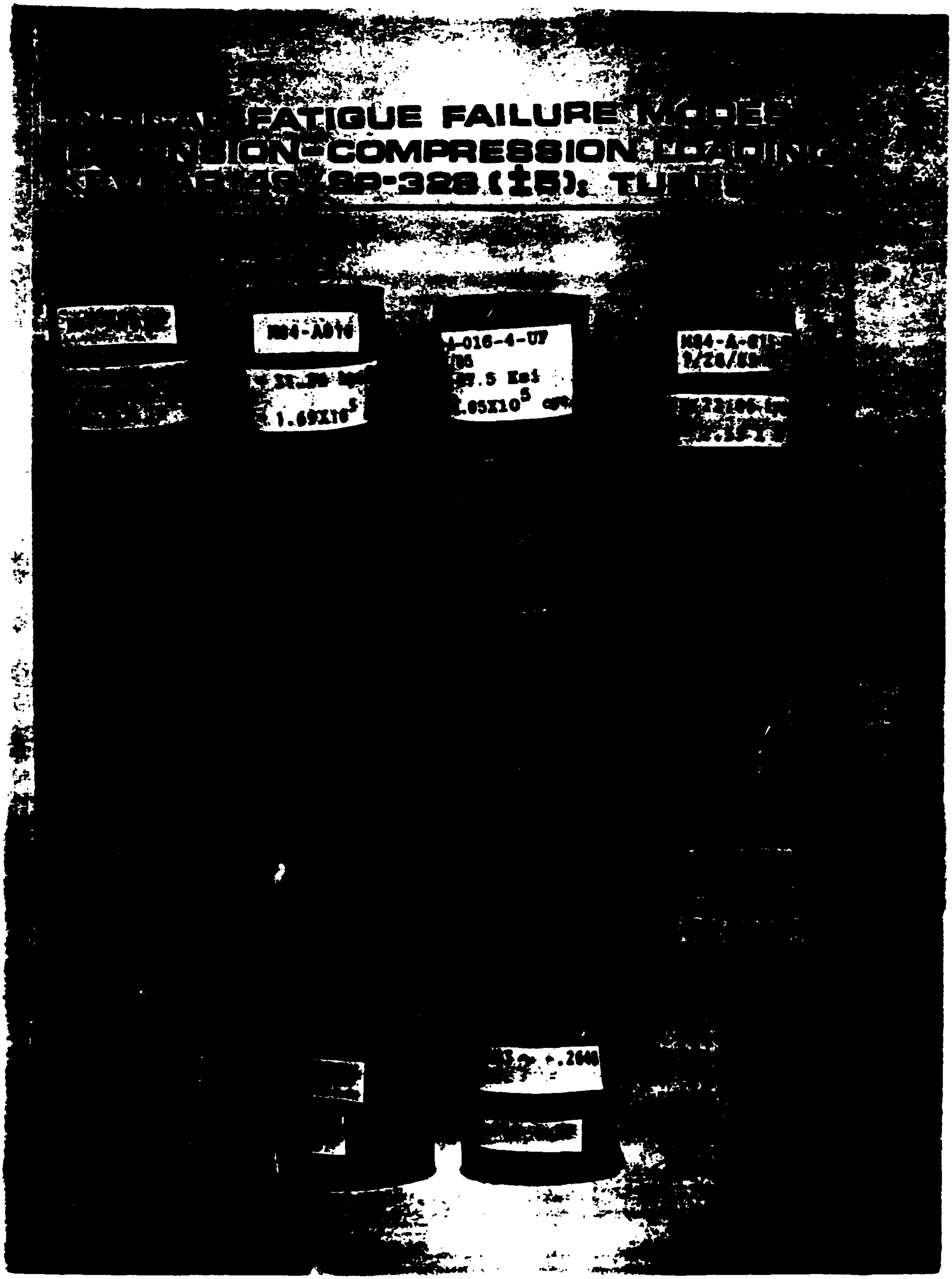
FATIGUE FAILURE
COMPRESSION
SP-328 (±5)
M84-A016
A-016-4-U7
1.69X10
1.05X10

Structural Tailoring Techniques for Increased Delamination Resistance of Laminated Composites

Anthony J. Vizzini
Assistant Professor

William R. Pogue, III
Research Engineer

2nd ARO–AHS-RPI Workshop on Composite Materials and Structures for Rotorcraft
September 14–15, 1989

Composites Research Laboratory
Center for Rotorcraft Education and Research
Department of Aerospace Engineering
University of Maryland
College Park, Maryland

Bearingless Rotor Hub

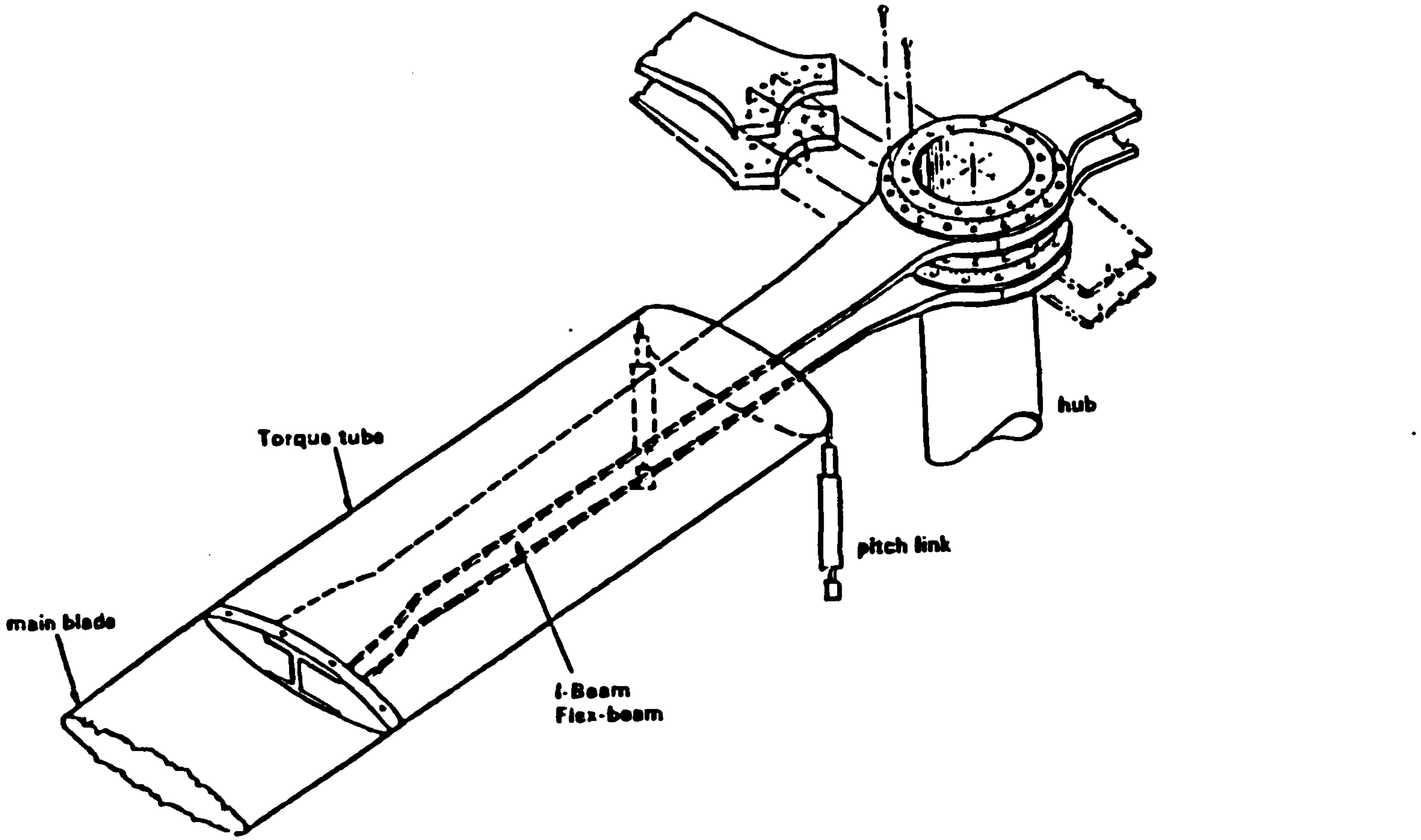

Motivation

To increase the service strength of delamination-critical structures

1. Performance can be increased by delaying or preventing the occurrence of delamination.
2. Techniques include the introduction of other materials, geometric changes, stacking sequence changes.
3. Method should be easily integrated in design and manufacturing phases.

Objectives

Alter significantly the state of interlaminar stress without altering *significantly* the component

1. Interlaminar effects occur within a small boundary layer.
2. Certain interfaces more critical than others.
3. Alter by removal, addition, replacement and/or relocation of material near edge.

RPI89–4

Delamination Mechanism

1. Mismatch of elastic properties
   Solution: Affect elastic moduli, stacking sequence, material choice

2. Stress-free edge, Discontinuity
   Solution: Remove discontinuity

3. Interlaminar stresses
   Solution: Alter interlaminar stress state

4. Interply failure, Delamination
   Solution: Increase interface strength

Discontinuity==>

Interlaminar Stress==>

Failure of Interface

Stronger interface prevents delamination by treating the symptom, *i.e.*, interfacial failure.

Alter the stress state and delamination is prevented by treating the primary cause.

Current Techniques

1. **Stacking sequence**
   Alteration of performance, particularly bending
2. **Softening strip**
   Nonhomogeneous component, thickness gradient
3. **Stitching**
   Delamination arrester, not interlaminar shear
4. **Ply wrap**
   Precludes trimming, inspection, monitoring
5. **Vertical ply drop**
   Thickness gradient, fewer load carrying fibers
6. **Angle alteration**
   Internal discontinuity

Schematic of Edge Alteration

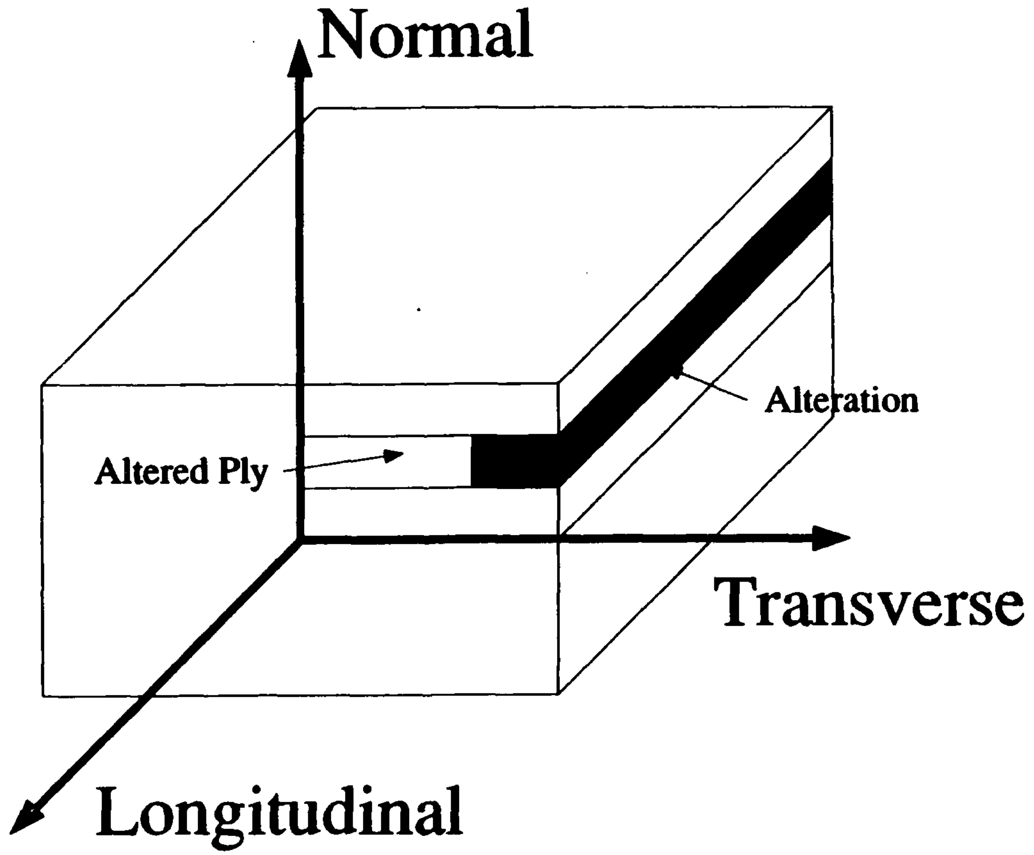

RPI89-8

Types of Edge Alterations

1. Discontinuous Alterations:
   - Vertical Ply Drop
   - Hybridization
   - Angle Alteration
2. Continuous Alteration:
   - Skewed Angle Alteration
   - Unaltered

Overall Approach

Analytical:

1. Model edge alterations
2. Calculate full 3–D states of stress at the free and internal edges via FEM
3. Select appropriate alterations
4. Determine expected performance

Experimental:

1. Develop edge-alteration specimens for each type of alteration
2. Manufacture specimens, unaltered and edge-altered
3. Evaluate stresses and strains

Analytical Program

1. Quasi-three-dimensional finite element model with assumed constant uniaxial strain
2. Assumed-stress hybrid element, 4 node, 12 dof
3. Two mesh schemes, one refined at the free edge, the other refined at the internal edge
4. Results in the interlaminar state of stress at the free and internal edges

Interlaminar Shear Stresses

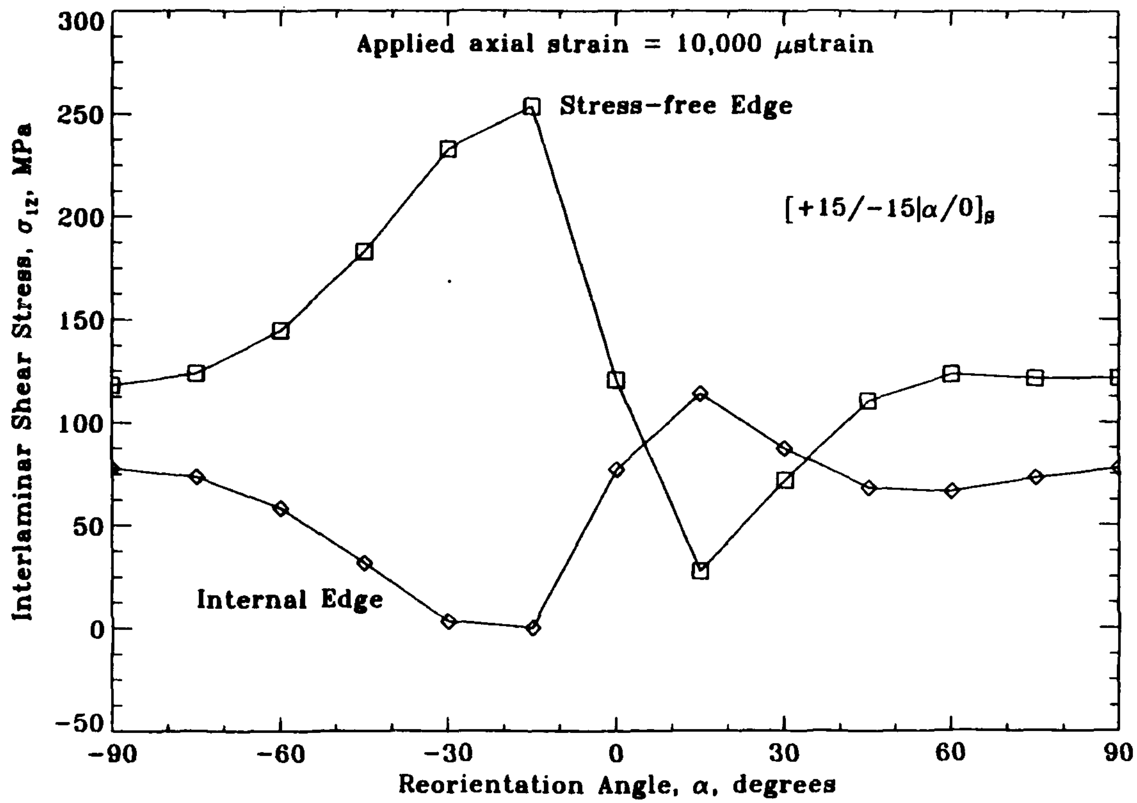

RPI89-12

Analytical Results

1. Introduction of edge alteration redistributes interlaminar stresses over the two interfaces.

2. Qualitative interlaminar states of stress at free and internal edges

3. Optima exist for specific edge alterations, *e.g.*, filler modulus, angle reorientation

Experimental Program

1. 20 unaltered, 75 edge-altered specimens
   - AS4/3501–6 Graphite/Epoxy
   - $[0/\pm15]_S$; $+15°$ or $-15°$ plies altered
   - $[\pm15/0]_S$; $-15°$ or $0°$ plies altered
   - Vertical ply drop, hybridization, angle alteration (replacement and skewing)

2. Quasistatic uniaxial tension to failure

3. Delamination initiation monitored visually, audibly, and via strain gage and load cell data

Schematic of Edge Alteration Specimen

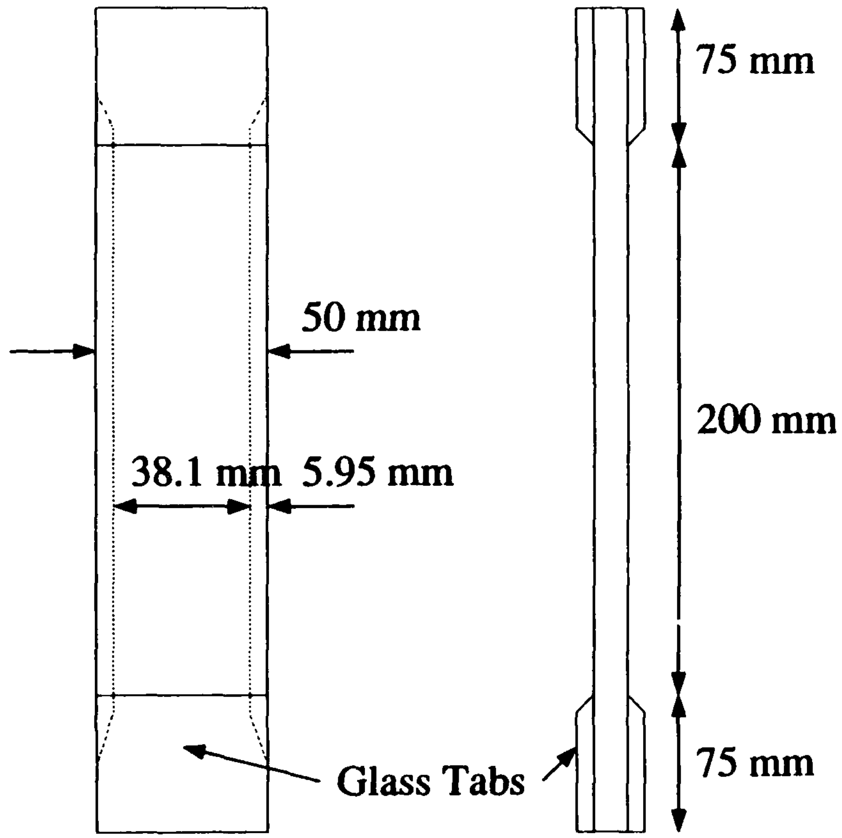

RP189–15

Skew Manufacturing Process

1. Angle ply is clamped between sets of parallel plates.
2. Backing paper is removed and skew area is heated via hot air gun.
3. Plates are then skewed up to 15°.
4. Ply is then transferred to the laminate.

Strain Gage Locations

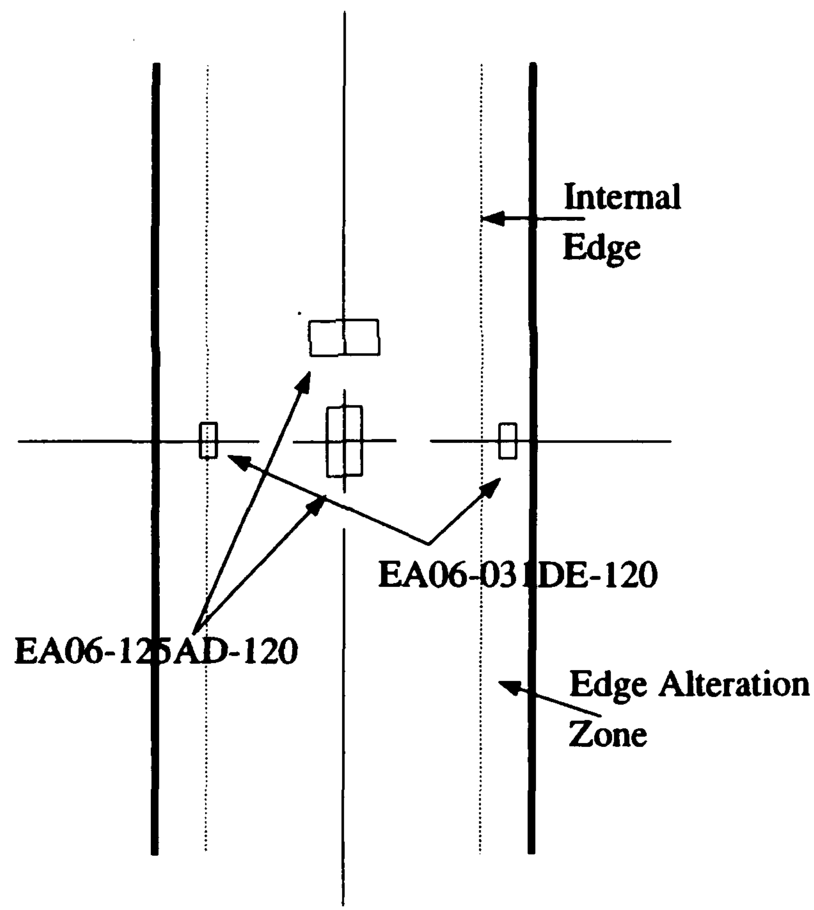

RPI89-17

Testing Procedure

1. MTS 810 220 kip testing machine with hydraulic grips.

2. Specimen edges painted white to highlight damage.

3. Stroke rate of 0.762 mm/min, equivalent to a strain rate of 3800 μstrain/min.

4. Test held at first indication of damage and visually inspected.

5. Test resumed, specimen loaded to final failure, photographed, and removed.

Experimental Results

1. Failure Mode
2. Delamination Onset Stress
3. Ultimate Failure Stress
4. Internal Edge Performance

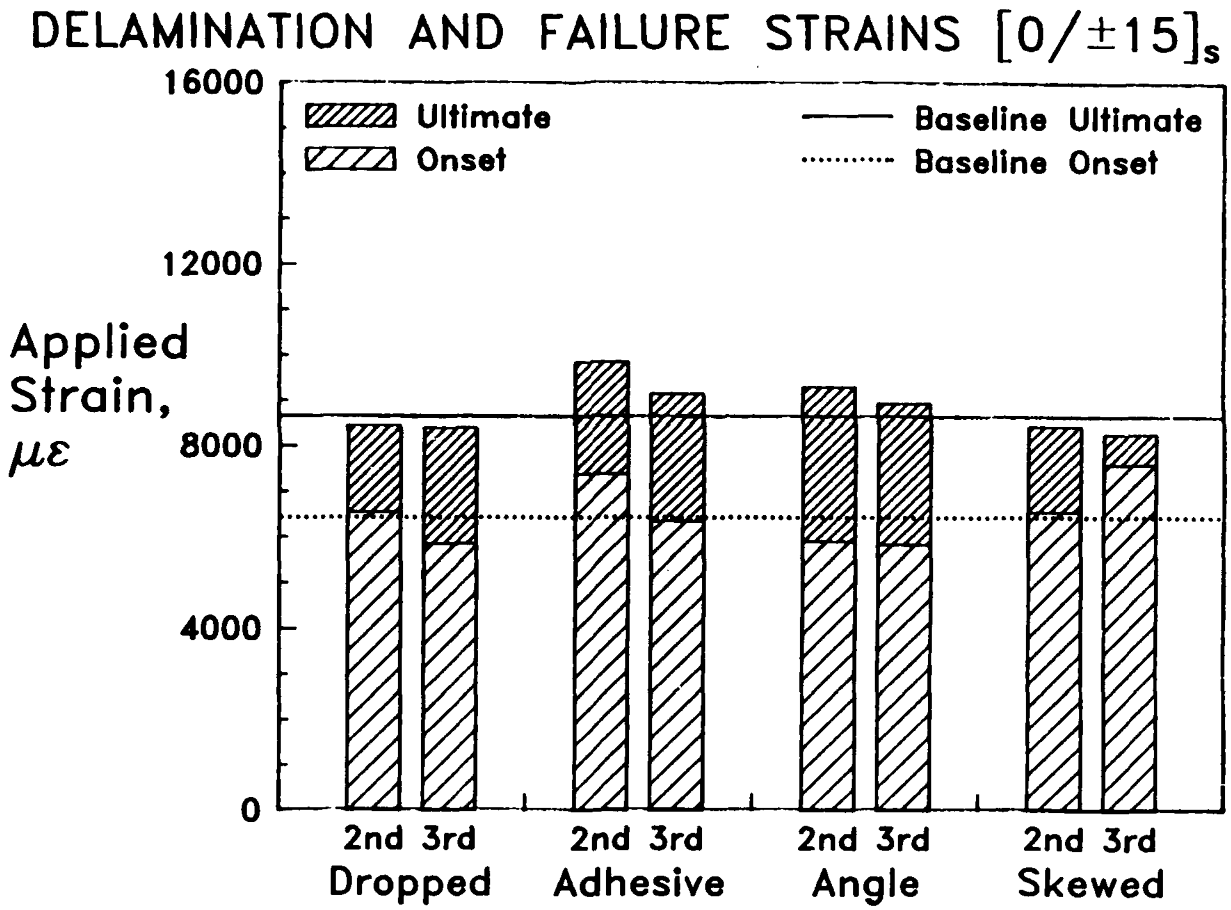
DELAMINATION AND FAILURE STRAINS [0/±15]s
Applied Strain, $\mu\varepsilon$
16000
12000
8000
4000
0
Ultimate
Onset
Baseline Ultimate
Baseline Onset
2nd 3rd
Dropped
2nd 3rd
Adhesive
2nd 3rd
Angle
2nd 3rd
Skewed

Front and side photographs of unaltered and skewed $[0/\pm 15]_S$ laminates

RP189–21

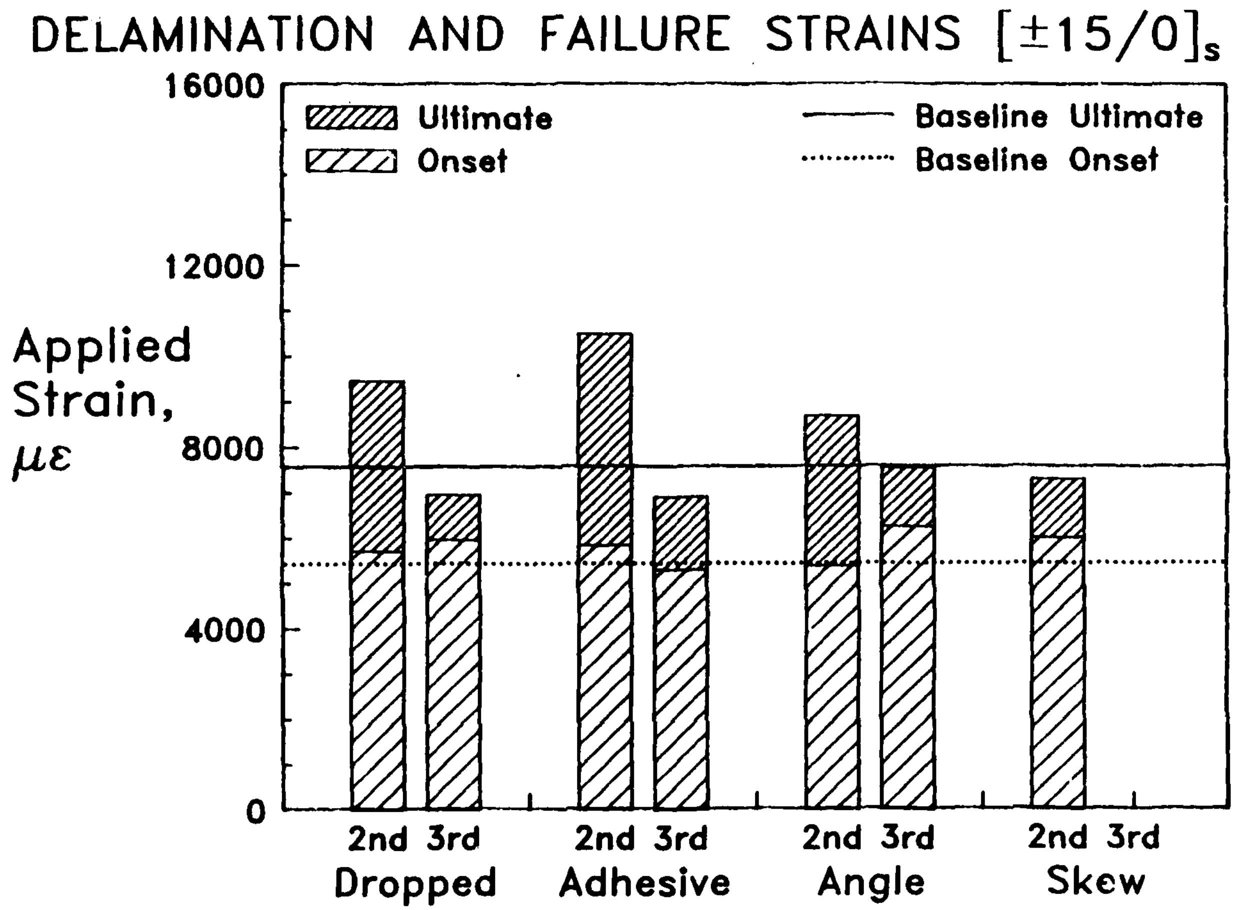

DELAMINATION AND FAILURE STRAINS [±15/0]s
Applied Strain, με
16000
12000
8000
4000
0
Ultimate
Onset
Baseline Ultimate
Baseline Onset
2nd 3rd
Dropped
2nd 3rd
Adhesive
2nd 3rd
Angle
2nd 3rd
Skew

Front and side photographs of unaltered and skewed $[\pm 15/0]_S$ laminates

RPI89–23

Interlaminar Stresses at the Internal Edge

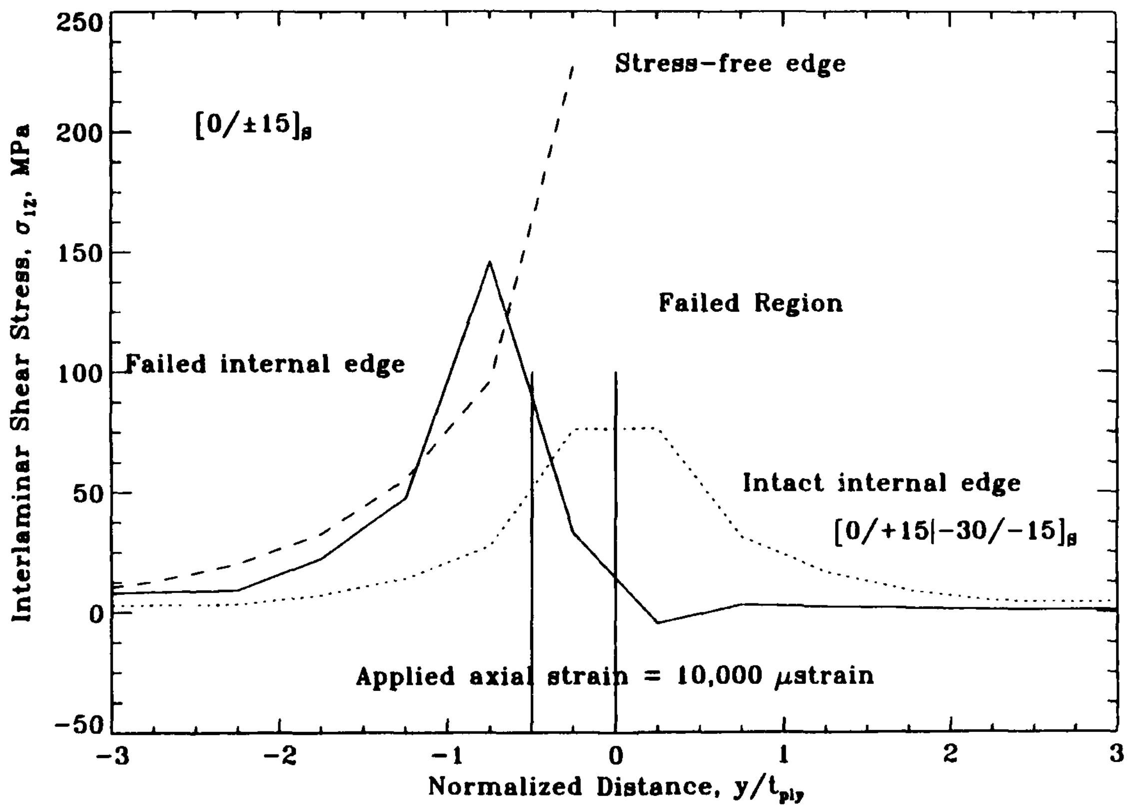

RPI89–24

In-Plane Stresses at Internal Edge

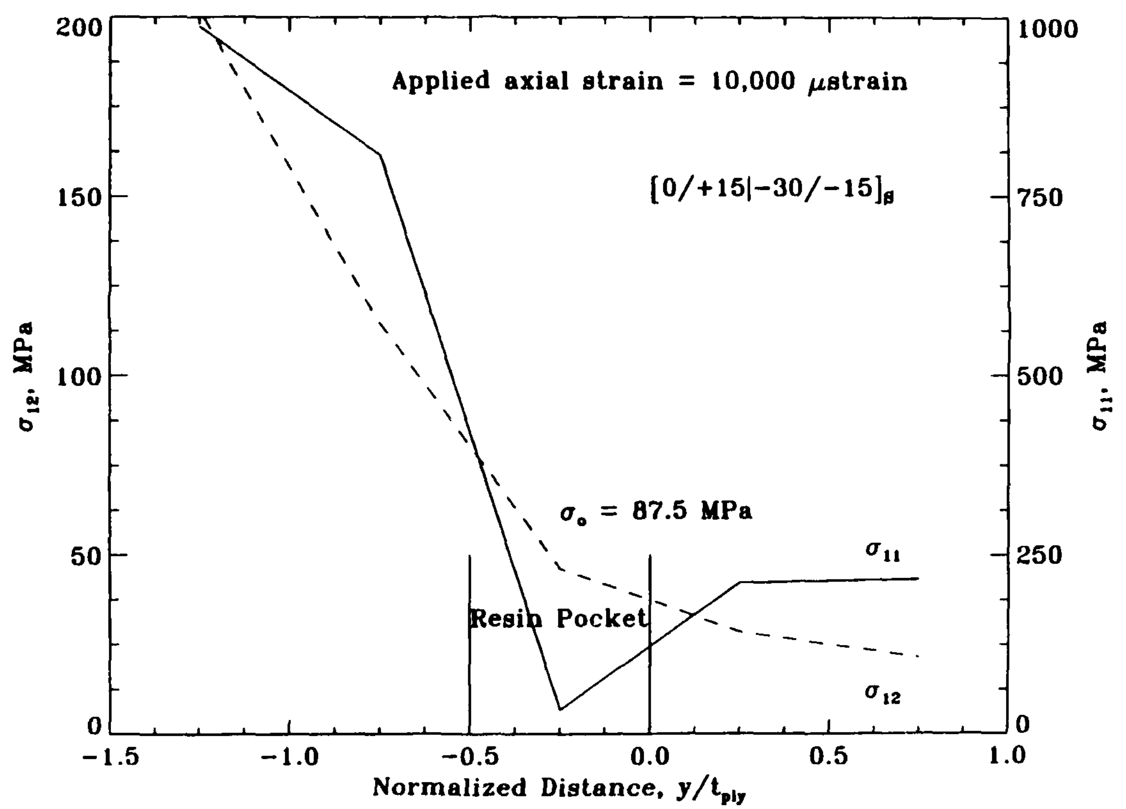

RPI89–25

Conclusions

1. Structural tailoring is effective in preventing the occurrence of delamination by changing beneficially the overall state of stress at the discontinuities.

2. The effect of a edge alteration is dependent upon stacking sequence and location of the alteration.

3. The internal edge create by discontinuous edge alterations may fail in plane resulting in an increase in the interlaminar stress state and a decrease in the apparent delamination onset strain.

Conclusions (cont.)

4. An undelaminated edge zone constrains delamination growth by constraining the sublaminates more so than a free-edge delamination.

5. Although certain alterations work in most instances, *extreme* care must be taken to avoid errant “fixes”.

GENERALIZED STRUCTURAL INTEGRITY ASSURANCE APPLICATION TO ROTORCRAFT

WILLIAM T. MATTHEWS
ARMY MATERIALS TECHNOLOGY LABORATORY
WATERTOWN, MA

ARO-AHS-RPI WORKSHOP ON COMPOSITE
MATERIALS AND STRUCTURES FOR ROTORCRAFT
SEPTEMBER 14 & 15, 1989

US ARMY
LABORATORY COMMAND
MATERIALS TECHNOLOGY LABORATORY

OUTLINE

- MTL INVOLVEMENT IN SIA
- STRUCTURAL DESIGN & INTEGRITY ISSUES
- GENERALIZED SIA
- DISCUSSION OF APPLICATION TO ROTORCRAFT

MTL - SIA INVOLVEMENT

- METALS - FRACTURE MECHANICS R&D
- COMPOSITES - JOINT STUDIES, SPECIMEN DEVELOPMENT FRACTURE STUDIES, MIL-STD-17/ STATISTICS
- ARMY MATERIEL FAILURE STUDIES
- SPONSORED NATIONAL MATERIAL ADVISORY BOARD STUDY "ASSURING STRUCTURAL INTEGRITY IN ARMY SYSTEMS"
  NMAB- 417, 1985
- DRAFTED AMC POLICY GUIDANCE STATEMENT REQUIRING SIA FOR ARMY MATERIEL SYSTEMS
  ADOPTED- 1986
  LAPSED - 1987

NATIONAL MATERIAL ADVISORY BOARD STUDY

CONCLUSION:

"A formal structural integrity program would be highly desirable in Army system development and procurement"

RECOMMENDATION:

"The development of a standard defining a structural integrity program considered as generic for all Army equipment"

5

SIA DEFINITION:

THE ASSURANCE THAT CRITICAL STRUCTURE WILL NOT FAIL IN SERVICE ENVIRONMENT DURING SPECIFIED LIFETIME

GENERALIZED SIA TECHNOLOGY PROGRAM:

A SET OF FORMAL REQUIREMENTS & GUIDELINES EXPRESSING FUNDAMENTAL SIA CONCEPTS & METHODS APPLICABLE TO ALL STRUCTURAL DESIGNS

6

SURVEY OF SIA- AIRWORTHINESS ACTIVITIES

- U.S. AIRFORCE
  AIRFRAMES: MIL-STD-1530,MIL-STD-87221
  ENGINES: MIL-STD-1783
  PUBLICATIONS: "Lessons Learned"
- NAVY AIRFORCE
  NMAB-417 SUMMARY
  CONTRACTOR REPORTS
  NASIP
- FAA
  AIRWORTHINESS STANDARDS:
  AIRPLANES, ROTORCRAFT, AIRCRAFT ENGINES
  ADVISORY CIRCULARS
- U.K. MILITARY AIRWORTHINESS
  TECHNICAL SPECIALIST PUBLICATIONS
- U.S. INDUSTRY - POWER GENERATION, PIPELINE
  NMAB-417 SUMMARY

7

SIA SURVEY CONCLUSION

* NO WIDELY ACCEPTED FUNDEMENTAL SERVICE LIFE SIA APPROACH OR CONCEPT

* ALL PROGRAMS DRIVEN BY AD HOC CONSIDERATIONS

MAJOR ELEMENTS OF STRUCTURAL DESIGN
ROLE OF STRUCTURAL INTEGRITY

* INITIAL IMPLICIT <u>FACTORS</u>	<u>ANALYSIS</u>	<u>TESTING</u>	IN-SERVICE <u>PROGRAM</u>
Failure Consequences System Performance Precision of Information Material "Quality" In-Service "Abuse" Factor of Safety	•Formulations •Computations	•Lab Structural Failure Criteria?	Usage Monitoring Inspection Maintenance

•EMPHASIS IN CONVENTIONAL DESIGN & MECHANICS STUDIES

√ AIR FORCE STRUCTURAL INTEGRITY METALLIC AIRFRAME PROGRAM DEVELOPMENT & EMPHASIS

* TYPICALLY CONSIDERED ON AD HOC BASIS

9

INFLUENCE OF IMPLICIT FACTORS IN GENERALIZED SIA

IMPLICIT FACTORS → MODELING → QUALIFICATION TEST DEFINITION & EVALUATION

MODELING DEPENDS UPON <u>ENGINEERING JUDGEMENT</u>

- MATERIAL: "Quality", Toughness, Variabilty, Etc.
- LOADING: "Precision", Amplitude, Rate, Etc.
- ENVIRONMENT:"Precision", Temperature, Humidity,Etc.
- IN-SERVICE "ABUSE": Surface Damage, Impact
- IN-SERVICE PROGRAM: Usage Monitoring, Etc.
- FACTOR OF SAFETY: All Uncertainties Quantified

QUALIFICATION TEST DEFINITION & INTERPRETATION
(TESTS ARE QUITE ARTIFICIAL)

- SIMULATION ? MATERIAL QUALITY, IN-SERVICE "ABUSE"
- TIME DURATION: Drastically Reduced -Loading Deleted
- ENVIRONMENTAL EFFECTS: Simulated By Load Adjustments
- ONE/ FEW TESTS REPRESENT ENTIRE POPULATION
  - Time Duration Adustment
  - Load Level Adustment
  - Load-Time Adjustments

10

INFLUENCE OF IMPLICIT FACTORS IN GENERALIZED SIA

ISSUES INITIALLY OMITTED (ON BASIS OF IMPLICIT FACTORS) ARE NOT LIKELY TO BE ASSESSED IN QUALIFICATION TESTING

11

SIA ACTIVITIES -
HARDWARE SYSTEM DEVELOPMENT

EVERY SIA ACTION & INACTION POTENTIALLY
INFLUENCES OVERALL HARDWARE SYSTEM ISSUES:

- SAFETY
- PERFORMANCE [f(Weight)]
- DOWNTIME / READINESS
- COST
- SCHEDULING

THUS:

HARDWARE SYSTEM AUTHORITY (NOT SIA EXPERTS ALONE)
MUST ESTABLISH CRITERIA FOR SIA IMPLEMENTATION -
WITHIN FRAMEWORK OF GENERALIZED
FUNDEMENTALLY SOUND SIA TECHNOLOGY

'2

DESIRABLE ATTRIBUTES
GENERALIZED SIA TECHNOLOGY PROGRAM

* INCLUDE IMPLICIT ISSUES
* <u>MOTIVATE MOST APPROPRIATE MODELING & CRITERIA</u>
* ESTABLISH PROPER RELATIONSHIPS BETWEEN TASKS
* PERMIT SPECIFIC HARDWARE SYSTEM AUTHORITY TO EXERCIZE ITS RESPONSIBILITY
* APPLICABLE TO ALL DESIGNS & MATERIALS (CONVENTIONAL & INNOVATIVE)
* PERMIT FLEXIBILITY: MODELING & METHODS
* ANALYTICAL CAPABILITY TO ASSESS AFTER FIELDING: IN-SERVICE DAMAGE,USAGE CHANGES,LIFE EXTENSION

:3

GENERALIZED SIA CONCEPT

1) DEFINE GENERALIZED SI PARAMETERS WHICH CHARACTERIZE SI

2) ESTABLISH REQUIREMENTS & GUIDELINES -
HARDWARE SYSTEM AUTHORITY SPECIFIES:
    - Measures of Generalized SI Parameters
    - Criteria/ Allowables of Measures
    - Modeling Methods(Optional)

3) GENERALIZED SIA PARAMETERS MUST BE <u>EVALUATED</u> WITH RESPECT TO ACCEPTANCE CRITERIA SPECIFIED BY HARDWARE SYSTEM AUTHORITY

4) CLARIFY:
    - INFLUENCE- IMPLICIT FACTORS,MEASURES & CRITERIA
    - APPLICATION & LIMITATIONS
        - Documented Basis & Rationale

GENERALIZED SIA CONCEPT

1) GENERALIZED SIA PARAMETERS DEFINED:

* RESISTANCE TO MAXIMUM LOADING
* SERVICE LIFE BASE LINE DESIGN
* SERVICE LIFE DESIGN SUFFERANCE

  LIMITED DURATION SERVICE LIFE:
* UNREPAIRED DAMAGE /SURVIVABILITY
* REPAIRED DAMAGE /BATTLE DAMAGE

15

1) GENERALIZED SI PARAMETERS

- SERVICE LIFE BASE LINE DESIGN:
  - Nominal Design Conditions
  - Majority of System Units
  - System Life Requirements
- SERVICE LIFE DESIGN SUFFERANCE (Must Be Evaluated) (CAPACITY TO ENDURE "HARDSHIP")

  Design Conditions Not Considered In Nominal Design

  GENERALIZED CHARACTERIZATION IN THE SPIRIT OF DAMAGE TOLERANCE OF CRACKS:
  AIR FORCE MIL STD- 1530
- MOTIVATE DETAILED CONSIDERATION OF DESIGN CONDITIONS IN BASE LINE & DESIGN SUFFERANCE MODELING
- BASIS & RATIONALE DOCUMENTED BY DEFINED GENERALIZED SIA SPECIFICATION PROCESS

16

1) DESIGN SUFFERANCE SI PARAMETER MODELING GUIDELINES

- EXPLICIT CRACK,FLAW,DAMAGE MODEL
  WHEN BASE LINE MODEL IS NON-FLAW BASED(Safe Life)
- LARGER THAN NOMINAL EXPLICIT INITIAL:
  CRACKS,FLAWS - Metals,Ceramics
  DAMAGE - Advanced/Engineered Materials
- LOSS OF NEAR SURFACE CONDITIONS WHICH PROMOTE SI:
  FAVORABLE RESIDUAL STRESSES
  ENVIRONMENTAL PROTECTION(Corrosion,Moisture)
- UNINTENDED OUT OF PLANE LOADING:
  ENGINEERED/ TAILORED MATERIALS
- LARGER THAN NOMINAL UNDETECTED IMPACT DAMAGE
- MULTIPLE SITE /WIDE SCALE DAMAGE & DEGRADATION
- HARDWARE SYSTEM AUTHORITY MAY SPECIFY MODELING OR
  MODELING MAY BE CHOSEN BY SYSTEM DEVELOPER:
  DOCUMENTATION OF BASIS & RATIONALE REQUIRED

OTHER THAN NOMINAL SERVICE CONDITIONS
GENERALIZED SIA APPROACH

- INNOVATIVE DESIGN/ EMERGING MATERIALS:

  QUANTITATIVE ESTIMATES OF "OTHER THAN NOMINAL" DESIGN CONDITIONS ARE UNCERTAIN

  EXPERIENCE BASE IS LACKING

- CONDITIONS BEST CHARACTERIZED BY DIRECT FUNDAMENTAL MODELING

- AS DEFINED BY DESIGN SUFFERANCE SI PARAMETER

- FACTOR OF SAFETY: ALL OTHER UNCERTAINTIES

  MODELING PRECISION
  MATERIAL QUALITY
  LOADING DEFINITION
  ENVIRONMENT DEFINITION
  QUALIFICATION BASED ON ONE/ FEW TESTS

8

2) ESTABLISH REQUIREMENTS & GUIDELINES HARDWARE SYSTEM AUTHORITY SPECIFIES:

FOR SPECIFIC CLASS OF STRUCTURE:
- Measures of Generalized SI Parameters
- Critical /Allowable Values

- RESISTANCE TO MAXIMUM LOADING
  - MEASURES
    - Strength, Strain Limit, Fracture, Displacement
    - Creep, Buckling
  - CRITERIA
    - Yield, Ultimate, Strain Limit Allowable,
    - KIC, JIC, R-Curve, Displacement Limit

- SERVICE LIFE
  - MEASURES
    - Life (Specified Loading)
    - Fatigue Strength (Specified Life)
  - CRITERIA
    - Time, Total, Dominant Load Cycle

9

3) SI PARAMETERS MUST BE <u>EVALUATED</u> WITH RESPECT TO ACCEPTANCE CRITERIA

ESTABLISHED BY HARDWARE SYSTEM AUTHORITY

- EVALUATION BASED ON <u>ALL</u> OF THE FOLLOWING:

  QUALIFICATION TEST RESULTS

  VALIDATED ANALYSIS
  Based On Design Development,
  Qualification Tests

  MANUFACTURING QUALITY CONTROL PROGRAM:
  Inherent Defects,Cracks,Surface Conditions

  IN-SERVICE PROGRAM:
  Usage Monitoring,Inspection,Maintenance

- HARDWARE SYSTEM AUTHORITY HAS OPTION:
  ACCEPTANCE NEED NOT BE BASED ON
  <u>ALL</u> DEFINED SI PARAMETERS

4) CLARIFY FACTORS,MEASURES,LIMITATIONS
Documented Basis & Rationale

- MOTIVATE MOST APPROPRIATE MODELING & CRITERIA
- DOCUMENT BUILDING BLOCK-ADV.MATERIAL DESIGN DEVELOPMEMT
- GENERALIZED SIA SPECIFICATION PROCESS
  - a)Generalized SIA Approach Documents:
    - Factors To Be Specified
    - Issues To Be Considered
  - b)Hardware Authority Specifies For Classes of Structure (To Extent Feasible)
  - c)If Factor Can Not Be Specified By Hardware System Authority
    - Materiel System Developers Make Interim Determinations of SIA Factors Based on Issues Cited by Generalized SIA Technology Program
  - d)Specifications of SIA Factors Shall Be Supported By Documentation of Basis & Rationale

GENERALIZED STRUCTURAL INTEGRITY ASSURANCE TECHNOLOGY PROGRAM

TASK I DESIGN INFORMATION	TASK II DESIGN ANALYSES AND MATERIAL CHARACTERIZATION	TASK III DESIGN DEVELOPMENT TESTING	TASK IV QUALIFICATION TESTS FORCE MANAGEMENT DATA	TASK V FORCE MANAGEMENT
A. SIA PLAN B. SI CHARACTERIZATION • MAX LOADING RESISTANCE • SERVICE LIFE BASE LINE DESIGN SUFFERANCE • LIMITED DURATION SERVICE LIFE C. DESIGN FOR SIA D. SERVICE LIFE SIA PLAN E. DESIGN SERVICE LIFE AND DESIGN USAGE F. MATERIALS, PROCESSES, JOINING METHODS SELECTION	A. MAX LOAD ANALYSIS B. SERVICE LOAD ANALYSES C. CHEMICAL/THERMAL ENVIRONMENT D. MECHANICAL PROPERTIES CHARACTERIZATION E. MECHANICS ANALYSES F. SIA ANALYSES AT MAX LOADING G. SERVICE LIFE ANALYSES • BASE LINE • DESIGN SUFFERANCE H. LIMITED DURATION SERVICE LIFE ANALYSES/SURVIVABILITY	A. SERVICE LOAD AND ENVIRONMENTAL B. JOINTS-MECHANICAL TESTS C. BUILDING BLOCK: ADVANCE MATERIAL TESTING D. MAX LOADING RESISTANCE E. SERVICE LIFE o BASE LINE o DESIGN SUFFERANCE F. LIMITED DURATION SERVICE LIFE G. MANUFACTURING QUALITY CONTROL SUMMARY	A. MAX LOADING RESISTANCE B. SERVICE LIFE • BASE LINE o DESIGN SUFFERANCE C. LIMITED DURATION SERVICE LIFE D. QUALIFICATION TEST SUMMARY E. FORCE MANAGEMENT DATA PACKAGE o MANUFACTURING QUALITY CONTROL SUMMARY o SI ANALYSIS SUMMARY o OPERATIONAL ENVELOPE o FORCE SIA MAINTENANCE PLAN o IN-SERVICE MONITORING PLAN F. SIA EVALUATION	A. SIA MANAGEMENT B. OPERATION ENVELOPE IMPLEMENTATION C. FORCE SIA MAINTENANCE IMPLEMENTATION D. IN-SERVICE USAGE MONITORING E. IN-SERVICE SIA DATABANK: FEEDBACK TO ANALYSIS SUMMARY

DESIRABLE ATTRIBUTES
GENERALIZED SIA TECHNOLOGY PROGRAM

- <u>MOTIVATE MOST APPROPRIATE MODELING & CRITERIA</u>
  DEFINED SIA PARAMETERS,MEASURES,CRITERIA,RATIONALE
- ESTABLISH PROPER RELATIONSHIP BETWEEN ALL SIA TASKS
  TECHNOLOGY PROGRAM DOCUMENT- DRAFT
- PERMIT SPECIFIC HARDWARE SYSTEM AUTHORITY
  TO EXERSIZE ITS RESPONSIBILITY
  ACCEPTANCE CRITERIA -EVALUATION OF PARAMETERS
  SPECIFIES MEASURES& CRITERIA, MODELING
- APPLICABLE TO ALL DESIGNS
  FLEXIBILITY: MODELING & METHODS
  GENERALIZED SI PARAMETERS,
  MEASURES & CRITERIA,MODELING
- ANALYTICAL CAPABILITY TO ASSESS AFTER FIELDING:
  IN-SERVICE DAMAGE, USAGE CHANGES, LIFE EXTENSION
  EVALUATION BASIS- VALIDATED ANALYSIS
- INCLUDE IMPLICIT ISSUES
  DOCUMENTED BASIS & RATIONALE

23

BENEFITS

GENERALIZED SIA:

IMPROVED:
MODELING & EVALUATIONS "OTHER THAN NOMINAL" CONDITIONS

CLARIFIES:

LIMITATION OF METHODS-(Advanced Materials)
APPLICATION TO INNOVATIVE DESIGN

COMPLETE GENERALIZED/SPECIFIC SIA TECHNOLOGY PROGRAM

PROMOTE SAFETY
EARLY DISCOVERY OF SIA DEFICIENCES
COMMUNICATION BETWEEN AUTHORITIES & DEVELOPERS

CLARIFIES TECHNOLOGY GAPS /R&D FOCUS
RETAINS TECHNICAL EXPERTISE

24

GENERALIZED SIA SUMMARY

NEW GENERALIZED SIA TECHNOLOGY APPROACH

- DEFINITION OF NEW PARAMETERS CHARACTERIZING SIA
- NEW DESIGN SUFFERANCE PARAMETER CHARACTERIZING "OTHER THAN NOMINAL" SERVICE LIFE DESIGN CONDITIONS
- EVALUATION OF SIA: HARDWARE SYSTEM AUTHORITY ESTABLISHES CRITERIA FOR ACCEPTANCE
- GENERALIZED REQUIREMENTS ARE PERMANENT ; EXCEPTIONS FOR <u>PARTICULAR</u> MATERIAL/STRUCTURAL SYSTEMS
- DOCUMENTATION OF BASIS & RATIONALE REQUIRED

25

GENERALIZED SIA
APPLICATION TO ROTORCRAFT

ARMY

- FLEXIBILITY IN METHODS FOR AIRFRAME, DYNAMIC COMPONENTS
- CLARIFY APPLICATION OF LIFE ASSURANCE TESTS: FATIGUE, DAMAGE TOLERANCE, DURABILITY
- INNOVATIVE DESIGN/ ADVANCED MATERIALS: PROVIDES FOR FORMAL DOCUMENTATION TO PROMOTE UNDERSTANDING OF APPLICATIONS & LIMITATIONS
- STATISTICAL ISSUES: BASIS FOR DESIGN ALLOWABLES

TRI-SERVICE

- FLEXIBILITY: EACH SERVICE CONTROLS METHODS & CRITERIA
- PROVIDES BASIS FOR TRI-SERVICE "COOPERATION"
- PROMOTES TECHNOLOGY TRANSFER

BANQUET SPEAKER

Jack D. Floyd
Deputy Director
Super Team LHX Joint Program Office
Bell Helicopter/McDonnell-Douglas Helicopter Company

"LHX-- A New Composite Helicopter"

MCDONNELL DOUGLAS
SUPERTEAM
BELL HELICOPTER TEXTRON

LHX

A New Composite Helicopter

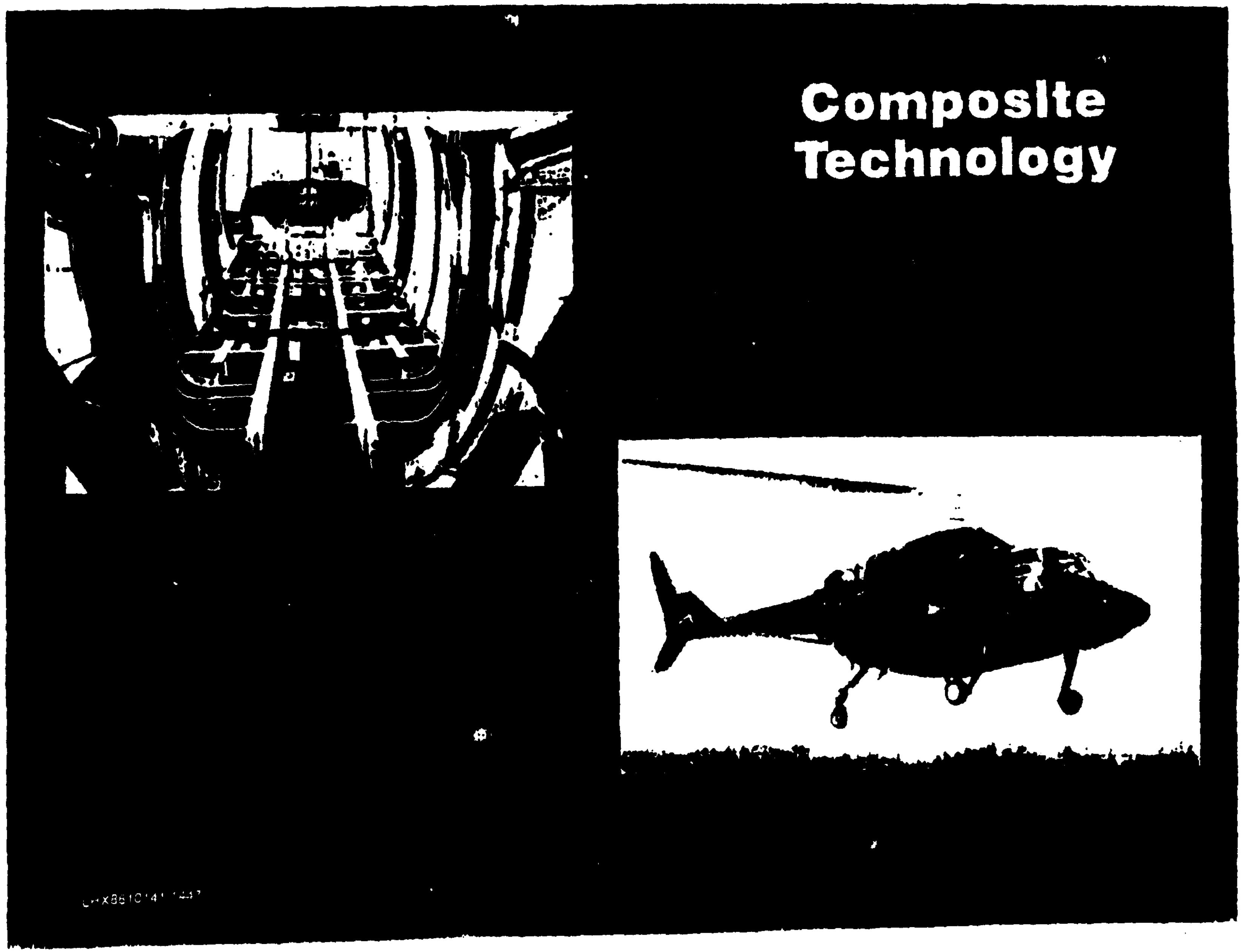
Composite
Technology

BELL ACAP PROGRAM APPROVED

-22% WEIGHT SAVINGS

-17% COST SAVINGS

- EXCEEDED ALL REQUIREMENTS

V-22

1) WING

2) FUSELAGE

PICTURE OF F/A 18

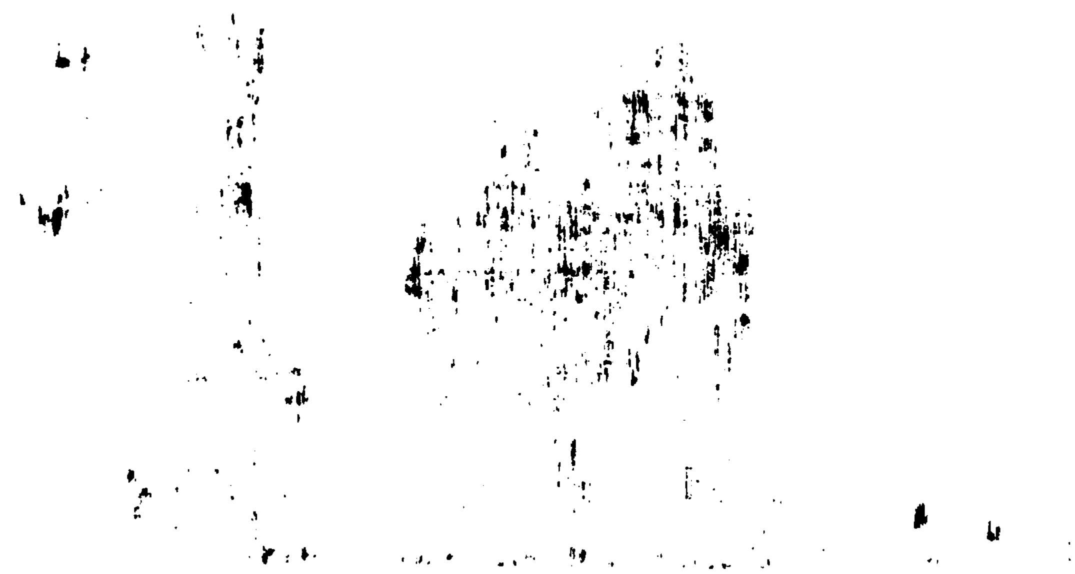

COMPETITION SENSITIVE

LHX McDONNELL DOUGLAS SUPERTEAM BELL HELICOPTER TEXTRON

LHX Concept Exploration

Concept Studies — 1983

Air Vehicle Preliminary Designs — 1984

ACAP; Wind Tunnel; T800 FSD — 1985

ADOCS; Single Pilot ARTI Simulations — 1986

RAND/IDA; Signature Reduction; 2nd Gen FLIR — 1987/1988

VHSIC, HMD, Multisensor Fusion Demonstrations; Target Acquisition, Night Pilotage Designs, Diagnostics

Dem/Val Oct 88

LHX8610141-1462B

COMPETITION SENSITIVE

LHX SUPERTEAM

$1B Risk Reduction for FSD

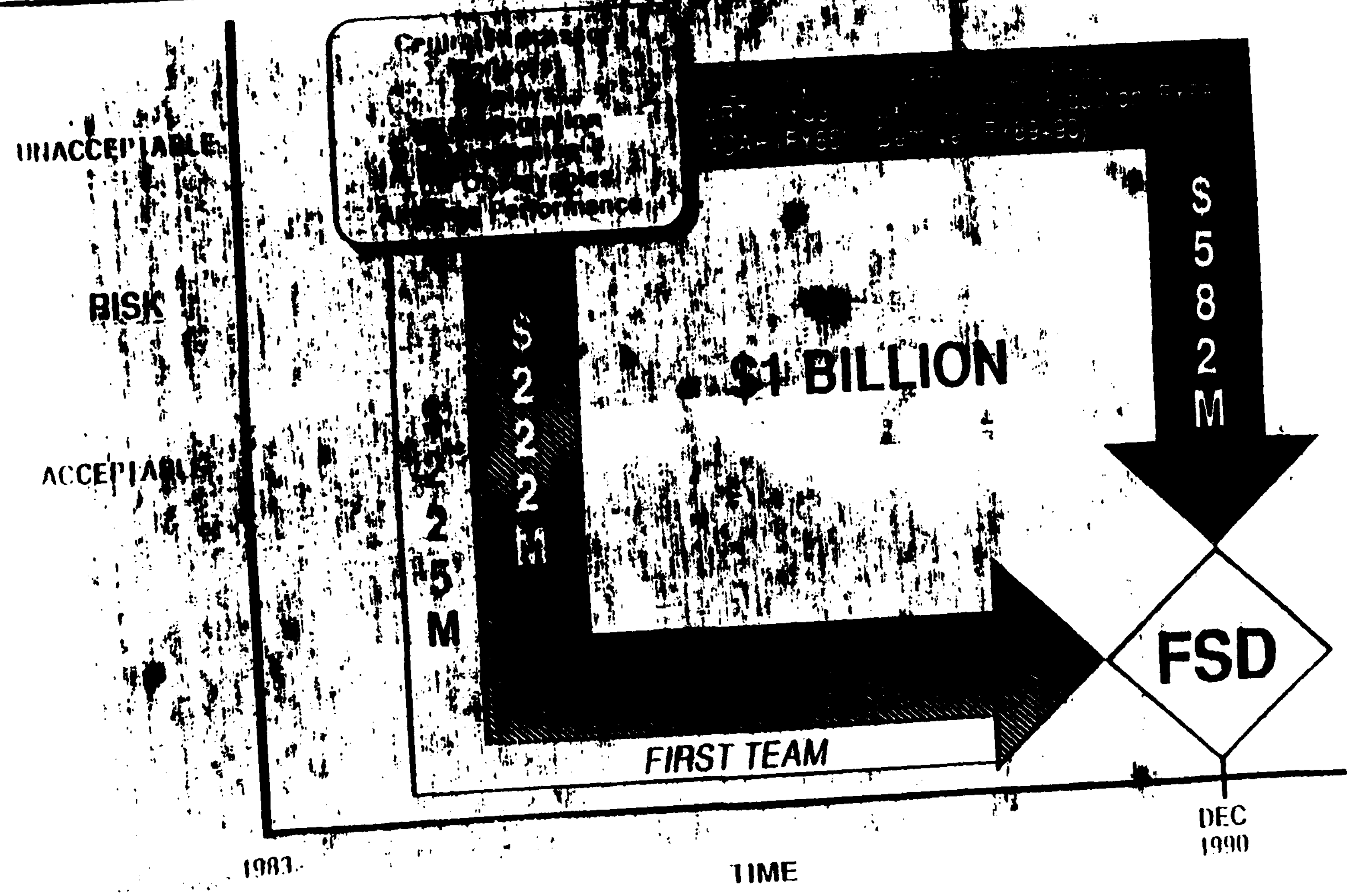


Emerging Threat
ZSU-X
Mi-24 HIND
SA-14 GREMLIN
Mi-28 HAVOC
Plus. ►Electro Optical Jammers ►Enhanced Radars ►Acoustic Detectors ►Nuclear Biological Chemical Threats

LHX ➡ MISSION LOADS
(MIDEAST MISSION)

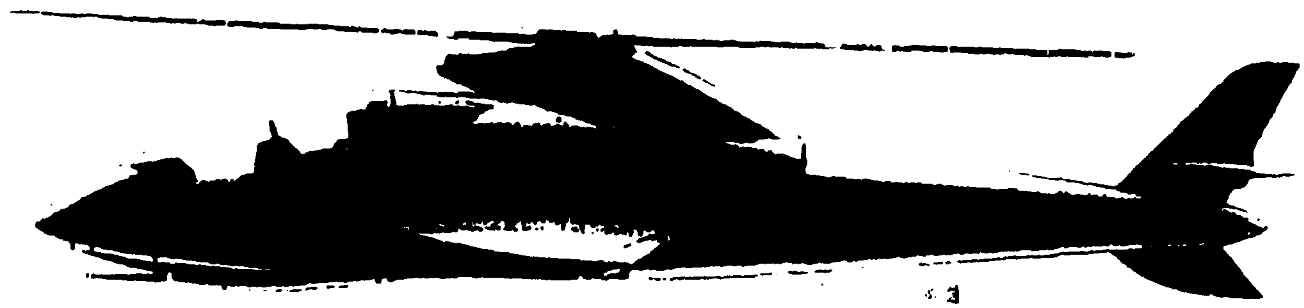

ATTACK	ARMED RECON
8 Hellfire	4 Hellfire
2 Stinger	4 Stinger
500 Rds Gun	320 Rds Gun
1.8 Hrs Fuel	2.5 Hrs Fuel

LHX

MCDONNELL DOUGLAS

SUPERTEAM

BELL HELICOPTER TEXTRON

LHX SuperTeam Organization

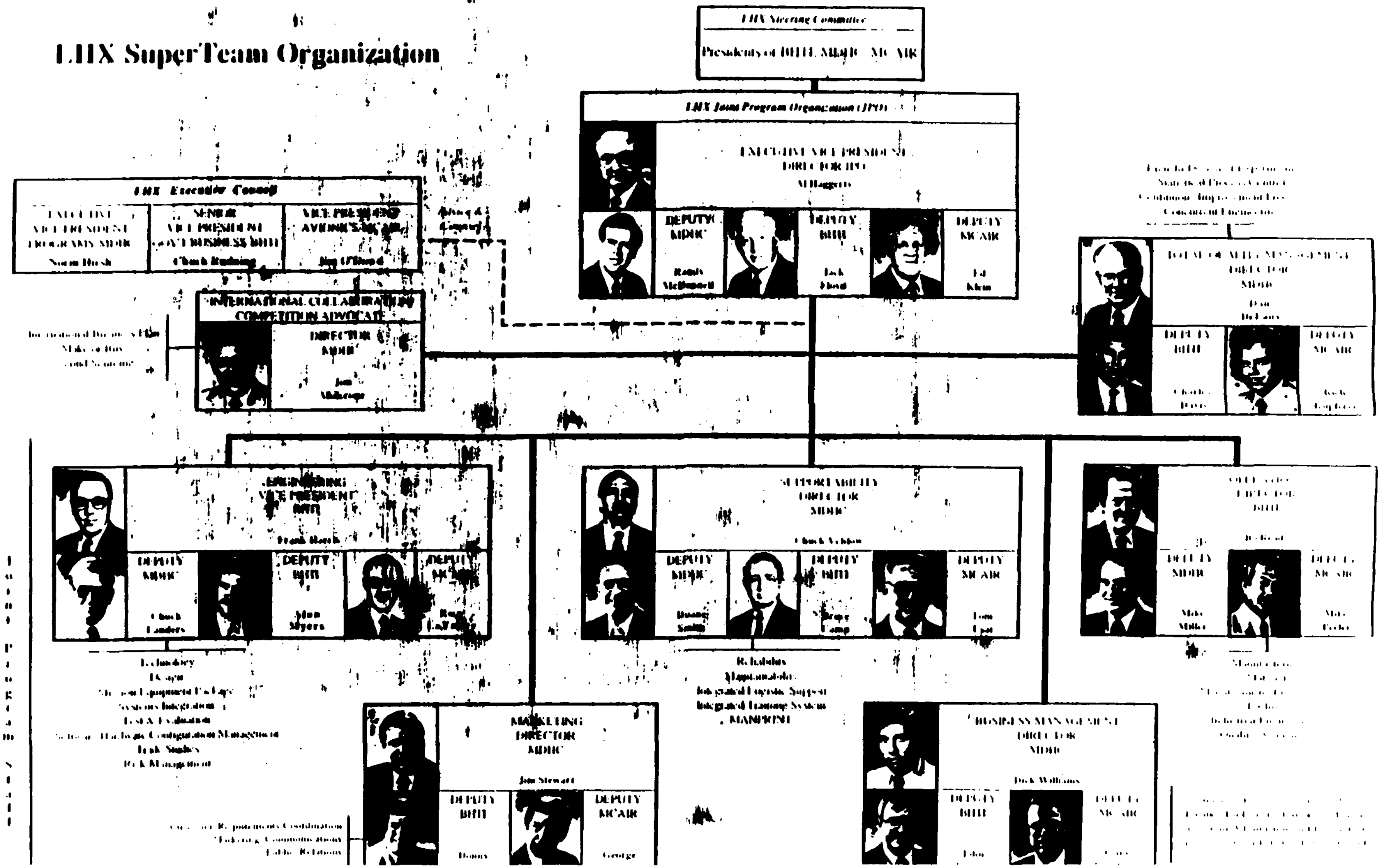

COMPETITION SENSITIVE

LHX SUPERTEAM

LHX - The Combat Helicopter

The SuperTeam

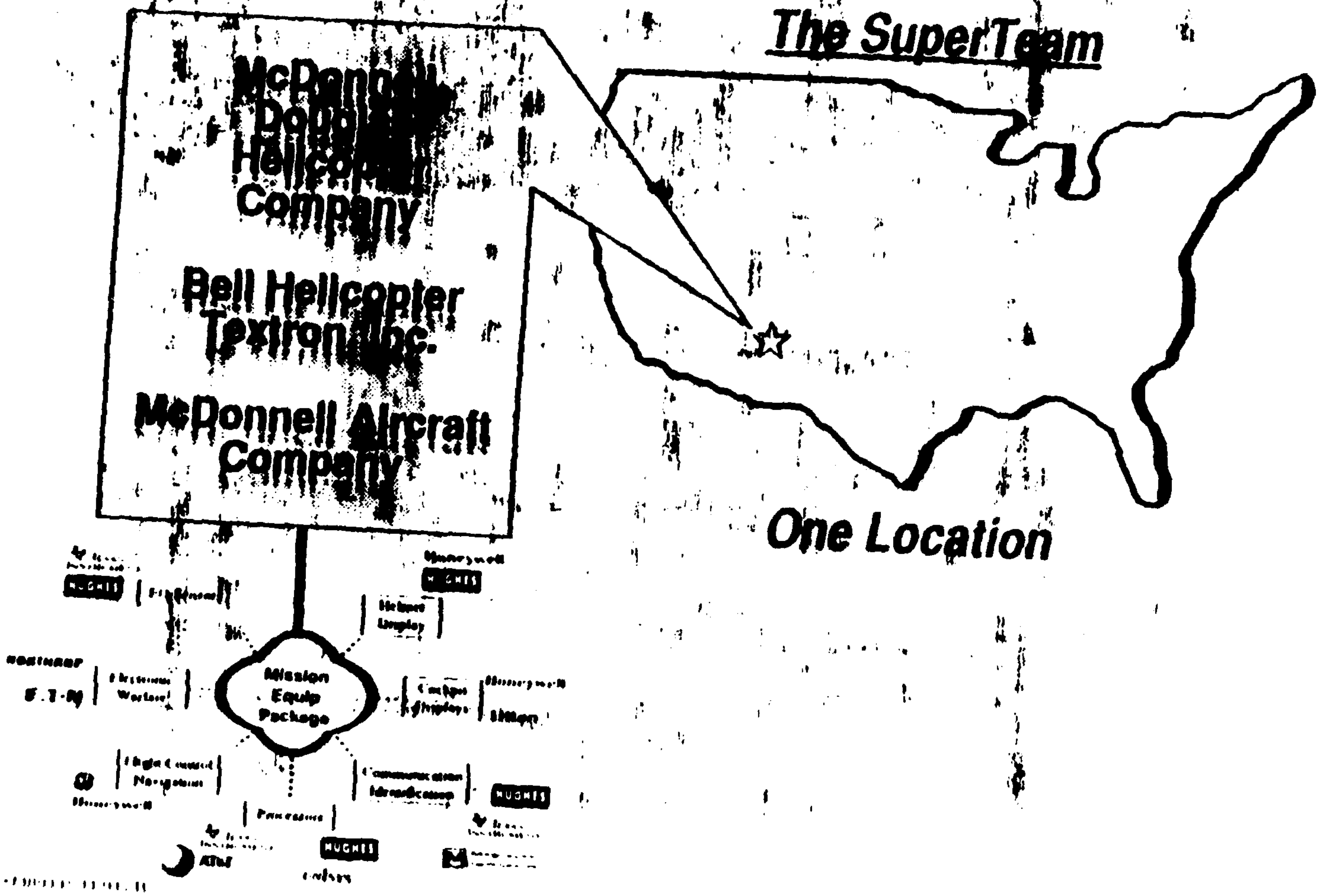

One Location

LHX | McDONNELL DOUGLAS SUPERTEAM BELL HELICOPTER TEXTRON

The Army's 30-Year LHX Plan

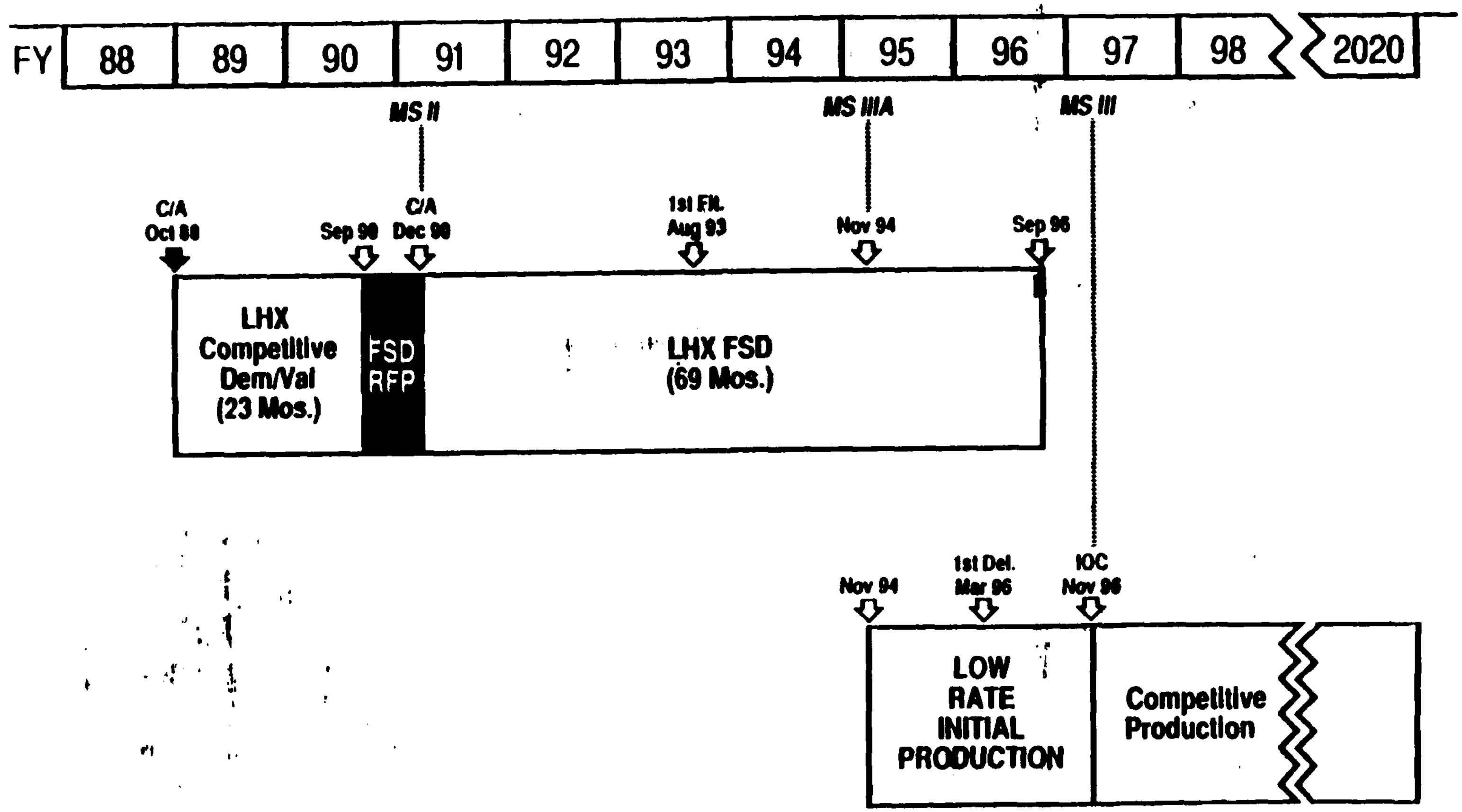

LHX SuperTeam's Dem/Val TQM Process

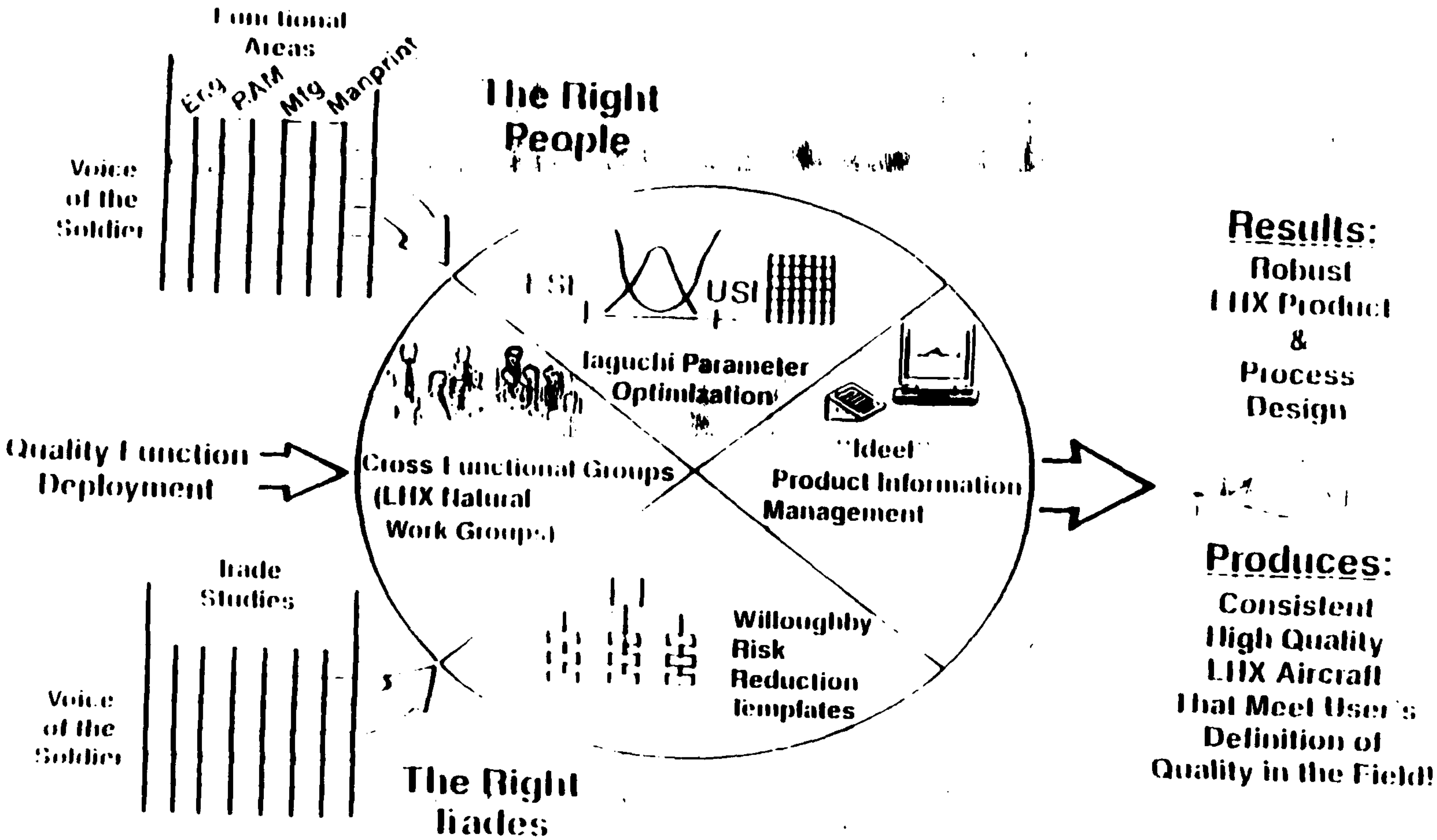

LHX SUPERTEAM

Voice of the Soldier – SuperTour

LHX SUPERTEAM

Voice of the Soldier – SuperTour

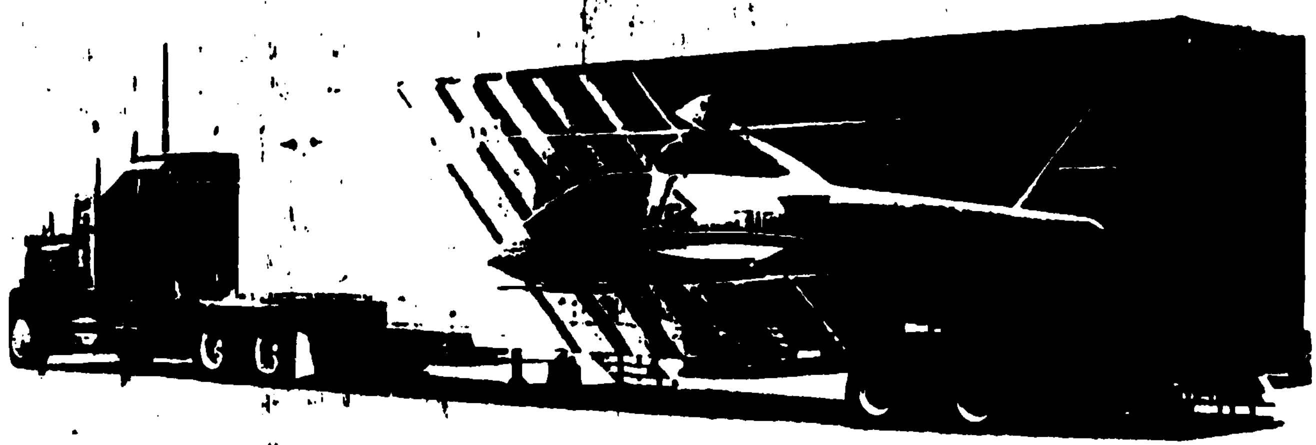

LH SUPERTEAM
McDONNELL DOUGLAS
BELL HELICOPTER TEXTRON

Air Vehicle Characteristics/Benefits

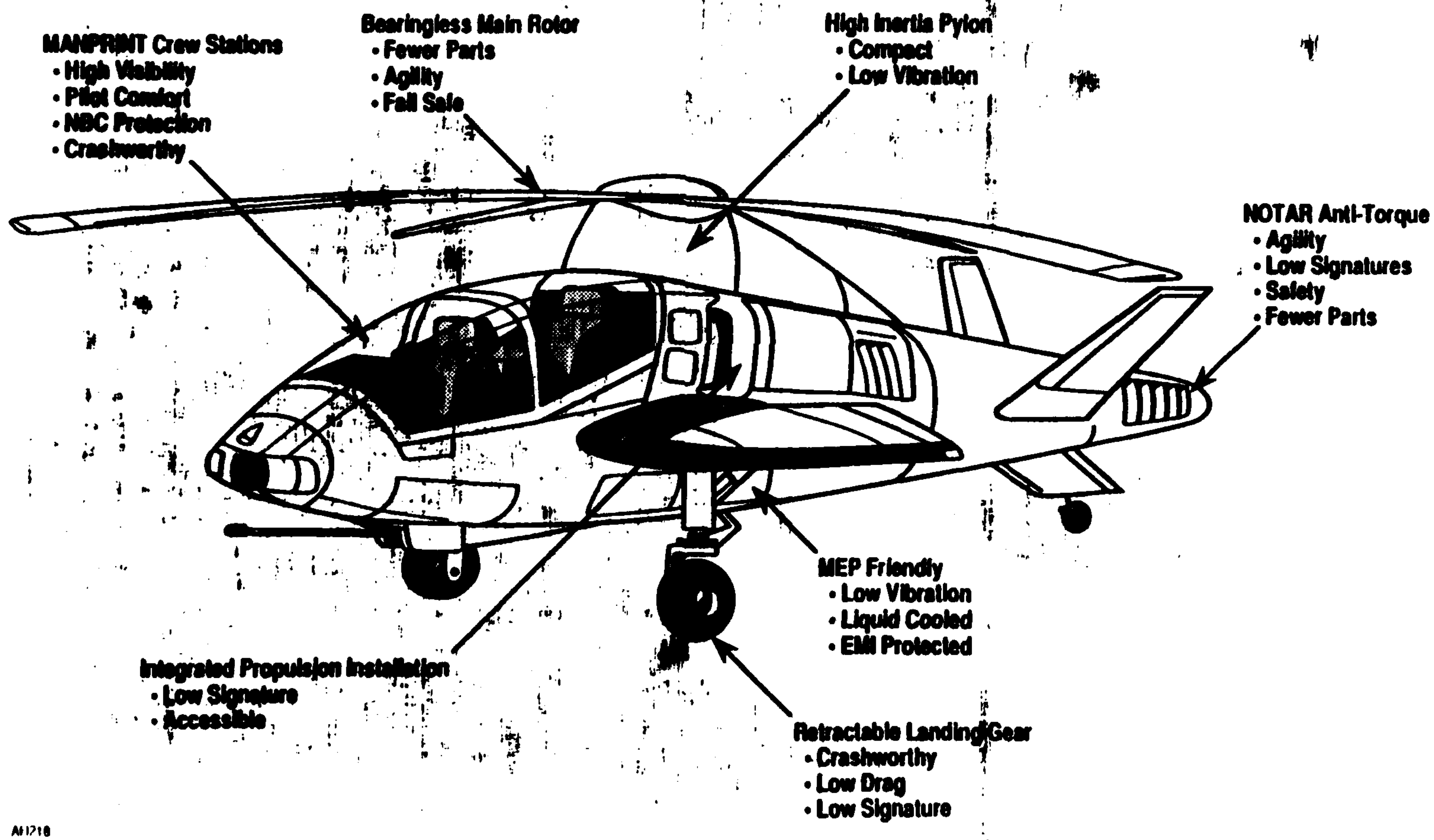

AI1218

LHX SUPERTEAM

MEP Characteristics/Benefits

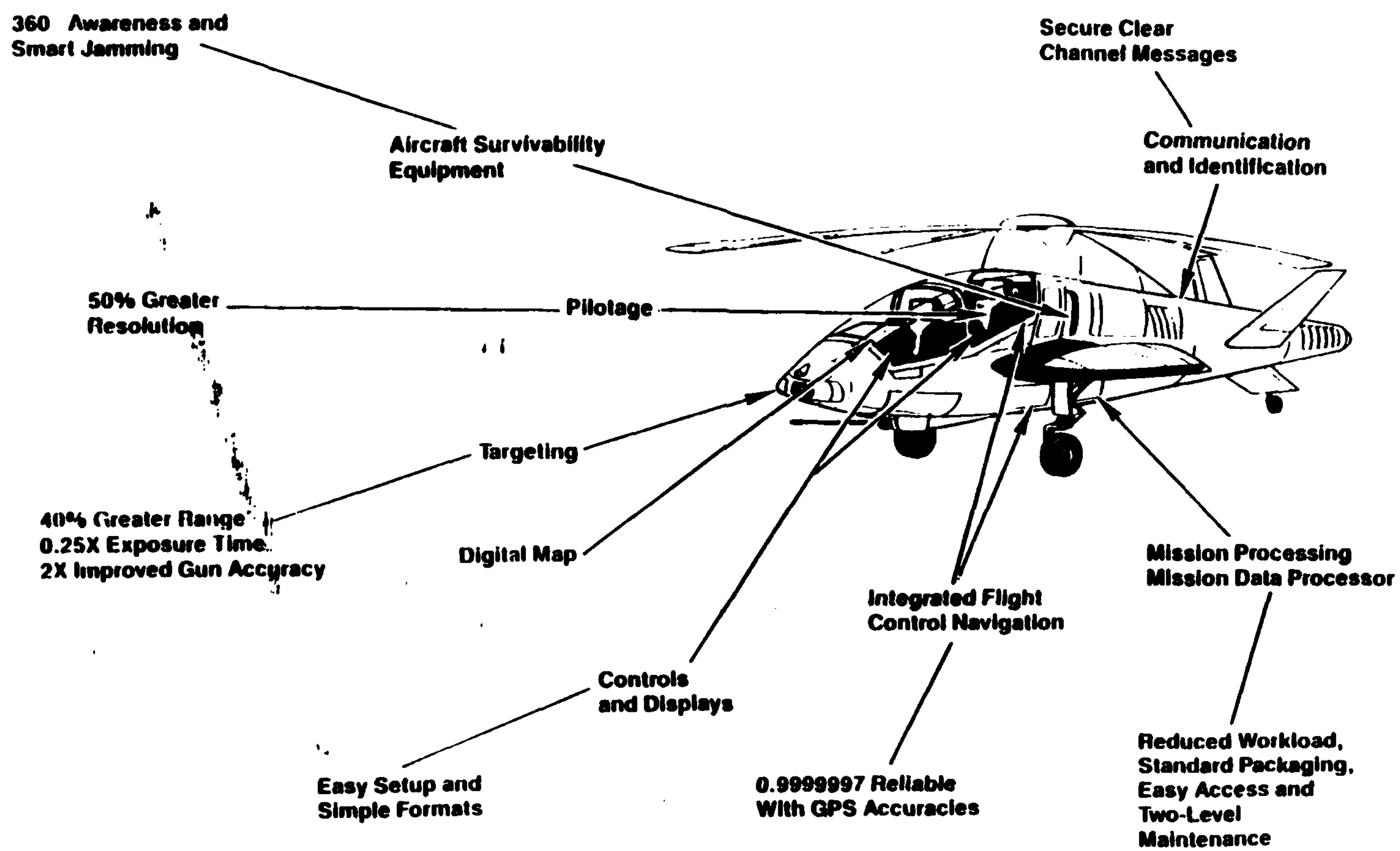

LHX
McDONNELL DOUGLAS HELICOPTER
SUPERTEAM
BELL HELICOPTER TEXTRON

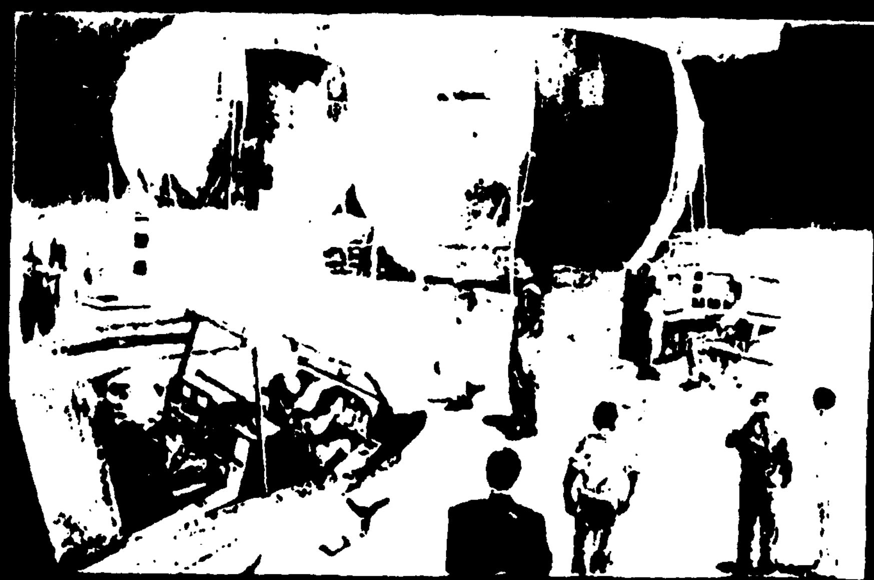

ADVANCED FLIGHT SIMULATION

6-1067

SuperTeam LHX

A Warfighter...by design

- A pilot's helicopter
- A maintainer's aircraft
- A commander's weapon system

LHX

SuperTeam

We Put the Fight

Into LHX

GEMINI

SESSION V

THERMOPLASTICS VERSUS THERMOSETS

Jeffrey A. Hinkley
NASA-Langley
Chairman

THE ADHESION OF CARBON FIBERS TO THERMOSET AND THERMOPLASTIC POLYMERS

W. D. Bascom
K-J. Yon

Materials Science and Engineering Department
University of Utah, Salt Lake City 84112

R. M. Jensen
L. Cordner

Graphite Fibers Development
Hercules Aerospace, Magna Ut

PRESENTED AT THE

2ND ARO-AHS-RPI WORKSHOP ON COMPOSITE MATERIALS AND STRUCTURES FOR ROTORCRAFT

THE SINGLE EMBEDDED FILAMENT TEST

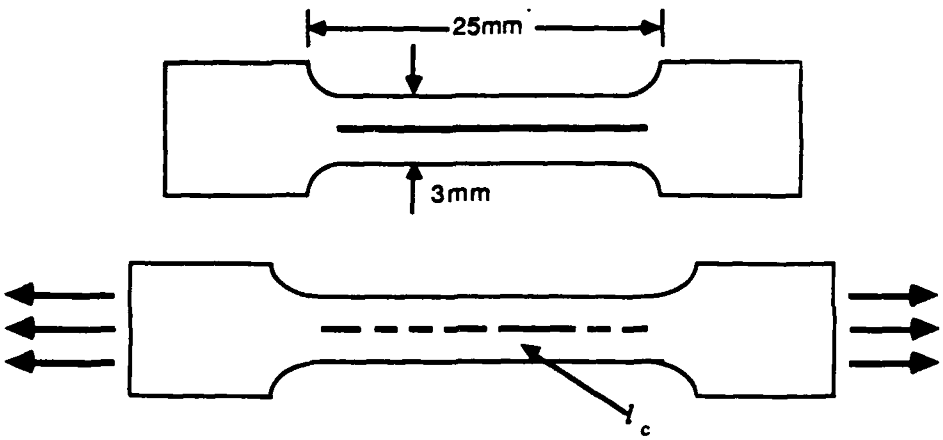

• micro-specimens are pulled in tension until the filament is fully fragmented and the length of the fragments (l_c) is then measured

• the critical length is related to the interphase shear strength by,

$$\tau_c = \frac{\sigma_c d}{2 l_c}$$

τ_c = interphase shear strength
σ_c = fiber strength
d = fiber diameter
l_c = fiber critical length

however the fiber strength has some statistical distribution $\Sigma\sigma_c$ so that,

$$\tau_c = \frac{d}{2 l_c}\Sigma\sigma_c$$

rearranging,

$$\frac{l_c}{d} = \frac{1}{2\tau_c}\Sigma\sigma_c$$

If $\Sigma\sigma_c$ is essentially constant then $\frac{l_c}{d}$ is an inverse measure of the interphase shear strength

EXPERIMENTAL TECHNIQUE

Epoxy specimens were made by placing the filament in a silicone mold, encapsulating in the liquid resin and heat curing.

The thermoset specimens were prepared by placing a single filament on a small plate of the polymer and then coating the filament with the same polymer from a volatile solvent;

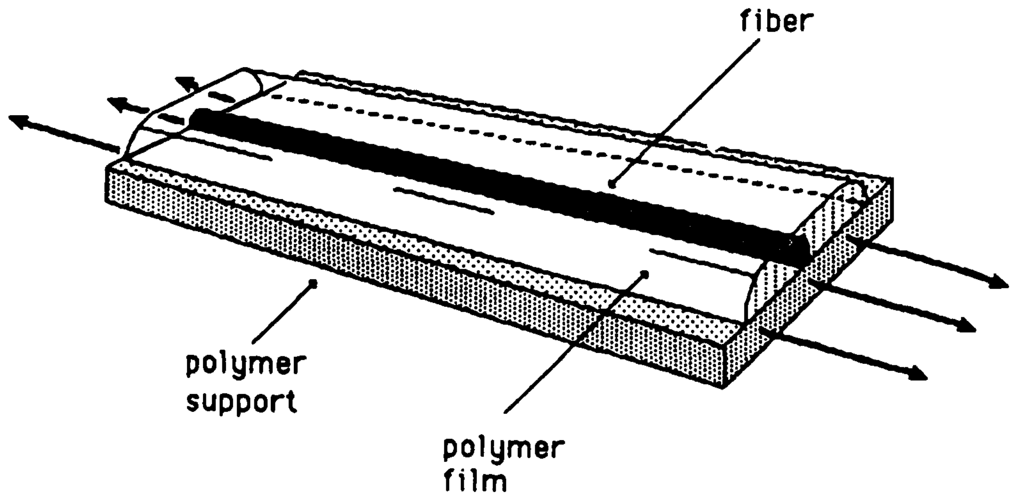

The specimens were placed in a tensile test fixture that fits on the stage of a light microscope;

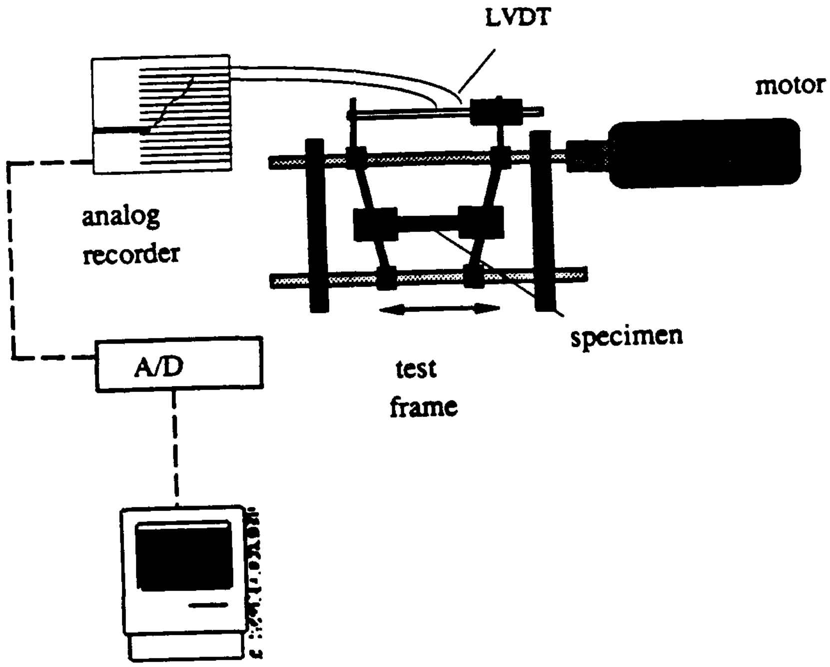

THE CRITICAL LENGTH DATA EXHIBIT A BROAD STATISTICAL DISTRIBUTION

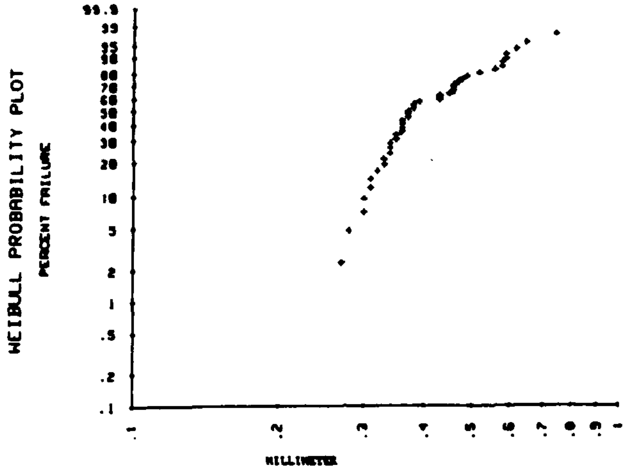

Typical lc data from one specimen

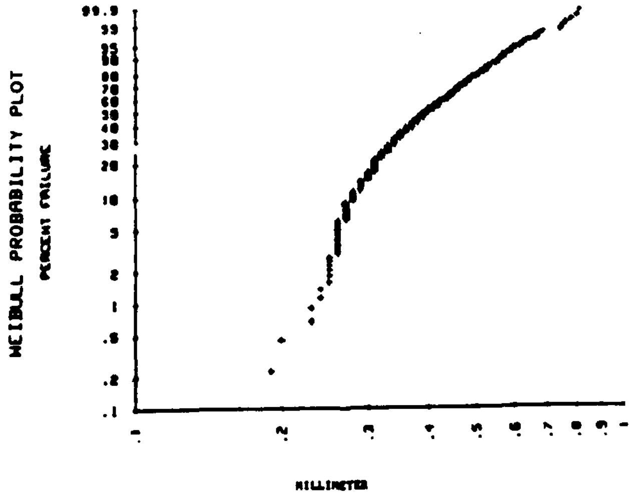

Combined lc data for 10 specimens

The data were analyzed by calculating the normal mean and the 99% confidence limits on the mean.

STRESS DISTRIBUTION AT FIBER BREAKS

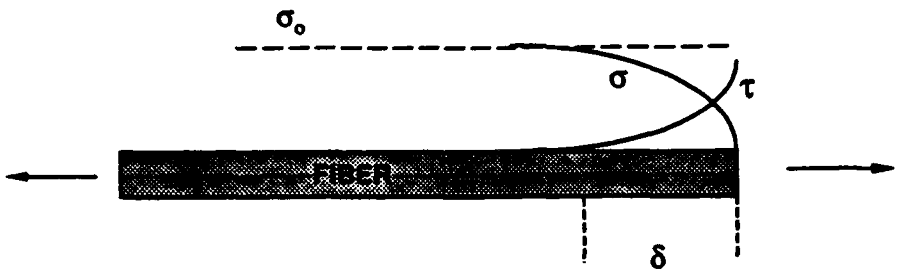

linear elastic analysis

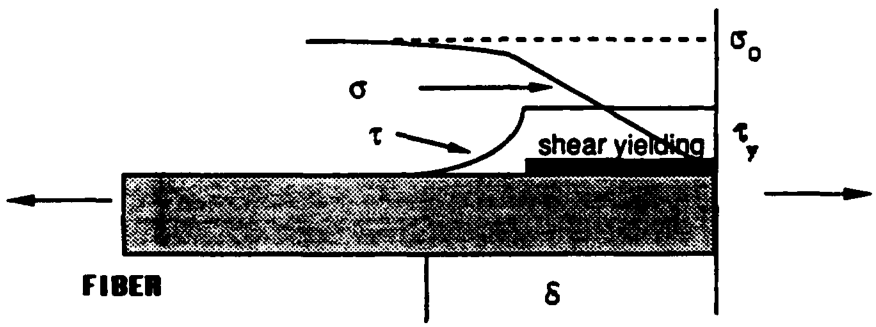

SHEAR YIELDING

A

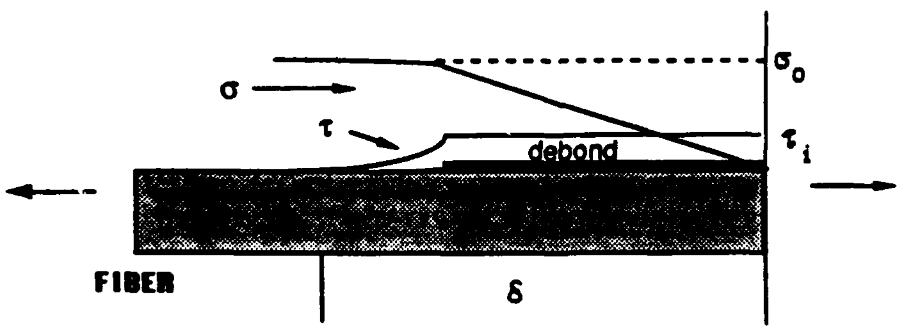

INTERFACIAL FAILURE

B

The polymers used in this study were transparent and stress birefringent and so the experiment revealed information about the stress distribution at fiber breaks.

A 64μ

B 64μ

STRESS BIREFRINGENCE PATTERNS

A Strong adhesion B Weak adhesion

EFFECT OF SURFACE TREATMENT ON ADHESION

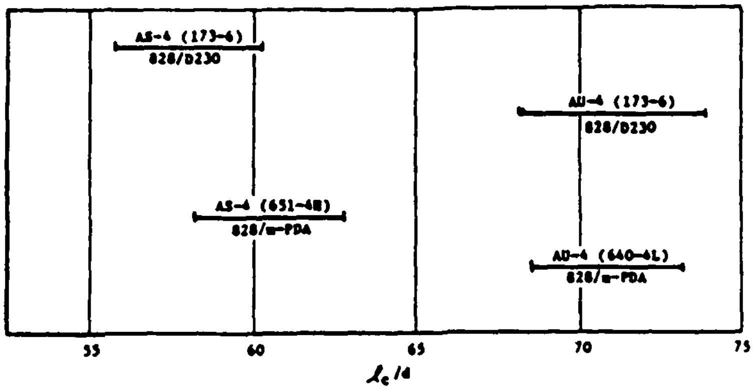

Confidence limits (99%) on lc/d AS-4 vs AU-4

EFFECT OF FIBER TYPE

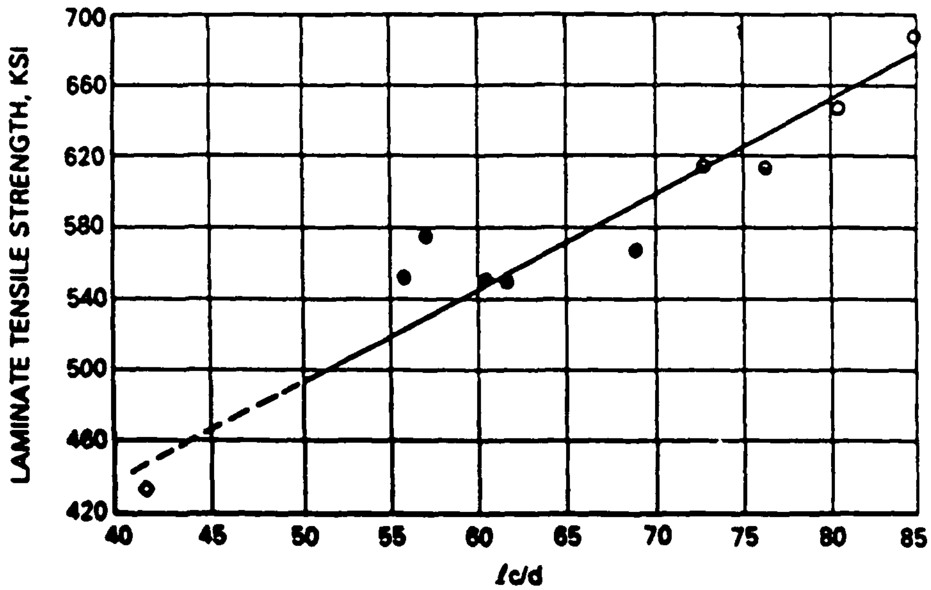

ADHESION TO THERMOPLASTICS

A Study of the adhesion of three fiber types,

Hercules AS1
Hercules AS4

Hysol-Grafil XAS[a]

revealed a similar adhesion to epoxy polymers but an unexpected difference in adhesion to thermoplastics

---

[a] now Courtaulds Grafil, 33-650

Critical Aspect Ratio for Carbon Fiber/Epoxy Systems

Carbon Fiber	Epoxy	Critical Lengths (mm)	Critical Aspect Ratio, l_c/d mean	99% confidence on the mean
AS1[a]	828/mPDA	0.3	42	-----------
AS4	828/mPDA	0.38	55	53 - 57
AS4	828/D230	0.41	60	58 - 62
XAS	828/m-PDA	0.21	32	31 - 33

[a] Drzal, L. T.; Rich, M.J.; and Lloyd, P.F.; "Adhesion of Graphite Fibers to Epoxy Matrices; I, The Role of Fiber Surface Treatment, "J. Adhesion, 16 1 (1983)

Critical Aspect Ratio for AS4 in Thermoplastic Polymers

Matrix	Critical	Critical Aspect Ratio, l_c/d	
	Lengths	mean	99% confidence
limits	mm		
polycarbonate	0.74	108	101-115
polyphenylene oxide	0.83	121	115-125
polyetherimide	0.64	93	90-96
polysulfone	0.83	121	114 - 128
PPO/PS (75/25)[a]	1.41	206	193 - 218

[a]wt.%

Critical Aspect Ratio for AS1 in Thermoplastics

Matrix	Critical Lengths mm	Critical Aspect Ratio, l_c/d	
		mean	99% confidence limits
polycarbonate	0.95	119	114 - 124
polyetherimide	0.67	84	80 - 88

Critical Aspect Ratio for XAS in Thermoplastic Polymers

Matrix	Critical Lengths mm	Critical Aspect Ratio, l_c/d mean	99% confidence limits
polycarbonate	0.36	54	52 - 56
polyphenylene oxide	0.37	55	53 - 58
polysulfone	0.36	55	--
polyetherimide	0.36	55	52 - 57
PPO/PS (75/25)[a]	0.41	61	58 -64

[a]wt.%

In all of the thermoplastics, the XAS gave a smaller l_c/d than the AS4 or AS1.

This indicates stronger adhesion of the XAS to these polymers than for the AS fibers.

The birefringence patterns confirmed this difference

WHY ?

We tested the following possibilities;

wettability

adsorbed specie on the AS fibers

surface roughness

None of these provided an explanation

SURFACE CHEMICAL ANALYSIS

XPS ANALYSIS REVEALED DIFFERENCES IN THE CHEMICAL CONSTITUTION OF THE FIBERS.

XPS ANALYSIS			
	C	O	N
	Atom Percent		
AS1	81.0	11.2	5.6
AS4	88.6	7.6	3.8
XAS	80.5	10.5	7.9

THE ONLY CORRELATION BETWEEN XPS RESULTS AND ADHESION WAS WITH THE O/N RATIO

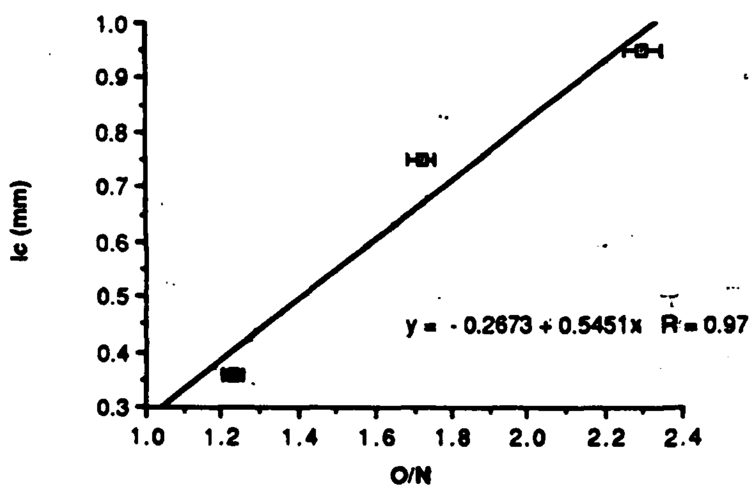

However, acid-base analysis of the fibers using inverse phase chromatography revealed a difference in basic character not evident from the HPS analyses.

γ_S^D = nonpolar surface energy

$I_{sp} = \Delta G^o_{sp}/aN$

I_{sp} = specific interaction
ΔG^o_{sp} = free energy of interaction
a = surface area of adsorbed molecule
N = Avogadro's number

ACID -BASE ANALYSIS[c]

probe molecule	character	I_{sp} (mJ/m^2)	
		AS4	XAS
$CHCl_3$	acidic	-	21.9
CCl_4	acidic	12.8	11.6
CH_3COCH_3	amphoteric	149	87.2
THF	basic	150	92.7
	....	γ_S^D (mJ/m^2)	
n-alkanes	nonpolar	40.0	39.3

[c] Determined by Prof. T. Ward, Virginia Tech

RETENTION TIME CHROMATOGRAPHY

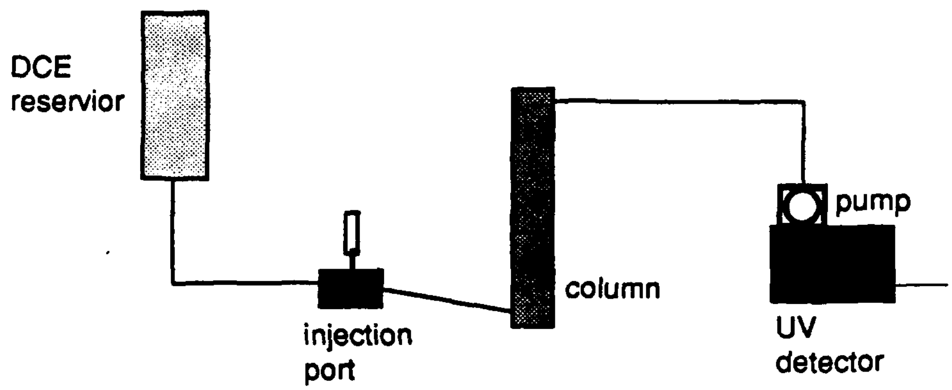

Statistical analysis of the data indicated a clear distinction in the absorptivity of polycarbonate on the different fibers:

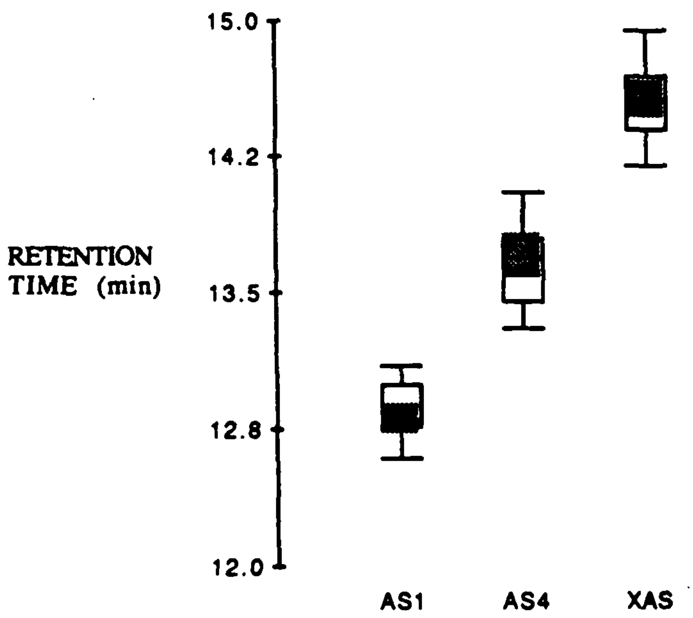

There was a good correlation between the retention time and the critical length

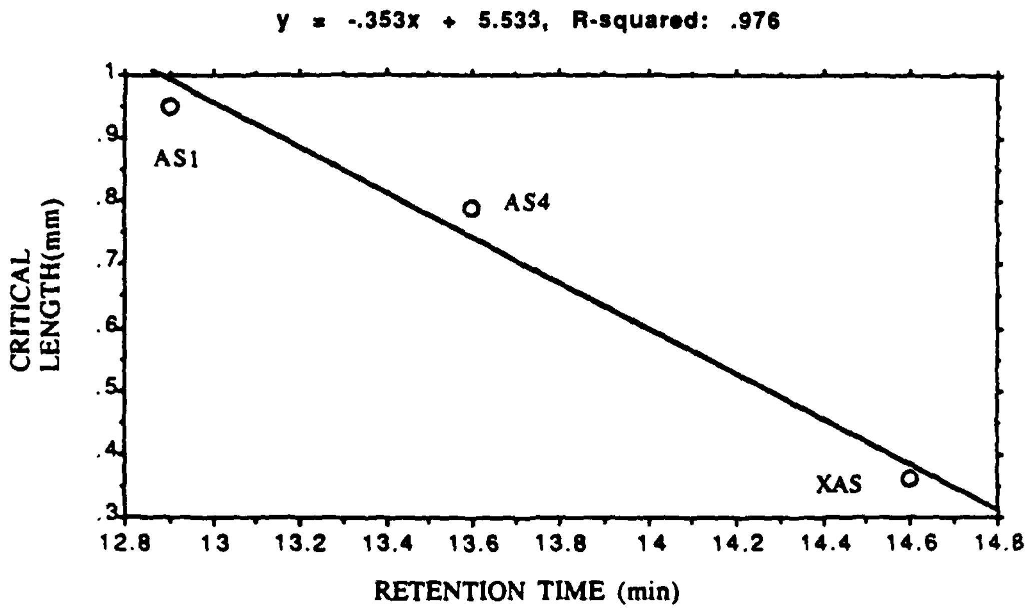

PRELIMINARY EXPERIMENTS SUGGEST THAT PLASMA TREATMENT IN AMMONIA IMPROVES THE ADHESION OF AS4 TO POLYCARBONATE

EFFECT OF PLASMA TREATMENT IN AIR
AS4/Polycarbonate

treatment time min	critical length, mm average	SD
control	0.71	0.22
1	0.80	0.20
2	074	0.21
5	0.75	0.23

EFFECT TO PLASMA TREATMENT IN AMMONIA GAS
AS4/Polycarbonate

treatment time min	critical length, mm average	SD
control	0.71	0.22
1	0.65	0.19
3	0.49	0.15
5	0.67	0.21

THE EFFECT OF THE NH_3 PLASMA APPEARS TO BE NONUNIFORM

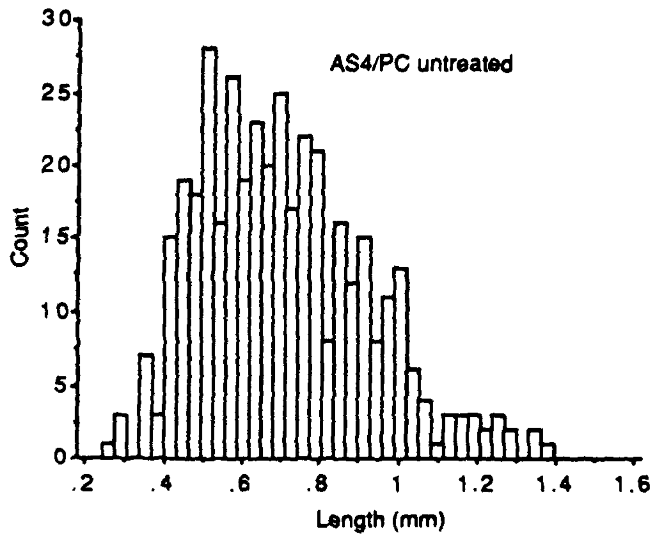

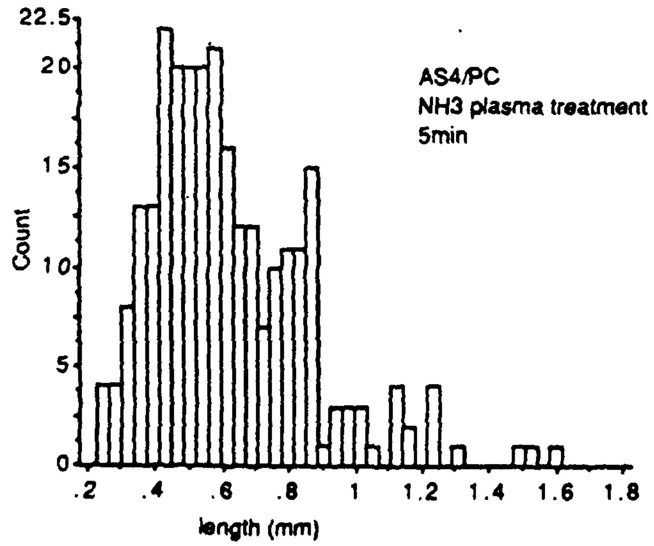

CONCLUSIONS

- Both the HAS and the AS fibers exhibit strong adhesion to the epoxy polymers

- The HAS exhibits strong adhesion to the thermoplastics whereas the AS4 and AS1 fibers exhibit weak adhesion to the thermoplastics

- The differences in adhesion to the thermoplastics could not be explained in terms of weak boundary layers, or differences in wettability or surface roughness

- The three fiber types differ in their surface chemistry
  - from XPS analysis
  - from acid-base characterization

- The only correlation found thus far between adhesion and surface chemical properties is with the XPS O/N ratio

- A correlation was found between the reverse phase LC retention time and the adhesion of polycarbonate.

- The difference in the adhesion of the three fibers to the thermoplastics appears to be due to a subtle but yet unidentified difference in their surface chemical composition

- Preliminary studies suggest that exposure of the AS4 fiber to NH_3 plasma improves the adhesion to polycarbonate

REFERENCES

Fraser, W. A, Ancker F. H. and DiBenedetto, A.T., Proc. Conf. on Reinforced Plastics, SPI , 1975, Section 22A, p.1

Fraser, W.A., Ancker, F. H., DiBenedetto, A. T. and Elbirli, B., Polym. Comp., 4 238 (1983)

Drzal, L.T., Rich, M.J. and Lloyd, P.F., J. Adhesion, 16 1 (1982)

Drzal, L. T., Rich, M. J. Koenig, M. F. and Lloyd, P. F. . J. Adhesion, 16 133 (1983)

Bascom W. D. and Jensen, R. M., J. Adhesion, 19 219 (1986)

Bascom, W. D., and Drzal, L. T., "The Surface Properties of Carbon Fibers and Their Adhesion to Organic Polymers", NASA Contractor Report 4084, NASA Scientific and Technical Information Office. Washington DC, 1987

COMPRESSION FAILURE AND DELAMINATION IN THERMOPLASTIC COMPOSITES

Prof. S. S. Sternstein
Rensselaer Polytechnic Institute
Troy, New York

Workshop on Composite Materials and
Structures for Rotocraft

Held at Rensselaer Polytechnic Institute
14-15 September, 1989

IDEALIZED IN PLANE AND OUT OF PLANE COMPRESSION FAILURE

IN PLANE 'MICROBUCKLING'

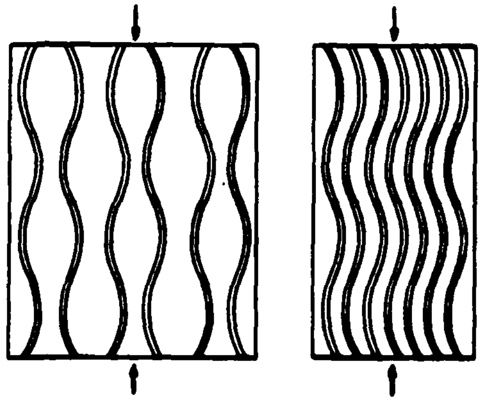

OUT OF PLANE FAILURE

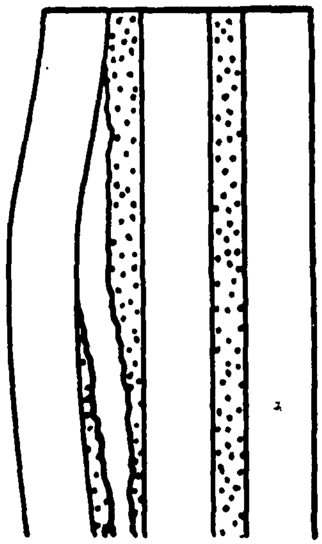

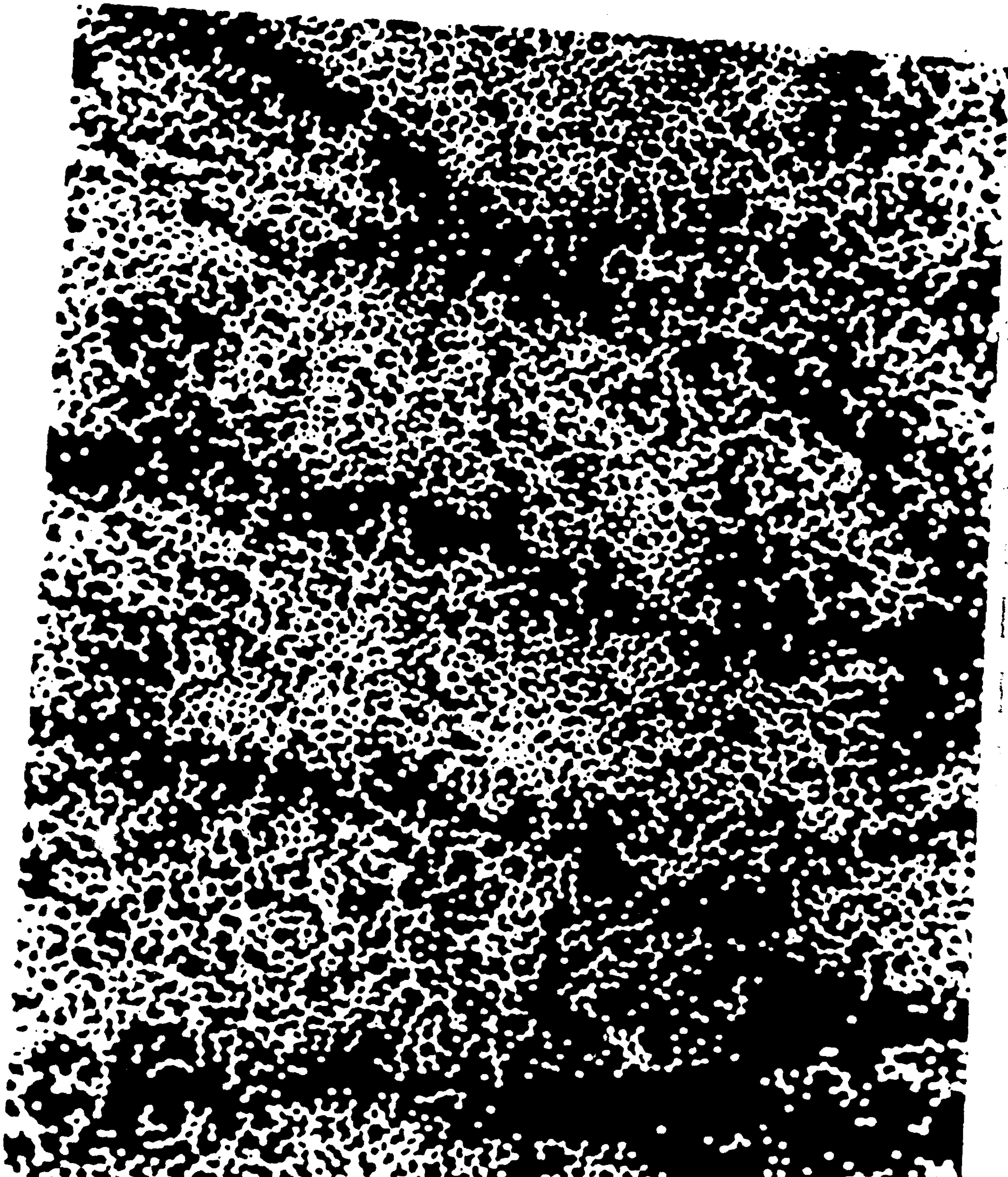

THE MICROBUCKLING ELEMENT

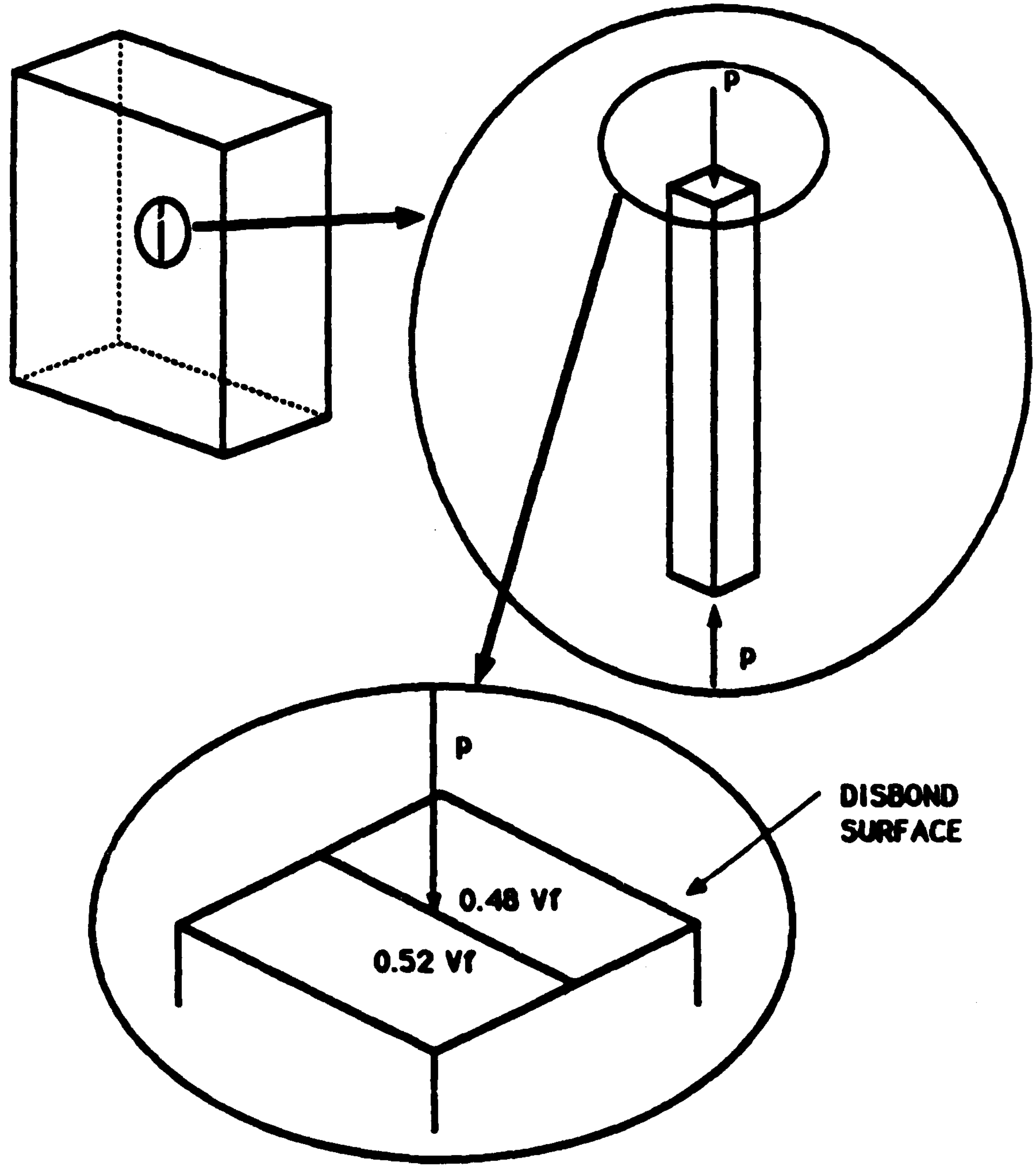

TRANFORMATION TO EQUIVALENT CROSS SECTION

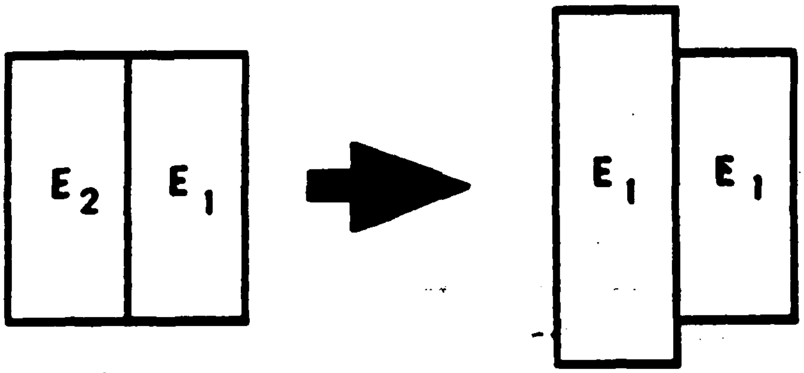

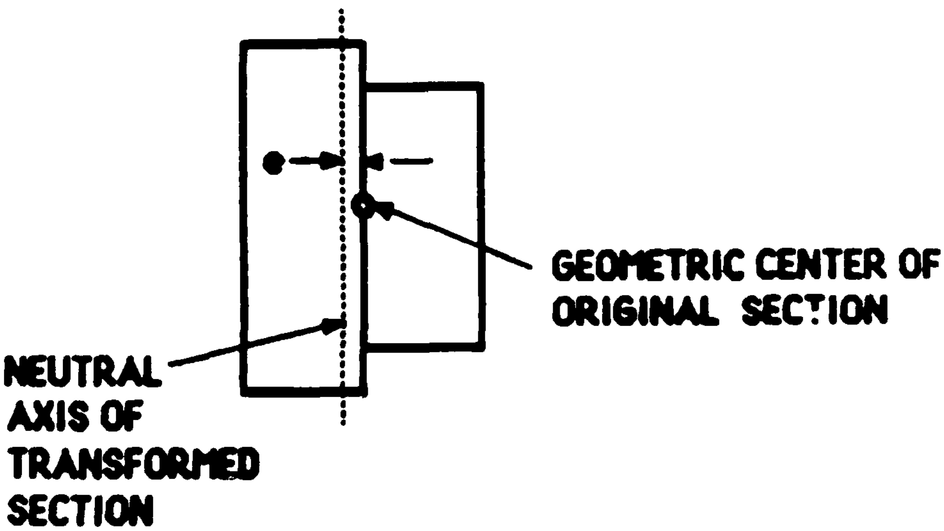

DEVELOPMENT OF AN INTERNAL MOMENT DUE TO NONUNIFORM STRUCTURE

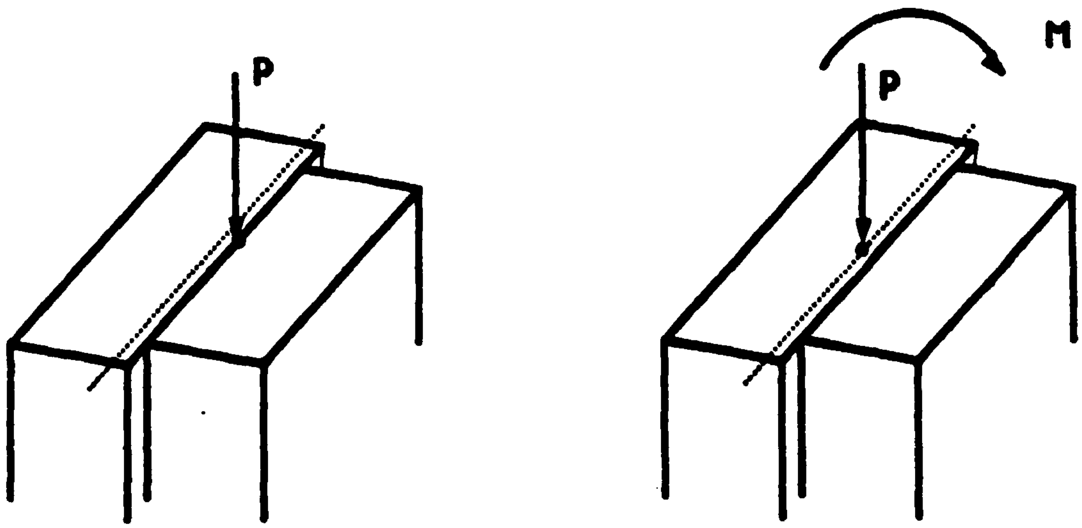

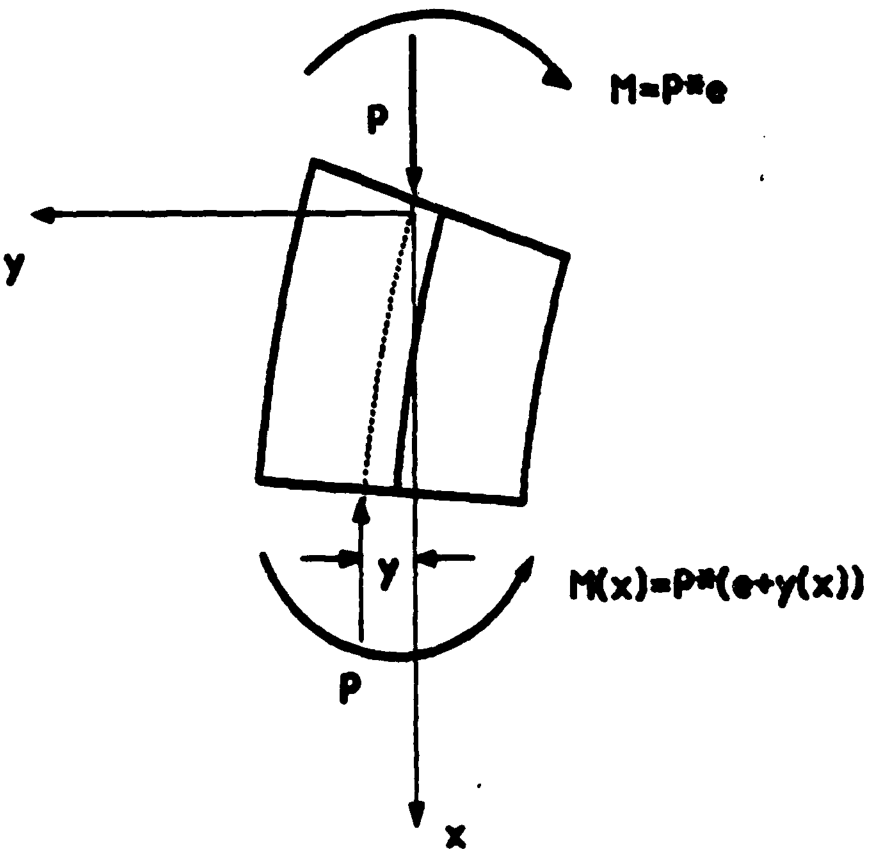

OUT OF PLANE DEFORMATION OF THE SURFACE PAIR

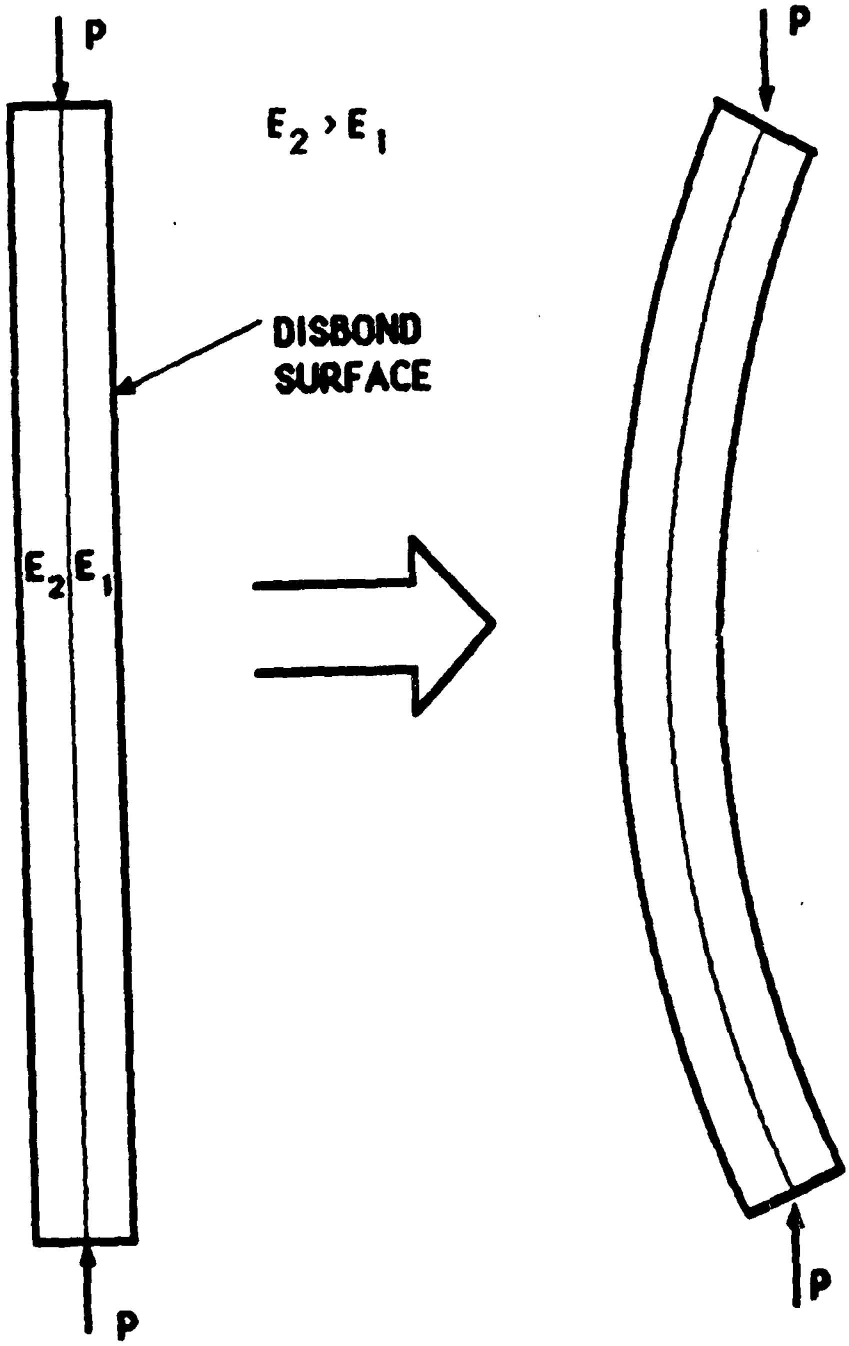

PERCENT STIFFNESS LOST vs P/P_{cr}

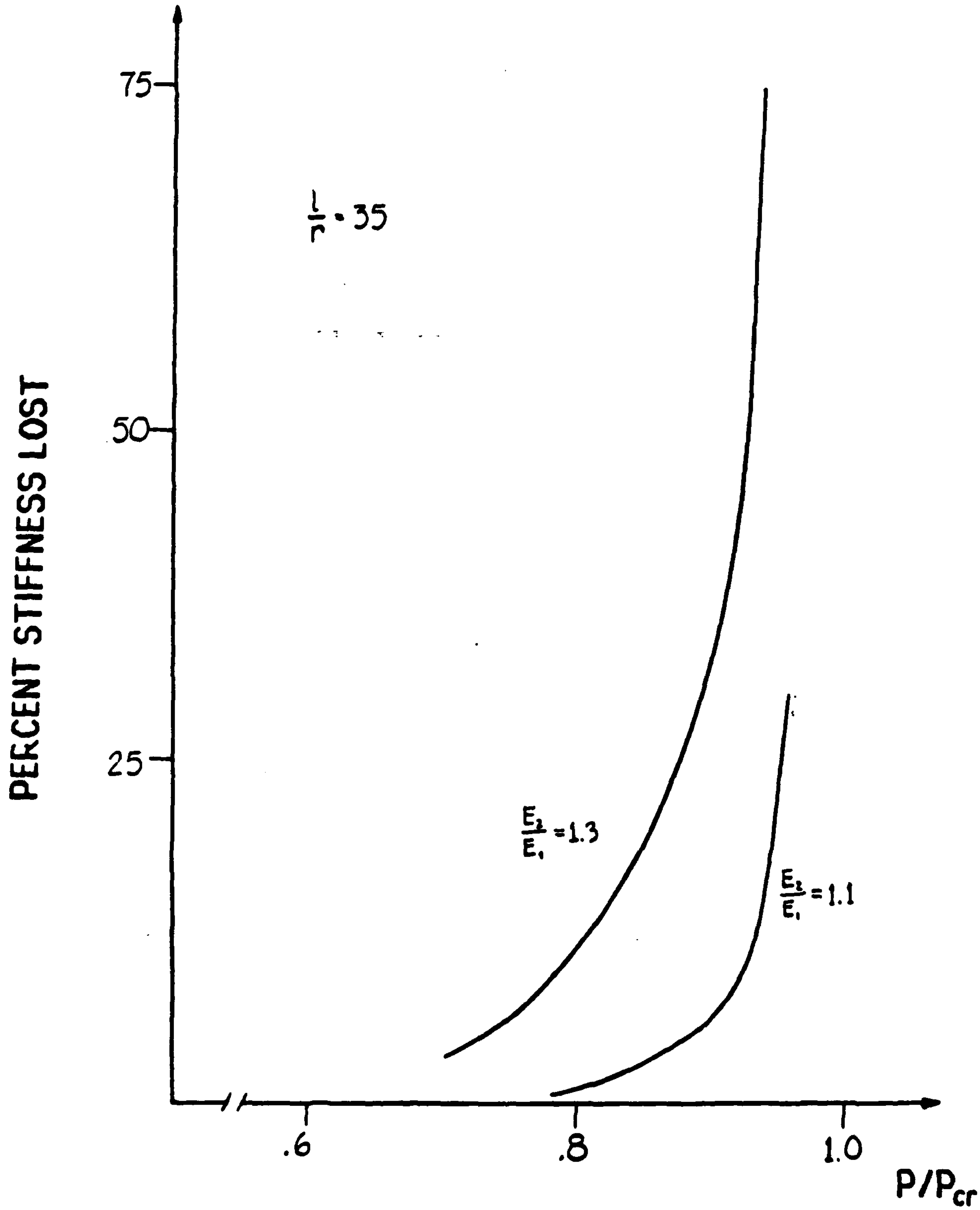

ORIGIN OF THE SHEAR LAG PROBLEM

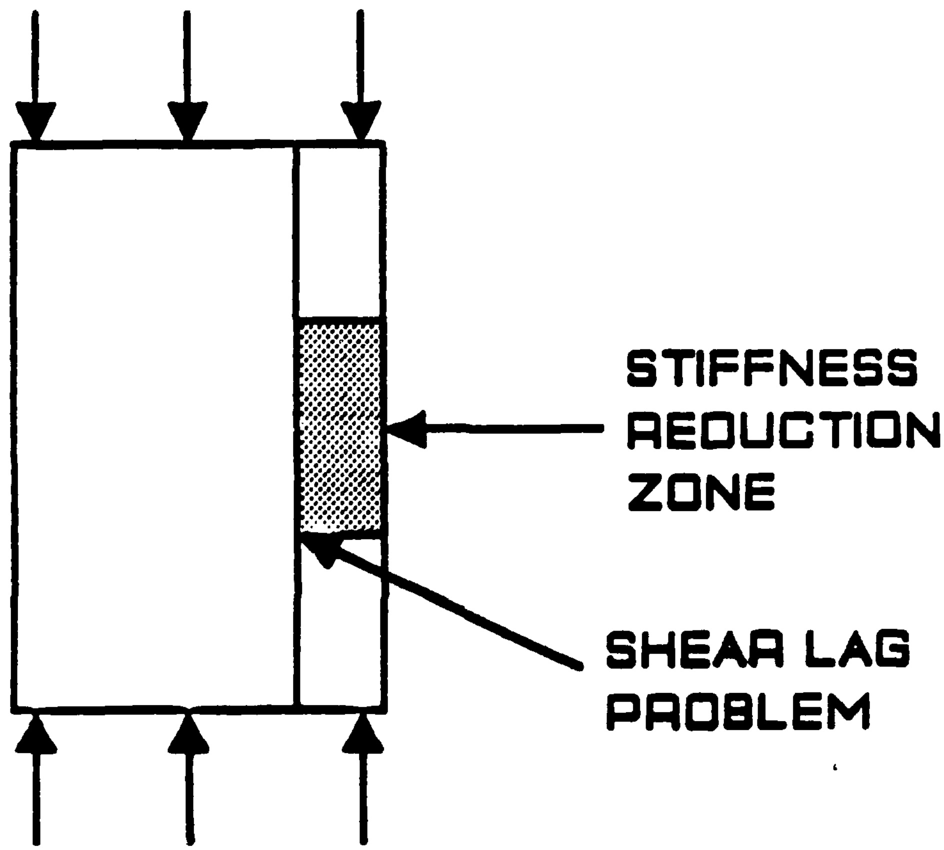

END CONDITIONS DETERMINE THE BOUNDARY CONDITIONS FOR THE SHEAR LAG PROBLEM

BASIC SHEAR LAG MODEL

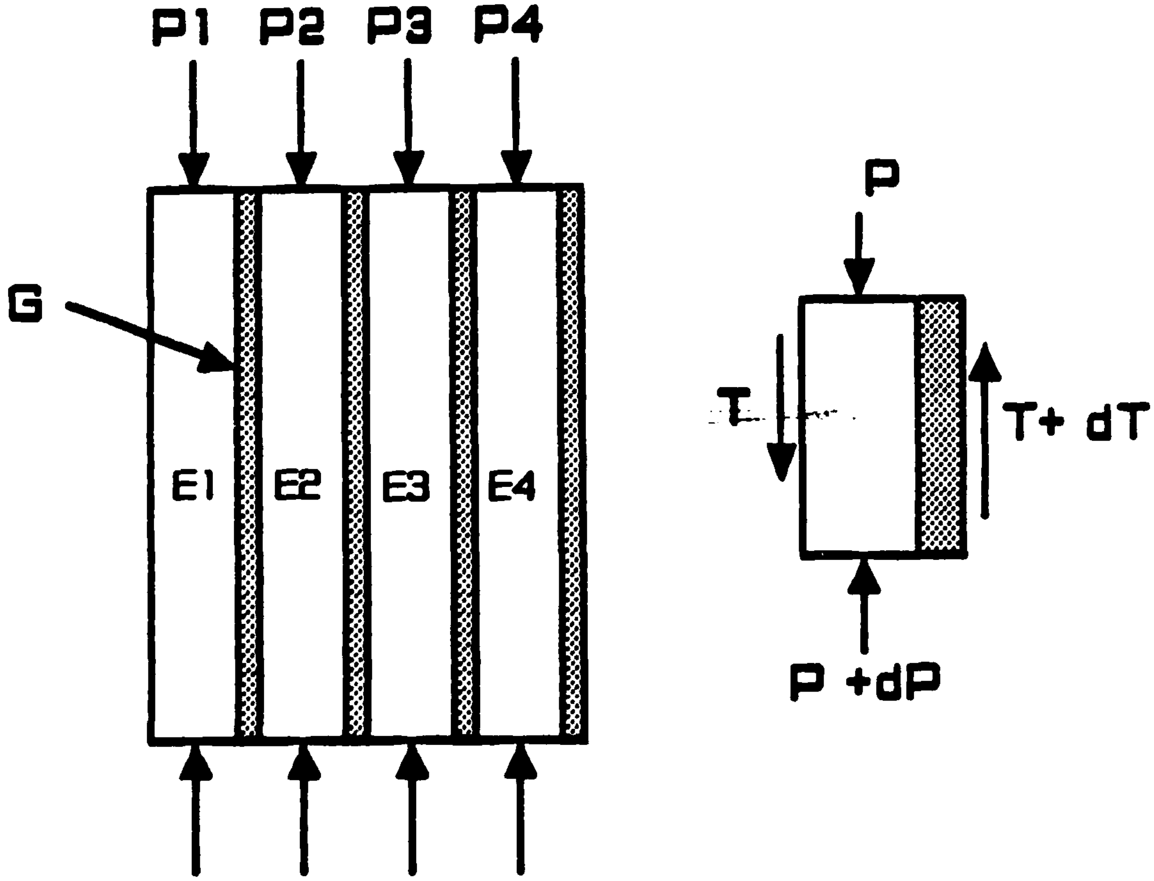

ASSUMPTIONS

NO SHEAR IN E LAYERS

ONLY SHEARS IN G LAYERS

AXIAL (NO TRANSVERSE) GRADIENTS WITHIN LAYERS

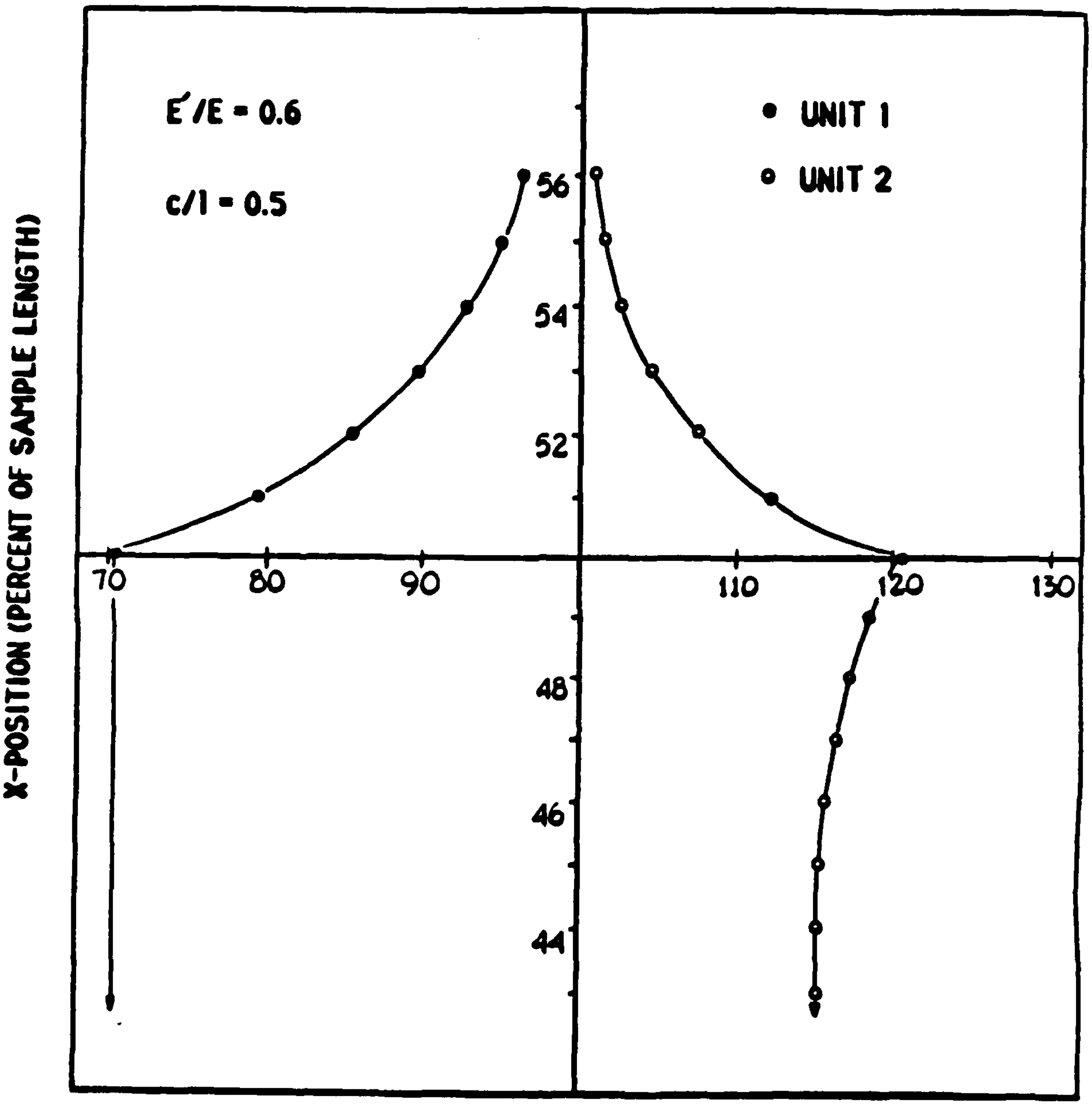

PERCENT OF APPLIED LOAD BEING CARRIED

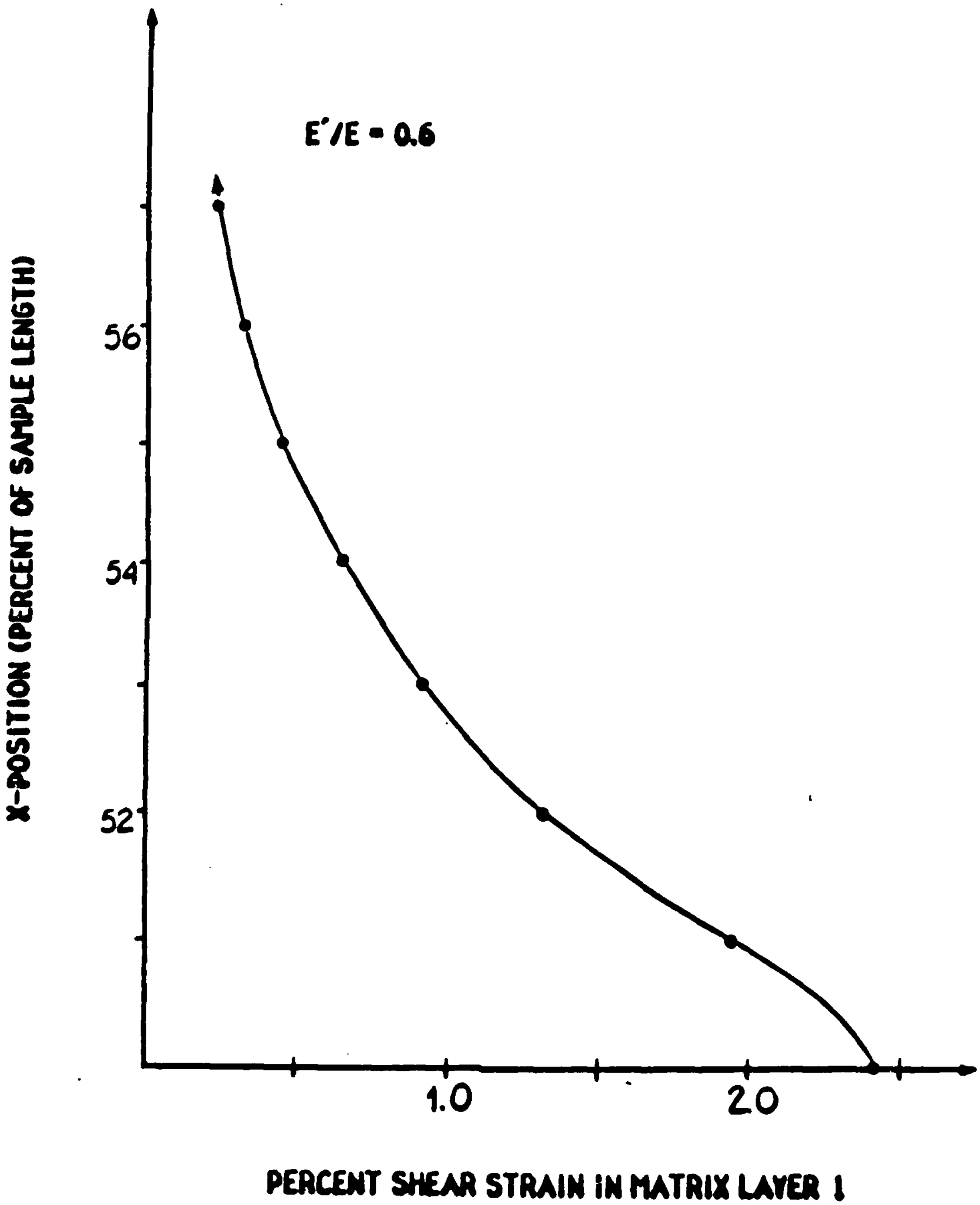

E'/E = 0.6
56
54
52
1.0
2.0
X-POSITION (PERCENT OF SAMPLE LENGTH)
PERCENT SHEAR STRAIN IN MATRIX LAYER 1

DISSIPATED ENERGY DENSITY RATE

0.8 CRACK RADII LAYER THICKNESS.

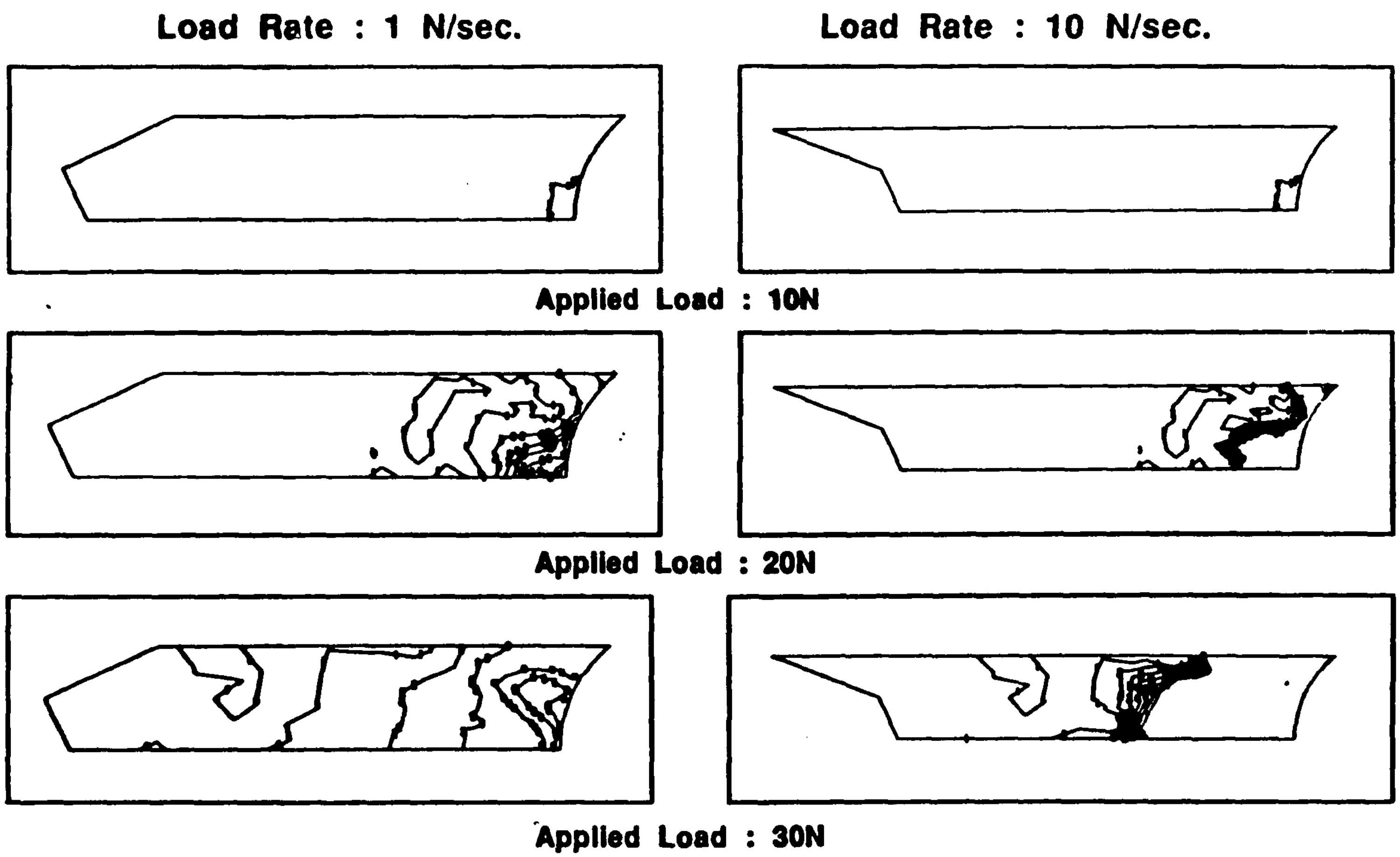

Dissipated Energy Density Rate Contours. (J/m3/sec)

1	0.051	4	1.50E+05	7	3.00E+05
2	5.00E+04	5	2.00E+05		
3	1.00E+05	6	2.50E+05		

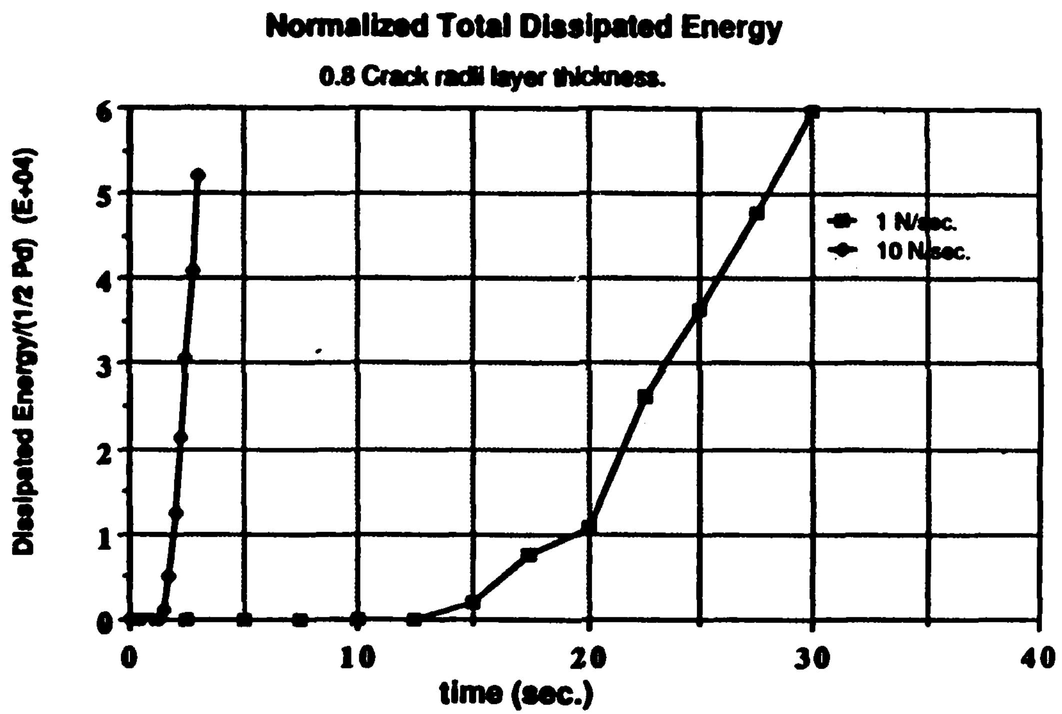
Normalized Total Dissipated Energy
0.8 Crack radii layer thickness.
Dissipated Energy/(1/2 Pd) (E+04)
time (sec.)
1 N/sec.
10 N/sec.
0
1
2
3
4
5
6
0
10
20
30
40

CONCLUSIONS

(DESTINED TO BE CONTROVERSIAL)

COMPRESSION STRENGTH IS NOT A MATERIAL PROPERTY, INSOFAR AS REAL ENGINEERING STRUCTURES ARE CONCERNED.

MICROSTRUCTURE WILL DETERMINE COMPRESSION PERFORMANCE, BUT MUST BE CONSIDERED IN CONJUNCTION WITH LOAD AND GEOMETRY GRADIENTS.

MATRIX VISCOELASTICITY WILL AFFECT COMPRESSION PROPERTIES THROUGH SHEAR REDISTRIBUTION OF LOAD CONCENTRATIONS.

PROCESS CONTROL FOR THE PREPEG AND LAMINATE MAY BE MORE IMPORTANT FOR COMPRESSION PERFORMANCE THAN FOR ANY OTHER ULTIMATE PROPERTY.

MICROSTRUCTURE UNIFORMITY REQUIREMENTS MUST BE QUANTIFIED.

ADVANCE THERMOPLASTIC COMPOSITE STRUCTURES FOR ROTORCRAFT APPLICATIONS

J. F. PRATTE
E. I. DU PONT DE NEMOURS & CO.
SEPTEMBER 15, 1989

Outline

- Rotorcraft Needs
- Thermoplastic Composites
  - Features
  - Du Pont's Material Systems
  - PEKK Resin System
  - Low Cost PEKK Composite Parts
- LDF™ Technology
  - Overview
  - General Thermoforming Process
  - Structural Component Configurations
  - Composite Performance
- Summary

Rotorcraft Structural/Operational Needs

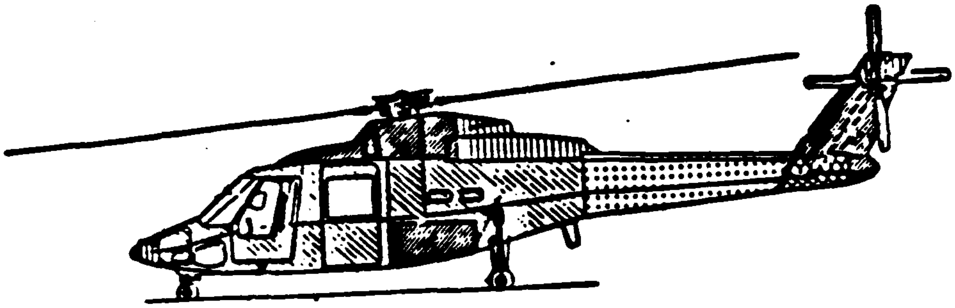

- Damage Tolerance
- Lightweight
- Good Fatigue Life
- Good Vibration Characteristics
- Crashworthiness
- Low Cost (Acquisition & Life Cycle)

Thermoplastic Composite Features

- High Toughness
  - Improved Damage Tolerance Characteristics
- Lower Cost Composite Structures
  - Less Labor Intensive Part Fabrication
  - Parts Consolidation
  - Unlimited Out Time
  - Reprocessible (increased yields)
  - No Cure (shorter cycle time)
  - Simplified Repair (welding)
  - Recyclable Scrap

THE DU PONT HIGH PERFORMANCE FAMILY

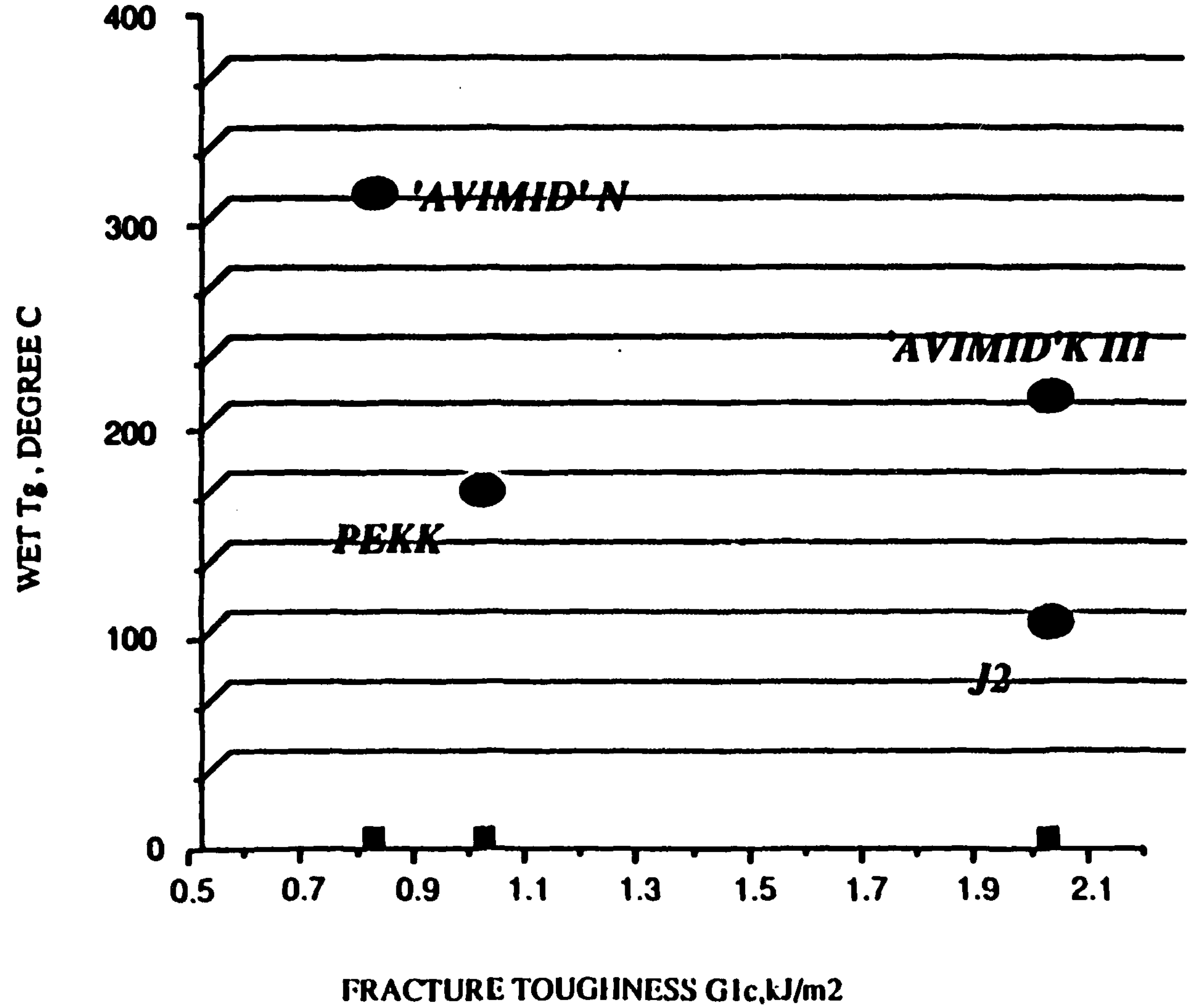

PEKK Matrix Features

- High Tensile Modulus (650 KSI)
- Suitable for composite use temperatures up to 300°F
- Flammability properties meet FAA requirements with heat release less than OSU 65/65
- Resistant to aircraft fluids
- Resin toughness adequate for good composite damage tolerance
- Low water absorption
- Melt viscosity compatible for thermo-forming processes

Low Cost PEKK Composite Parts

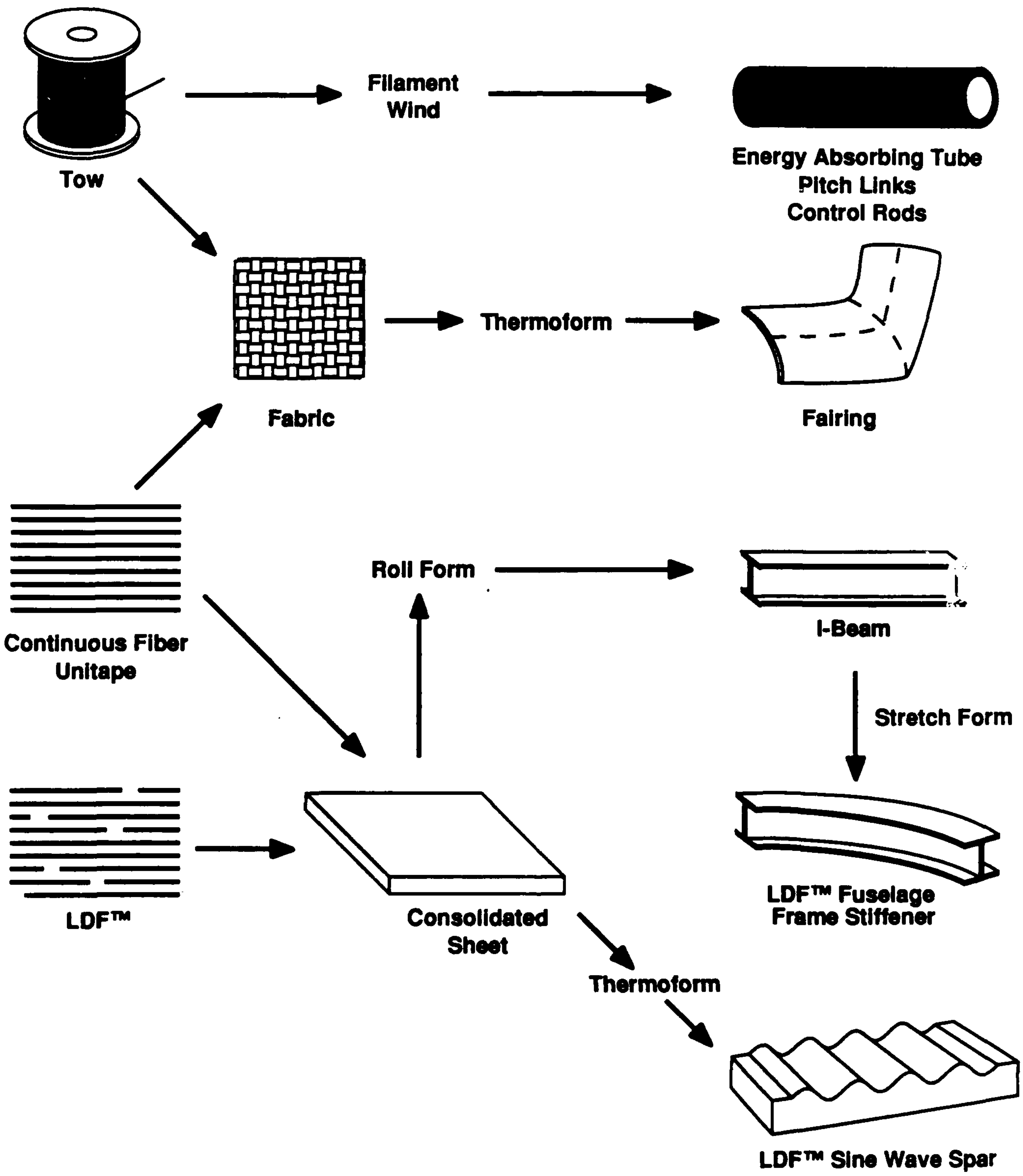

Du Pont LDF™ Technology

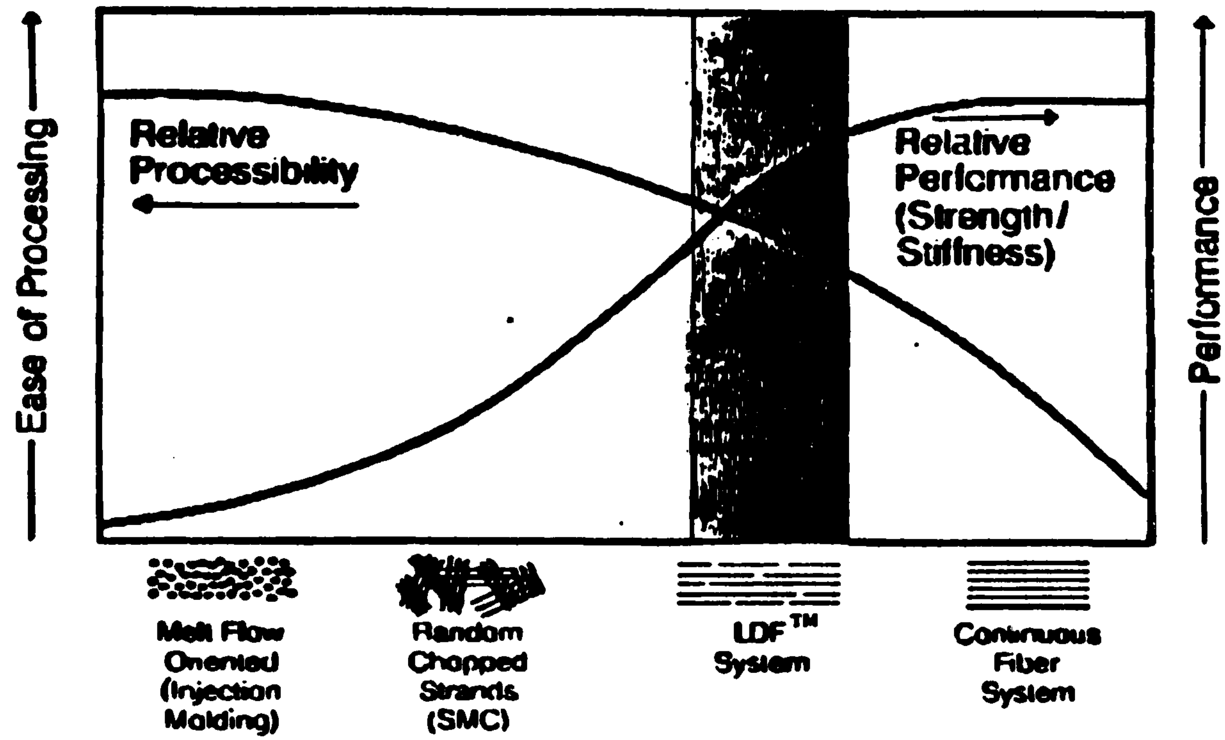

LDF™ TECHNOLOGY DEVELOPMENT

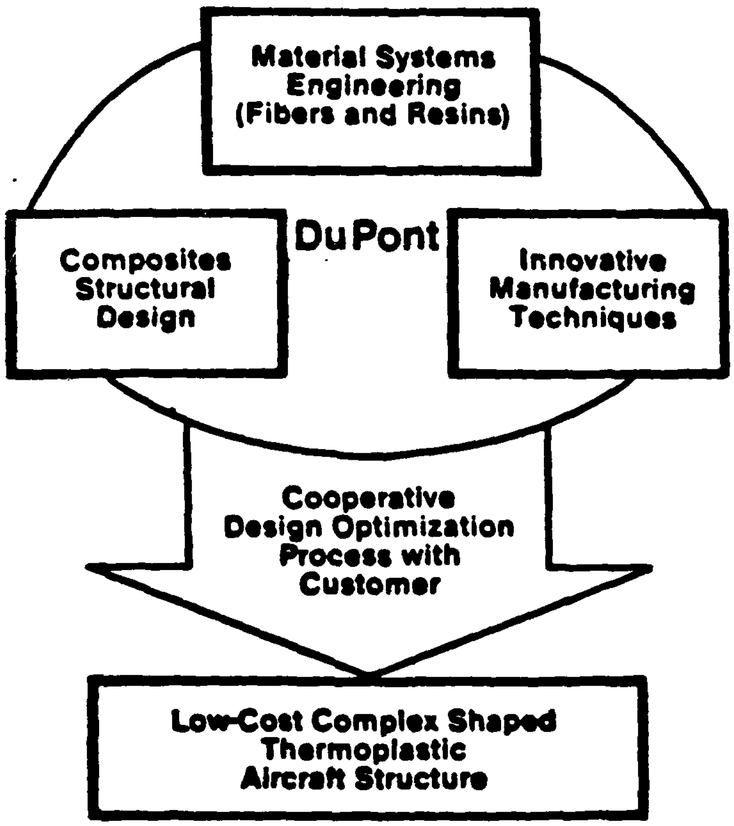

LDF™ Technology Goals

- Exploit material's "metal-like" drawability through processes such as:

  - Match die press forming
  - Rubber pad press forming
  - Diaphragm forming
  - Stretch forming

  leading to weight efficient structures at lower cost

- Composite performance equal to continuous fiber reinforcement

General Thermoforming Concept

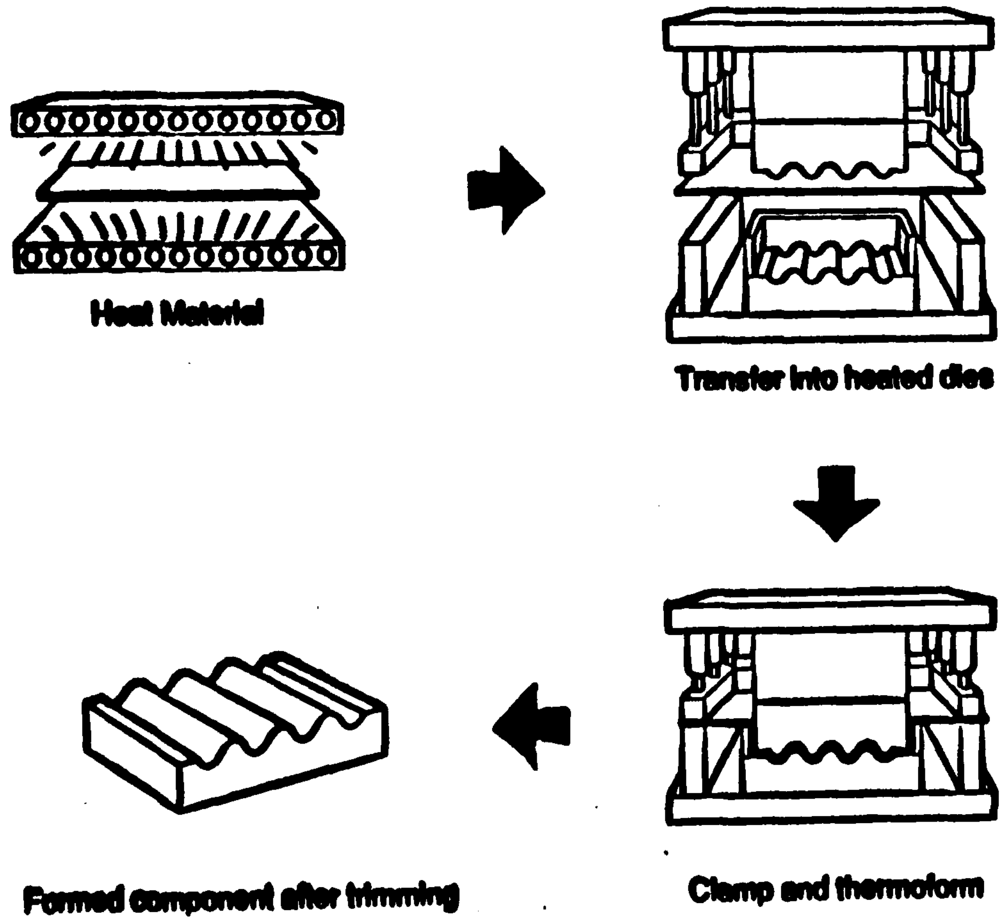

Structural Component Configurations

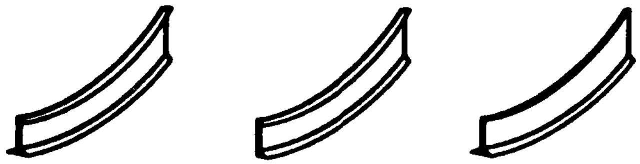

Contoured 'J', 'C', 'I' or Blade Section Stiffeners

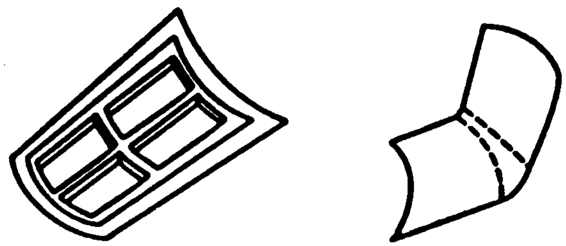

Stiffened Skin Panels
and Fairings with Complex Contour

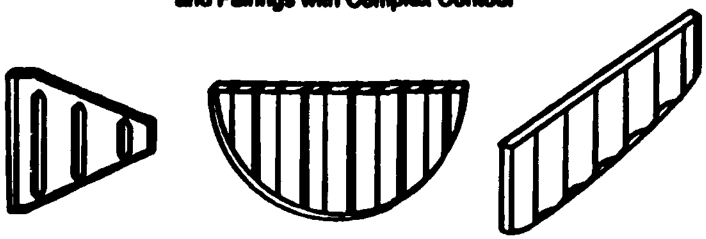

Stiffened Ribs, Formers, Bulkheads
or Support Beams

Key Performance Criteria

- Fiber length greater than 50 times critical length
- Consistent fiber volume fraction and thickness control
- Post formed fiber orientation meeting design requirements

Unidirectional Mechanical Properties of AS-4 Carbon Fiber/PEKK Laminates*

Property		LDF™**	Continuous	ASTM Test
Tensile				D3039
Strength (0°)	KSI	234	243	
Modulus (0°)	MSI	17.9	18.8	
Poisson Ratio		0.35	0.33	
Strength (90°)	KSI	13.2	10.6	
Modulus (90°)	MSI	1.5	1.2	
Compressive				D695
Strength (0°)	KSI	183	202	
Modulus (0°)	MSI	16.1	17.6	

*Fiber volume fraction 58%, 75°F dry
**Average fiber Length 2.2"

Unidirectional Mechanical Properties of AS-4 Carbon Fiber/PEKK Laminates* (Cont'd)

Property		LDF™**	Continuous	ASTM Test
Flexural				
Strength (0°)	KSI	240	280	D790
Modulus (0°)	MSI	18.0	18.5	
Shear				
Inplane Strength	KSI	21.2	20.6	D3518
Inplane Modulus	MSI	0.8	0.84	
Short Beam Strength	KSI	16.0	17.0	D2344

*Fiber volume fraction = 6[illegible]%, 75°F dry
**Average fiber length = 2.2"

Toughness Behavior - Carbon Fiber (AS-4) PEKK

Prcoerty	LDF™ System	Continuous Fiber System
Edge Delamination* Strength MPa (KSI)	422 ± 23 (61.2 ± 3.4)	405 ± 37 (58.7 ± 5.4)
G_{Ic}, Interlaminar Fracture Toughness KJ/m² (in-lb/in²)	1.4 (7.5)	1.4 (7.5)

*Laminate Layup: $[(\pm 25)_2, 90]_s$

Damage Tolerant Behavior

Fiber:	AS-4
Resin:	PEKK
FVF:	58%
Condition:	75°F dry

	LDF™	Continuous
Open Hole Compression Strength	44.5 KSI	47.2 KSI
Open Hole Tensile Strength	46.1 KSI	48.6 KSI
Compression after Impact (1500 in-lb/in)	39.5 KSI	40.0 KSI
Strain to Failure	0.59%	0.60%

Moisture Absorption

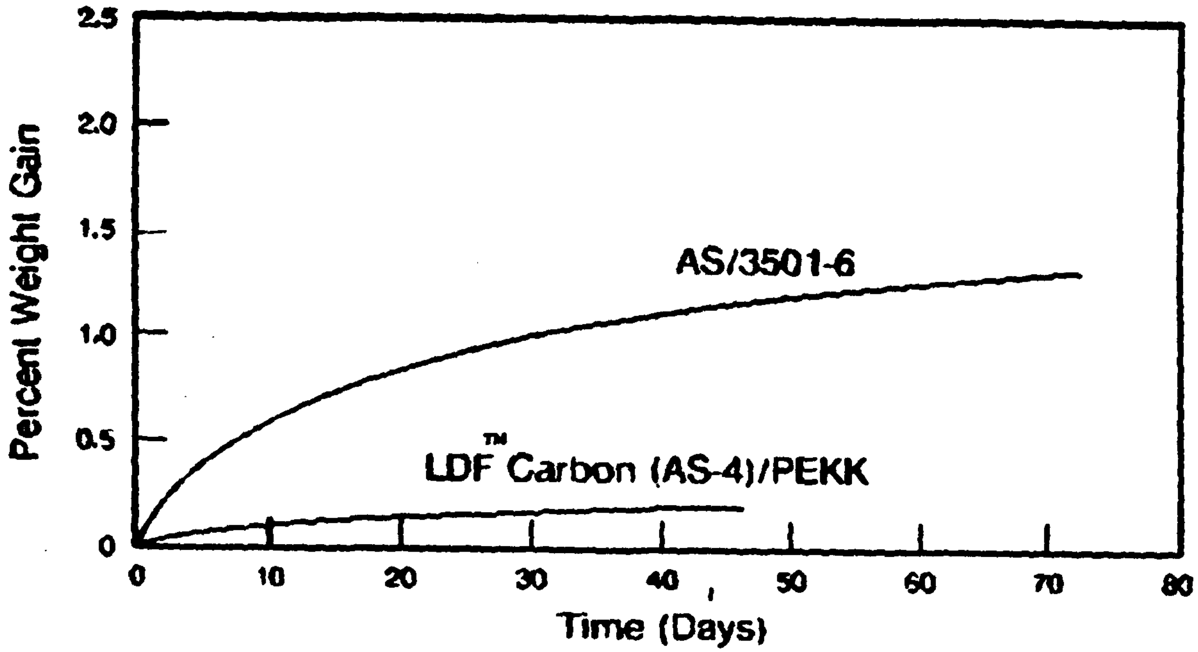

Open Hole Compression

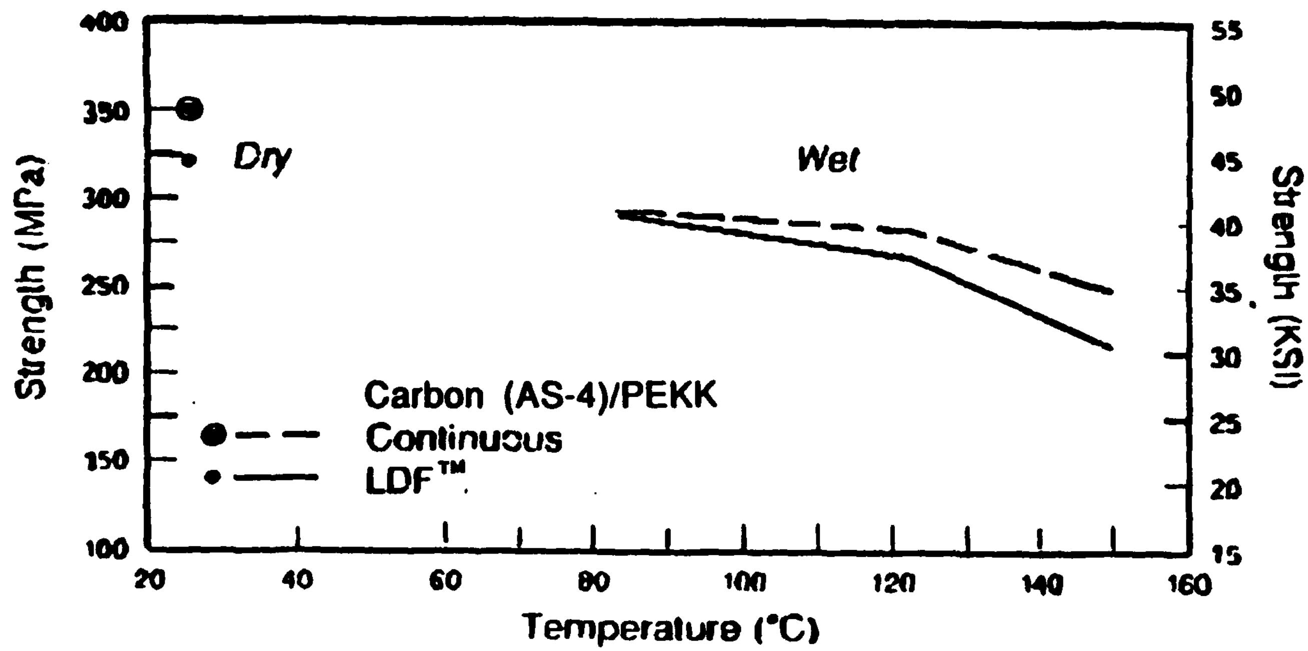

LDF™ SUMMARY/PATH FORWARD

- Lower cost structures versus thermosets
- Capability to thermoform a wider range of complex shape parts than continuous fiber materials
  - Greater Design Freedom
  - Parts Consolidation
- Static mechanical and damage tolerance properties similar to continuous fiber materials
- Dynamic measurements in progress
- Development programs are being established to validate LDF™ technology

BASF

Thermoplastic Prepreg Product Forms

Thermoplastic Composites

BASF

- **Products**
- **Processing**
- **Manufacturing**

Drapeable Materials

- Conformability
- Preforms
- Predictable Fiber Orientation
- Co-Consolidation

BASF

Prepregging Technologies

- Commingled Yarns and Fabrics
- Powder Prepregs

BASF

Commingled Yarns

Thermoplastic Composites

Commingled Yarn Advantages

- **Flexible/Drapeable Materials**
- **No Solvents**
- **Broad Goods**
- **Preforms**
    - Multilayer
    - Near Net Shape

Commingled Products

Polymers	Reinforcements
PEEK	AS4, IM7 S2 Glass® HT
PEKEKK	AS4, IM7

BASF

Powder Prepregs

Thermoplastic Composites

Unconsolidated Powder Prepreg Schematic

BASF

- ● Fiber
- ○ Powder

12 mils

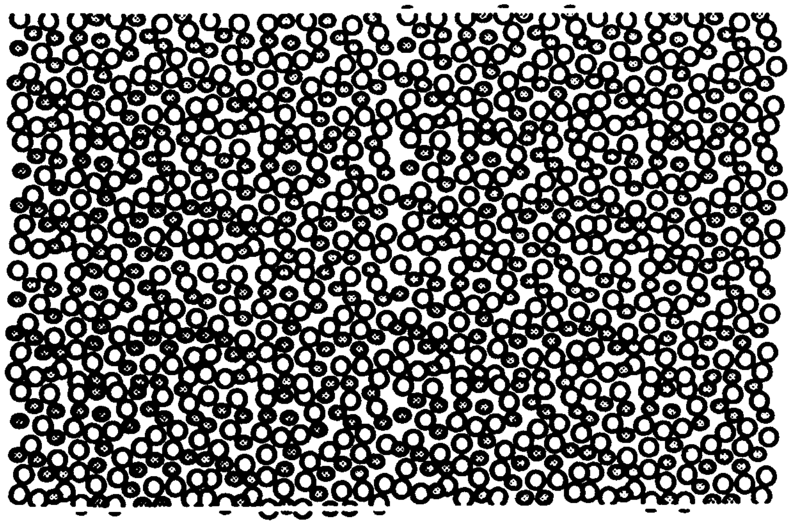

Powder Prepreg Advantages

- **Polymers Not Spinnable As Fine Denier Fibers**
  - High Melt Viscosities
  - Thermosets
- **Flexible/Drapeable**
- **No Solvents**
- **Polymer Alloys**

Powder Products

Polymers	Reinforcements
TPI	AS4, IM7, IM8
PMR-15	G30-500, AS4

Powder Product Forms

- **Unidirectional Tapes**
- **Towpreg**
- **Impregnated Fabrics**
    - PMR-15 (under development)

BASF

PMR-15 Powder Prepreg

- **Pre-imidized Polymer**
  - Reduced MDA Exposure
  - Unlimited Shelf Life
  - Simplified Processing

BASF

- Products
- Processing
- Manufacturing

PEEK Processing

BASF

TYPICAL AUTOCLAVE CYCLE FOR PEEK 150G

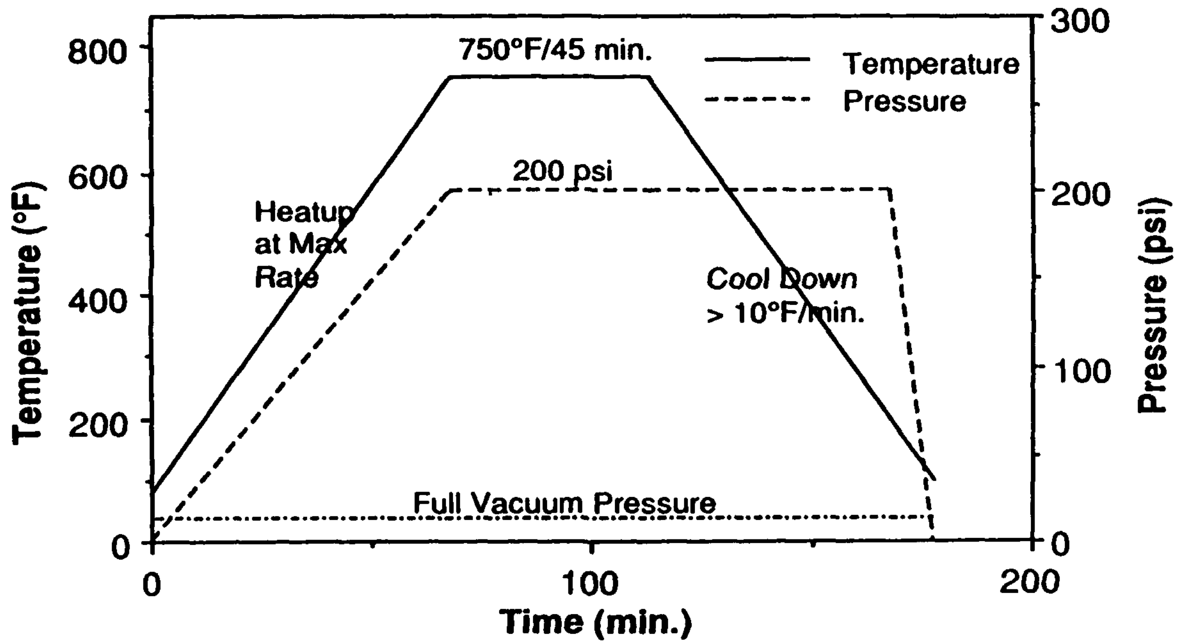

PMR-15 Processing Cycle

BASF

PMR-15 Press Molding Cycle

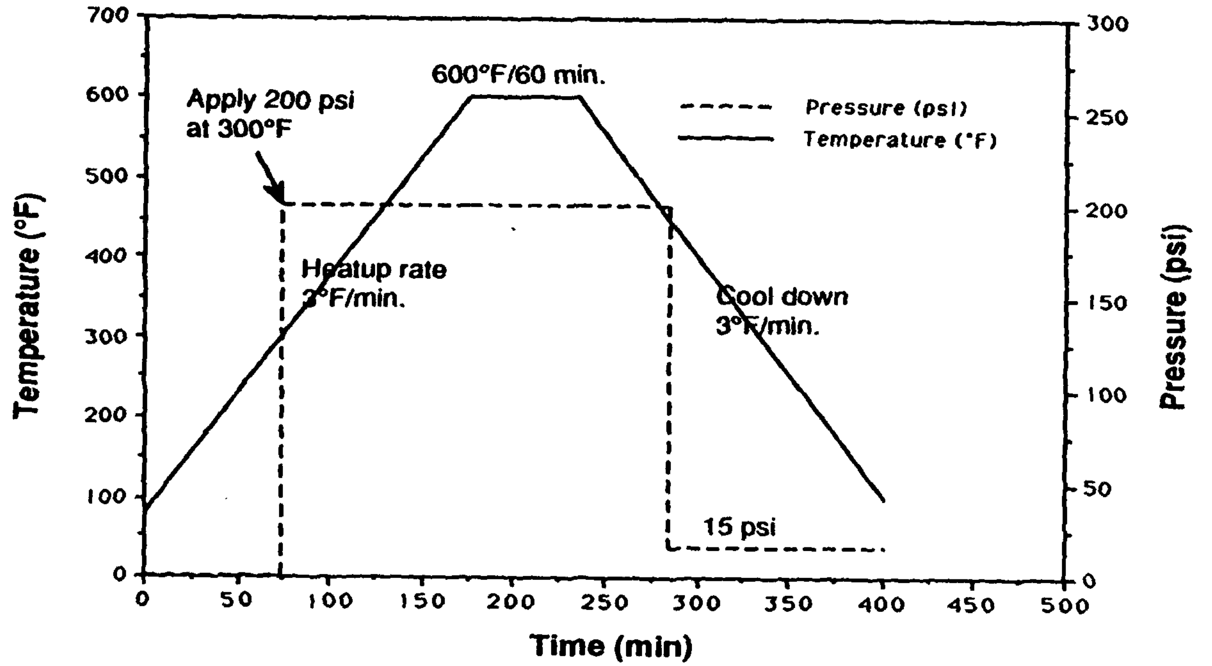

BASF

- Products
- Processing
- Manufacturing

BASF

Preforms

- Stitched
- Multi-layer
- Braided
- Woven

High Temperature Autoclave Consolidation

BASF

- Drapeability
- Complex Shapes
- Co-Consolidation
- Preforms

Low Temperature Autoclave Consolidation

BASF

- Integrally Heated/Cooled Tools
- Faster Cycles
- Low Temperature Sealants
- Preforms

Diaphragm Consolidation

BASF

- Single Diaphragm Process
- Integrally Heated/Cooled Tools
- Faster Cycles

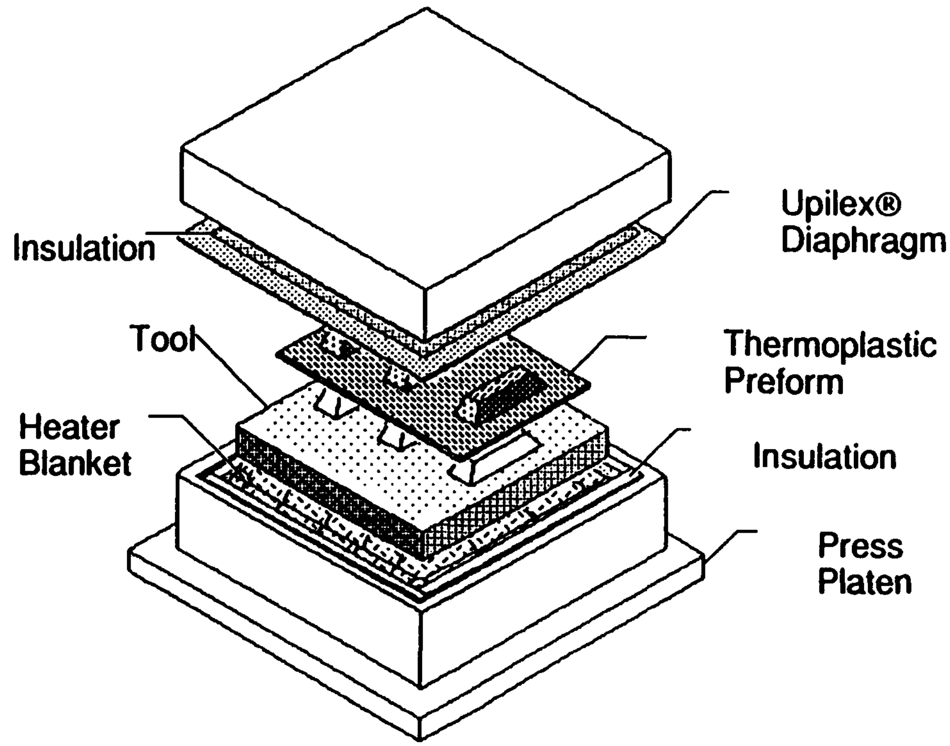

Stitched Preforms

- **Near-Net Shape**
- **Complex Geometry**
- **Multi-Layer Preforms**
  - Quasi-isotropic Fabrics

BASF

Diaphragm Consolidation

- Preforms
- Co-Consolidation

Pultrusion

BASF

- Preforms
- Quasi-isotropic Orientation

Compression Molding

BASF

- Drapeability
- Simple Processing
- Preforms

BASF

Hot Head Filament Winding

- Flexible Tow for Complex Geometries
- In-Situ Consolidation
- Wide Range of Fibers/Polymers

Fiber Placement/Tape Laying

- Room Temperature
- Fast Placement
- Utilize Existing Thermoset Equipment

"Advanced Thermoset Resin Systems"

William T. McCarvill

Hercules Inc., Magna, Utah

ARO-AHS-RPI 2nd International Workshop on COMPOSITE MATERIALS AND STRUCTURES FOR ROTORCRAFT

September 14 and 15, 1989

Rensselaer Polytechnic Institute
Troy, New York

IMPROVED RESINS ARE BEING DEVELOPED

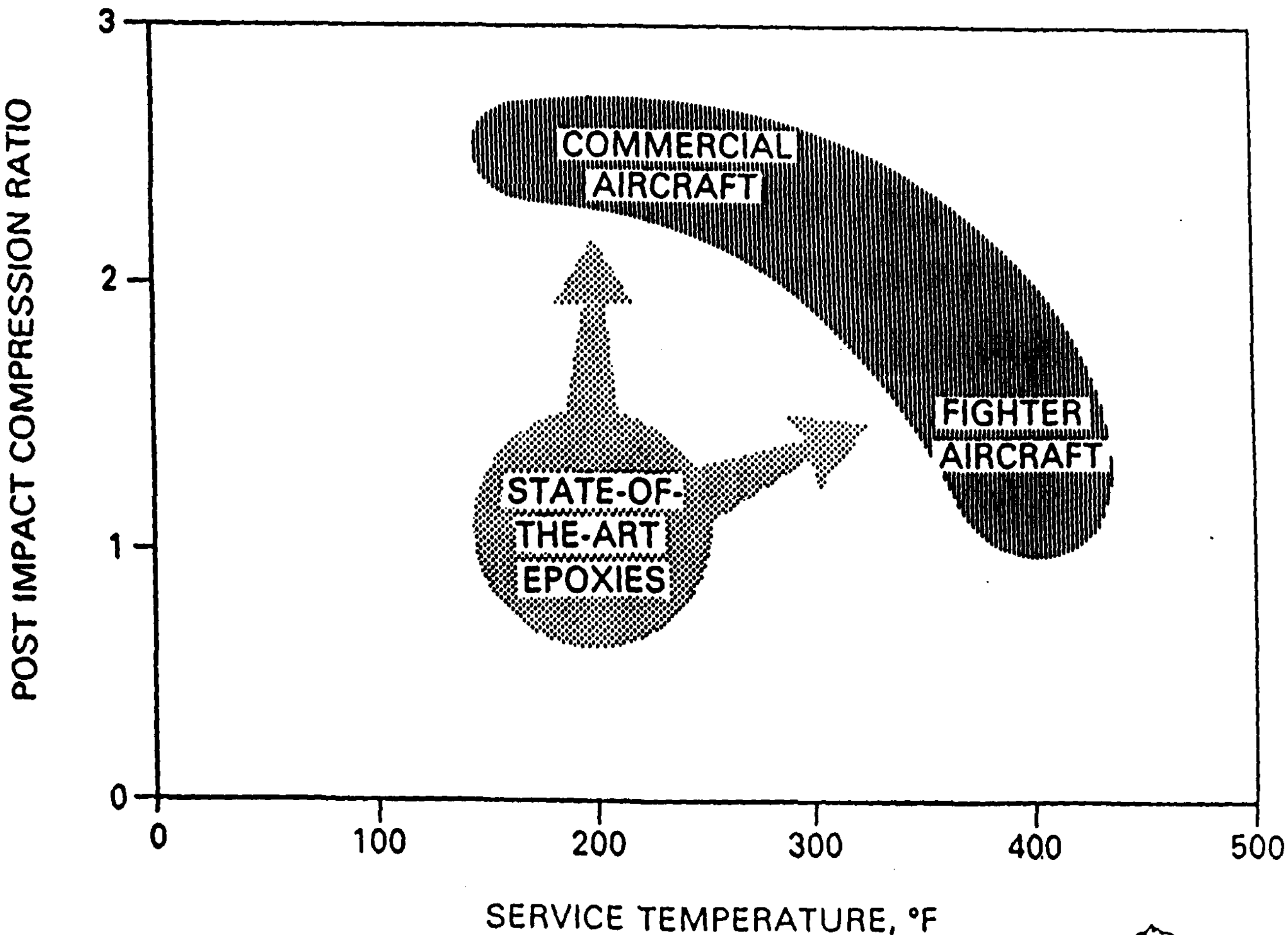

HERCULES

ADVANCED THERMOSETS

- MATERIAL CHOICE IS ALWAYS A COMPROMISE
  - RAW MATERIAL COSTS
  - PERFORMANCE
  - FACILITY COSTS
  - PRODUCTION RUN
  - TOOLING COSTS
  - MATERIAL AVAILABILITY
- SHORT RUN SPECIALITY PRODUCTS USUALLY REQUIRE MATERIAL/PROCESS TAILORING OF EXISTING TECHNOLOGY.
- LONG RUN COMMODITY PRODUCTS CAN PAY FOR DEVELOPMENT OF NEW MATERIALS/PROCESSES DESIGNED SPECIALLY FOR PRODUCT LINE.

WHY THERMOSETS FOR HI PERFORMANCE COMPOSITES?

PERFORMANCE - IN THE 1970'S THERE WERE NO HIGH PERFORMANCE THERMOPLASTICS.

- TEMPERATURE, MOISTURE AND SOLVENT RESISTANCE.

COST NOT AN ISSUE - MILIARY APPLICATIONS WERE PERFORMANCE DRIVEN.

THERMOSETS BEST ADAPTED TO PREPREG AND FILAMENT WINDING PROCESSES.

LOW VISCOSITY - EASY FIBER IMPREGNATION ON SIMPLE EQUIPMENT.

TAILORED CHEMISTRY - GEL, CURE ADAPTED TO PROCESS.

SMALL VOLUME DICTATED HAND LAYUP.

- TACK
- DRAPE
- EASY TO CHANGE LAYUP

LABOR INTENSIVE, BUT CHEAP EQUIPMENT.

- AUTOCLAVE
- OVENS
- TABLES
- FILAMENT WINDER

VISCOSITY

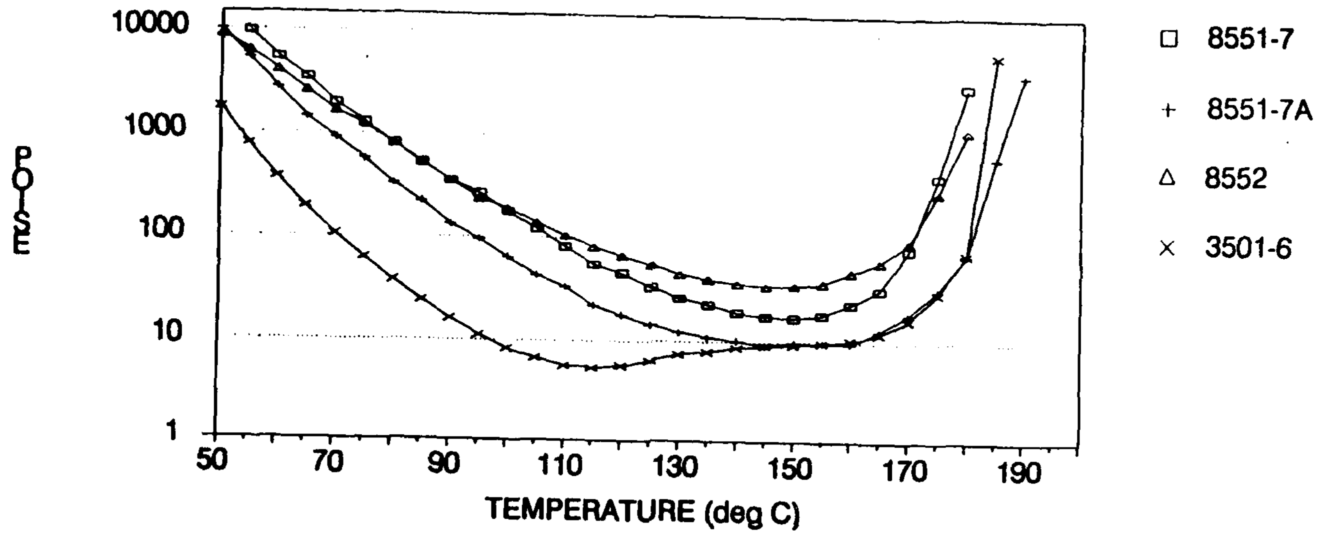

RESIN PROPERTIES	8551-7	8551-7A	8552	3501-6
MIN. VISCOSITY (POISE)	19	10	32	6
MIN. VISCOSITY TEMP (deg C)	149	143	145	115
DYNAMIC GEL TEMP (deg C)	178	187	179	185
FLOW NUMBER (MIN/POISE)	1.2	3.3	0.7	7.6
HEATING RATE (deg C/MIN)	1.75	1.56	1.87	1.71

HERCULES

MEP/bdm GDF-M.DRW

COMPOSITE APPLICATIONS ARE CHANGING
MILITARY TO COMMERCIAL AIRCRAFT
SPECIALITY TO COMMODITY
PERFORMANCE TO COST

- MATERIAL COST
  - SPECIALITY MATERIALS $10-$50/LB.
  - LOW VOLUME INGREDIENTS, 10^6 LBS/YEAR
  - MONOMER - TOXICITY COMPLIANCE COSTS
  - EXOTHERM HAZARD
  - SHELF LIFE LIMITATIONS
- PROCESSING COSTS
  - LONG CURE CYCLES
  - HAND LAYUP, NOT AUTOMATED
  - LARGER PART = LARGER AUTOCLAVES
  - REPAIR OR SCRAP
- PERFORMANCE LACKS
  - TOUGHNESS
  - OUTTIME FOR INCREASINGLY LARGE PARTS.
- LIFE TIME COSTS
  - REPAIR

TYPICAL MECHANICAL TEST CURE CYCLE

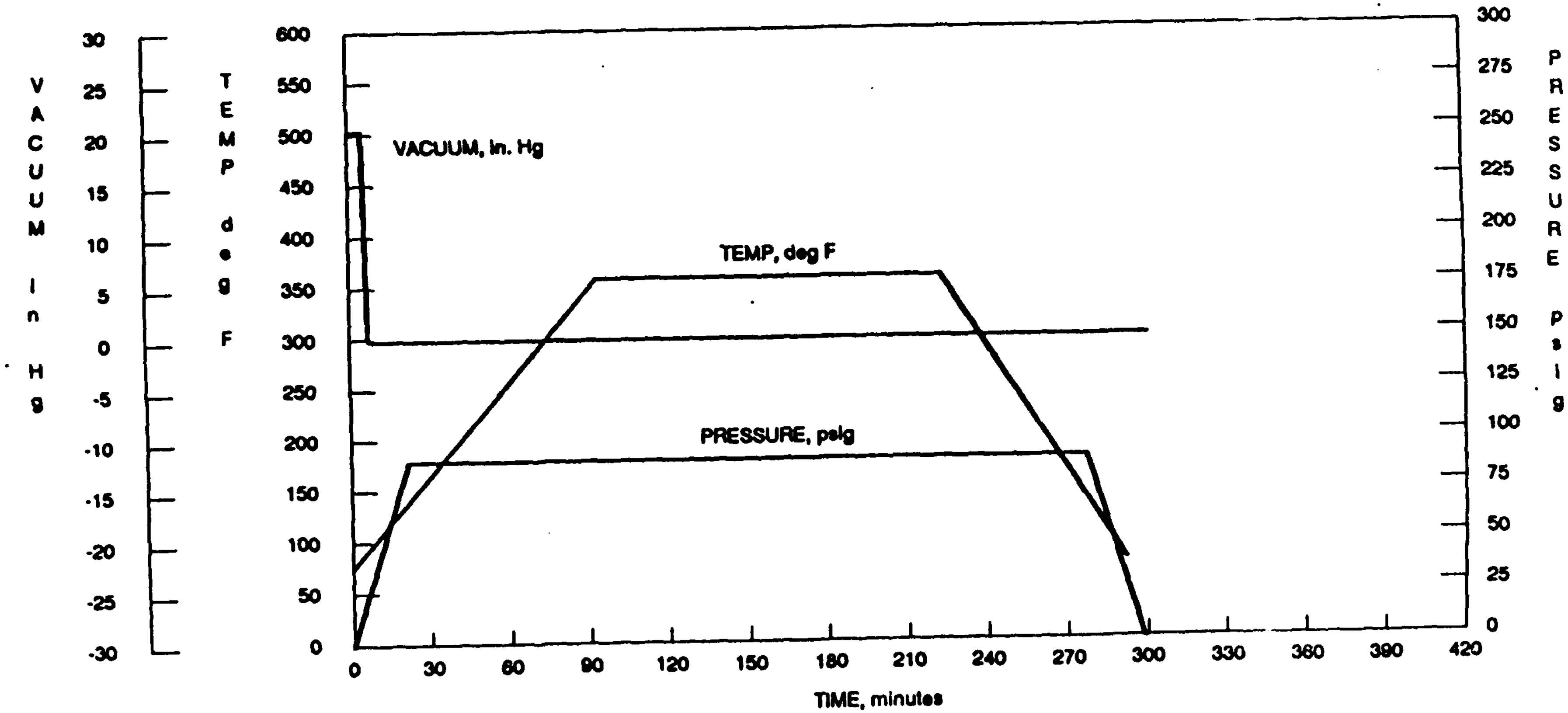

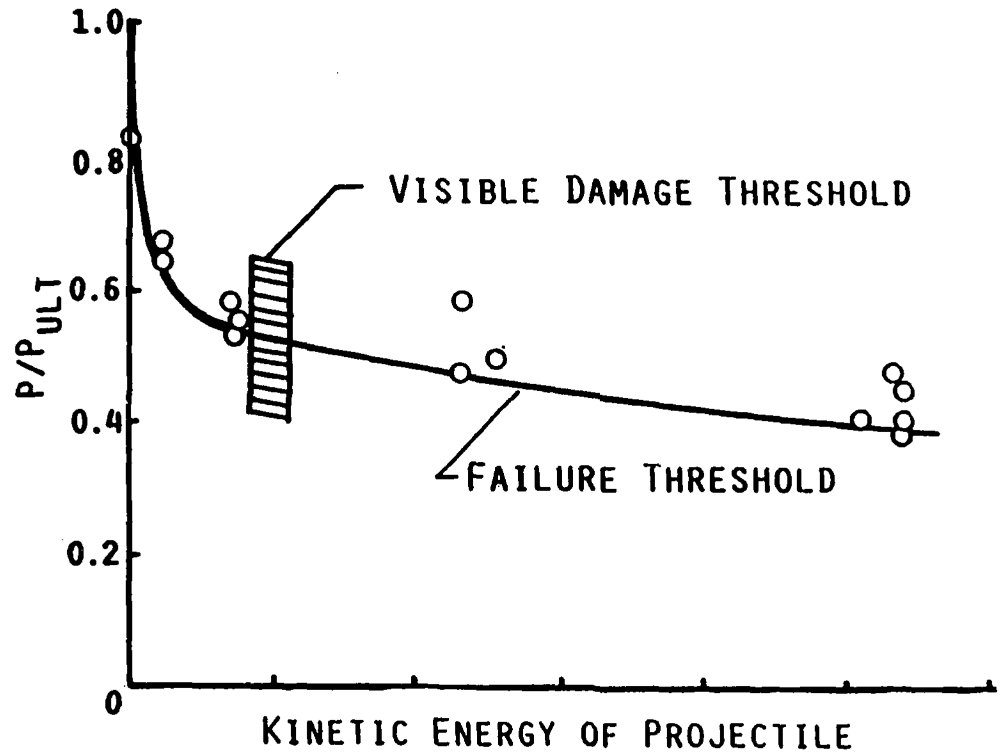
1.0
0.8
0.6
0.4
0.2
0
P/P_{ULT}
VISIBLE DAMAGE THRESHOLD
FAILURE THRESHOLD
KINETIC ENERGY OF PROJECTILE

THERMOPLASTICS HAVE POTENTIAL TO SOLVE DEFFICIENCIES

- HIGH NEAT RESIN TOUGHNESS
- FULLY POLYMERIZED
  - NO EXOTHERM
  - NO TOXICITY
  - NO 'CURE' TIME
- LOW COST MATERIALS (10^{10} LB/YEAR)
- AUTOMATABLE PROCESSES
- COMPACTION NOT POLYMERIZATION

THERMOSETS TODAY HAVE RESPONDED TO THREATS

- PRIMARY PERFORMANCE LACK HAS BEEN ADDRESSED.
- DAMAGE TOLERANCE AND RESISTANCE EQUAL TO THERMPLASTICS.

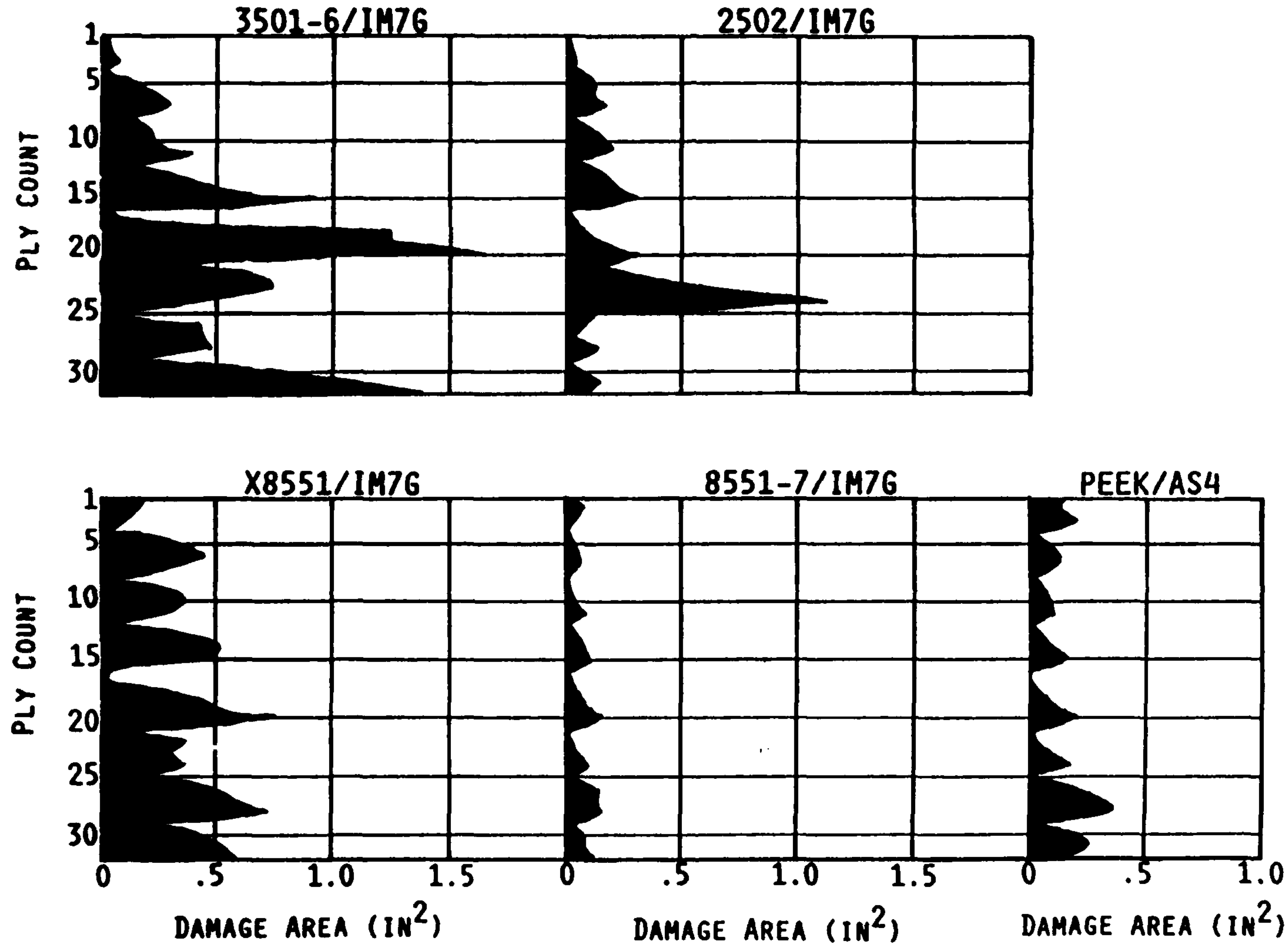

3501-6/IM7G
2502/IM7G
X8551/IM7G
8551-7/IM7G
PEEK/AS4
PLY COUNT
PLY COUNT
1
5
10
15
20
25
30
0
.5
1.0
1.5
DAMAGE AREA (IN2)
DAMAGE AREA (IN2)
DAMAGE AREA (IN2)

8551-7 CAI STRAIN BETTER THAN THERMOPLASTIC

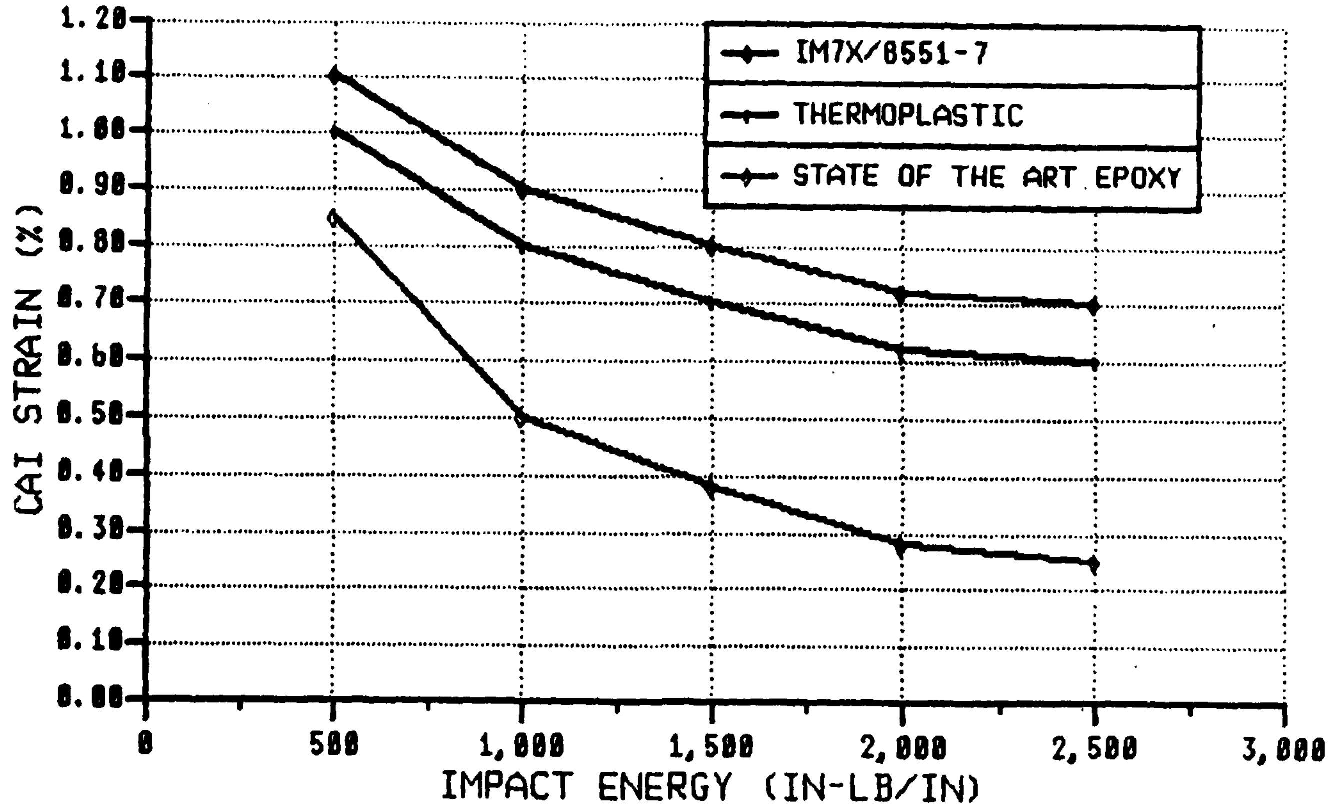

HERCULES

THERMOSETS TODAY AND IN THE FUTURE
WILL USE VARIOUS TOUGHENING TACTICS

- DISSOLVED THERMOPLASTICS
- REDUCED X-LINK DENSITY
- OLIGOMERS
- COMPOSITE TOUGHENING

FIGURE 1

8551-7/IM7XG COMPOSITE

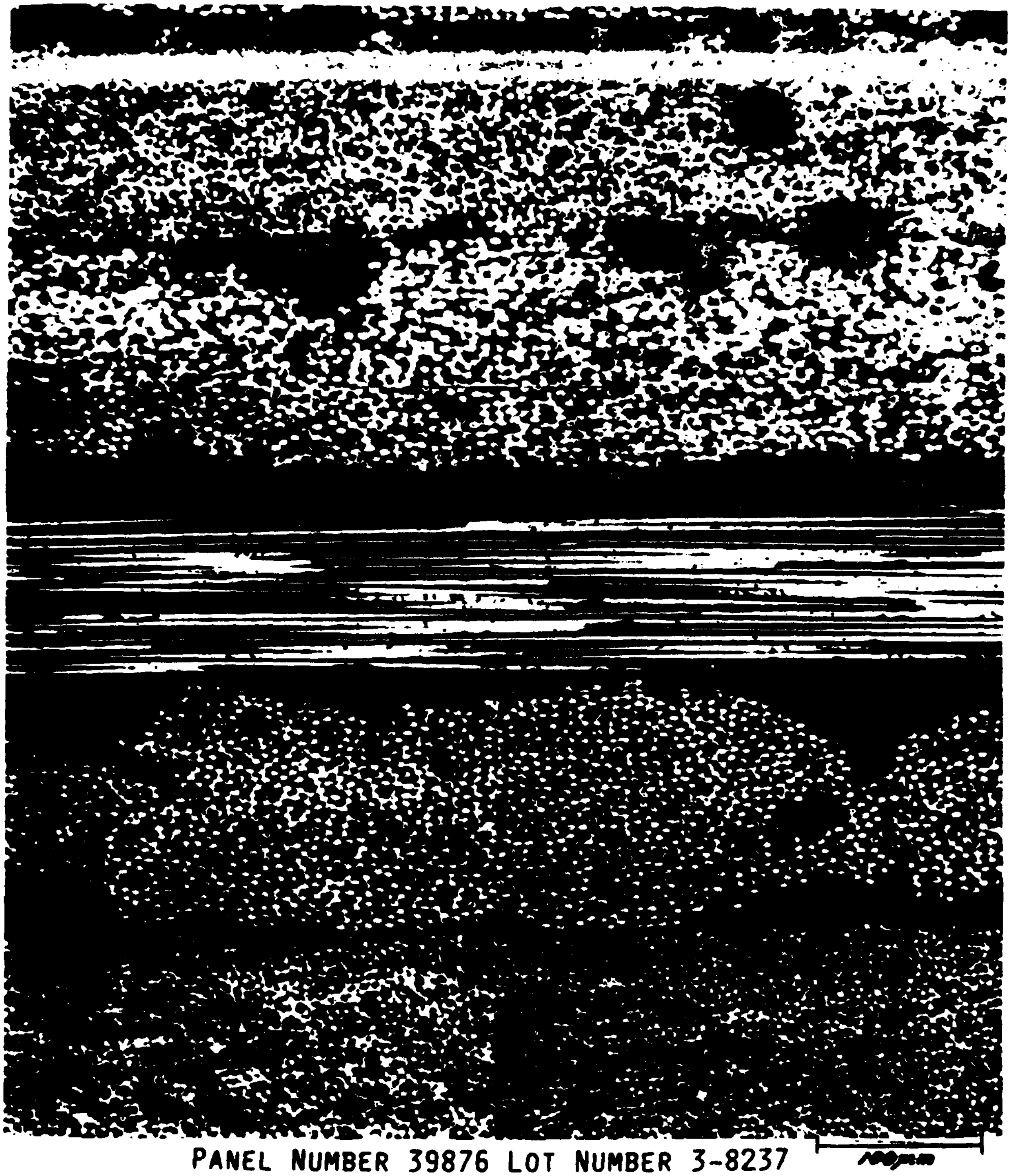

PANEL NUMBER 39876 LOT NUMBER 3-8237

52.2 KSI PIC

DECISIONS, DECISIONS
WHEN WILL THERMOSETS BE USED?

- ULTIMATE PROPERTIES, BALANCED PROPERTIES ARE REQUIRED.
  - COMPRESSION STRENGTH
  - INTERLAMINAR STRENGTH
  - SOLVENT RESISTANCE

- HIGHEST TEMPERATURES ARE NEEDED.
  - CURE TEMPERATURE = PERFORMANCE TEMPERATURE FOR THERMOSETS
  - PROCESS TEMPERATURE >> PERFORMANCE TEMPERAUTRE FOR THERMOPLASTICS

- OTHER PARTS OF THE SYSTEM ARE TEMPERATURE LIMITED
- SMALL PRODUCTIONS RUNS - HAND OPERATIONS
- NOT STOCK FORMS

- NEW FABRICATION TECHNIQUES SUCH AS RESIN TRANSFER AND INJECTION MOLDING
  - RAPID, EASY FIBER WETTING AND LOW PRESSURE MOLD FILLING
  - MIX TWO INERT INGREDIENTS, LONG OUTTIME
  - RAPID POLYMERIZATION CHEMISTRY FOR SHORT CYCLES

Fatigue Compression of OHC

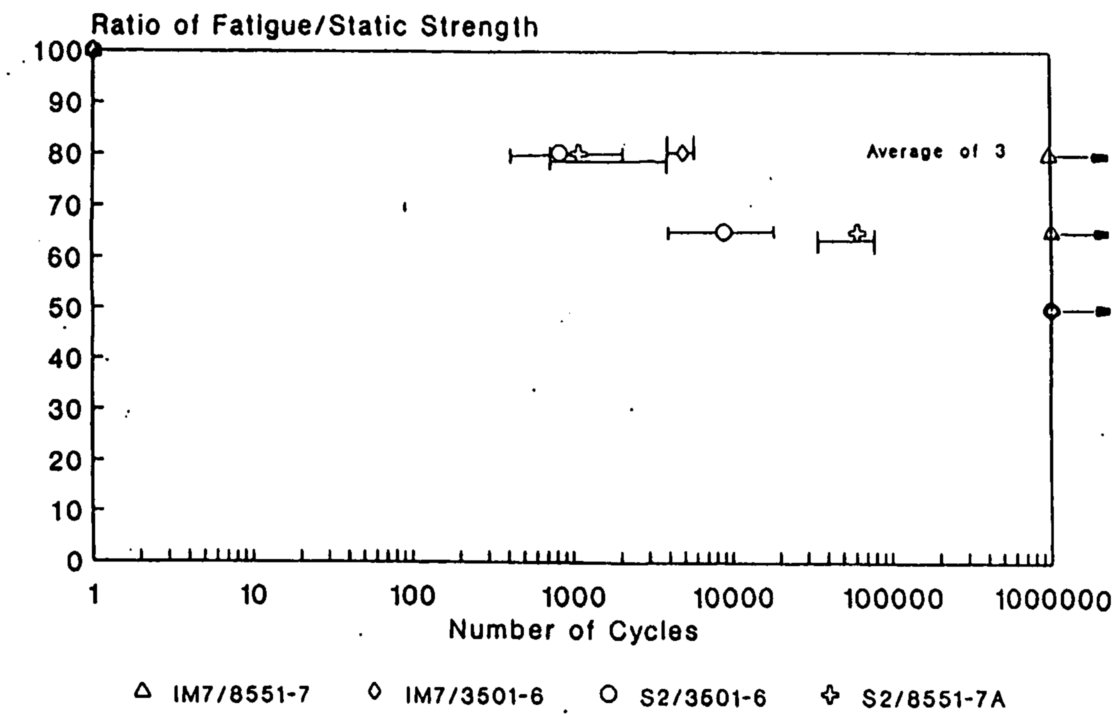

SESSION VI

INTELLIGENT STRUCTURES AND ACTIVE CONTROL

George Schneider
Sikorsky Aricraft Division, UTC
Chairman

Embedded Actuation and Processing in Intelligent Materials

Edward F. Crawley
Kenneth B. Lazarus
David J. Warkentin

Space Engineering Research Center
Department of Aeronautics and Astronautics
Massachusetts Institute of Technology

Abstract

This presentation describes some of the work recently performed at the Space Engineering Research Center in an area which has come to be known as intelligent materials, i.e., materials integrated with highly distributed actuators, sensors, and processing networks. In this work, models are derived of the *actuation of composite* structures by generic induced strain mechanisms, and the predicted bending and twisting of plates thus achieved is compared to experimental results using piezoceramics bonded to graphite/epoxy laminates. Some fundamental criteria for the selection of an induced strain actuator are discussed, followed by the presentation of a manufacturing technique for embedding piezoceramic actuators within the composite structures. Finally, similar work involving the embedding of electronic devices (eventually to include microprocessors) is presented.

Embedded Actuation and Processing in Intelligent Composite Materials

Edward F. Crawley
Kenneth B. Lazarus
David J. Warkentin

M.I.T.

September 1989

Intelligent Materials

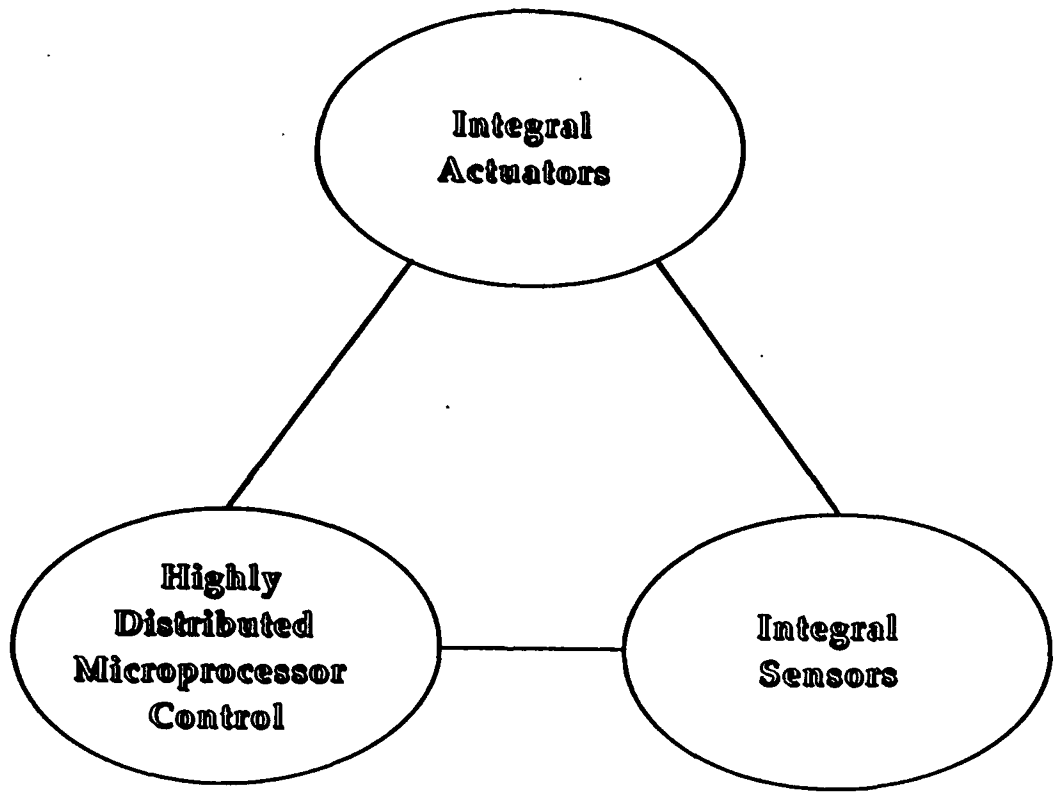

Plus - Modeling and Analysis Techniques

Outline

- Models of induced strain actuation
- Bending and twisting of plates
- Selection of induced strain actuator
- Embedding of actuators
- Embedding of microelectronic devices

INDUCED STRAIN ACTUATION SYSTEM

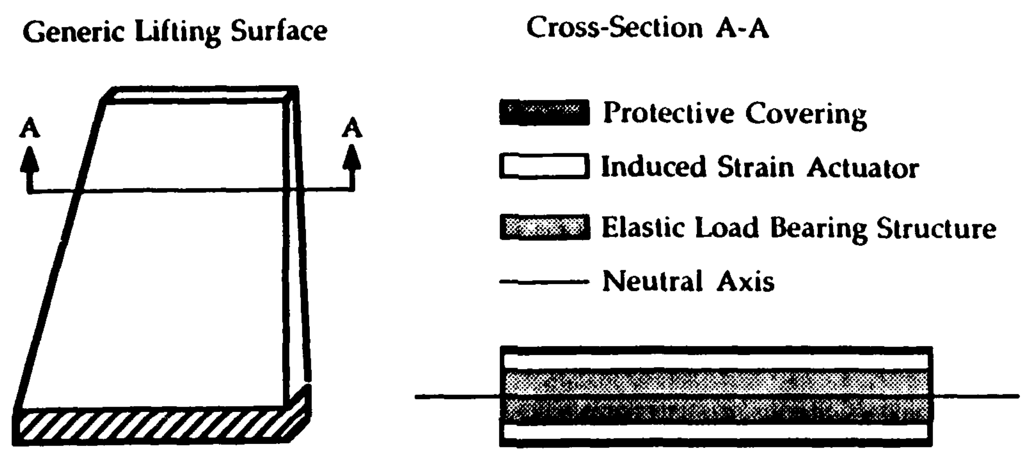

- **Applications**
  - Shape control of aeroelastic structures
  - Reflector or mirror contour control
  - Pointing of precision instruments
  - Acoustical control of structure borne noise

CONSISTENT PLATE MODEL

- **Actuators and Substrates are Integrated as Plies of a Laminate Plate**
- **Consistent Deformations Assumed in the Actuators and Substrates**
- **Thin Classical Laminated Plate Theory Assumptions Made**
- **Strain-Displacement Relation**

$$\varepsilon = \varepsilon^{o} + z\kappa$$

- **Stress-Strain**

$$\sigma = Q\,(\varepsilon - \Lambda)$$

where Λ is the actuation strain $\Lambda = [\,\Lambda_x \;\; \Lambda_y \;\; \Lambda_{xy}\,]^T$

CONSISTENT PLATE MODEL

- **Governing Force and Moment Equations**

$$\begin{bmatrix} \bar{\mathbf{N}} \\ \bar{\mathbf{M}} \end{bmatrix} = \begin{bmatrix} \mathbf{A} & \mathbf{B} \\ \mathbf{B} & \mathbf{D} \end{bmatrix} \begin{bmatrix} \varepsilon^o \\ \kappa \end{bmatrix} - \begin{bmatrix} \mathbf{N}_\Lambda \\ \mathbf{M}_\Lambda \end{bmatrix}$$

$$\bar{\mathbf{N}} = \int_t \sigma \, dz \qquad \bar{\mathbf{M}} = \int_t \sigma z \, dz$$

$$\mathbf{N}_\Lambda = \int_t \mathbf{Q} \Lambda \, dz \qquad \mathbf{M}_\Lambda = \int_t \mathbf{Q} \Lambda z \, dz$$

  - Integrate only through actuator plies for $\mathbf{N}_\Lambda$ and $\mathbf{M}_\Lambda$
  - Numerous coupling terms provide for a variety of deformations

- **Alternative Formulation Using the Plate Strain Energy**

$$U = \frac{1}{2} \iint_A \{\varepsilon^{oT} \ \kappa^T\} \begin{bmatrix} \mathbf{A} & \mathbf{B} \\ \mathbf{B} & \mathbf{D} \end{bmatrix} \begin{Bmatrix} \varepsilon^o \\ \kappa \end{Bmatrix} d\,(A) - \iint_A [\mathbf{N}_\Lambda \ \mathbf{M}_\Lambda] \begin{Bmatrix} \varepsilon^o \\ \kappa \end{Bmatrix} d\,(A)$$

EXACT SOLUTIONS

- **For Symmetric Actuation of Isotropic Substrates with Free-Free Boundary Conditions, No Externally Applied Loads, and Linear Isotropic Actuation Strain**

$$\varepsilon = \frac{\alpha_1}{\alpha_1 + \psi}\begin{bmatrix} 1 & 0 & 0 \\ 0 & 1 & 0 \\ 0 & 0 & 1 \end{bmatrix}\Lambda \qquad \kappa = \frac{2}{t_s}\left[\frac{1}{T} + 1\right]\frac{\alpha_2}{\alpha_2 K + \psi}\begin{bmatrix} 1 & 0 & 0 \\ 0 & 1 & 0 \\ 0 & 0 & 1 \end{bmatrix}\Lambda$$

$$T = \frac{t_s}{t_a} \qquad K = \frac{4}{3}\left(\frac{1}{T}\right)^2 + 2\left(\frac{1}{T}\right) + 1 \qquad \psi = \frac{E_s t_s}{E_a t_a} \qquad \Lambda = [\Lambda \ \Lambda \ 0]^T$$

- **Magnitude of Induced Strain and Curvature Depends On**
  - The actuation strain
  - The relative stiffness ratio
  - The actuator/substrate geometry
- **Equations Uncouple and Poisson's Ratio Not Present**

RITZ SOLUTION FOR TWIST CURVATURE OF ANISOTROPIC PLATES

- **Choose Minimum Set of Modes**
  - Extension
  - Bending
  - Twist

- **In General, Can Not Actuatate κ_{xy} Directly, Since $\Lambda_{xy} = 0$**

- **Twist for a Plate with Bending/Twist Coupling**

$$\kappa_{xy} = -\frac{1}{2}\left[\frac{D_{16}}{D_{11}D_{66} - D_{16}^2}\right](M_\Lambda)_x \qquad \psi_D = \frac{D_{16}}{\sqrt{D_{11}D_{66}}}$$

- **Twist for a Plate with Extension/Twist Coupling**

$$\kappa_{xy} = \frac{1}{2}\left[\frac{B_{16}}{A_{11}D_{66} - B_{16}^2}\right](N_\Lambda)_x \qquad \psi_B = \frac{B_{16}}{\sqrt{A_{11}D_{66}}}$$

EXPERIMENTATION: PLATE ARTICLES

- **Objective: To Verify the Consistent Plate Model for Systems with External Loads and More Complicated Boundary Conditions and to Verify the Accuracy of the Ritz Solution**

- **Plate construction**

Aluminum:	Bench mark specimen	
G/E $[0/\pm45]_s$:	Increased transverse bending	ψ_D=0.06
G/E $[30_2/0]_s$:	Bending/twist coupling	ψ_D=0.31
G/E $[+45_3/-45_3]$:	Extension/twist coupling	ψ_B=0.36

- **Testing**
  - Cantilever boundary condition
  - Deflections measured at 3 three transverse positions

$$W_1 = \frac{M_2}{C} \qquad W_2 = \left[\frac{M_3 - M_1}{C}\right] \qquad W_3 = \frac{M_2 - \left[\dfrac{M_3 + M_1}{2}\right]}{C}$$

EXPERIMENTATION: PLATE ARTICLES

- **Cantilever Plate Configuration: Actuators Cover 71% of Plate**

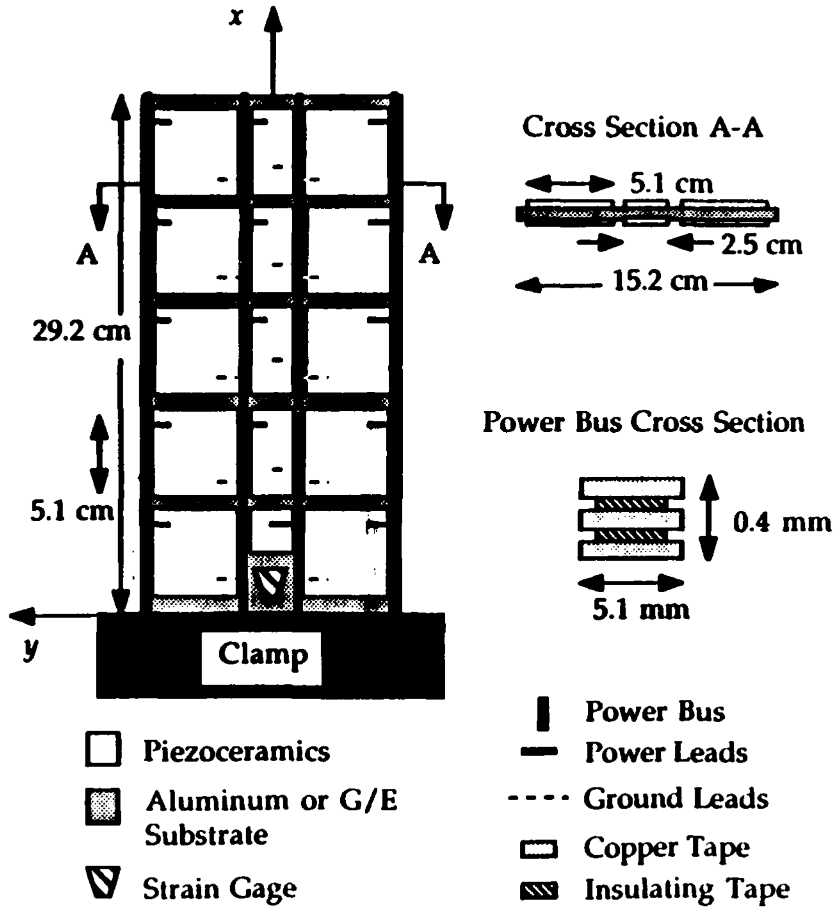

EXPERIMENTATION: PLATE ARTICLES

- **Cantilever Plate Mode Shapes**

Mode Number	Deflection	Shape Function $\phi(x)$	$\phi(y)$
In-Plane Modes			
1	longitudinal extension	x/L	1
2	longitudinal shear	x/L	y/C
3	transverse extension	1	y/C
4	transverse shear	x/L	1
Out-Of-Plane Modes			
5	longitudinal bending	$(x/L)^2$	1
6	twist	x/L	y/C
7	transverse bending	x/L	$(y/C)^2$

EXPERIMENTATION: PLATE ARTICLES

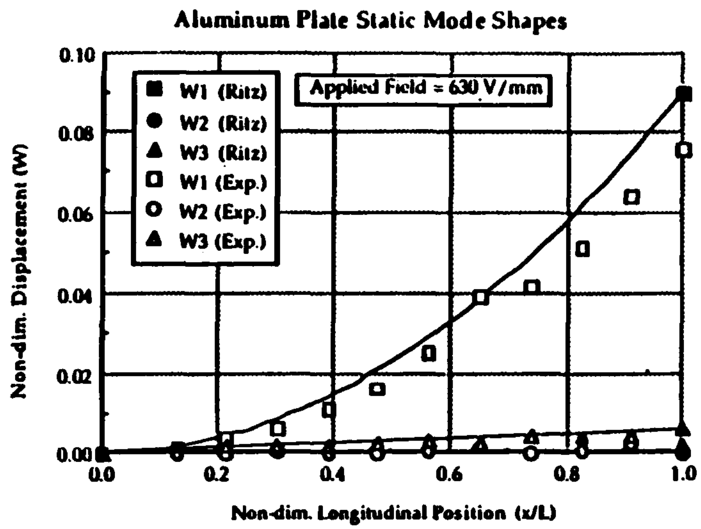

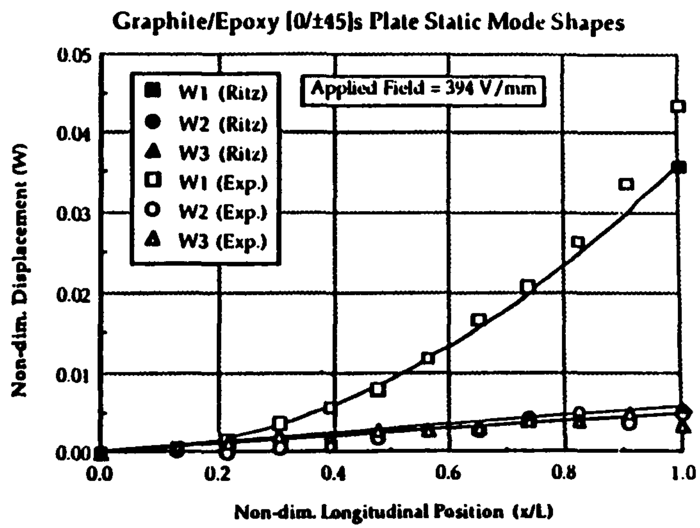

- Quadratic Longitudinal Bending
- Transverse Bending Deflection Drops Off at the Tip
- Longitudinal Bending Greater Than Transverse Bending

EXPERIMENTATION: PLATE ARTICLES

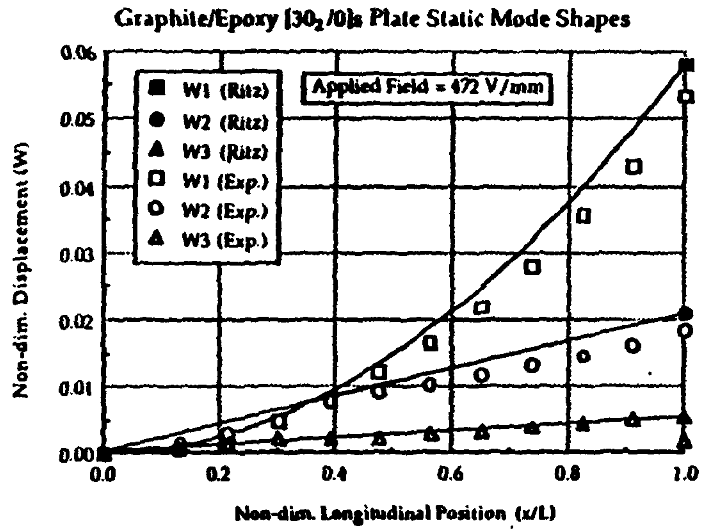

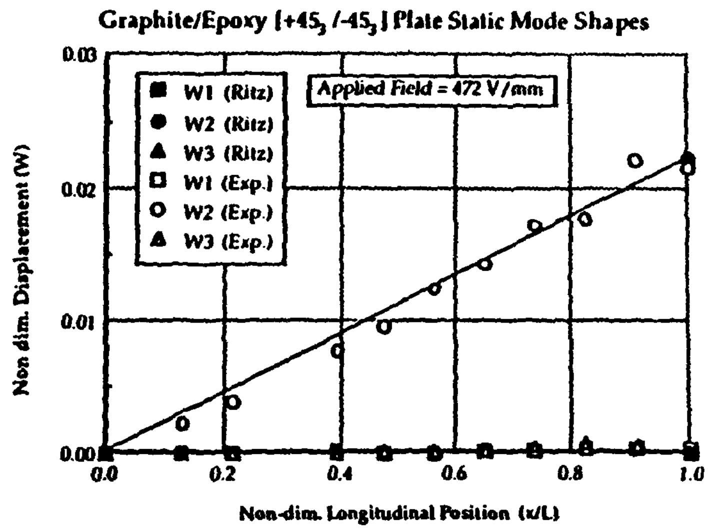

- **Twist Distribution Nearly Linear**
- **Good Agreement with Assumed Modes**

WIND TUNNEL TESTING

- G/E $[30_2/0]_s$ Plate: $\frac{\partial C_l}{\partial \alpha} = 5 \qquad \alpha_0 = 0$

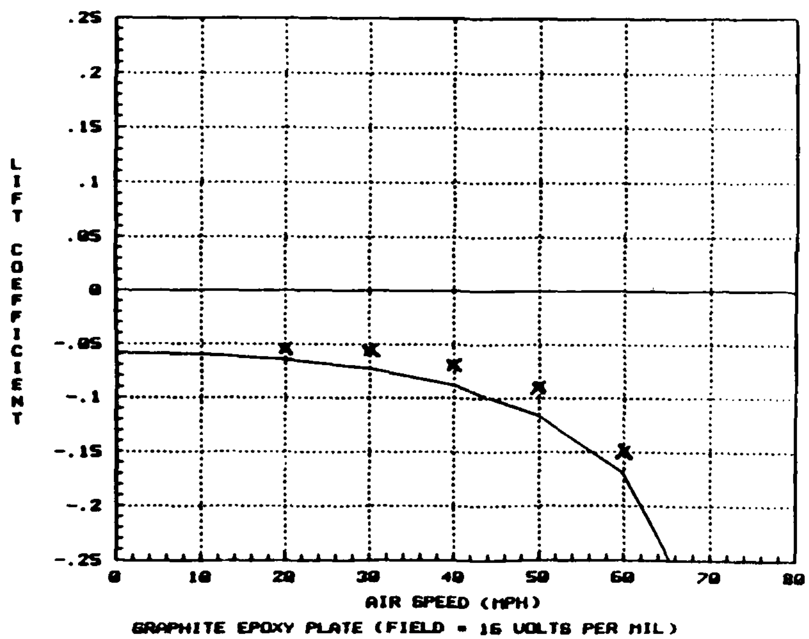

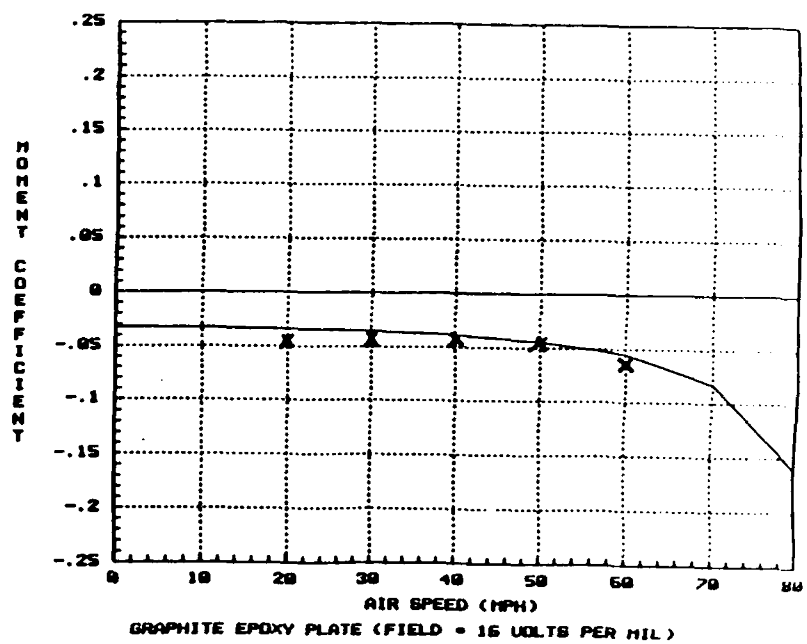

CONCLUSIONS

- **Analytical Models of Induced Strain Actuation Developed for Systems with Arbitrary Stiffness Coupling, Boundary Conditions, and Externally Applied Forces**

- **Design Parameters Obtained for Particular Desired Deformations**

- **The Analytic Model was found to Correlate Well with Experimental Results**

- **Significant Deflections were Obtained**
  - Longitudinal bending deflections over 15 times the plate thickness (one-sided, 67% of $\mathcal{E}_{max}$)
  - Camber change of 0.5% (one-sided, 50% of $\mathcal{E}_{max}$)
  - Tip twist of 1.8 degrees (one-sided, 67% of $\mathcal{E}_{max}$)
  - Lift coefficient of 0.16 (peak-to-peak, 67% of $\mathcal{E}_{max}$)

Characterization of Piezoceramic Actuation Strain

- Actuation strain may be a result of:
  - temperature
  - moisture
  - piezoelectricity
  - electrostriction
  - magnetostriction
  - shape memory

- Linear Piezoelectric Constitutive Relations
  - One-dimensional piezoelectric actuation strain

$$\varepsilon = \frac{\sigma}{E} + \Lambda$$

$$\Lambda = d_{31}\mathcal{E}_3$$

Manufacturing: Selection Criteria

- Piezoelectrics are available in ceramic or polymer form.
- Large variation in modulus, Curie temperature, maximum field.
- Effectiveness of piezoelectric (in bending):

$$E_{max}\, d_{31} \left(\frac{6}{6 + \frac{E_b t_b}{E_c t_c}} \right)$$

  - large E_{max}
  - large d_{31}
  - large stiffness compared to substructure
- If voltage available is limited, must examine effectiveness/field.
- For embedding, Curie temperature must be higher than cure temperature of composite.
- Piezoelectric must be available in sizes comparable to composite plies.

Comparison of Piezoelectric Materials

	PZT G-1195	PZT HST-41	PZT G-1278	PVDF	
Curie Temperature (°C)	360	270	190	100	
E_{max} (kV/m)	600	600	600	40000	
d_{31} (pm/V)	190	157	250	23	
E_c (GPa)	63	70	60	3	
Effectiveness ($\times 10^{-6}$)	40	34	50	21	(typical
Effect./Field (pm/V)	67	56	83	.553	case)

- Ceramics offer a wider operating temperature range, higher effectiveness, and a higher effectiveness per field.
- Film is applied easily to complex surfaces.
- G-1195 is best choice for embedding inside composites.

Manufacturing: Procedure

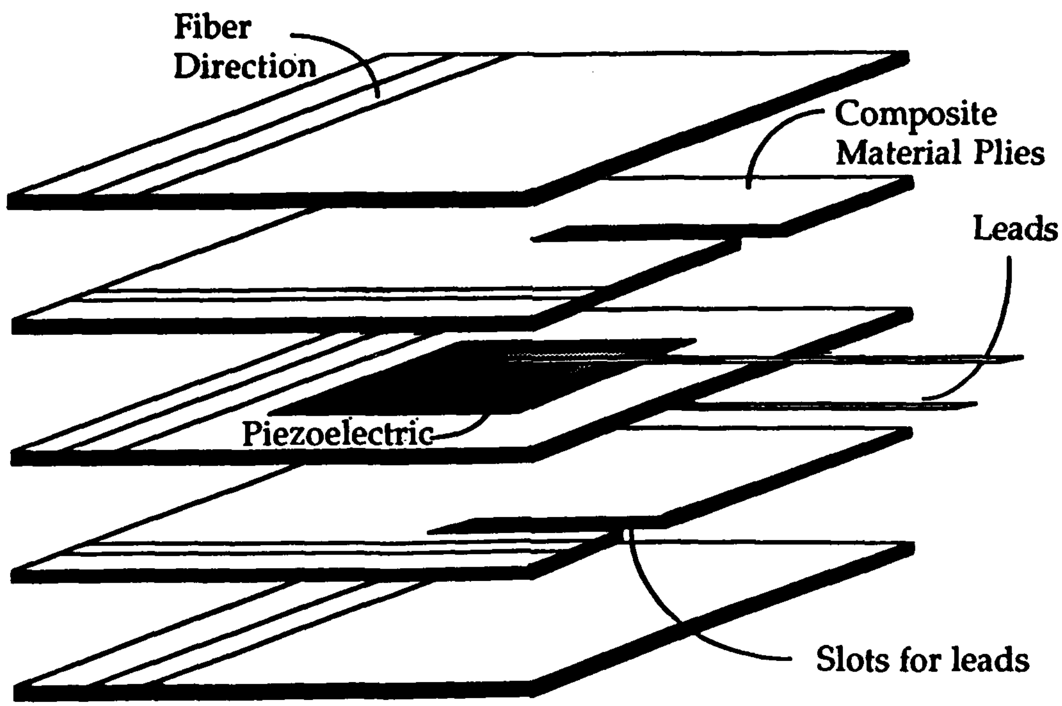

- Hole and slots for piezoelectric and leads are cut out of composite plies.
- Thickness of laminate remains approximately constant.

Manufacturing: Insulation

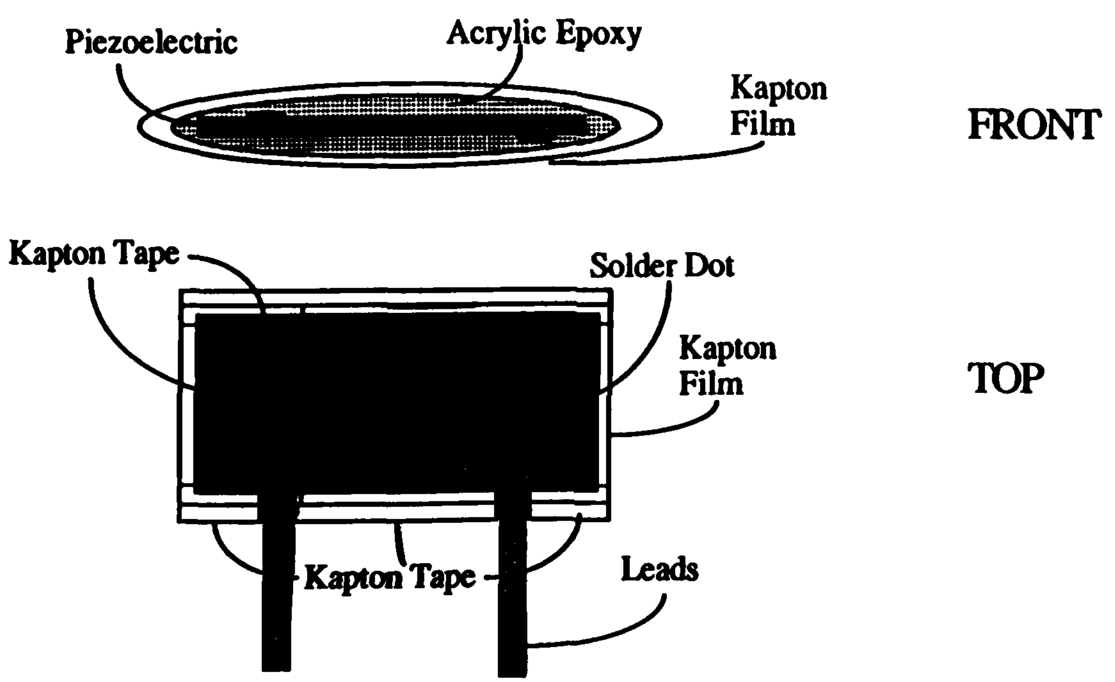

- Piezoelectrics cannot be inserted directly into graphite/epoxy without electrically shorting the actuator.
- Problem: how to embed the piezoelectrics while maintaining a hard bond between the actuator and the surrounding composite?

Distributed Processing

Motivation for Distributed Processing

- Alleviates processing burden for systems with large numbers of sensors and actuators
- Lowers operating speed of global processor by relegating high bandwidth control to local processors
- Simplifies communications links among sensors, actuators, and controllers

Issues in Implementation

- Balance packaging and hardening vs. access and lifetime
- Find most effective distribution of processing and signal conditioning

Examination of Electrical and Mechanical Compatibility

Issues:

- Temperature – Autoclave, operating
- Pressure – Isostatic autoclave pressure
- Operational mechanical stress – brittle Si, delicate SiO_2 and metal structures
- Ionic contamination – device lifetime is primarily limited by corrosion
- Electrical insulation from graphite fibers
- Minimal disruption of structural plies

Technique for Embedding Devices

- Tape Automated Bonding (TAB) connects the chip to flat copper conductors on polyimide film which leads to other similarly attached devices, thus providing a minimum-volume interconnect

- Plies are cut to make room for interconnect and chips

- Before layup, chip is coated with a electronics-grade epoxy which will cure during the autoclave cycle

- The chip epoxy must be chosen for chemical purity and for its compliance so that the chip is sufficiently protected from the structure

- Silicone gel might be used as an alternative to epoxy for mechanical strain relief

Technique for Embedding Devices

TAB bonding:

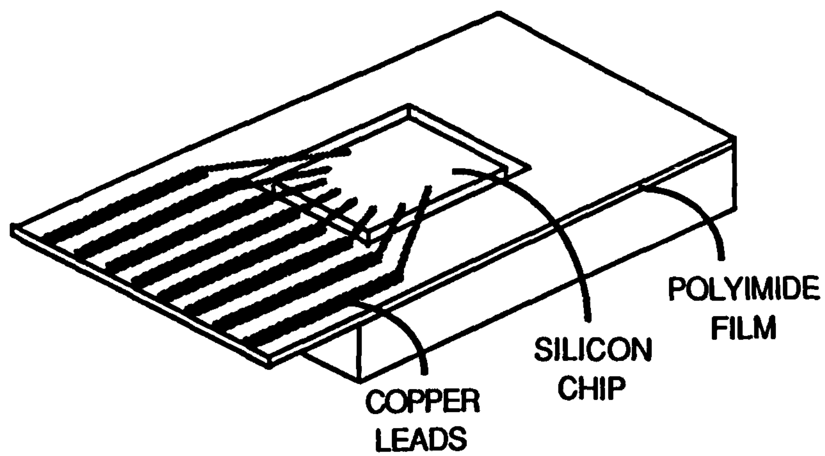

Tests of Embedded Silicon Devices

- Temperature - Humidity - Bias

  Electrical operation at 85°C, 85% rel. hum. to provoke corrosion failures

- Temperature Cycling

  Thermal stress induced by CTE mismatch to cause immediate and fatigue failure of lead connections

- Static Mechanical Loading

  4-point bending test of load transfer to lead connections and silicon substrate

- Cyclic Mechanical Loading

  Piezoelectric excitation at first cantilever beam mode for fatigue testing

DYNAMICALLY-TUNABLE SMART COMPOSITES FEATURING ELECTRO-RHEOLOGICAL FLUIDS

Mukesh V. Gandhi and Brian S. Thompson
Intelligent Materials and Structures Laboratory
Composite Materials and Structures Center
Michigan State University
East Lansing, MI 48824

Photomicrograph of ER-Fluid with 0 kV/mm Field Strength

Photomicrograph of ER-Fluid with 2 kV/mm Field Strength

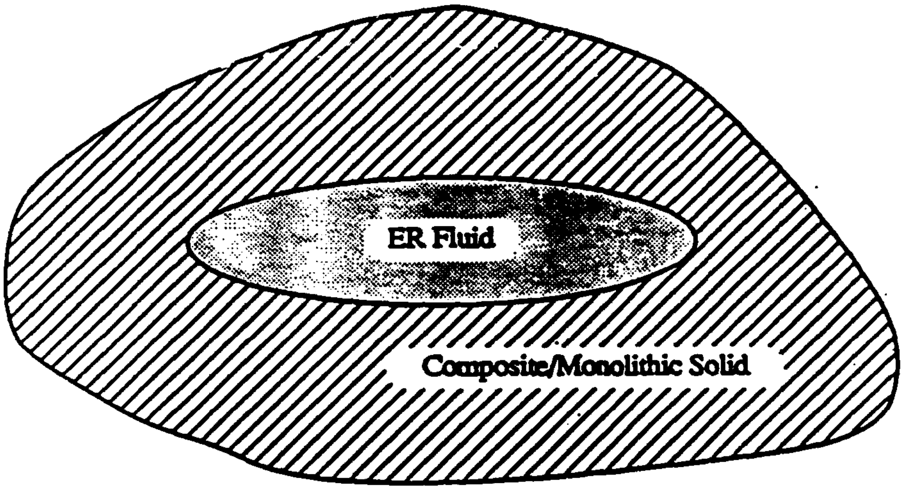

ER Fluids
Fluid 1
Fluid 2
Fluid 3

Structural Materials
Aluminum Alloys
Carbon Steels
Magnesium Alloys
Graphite/Epoxy Materials
Glass/Epoxy Materials
Hybrid Composite Materials

ER-based Smart Structure

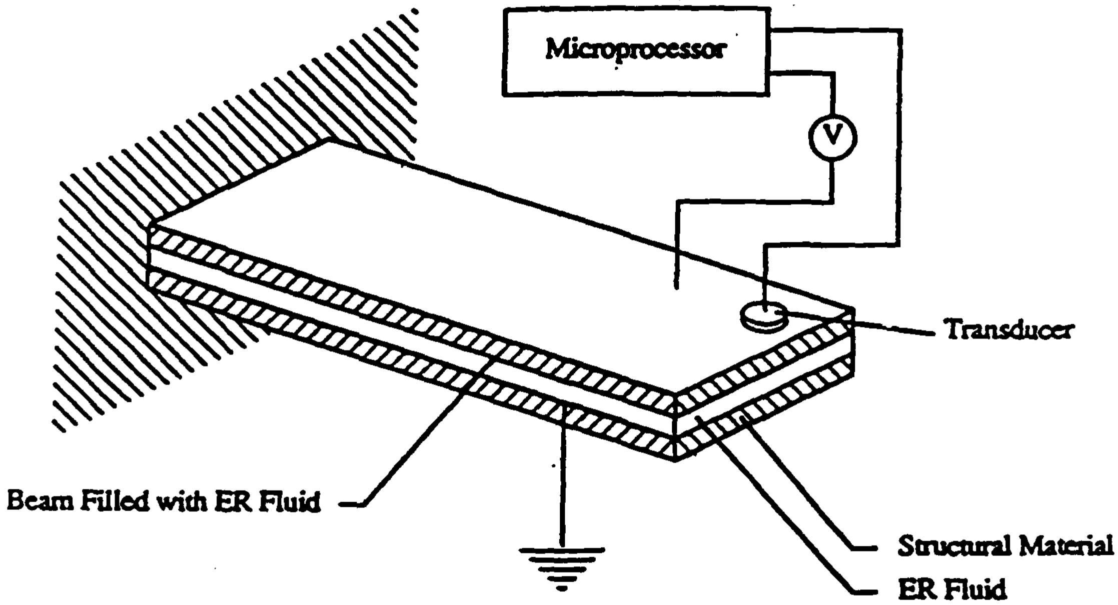

Ability of Smart ER-based Beams to Dramatically Change their Vibration Characteristics: Schematic of the Beam

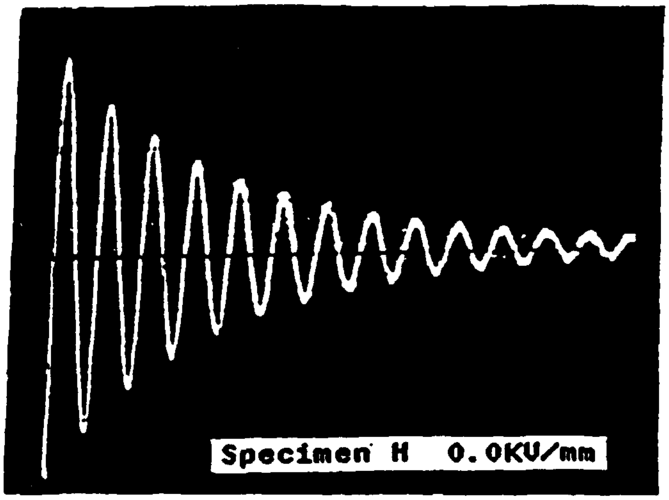

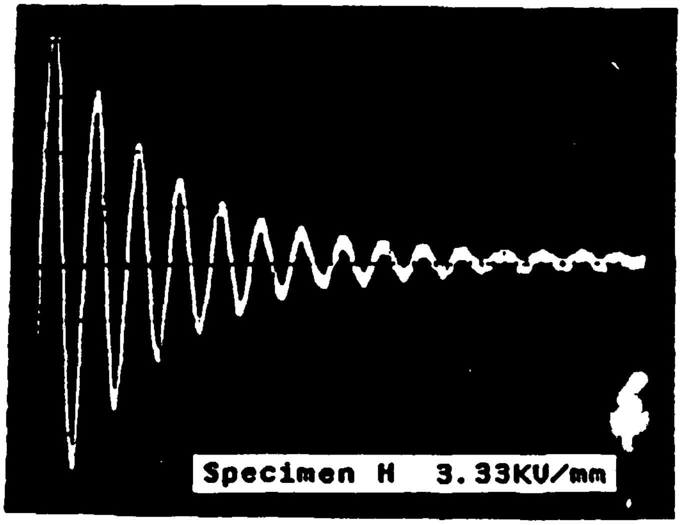

Ability of Smart ER-based Beams to Dramatically
Change their Vibration Characteristics:
Experimental Results

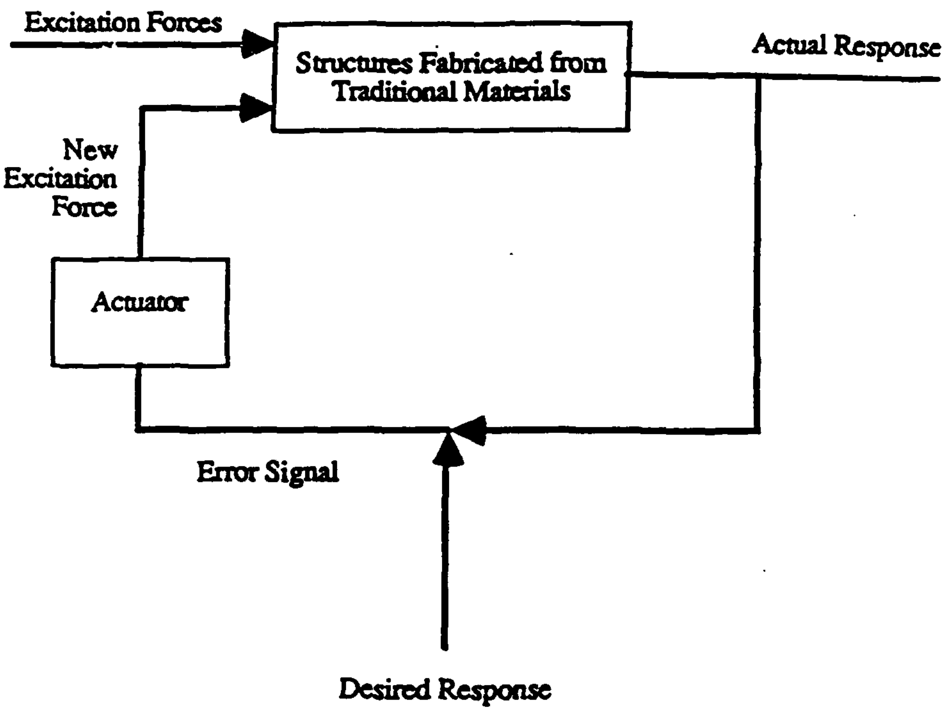

Traditional Control Strategies

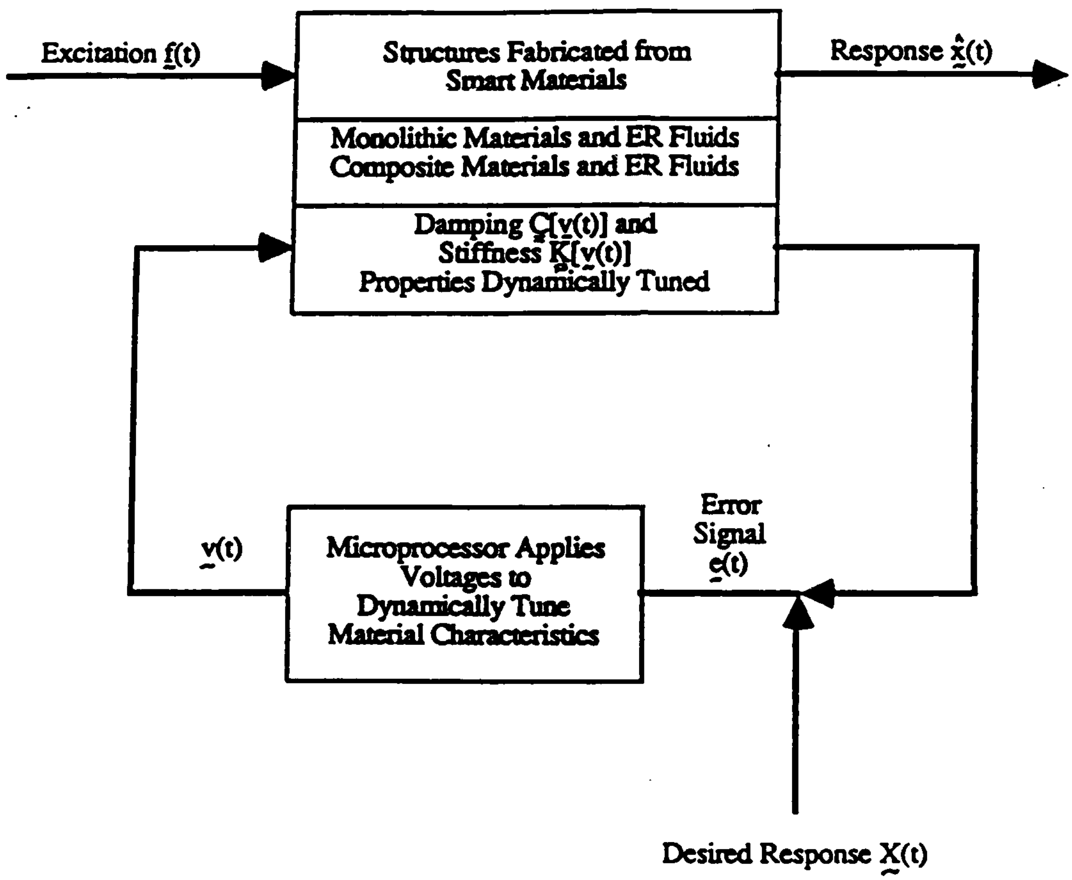

Control Strategies For Smart Materials And Structures

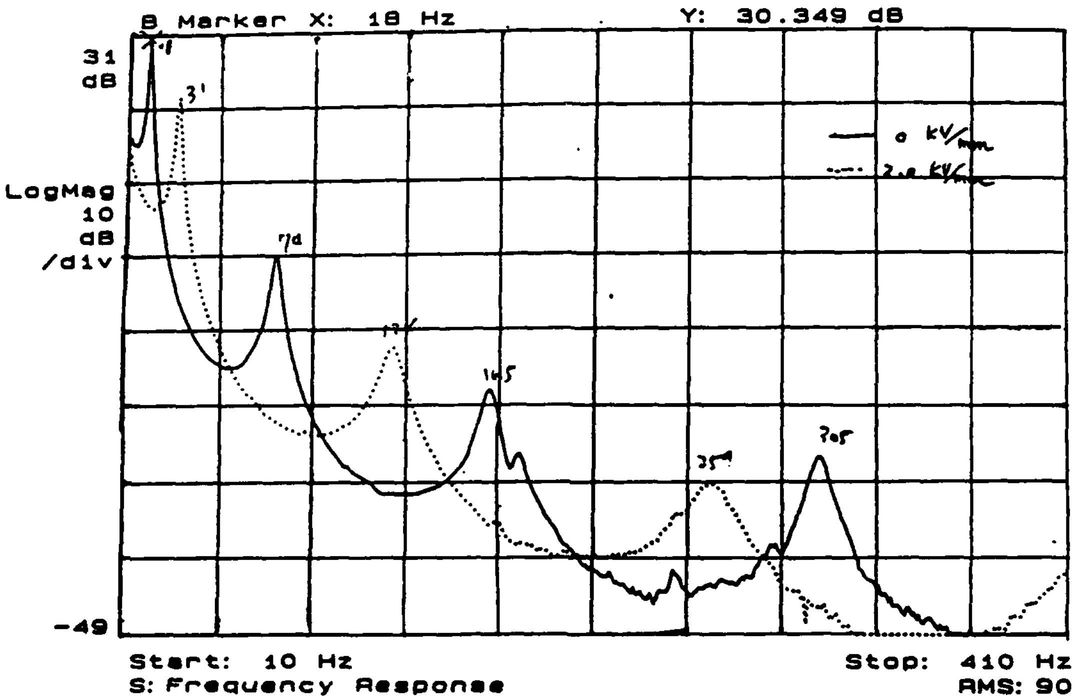

Unique Capability of ER-based Smart Beams to Dramatically Change Their Natural Frequencies and Damping Characteristics in Real-time

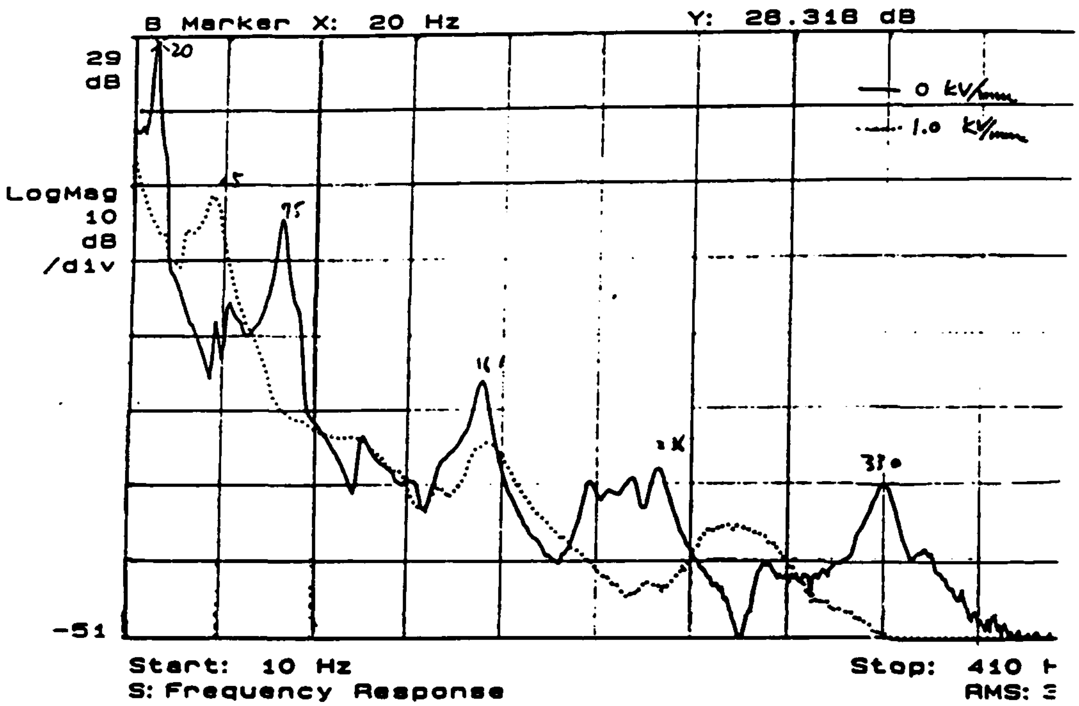

Unique Capability of ER-based Smart Plates to Dramatically Change their Natural Frequencies and Damping Characteristics in Real-time

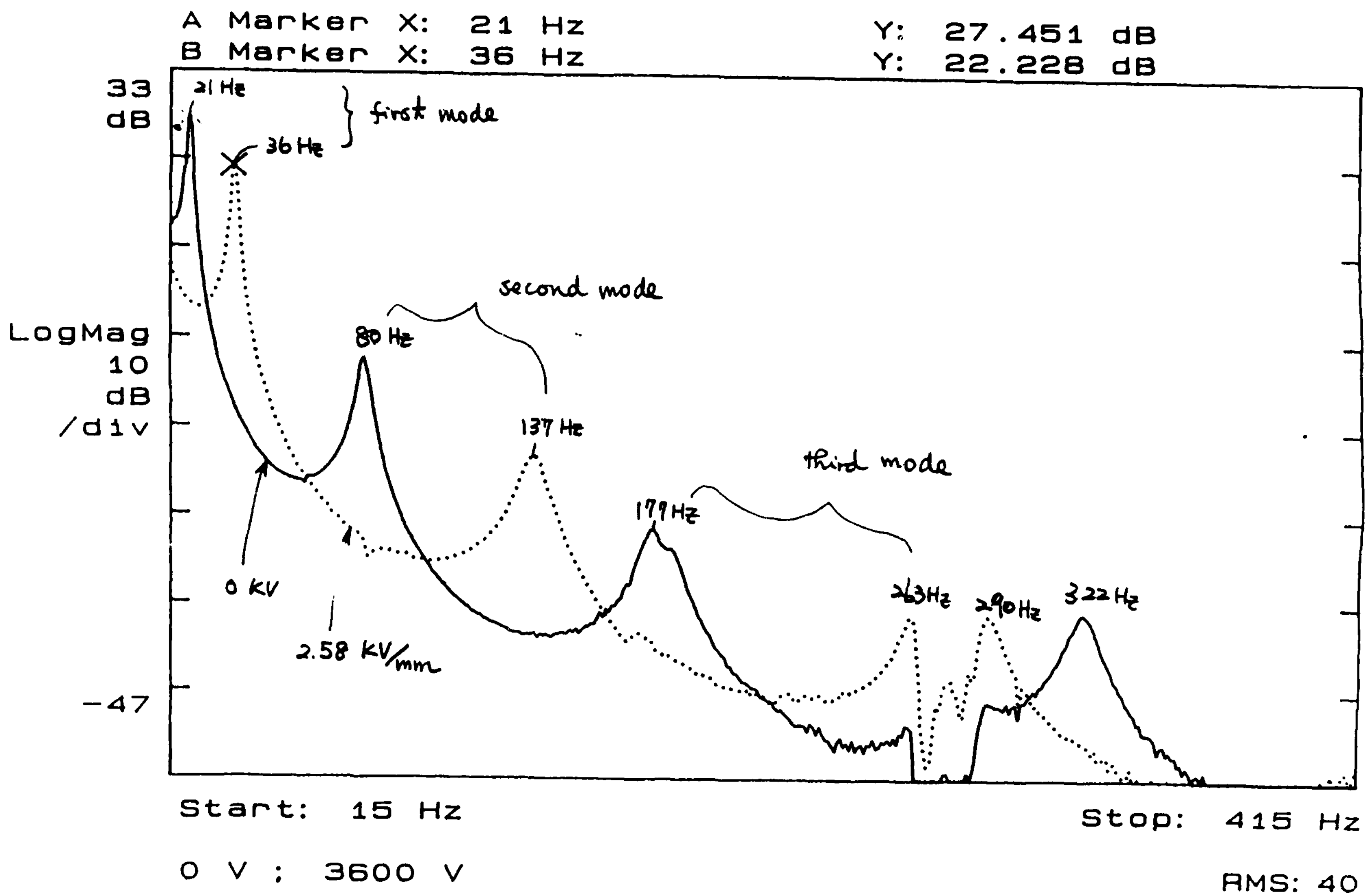

A Marker X: 21 Hz
B Marker X: 36 Hz
Y: 27.451 dB
Y: 22.228 dB
33
dB
LogMag
10
dB
/div
-47
21 Hz
36 Hz
first mode
80 Hz
second mode
137 Hz
179 Hz
third mode
263 Hz
290 Hz
322 Hz
0 KV
2.58 KV/mm
Start: 15 Hz
Stop: 415 Hz
0 V ; 3600 V
RMS: 40

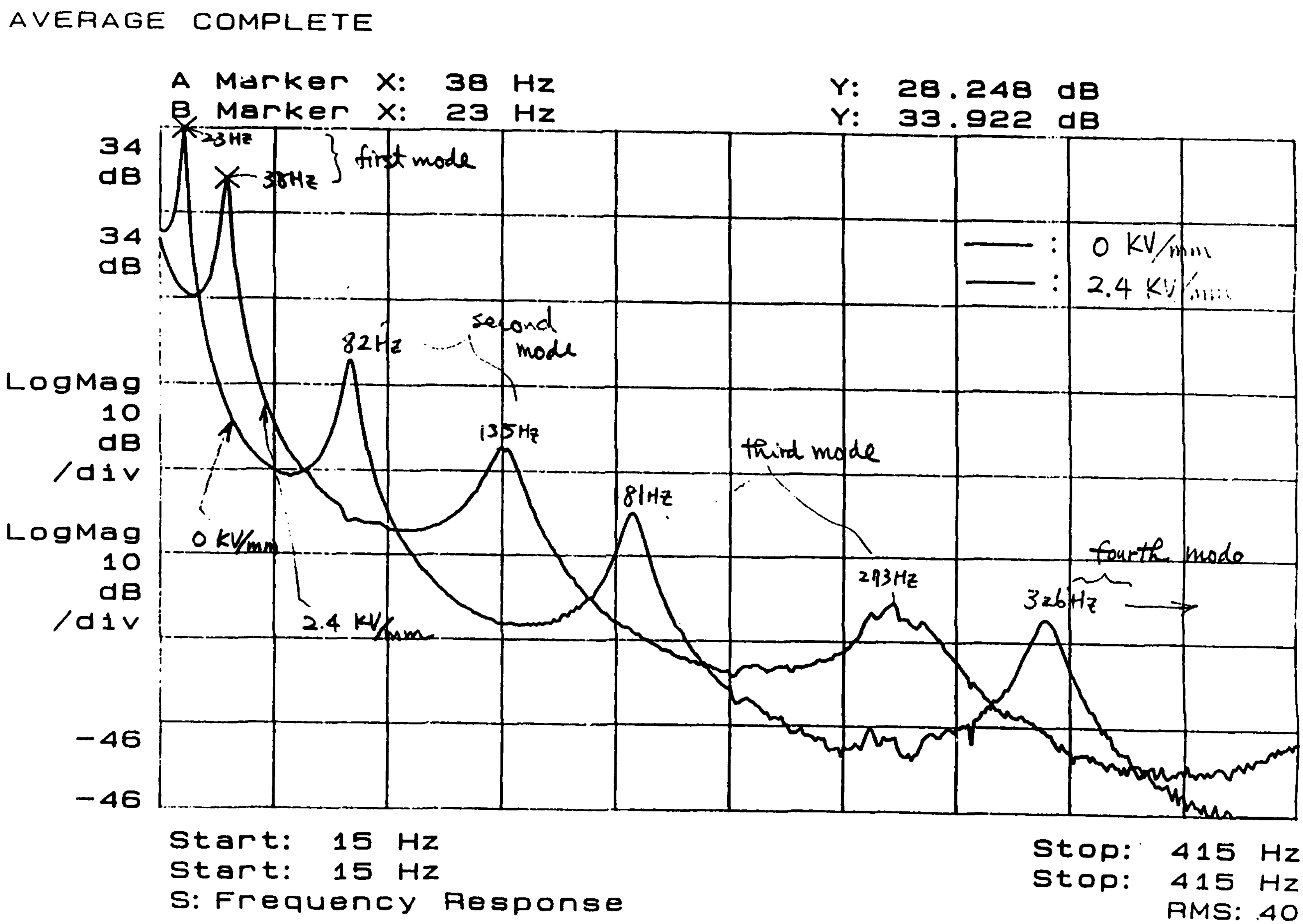
AVERAGE COMPLETE
A Marker X: 38 Hz Y: 28.248 dB
B Marker X: 23 Hz Y: 33.922 dB
34 dB
34 dB
LogMag 10 dB /div
LogMag 10 dB /div
-46
-46
23Hz
38Hz
first mode
82Hz
second mode
135Hz
81Hz
third mode
293Hz
326Hz
fourth mode
0 KV/mm
2.4 KV/mm
Start: 15 Hz
Start: 15 Hz
S: Frequency Response
Stop: 415 Hz
Stop: 415 Hz
RMS: 40

A typical representation for a BKZ-type constitutive model for describing the properties of field-dependent ER fluids is anticipated to take the following qualitative form:

$$\underset{\sim}{\sigma}\,[E(\underset{\sim}{x},t)] = -p\underset{\sim}{I} + q\left[\int_{-\infty}^{t}\left\{U_1\underset{\sim}{C}_t^{-1}(\varsigma) - U_2\underset{\sim}{C}_t(\varsigma)\right\}d\varsigma\right.$$

where σ are the components of the stress tensor for the ER fluid, p is an indeterminate scalar, q is a function, and U_i and $\underset{\sim}{C}_t$ are defined as follows:

$$U_i = \frac{\partial U}{\partial I_i}\;,\; i = 1,2$$

where U(E(x,t)), is the electrical field-dependent strain energy potnetial of the ER Ifuid, and I_1 and I_2 are the first and second invariants of the right relative Cauchy-Green deformation tensor

$$\underset{\sim}{C}_t(\varsigma) = \underset{\sim}{F}_t^{T}(\varsigma)\underset{\sim}{F}_t(\varsigma)$$

where $\underset{\sim}{F}_t$ are the components of the relative deformation gradient tensor. Clearly the electrical field $E(\underset{\sim}{x},t)$ imposed upon the ER fluid would be a function of the geometry of the electrodes, their distribution in space and the potential difference, and can be determined from the classical theory of electro-magnetism.

$$
\begin{aligned}
0 = \delta\hat{J} = \int_t \Bigg\{ & \int_{V^f} \delta v_i^f \left[X_i^f + \sigma_{ij,j}^f - \rho^f \dot{v}_i^f\right] dV^f - \int_{V^f} \delta p e_{kk}^f dV^f \\
& + \int_{V^f} \delta\sigma_{ij}^f \left[e_{ij}^f - \frac{1}{2}\left(v_{i,j}^f + v_{j,i}^f\right)\right] dV^f + \int_{S_1} \delta v_i^f \left(\bar{g}_i^f - g_i^f\right) dS_1 \\
& + \int_{S_2} \delta g_i^f \left(\bar{v}_i^f - v_i^f\right) dS_2 \Bigg\} dt \\
& - \int_t \Bigg\{ \int_{S^*} \delta g_i \left(\dot{u}_i^s - v_i^f\right) dS^* - \int_{S^*} \delta v_i^f \left(g_i^s + g_i^f\right) dS^* \Bigg\} dt \\
& + \int_t \Bigg\{ \int_{V^s} \delta\dot{u}_i^s \left[X_i^s + \sigma_{ij,j}^s - \rho^s \ddot{u}_i^s\right] dV^s + \int_{V^s} \delta\dot{\gamma}^s \left[\gamma_{ij}^s - \frac{\partial W}{\partial\gamma_{ij}}\right] dV^S \\
& + \int_{V^s} \delta\sigma_{ij}^s \left[\dot{\gamma}_{ij}^s - \frac{1}{2}\left(\dot{u}_{i,j}^s + \dot{u}_{j,i}^s\right)\right] dV^s + \int_{S_1} \delta\dot{u}_i^s \left(\bar{g}_i^s - g_i^s\right) dS_1 \\
& + \int_{S_2} \delta g_i^s \left(\bar{\dot{u}}_i^s - \dot{u}_i^s\right) dS_2 \Bigg\} dt
\end{aligned}
$$

solid (elastic)

$$[M^s]\{\ddot{U}^s\} + [K^s]\{U^s\} = \{F^s\} - [M^s]\{\dot{V}_R^s\} + \{F_i^s\}$$

fluid (Bingham plastic)

$$[M^f]\{\ddot{U}^f\}+[Q^f(E)]\{\dot{U}^f\}-[Q_p^f]\{P^f\} = \{F^f\}-[Q_\tau^f]\{\tau_o(E)\}-[M^f]\{\dot{V}_R\}+\{F_i^f\}$$

$$[R^f]\{\dot{U}^f\} = \{0\}$$

interface

$$\{F_i^s\} + \{F_i^f\} = \{0\}$$

$$\{\dot{U}_i^s\} = \{\dot{U}_i^f\}$$

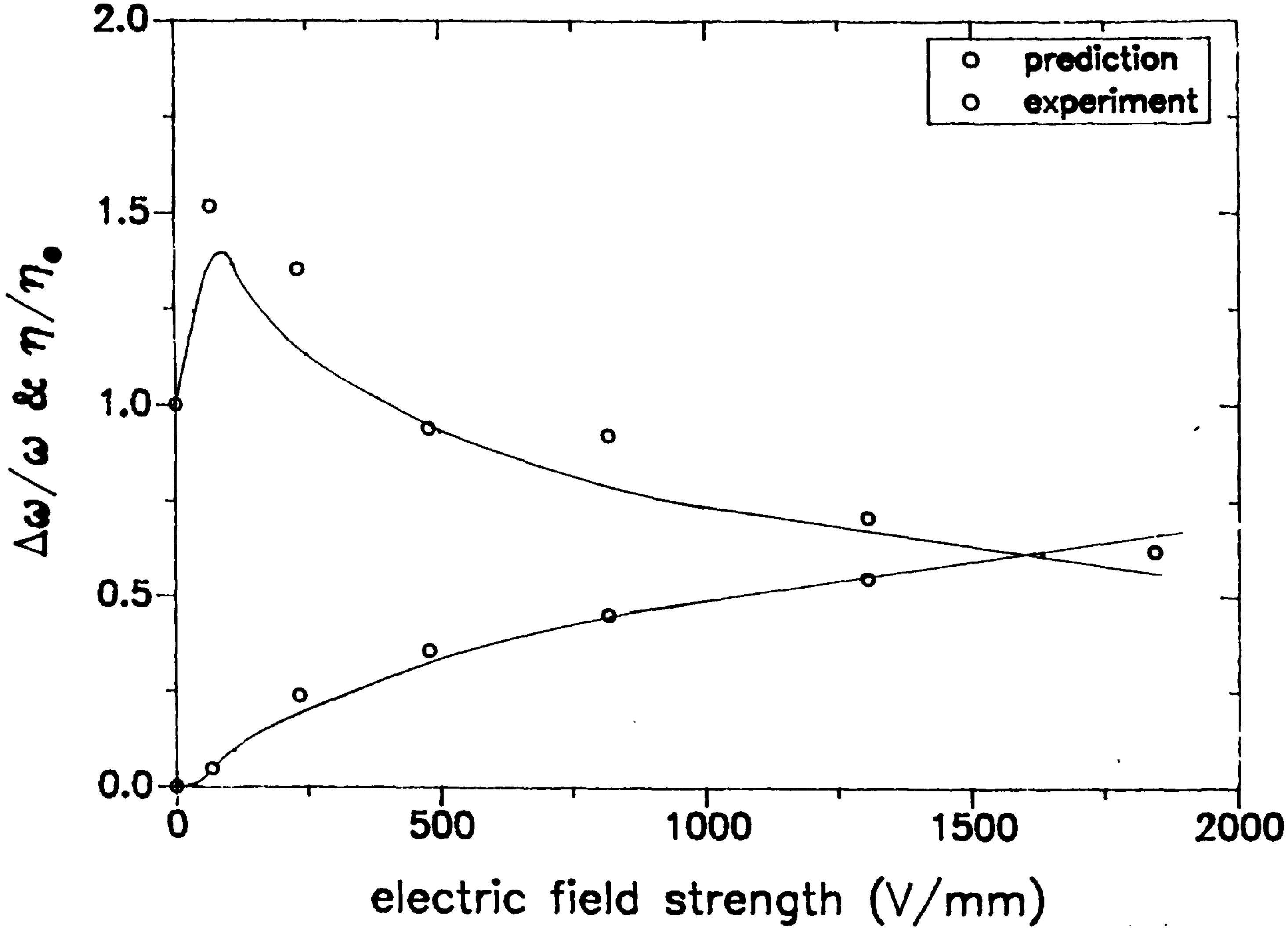

2.0
1.5
1.0
0.5
0.0
Δω/ω & η/η₀
0
500
1000
1500
2000
electric field strength (V/mm)
prediction
experiment

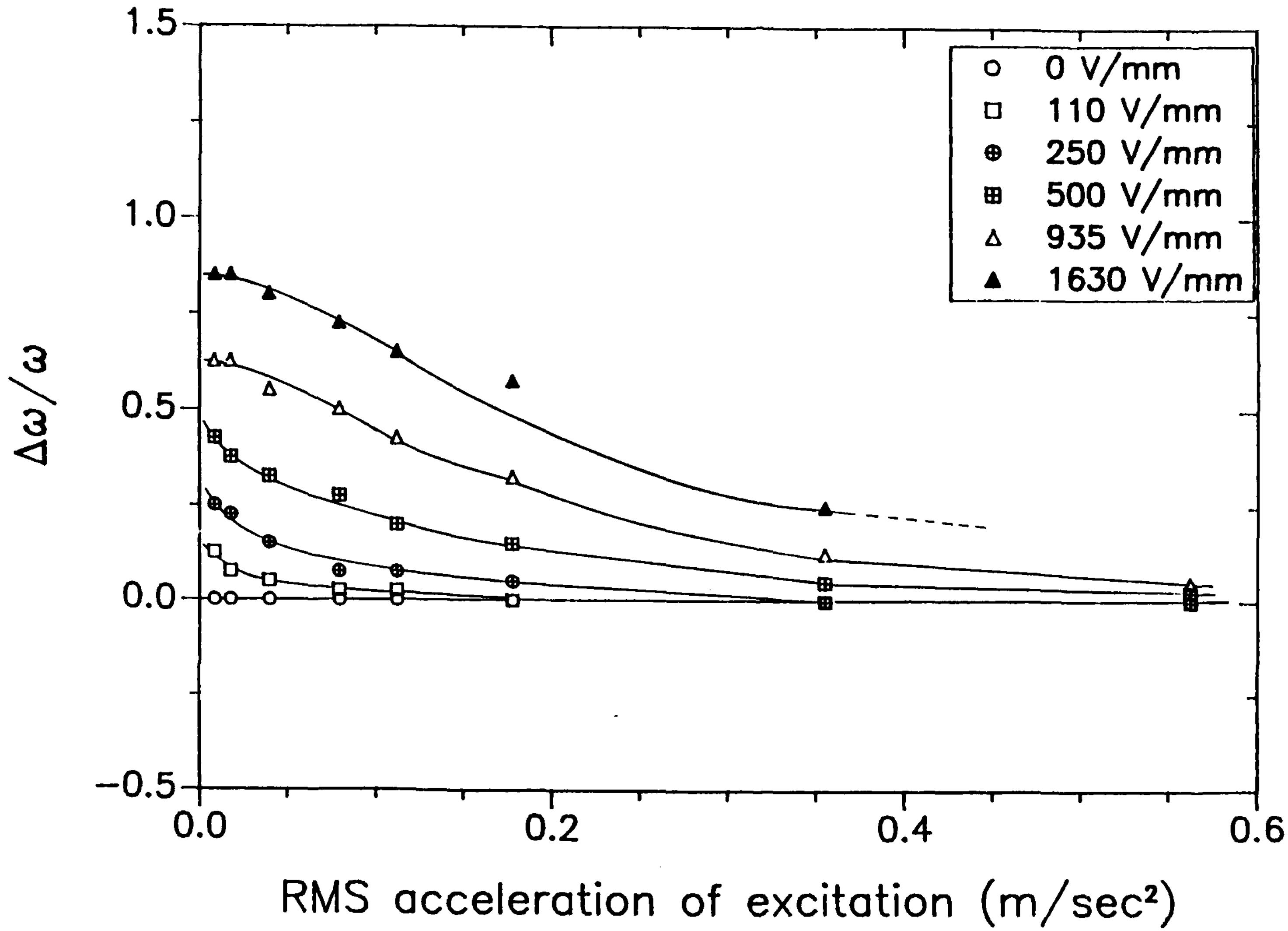

0 V/mm
110 V/mm
250 V/mm
500 V/mm
935 V/mm
1630 V/mm
$\Delta\omega/\omega$
1.5
1.0
0.5
0.0
−0.5
0.0
0.2
0.4
0.6
RMS acceleration of excitation (m/sec²)

ACTIVE DYNAMIC TUNING UTILIZING SMA COMPOSITES

Dr.Craig A. Rogers
Smart Materials & Structures Laboratory
Mechanical Engineering Department
Virginia Polytechnic Institute & State University
Blacksburg, Virginia 24061

2nd ARO-AHS-RPI Workshop on Composite Materials And Structures for Rotorcraft

September 14 & 15, 1989

Ransselaer Polytechnic Institute
Troy, New York

ACTIVE DYNAMIC TUNING UTILIZING ADAPTIVE COMPOSITES
SMART MATERIALS & STRUCTURES RESEARCH AT VPI&SU

- Shape Memory Alloy Composites
  - Introduction to Nitinol
  - Active Modal Modification
  - Active Structural Acoustic Control
  - Nitinol Characterization
  - Constitutive Modelling
  - Modal Analysis Techniques
  - Thermo-mechanical Modelling
  - Distributed Nitinol Sensors
- Piezoelectric Investigations

INTRODUCTION TO NITINOL

- NITINOL - Nickle-Titanium - Naval Ordinance Laboratory
- Discovered in the late 1950's
- Near-equiatomic composition of Nickel and Titanium
- Utilizes a martensitic phase transformation (twinning)
  - low temperature phase = Martensite
  - high temperature phase = Austenite
- The transition temperature(s) can be selected over a range from 50°C to 155°C
- Capable of recovering 8% plastic strain
- Capable of recovery stress of 100,000 psi
- Young's modulus changes by a factor of 4 during phase transformation
- Superelastic Nitinol has an elastic limit of 6%

MAPPING OF THE VARIATION OF STIFFNESS
WITH TEMPERATURE AND STRAIN

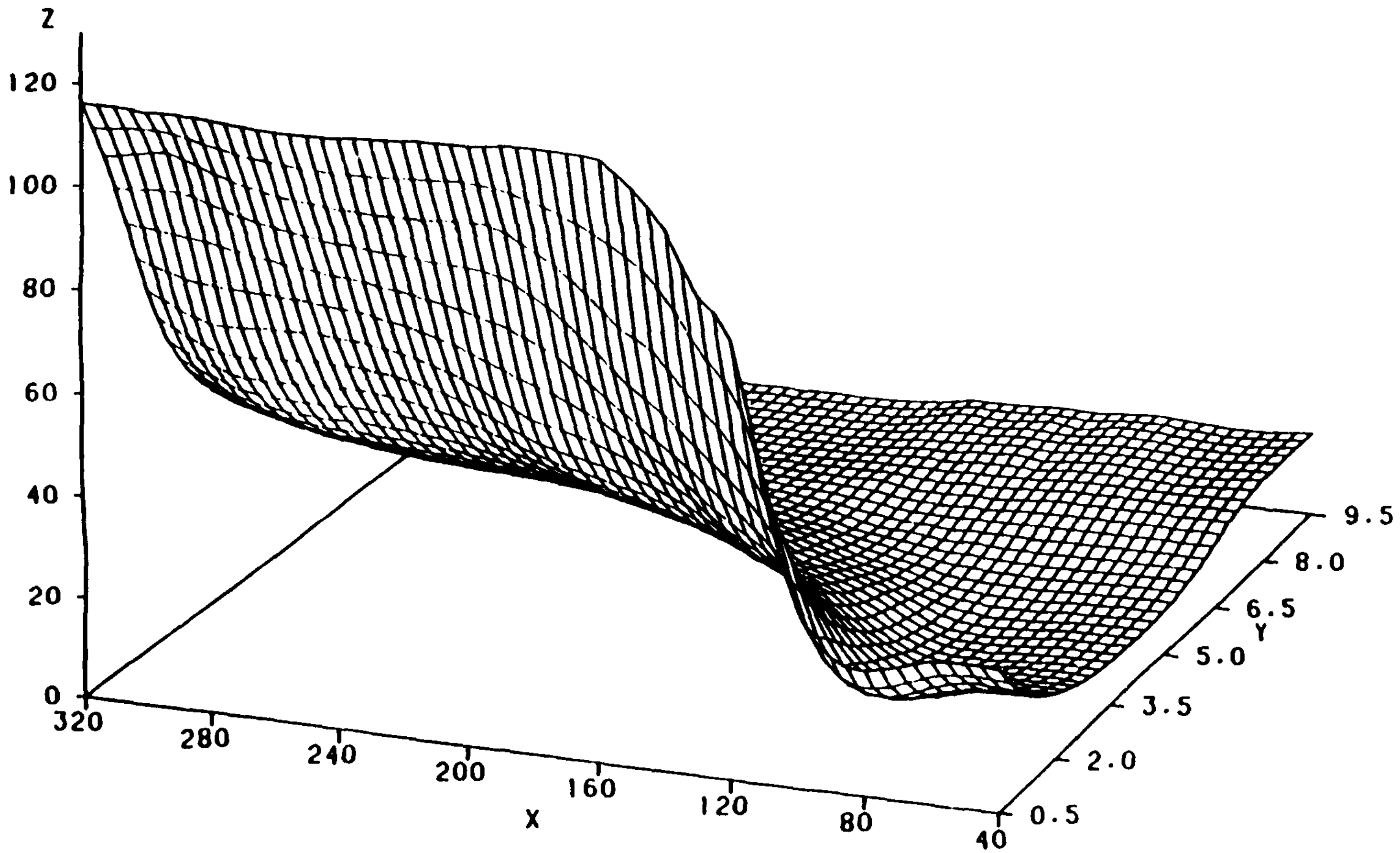

X=TEMPERATURE Y=STRAIN Z=STIFFNESS

ACTIVE MODAL MODIFICATION

The use of shape memory alloy fibers embedded in composite materials to alter the dynamic behavior and characteristics of structures

ACTIVE PROPERTY TUNING (APT)

- Employs embedded unstrained Nitinol fiber actuators
- Exploits the change in Young's modulus of the Nitinol fibers

ACTIVE STRAIN ENERGY TUNING (ASET)

- Employs embedded plastically prestrained nitinol fiber actuators
- Exploits change in apparent strain state (recovery stress) of the nitinol fibers

LAY-UP SCHEME FOR NITINOL REINFORCED COMPOSITE BEAM

Specifications

Graphite epoxy:	5245 prepreg system	
Dimensions:	Length (L)	= 32.0 in. (86.4 cm)
	Width (W)	= 13/16 in. (2.06 cm)
	Spacing (S)	= 1/32 in. (0.79 mm)
No. of actuators	= 24 x .015 in. (.381 mm) dia	
Nitinol volume fraction	= 15%	

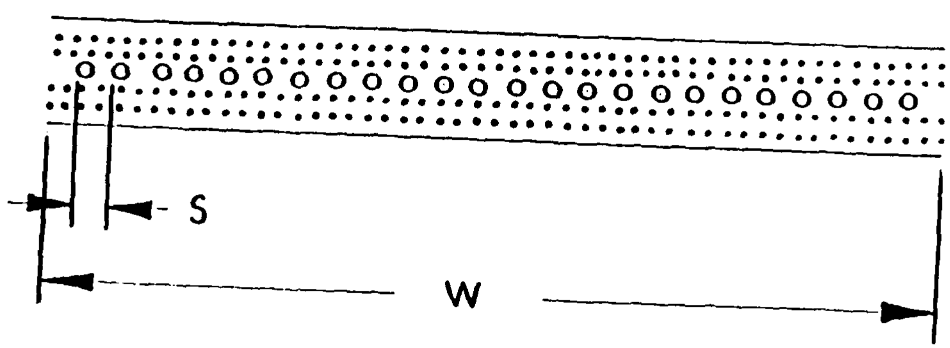

FFT of Unactivated Beam

vf = .1, As = 100 F, temp = 76.5 F

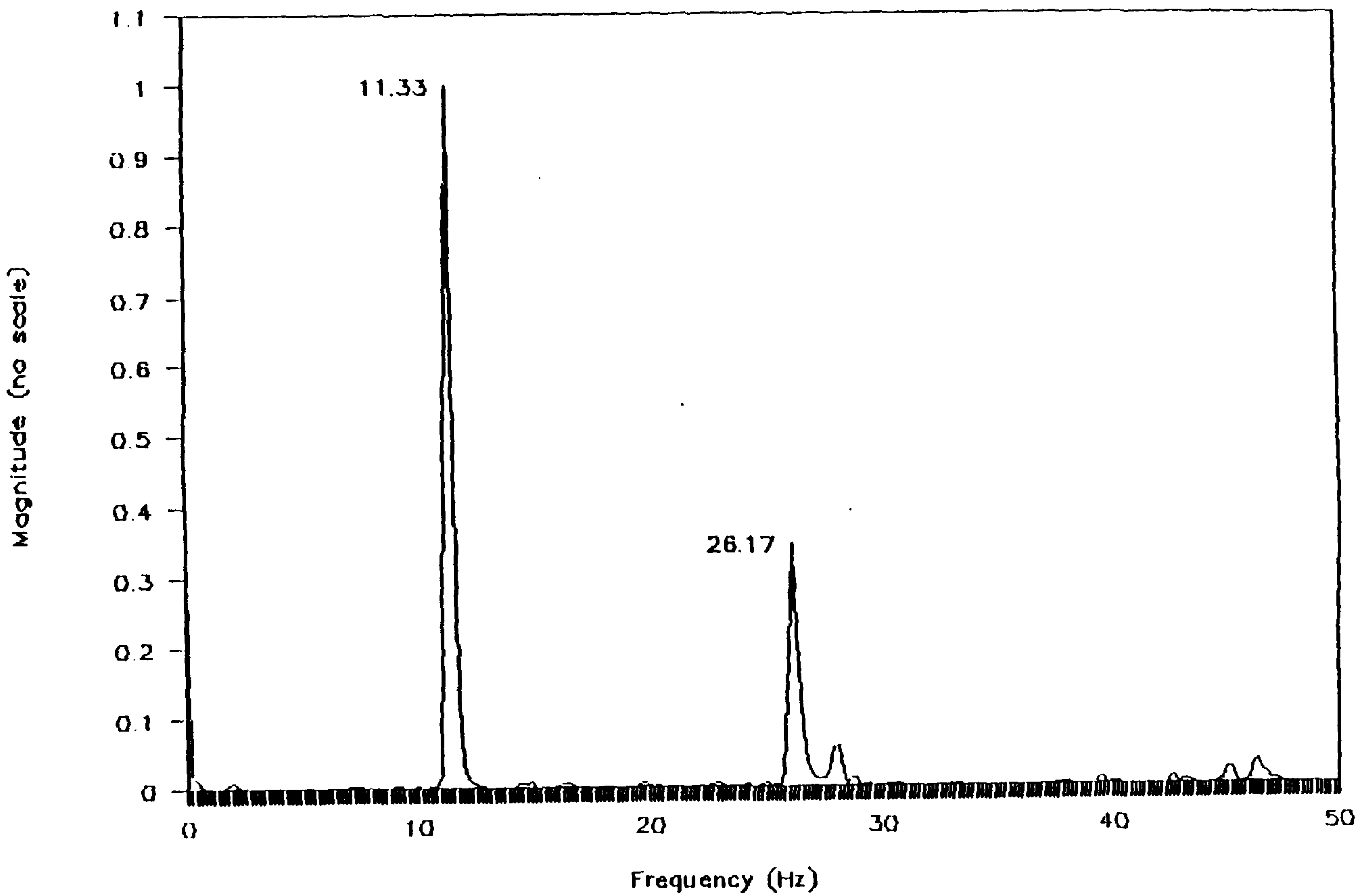

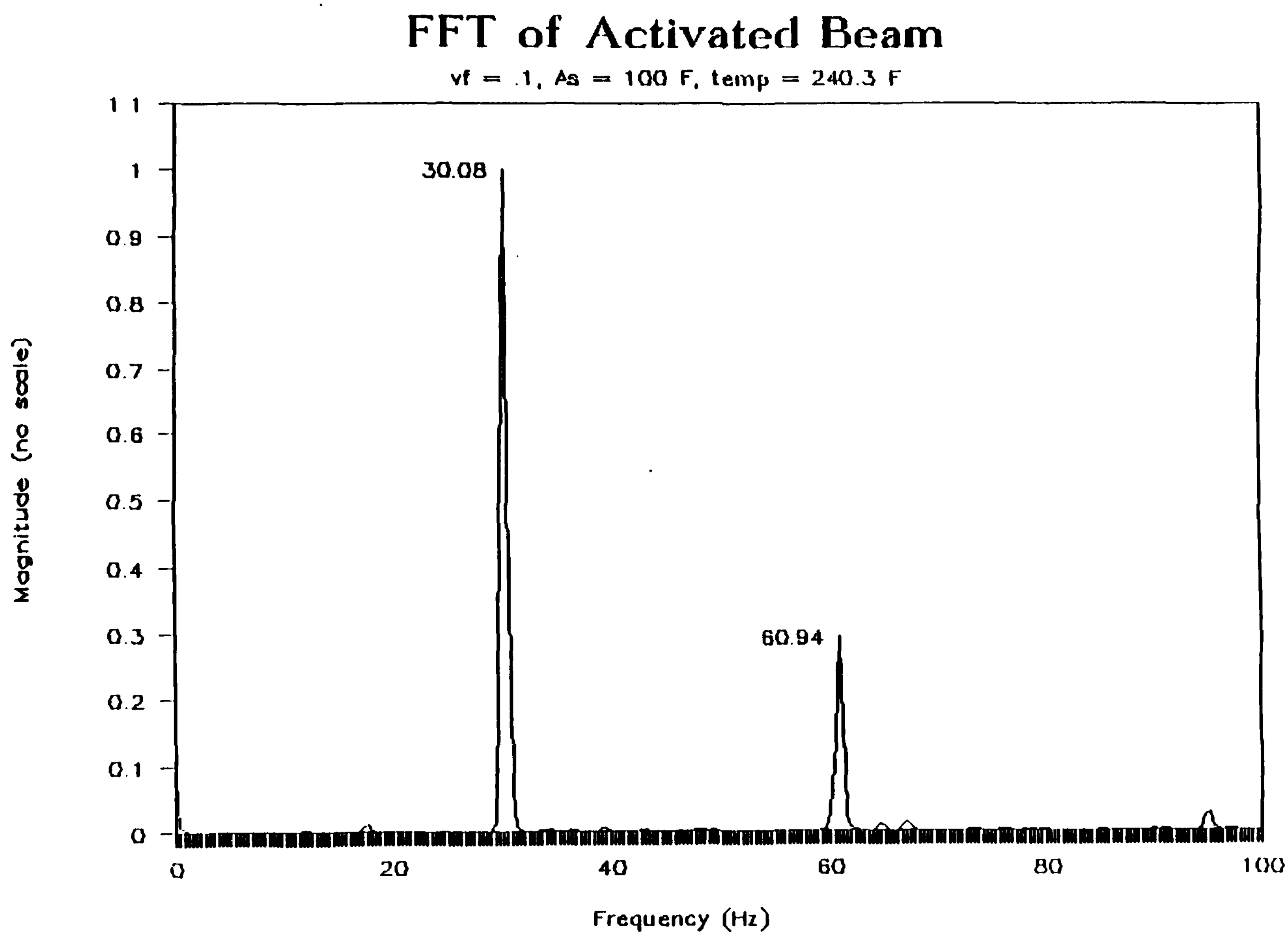
FFT of Activated Beam
vf = .1, As = 100 F, temp = 240.3 F
30.08
60.94
1 1
1
0.9
0.8
0.7
0.6
0.5
0.4
0.3
0.2
0.1
0
Magnitude (no scale)
0
20
40
60
80
100
Frequency (Hz)

NITINOL CHARACTERIZATION SET-UP

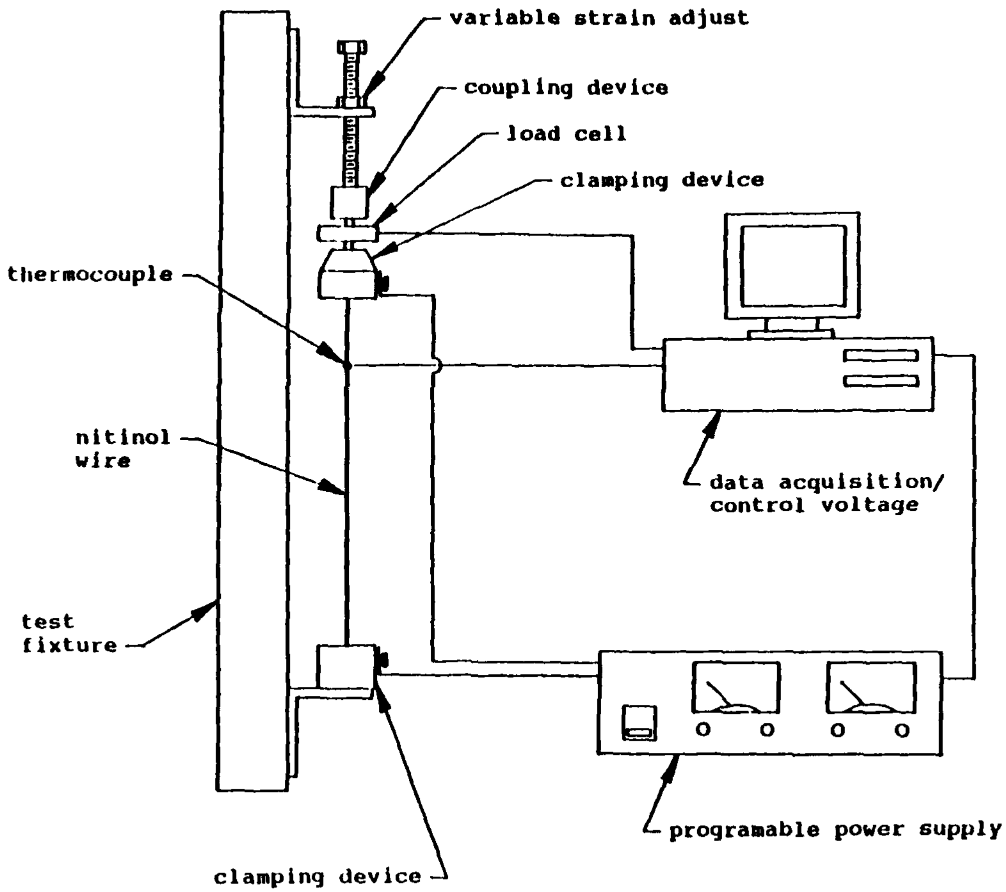

RECOVERY STRESS FOR CONSTRAINED NITINOL

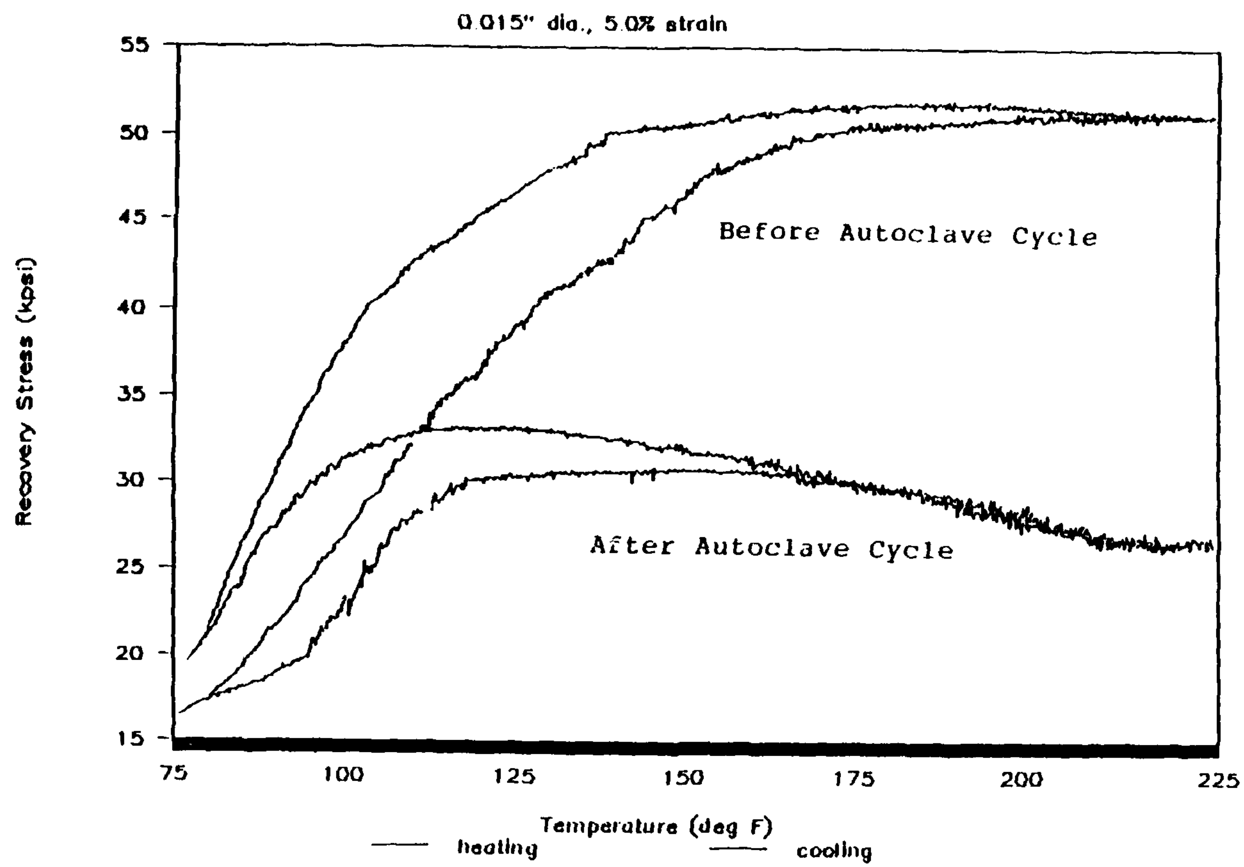

ACOUSTIC RADIATION/TRANSMISSION OF SMA COMPOSITE PLATES

- Change of the first ten natural frequencies of a quasi-isotropic plate with an activated 45° ply

	Natural Frequencies (Hz)									
	1	2	3	4	5	6	7	8	9	10
Inact.	41.3	82.8	114.8	144.4	166.9	224.0	233.7	245.5	290.7	317.9
Act.	71.5	129.7	146.6	203.4	239.5	246.9	296.5	322.4	355.4	403.4

Table 1. Change of the First Ten Natural Frequencies (Hz)

- Change of the first ten mode shapes

Act.	Inactivated Modes									
	1	2	3	4	5	6	7	8	9	10
1	1.00	.000	.000	.005	.009	-.001	.000	.000	.000	0.002
2	.000	.327	.945	.000	.000	.000	.000	.010	.006	0.000
3	.000	.945	-.327	.000	.000	.000	.000	.007	-.004	0.000
4	-.011	.000	.000	.505	.861	.028	.051	.000	-.000	0.000
5	.000	.000	.000	.856	-.493	-.143	-.151	.000	-.000	0.019
6	.001	.000	.000	.105	-.120	.989	.987	.000	.000	-.014
7	.000	-.014	.000	.000	.000	.000	.000	.600	.281	0.000
8	.000	.006	-.009	.000	.000	.000	.000	-.038	.945	0.000
9	.000	.002	.009	.000	.000	.000	.000	-.799	.167	0.000
10	.000	-.001	.000	.000	.000	.000	.000	.008	-.028	0.000

- Change of the Transmitted Intensity Pattern (220 Hz)

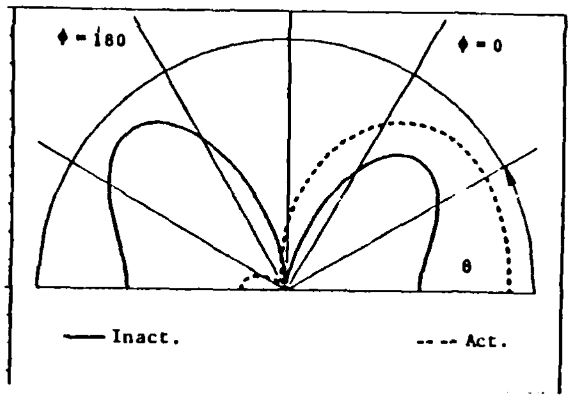

- Transmission Loss

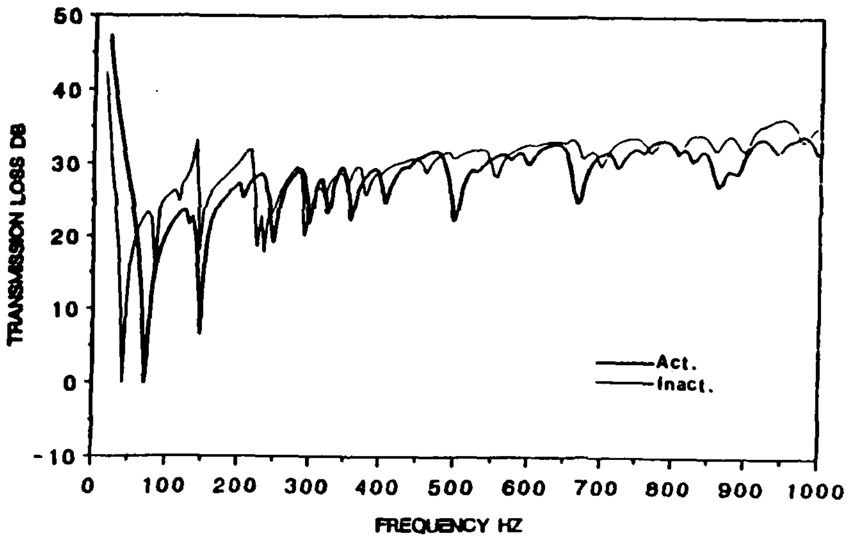

EXPERIMENTAL RESULTS OF ACTIVE STRUCTURAL ACOUSTIC CONTROL

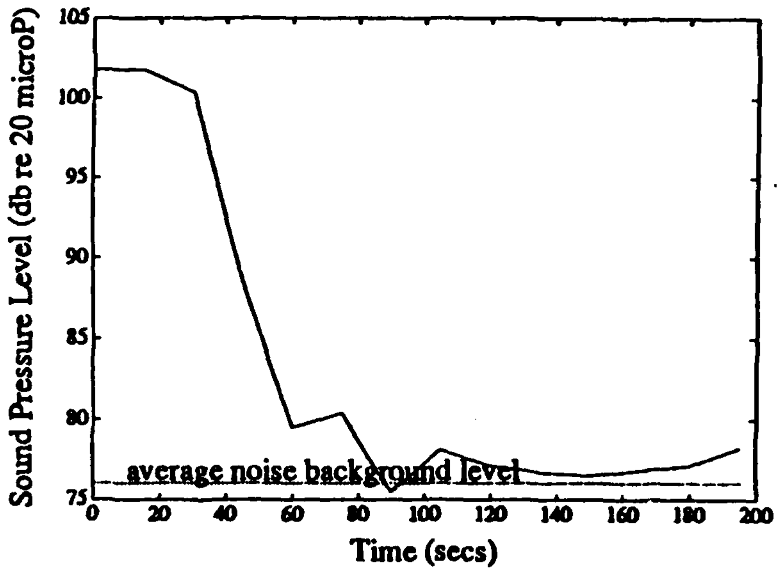

Figure 4: Controlled Sound Pressure ($f_o = 35Hz$)

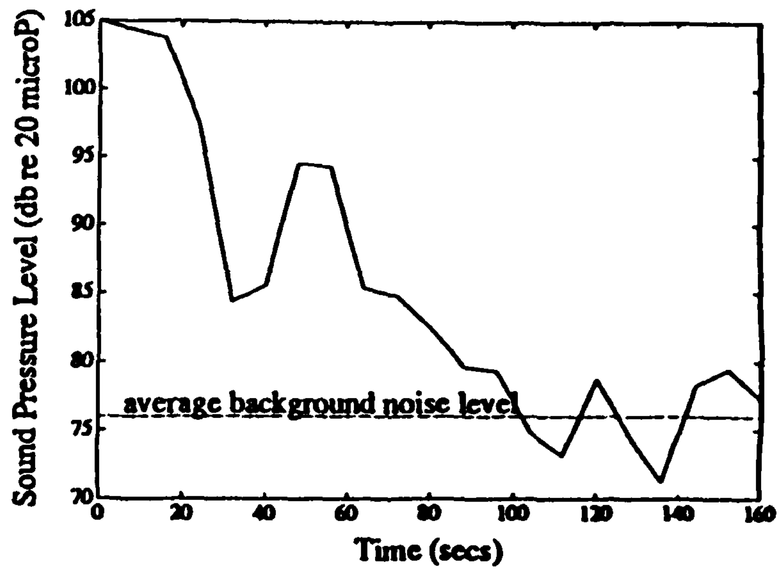

Figure 5: Controlled Sound Pressure ($f_o = 145Hz$)

INVESTIGATIONS OF INTERFACIAL SHEAR STRENGTH

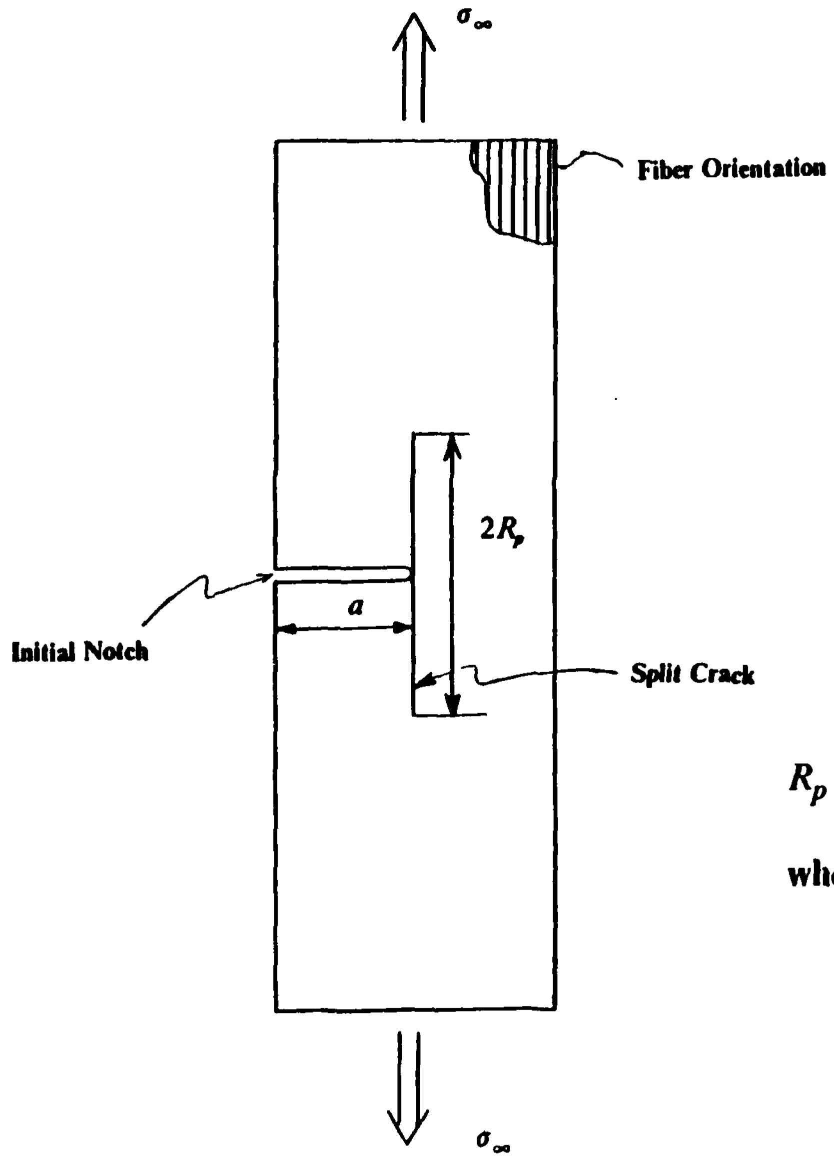

$$R_p = \frac{\pi}{4} a \left(\frac{\sigma_\infty}{\tau_0}\right)^2 \frac{G_{12}}{E_{11}} \alpha \left[\frac{(\alpha + \beta)}{2}\right]^{1/2},$$

where

$\alpha = [E_{11}/E_{22}]^{1/2}$
$\beta = E_{11}/2G_{12} - \nu_{12}$
σ_∞ = **Applied Stress**
τ_0 = **Interfacial Shear Yield Stress**

Failed Tensile Coupons

0° Specimen

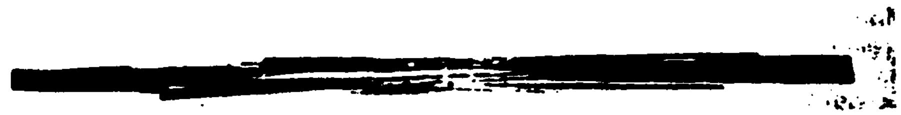

45° Specimen

90° Specimen

THERMOMECHANICAL CONSTITUTIVE RELATION OF SMA

- Utilizes the Helmholtz free energy associated with the two-state phase transformation. It is a unified theory which also satisfies the first and second law of thermodynamics.

- Capabilities include
  - Stress-strain relations
  - Recovery stress-strain-temperature relations
  - Hysteresis characteristics of SME
  - Energy dissipation/consumption during recovery

FREE RECOVERY

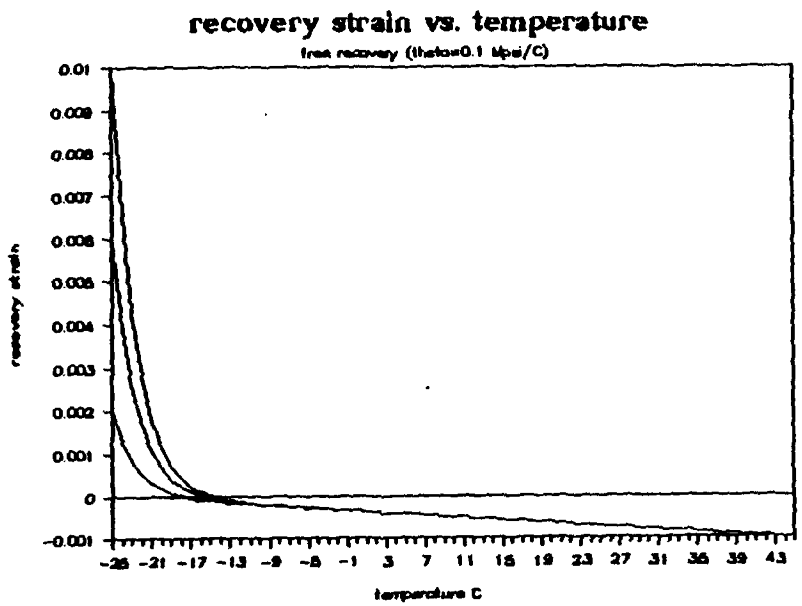

$$\bar{\varepsilon}_r = \bar{\varepsilon}_{res} - \frac{1}{D}\left[\Theta(T - A_s) + \Omega\frac{\bar{\varepsilon}_{res}}{\bar{\varepsilon}_L}\left(e^{a_A(A_s - T)} - 1\right)\right]$$

RESTRAINED RECOVERY

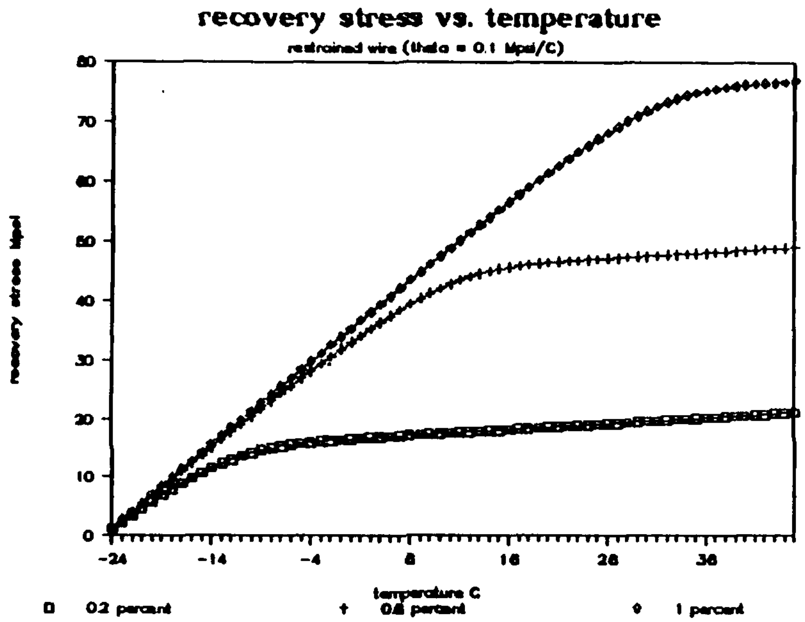

$$\overline{\sigma}^r = \Theta(T - A_s) + \Omega \frac{\overline{\varepsilon}_{res}}{\overline{\varepsilon}_L} (e^{[a_A(A_s - T) + b_A \overline{\sigma}^r]} - 1)$$

IN-SITU DETERMINATION OF ELASTIC PROPERTIES

AIMS:

- To provide a reliable data-base which the researchers in this field can draw upon
- To determine the contribution of SMA fibers on active control of structures
- To determine the nature of residual stresses in the laminates
- To provide a quick and non-destructive means of verifying material properties

PROCEDURE:

- Mathematical model based on Rayleigh-Ritz technique
- Use an iterative procedure where seven natural frequencies of structure determined from modal analysis are used to compute the four elastic constants E_x, E_y, G_{xy}, and ν_{xy} and the three in-plane loads
- Study the sensitivity of technique to the initial assumed values of these elastic constants and in-plane loads

Determination of Elastic Constants Using Modal Analysis/Rayleigh-Ritz Technique

B.C. => C-F-F-F

	E_x Gpa	E_y Gpa	G_{xy} Gpa	ν_{xy}
Exact Values	127.94	10.27	7.31	0.2212
Mean from 50 % higher initial guesses (13 comb. of freqs.)	127.95	10.27	7.30	0.2246
Standard deviations	0.2220E-01	0.3790E-02	0.1379E-02	0.4376E-03
Mean from 50 % lower initial guesses (13 comb. of freqs.)	127.94	10.27	7.32	0.2162
Standard deviations	0.2160E-01	0.4678E-02	0.1058E-01	0.5213E-03

% MEAN AND STANDARD DEVIATION OF E_x AND E_y AGAINST % RANGE OF INITIAL GUESS

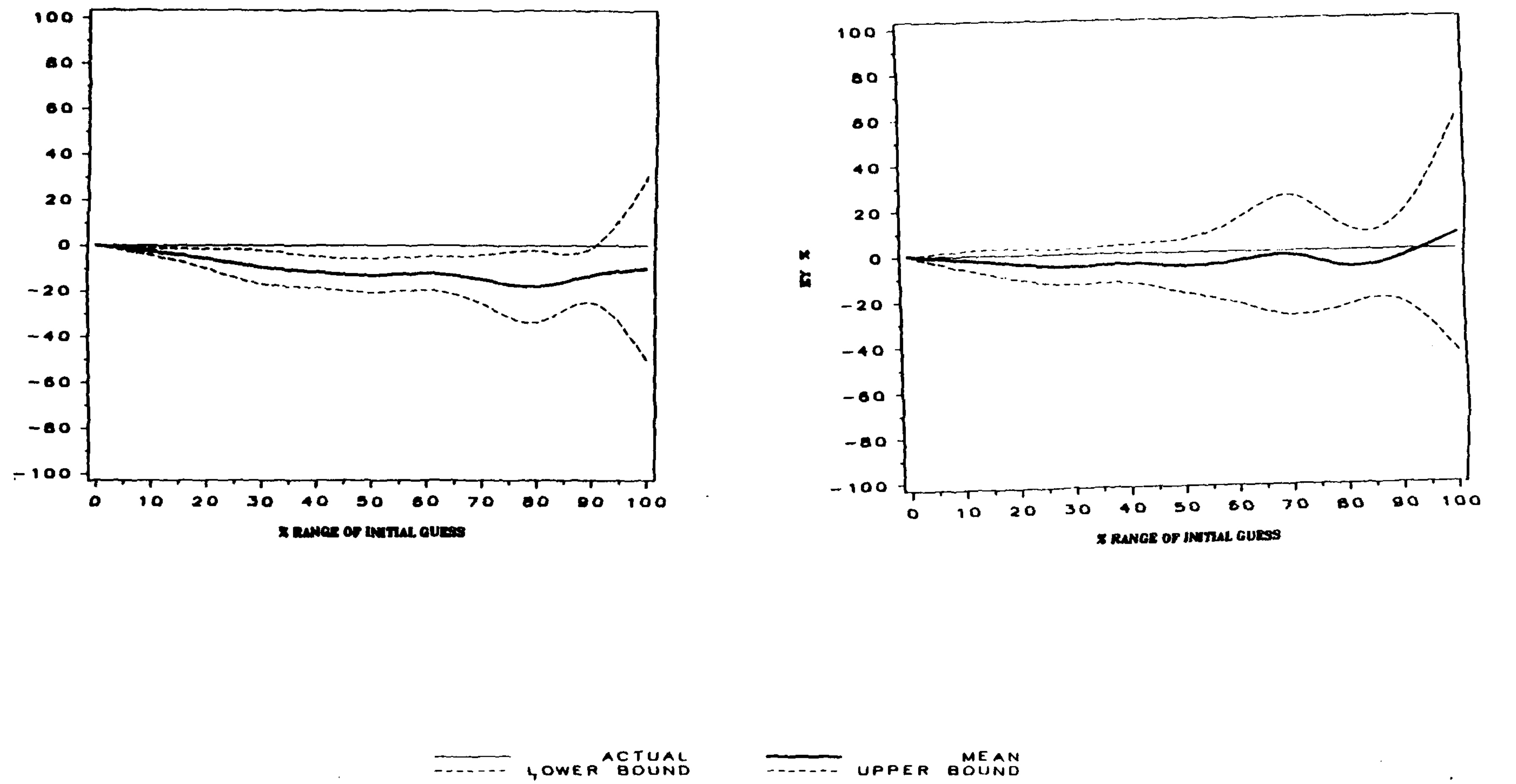

% MEAN AND STANDARD DEVIATION OF N_x AND N_y AGAINST % RANGE OF INITIAL GUESS

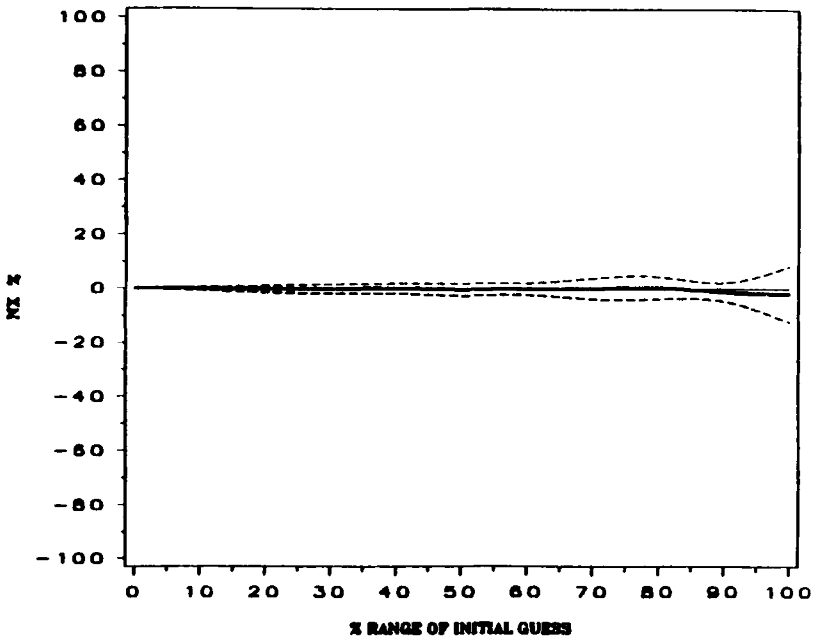

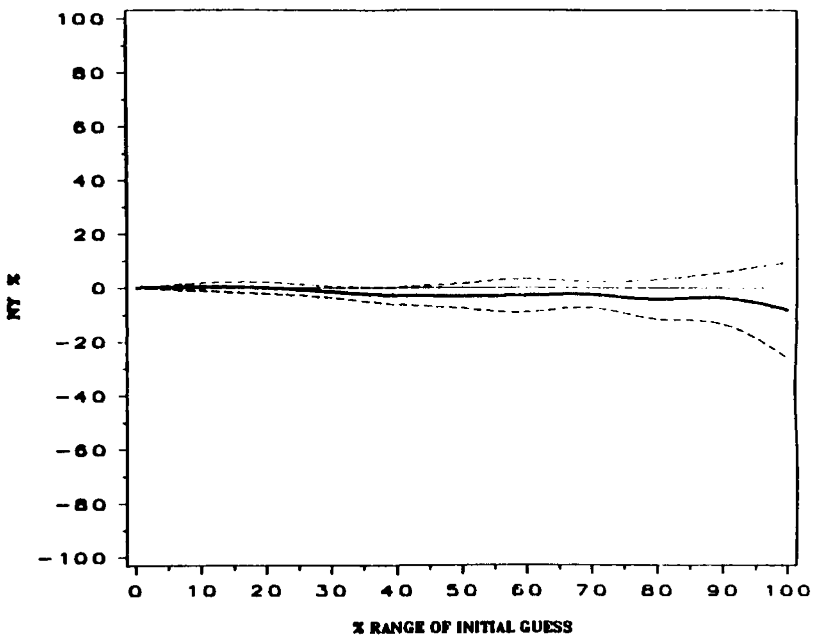

TRANSIENT THERMAL RESPONSE OF AN SMA COMPOSITE

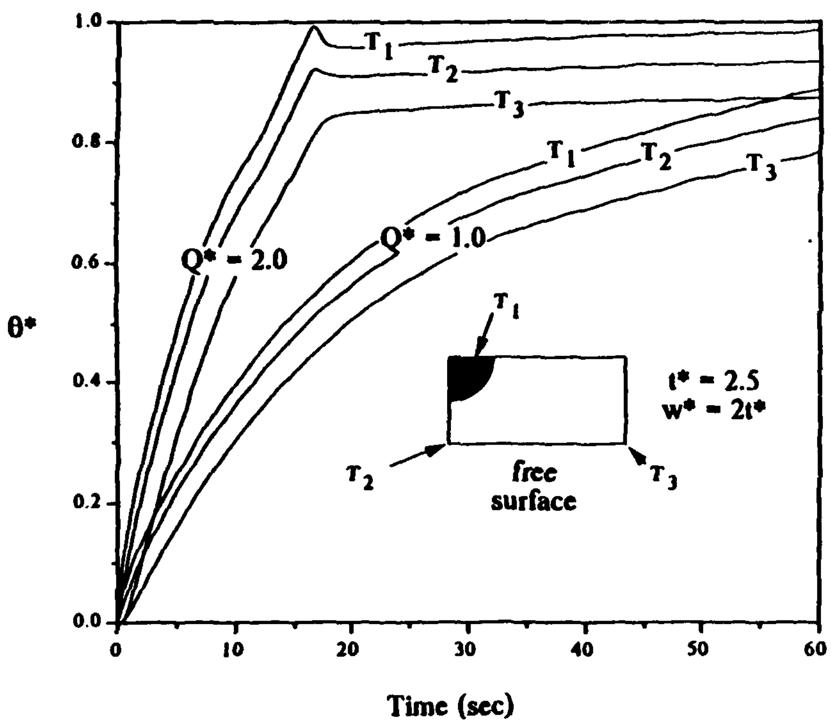

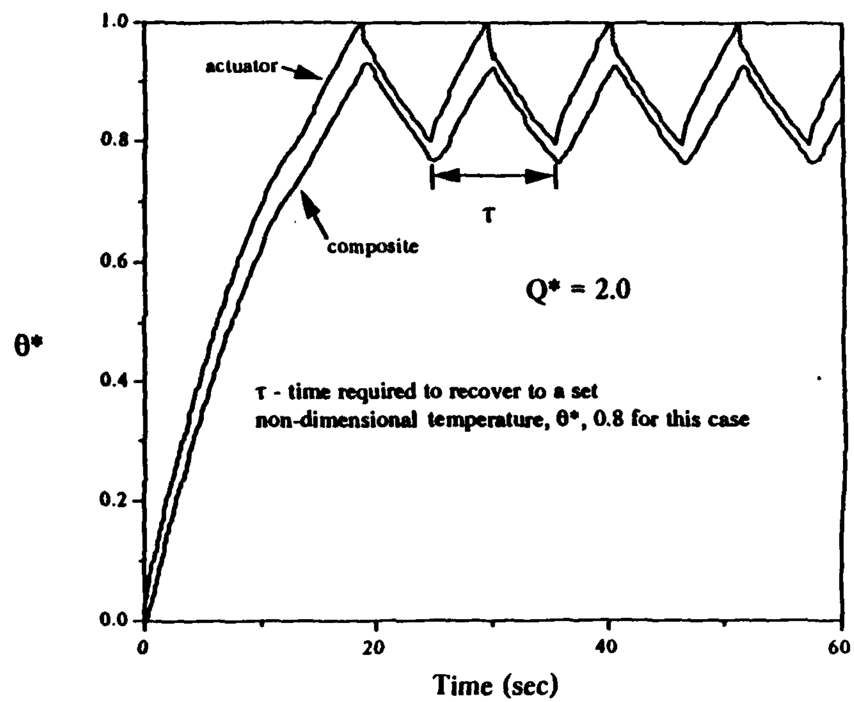

Figure 8. Actuator Response to a Square Pulse Power Input Level of 2.0

Distributed Strain Sensing Using 'Superelastic' Nitinol

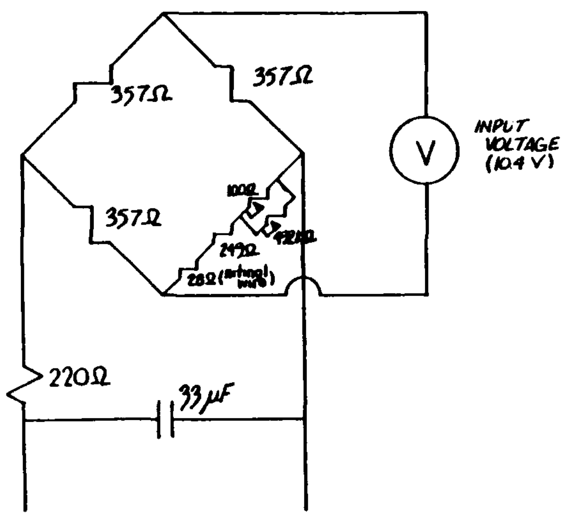

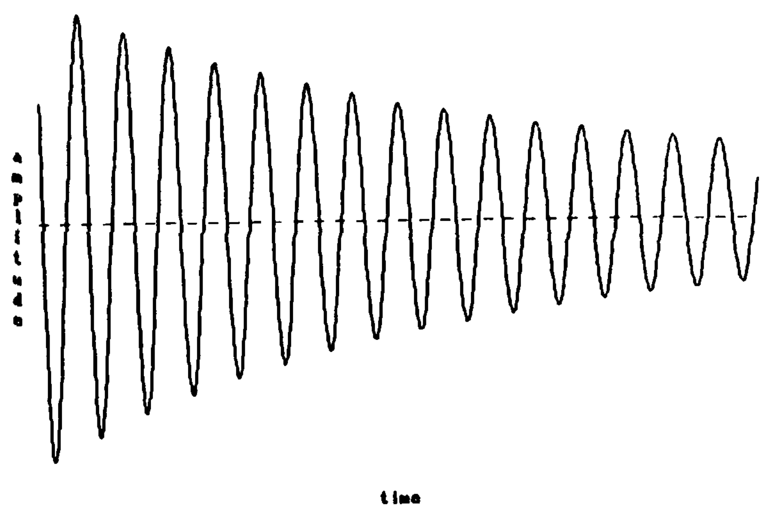

Figure 4. Typical curve generated by oscillation of beam.

CONCLUSIONS

- **Developed and evaluated fabrication techniques for embedding nitinol actuators**
- **Experimentally determined the effect of thermoset processing on nitinol behavior**
- **Developing a unified constitutive model for nitinol**
- **Experimentally demonstrated Active Structural Acoustic Control using SMA composites**
- **Developed *in – situ* methods for determining laminate properties of SMA composites**
- **Experimentally demonstrated the use of nitinol strain and temperature sensors**

SMA ACTUATOR and SMA REINFORCED COMPOSITES

supported by

ONR-YIP N00014-88-K-0566
and
ONR/DARPA N00014-88-K-0721

Leveraged with support from

Virginia Center for Innovative Technology

6

An Abstract for the
Second International Workshop on
Composite Materials and Structures for Rotorcraft

A REVIEW OF ACTIVE NOISE CONTROL STRATEGIES FOR REDUCTION OF ROTORCRAFT INTERIOR NOISE

J. D. Jones
Ray W. Herrick Laboratories
School of Mechanical Engineering
Purdue University
West Lafayette, IN 47907

Source mechanisms and transmission paths of rotorcraft interior noise are well defined. Rank ordering of these sources has established the main rotor gearbox as the primary contributor to the cabin noise levels. Gear-mesh vibrations generate a series of harmonic tones within the cabin, the most significant of which is typically the fundamental mesh tone at approximately 700-800 Hz. Current passive noise control methods (e.g., the fuselage sidewall treatments) do not adequately reduce cabin noise levels to provide passenger comfort, especially for extended flights. Further sidewall treatments can add substantially to weight penalities and cost. Thus, new lightweight noise control methods are needed to reduce rotorcraft interior noise.

Much recent work has focused on alternative methods for interior noise reduction in aerospace vehicles (e.g., propeller-driven aircrafts, rotorcraft, and space station). Current efforts in this area emphasize the use of active noise control (ANC) strategies in conjunction with passive methods for broadband noise reduction. Active noise control pertains to a family of techniques which use a controller to "actively" create a secondary sound field out-of-phase with the primary noise field so that superposition of the two sound fuels results in an overall reduction in the noise levels. Active noise control (ANC) is ideally suited to such applications due to its complementary effectiveness with minimum weight penalities at potentially lower costs.

In the proposed paper, a review of two active noise control strategies for reduction of rotorcraft interior noise is presented. First the conventional ANC strategy consists of implementing an array of interior acoustic sources (e.g., audio speakers) as secondary controllers to reduce the interior cabin levels. Second, a more recent ANC strategy involves applying secondary vibration actuators directly to the rotorcraft fuselage in the vicinity of the gearbox supports so as to reduce the transmission of structureborne gear mesh vibrations into the cabin interior. The second strategy is especially promising when the power flow into the structure is localized such as with the rotorcraft gearbox vibrations. Advantages and disadvantages of these two active noise control strategies will be discussed along with their potential for providing global reduction of rotorcraft interior cabin noise.

A REVIEW OF ACTIVE NOISE CONTROL STRATEGIES FOR REDUCTION OF ROTORCRAFT INTERIOR NOISE

by

J.D. Jones
Ray W. Herrick Laboratories
School of Mechanical Engineering
Purdue University
West Lafayette, IN 47907

ACTIVE NOISE CONTROL STRATEGIES

ACTIVE NOISE CONTROL: is a family of techniques which use some type of secondary controller to generate a sound field which then superimposed on an existing noise field will result in overall noise reduction.

TWO TYPES OF SECONDARY CONTROLLERS

- Acoustic Control Sourses (Loudspeakers)
- Vibration Control Sources (Shakers)

LOCAL CONTROL

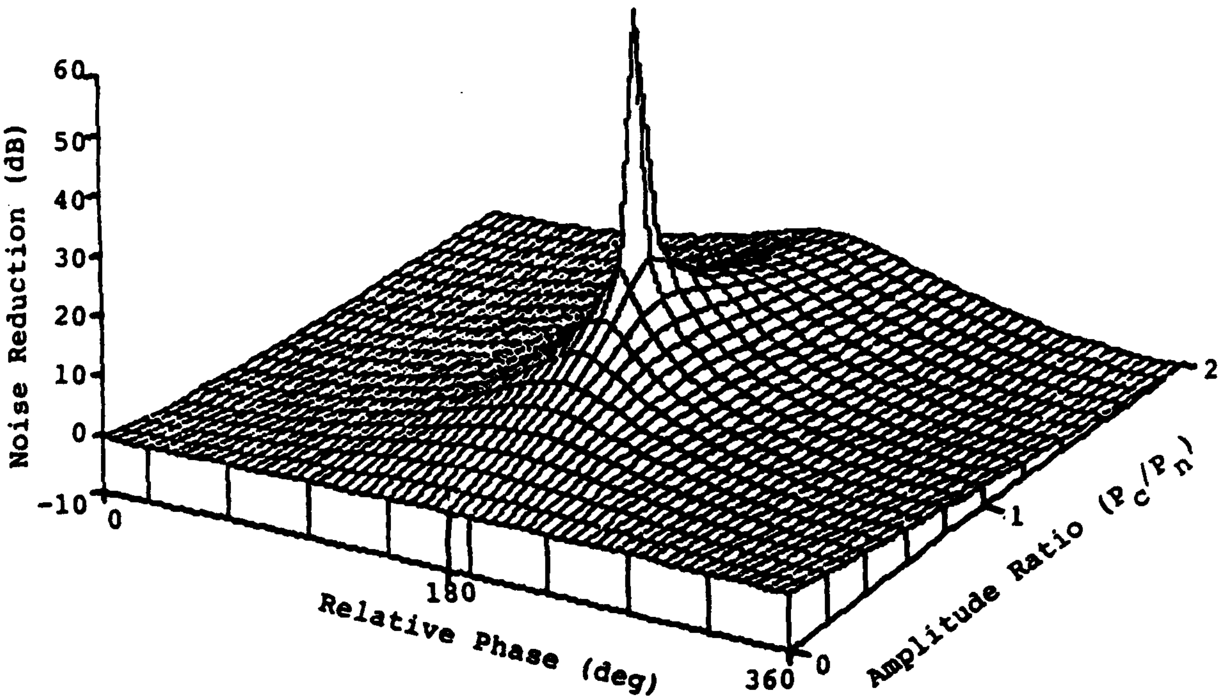

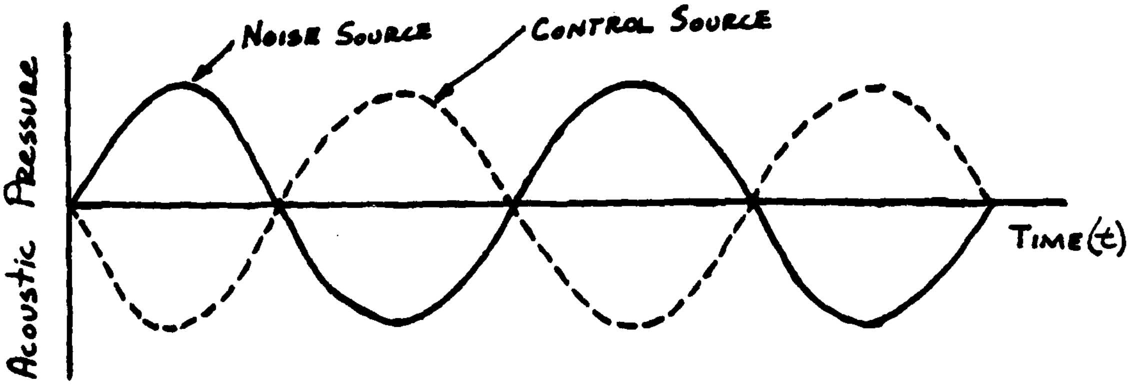

FREQUENCY LIMITATIONS

Active noise control systems perform <u>best</u> at low frequencies (generally $<$500-600 Hz) where traditional passive techniques for noise control (e.g., acoustic foams, fiberglass, etc.) are frequently inadequate.

Active and passave techniques are spectrally complementary noise control strategies.

AN APPLICATION OF ACTIVE NOISE CONTROL USING ACOUSTIC SOURCES

from

Elliott, S., Nelson, P., Stothers, I., Boucher, C., Evers, J., and Chidley, B., "In-Flight Experiments on the Active Control of Propeller-Induced Cabin Noise," AIAA Paper 89-1047.

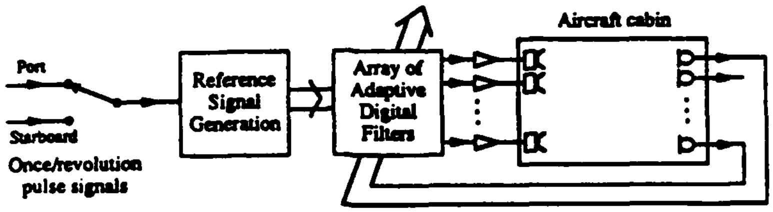

Figure 1. Block diagram of the control system.

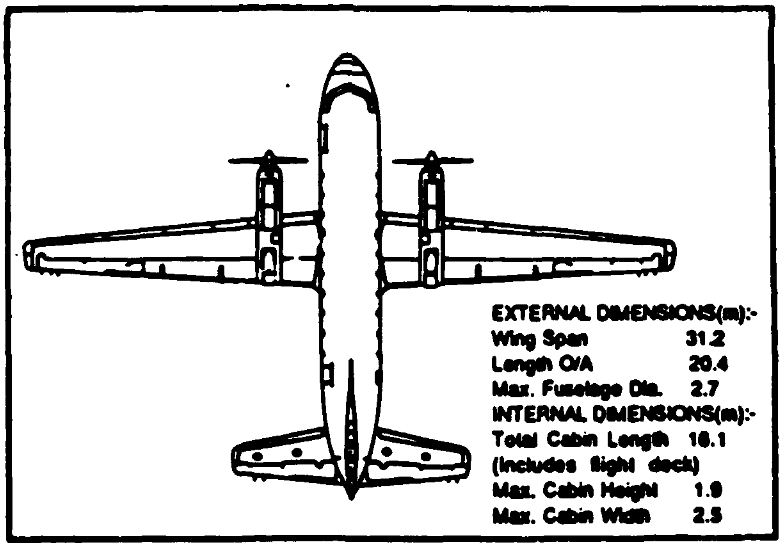

FIGURE 1. Plan view of a British Aerospace 748 twin turboprop, 48 seat aircraft.

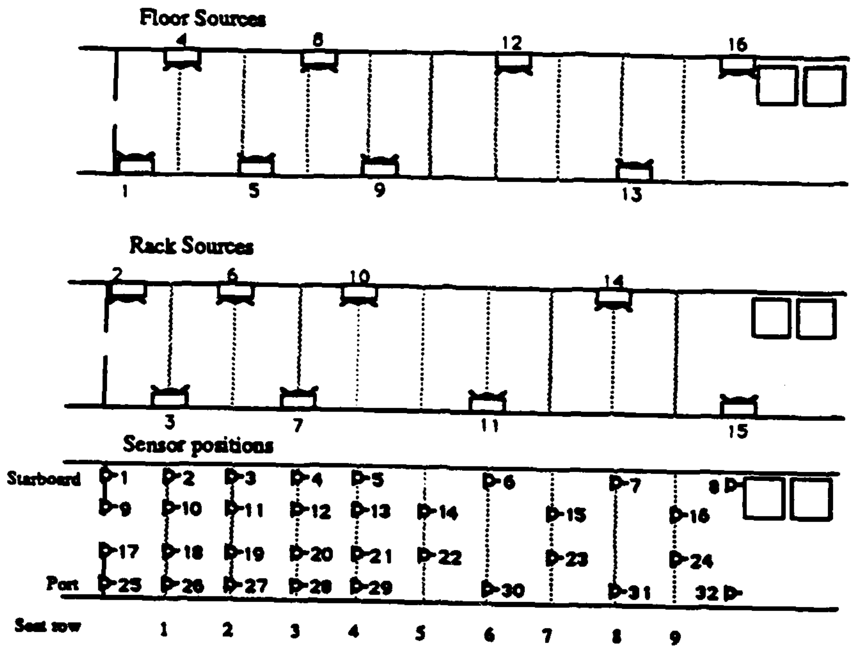

Figure 2. Microphone and loudspeaker arrangement, showing a plan view of the internal passenger cabin at three levels: (upper graph) floor level showing loudspeaker positions, (middle graph) rack level showing further loudspeaker positions, (lower graph) seated head height showing microphone positions.

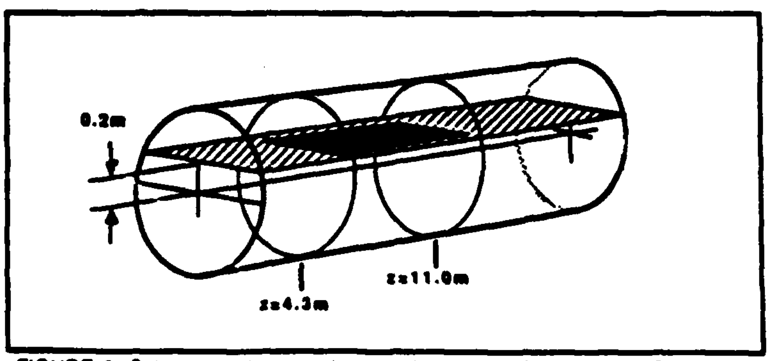

FIGURE 8. Schematic diagram showing the head height plane (0.2m above the fuselage centreline)

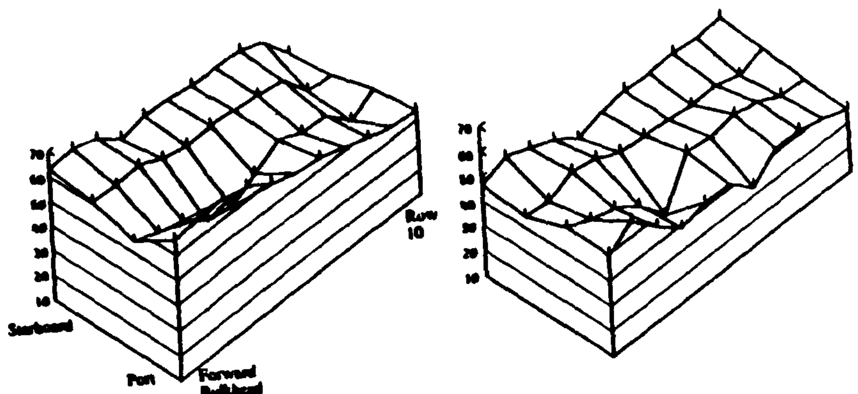

Figure 3. Pressure distribution at 88 Hz, measured at the 32 control microphones illustrated in Figure 2 with the control system off (left hand plot) and on (right hand plot).

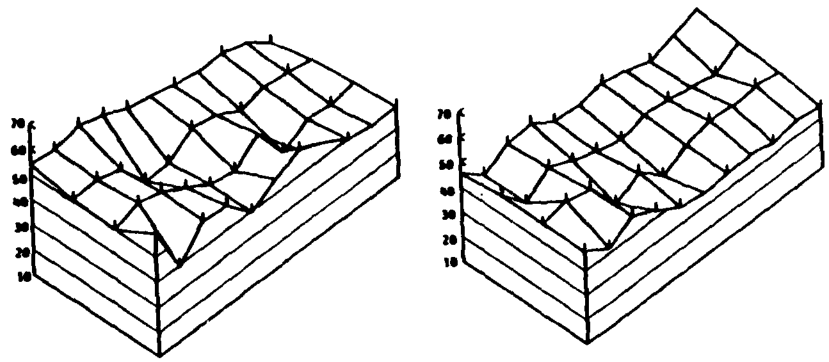

Figure 4. Pressure distribution at 176 Hz, measured at the 32 control microphones.

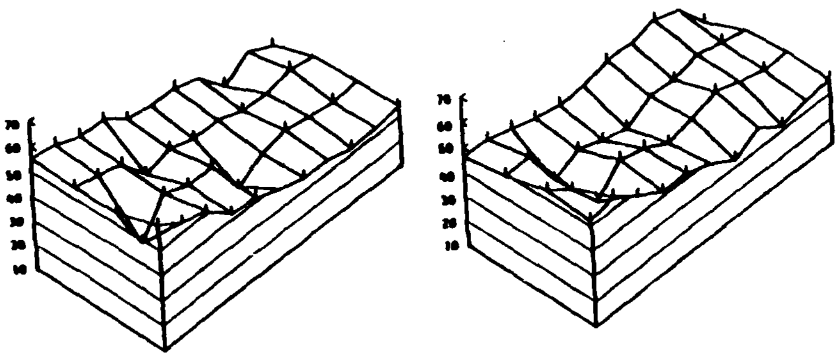

Figure 5. Pressure distribution at 264 Hz, measured at the 32 control microphones.

Control system configuration	Propeller producing sound field	88 Hz ΔJ_{p32}	176 Hz ΔJ_{p32}	264 Hz ΔJ_{p32}
Loudspeakers fully distributed (Fig. 2)	Port	-13.8	-7.1	-4.0
	Starboard	-10.9	-4.9	-4.8

Table 1. Changes in the sum of the squares of the pressures at 32 microphones (ΔJ_{p32}); loudspeakers positioned on the floor and in the overhead bins only, as in Figure 2.

AN APPLICATION OF ACTIVE NOISE CONTROL USING VIBRATIONAL FORCE INPUTS

from

Simpson, M.A., Luong, T.M., Fuller, C.R., and Jones, J.D., "Full-Scale Demonstration Tests of Cabin Noise Reduction Using Active Vibration Control," AIAA Paper 89-1074.

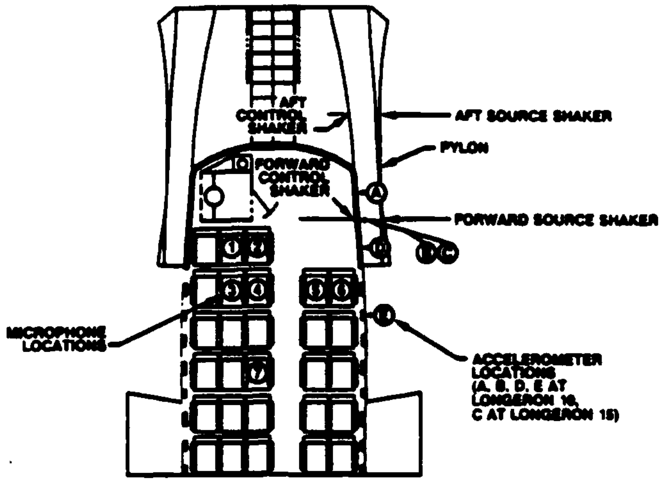

FIGURE 2a. SHAKER, MICROPHONE, AND ACCELEROMETER LOCATIONS IN THE TEST FUSELAGE

FIGURE 2b. CABIN INTERIOR, FACING AFT, SHOWING PLACEMENT OF MICROPHONES

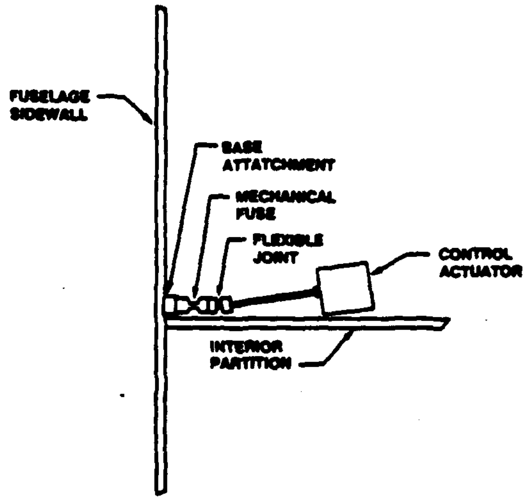

FIGURE 3a. CONFIGURATION OF CONTROL SHAKER ATTACHMENT

FIGURE 3b. CONTROL SHAKER IN PLACE

TABLE 1
ACTIVE VIBRATION CONTROL
TEST CONFIGURATIONS

TEST SET	TEST NO.	SOURCE FREQUENCY	SOURCE LOCATION	CONTROL LOCATION	ERROR SENSORS	MEASUREMENT SENSORS	TEST PARAMETERS EVALUATED
I	1	170 Hz	FORWARD	FORWARD	1 MIC	7 MICS	NUMBER OF ERROR SENSORS
	2	170 Hz	FORWARD	FORWARD	2 MICS	7 MICS	
	3	170 Hz	FORWARD	FORWARD	4 MICS	7 MICS	
II	4	185 Hz	FORWARD	FORWARD	4 MICS	7 MICS	SOURCE FREQUENCY
	5	120 Hz	FORWARD	FORWARD	4 MICS	7 MICS	
III	6	170 Hz	FORWARD	FORWARD	1 ACCEL	5 ACCELS	ACCELEROMETER ERROR SENSOR
	7	170 Hz	FORWARD	FORWARD	1 ACCEL	7 MICS	
IV	8	170 Hz	AFT	AFT	1 MIC	7 MICS	SOURCE LOCATION/ NUMBER OF CONTROL SHAKERS
	9	170 Hz	AFT	AFT	4 MICS	7 MICS	
	10	170 Hz	AFT	FORWARD AND AFT	4 MICS	7 MICS	

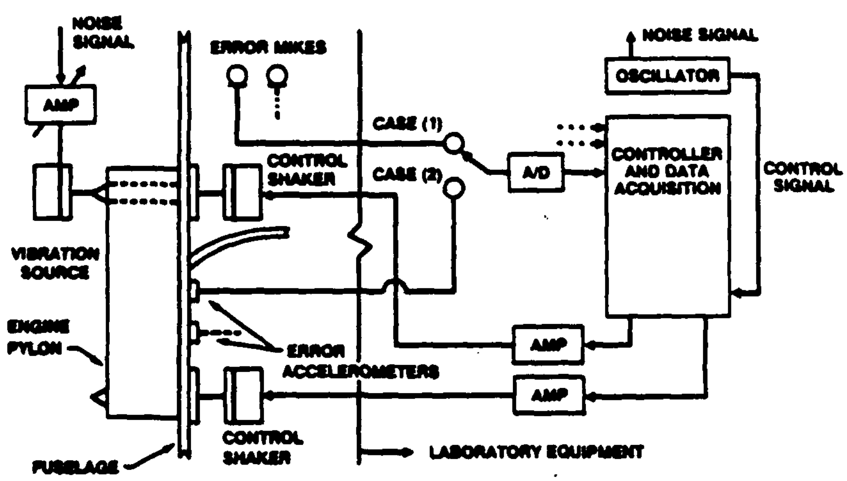

FIGURE 4. EXPERIMENTAL TEST ARRANGEMENT

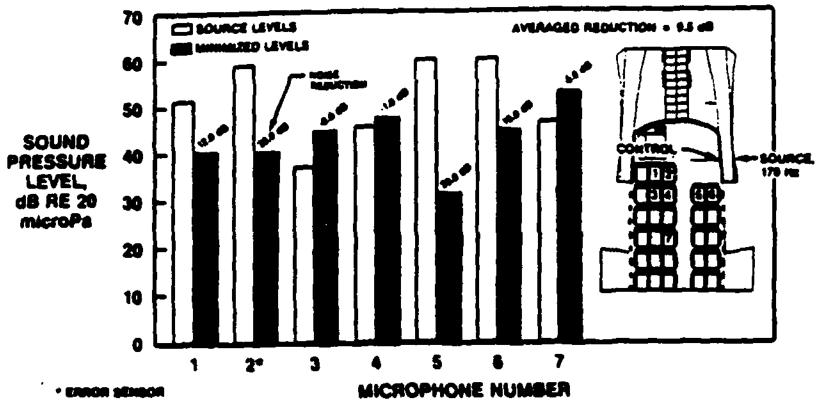

FIGURE 5. MEASURED NOISE LEVELS, ONE ERROR SENSOR (TEST 1)

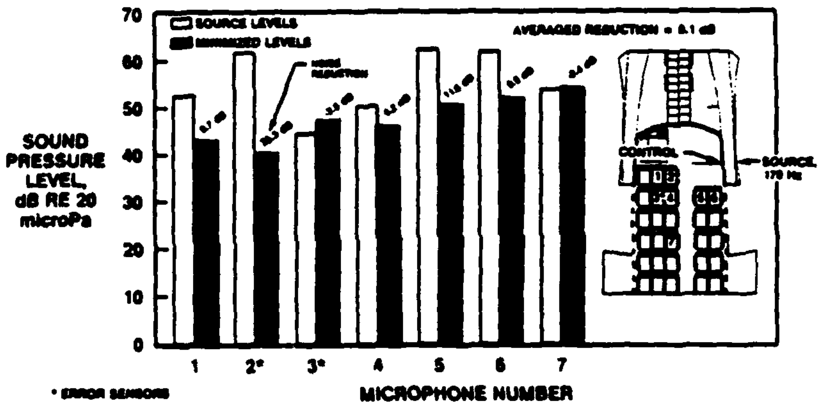

FIGURE 6. MEASURED NOISE LEVELS, TWO ERROR SENSORS (TEST 2)

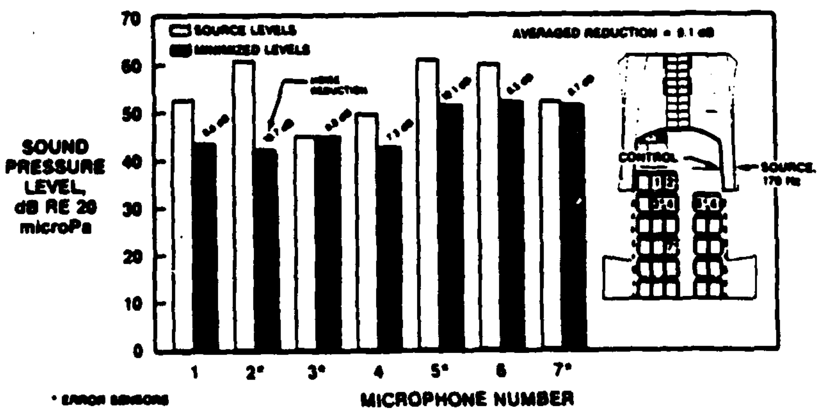

FIGURE 7. MEASURED NOISE LEVELS, FOUR ERROR SENSORS (TEST 3)

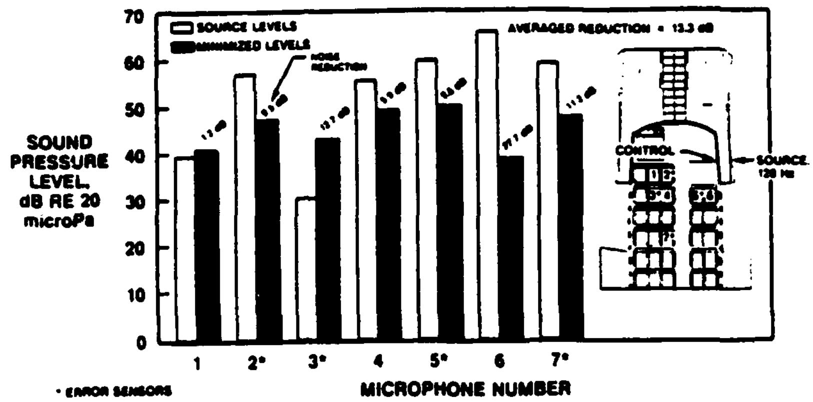

FIGURE 9. MEASURED NOISE LEVELS, 120 Hz (TEST 5)

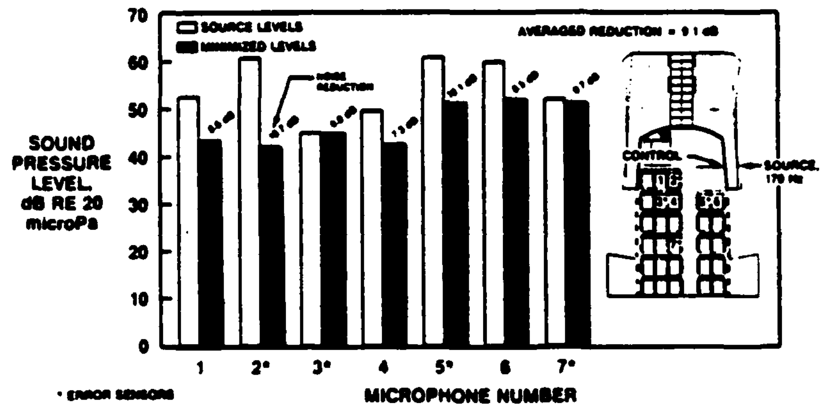

FIGURE 7. MEASURED NOISE LEVELS, FOUR ERROR SENSORS (TEST 3)

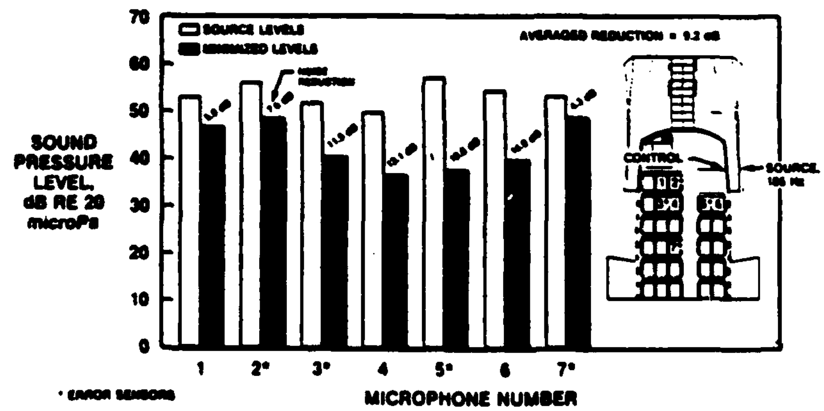

FIGURE 8. MEASURED NOISE LEVELS, 185 Hz (TEST 4)

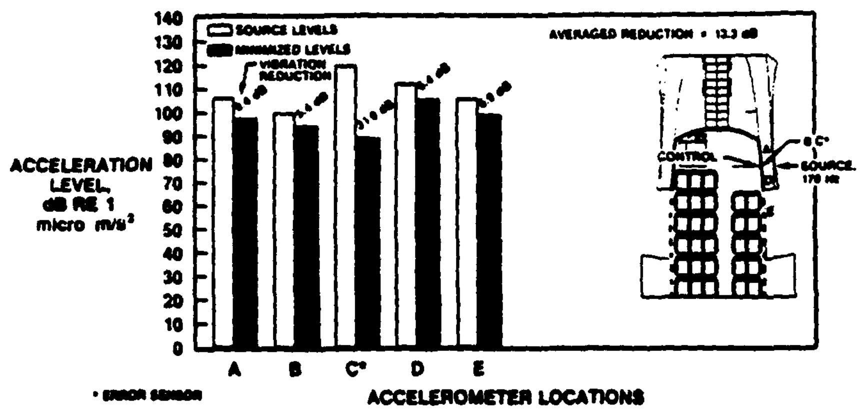

FIGURE 10. MEASURED VIBRATION LEVELS, ONE ACCELEROMETER ERROR SENSOR (TEST 6)

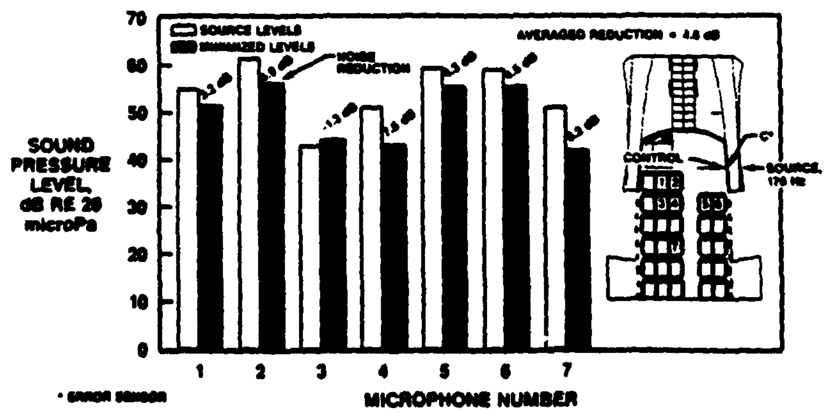

FIGURE 11. MEASURED NOISE LEVELS, ONE ACCELEROMETER ERROR SENSOR (TEST 7)

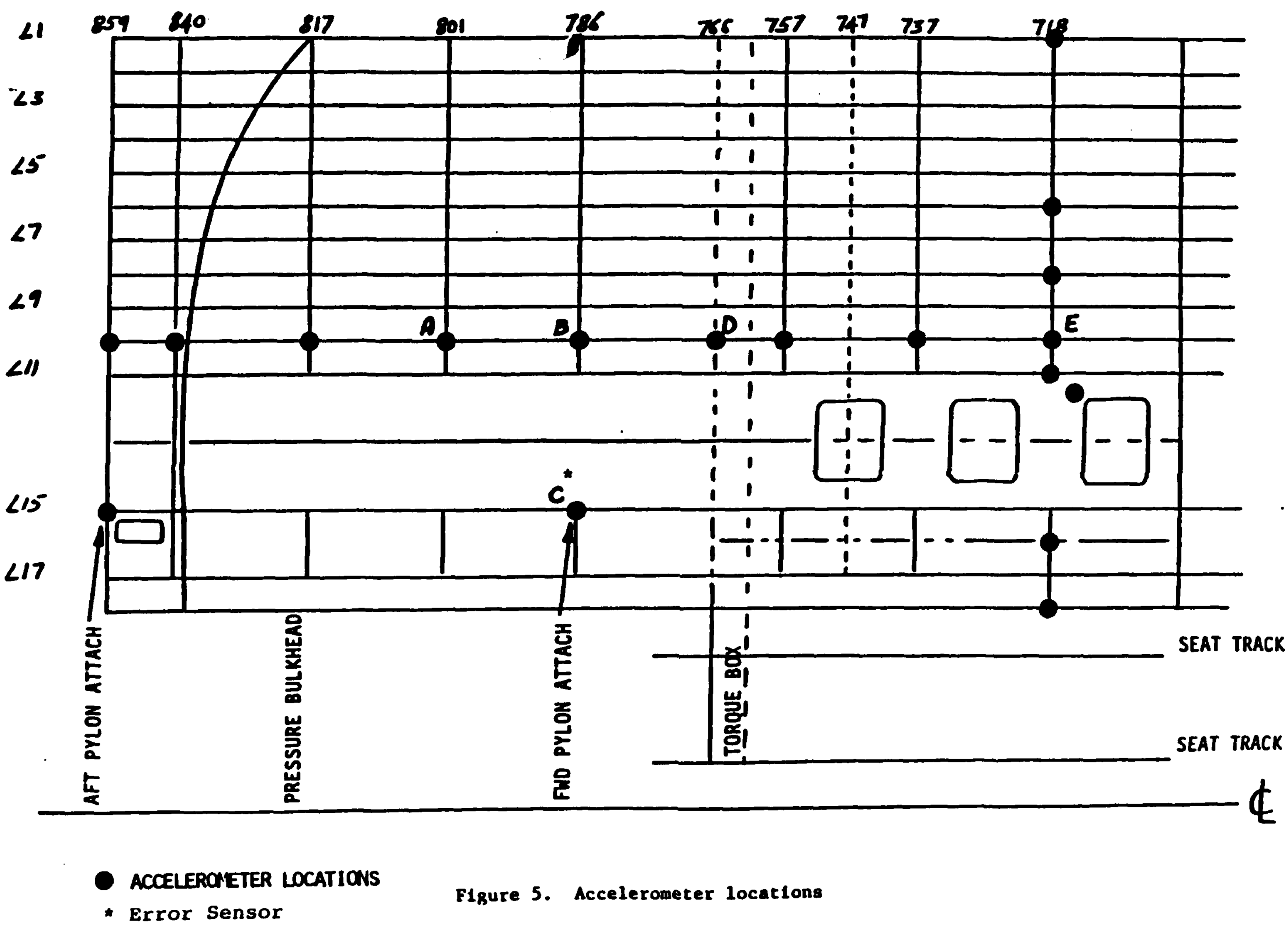

Figure 5. Accelerometer locations

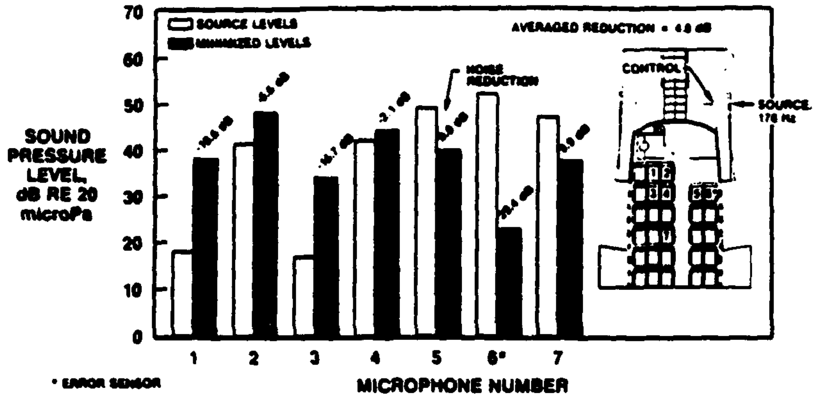

FIGURE 12. MEASURED NOISE LEVELS, AFT SOURCE AND CONTROL SHAKERS, ONE ERROR SENSOR (TEST 8)

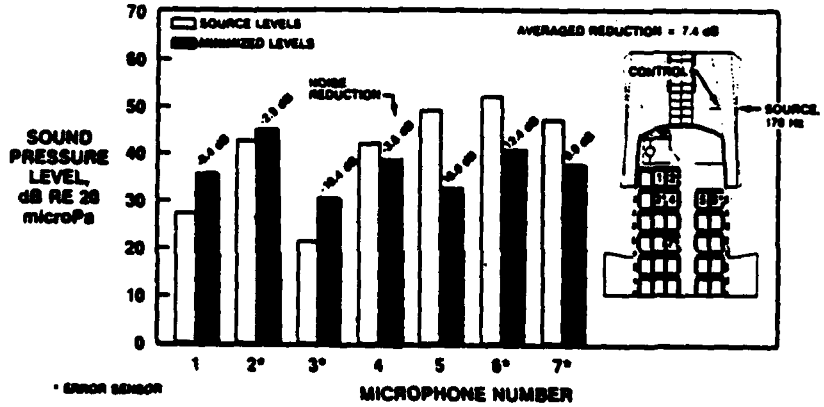

FIGURE 13. MEASURED NOISE LEVELS, AFT SOURCE AND CONTROL SHAKERS, FOUR ERROR SENSORS (TEST 9)

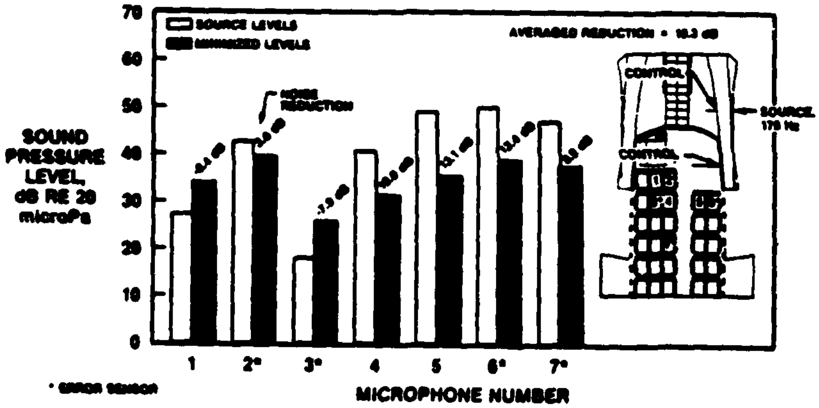

FIGURE 14. MEASURED NOISE LEVELS, FORWARD AND AFT CONTROL SHAKERS (TEST 10)

ACTIVE NOISE CONTROL STRATEGIES FOR THE ROTORCRAFT ENVIRONMENT

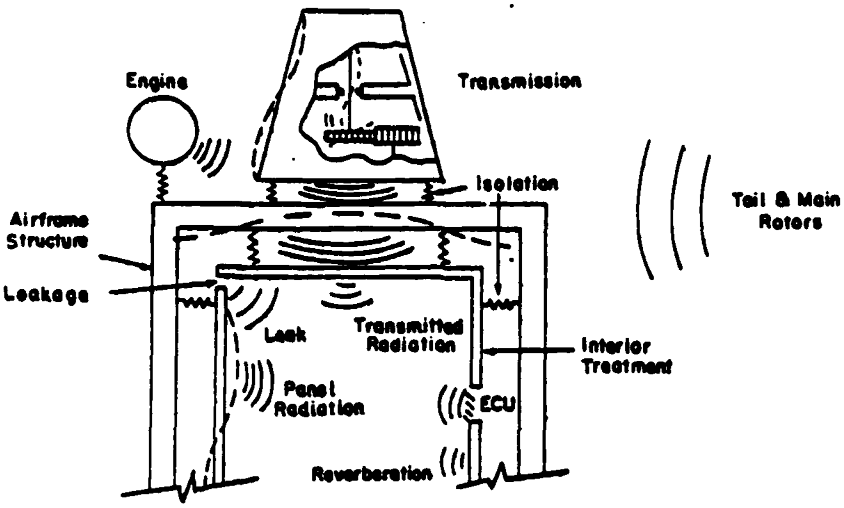

Figure 1. Internal Noise Sources and Paths.

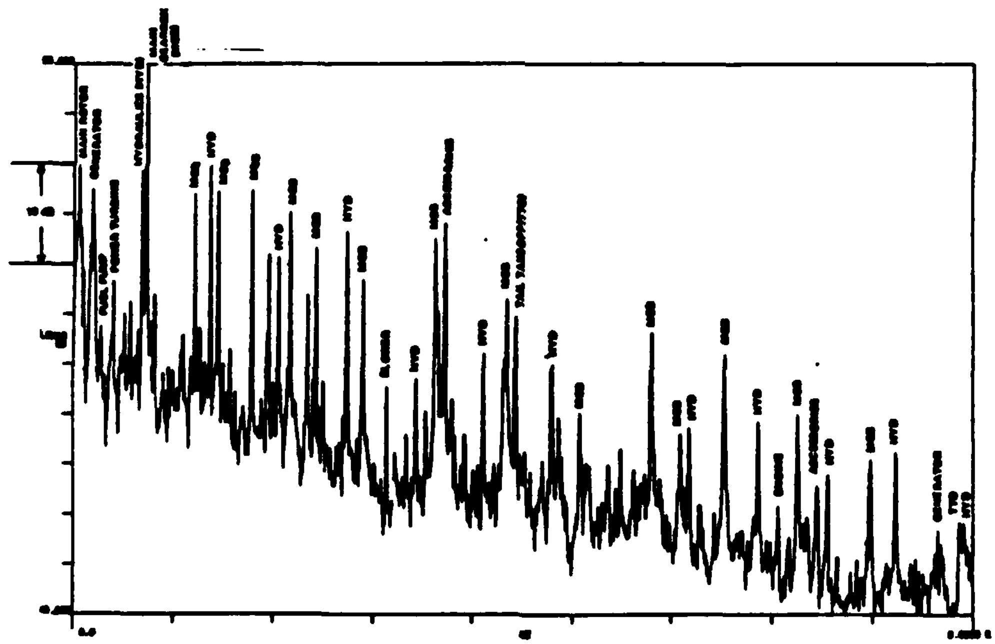

Figure 13. S-76 Bare Cabin SPL-75 m/s LFO 100% N_R .

Yoerkie, C.A., Moore, J.A., Manning, J.E., "Development of Rotorcraft Interior Noise Control Concepts - Phase 1: Definition Study," NASA Contractor Report 166101, May 1983.

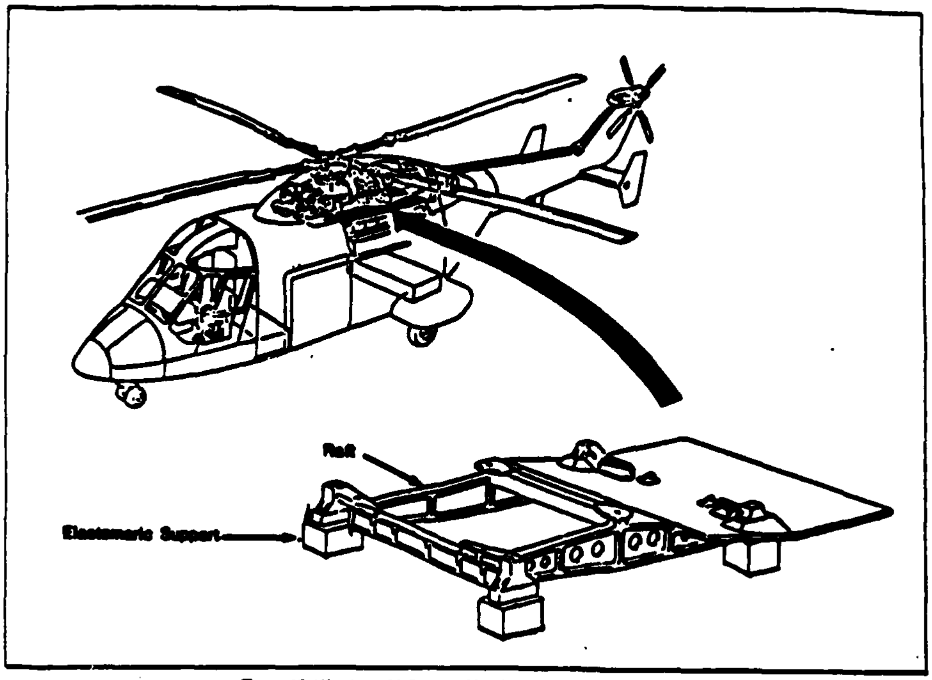

Figure 13. Westland 30 Series 100 raft construction and location.

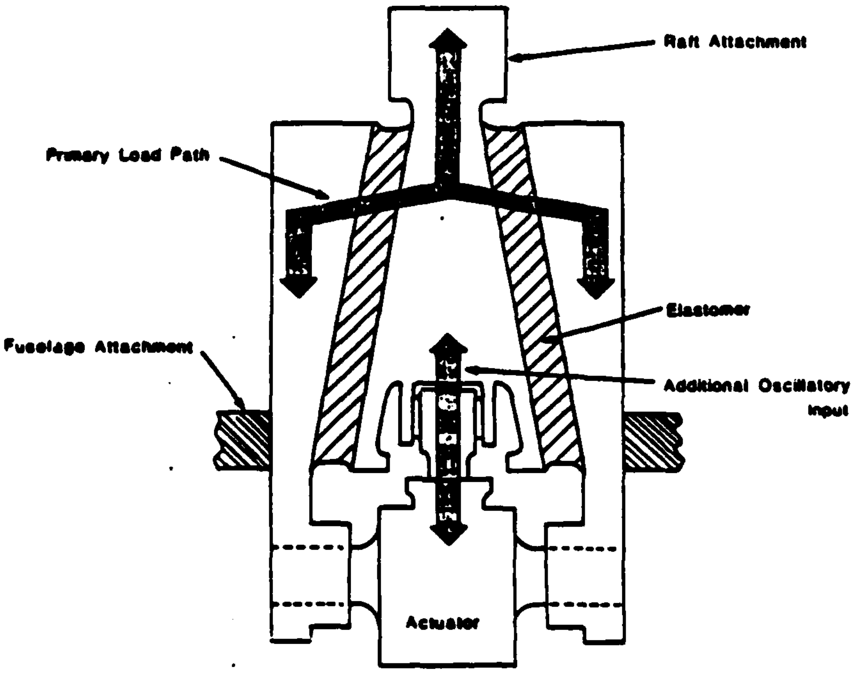

FIGURE 8. Modified Elastomeric Support (including Force Actuator)

King, S.P., "The Minimization of Helicopter Vibration Through Blade Design and Active Control," Aeronautical Journal, pp. 247-263, August/September 1988.

ACTIVE NOISE
CONTROL STRATEGIES

ACOUSTIC CONTROL SOURCES (LOUDSPEAKERS)

- *Acoustic Controllers can be used for either airborne or structureborne noise.*
- Acoustic controllers are simpler to implement.
- Generally, a large array of acoustic controllers are needed for global reduction over a reasonable spatial region.

VIBRATION CONTROL SOURCES (SHAKERS)

- Vibration controllers can be used for structureborne noise only.
- Vibration controllers are more difficult to implement.
- Generally, a smaller array of vibration controllers are needed for global reduction.
- Vibration controllers are most effective when power flow into the structure is localized.

LUNCHEON ADDRESS

Joseph Goldberg
Program Manager
Sikorsky Aircraft-UTC

"What Rotorcraft Composite Manufacturers Now Require from the Research Community"

"What Rotorcraft Composite Manufacturers Now Require from the Research Community"

o The philosopher Ralph Waldo Emerson once wrote, "If a man can make a better book, preach a better sermon, or make a better mousetrap than his neighbor, though he builds his house in the woods, the world will make a beaten path to his door". But Emerson was wrong! You must beat a path to the customer's door *to find out what he wants and needs.* Stunning innovation and brilliantly designed new products are only part of the answer. Fortunately Mr. Emerson made his living as a philosopher - not as a company president.

o Up to now, led by the rotorcraft industry, Mr. Emerson's error was not significant. However, today it has become significant and I'd like to discuss the impact.

o First, why have rotorcraft designers led the way and what have they done?

Rotorcraft customers wanted long life (durability) and low weight in a very demanding environment. Historically, wet layup composites found A/C application including helo in the late 50's. The marginal nature of the material form for both performance and processing severely limited use. Fibers and fiber volume severely limited specific strengths and stiffness plus quality problems of wet layup. Driven by these issues the materials industry started engineering these materials: prepreg epoxies, kevlar, boron, graphite, uni tape. Glass thermoset prepregs found simple applications in the '60s for fairings and non-critical structure. Rotor blades provide the first major technical applications for composites. Glass was the material that was created for rotor blades. Tough, fatigue strain resistant, no corrosion, relatively easily drilled, adaptable to shapes, low cost.

Other technology breakthroughs that composites achieved through rotor craft in the '70s were the flexbeam and bearingless rotor notably the tail rotors of UTAS and AAH Aircraft. The very high fatigue strain allowable and anisotropic properties of these materials allowed them to be engineered for unique capabilities. As with the rotor blades these structures provided superb improvements in performance and reliability over the previous generation of metal structures. With the level of success in the heart of the rotor craft composite appeared to be a relatively easy transition into the airframe. Thus, birth was given to a series of Government and contractor funded programs. These, of course, culminated in the '80s with the ACAP aircraft and the Boeing 360. They looked and flew like any other aircraft, saved 20% plus weight, were more survivable and were projected to cost 20% less as well. Unfortunately engineers are less well accomplished at cost reduction than weight predictions and in the light of five (5) years of hind sight the cost saving advantages may not have been achieved; at least not with Thermoset Prepreg in Autoclave cure.

Epoxy prepregs were limited to about 300°F applications, are significantly effected by moisture, suffer major degradations in strength from low velocity impact, and have many characteristics that impeded automation and repeatable processing. The realization is that composite materials require significant additional engineering if their market applications were to continue to expand. Other composite material forms and applications attacked these problems.

In summary, there have been three (3) distinct generations:

Generation 1: Original Non-Structural parts and rotor blades **(VG 1 & 2)**
Advantage: Weight Savings
Cost

Generation 2: Airframe Structural Parts **(VG 3 through 9)**
Advantage: Weight Savings

Generation 3: High Performance Parts **(VG 10 through 13)**
Advantage: Cost/Producibility
Weight Savings

We are in Generation 3 and applications are growing.

o **Where are composites in the Rotorcraft Industry going?**
- **They are becoming pervasive through the airframe**
- **Airframe fittings are the next challenge. They require high rate/low cost production of smaller, more complex components. (Re-show VG 11)**

Two significant alternatives to classic prepreg processing are receiving broad attention: Thermoplastic Forming and Liquid Resin Molding/Resin Transfer Molding. The Thermoplastic advocates hope to produce low cost details for assembly similar to sheet metal airframe manufacture. The goal of RTM is the comolding of very complex assemblies from relatively low cost raw materials.

In summary, composites are proven for structural weight savings.

However, Composites are unproven for:
- **Producibility/Quality**
- **Labor Cost**

These problems stem from the MANTEC dilemma

o **The MANTEC Dilemma**
- **ACAP, CRF were MANTEC Programs** **(VG 14)**
- **MANTEC was cancelled through lack of funding in 1986**
- **This left Manufacturing Development to Industry**
- **Customers want products and product development is not included in the research agenda. If the Government is the customer, the MANTEC omission makes it difficult to supply to them in the manner they would like.**
- **Manufacturing innovation is not encouraged and that is a serious problem.**

- Examples of MANTEC areas now not attended and that are dictated by customer needs
  - Fitting type missile body parts (VG 15)
  - Automated manufacturing processing (with its incumbent analysis)
    - Preforming
    - Cure Speed/Heat Up/Down Speed (Computational Fluid Dynamics)
    - Post Cure Processing and Automation

- Cost Goals to be Attained by Dictate of the Customer
  - LHX goal is \$1 to \$2/lb of Airframe Structure
  - Missile Body Parts at 20 to 30 per day
  - Transverse Shear Enhancements at no Expense

- These challenges, again, are from the customer and the rotorcraft industry is rising to the challenge.

KEY SELECTION FACTORS

SCATTER

DAMAGE TOLERANCE

MANUFACTURING EASE

COST

FAILURE MODES

COMPRESSIVE LOADING SIGNIFICANCE

WEIGHT

STIFFNESS

SPACE ENVELOPE

STRENGTH

Double Wound Lug

J5406/01

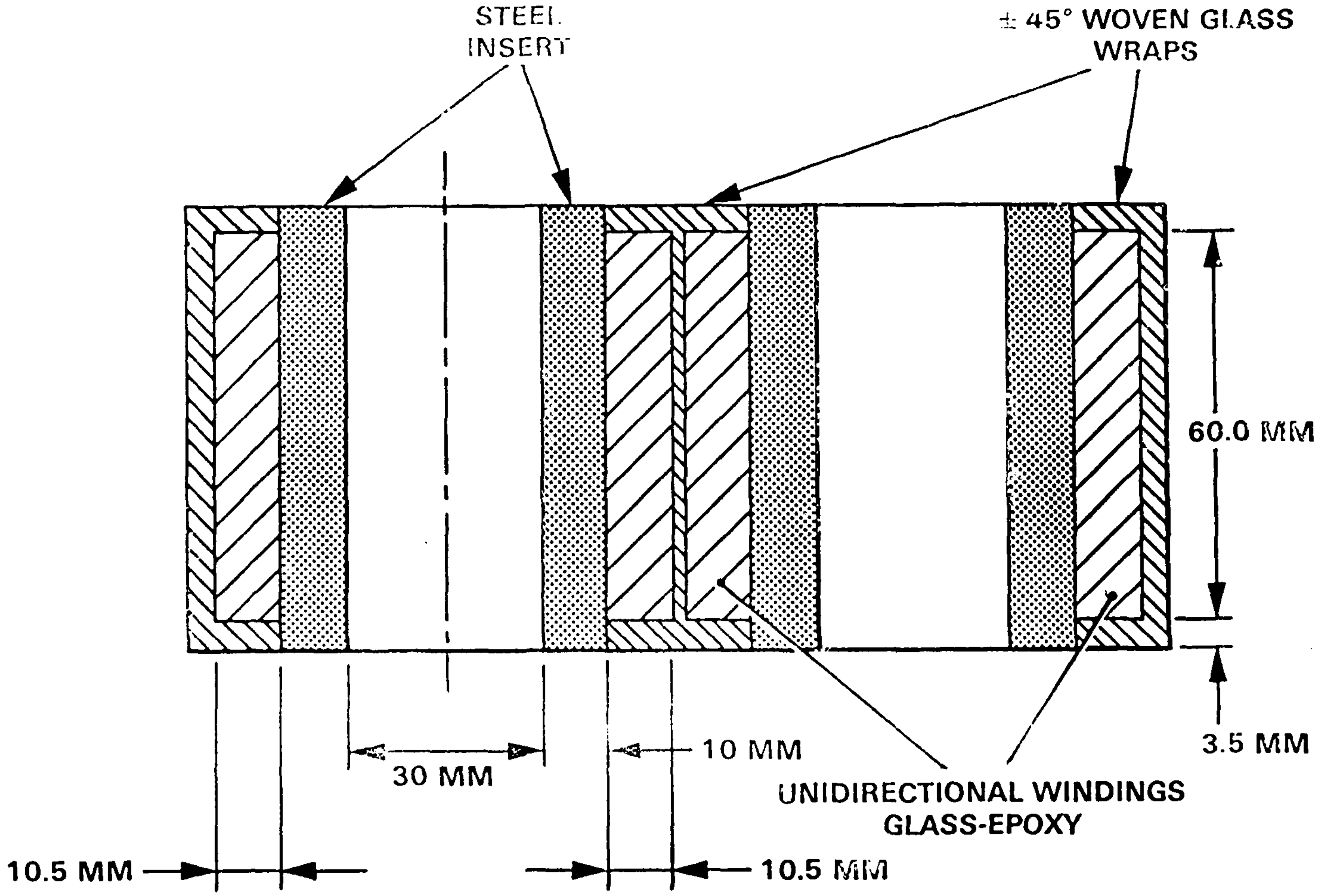

SINGLE WOUND LUG

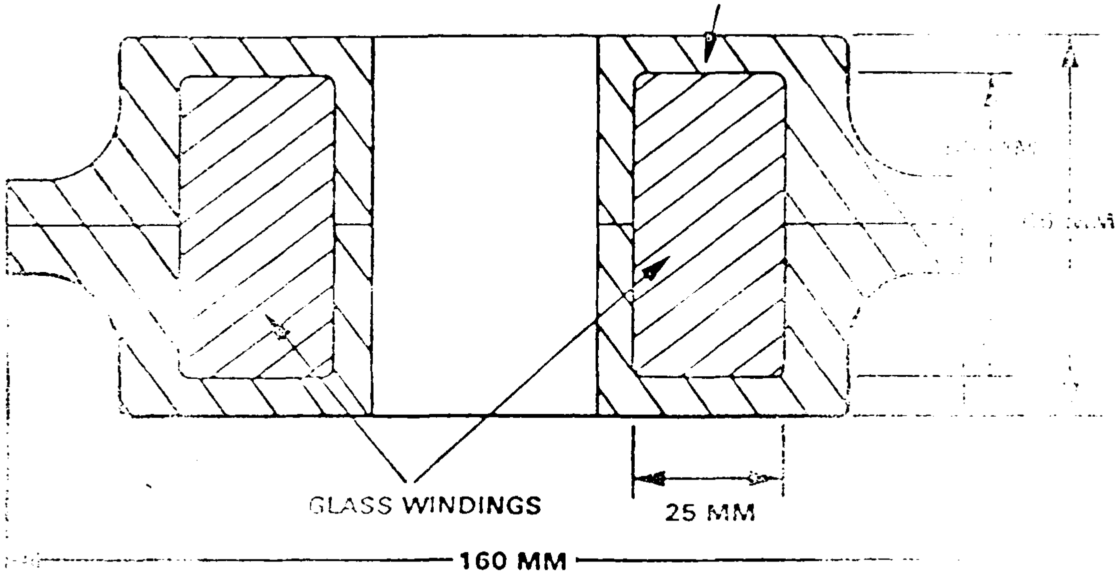

DOUBLE DRILLED LUG

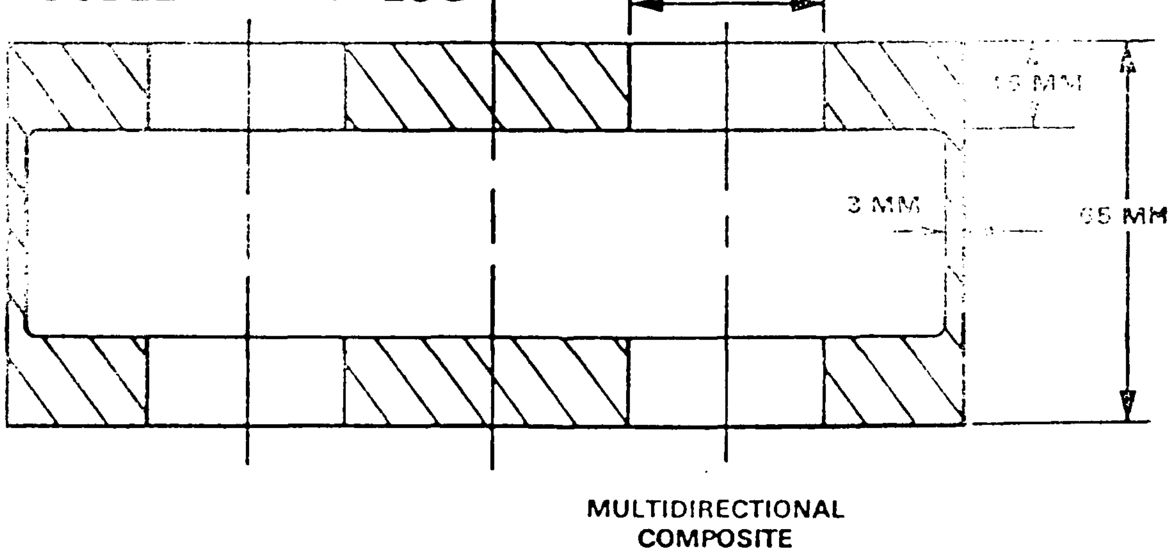

COMPARISON ... ELEMENTS

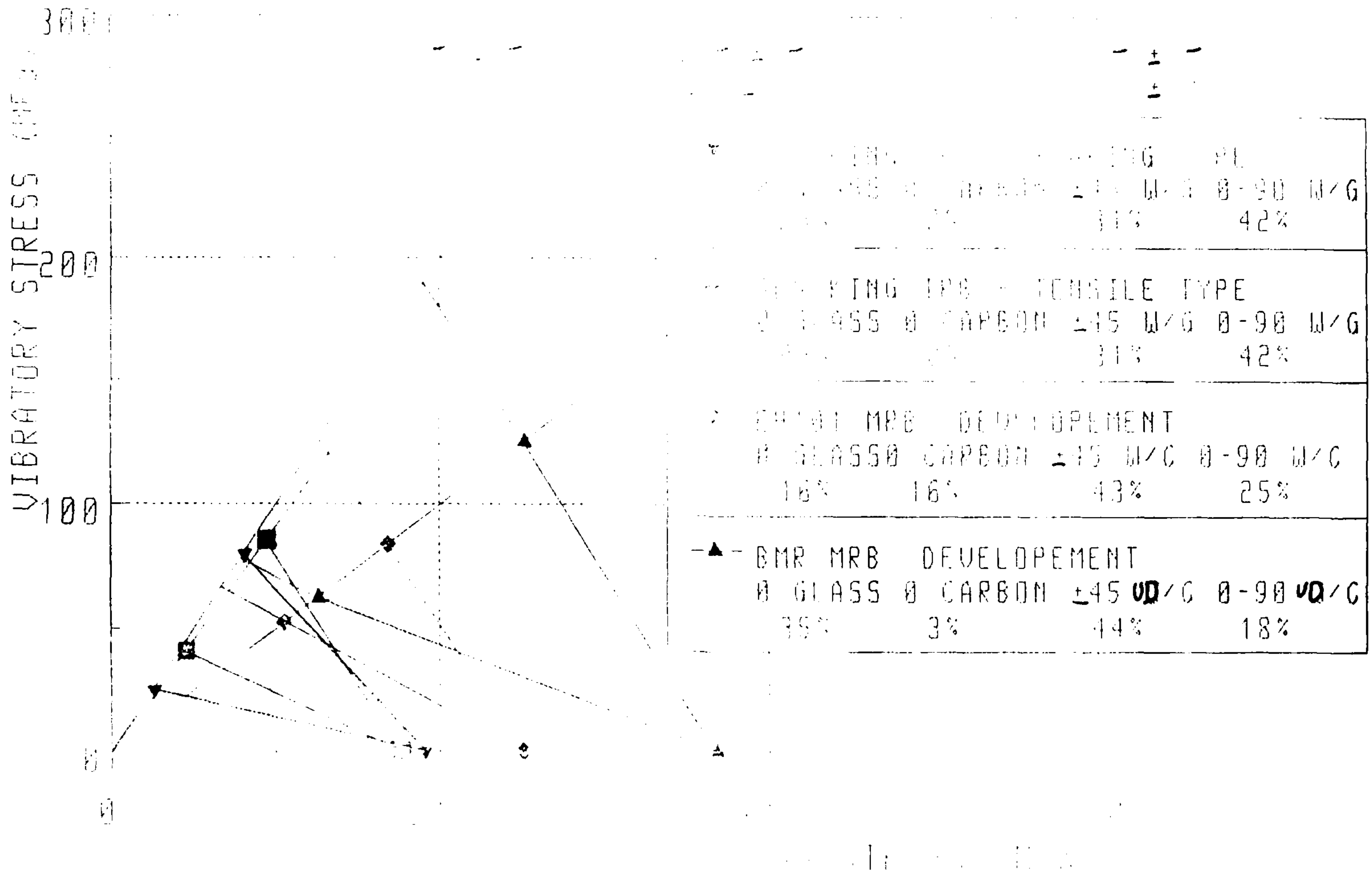

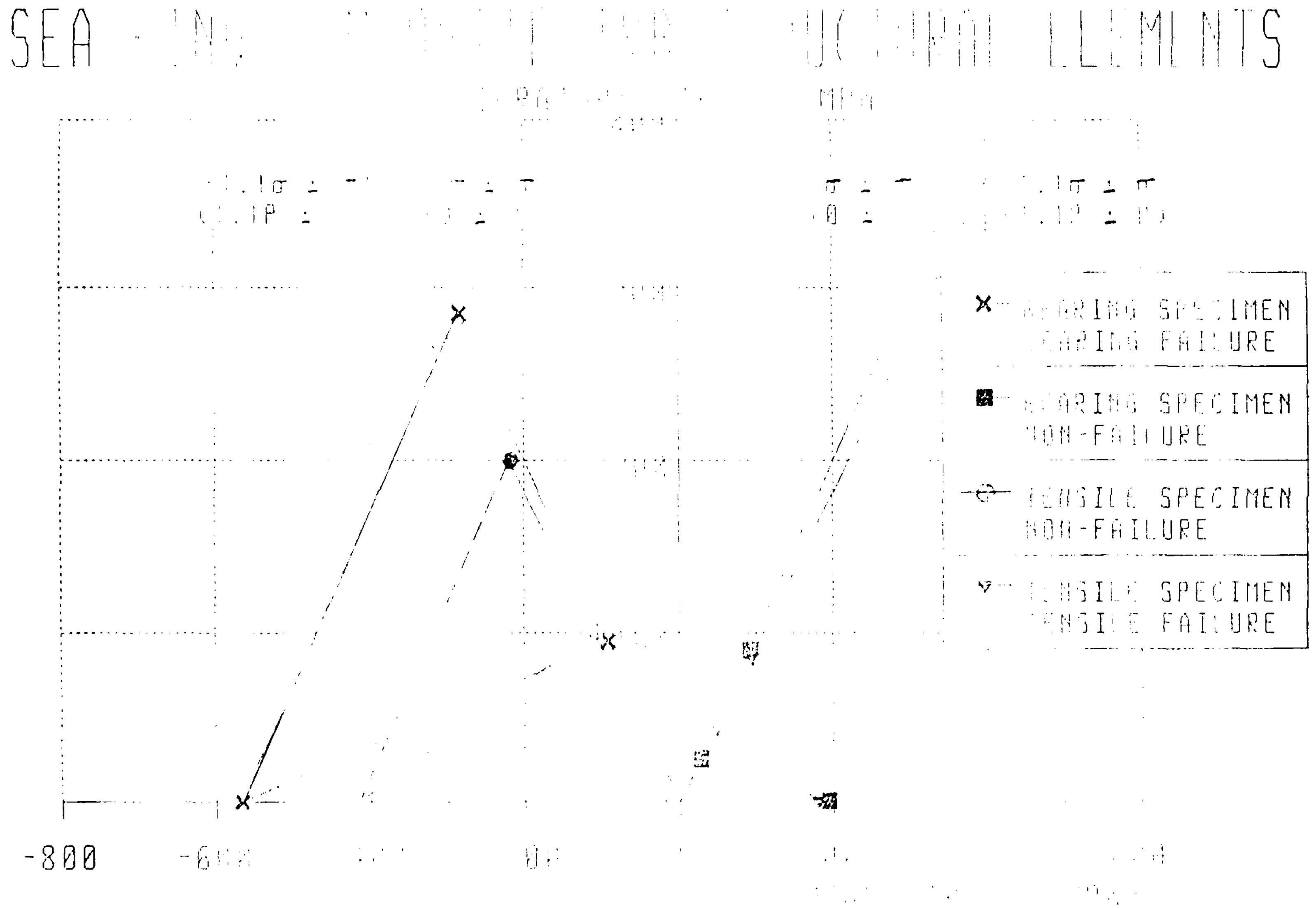

SEA
ELEMENTS
MPa
BEARING SPECIMEN
BEARING FAILURE
BEARING SPECIMEN
NON-FAILURE
TENSILE SPECIMEN
NON-FAILURE
TENSILE SPECIMEN
TENSILE FAILURE
-800

EH101 MRB ROOT END STRUCTURAL ELEMENTS

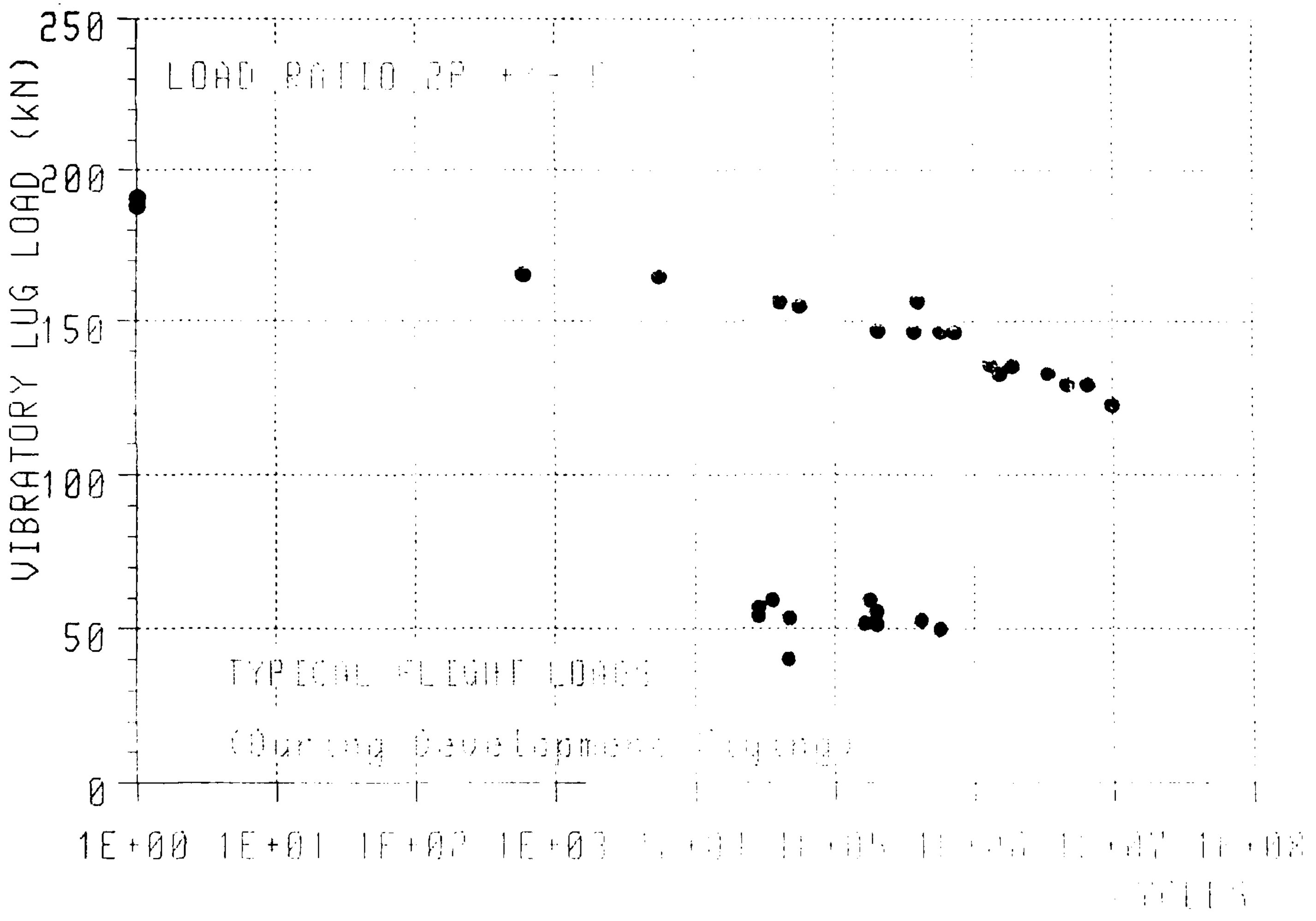

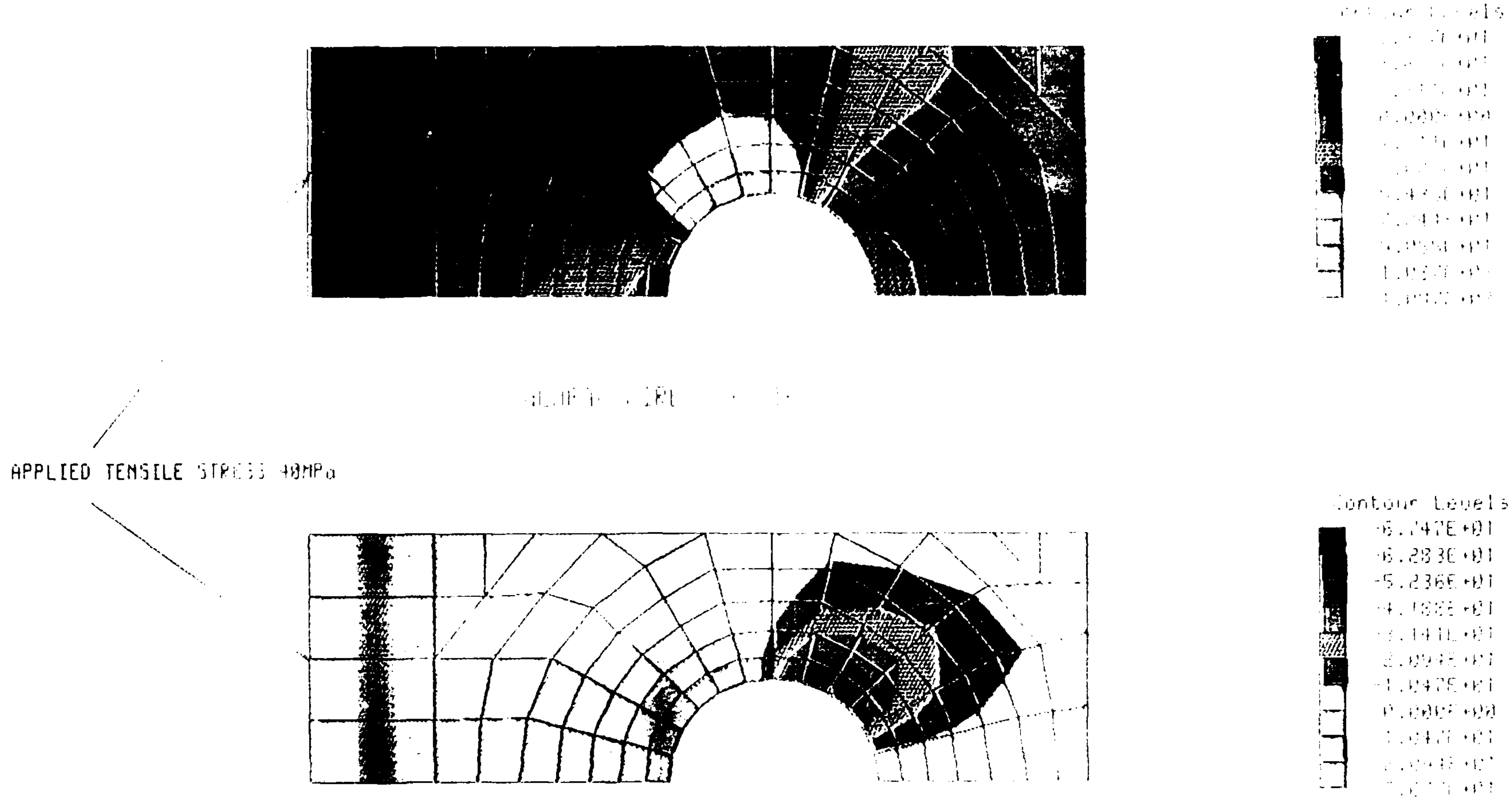
APPLIED TENSILE STRESS 40MPa
Contour Levels
-5.236E+01

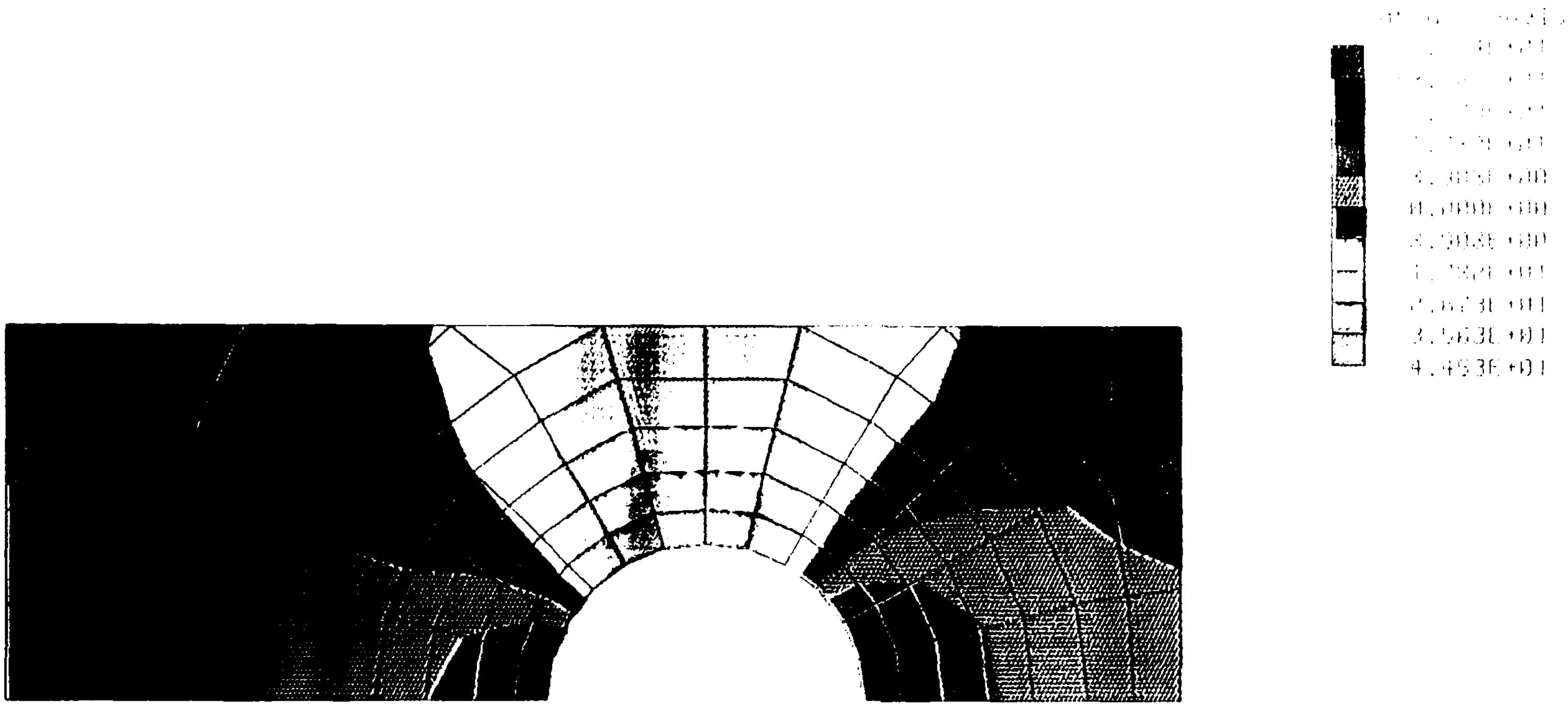

ORILL

Drilled Lug Geometry

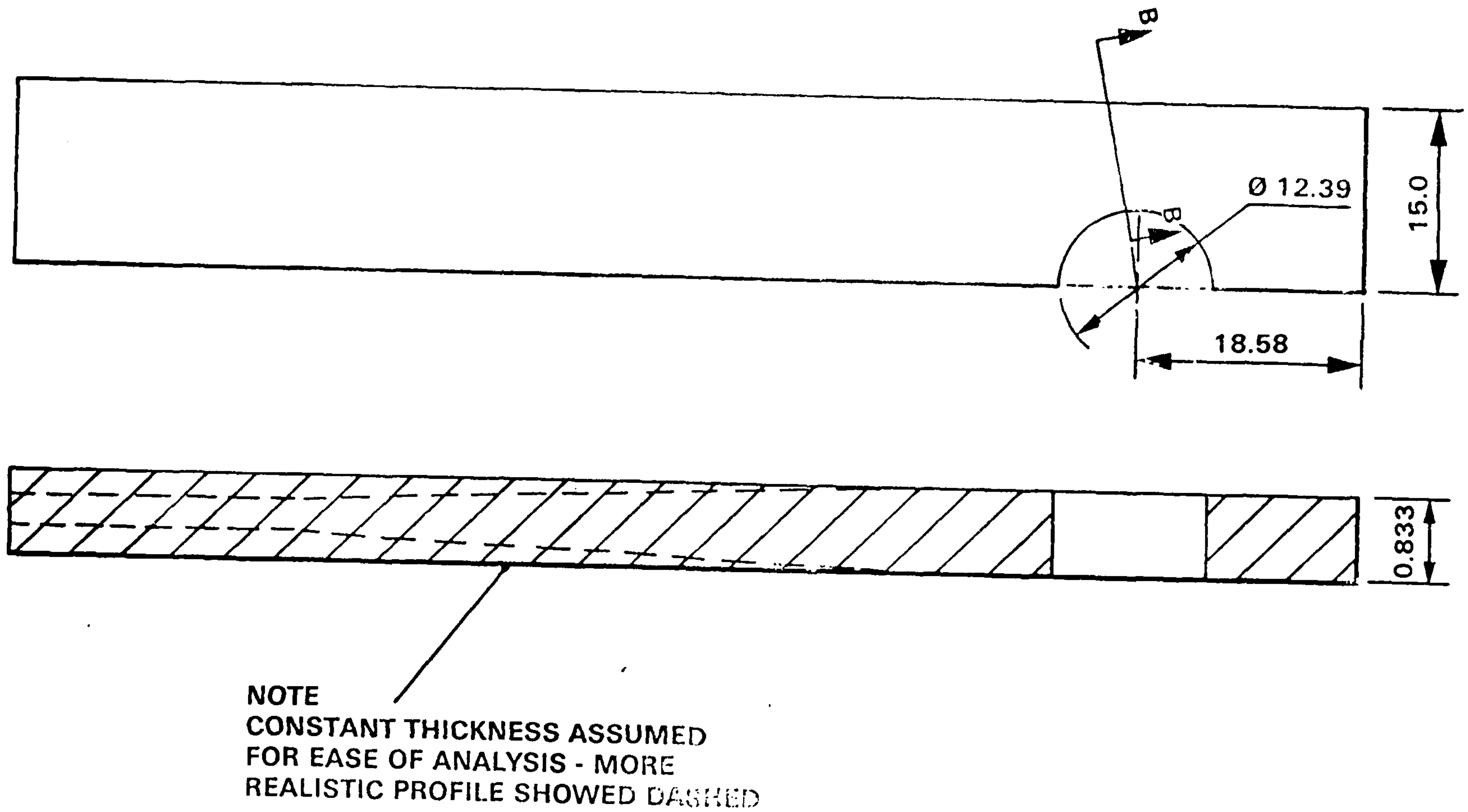

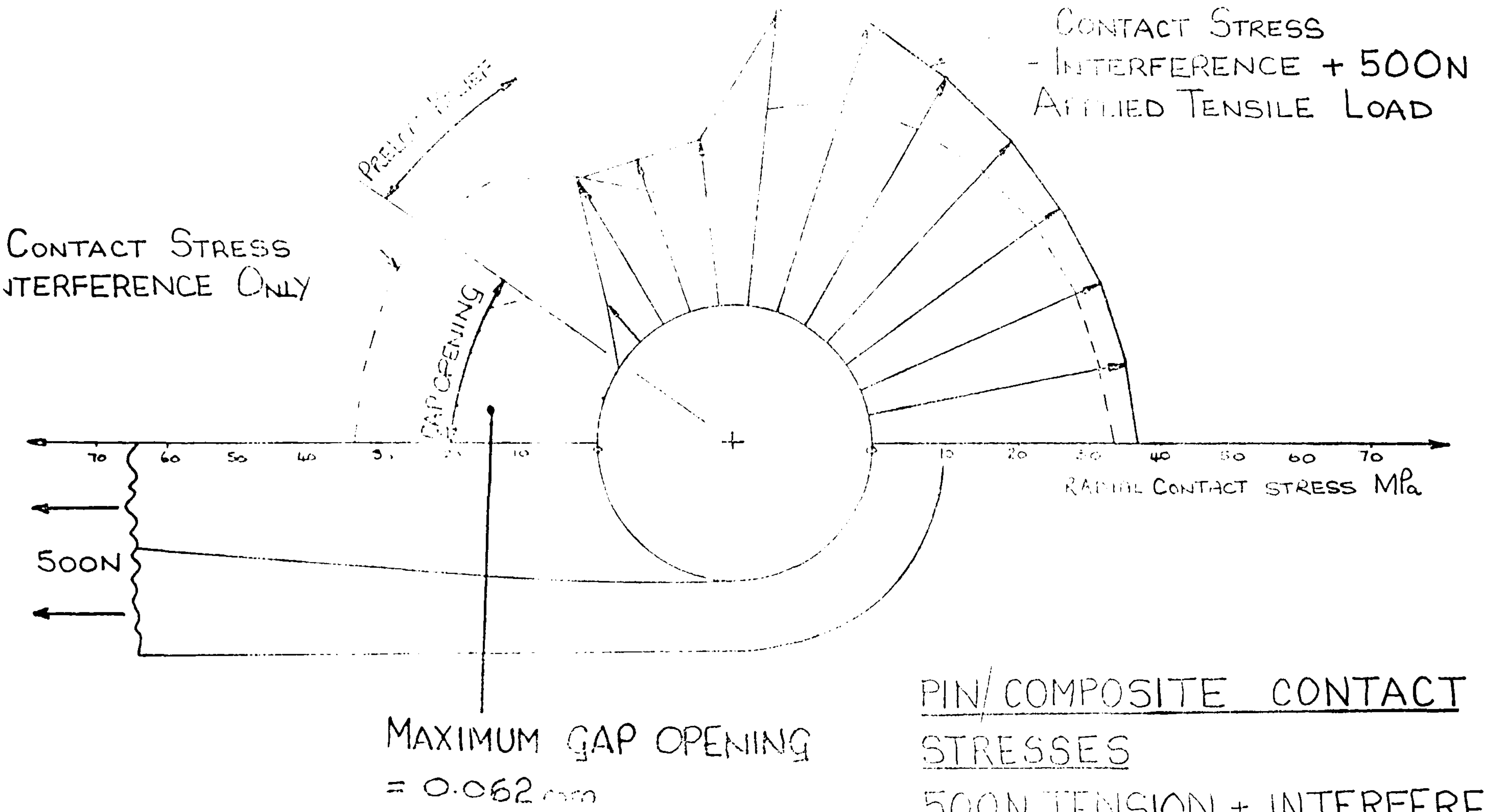

PIN/COMPOSITE CONTACT STRESSES

500N TENSION + INTERFERENCE

Double Wound Lug

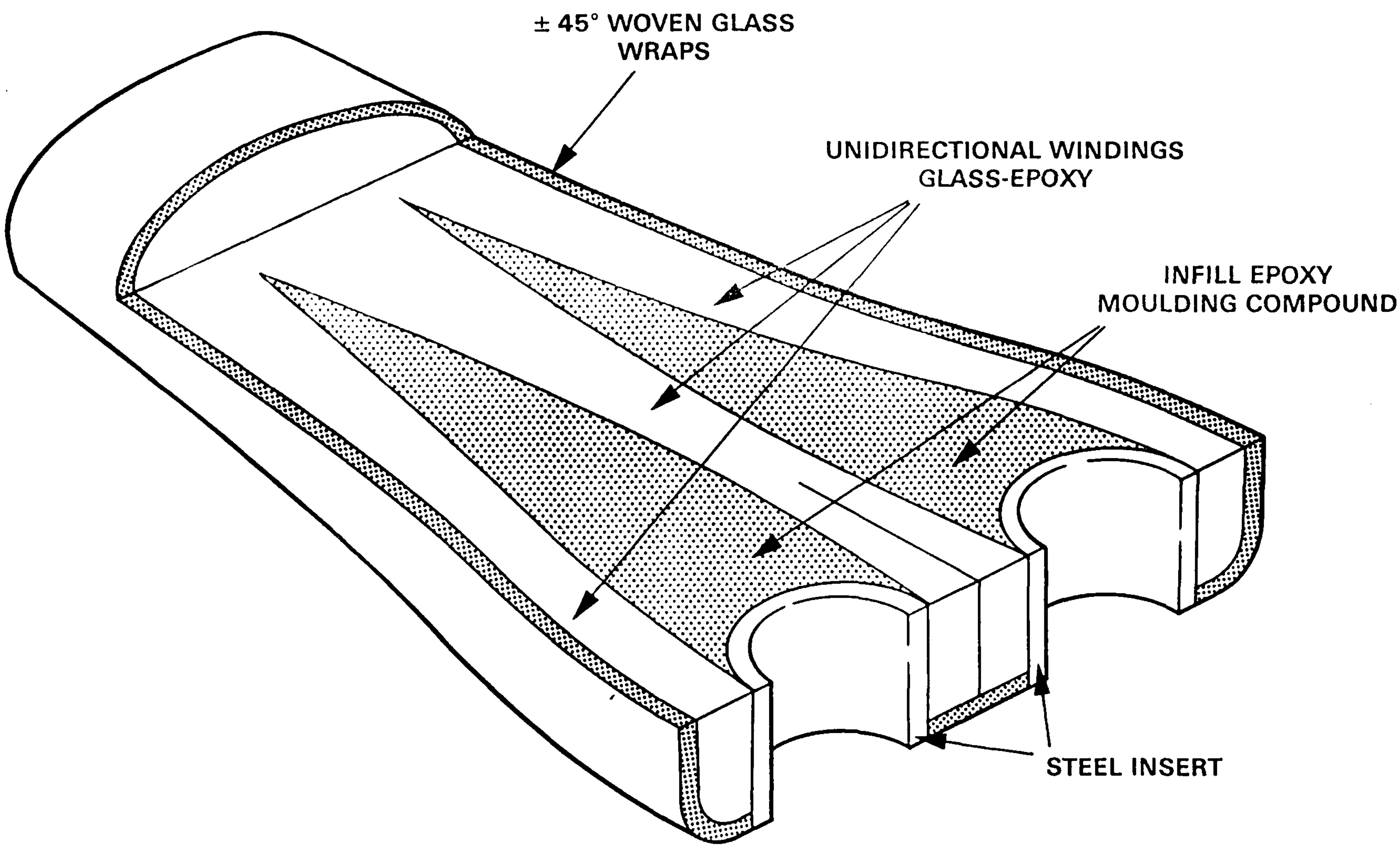

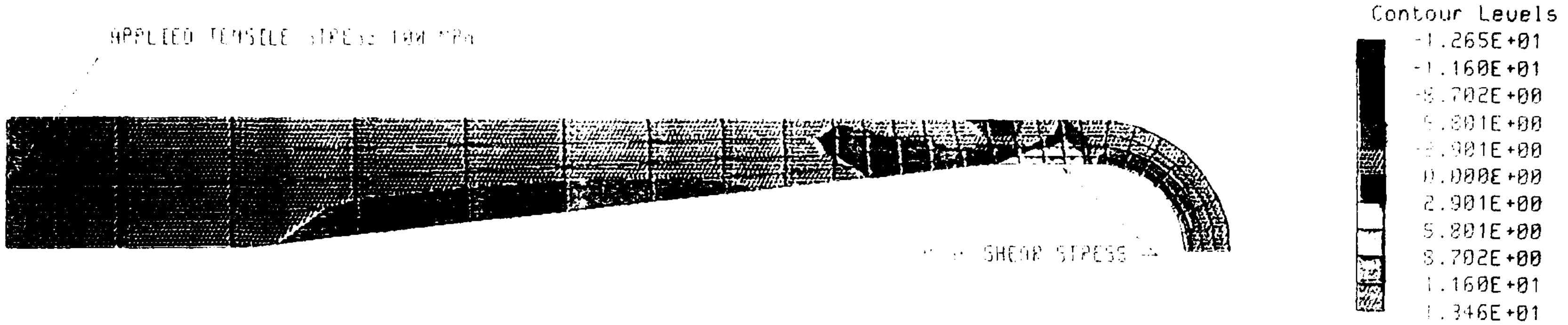

WOUND LUG LOCAL XY SHEAR STRESS

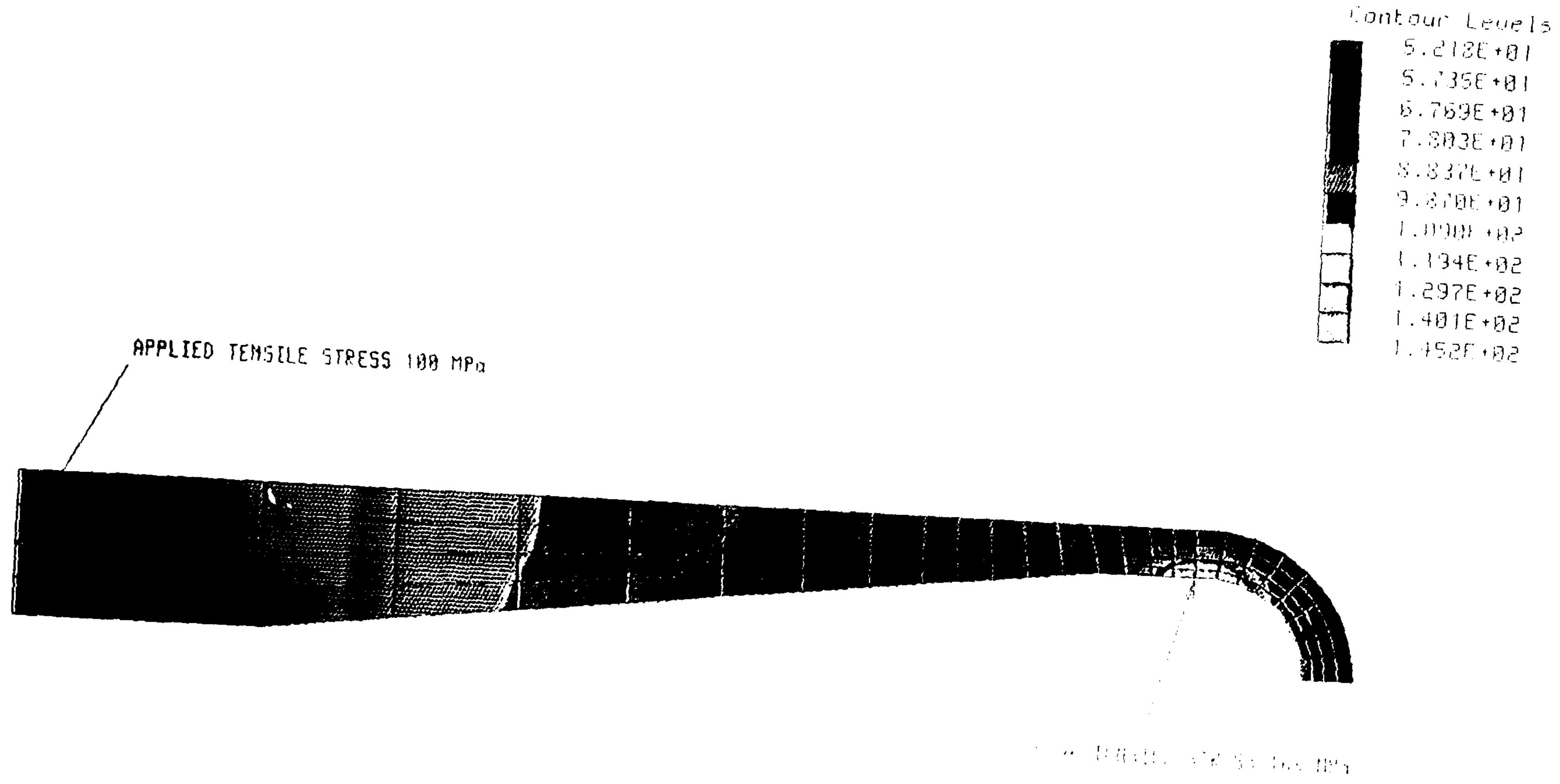

WOUND LUG, LOCAL DIRECT X STRESS

Wound Lug Geometry & Axis Systems

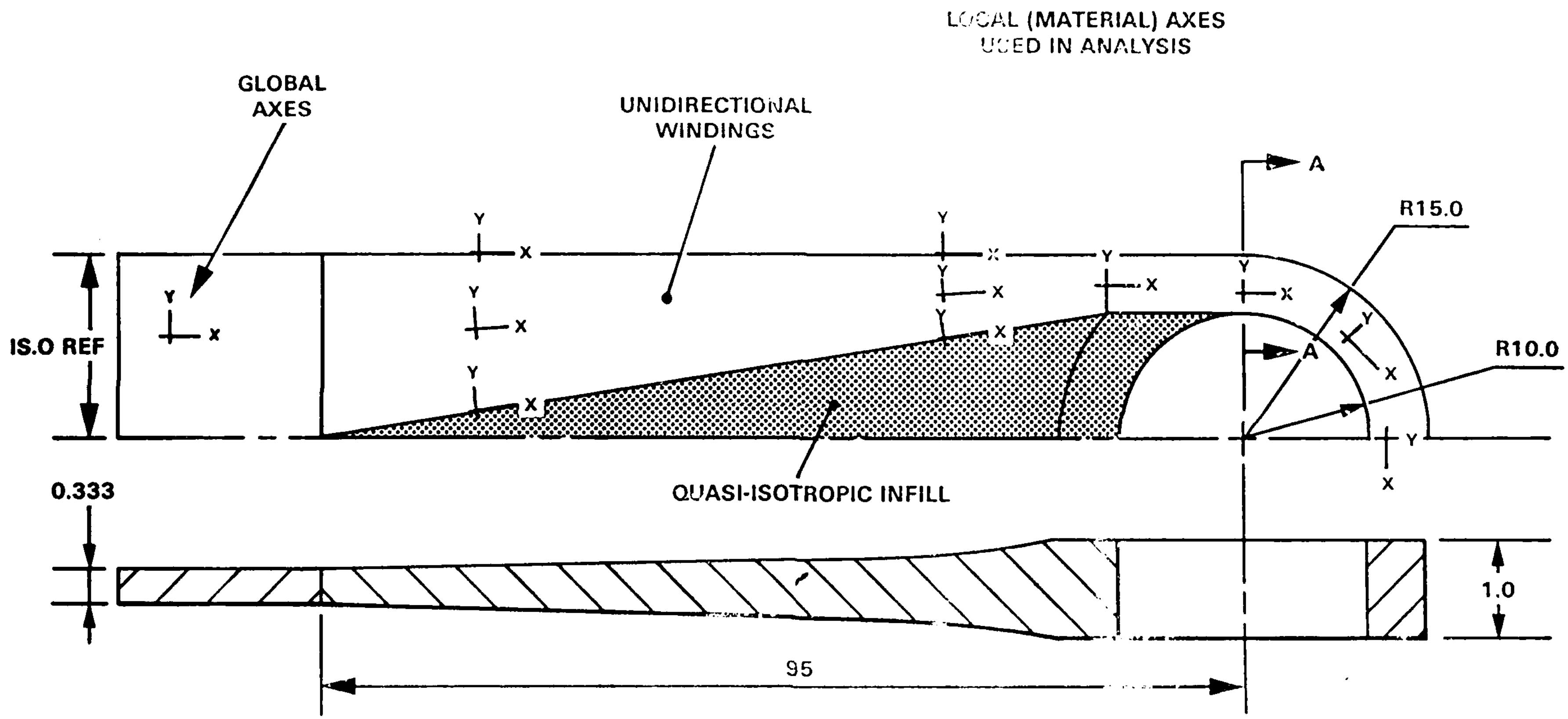

NOT TO SCALE

DISCLAIMER NOTICE

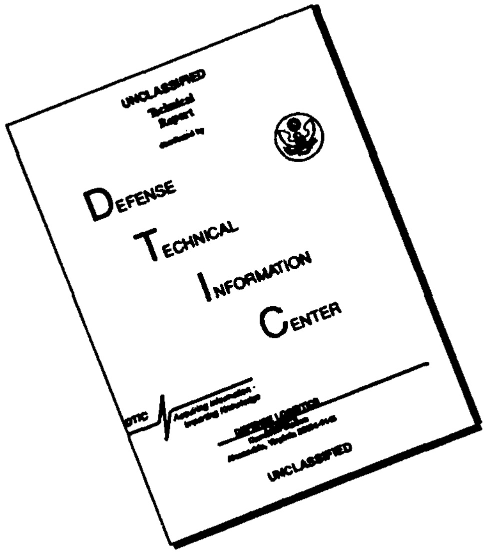

THIS DOCUMENT IS BEST QUALITY AVAILABLE. THE COPY FURNISHED TO DTIC CONTAINED A SIGNIFICANT NUMBER OF PAGES WHICH DO NOT REPRODUCE LEGIBLY.